



Natural Resources  
Canada

Ressources naturelles  
Canada

**GEOLOGICAL SURVEY OF CANADA  
OPEN FILE 7049**

***In Situ* Stress Orientations and Magnitudes in the Liard  
Basin of Western Canada**

**J.S. Bell**

**2015**

**Canada**



**GEOLOGICAL SURVEY OF CANADA  
OPEN FILE 7049**

***In Situ* Stress Orientations and Magnitudes in the Liard  
Basin of Western Canada**

**J.S. Bell<sup>1</sup>**

<sup>1</sup> Sigma H Consultants Ltd.,  
P. O. Box 2797,  
Invermere, BC V0A 1K0

**2015**

© Her Majesty the Queen in Right of Canada, as represented by the Minister of Natural Resources Canada,  
2015

doi:10.4095/295742

This publication is available for free download through GEOSCAN (<http://geoscan.nrcan.gc.ca/>).

**Recommended citation:**

Bell, J.S., 2015. *In Situ* Stress Orientations and Magnitudes in the Liard Basin of Western Canada;  
Geological Survey of Canada, Open File 7049, 410p. doi:10.4095/295742

Publications in this series have not been edited; they are released as submitted by the author.

## TABLE OF CONTENTS

### Part 1:

Abstract	3
Disclaimer	4
1. Introduction	5
2. Describing the state of stress	7
3. Measuring stress orientations in sedimentary basins	8
4. Breakout Identification, analysis and population selection	12
5. Stress axes and trajectories in the Liard Basin	12
6. Conclusions and Implications	20

### Part 2:

7. Introduction	28
8. Describing the state of stress	28
9. Measuring stress orientations in sedimentary basins	29
10. The value of <i>in situ</i> stress magnitude information	32
11. Mapping vertical stress, $S_v$	35
12. Mapping the smaller horizontal stress, $S_{Hmin}$	54
13. Estimating the larger horizontal stress, $S_{Hmax}$	70
14. Estimating and mapping effective stresses	93
15. Trans-basinal relationships	105

16. Overview and Conclusions	108
17. Acknowledgements	109
18. References	110
19. Appendix Notes	113
Appendix 1	114
Appendix 2	189
Appendix 3	253

## FIGURES

Fig. 1. <i>In situ</i> stress at a point in the subsurface	14
Fig. 2. Stress orientations beneath sedimentary basins	16
Fig. 3. Principal stress axes in hydraulic fractures	17
Fig. 4. Downhole view of borehole breakouts	17
Fig. 5. Azimuths of breakout populations in the Liard Basin	22
Fig. 6. Breakout populations in wells in the Liard Basin	23
Fig. 7. Stress trajectories inferred from breakouts and fractures in the Liard Basin	24
Fig. 8. Horizontal stress trajectories inferred from breakouts and fractures in the Liard Basin	25
Fig. 9. Non-regional stress orientations	26
Fig. 10. Relationship between preferred fluid flow and stress in Reservoirs	27
Fig. 11. <i>In situ</i> stress at a point in the subsurface	29
Fig. 12. Stress orientations beneath sedimentary basins	30
Fig. 13. Permeability related to confining pressure in sandstone	33
Fig. 14. Coal seam permeability in the Bowen Basin, Australia	34
Fig. 15. <i>In situ</i> stress and gas production in the Black Warrior Basin	34
Fig. 16. Determination of vertical stress from a density log	35
Fig. 17. Locations of wells that provided density logs for $S_v$ magnitude calculations	36
Fig. 18. $S_v$ magnitudes at 250m depth in the Liard Basin	38
Fig. 19. $S_v$ magnitudes at 500m depth in the Liard Basin	39

Fig. 20. $S_V$ magnitudes at 1000m depth in the Liard Basin	40
Fig. 21. $S_V$ magnitudes at 1500m depth in the Liard Basin	41
Fig. 22. $S_V$ magnitudes at 2000m depth in the Liard Basin	42
Fig. 23. $S_V$ magnitudes in MPa at the top of the Scatter Formation	46
Fig. 24. $S_V$ magnitudes in MPa at the top of the Bluesky Formation	47
Fig. 25. $S_V$ magnitudes in MPa at the top of the Paleozoic strata	48
Fig. 26. $S_V$ magnitudes in MPa at the top of the Debolt Formation	49
Fig. 27. $S_V$ magnitudes in MPa at the top of the Banff Formation	50
Fig. 28. $S_V$ magnitudes in MPa at the top of the Kotcho Formation	51
Fig. 29. $S_V$ magnitudes in MPa at the top of the Jean Marie Formation	52
Fig. 30. Schematic representation of a leak-off test and a pressure/volume plot	55
Fig. 31. Massive fracture record for well D-055-G/094-O-14	59
Fig. 32. Gradients of leak-off test pressures in the Liard Basin	62
Fig. 33. Gradients of fracture breakdown pressures measured in wells in the Liard Basin	63
Fig. 34. Gradients of leak-off and fracture breakdown pressures	64
Fig. 35. Magnitudes of $S_{Hmin}$ at the top of the Scatter Formation	67
Fig. 36. Magnitudes of $S_{Hmin}$ at the top of the Montney Formation	68
Fig. 37. Magnitudes of $S_{Hmin}$ at the top of the Banff Formation	69
Fig. 38. Wells analysed for breakouts showing the mean azimuths	72
Fig. 39. Wells selected for failure simulations to estimate $S_{Hmax}$	73

Fig. 40. Wells that exhibit breakouts suitable for determining $S_{Hmax}$ magnitudes and $S_V$ gradients at 500m depth	76
Fig. 41. Wells that exhibit breakouts suitable for determining $S_{Hmax}$ magnitudes and $S_V$ gradients at 1000m depth	77
Fig. 42. Wells that exhibit breakouts suitable for determining $S_{Hmax}$ magnitudes and $S_{Hmin}$ gradients at 1000m depth	78
Fig. 43. Cohesive strength plotted against depth	79
Fig. 44. Map of $S_{Hmax}$ gradients derived from modelling breakouts	81
Fig. 45. Map of $S_{Hmax}$ gradients derived from: $S_{Hmax} = 2(S_{Hmin}) - P_o$	82
Fig. 46. $S_{Hmax}$ magnitudes at the top of the Scatter Formation	86
Fig. 47. $S_{Hmax}$ magnitudes at the top of the Bluesky Formation	87
Fig. 48. $S_{Hmax}$ magnitudes at the top of the Mattson Formation	88
Fig. 49. $S_{Hmax}$ magnitudes at the top of the Debolt Formation	89
Fig. 50. $S_{Hmax}$ magnitudes at the top of the Banff Formation	90
Fig. 51. $S_{Hmax}$ magnitudes at the top of the Kotcho Formation	91
Fig. 52. $S_{Hmax}$ magnitudes at the top of the Jean Marie Formation	92
Fig. 53. Effective vertical stress at 250m depth in the Liard Basin	97
Fig. 54. Effective vertical stress at 500m depth in the Liard Basin	98
Fig. 55. Effective vertical stress at 1000m depth in the Liard Basin	99
Fig. 56. Effective horizontal stress at 250m depth in the Liard Basin	100
Fig. 57. Effective horizontal stress at 500m depth in the Liard Basin	101
Fig. 58. Effective horizontal stress at 1000m depth in the Liard Basin	102
Fig. 59. Post-1985 earthquakes in the Liard Basin and effective horizontal stress magnitudes at 1000m depth	103

- Fig. 60. Post-1985 earthquakes in the Liard Basin and effective vertical stress magnitudes at 500m depth 104
- Fig. 61. North-south cross sections of stress magnitude and pore pressure profiles across the Liard Basin 106
- Fig. 62. West-east cross sections of stress magnitude and pore pressure profiles across the Liard Basin 107



## TABLES

Table 1. Mean azimuths of breakout and fracture populations in Liard Basin wells	21
Table 2. Vertical stress magnitudes (SV) at specific depths	37
Table 3. Formation tops in wells that provide SV magnitudes	44
Table 4. Vertical stress magnitudes at formation tops	45
Table 5. Leak-off test results for wells in the Liard Basin	56
Table 6. Fracture breakdown pressures and gradients for wells in the Liard Basin	58
Table 7. Formation tops for wells providing $S_{Hmin}$ magnitudes	65
Table 8. $S_{Hmin}$ magnitudes at formation tops in the Liard Basin	66
Table 9. Breakout intervals selected for failure simulations	74
Table 10. Details of breakouts selected for failure simulation	80
Table 11. Formation tops for wells in which failure simulations of breakouts were conducted	84
Table 12. Estimated $S_{Hmax}$ magnitudes at selected formation tops	85
Table 13. Effective vertical stresses for wells in the Liard Basin	95
Table 14. Effective horizontal stresses for wells in the Liard Basin	96
Table 15. Formation tops for wells in cross sections in Figures 61 and 62	105

## ABSTRACT

Part 1 of this report presents the conclusions reached from identifying and recording the orientations of borehole breakouts recorded on 4-arm dipmeter logs from 47 wells in the Liard Basin of western Canada. Two borehole imagery logs were also examined and they provided orientation data for breakouts and drilling-induced fractures. Twenty-seven of the forty-seven wells exhibited 2 breakout populations. In the majority of wells, the major breakout populations exhibited mean azimuths that cluster between NW-SE and NNW-SSE. These orientations are interpreted to reflect the direction of  $S_{Hmin}$ , the smaller horizontal principal stress. A few wells exhibited significant breakout populations that were at high angles to this regional trend. It is suspected that, in these cases, nearby fault zones may have deflected the stress trajectories. A table of results has been prepared and all the supporting data are recorded in the Appendix. Figures showing breakout population axes, stress trajectories, and areas where fault zones may be deflecting stresses are included in the text. All the data presented in the report are available in digital format.

Part 2 of this report describes gathering and processing subsurface pressure data from the records of wells drilled in the Liard Basin in northwestern Canada. Part 2 of the Liard Basin Study is concerned with establishing principal stress magnitudes at as many locations as possible across the basin and mapping how these parameters vary laterally at strategic horizons. Information from laboratory tests and field observations in numerous oil and gas fields worldwide indicate that oil and gas reservoir permeability is inversely related to rock stress. The less a rock body is compressed, the greater will be its permeability, all other factors being equal. That is the operational justification for this investigation, but it is also anticipated that the findings will contribute to an improved understanding of the tectonic evolution of that part of the Canadian landmass occupied by the Liard Basin.

All the data analyzed here are in the public domain and come from well logs, drilling histories and well history reports. These sources of information provided data that was used to estimate the magnitudes of the vertical stress ( $S_V$ ) and the smaller horizontal stress ( $S_{Hmin}$ ). The interpretation of vertical stress variation across the Liard Basin employed density logs from 64 wells. Analysis of these logs allowed a lateral variation in vertical stress magnitude ( $S_V$ ) to be mapped at various depths. The smaller horizontal stress ( $S_{Hmin}$ ) was mapped using leak-off test pressure and fracture breakdown pressures. The larger horizontal stress ( $S_{Hmax}$ ) was determined via numerical simulation of breakout failure, as well as being calculated algebraically. Horizontal and vertical effective stresses were calculated and mapped and their relationship to seismic activity was speculated upon.

**DISCLAIMER**

This study has been carried out with all due professional diligence and the interpretations offered are based only on data and information in the public domain. Sigma H Consultants Ltd. assumes no responsibility for the consequences of any action taken on the basis of material contained in this report.

## **PART 1**

### **1. INTRODUCTION**

Over the last two decades, the oil industry has been paying progressively more attention to *in situ* stress, as it affects the hydrocarbon-rich rocks through which they drill. Why is there this interest in quantifying the subsurface stresses?

In large part, it is due to the rise in the costs of exploring for, and developing, hydrocarbon prospects in increasingly hostile environments. Most of the easily accessible oil and gas has been found and is either on stream, and/or subject to declining production levels. The new resources are much more expensive to find and more expensive to produce.

North America has not led the way in exploiting the potential insights offered by *in situ* stress data. The major advances have come from European operators in the North Sea. There, stress data have been gathered for two purposes: to increase the safety and efficiency of drilling, and to assist in designing optimal production scenarios. Success has been achieved in both areas.

The most focused Canadian study that has been published is Imperial Oil's assessment of *in situ* stress at Norman Wells in the Northwest Territories, and this led to significant modifications to their oil production strategy (Gronseth and Kry, 1987). Elsewhere in western Canada, there has never been a sustained effort to gather *in situ* stress data over a significant volume of buried sediments. Here and there, measurements have been made (e.g. McLellan, 1988), but it is not clear if these have provided any significant operational benefits. An understanding of the stress regime(s) of a sedimentary basin gives oil companies significant operational advantages. These relate to the production of hydrocarbons and to the successful drilling of wells.

Specific insights that *in situ* stress orientations can provide include:

Knowing the orientation of the principal stresses permits prediction of the propagation directions of induced hydraulic fractures.

Knowledge of principal stress orientations will indicate whether or not a network of natural fractures will assist fluid flow through a reservoir and thereby assist hydrocarbon recovery.

It has been widely demonstrated that preferred fluid flow directions in reservoirs, fractured and unfractured, are aligned with the axis of the larger horizontal principal stress (Heffer and Lean, 1993). This information is enormously useful because it can help design configurations of production wells that will provide optimal hydrocarbon recovery at least cost. Regional stress orientations need to be known and also whether

there are local deflections of principal stress axes caused by lateral variations in rock mechanical properties associated with such features as faults and diapirs. Given structural information on fault geometry, stress orientations may indicate which faults, or sections of faults, are likely to be sealed.

In this study, the orientations and trajectories of the stress regime in the Liard Basin are determined and mapped. It is proposed that these data, together with what are gathered in future exploration programs, will aid in sustaining the economic production of hydrocarbons from this structural province.

## 2. DESCRIBING THE STATE OF STRESS

In any solid, the state of three-dimensional compressive stress at a point can be fully described by the magnitudes and directions of three principal stresses that are orthogonal to each other. By convention in earth sciences, compressive stress magnitudes are positive. The nomenclature of  $\sigma_1$ ,  $\sigma_2$  and  $\sigma_3$ , is assigned for, respectively, the larger, intermediate and smaller principal stress (Fig. 1). In a triaxial cell in a laboratory, it is straightforward to determine which is which and how the principal stresses are oriented with respect to the sample being tested.

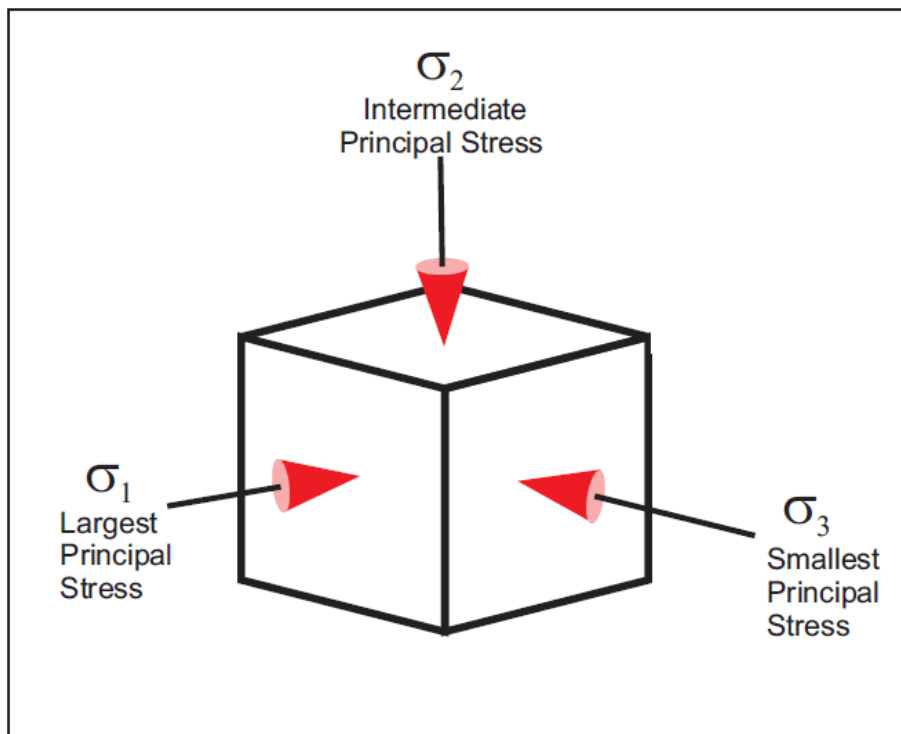


Fig.1. *In situ* stress at any point in the subsurface can be fully described by the magnitudes and orientations of three orthogonal principal stresses, designated by  $\sigma_1$ ,  $\sigma_2$ , and  $\sigma_3$  for, respectively, the largest, the intermediate and the smallest principal stress.

In the Earth, it is more difficult. In mines, multiple overcoring measurements have established the orientations and magnitudes of all three principal stresses (McGarr and Gay, 1978). To date, the overcoring technique is the only method that will recover data on all three principal stresses and, to do so, several core holes have to be drilled in different directions. Experience worldwide has shown that the *in situ* stress in the subsurface is usually anisotropic, in other words, none of the principal stresses is of the same magnitudes (McGarr and Gay, 1978; Hoek and Brown, 1980).

### 3. MEASURING STRESS ORIENTATIONS IN SEDIMENTARY BASINS

Whereas it is possible to measure the stress tensor in a mine shaft or a corridor, this is not yet feasible in a small diameter borehole. No tools have been developed that can record the complete stress tensor. However, oil field logging and drilling practices do allow much of this information to be estimated with reasonable precision; and there is one important favourable factor.

In general, a principal stress trajectory tends to reorient so that it approaches a free surface at right angles. Most continental sedimentary basins, like the Liard Basin, exhibit relatively low surface relief, so that the contact between the ground and the atmosphere approximates a horizontal free surface at a regional scale. Thus, one principal stress will be approximately vertical, particularly if the measurements are made at some depth. While not 100% rigorous, this reasoning allows us to infer that, if one of the principal stresses is essentially vertical, the other two will be approximately horizontal. This rationale has spawned the following terminology:  $S_V$ , for the vertical stress, and  $S_{Hmax}$  and  $S_{Hmin}$ , for the larger and smaller horizontal stresses (Fig. 2).

Since principal stresses are orthogonal, if we can determine the azimuth of one of the horizontal principal stresses and identify it as either  $S_{Hmax}$  or  $S_{Hmin}$ , we can identify the other horizontal stress oriented at  $90^\circ$  to the first. Ideally, an induced hydraulic fracture will propagate in a plane normal to the smallest principal stress which is parallel to the plane of the intermediate and larger principal stresses (Fig. 3). Impression packers and borehole image logs will record the traces of such fractures on the sides of a well bore. The long axes of breakouts are aligned with the smaller of the two principal stresses acting at high angles to a borehole, so breakouts in vertical, or near vertical wells, provide reliable measures of the orientations of  $S_{Hmin}$  (Fig. 4).

Over the past thirty years, it has become apparent that the most accurate indicators of subsurface horizontal stress orientations are borehole breakouts. Breakouts are caved intervals where the spalling has led to asymmetric lateral elongation of the wellbore, so that it has become “ovalised”. This “ovalisation” is due to compressive failure around the wellbore in response to unequal lateral compression. The long axis of a breakout interval is aligned with the axis of the smaller principal stress. Thus the presence of breakouts not only indicates that asymmetric compression exists but allows one to determine one principal stress orientation.

Since the surface of the Liard Basin is a semi-horizontal surface over most of its extent, one principal stress will be close to vertical and the other two approximately horizontal. Hence, in the semi-vertical wells that are being studied here, breakouts will diagnose the orientation of  $S_{Hmin}$ , and  $S_{Hmax}$ , the smaller and larger horizontal stresses.

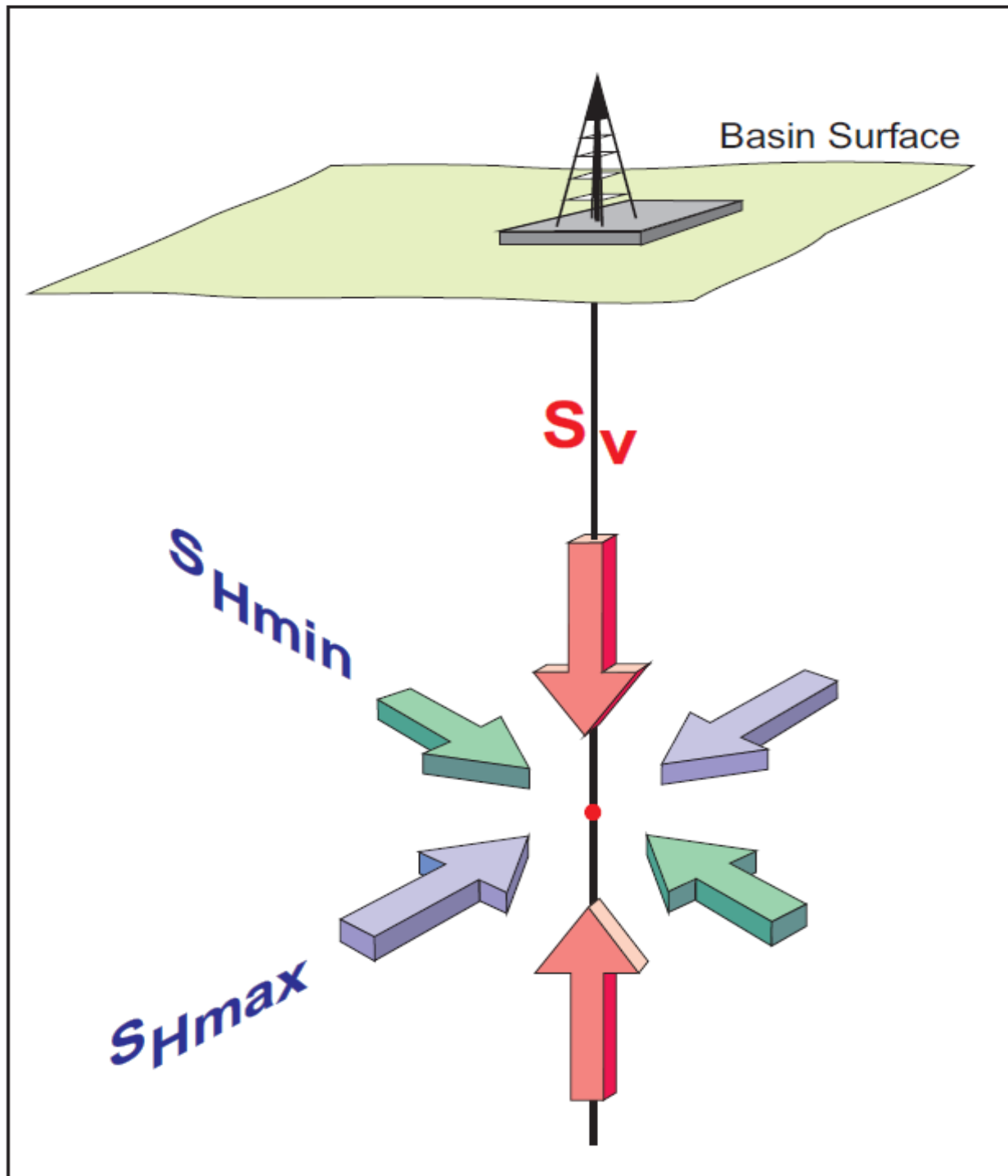


Fig. 2. A principal stress tends to intersect a free surface at right angles. The interface between the ground surface and the atmosphere is a free surface and, over most basins, closely mimics a horizontal plane, so one can infer that one of the principal stresses is nearly vertical and the other two are approximately horizontal.



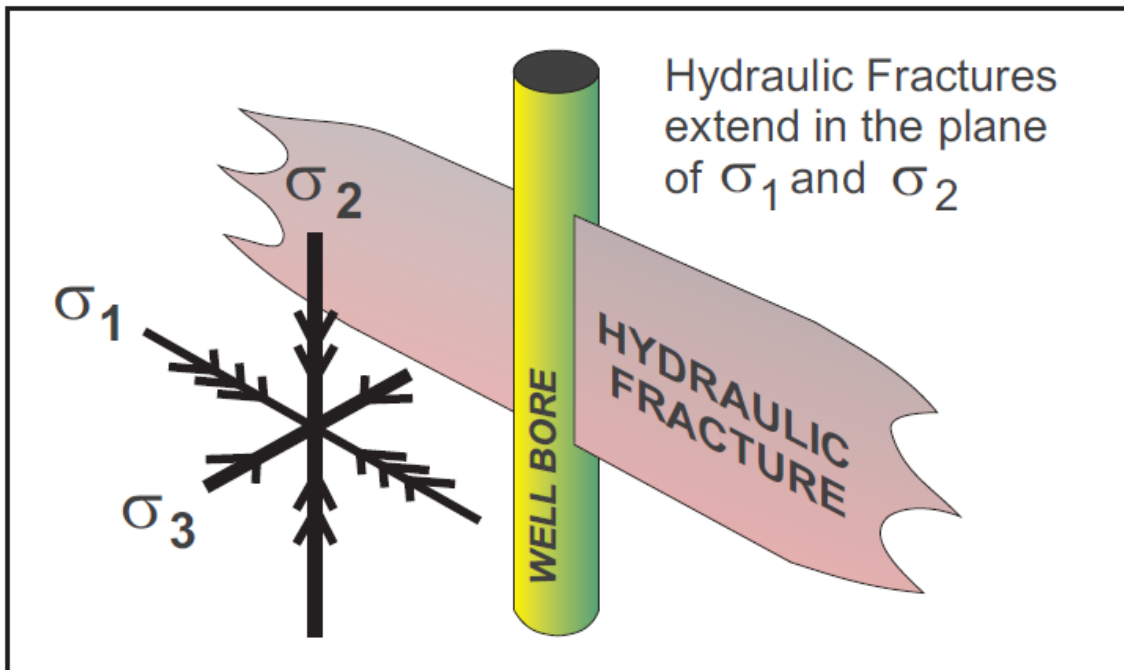


Fig. 3. Hydraulic fractures open along fracture planes that are perpendicular to the smallest principal stress. If their axial traces are recorded in a well, this will indicate the  $S_{Hmax}$  axes. In 2 wells in the Liard Basin, several drilling-induced fractures were identified and they were used to infer orientations of  $S_{Hmax}$

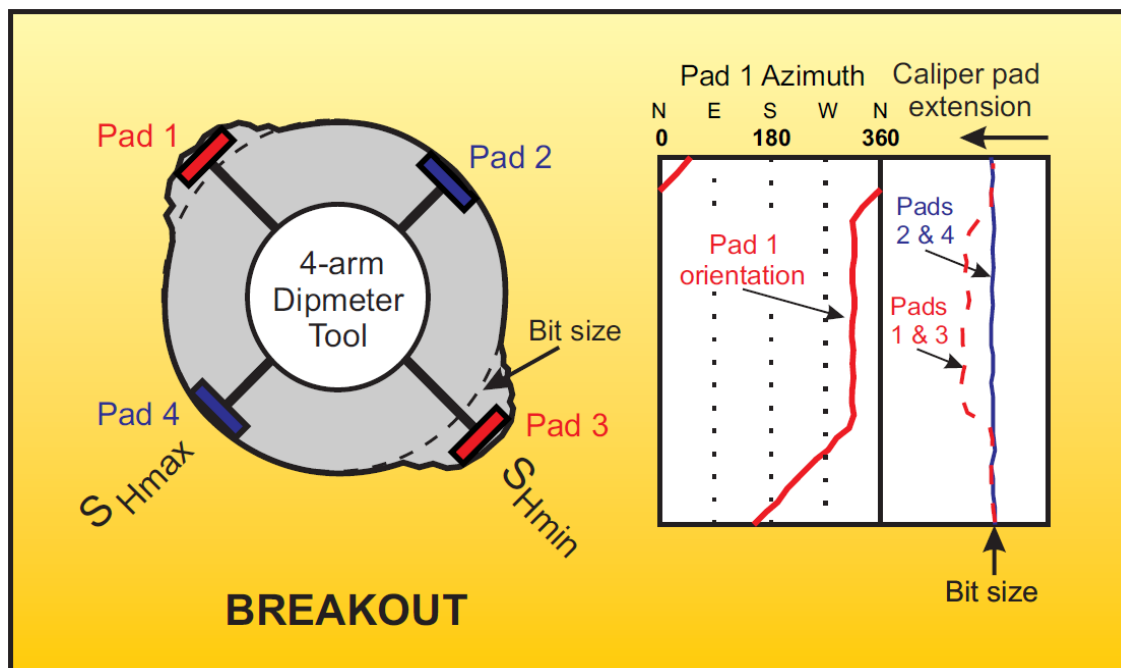


Fig. 4. Downhole view of a borehole breakout. Amplification of anisotropic stress in the country rock causes the borehole wall to spall on opposite sides. The long axis of lateral extension is aligned with the smaller principal stress. In vertical wells, this is  $S_{Hmin}$ . The presence of breakout intervals and the orientations of their long axes are identified by differential extension of the pads of the four-arm dipmeters and by the cessation of tool rotation, as shown here diagrammatically.

Four-arm dipmeter tools are ideal for recognising breakouts and for recording their orientations. They are equipped with two sets of extendable pads that record borehole geometry. The orientation of Pad 1 is recorded, as is the vertical deviation of the well and an azimuth known as the relative bearing that enables the directional azimuth of the well (drift) to be calculated. Moreover, the cable is torqued and this causes the dipmeter tool to rotate in a clockwise direction as it is drawn up a well. This rotational behaviour is very important because, when one or other of the extendable pad sets enters an asymmetrically caved interval (breakout), rotation ceases and only restarts at the top of the breakout interval when the hole is once more approximately circular (Fig. 4). The ability of the four-arm dipmeter tool to record the directional azimuth of the hole is also critical because some ovalised intervals have their long axes aligned in the direction of “drift” of the well. Such intervals may indeed be true stress-induced breakouts, but there is also the possibility that they are simply the result of drill pipe wear on an inclined borehole. As such they are considered to be “key seats”, the term being derived from keyhole geometry, and should not be assigned breakout status. Key-seating is found most frequently in wells with high vertical deviations and, in this study, no breakouts were identified in sections of wells that exceeded  $10^\circ$  of vertical deviation, except in one instance. There is another reason for applying these cut-offs. Assuming that breakouts form through Mohr-Coulomb failure, the breakout long axes could be yielding inaccurate  $S_{Hmin}$  orientations in wells that are vertically deviated more than  $10^\circ$  (Mastin, 1988).

Assuming that one principal stress is vertical ( $S_V$ ), the long axis of a borehole breakout will determine the azimuth of  $S_{Hmin}$ ; and  $S_{Hmax}$  will be aligned at  $90^\circ$  to the latter direction.

Borehole imagery logs record all the same parameters as four-arm dipmeter tools, so they too can be used to identify and orient breakouts. Imagery logs have the advantage of showing the actual images of breakouts, which allows their bipolar geometry to be confirmed. Image logs allow breakouts to be distinguished from key seats, which exhibit one-sided caving of the wellbore. A further advantage of borehole imagery logs is that they display drilling-induced fractures that can be identified and oriented. These are predominantly near-vertical features and their propagation axes are aligned with  $S_{Hmax}$ .

In this study, most of the reported horizontal stress orientations have been determined by identifying and orienting breakouts from uncomputed four-arm dipmeter logs. Borehole imagery logs were also available allowing for identification of breakouts and drilling-induced fractures and the recording of their orientations.

#### 4. BREAKOUT IDENTIFICATION, ANALYSIS AND POPULATION SELECTION

In this report, breakouts were identified and oriented by the PFAS (Planning and Field Application Software) of ITC a.s. of Tonsberg, Norway. Digital LAS files of four-arm dipmeter records were entered into this software and breakouts were identified according to the criteria set out by Plumb and Hickman (1985). The PFAS software compresses log data and reduces it to numerical readings for each meter of depth in a well. The mean azimuths of each breakout interval are determined using the circular variance methodology of Mardia (1972), and mean azimuths of breakout populations determined in the same manner.

In most wells, the individual breakout azimuths indicate clearly which breakouts compose the major population and these were selected manually for averaging in order to generate mean azimuths. In this study, this was determined by data inspection and, where required, through examination of histograms of the breakout orientations. In a few instances, a minor population (with respect to net breakout interval) was interpreted as representing the regional orientation for  $S_{Hmin}$ , and the rationale for doing so is described in the well commentaries.

Basinwide stress orientation studies support the concept of reasonably uniformly oriented regional stress axes (e.g. Bell and Babcock, 1986; Bell, 1990). Further, it has been shown that such  $S_{Hmax}$  axes are closely aligned with absolute crustal plate motions. Therefore, confidence can be placed in the interpretation of the regional horizontal stress axes based on major breakout populations that have been mapped in the Liard Basin. The meaning of the minor breakout populations is less clear. There are numerous factors that influence local deviations of regional horizontal stress orientations including: lateral variations in geomechanical properties associated with diapirs (Schneider, 1985) or fault zones and other lateral inhomogeneities such as natural and induced fracture collapse (Bell et al., 1992). Also, many minor populations consist of breakouts that occur at widely separated depths in wells and thus may be due to several different causes. Little work has been done investigating indicators of non-regional horizontal stress axes. Because  $S_{Hmax}$  axes define preferred fluid flow axes (Heffer and Lean, 1993) this is a field of enquiry that will yield significant economic benefits for designing production scenarios for hydrocarbon recovery from oil and gas fields that exhibit significant differences in stress orientations.

## 5. STRESS AXES AND TRAJECTORIES IN THE LIARD BASIN

Four-arm dipmeter logs were analysed from 49 wells in the Liard Basin. Except for two logs, they all revealed breakouts. In two wells, borehole imagery logs were available and they provided orientation data on breakouts and drilling-induced fractures. The results of the analyses are presented in commentary texts, tables and graphic logs for each well in the Appendix of this report. They are summarised in Table 1.

For each well, Table 1 lists the total net metres of breakouts, their mean azimuths and their standard deviations in columns 3, 4 and 5, respectively. Twenty-two wells exhibited breakouts and/or drilling-induced fractures that were consistently oriented and statistically represented a single population. However, in twenty-seven of the wells, breakouts were sufficiently varied in the long axis orientations that two populations were recognised. These are listed in columns 6 to 11 in Table 1. The designation of populations 1 and 2 was based on the net metres of breakouts in each.

The mean breakout azimuths of Populations 1 and 2 are plotted geographically on Figure 5. The major populations trend NW-SE to NNW-SSE. This is an expected finding, since the northern part of the Western Canadian Sedimentary Basin, immediately to the south, exhibits a similar trend.

The secondary populations exhibit mean azimuths that are generally at high angles to the major populations. This is likely due to a variety of causes. Fault zones that are weaker than the surrounding rock can deflect stresses locally and this may be the cause of some of the non-regional breakout orientations. As Figure 6 shows, some of these orientations are spatially associated with mapped faults along the western side of the Liard Basin. It is also possible that, where one population's mean azimuth is approximately 90° different from the other, the dipmeter tool has failed to reorient itself correctly between breakouts as it was drawn up the well. Furthermore, non-regional orientations could also be due to the collapse of drilling-induced fractures. The latter two possibilities can be investigated by examining borehole imagery logs. Unfortunately, four-arm dipmeter records are inadequate for resolving such issues. To summarise, some of the non-regional breakout long axes may be due to fault zone influence, but others may be spurious.

No.	Well Name	All Breakouts			Population 1			Population 2			Sources of Data Breakouts or Drilling-induced Fractures (DIFs)
		Net metres	Mean Azimuth	Standard Deviation	Net metres	Mean Azimuth	Standard Deviation	Net metres	Mean Azimuth	Standard Deviation	
1	A-006-C/094-O-08	112	71.2	34.4	85	64.3	15.8	27	137.8	7.9	Breakouts
2	A-045-E/094-O-10	212	146.9	6.2	212	146.9	6.2				Breakouts
3	A-067-D/094-O13	861	108.5	14.9	861	108.5	14.9				Breakouts
4	A-081-J-094-P-04	73	21.3	26.6	59	22.4	8.1	14	118.2	25.5	Breakouts
5	A-085-E-094-P-12	107	54.7	31.1	70	160.7	5.9	37	100.6	5.3	Breakouts
6	B-019-K-094-N-16	448	95.7	38.2	286	78.9	22.6	162	138.3	23.3	Breakouts
7	B-021-K-094-O-14	509	102.6	29.0	412	98.3	14.8	97	169.6	12.0	Breakouts
8	B-029-A-094-J-15	38	122.5	40.6	23	42.2	1.7	15	144.7	23.1	Breakouts
9	B-038-60-10-124-00	29	147.8	6.2	29	147.8	6.2				Breakouts
10	B-044-B-094-P-05	145	48.3	36.9	56	149.1	34.9	89	51.5	3.1	Breakouts
11	B-044-L-094-O-10	84	57.4	15.8	78	56.7	1.8	6	137.9	3.2	Breakouts
12	B-055-60-30-123-45	827	113.9	33.6	488	135.4	18.2	339	80.9	13.8	Breakouts
13	B-058-A-094-I-13	26	22.0	13.7	26	22.0	13.7				Breakouts
14	B-066-I-094-O-08	721	41.2	26.0	555	50.6	16.9	166	4.8	15.6	Breakouts
15	B-085-H-094-O-11	318	121.6	7.0	318	121.6	7.0				Breakouts
16	B-093-C-094-I-14	287	152.2	11.5	287	152.2	11.5				Breakouts
17	B-096-E-094-O-10	4	128.2	7.0	4	128.2	7.0				Breakouts
18	C-24-H-04-O-16	37	139.1	1.8	37	139.1	1.8				Breakouts
19	C-028-H-094-O-16	51	138.0	17.9	51	138.0	17.9				Breakouts
20	C-051-D-094-P-12	190	120.6	27.8	112	140.1	7.0	78	88.8	5.6	Breakouts
21	C-054-K-094-N-16	78	111.8	4.3	78	111.8	4.3				Breakouts
22	C-060-60-10-121-15	34	164.6	14.3	32	164.7	1.5	2	76.4	6.0	Breakouts
23	C-086-A-094-I-14	281	3.1	38.9	188	8.8	11.0	93	108.1	22.3	Breakouts
24	D-007-J-094-O-09	12	143.7	5.2	12	143.7	5.2				Breakouts
25	D-016-A-094-N-15	331	162.7	13.7	331	162.7	13.7				Breakouts
26	D-025-61-20-121-45	27	149.2	18.8	23	154.1	2.2	4	97.7	5.5	Breakouts
27	D-057-K-094-N-02	453	83.5	24.5	348	74.9	10.9	105	126.6	12.3	Breakouts
28	D-064-K-094-N-16	644	55.1	30.1	527	55.3	14.3	117	145.7	18.7	Breakouts
29	D-069-L-094-P-04	231	162.3	22.1	212	162.5	13.3	19	74.1	13.2	Breakouts
30	D-074-F-094-P-05	548	141.7	57.1	316	156.3	21.0	232	72.2	20.5	Breakouts
31	D-087-A-094-O-11	11	129.6	9.4	11	129.6	9.4				Breakouts
32	D-087-C-094-P-05	126	66.6	47.4	57	130.6	12.3	69	43.7	0.8	Breakouts
33	D-087-G-094-O-06	224	8.4	21.3	224	8.4	21.3				Breakouts
34	D-092-J-094-O-06	89	86.1	15.5	89	86.1	15.5				Breakouts
35	D-095-F-094-P-05	0			0						No data
36	E-072-61-20-122-00	124	167.0	13.3	124	167.0	13.3				Breakouts
37	F-008-60-40-124-30	0			0						No data
38	F-038-60-30-123-45	113	133.8	11.6	113	133.8	11.6				Breakouts
39	G-001-60-10-124-15	841	114.5	49.9	513	145.5	30.0	328	74.4	18.5	Breakouts
40	G-032-61-10-121-15	70	5.3	18.2	64	3.1	4.5	6	103.3	0.0	Breakouts
41	G-042-69-20-121-00	102	25.7	50.9	69	10.9	27.7	33	89.5	18.2	Breakouts
42	L-060-60-20-124-15	414	28.7	56.5	243	155.5	31.7	171	55.0	11.0	Breakouts
43	M-051-60-30-121-00	125	170.2	26.2	125	170.2	26.2				Breakouts
44	N-019-60-40-123-45	5	164.2	0.0	5	164.2	0.0				Breakouts
45	N-033-61-00-122-30	33	164.1	22.1	29	168.4	6.1	4	86.4	0.0	Breakouts
46	O-046-60-30-123-45	22	150.0	50.4	15	158.0	21.1	7	72.3	1.6	Breakouts
47	P-024-60-30-123-45	283	64.6	21.1	252	62.3	8.8	31	135.2	3.0	Breakouts
48	B-094-H-094-J-14	666	172.2	26.5	637	172.7	23.1	29	90.7	13.4	Breakouts
49	C-070-H-094-I-11	10.0	146.0	7.4	10.0	146.0	7.4				Breakouts
		101.0	146.2	7.0	101.0	146.2	7.0	101 measurements			DIFs
50	D-098-J-094-I-01	5.0	158.8	1.6	5.0	158.8	1.6	5 measurements			DIFs
51	D-099-I-094-I-01	49.0	139.9	6.9	49.0	139.9	6.9				Breakouts

Table 1. Mean azimuths of breakout and drilling-induced fracture populations in Liard Basin wells.

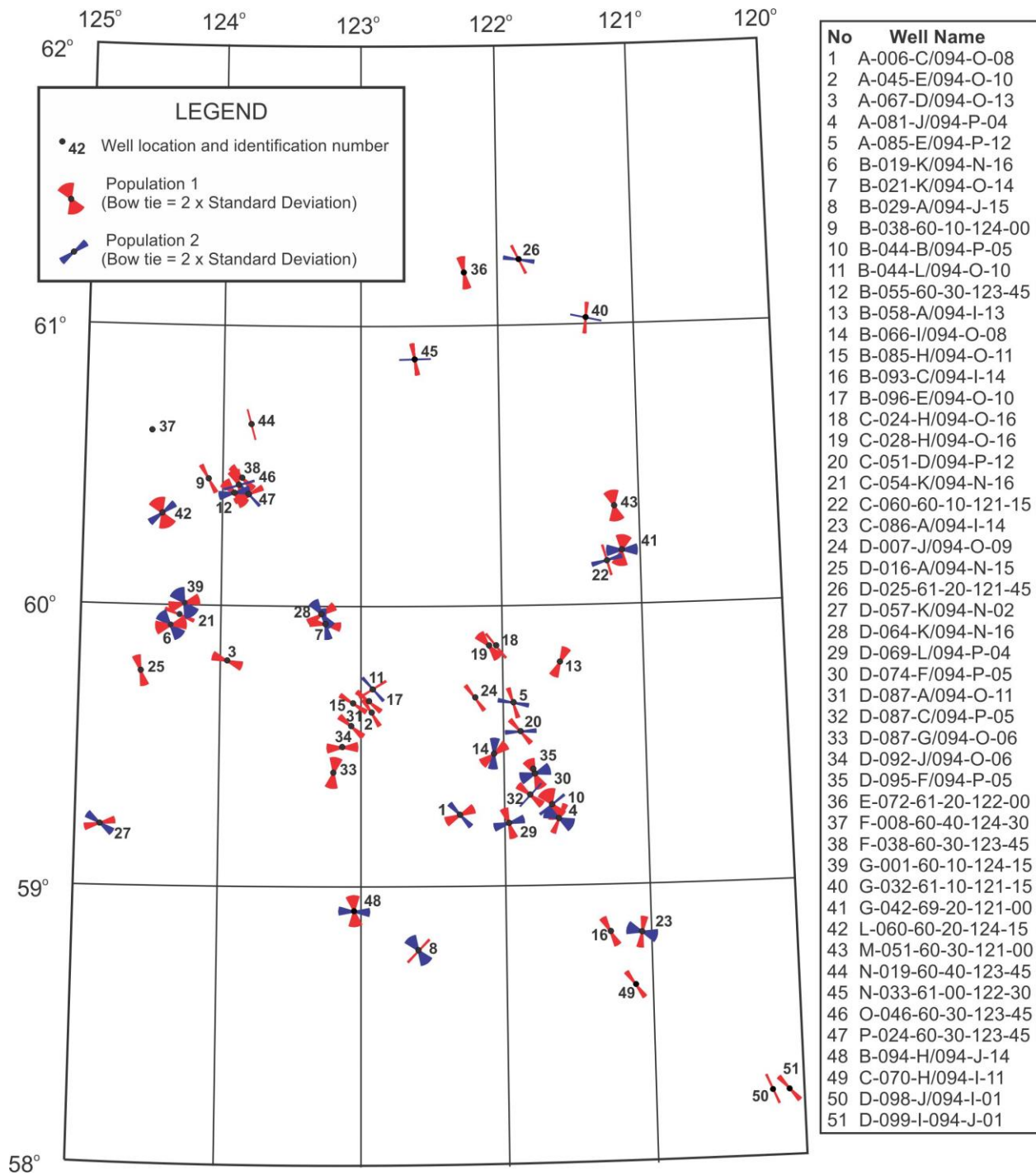


Fig. 5. Orientations of breakout populations in the Liard Basin

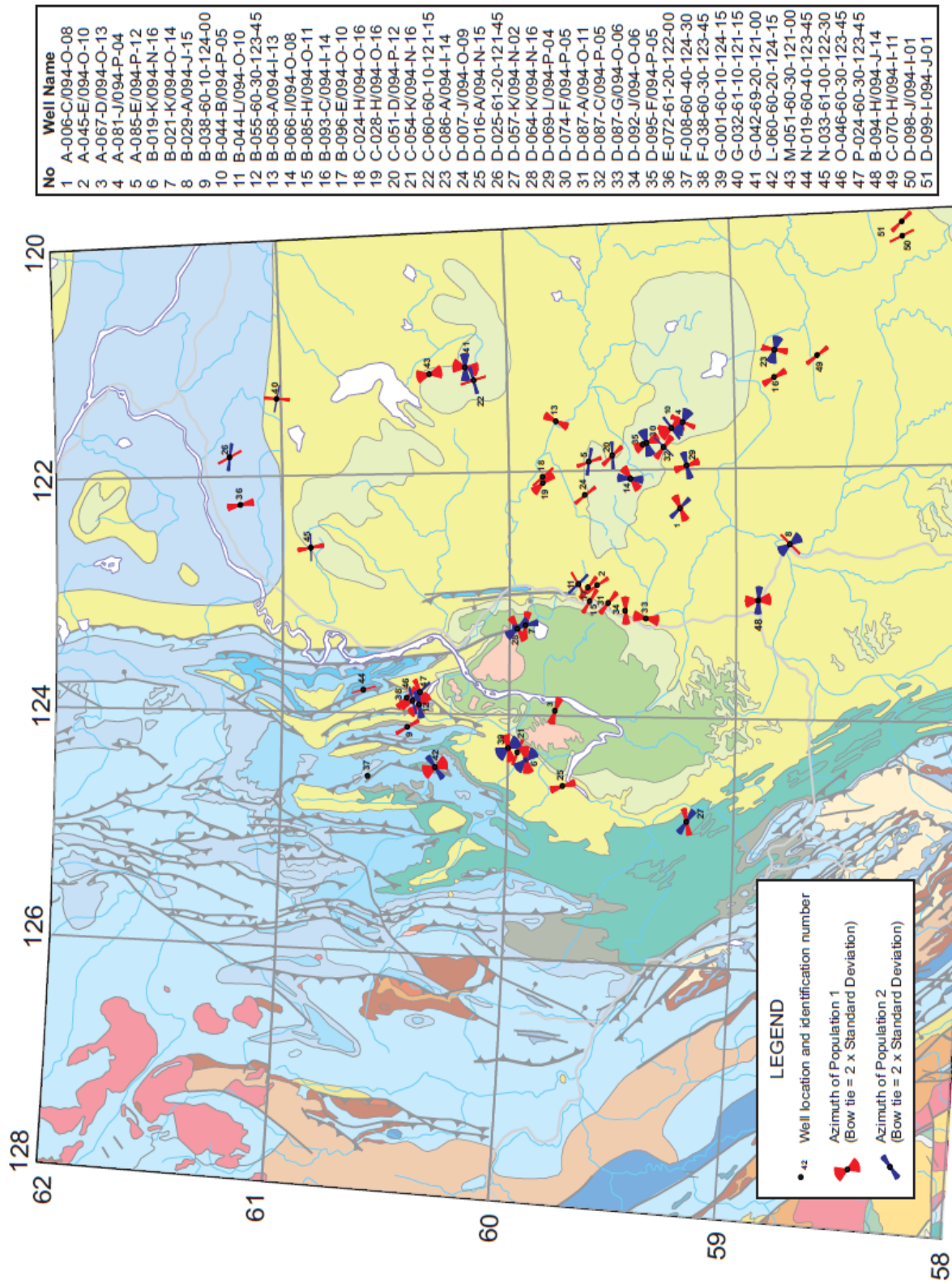


Fig. 6. Breakout populations in wells in the Liard basin

The breakout mean azimuths were used to interpret horizontal stress trajectories across the Liard Basin, as shown in Figure 7.

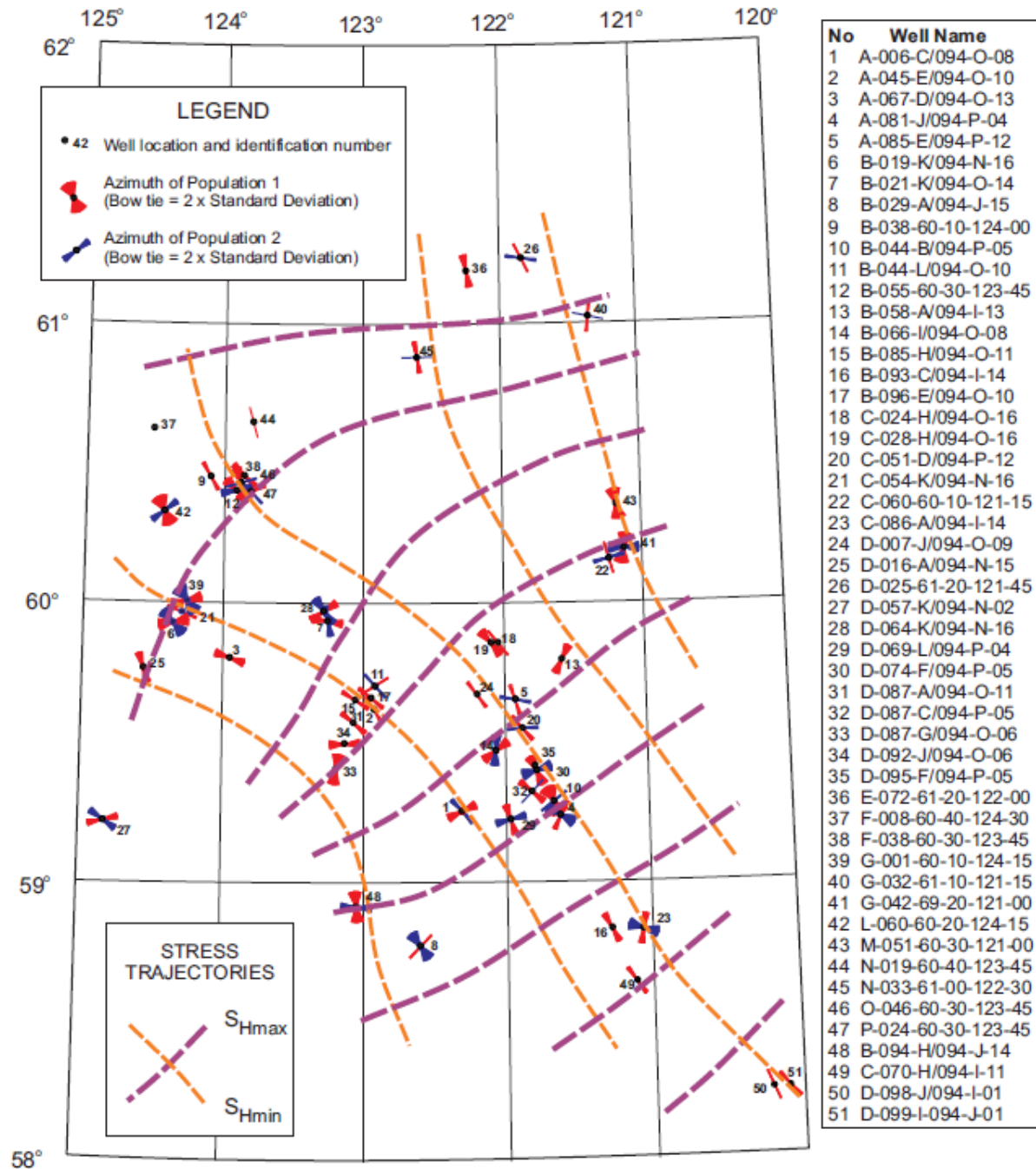


Fig. 7. Stress trajectories from breakouts and drilling-induced fractures in the Liard Basin



Figure 8 shows the stress trajectories projected across the surface geology of the Liard Basin. The  $S_{Hmin}$  trajectories are interpreted to deflect as they approach the salient of the deformation front north of latitude  $60^{\circ}$ .

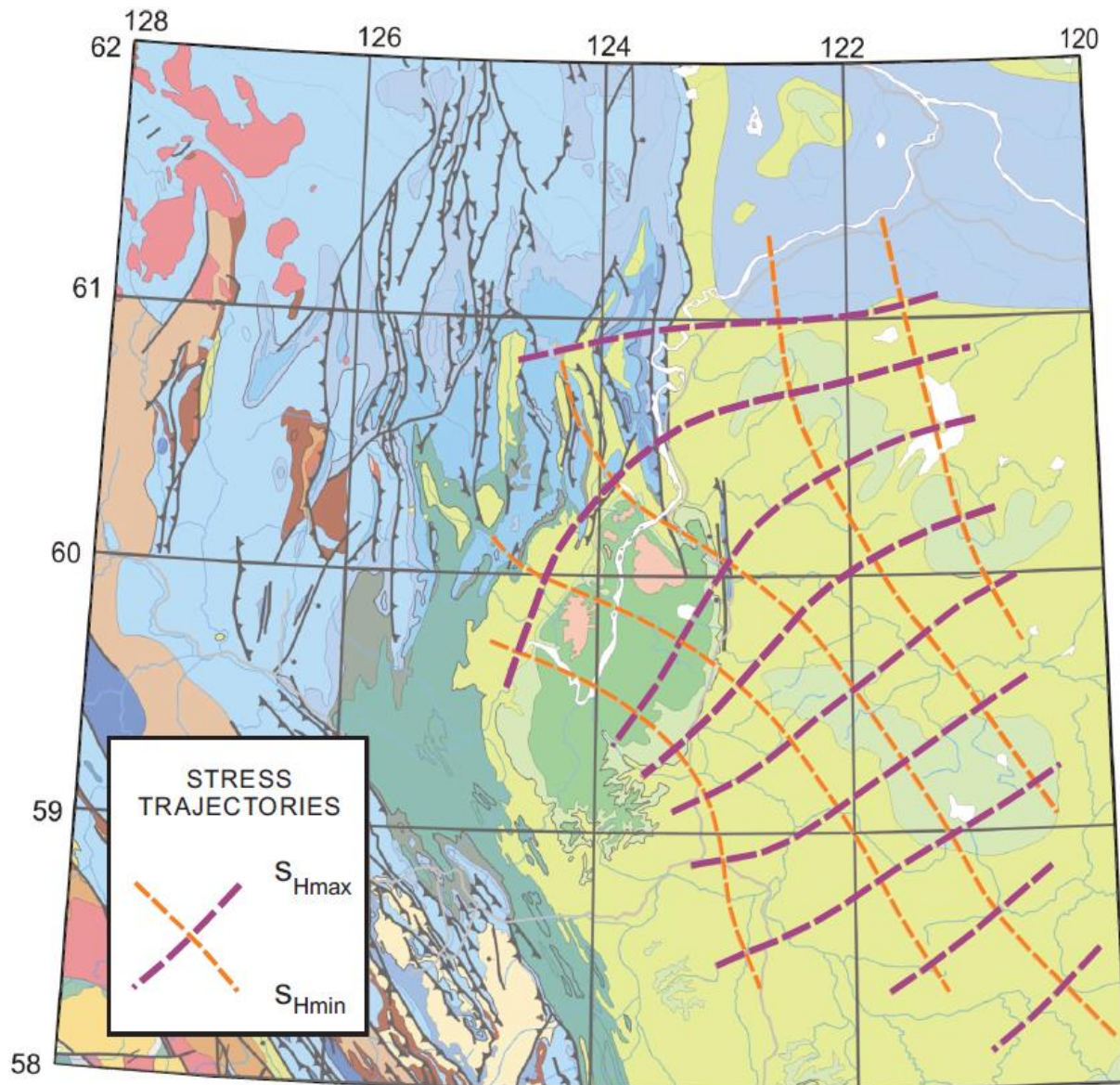


Fig. 8. Horizontal stress trajectories across the Liard Basin inferred from orientations of breakouts and drilling-induced fractures

Figure 9 highlights those areas where non-regional breakout azimuths suggest that there may be fault zones present. As indicated earlier, this is speculative in many cases.

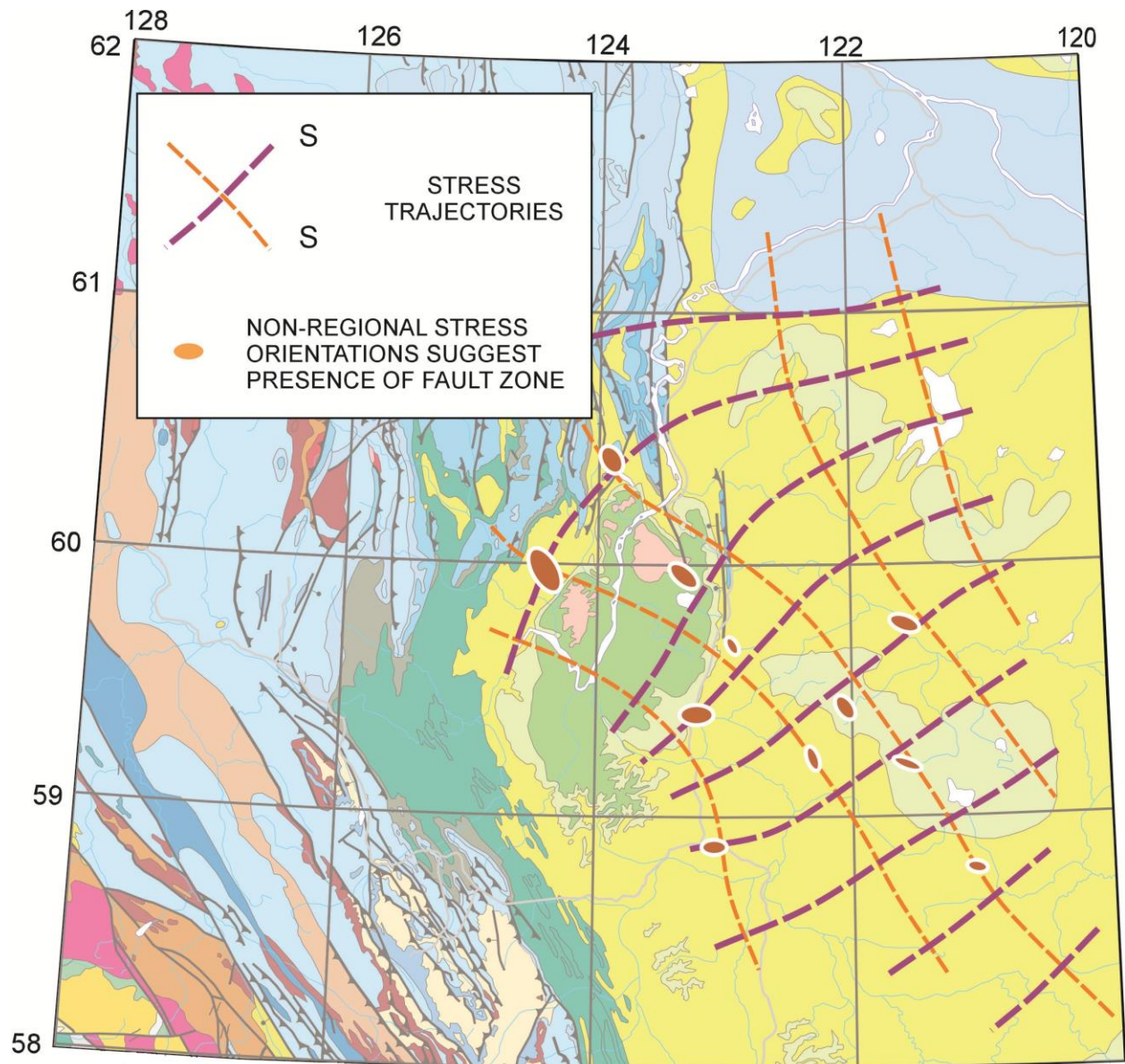


Fig. 9. Non-regional stress orientations can be due to deflection by fault zones. The light brown areas outlined in white mark regions where breakouts indicated that non-regional

## 6. CONCLUSIONS AND IMPLICATIONS

The stress trajectory maps provide key information for hydrocarbon production strategy.

Induced fractures at depth are likely to be vertical and aligned with  $S_{Hmax}$ . Moreover, any open fractures in reservoirs are likely to be sub-vertical and oriented within  $30^\circ$  of the  $S_{Hmax}$  axis. This means that inclined and horizontal wells are more likely to encounter such fractures if they are drilled sub-parallel to the  $S_{Hmin}$  stress trajectories. Furthermore, the preferred flow axes for fluids in reservoirs will be aligned with  $S_{Hmax}$  trajectories (Fig. 10), where formation fractures may be open. These insights could lead to significant cost savings as drilling scenarios are devised to maximise hydrocarbon production. This has been the case for some oil fields in the North Sea.

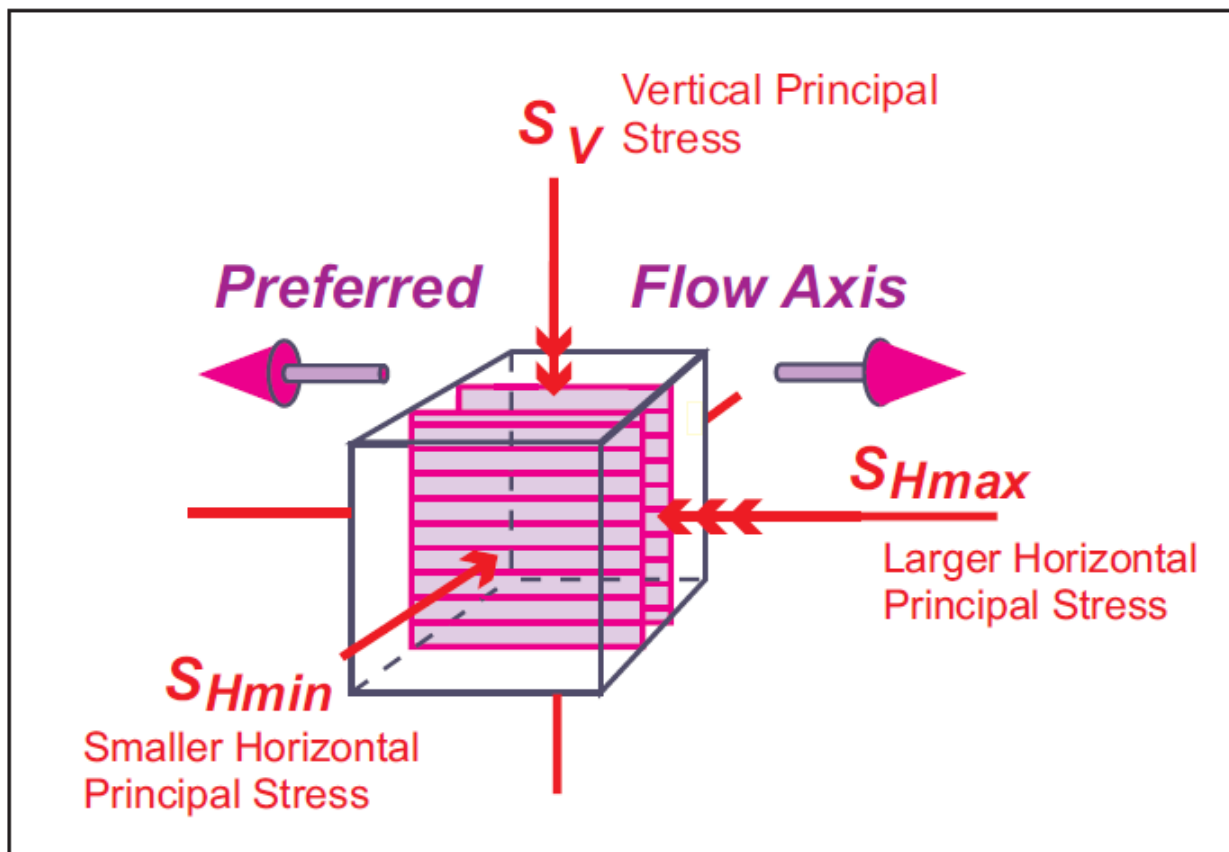


Fig. 10. Relationship between preferred fluid flow axes and stress in reservoirs, documented by Heffer and Lean (1993). Permeability is greatest along the axis of  $S_{Hmax}$ .

## PART 2

### 7. INTRODUCTION

Over the last two decades, the oil industry has been paying progressively more attention to *in situ* stress, as it affects the hydrocarbon-rich rocks through which they drill. Why is there this interest in quantifying the subsurface stresses?

In large part, it is due to the rise in the costs of exploring for, and developing, hydrocarbon prospects in increasingly hostile environments. Most of the easily accessible oil and gas has been found and is either on stream, and/or subject to declining production levels. The new resources are much more expensive to find and more expensive to produce.

North America has not led the way in exploiting the potential insights offered by *in situ* stress data. The major advances have come from European operators in the North Sea. There, stress data have been gathered for two purposes: to increase the safety and efficiency of drilling, and to assist in designing optimal production scenarios. Success has been achieved in both areas.

The most focused Canadian study that has been published is Imperial Oil's assessment of *in situ* stress at Norman Wells in the Northwest Territories, and this led to significant modifications to their oil production strategy (Gronseth and Kry, 1987). In the Western Canadian Sedimentary Basin, there has never been a sustained effort to gather *in situ* stress data over a significant volume of buried sediments. Here and there, measurements have been made (e.g. McLellan, 1988), but it is not clear if these have provided any significant operational benefits.

### 8. DESCRIBING THE STATE OF STRESS

In any solid, the state of three-dimensional compressive stress at a point can be fully described by the magnitudes and directions of three principal stresses that are orthogonal to each other. By convention in earth sciences, compressive stress magnitudes are positive. The nomenclature of  $\sigma_1$ ,  $\sigma_2$  and  $\sigma_3$ , is assigned for, respectively, the larger, intermediate and smaller principal stress (Fig. 11). In a triaxial cell in a laboratory, it is straightforward to determine which is which and how the principal stresses are oriented with respect to the sample being tested.

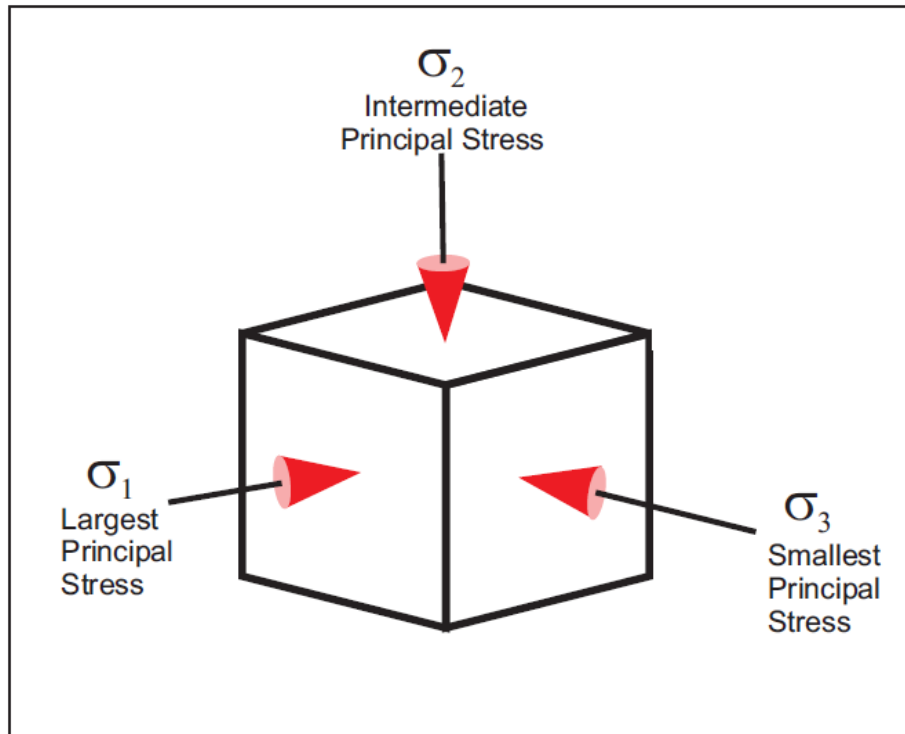


Fig.11. In situ stress at any point in the subsurface can be fully described by the magnitudes and orientations of three orthogonal principal stresses, designated by  $\sigma_1$ ,  $\sigma_2$ , and  $\sigma_3$  for, respectively, the largest, the intermediate and the smallest principal stress.

## 9. MEASURING STRESS ORIENTATIONS IN SEDIMENTARY BASINS

Whereas it is possible to measure the stress tensor in a mine shaft or a corridor, this is not yet feasible in a small diameter borehole. No tools have been developed that can record the complete stress tensor. However, oil field logging and drilling practices do allow much of this information to be estimated with reasonable precision; and there is one important favourable factor.

In general, a principal stress trajectory tends to reorient so that it approaches a free surface at right angles. Most continental sedimentary basins, like the Liard Basin, exhibit relatively low surface relief, so that the contact between the ground and the atmosphere approximates a horizontal free surface at a regional scale. Thus, one principal stress will be approximately vertical, particularly if the measurements are made at some depth. While not 100% rigorous, this reasoning allows us to infer that, if one of the principal stresses is essentially vertical, the other two will be approximately horizontal. This rationale has spawned the following terminology:  $S_V$ , for the vertical stress, and  $S_{Hmax}$  and  $S_{Hmin}$ , for the larger and smaller horizontal stresses (Fig. 12).

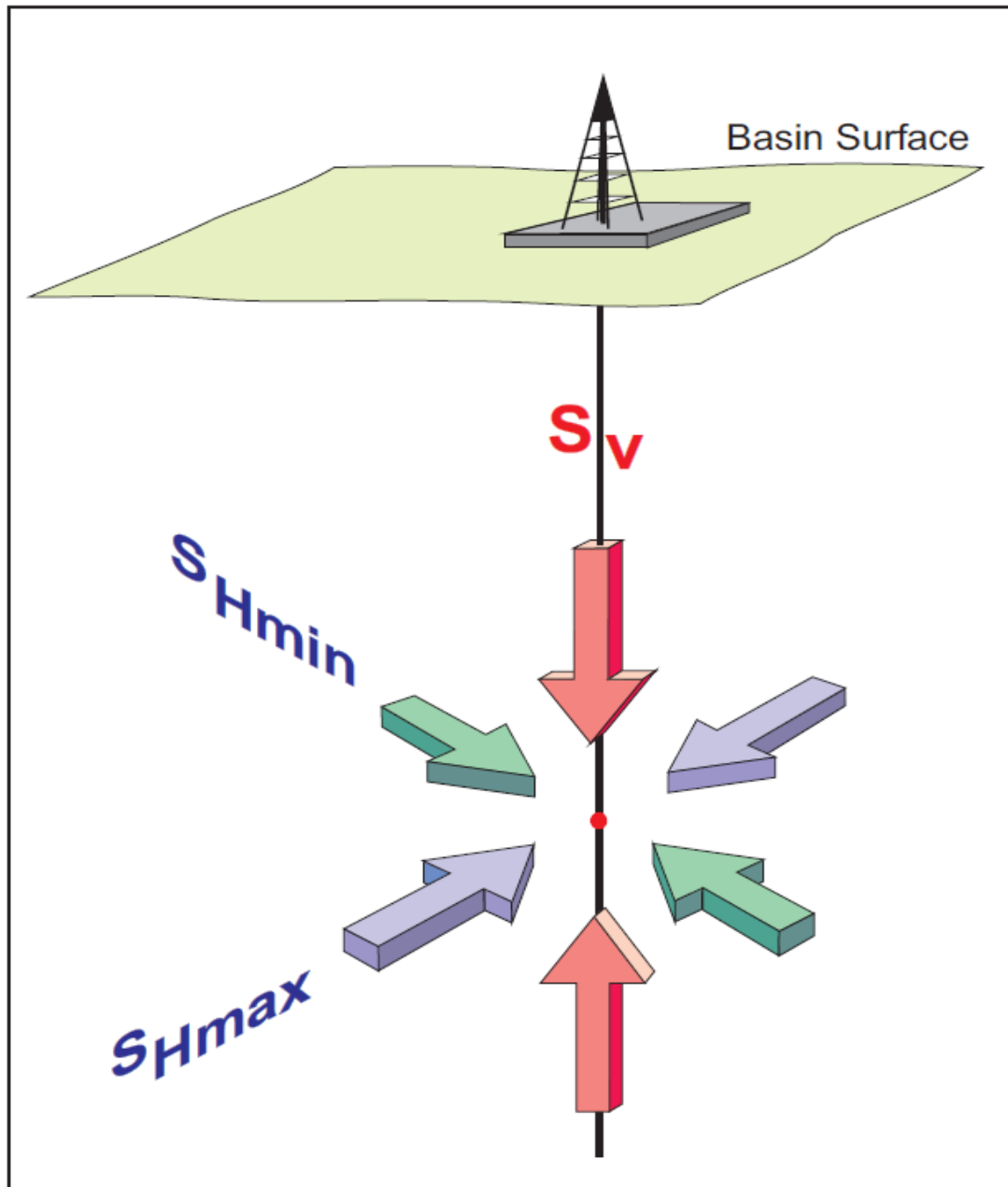


Fig. 12. A principal stress tends to intersect a free surface at right angles. The interface between the ground surface and the atmosphere is a free surface and, over most basins, closely mimics a horizontal plane, so one can infer that one of the principal stresses is nearly vertical and the other two are approximately horizontal.

It is assumed that the vertical stress will be equivalent to the pressure exerted by the weight of the rocks above the point of measurement. Rock density data from vertical wells are required and can be supplied by density logs. Fortunately, these logs have been run in a large number of wells in western Canada.

Calculating horizontal stress magnitudes is more difficult. The ideal method is to open a small hydraulically induced fracture within a packed off interval in a well and to monitor the induced pressure as the process proceeds. After a fracture has been initiated it is then opened and closed several times until a consistent closure pressure has been achieved. This procedure is known as micro-fracturing and is undertaken specifically to measure the magnitude of the smallest principal stress acting at the depth of fracturing. The smallest principal stress is equated with the closure pressure. If the closure pressure is less than the estimated vertical stress magnitude at the depth of measurement, it is assumed that  $S_{Hmin}$  has been measured.

Micro-fracturing stress measurement is expensive and, to date, no such measurements are reported to have been made in wells in the Liard Basin. The next best technique for measuring the smallest principal stress is provided by the closure pressures of mini-fractures that are initiated prior to massive hydraulic fracture jobs run to improve productivity of hydrocarbon reservoirs. Again, no such information has yet been obtained for wells drilled in the Liard Basin.

Initiating a fracture requires that the cohesive strength of the rock must be overcome, thus more pressure is required to fracture a formation than is required to keep open that fracture once it has been created. The leading source of fracturing pressures in most jurisdictions is leak-off tests. These are run below a newly installed casing string to determine what pressures the rocks will withstand as the well is drilled ahead. They are a safety measure and, once the leak-off pressure has been determined, mud weights will not be increased beyond that pressure as drilling proceeds. Thus an ideal leak-off test will provide a pressure that will be slightly higher than the smallest principal stress. The same rationale can be applied to the fracture breakdown pressures recorded during massive fracture operations. They, too, should record pressures slightly higher than the smallest principal stress. However these are not plentifully recorded for Liard Basin wells.

Many of the wells in the Yukon and NWT were drilled in the 1970s and 1980s. Overpressuring was not anticipated, so there was no pressing need to obtain precise rock fracture pressures before drilling ahead after setting casing. Leak-off tests may have been run but, at that time, COGLA did not require them in this region and the daily drilling report forms contained no boxes for recording leak-off test information. In a few cases, leak-off test results were recorded in well history reports.

Historically, in British Columbia, drilling regulations have not stipulated that leak-off tests must be run in oil and gas wells, or that the results be reported. Therefore, only two reports of leak-off tests run in wells drilled in the Liard Basin in British Columbia were located, despite examining several thousand well files.

The situation was slightly better with respect to hydraulic fracture records, although fracture completions of Liard Basin wells are not common. However, the British Columbia Ministry of Energy and Mines requires that reports be submitted, and they are most diligently curated at the Ministry's record centre in Victoria. It is hoped that further data can be obtained as exploration activities proceed in coming years, and that this will enhance the information bearing on  $S_{Hmin}$  magnitudes that is presented here.

In summary, the data used to map stress magnitudes in the Liard Basin come from vertical, or near vertical wells, their logs, their drilling histories and from reports of hydraulic fracturing.

## 10. THE VALUE OF *IN SITU* STRESS MAGNITUDE INFORMATION

As noted above, stress magnitudes enable reservoir permeability to be assessed. Mapping stress magnitudes, and particularly the lateral variations, will help identify those areas with the best productivity potential. Stress magnitude data will help forecast what is required to achieve optimal borehole stability and thereby reduce drilling costs. It also has potential applications for helping assess seismic risk.

There is much evidence that permeability is inversely proportional to stress magnitude. David and Darot (1989) performed laboratory experiments in which sandstone plugs were tested in an apparatus that allowed for control of the pore pressure inside the sample independently from the confining pressure applied externally. Permeability to water was measured at varying pressures. Figure 13 portrays the decrease in permeability when increasing confining pressure was applied to porous sandstone in which the pore fluid pressure was kept constant.

Enever et al. (1994) reported field studies that showed stress being a major control of permeability. They participated in a program where stress and permeability measurements were made at common depths in wells in the Bowen Basin in Queensland, Australia. The measurements were made in coal seams between depths of 300 and 750 metres, and the relationship between *in situ* stress and permeability is well demonstrated in Figure 14. The stress magnitudes, being less than the inferred overburden loads, implied that  $S_{Hmin}$  was being measured.



An even more impressive demonstration, again from coal seams, comes from the Black Warrior Basin in Alabama, U.S.A, where Sparks et al. (1995) made *in situ* stress measurements in numerous coal bed methane wells and mapped the  $S_{Hmin}$  magnitudes against production rates. Figure 15 shows the remarkable correspondence in the Oak Grove coal field.

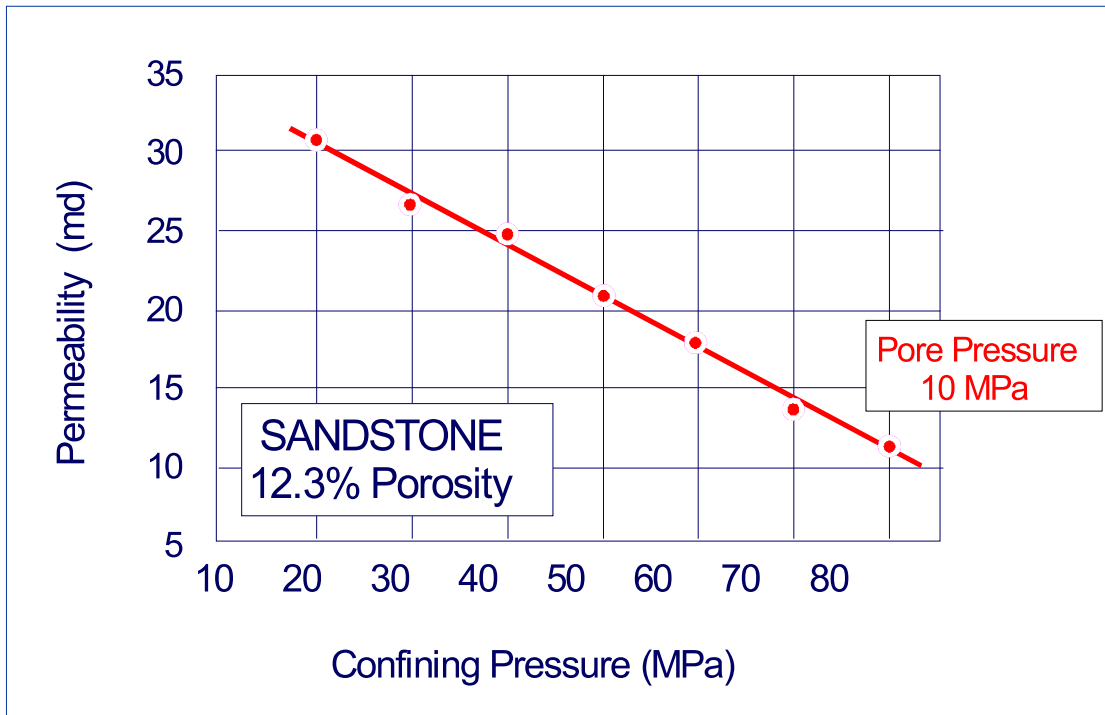


Fig. 13. A sandstone with 12.3% porosity was subjected to increasing confining pressure while the pore pressure was held constant at 10 MPa. Note how permeability decreases in response to increases in pressure (modified from Darot and David, 1989).

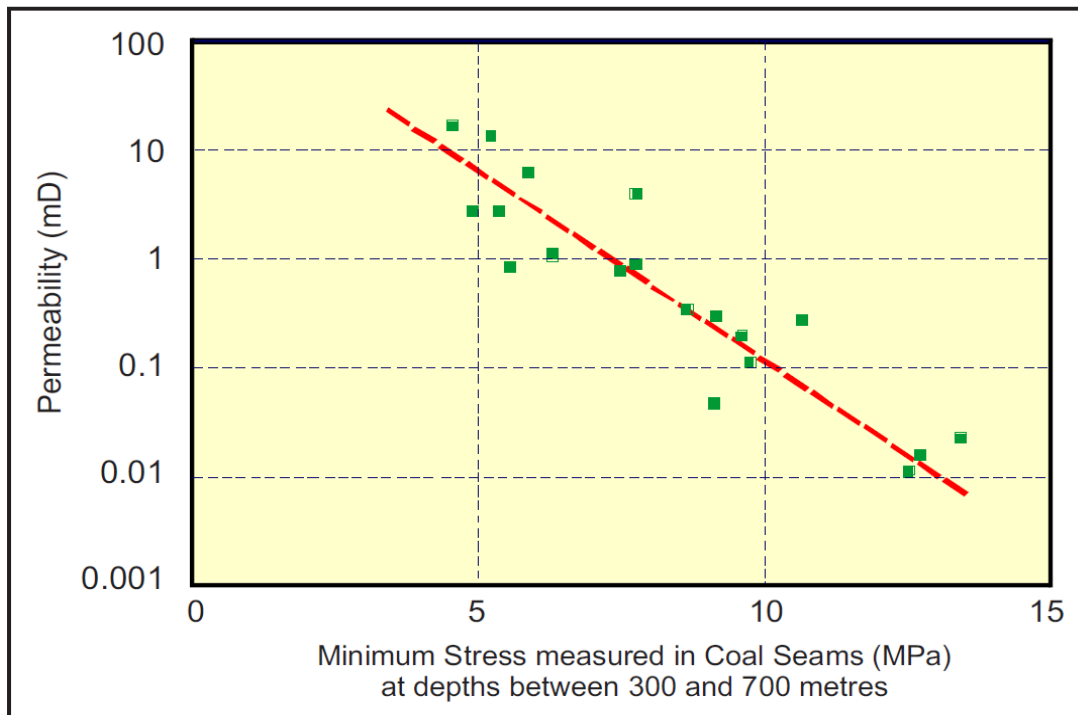


Fig. 14. Coal seam permeability plotted against  $S_{Hmin}$  magnitudes for the Bowen Basin, Australia, showing a well-defined inverse log normal relationship (Enerver et al., 1994).

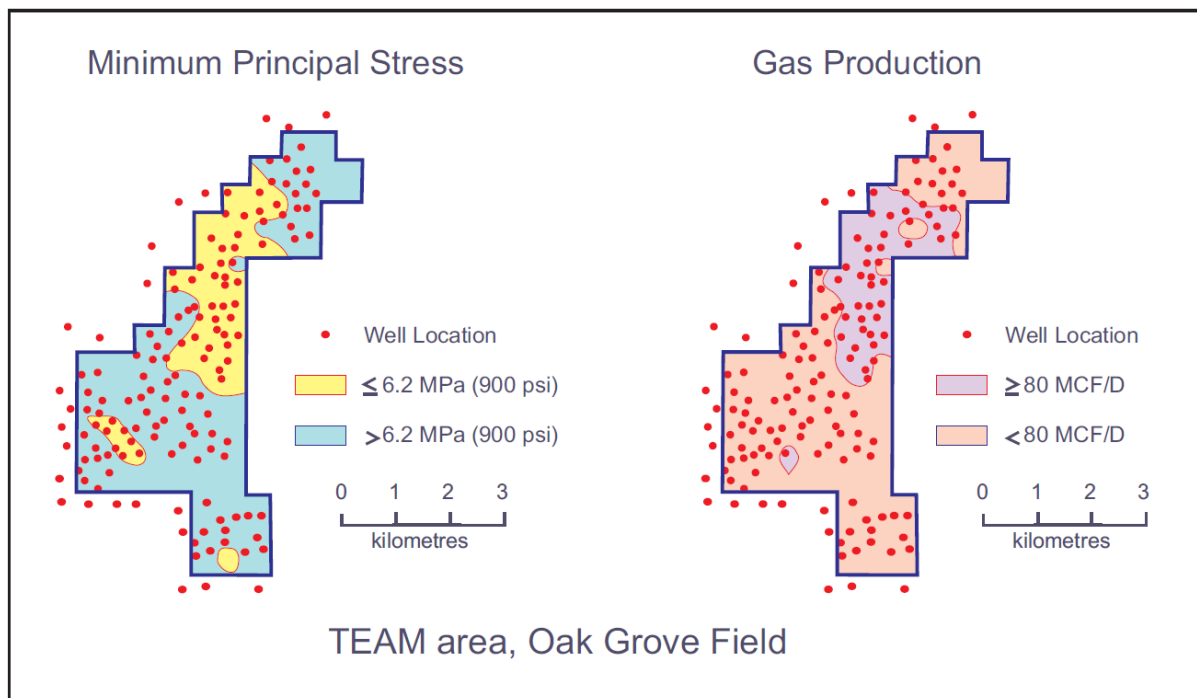


Fig. 15. Relationship between *in situ* stress and gas production from coal in the Mary Lee Group (depth ~ 700 m) in the Black Warrior Basin, Alabama (modified from Sparks et al., 1995).

## 11. MAPPING VERTICAL STRESS, $S_V$

Mapping vertical stress involves determining its magnitude at specific depths in various wells and contouring the results. Since the vertical stress,  $S_V$ , corresponds to the weight of the overburden at a specified depth, density logs provide the basic data.

Ideally, density logs would record values continuously from the surface to the depth of investigation, and integrating such a log would give us the overburden load over the depths that the log was run. However, such coverage is rarely recorded and, in every well used here, there were unlogged gaps between the ground surface and the first density value. In order to determine overburden loads ( $S_V$  magnitudes) at depth, it was necessary to estimate the densities of the rocks in the unlogged sections. Hence, a linear trend was established for the upper several hundred metres of the logged section, and this trend was then used to extrapolate density values for the unlogged sections at the top of each well (Fig. 16).

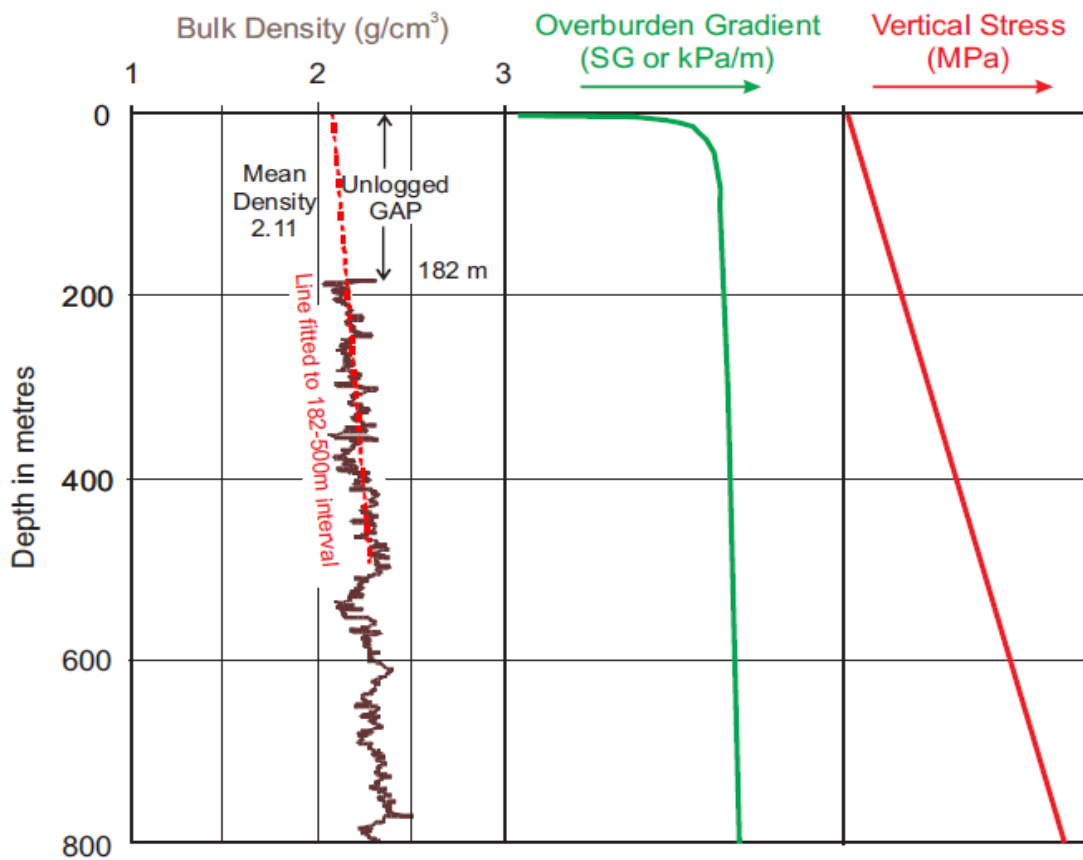


Fig.16. Determination of vertical stress from a density log.

As Figure 17 shows, the 64 wells that were selected in order to map  $S_V$ , the vertical stress, do not provide a perfect areal distribution of data points across the Liard Basin, but it was the best that could be achieved. North of the British Columbia border, drilling has not been extensive, except where gas has been produced. Table 2 lists the 64 wells, and the  $S_V$  magnitudes calculated for depths of 250, 500, 1000, 1500 and 2000 metres.

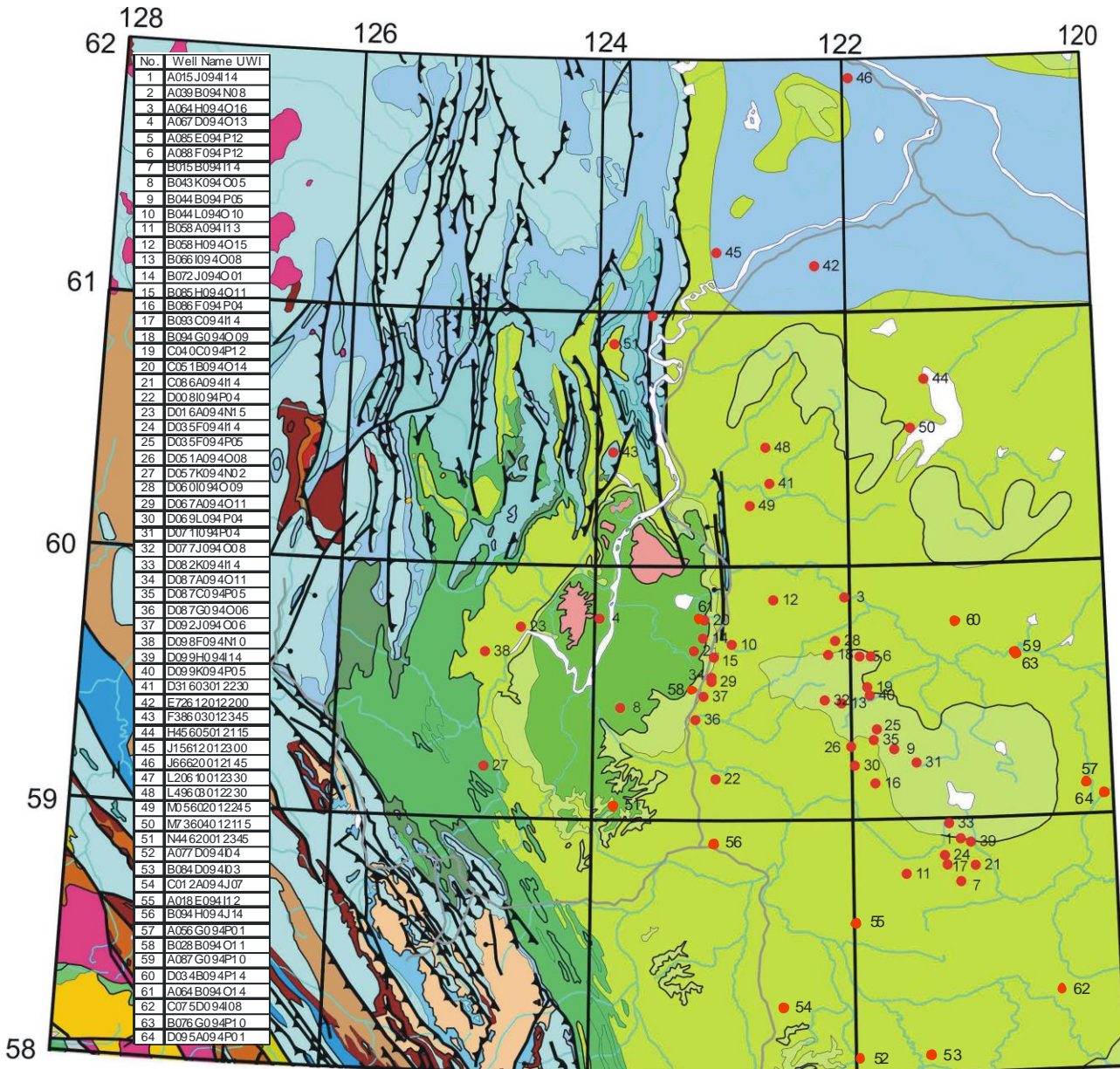


Fig. 17. Locations of wells that provided density logs used for  $S_V$  magnitude calculations.

No.	Well Name UWI	Latitude	Longitude	Sv at 250m (MPa)	Sv at 500m (MPa)	Sv at 1000m (MPa)	Sv at 1500m (MPa)	Sv at 2000m (MPa)
1	A015J094I14	58.927	121.178	6.0	12.2			
2	A039B094N08	59.277	124.228	6.5	13.1	39.4		
3	A064H094O16	59.885	122.041	6.0	12.3	25.1	38.3	50.9
4	A067D094O13	59.802	123.953	6.0				
5	A085E094P12	59.652	121.928	6.0	12.1	25.0	38.1	50.5
6	A088F094P12	59.652	121.841	6.1	12.2	24.9	37.7	49.5
7	B015B094I14	58.760	121.184	6.0	12.2	25.1	38.0	50.5
8	B043K094O05	59.452	123.784	5.9	12.0	24.6	37.4	49.8
9	B044B094P05	59.285	121.672	5.9	12.0	24.9	38.1	51.1
10	B044L094O10	59.702	122.922	6.2	12.6			
11	B058A094I13	58.794	121.597	5.8	11.9	24.7	37.8	
12	B058H094O15	59.877	122.597	6.2	12.7	25.5	38.4	51.2
13	B066I094O08	59.469	122.072	5.4	11.0	23.6	36.8	49.9
14	B072J094O01	59.727	123.147	5.8	11.7	24.7	37.6	50.4
15	B085H094O11	59.652	123.059	5.9	12.0	24.5		
16	B086F094P04	59.152	121.822	5.5	11.1	23.6	36.0	
17	B093C094I14	58.827	121.284	5.6	11.6	24.5	37.5	50.1
18	B094G094O09	59.660	122.172	5.8	11.6	24.2	37.1	49.7
19	C040C094P12	59.531	121.872	5.5	11.1	23.8	36.2	48.8
20	C051B094O14	59.798	123.134	5.6	11.3	23.1	35.0	47.6
21	C086A094I14	58.823	121.072	5.3	10.8	23.6	36.4	49.6
22	D008I094P04	59.173	121.591	6.1	12.3	25.3	38.5	50.8
23	D016A094N15	59.765	124.566	6.1	12.4	24.8	37.2	
24	D035F094I14	58.865	121.303	5.9	12.0			
25	D035F094P05	59.365	121.803	5.8	11.9	24.6	37.8	
26	D051A094O08	59.298	122.003	6.0	12.0	25.1	38.2	51.2
27	D057K094N02	59.215	124.828	6.6	13.3	26.5	40.3	54.5
28	D060I094O09	59.715	122.116	6.1	12.4	25.4	38.4	51.5
29	D067A094O11	59.556	123.078	5.7	11.7			
30	D069L094P04	59.223	121.978	5.9	11.9	24.7	37.4	49.6
31	D071I094P04	59.231	121.503	6.0	12.1	25.0	38.2	51.3
32	D077J094O08	59.481	122.203	5.4	10.9	23.5	36.0	48.9
33	D082K094I14	58.990	121.266	5.3	10.9	23.2	36.0	49.1
34	D087A094O11	59.573	123.078	6.0	12.2			
35	D087C094P05	59.323	121.828	6.1	12.3	25.0	37.9	49.9
36	D087G094O06	59.406	123.203	5.8	11.7	24.3		
37	D092J094O06	59.498	123.141	5.6	11.5	24.2	37.3	
38	D098F094N10	59.665	124.841	5.7	12.0	24.2	36.5	49.4
39	D099H094I14	58.915	121.103	5.8	12.0			
40	D099K094P05	59.498	121.853	6.0	11.9	24.7	37.5	50.4
41	D316I03012230	60.335	122.621	5.7	11.8			
42	E726I2012200	61.190	122.246	6.2	12.5	25.6		
43	F386J03012345	60.456	123.863	6.3	12.6	25.6	38.7	51.9
44	H456J05012115	60.740	121.379	5.1	9.7	21.9	34.8	
45	J156I2012300	61.244	123.043	6.2	12.4			
46	J666J2012145	61.927	121.949	6.0	12.5			
47	L206I0012330	60.994	123.559	6.3	12.6	25.7		
48	L496J03012230	60.477	122.652	5.9	12.0			
49	M056J02012245	60.248	122.777	5.9	12.0			
50	M736J04012115	60.548	121.496	5.8	11.6	24.0	37.0	
51	N446J20012345	61.898	123.895	6.8	13.8			
52	A077D094I04	58.060	121.953	5.0	10.5	22.3		
53	B084D094I03	58.069	121.422	5.6	11.4			
54	C012A094J07	58.265	122.522	5.6	11.4	23.3		
55	A018E094I12	58.594	121.966	5.8	11.9	24.6	37.3	49.7
56	B094H094I14	58.910	123.047	5.6	11.7			
57	A056G094P01	59.127	120.191	5.0	11.1	24.0		
58	B028B094O11	59.519	123.222	6.0	12.2	24.7	37.1	
59	A087G094P10	59.652	120.703	6.0				
60	D034B094P14	59.781	121.166	5.8	11.9			
61	A064B094O14	59.802	123.166	6.0	12.2	24.7		
62	C075D094I08	58.315	120.434	5.8	11.8			
63	B076G094P10	59.644	120.697	5.9				
64	D095A094P01	59.081	120.053	4.8	9.9	22.3	34.4	46.2

Table 2. Vertical stress magnitudes ( $S_V$ ) at specific depths for 64 wells in the Liard Basin.  
Magnitudes in italics refer to values extrapolated from higher in that well

Figure 18 portrays the variation in vertical stress magnitude across the Liard Basin at a depth of 250 metres. All 64 wells contributed data to this map.

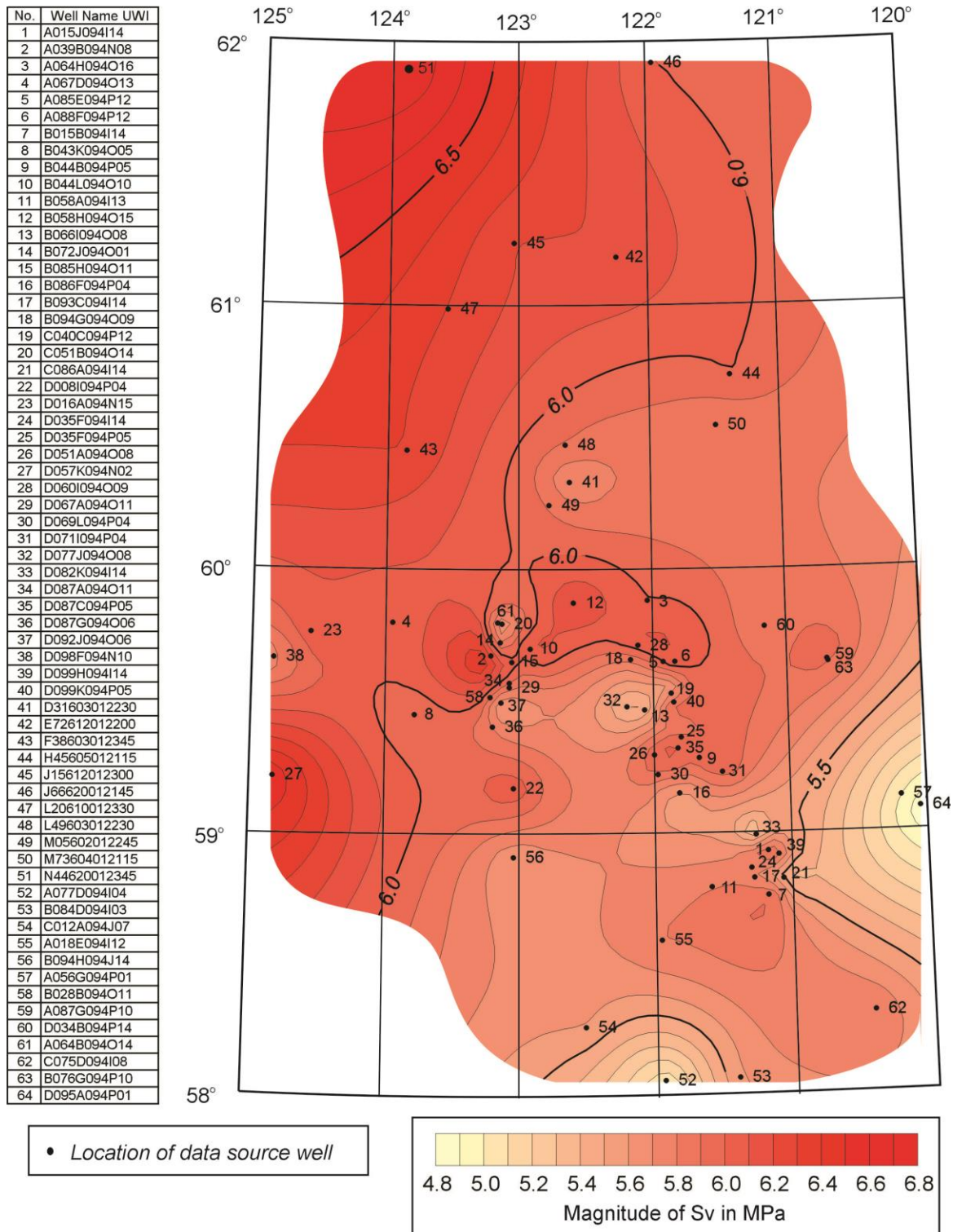


Fig. 18. Sv magnitudes at 250 m depth in the Liard Basin

At 500 metres depth, 61 wells supplied  $S_v$  data (Fig. 19).

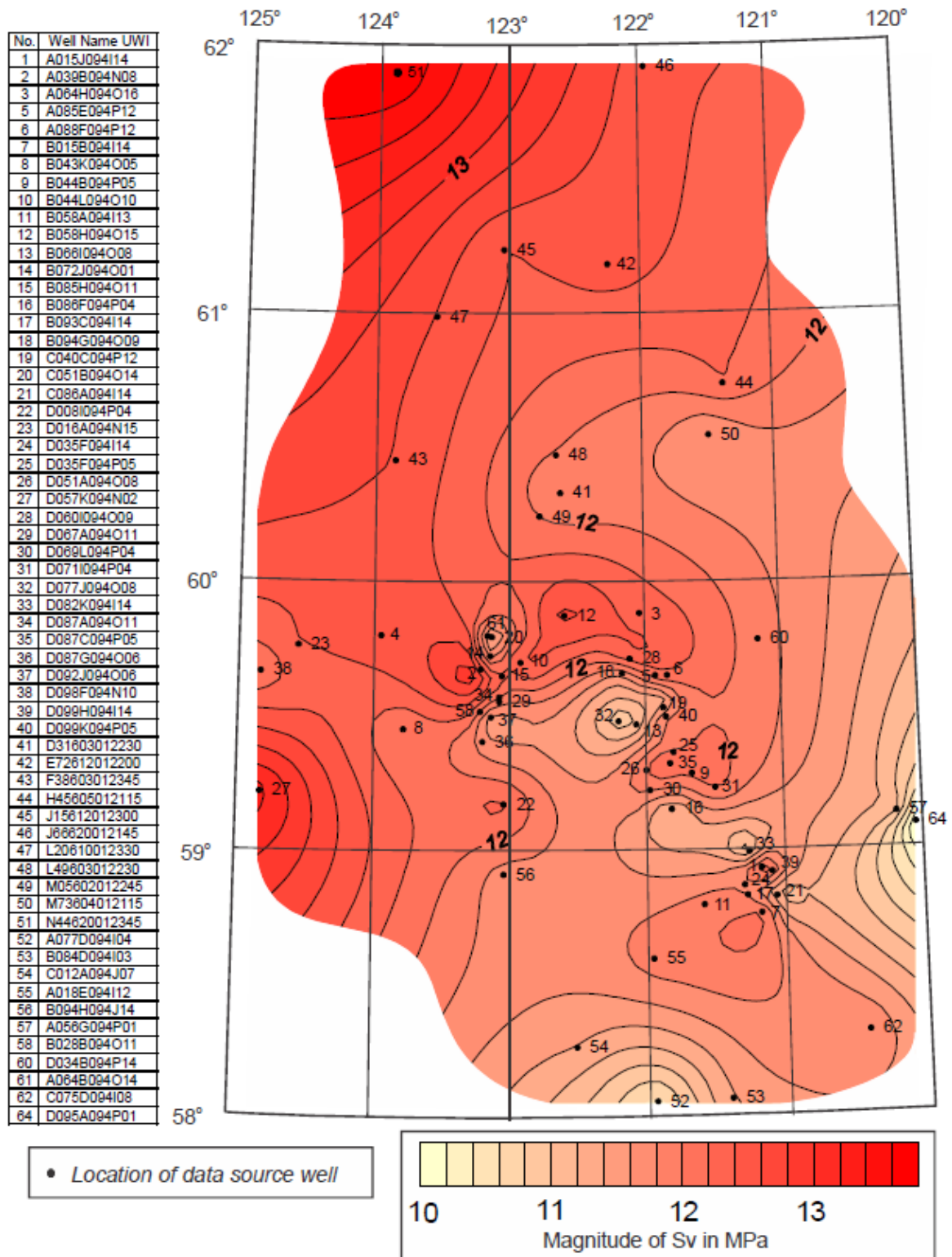


Fig. 19.  $S_v$  magnitudes at 500 m depth in the Liard Basin

At 1000 metres depth, 47 of the 64 wells provided  $S_v$  magnitudes (Fig. 20).

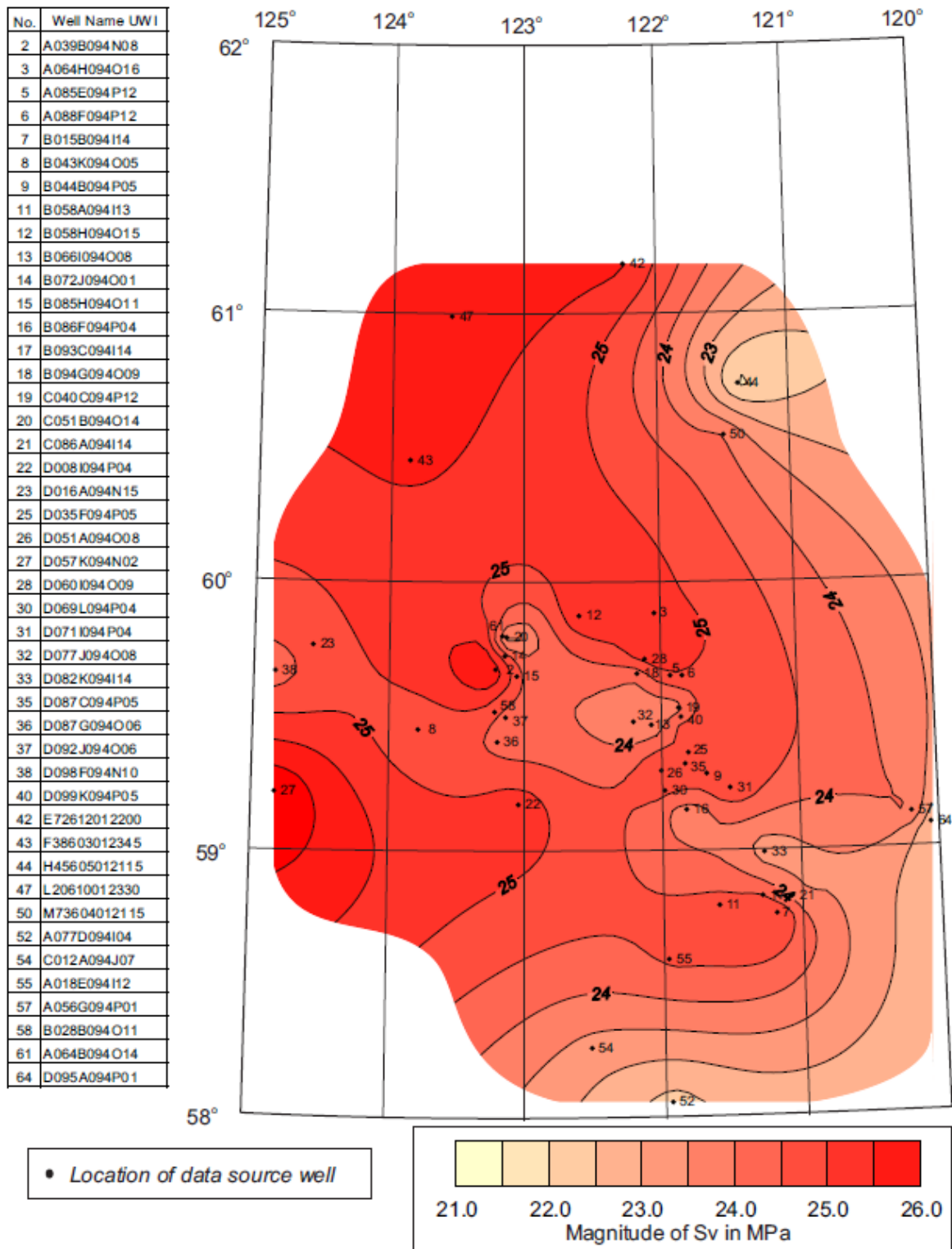


Fig. 20.  $S_v$  magnitudes at 1000 m depth in the Liard Basin



At 1500 metres depth, the number of wells providing  $S_v$  magnitudes was reduced to 36, due to a lack of deeper drilling (Fig. 21).

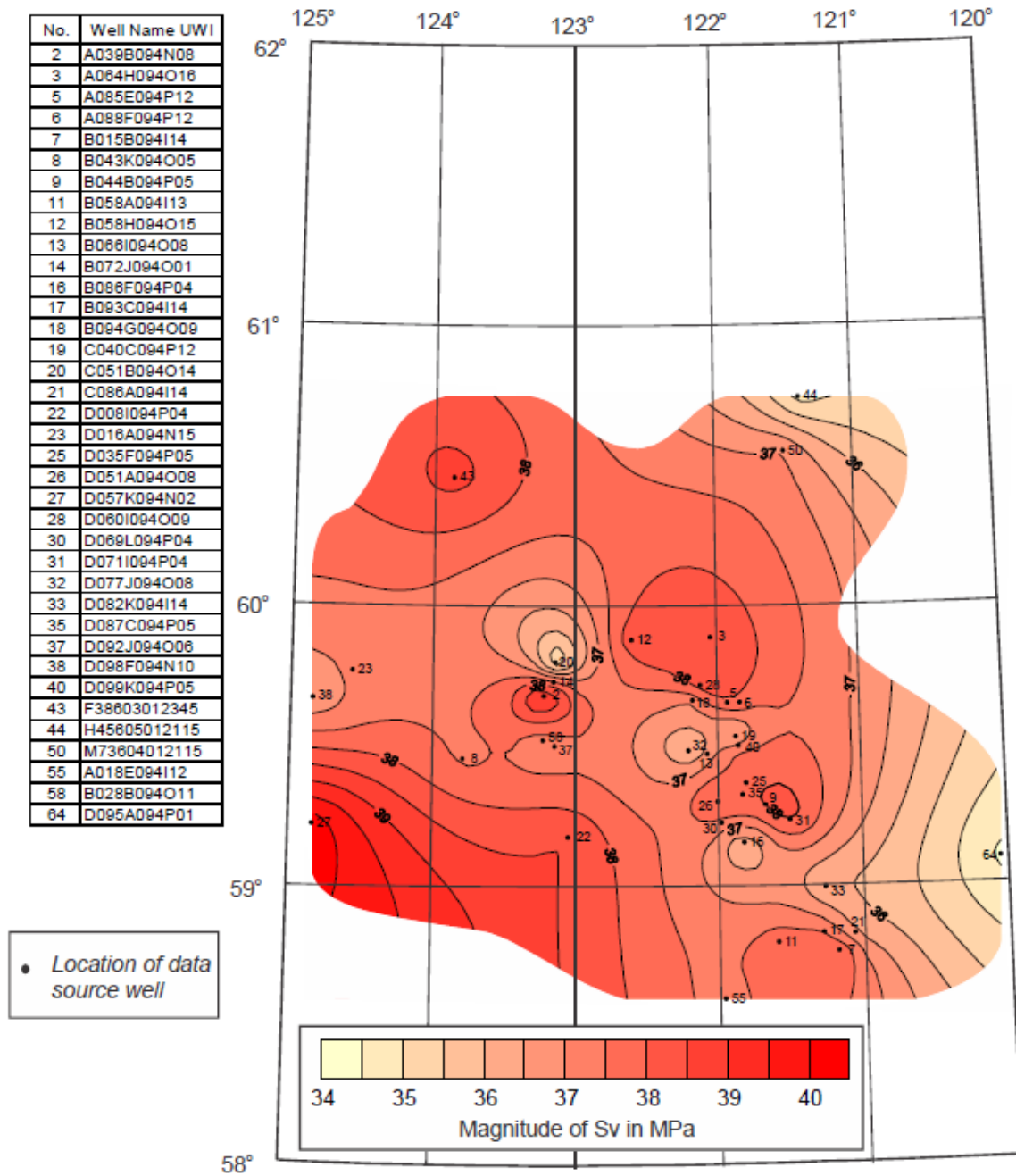


Fig. 21.  $S_v$  magnitudes at 1500 m depth in the Liard Basin

At 2000 metres depth, only 28 wells contributed  $S_v$  magnitudes (Fig 22). As Figures 10 to 12 indicate, deep wells are not present in all parts of the basin.

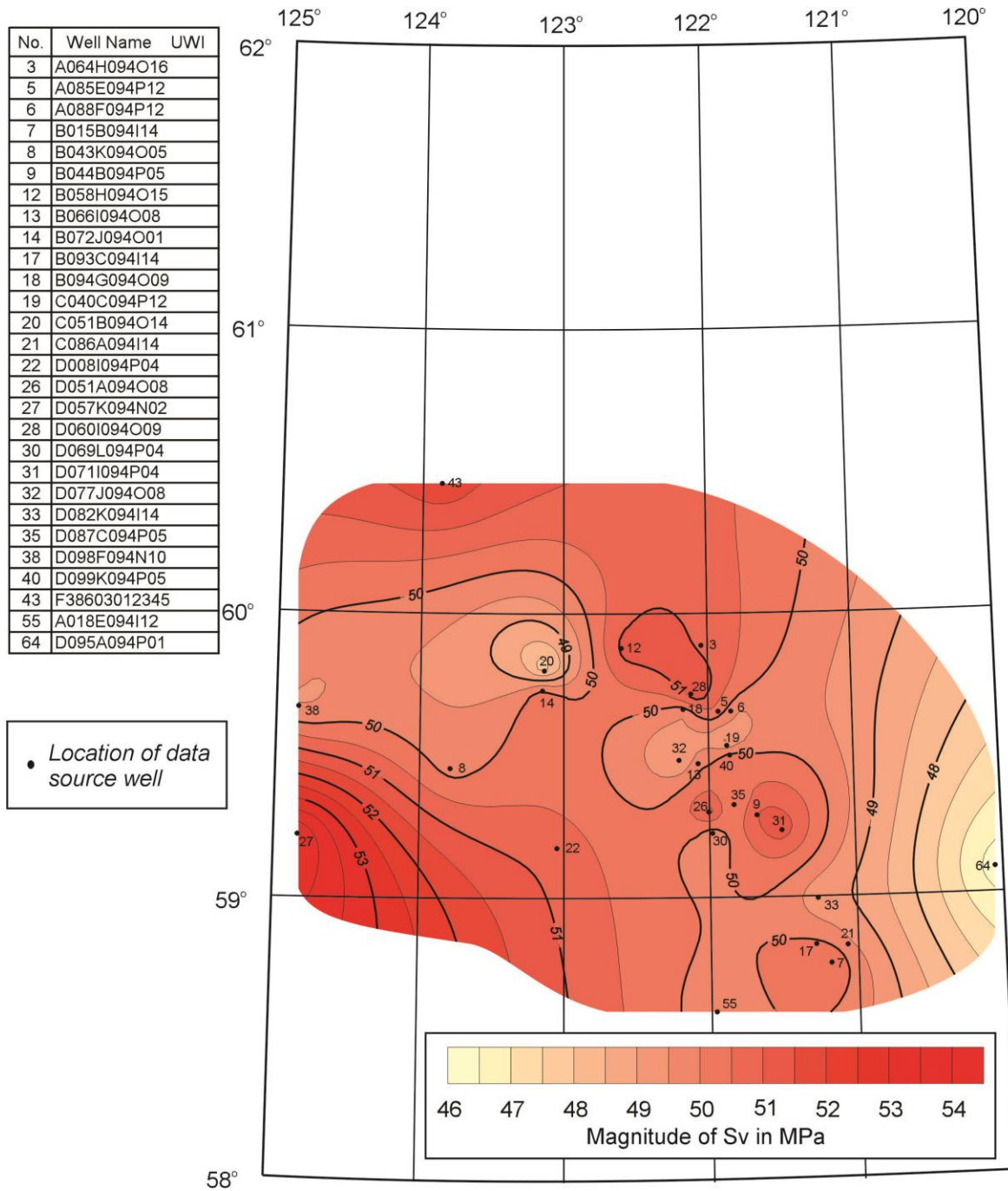


Fig. 22.  $S_v$  magnitudes at 2000 m depth in the Liard Basin

Interpreting the  $S_V$  magnitude maps is not a completely straightforward exercise. They represent the overburden load represented by the sum of the densities of the rocks above the depth of investigation. Rock densities reflect: 1) the composition of the rocks, 2) vertical compaction and 3) lateral compression. In the Western Canadian Sedimentary Basin, rocks close to the Laramide overthrust belt exhibit high  $S_V$  gradients that can only be accounted for by the effects of lateral compression.

Vertical compression results not only from today's overburden load but also from former loads that have been eroded. In other words, it can reflect, in part, paleotopography and its time scale. Long existent valleys can exert lesser loads on buried rocks than adjacent highlands.

Figures 18 and 19 contour, respectively, the vertical stress magnitudes at 250 metres depth based on data from 64 wells and at 500 metres depth based on data from 61 wells. The values of the  $S_V$  gradients and magnitudes for all of these wells are presented in graphic plots in Appendix 2 and are also available in digital format. In Figures 18 and 19, low  $S_V$  magnitudes are present between latitudes  $59^\circ$  and  $59^\circ 30'$  and there is also an indication of low magnitudes around latitude  $58^\circ$ . The more northerly low magnitude area has a west-east semi-linear trend that suggests it may owe its lesser compaction to a Cenozoic valley system that drained emergent mountains to the west, where today there is a prominent salient in the overthrust terranes (Fig. 17). Similarly, both maps show higher  $S_V$  magnitudes rimming the western margin of the Liard Basin. These elevated magnitudes may be due, in part, to lateral compression exerted by the eastward overthrusting that defines the western margin of the basin.

Figures 20, 21 and 22 portray essentially the same configurations at 1000 m, 1500 m and 2000 m depth, but with less control because many of the wells did not penetrate to these depths.

The vertical stress profiles derived from the density logs also offer the opportunity to construct contour maps of  $S_V$  magnitudes at specific geological horizons. Table 3 lists the most frequently picked Mesozoic and Paleozoic formation tops in metres KB for the wells featured in Figures 18 – 22. Seven of the tops were recognised in enough wells to make it feasible to contour  $S_V$  magnitudes at these stratigraphic horizons. The  $S_V$  magnitudes at these formation tops are listed in Table 4, and the related  $S_V$  magnitude maps are presented in Figures 23 to 29.

Number	Well Name UWI	Latitude	Longitude	Sikanni	Scatter	Garbutt	Bluesky	Fantasque	Mattson	Debolt	Banff	Kotcho	Trout River	Jean Marie	Slave Point	Keg River
1	A015J094I14	58.927	121.178				617			634						
2	A039B094N08	59.277	124.228	546	1349	1703										
3	A064H094O16	59.885	122.041							299.5	496.5	921.7	1226	1420		2325
4	A067D094O13	59.802	123.953	370	1284	1594		2253.3	2427.9	3659.9	3659.9					
5	A085E094P12	59.652	121.928							519	724	1117	1380	1656.5		
6	A088F094P12	59.652	121.841											1574	2165.2	
7	B015B094I14	58.760	121.184				566.9			603.2	675.4	1048.5	1229.8	1387.4		2283.5
8	B043K094O05	59.452	123.784	791	1330	1601		2418		2750						
9	B044B094P05	59.285	121.672				641.3			667.5	807.1	1170.4	1367.6	1422.1		
10	B044L094O10	59.702	122.922						394.4							
11	B058A094I13	58.794	121.597							640	825	1112	1280	1461		
12	B058H094O15	59.877	122.597							430.5		1271.5	1608		2710.5	2762
13	B066I094O08	59.469	122.072				624			634	843	1223	1464	1844		
14	B072J094O01	59.727	123.147													
15	B085H094O11	59.652	123.059						958.5	1356.3						
16	B086F094P04	59.152	121.822							551.7	740.3	1074.1	1236.8	1422.1		
17	B093C094I14	58.827	121.284								773	1076.5	1259	1426.5		2210
18	B094G094O09	59.660	122.172				401.5			470.5	761.6	1193.6	1461	2022		2580.5
19	C040C094P12	59.531	121.872								636.5	1107	1341.4	1507.8		
20	C051B094O14	59.798	123.134		947.6	1089										
21	C086A094I14	58.823	121.072				542			568	732.5	1039.2		1376.2	1874	
22	D008I094P04	59.173	121.591							649	760	1172	1346	1533	2138	
23	D016A094N15	59.765	124.566					1502	1653							
24	D035F094I14	58.865	121.303				613.8			625.7						
25	D035F094P05	59.365	121.803							678	831	1218.5	1501	1736		
26	D051A094O08	59.298	122.003													2469.5
27	D057K094N02	59.215	124.828													
28	D060I094O09	59.715	122.116					406		438	608	1087	1382	1864		2453
29	D067A094O11	59.556	123.078		330.4	437.7			462.7	681.2						
30	D069L094P04	59.223	121.978				520			538	1092	1092	1256	1575		
31	D071I094P04	59.231	121.503							704	879	1230	1438.5	1600.5	2164	
32	D077J094O08	59.481	122.203							658.9	865.6	1307.2				
33	D082K094I14	58.990	121.266								811	1152.5	1334.3	1486.5		
34	D087A094O11	59.573	123.078		310.9				434.6	749.8						
35	D087C094P05	59.323	121.828							612.8	775.6	1130	1324.4	1477.8	2313.6	
36	D087G094O06	59.406	123.203		385.2	537	578.5		623	1010.1						
37	D092J094O06	59.498	123.141					852.8	975.3	1611.7						
38	D098F094N10	59.665	124.841					1473	1538.9							
39	D099H094I14	58.915	121.103				602			616	767					
40	D099K094P05	59.498	121.853							563	754	1136	1387	1538		
41	D31603012230	60.335	122.621	150.9	369.4	409.3										
42	E72612012200	61.190	122.246											27.4		
43	F38603012345	60.456	123.863								1429.4					
44	H45605012115	60.740	121.379								280.4	400.5	759	968.3	1492	1609.3
45	J15612012300	61.244	123.043												c. 422	
46	J66620012145	61.927	121.949												c. 356	384
47	L20610012330	60.994	123.559												c. 835	
48	L49603012230	60.477	122.652	211.2	419.4	466	570.3		576.1							
49	M05602012245	60.248	122.777		332.2	396.2	488		507.2							
50	M73604012115	60.548	121.496		311.2						395.6	676	1045.5	1266.1	1761.7	1900.7
51	N44620012345	61.898	123.895													
52	A077D094I04	58.060	121.953							1074	1364	1634	1748	1906.5	2443.5	
53	B084D094I-03	58.069	121.422							856	1084.5	1389		1690		
54	C012A094J07	58.265	122.522							1108	1407	1695	1778.5		2426	2603.5
55	A018E094I12	58.594	121.966							623	846	1152	1296	1487	1975	
56	B094H094J14	58.910	123.047							605	961	1333.4	1398.7		2028	2331.6
57	A056G094P01	59.127	120.191				345				349	646	864	1009		
58	B028B094O11	59.519	123.222		1150	1265										
59	A087G094P10	59.644	120.697								409.5	727.5	968	1203		
60	D034B094P14	59.781	121.166								482	889	1143	1324.3		
61	A064B094O14	59.802	123.166		1002	1122										
62	C075D094I08	58.315	120.434													
63	B076G094P10	59.644	120.697													
64	D095A094P01	59.081	120.053													


 = No information available

Table 3. Formation tops in metres in wells that provide  $S_v$  magnitudes

Number	Well Name UWI	Scatter Sv (MPa)	Bluesky Sv (MPa)	Top Paleozoic Sv (MPa)	Debolt Sv (MPa)	Bantff Sv (MPa)	Kotcho Sv (MPa)	Jean Marie Sv (MPa)
32	D077J094O08			14.5	14.5	20.0	31.5	
33	D082K094I14			14.6		13.5	27.1	35.7
34	D087A094O11	7.5		10.7	18.7			
35	D087C094P05			15.0	15.0	19.3	28.4	37.3
36	D087G094O06	9.0	13.5	14.6	24.5			
37	D092J094O06			20.4	40.2			
38	D098F094N10			35.8				
39	D099H094I14		14.4	14.7	14.7	18.7		
40	D099K094P05			13.4	13.4	18.3	28.0	38.5
41	D31603012230	9.2						
42	E72612012200							
43	F38603012345							
44	H45605012115			5.7		5.7	7.4	21.1
45	J15612012300							
46	J66620012145							
47	L20610012330							
48	L49603012230	10.0	13.7	13.9				
49	M05602012245	7.9	10.7	12.2				
50	M73604012115	7.2		9.2		9.2	15.8	31.1
51	N44620012345							
52	A077D094I04			24.2	24.2	np	np	np
53	B084D094I-03			np	np	np	np	np
54	C012A094J07			np	np	np	np	np
55	A018E094I12			14.8	14.8	20.6	28.4	36.9
56	B094H094J14			14.1	14.1	np	np	
57	A056G094P01		7.2	7.2		7.2	14.7	24.2
58	B028B094O11	25.9						
59	A087G094P10					np	np	np
60	D034B094P14					np	np	np
61	A064B094O14	24.8						

np = not penetrated. The density log did not extend to the formation top.

Number	Well Name UWI	Scatter Sv (MPa)	Bluesky Sv (MPa)	Top Paleozoic Sv (MPa)	Debolt Sv (MPa)	Bantff Sv (MPa)	Kotcho Sv (MPa)	Jean Marie Sv (MPa)
1	A015J094I14		15.1	15.5	15.5			
2	A039B094N08	35.4						
3	A064H094O16			7.2	7.2	12.3	23.0	36.1
4	A067D094O13	np		np	np	np		
5	A085E094P12			12.5	12.5	17.8	28.0	41.9
6	A088F094P12							39.5
7	B015B094I14		13.9	14.7	14.7	16.7	26.4	35.2
8	B043K094O05	33.0		60.1	69.0			
9	B044B094P05		15.5	16.4	16.4	19.9	26.7	36.1
10	B044L094O10			9.9	9.9			
11	B058A094I13			15.3	15.3	20.2	27.5	36.8
12	B058H094O15			10.8	10.8		32.4	
13	B066I094O08		13.8	14.1	14.1	19.5	29.5	45.8
14	B072J094O01			11.4	11.4	19.0	25.5	
15	B085H094O11			23.5	np			
16	B086F094P04			12.2	12.2	17.1	25.4	33.9
17	B093C094I14			18.6		18.6	26.5	35.6
18	B094G094O09		9.2	10.8	10.8	18.4	29.2	50.2
19	C040C094P12			14.5		14.5	26.3	36.4
20	C051B094O14	21.9						
21	C086A094I14		11.8	12.4	12.4	16.8	24.5	33.3
22	D008I094P04			15.9	16.0	19.0	29.8	39.4
23	D016A094N15			37.2				
24	D035F094I14		14.8	15.1	15.1			
25	D035F094P05				16.1	20.2	32.0	44.0
26	D051A094O08							
27	D057K094N02							
28	D060I094O09			9.9	10.7	15.2	27.6	np
29	D067A094O11	7.7		10.8	16.4			
30	D069L094P04		12.3	12.8	12.8	27.0	27.0	39.3
31	D071I094P04			17.2	17.2	21.8	31.0	40.9

Table 4. Vertical stress magnitudes at formation tops in wells in the Liard Basin.

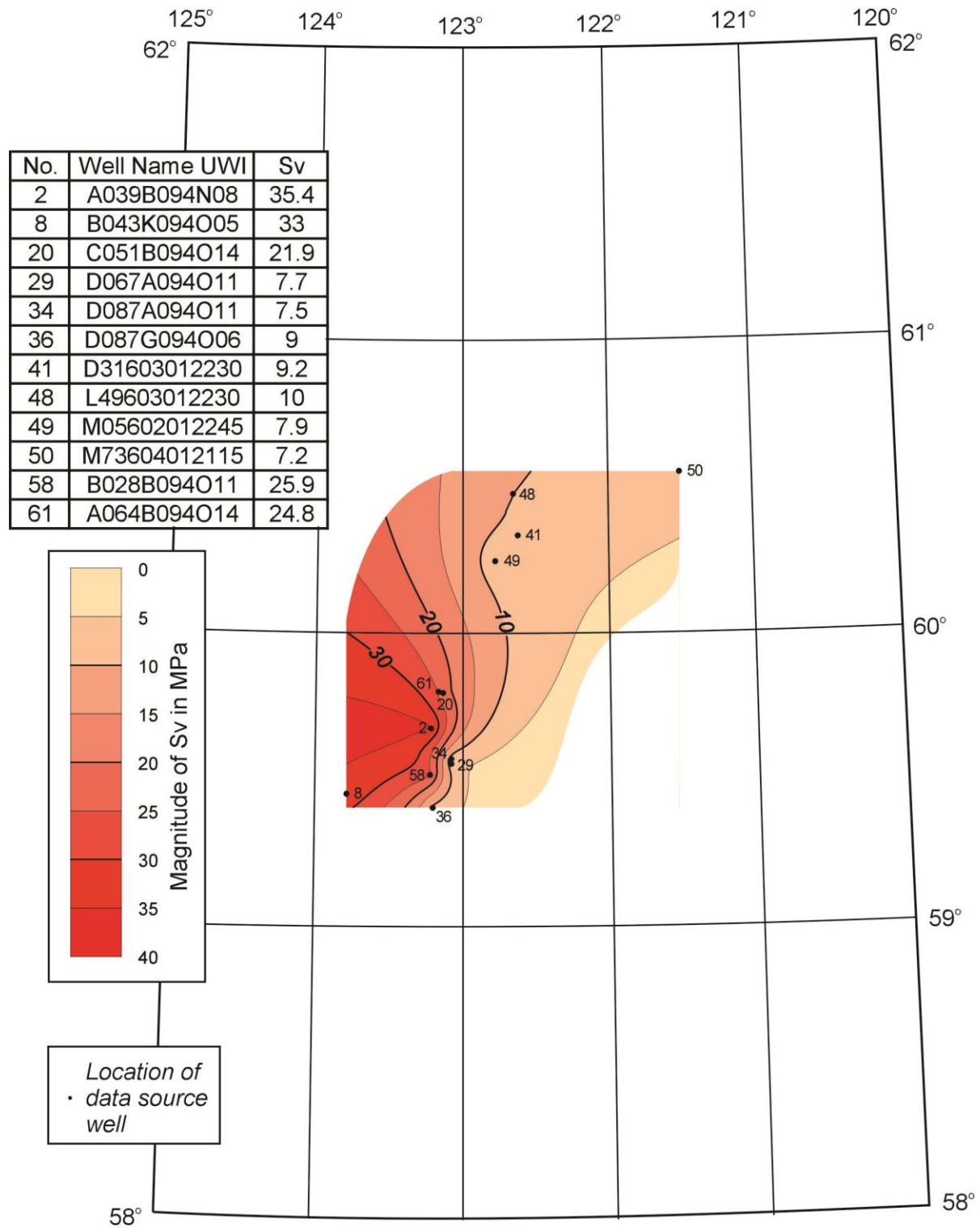


Fig. 23. Sv magnitudes in MPa at the top of the Scatter Formation in the Liard Basin

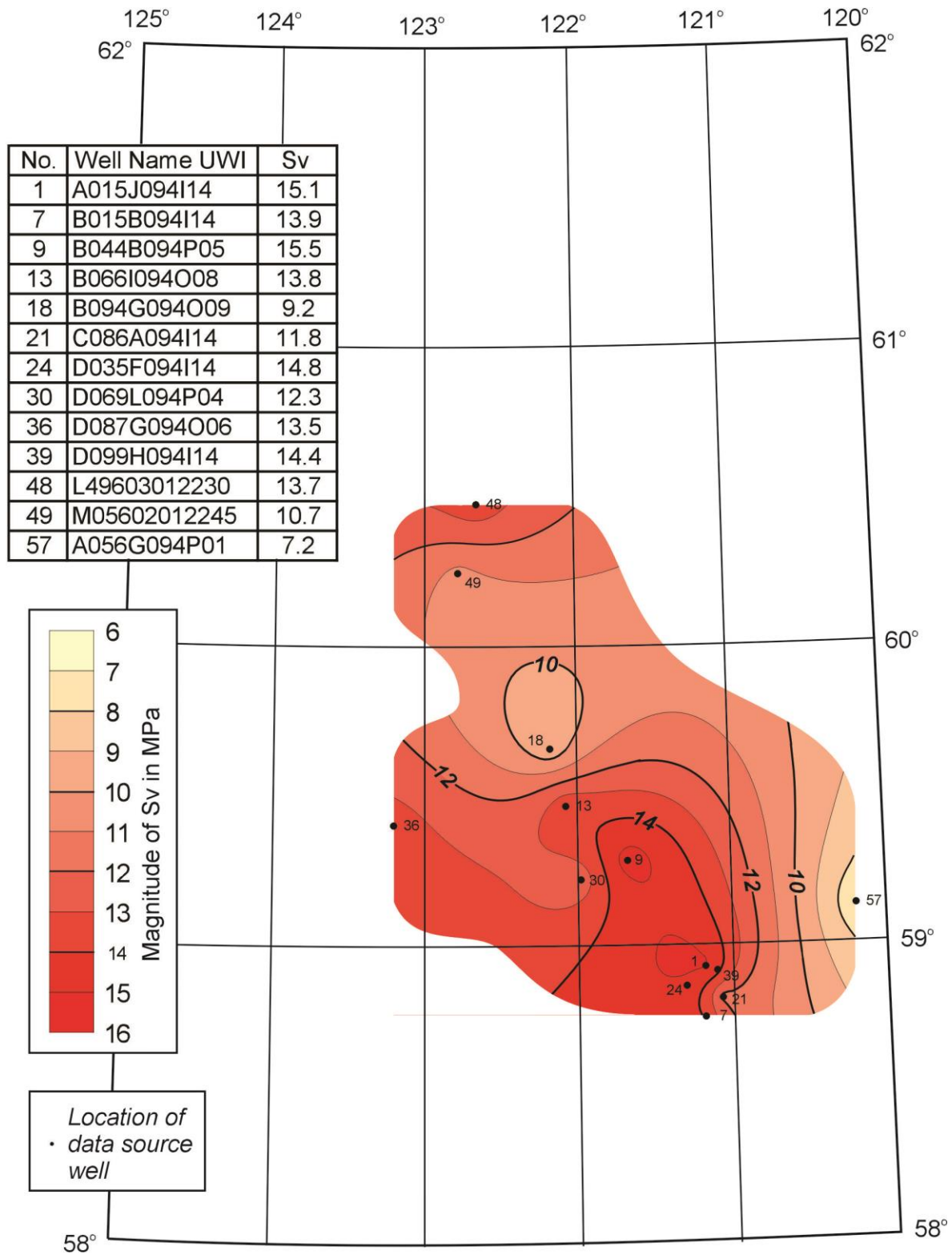


Fig. 24. Sv magnitudes in MPa at the top of the Bluesky Formation in the Liard Basin

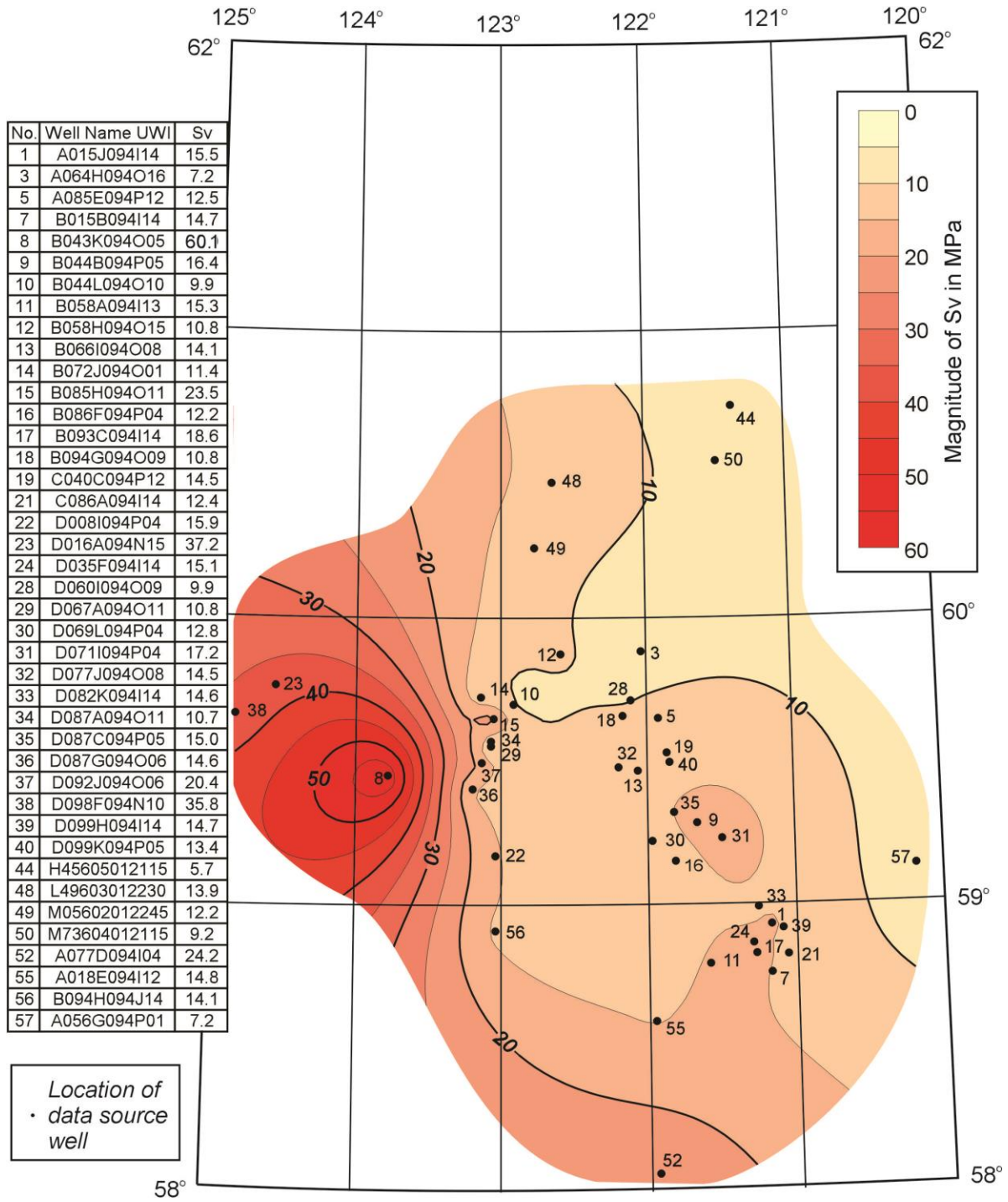


Fig. 25. Sv magnitudes in MPa at the top of the Paleozoic strata in the Liard Basin



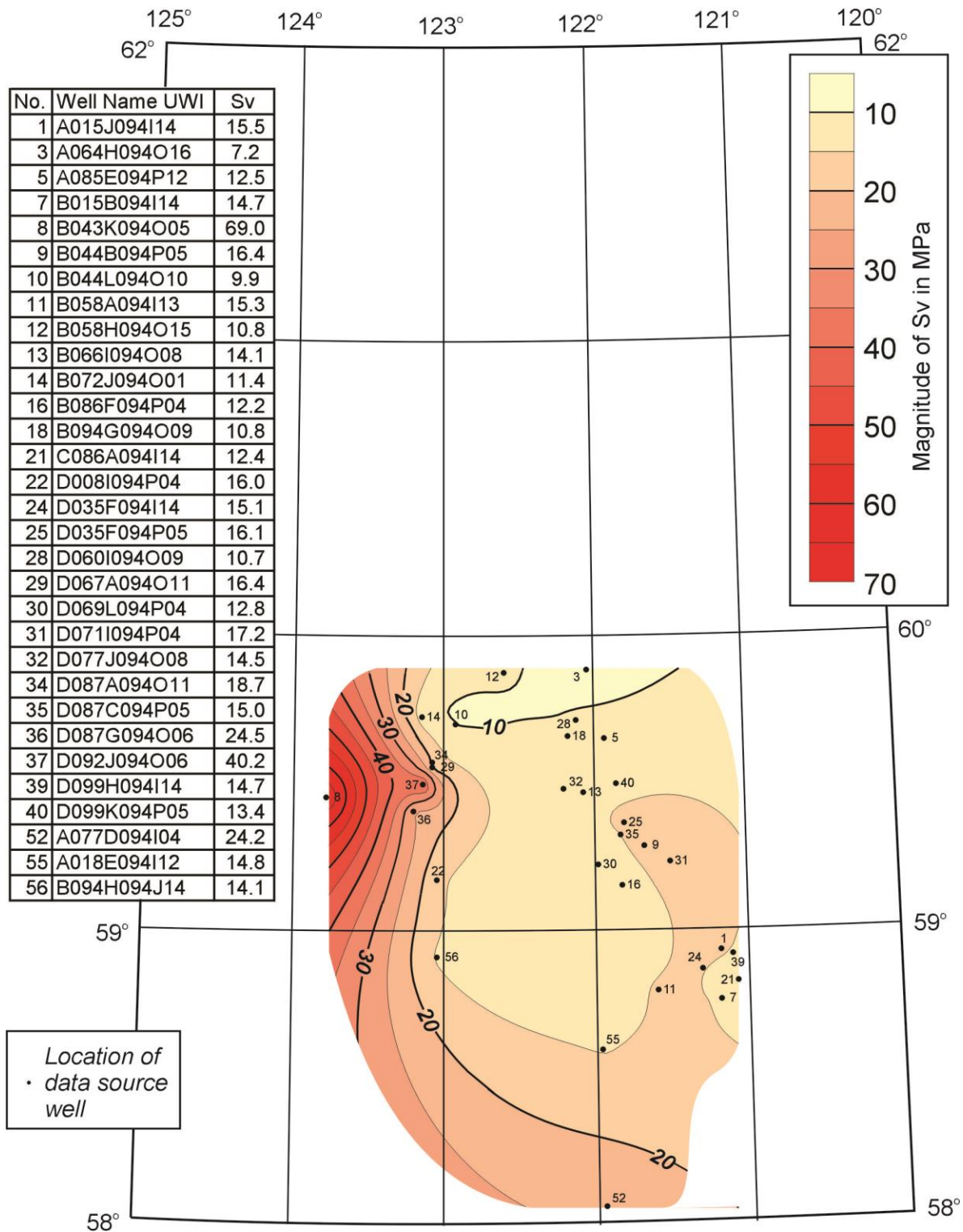


Fig. 26. Sv magnitudes in MPa at the top of the Debolt Formation in the Liard Basin

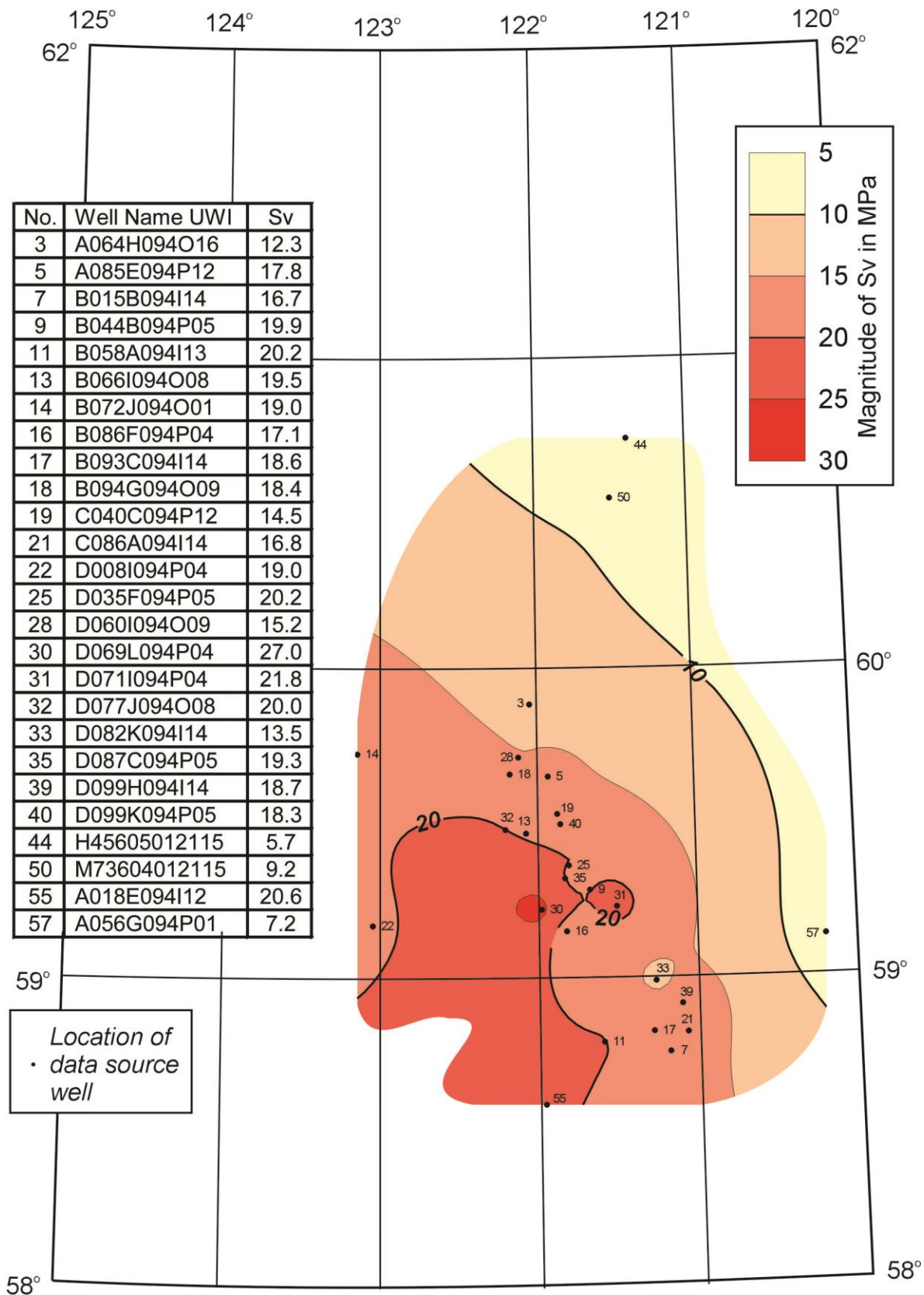


Fig. 27. Sv magnitudes in MPa at the top of the Banff Formation in the Liard Basin

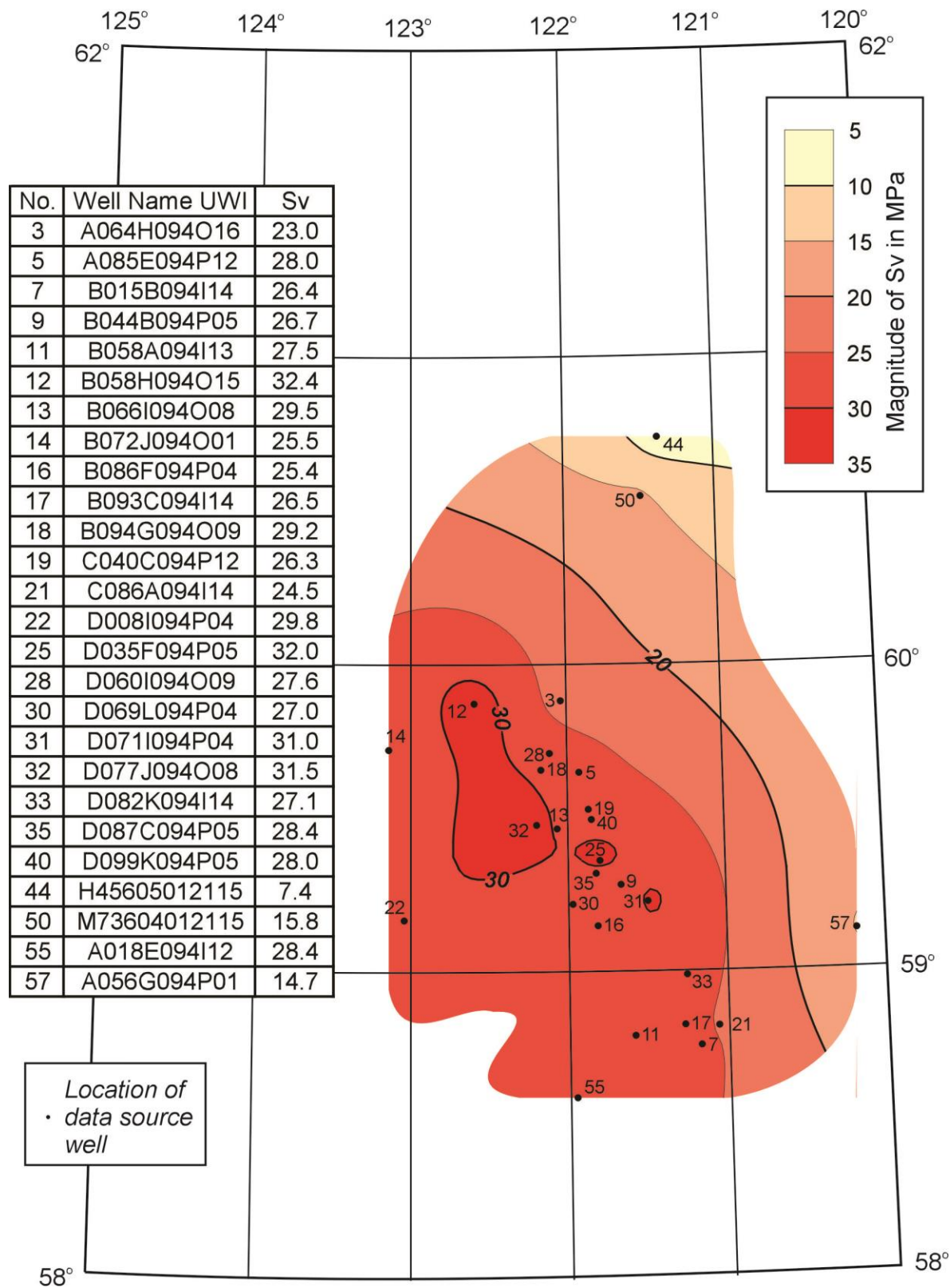


Fig. 28. Sv magnitudes inMPa at the top of the Kotcho Formation in the Liard Basin

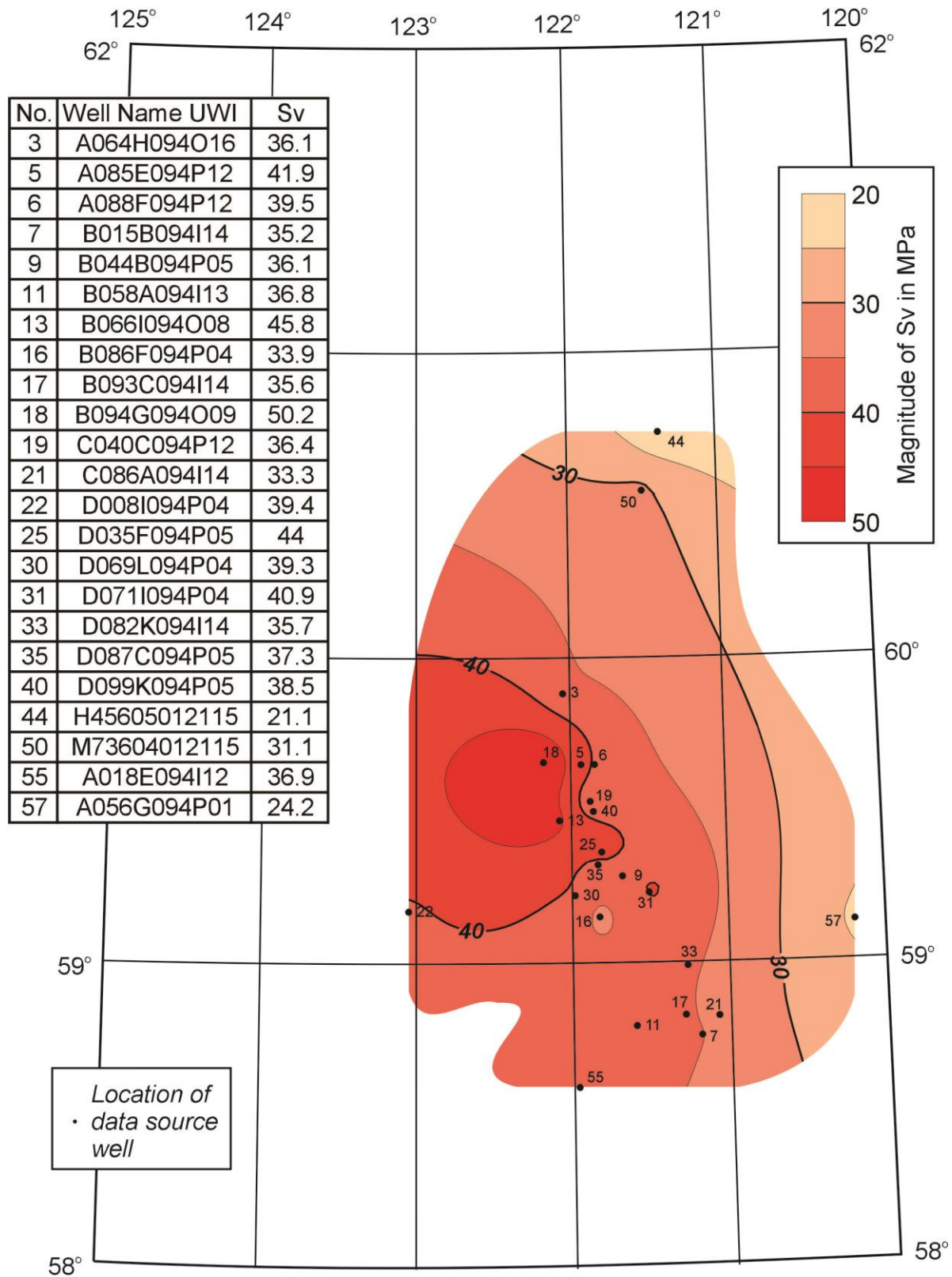


Fig. 29. Sv magnitudes in MPa at the top of the Jean Marie Formation in the Liard Basin

Figure 23 portrays the areal variation of  $S_V$  magnitude at the top of the Scatter Formation. The unit was only penetrated in 12 wells, largely in the west central part of the Liard Basin, where its westward increase in burial results in higher  $S_V$  magnitudes.

The 13 wells in which the Bluesky Formation is recognised are nicely distributed for mapping the areal variation of  $S_V$  magnitude at this horizon (Fig. 24). The low gradient salient at latitude  $60^\circ$  is comparable to a similar feature seen on Figures 18 to 22, and probably reflects differential paleoburial, since there is a limited range of burial depths for the tops of the Bluesky Formation. As Table 3 indicates, apart from well A-056-G/094-P-01 on the eastern edge of the map area, Bluesky tops range in depth from 401.3 to 641.3 metres KB.

The top of the Paleozoic sequence is an unconformity below which a number of different formations abut. Figure 25 contours  $S_V$  magnitudes from 40 wells. Magnitudes become greater to the west with increasing depth of burial. There is a “bull’s eye” around well B-043-K/094-O-05 (Well 8 on Figure 25), which may be due to down-faulting.

The top Debolt Formation  $S_V$  magnitude map (Figure 26) also contains the “bull’s eye” around well B-043-K/094-O-05, as well as the east-west low magnitude salient south of latitude  $60^\circ$ . Although the Debolt  $S_V$  magnitude map benefits from information from 31 wells, unfortunately no data were available north of  $60^\circ$ .

The maps contouring  $S_V$  magnitudes at the tops of the Banff, Kotcho and Jean Marie Formations all display similar configurations with westward increases in magnitude consistent with deeper burial. Data points are reasonably abundant with 26 for the Banff Formation (Fig. 27), 26 for the Kotcho Formation (Fig. 28) and 23 for the Jean Marie Formation (Fig. 29).

## 12. MAPPING THE SMALLER HORIZONTAL STRESS, $S_{Hmin}$

The most accurate method for determining the magnitude of the smallest principal stress in the subsurface involves micro-fracturing. In micro-fracture tests a hydraulic fracture is initiated within a short packed-off interval by injecting low viscosity fluids slowly through perforated casing or in open hole (Kry and Gronseth, 1982). The volume injected is usually approximately  $1 \text{ m}^3$ , and the fracture is opened and closed several times so that successive pressure declines can be monitored until a consistent Fracture Closure Pressure is obtained. This pressure is equated with the smallest principal stress acting on the interval concerned (Gronseth and Kry, 1983). If the closure pressure is less than the overburden load, it is assumed that the smaller horizontal principal stress has been measured.

Micro-fracture tests provide reliable, repeatable, measurements of *in-situ* stress. They are regarded as costly and time-consuming to run and, for these reasons, few such stress measurements have been made in western Canada. None have been reported from wells drilled in the Liard Basin.

The next best measurements are provided by mini-fractures. Mini-fracture tests are pre-fracture stimulation tests. They typically involve higher rate injection of viscous fluids in excess of  $10 \text{ m}^3$  (McLellan, 1988). In-situ stress magnitudes can be inferred from their pressure/time records, but the procedures are designed to measure an average in-situ stress over a larger interval than a micro-fracture test (Nolte, 1988 a, b).

Mini-fractures propagate small fractures in reservoirs that are candidates for subsequent massive fracture treatments. This can lead to problems in using their closure pressures to estimate stress magnitudes. In many cases, mini-fractures are run in reservoirs that have already produced substantial quantities of hydrocarbons, and thereby lowered the reservoir fluid pressures. Production of hydrocarbons will have lowered the virgin reservoir fluid pressures and this, in turn, is likely to lower the magnitudes of the stresses around the wellbore (Salz, 1977). Hence, the stress measured by the mini-fracture test may be less than the virgin magnitude. To avoid the problem, one should infer stress magnitudes only from mini-fracture closure pressures measured in rocks that have not suffered fluid depletion. At this stage, no wells have been located in the Liard Basin in which mini-frac pressures have been measured.

To this point, we have discussed using fracture closure pressures as measures of the smallest principal stress. Since no such measurements have been located at this stage, we are obliged to turn to fracture opening pressures, aware that these will always be greater than fracture closure pressures.

Leak-off tests record fracture opening pressures, and they are run in many exploration wells. In a leak-off test, pressure on the drilling mud column is raised slowly until the pressure build-up ceases to be linear, at which point a small volume (less than 1 m<sup>3</sup>) is interpreted to have begun to “leak-off” into the formation (Figure 30).

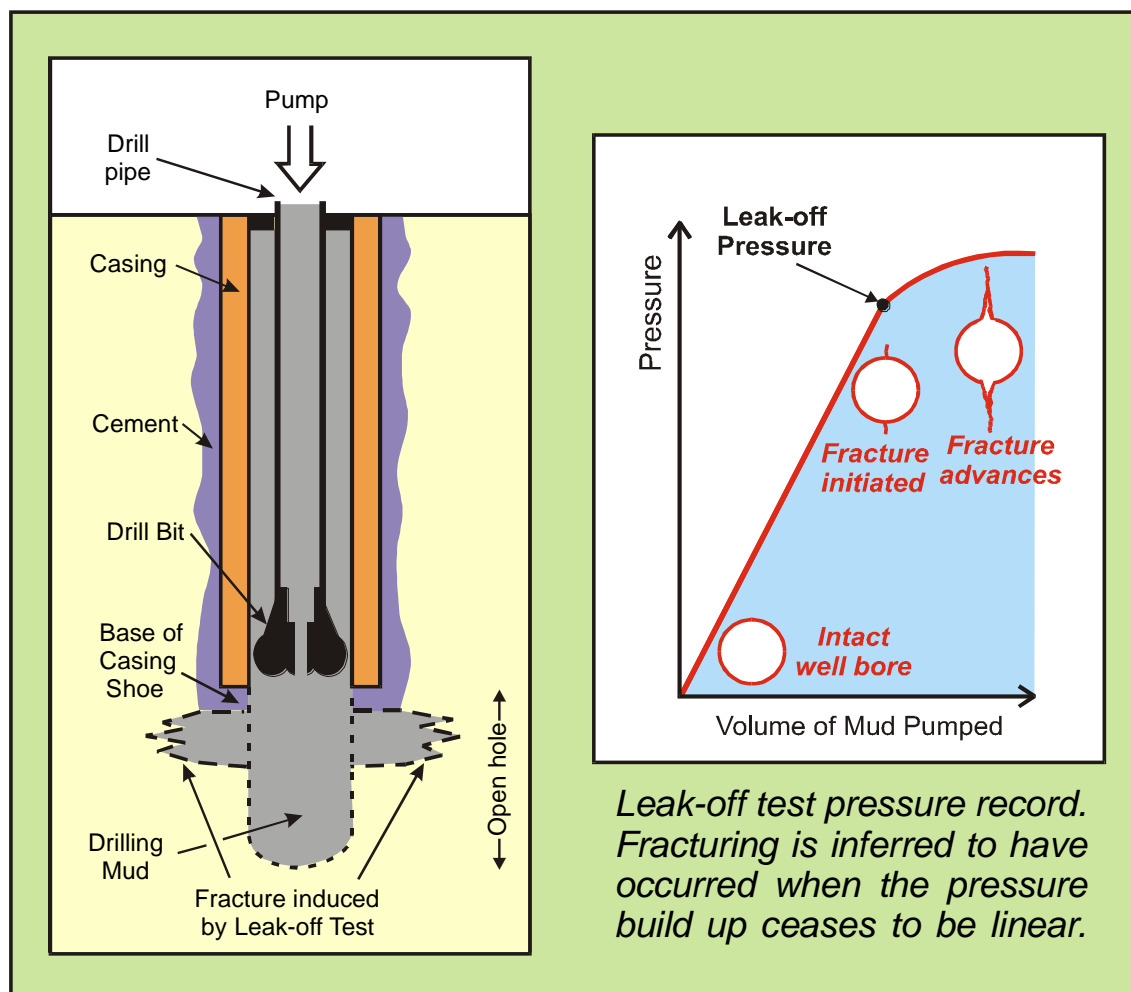


Fig. 30. Schematic representation of a leak-off test and a pressure/volume plot

Leak-off tests are run below casing in open hole to determine the maximum mud weight that can be used safely while drilling, and are used to infer the fracture gradient of a well. In a leak-off test, pressure on the drilling mud column is raised slowly until

the pressure build-up ceases to be linear, at which point a small volume (less than 1 m<sup>3</sup>) is interpreted to have begun to “leak-off” into the formation (Figure 30).

For an initial leak-off test, to a first approximation, this pressure is the sum of the fracture breakdown pressure and the rock’s tensile strength. If the latter is high, so is the leak-off pressure. Near surface rocks often exhibit high cohesive strengths and therefore generate leak-off pressures that are considerably higher than the *in situ* stresses to which they are subjected. Table 5, below, lists details of the leak-off tests reported for various wells within the Liard Basin. A leak-off test pressure gradient greater than 30 kPa/m was reported for well A01-60-10-123-15. This is clearly far higher than the  $S_{Hmin}$  magnitude and exceeds the overburden load ( $S_V$ ) by a considerable amount, so it cannot be used to infer a horizontal stress magnitude. Similarly, if leak-off pressure is very low and close to formation fluid pressure, it is assumed that no fracture was initiated and that the pressured drilling mud simply leaked off either into a very permeable rock, or into pre-existing open fractures. Such a pressure provides no *in situ* stress information, as was the case for well B41-60-40-122-45.

No.	Well Name UWI	Latitude	Longitude	Casing depth (metres KB)	Test Depth (metres KB)	Open Interval (metres)	LOT gradient (kPa/m)
1	D-011-E/094-I-11	58.598	121.378	nr	305.0	nr	24.0
2	B-057-I/094-O-15	59.960	122.984	nr	450.0	nr	16.4
3	A-01-60-10-123-15	60.002	123.254	503.0	508.0	5.0	>30.2
4	B-41-60-40-122-45	60.502	122.887	311.0	320.0	9.0	>9.8
5	B-25-60-30-122-30	60.402	122.574	207.5	209.0	1.5	17.8
6	I-02-60-20-123-30	60.194	123.504	514.0	525.0	11.0	>18.0
7	L-63-61-00-124-15	60.877	124.465	185.8	188.0	2.2	21.6
7	L-63-61-00-124-15	60.877	124.465	766.2	770.0	3.8	19.6
7	L-63-61-00-124-15	60.877	124.465	2602.0	2604.0	2.0	16.4
8	N-33-61-00-122-30	60.881	122.613	219.4	?224.4	?5	>17.8

Table 5. Leak-off test results for wells in the Liard Basin.  
(nr = not recorded on scout ticket)

A further relevant source of fracture pressure information comes from the records of massive fracture treatments of hydrocarbon reservoirs. Some of the completion reports curated by the Ministry of Energy and Mines of British Columbia included such information.



The Fracture Breakdown Pressure is the pressure recorded when the rock surrounding the wellbore first breaks down as it absorbs the injected fluid. According to Haimson and Fairhurst (1970):

$$P_b = T + 3 S_{Hmin} - S_{Hmax} - P_o$$

where:

$P_b$  = Fracture Breakdown Pressure

$T$  = tensile strength of the rock being fractured

$S_{Hmin}$  = smaller horizontal principal stress

$S_{Hmax}$  = larger horizontal principal stress

$P_o$  = pore pressure within the rock being fractured

This relationship assumes Mohr-Coulomb behaviour, as well as an isotropic response from the fractured rock, so it is somewhat idealised (Jaeger and Cook, 1976). However, it indicates clearly that the Fracture Breakdown Pressure will be greater in magnitude than  $S_{Hmin}$ , and considerably so, if the rock in question resists fracturing; in other words, exhibits a high cohesive strength. The equation also yields  $S_{Hmax}$  magnitudes, although their values are constrained within somewhat tight limits.

If the massive fracturing was applied to a reservoir where the fluid pressure has been reduced by earlier production, the fracture breakdown pressure could be less than the magnitude of the virgin *in situ* stress. The fracture breakdown pressures listed in Table 6 were all measured in wells that had not experienced prior production. As with the leak-off test pressures, fracture breakdown pressures with gradients less than 12 kPa/m were discounted, as it was assumed that no fracturing had occurred. Fracture breakdown pressures with gradients greater than 30 kPa/m were also disregarded on the grounds that the rocks involved probably exhibited high tensile strengths so that the fracturing pressure would have greatly exceeded the smallest principal stress acting on them.

Map No.	Well name UWI	Latitude	Longitude	Depth (m KB)	Pressure (MPa)	Gradient (kPa/m)	Formation
1	A-018-J/094-O-11	59.677	123.216	1886.0	33.2	17.6	Chinkeh
2	A-037-B/094-I-08	58.277	120.203	1336.5	17.2	12.9	Jean Marie
3	A-049-J/094-O-11	59.702	123.228	1629.7	38.5	23.6	Chinkeh
4	A-077-B/094-O-14	59.810	123.203	1681.0	33.1	19.7	Chinkeh
5	A-081-A/094-I-03	58.069	121.003	667.0	8.3	12.4	Montney
6	A-083-E/094-I-03	58.152	121.403	681.0	12.6	18.5	Montney
7	B-004-H/094-I-03	58.085	121.047	660.5	8.9	13.5	Montney
8	B-022-K/094-I-10	58.685	120.772	555.3	12.0	21.6	Banff
9	B-039-C-094-I-02	58.027	120.859	689.5	10.2	14.8	Montney
10	B-041-G-094-I-03	58.119	121.134	664.5	9.0	13.5	Montney
11	B-049-J/094-O-11	59.702	123.234	1862.5	27.5	14.8	Chinkeh
12	B-052-K-094-O-11	59.71	123.272	1665.5	28.0	16.8	Chinkeh
13	B-055-B/094-O-15	59.794	122.684	3300.7	61.4	18.6	Evie
14	B-058-B/094-O-14	59.794	123.222	1731.0	34.8	20.1	Chinkeh
15	B-088-D-094-I-02	58.069	120.972	682.0	19.6	28.7	Montney
16	B-099-D-094-I-02	58.077	120.984	657.0	16.2	24.7	Montney
17	C-009-C-094-I-02	58.006	120.859	708.5	11.2	15.8	Montney
18	C-018-J/094-O-11	59.681	123.222	1642.1	34.8	21.2	Chinkeh
19	C-026-G/094-O-14	59.856	123.197	1476.0	27.3	18.5	Chinkeh
20	C-026-G/094-O-14	59.856	123.197	1486.0	34.1	22.9	Chinkeh
21	C-028-C-094-I-02	58.023	120.847	698.0	11.4	16.3	Montney
22	C-054-G-094-I-03	58.131	121.172	674.0	9.9	14.7	Montney
23	C-084-F-094-I-03	58.156	121.297	668.0	10.7	16	Montney
24	D-006-H-094-I-03	58.09	121.066	667.0	9.7	14.5	Montney
25	D-024-D-094-I-02	58.023	120.916	698.5	14.5	20.8	Montney
26	D-026-H-094-I-03	58.106	121.066	663.0	11.9	17.9	Montney
27	D-030-H-094-I-03	58.106	121.116	669.0	12.5	18.7	Montney
28	D-042-D-094-I-02	58.04	120.891	687.5	14.7	21.4	Montney
29	D-055-G/094-O-14	59.881	123.178	1531.0	41.1	26.8	Chinkeh
30	D-070-D-094-I-02	58.056	120.991	671.0	19.1	28.4	Montney
31	D-086-K/094-I-08	58.490	120.316	407.5	9.6	23.6	Bluesky/Elkton

Table 6. Fracture breakdown pressures and gradients for wells in the Liard Basin

A typical massive fracture treatment summary is shown in Figure 31. The chart refers to well D-055-G/094-O-14, for which the reported fracture breakdown pressure is 41.1 MPa, as can be seen on the pressure plot.

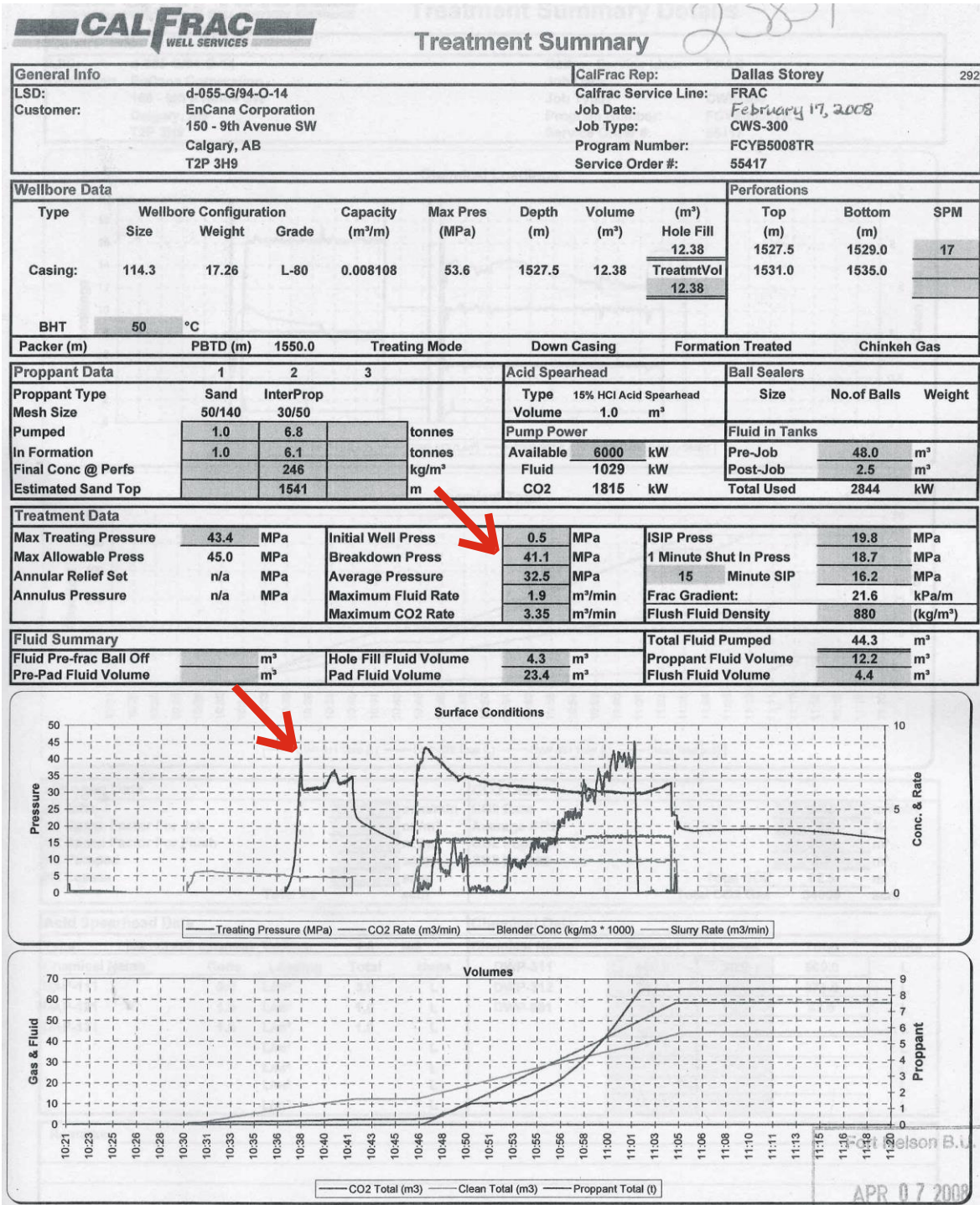


Fig. 31. Massive fracture record for well D-055-G/094-O-14

In the case of leak-off tests, some culling also is usually required, especially when the leak-off pressure is significantly higher than any conceivable overburden load. Intuitively, this seems illogical. How can a rock fracture at a pressure equivalent to over 30 kPa/m, when the overburden gradient is likely to be on the order of 25 kPa/m or less? Why wasn't a horizontal fracture initiated at a pressure approximating that exerted by the overlying rocks? If such a high pressure was applied, why did it not lift up the section?

Experience has shown that this situation is quite commonly encountered for rocks at shallow depths, below surface casing. What seems to be happening is that these rocks exhibit high tensile strengths and are extremely resistant to fracturing. When pressure is exerted on a section of the borehole wall of a vertical well and a fracture is finally initiated, that fracture tends to be vertical and to extend up and down opposite sides of the well. As it propagates away from the hole, it will flip and become horizontal and, after that has occurred, the propagation pressure will drop down to levels similar to the overburden pressure. Gronseth and Kry (1987) reported a case history of such an occurrence at Norman Wells.

In some wells, leak-off occurs after essentially zero pressure increase, in essence at level with the formation fluid pressure. As noted above, in such instances it is suspected that no fracturing occurs and the drilling mud is simply injected either into a very permeable rock or along a pre-existing open fracture. Thus, not all of the leak-off population is likely to provide reliable quantitative insights into stress magnitudes, and some culling is required, as was the case for wells A-01-60-10-123-15 and B-41-60-40-122-45 (Table 5).

The same principles apply to fracture breakdown pressures. The following wells were culled due to their gradients being too high or too low to be close to probable *in situ* stress pressures, and are therefore not listed in table 5: A-037-B/094-I-08, A-064-E/094-I-14, A-084-F/094-I-02, B-032-C/094-I-09, C-001-C/094-I-09, C-056-B/094-I-13 and D-015-J/094-P-04.

If fracturing has been initiated, both leak-off test pressures and fracture breakdown pressures will exceed the smallest principal stress, since it requires a greater pressure to initiate and open a fracture than it does to just prevent it from closing. So some reduction in gradients should be made. Normally, this is determined by comparing their magnitudes to those of micro-fracs and mini-fracs, these being interpreted as accurate measurements of the smallest principal stress. Unfortunately, in the Liard Basin, no such measurements were encountered. None are reported in the literature and none were discovered during an extensive examination of well history reports for Yukon, NWT and BC wells. With so few suitable leak-off pressures and fracture breakdown pressures available (Tables 5 and 6), and their limited geographic extent, it was decided not to adjust their gradients at this stage, but use all of the unaltered gradients as proxies for  $S_{Hmin}$  gradients. There is some precedent for such an approach.

It has been widely employed in the North Sea, where leak-off test pressures have been interpreted as  $S_{Hmin}$  and used successfully for predicting borehole stability in drilling operations (R. Bratli, pers. comm., 2001).

As noted earlier, density logs provide  $S_V$  magnitudes at all depths (in this study they are reported at 1 metre intervals). However, leak-off tests and hydraulic fracture treatments are conducted over a specific depth interval in a well and are equated with the top of that interval. Thus, a leak-off pressure or a fracture breakdown pressure provides an estimate of the smaller horizontal stress magnitude,  $S_{Hmin}$ , for only a single depth. Therefore, in order to map lateral variations of  $S_{Hmin}$  at common depths, it is necessary to employ gradients, and gradients have to be used when attempting to assess how  $S_{Hmin}$  magnitudes may vary laterally at specific stratigraphic horizons.

Figure 32 is a contour map of the leak-off test gradients in the Liard Basin. With only four wells providing firm data points, the control is minimal. Thirty wells provided fracture breakdown pressure gradients, but their geographic distribution is very limited and most of the wells are concentrated in two local areas (Fig. 33). Combining the two data sets generates a slightly better  $S_{Hmin}$  gradient map (Fig. 34), but the geographic coverage is still far from ideal. Note that the contour configuration of the  $S_{Hmin}$  gradients in kPa/m in Figure 24 corresponds to  $S_{Hmin}$  magnitudes at 1000 metres depth in MPa.

The lack of well data suitable to estimating  $S_{Hmin}$  magnitudes and paucity of formation tops (Tables 7 and 8) limits the maps that can be usefully created. The only maps of  $S_{Hmin}$  magnitudes that were constructed were for: 1) the top of the Scatter Formation (Fig. 35), where there is some suggestion of a westward increase in magnitude, 2) the top of the Montney Formation (Fig. 36) which is of no regional significance because all of the wells are closely spaced in one local area, and 3) the top of the Banff Formation (Fig. 37), which shows some lateral variation in  $S_{Hmin}$  magnitude, but no obvious trends.

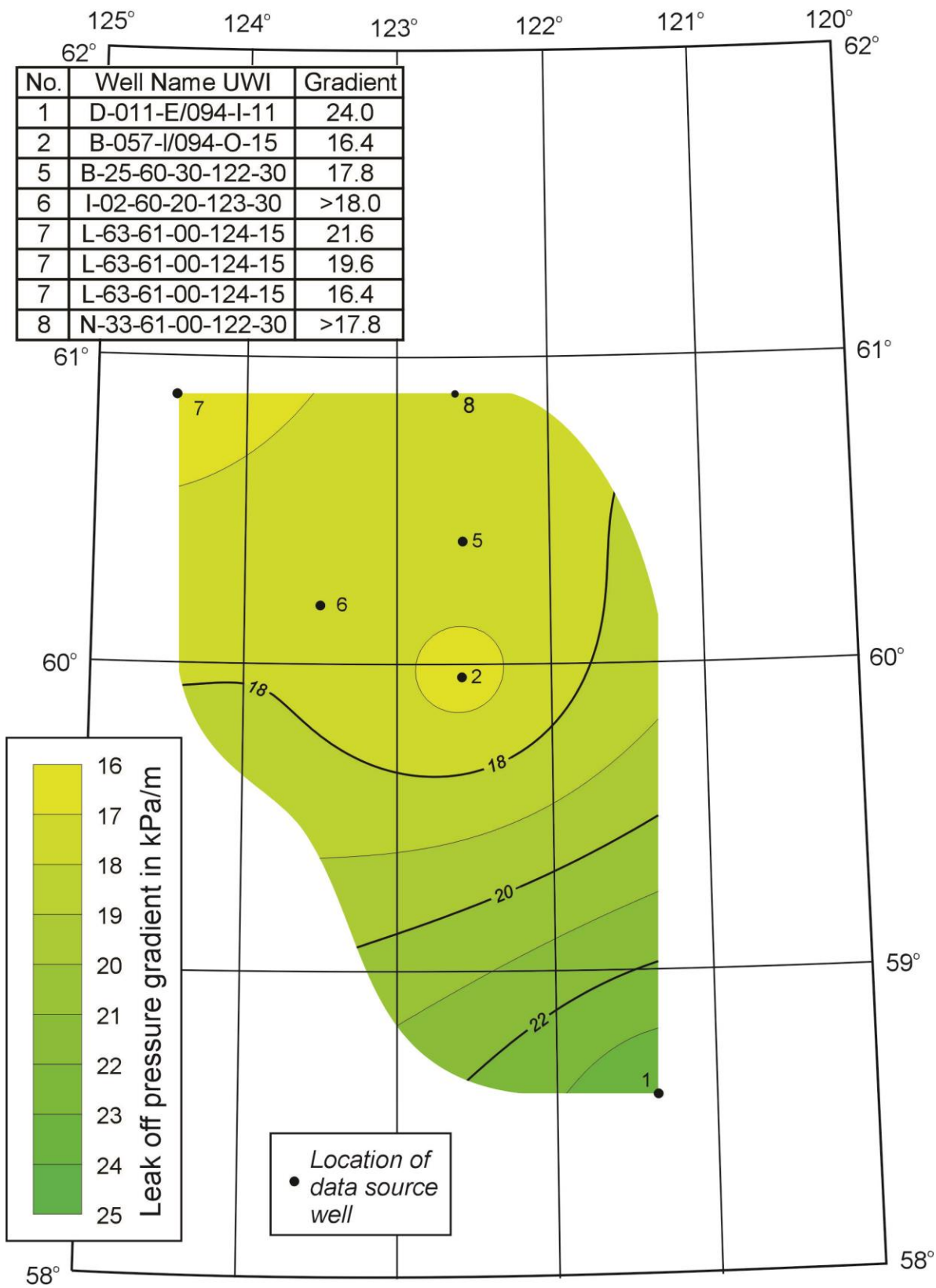


Fig. 32. Gradients of leak-off test pressures measured in wells in the Liard Basin

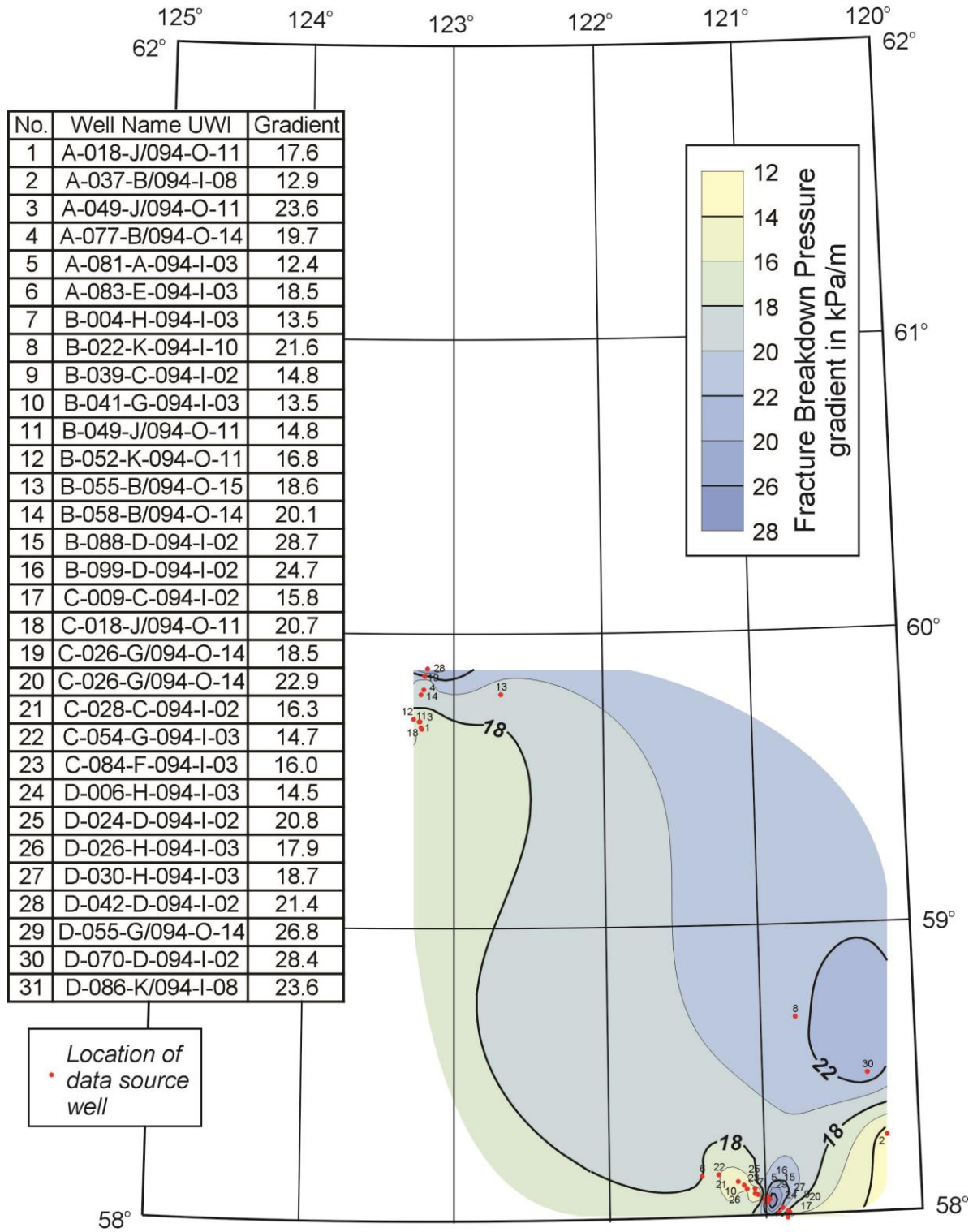


Fig. 33. Gradients of fracture breakdown pressures measured in wells in the Liard Basin

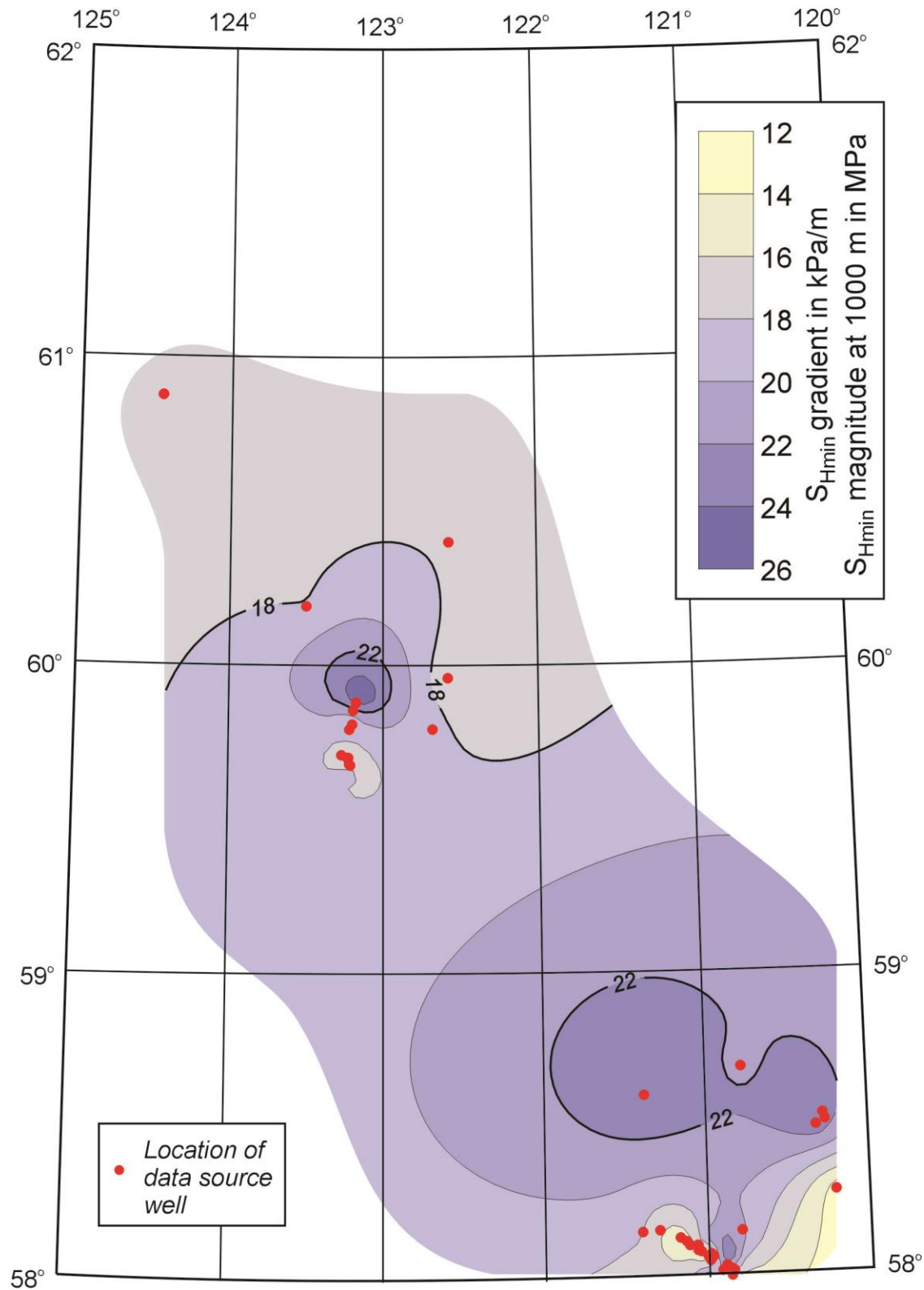



Fig. 34. Gradients of leak-off test pressures and fracture breakdown pressures measured in wells in the Liard Basin. Wells are identified on Figures 22 and 23. This map can also be interpreted as  $S_{Hmin}$  magnitude contours at 1000 m depth.



Map Number	Data Source	Well name UWI	Latitude	Longitude	Scatter	Garbutt	Bluesky	Montney	Debolt	Banff	Exshaw	Kotcho	Jean Marie	Fort Simpson	Slave Point
1	LOT	D-011-E/094-I-11	58.598	121.378					555.3		1050.9		1378.2	1400.2	
2	LOT	B-057-I/094-O-15	59.960	122.984											
5	LOT	B-25-60-30-122-30	60.402	122.574	311.0	366.0				717.0					
7	LOT	L-63-61-00-124-15	60.877	124.465							1775.0			1878.5	
1	FBP	A-018-J/094-O-11	59.677	123.216	1298.0	1441.0									
2	FBP	A-037-B/094-I-08	58.277	120.203						662.0		975.5	1327.5	1346.0	
3	FBP	A-049-J/094-O-11	59.702	123.228											
5	FBP	A-077-B/094-O-14	59.810	123.203	1263.5	1417.0									
6	FBP	A-081-A/094-I-03	58.069	121.003				664.5							
7	FBP	A-083-E/094-I-03	58.152	121.403				670.0							
9	FBP	B-004-H/094-I-03	58.085	121.047				653.0							
10	FBP	B-022-K/094-I-10	58.685	120.772			406.0			529.5					
12	FBP	B-039-C-094-I-02	58.027	120.859			676.8	685.0							
13	FBP	B-041-G-094-I-03	58.119	121.134	454.0	503.0		654.0		835.0	1350.0	1366.5		1895.0	2552.0
14	FBP	B-049-J/094-O-11	59.702	123.234	1439.5	1620.0									
15	FBP	B-052-K-094-O-11	59.71	123.272	1336.0	1526.5									
16	FBP	B-055-B/094-O-15	59.794	122.684											
17	FBP	B-058-B/094-O-14	59.794	123.222	1326.0	1548.0									
18	FBP	B-088-D-094-I-02	58.069	120.972				672.0							
19	FBP	B-099-D-094-I-02	58.077	120.984											
21	FBP	C-009-C-094-I-02	58.006	120.859			687.2	702.6							
22	FBP	C-018-J/094-O-11	59.681	123.222											
23	FBP	C-026-G/094-O-14	59.856	123.197	1077.0	1268.4									
25	FBP	C-028-C-094-I-02	58.023	120.847				682.0							
26	FBP	C-054-G-094-I-03	58.131	121.172				654.0							
27	FBP	C-056-B/094-I-13	58.798	121.697					646.0	801.0	1113.5	1121.0	1584.0		
28	FBP	C-084-F-094-I-03	58.156	121.297				657.0							
29	FBP	D-006-H-094-I-03	58.09	121.066											
31	FBP	D-024-D-094-I-02	58.023	120.916				674.2							
32	FBP	D-026-H-094-I-03	58.106	121.066				653.0							
33	FBP	D-030-H-094-I-03	58.106	121.116				659.0							
34	FBP	D-042-D-094-I-02	58.04	120.891				681.0							
35	FBP	D-055-G/094-O-14	59.881	123.178	1160.4	1450.5									
36	FBP	D-070-D-094-I-02	58.056	120.991				661.0							
37	FBP	D-086-K/094-I-08	58.490	120.316											

Table 7. Formation tops in meters in wells that provide  $S_{Hmin}$  magnitudes in the Liard Basin

 = No information available

Map Number	Data Source	Well name UWI	Latitude	Longitude	SHmin Gradient (kPa/m)	Scatter SHmin (MPa)	Montney SHmin (MPa)	Banff SHmin (MPa)	Kotcho SHmin (MPa)	Jean Marie SHmin (MPa)
1	LOT	D-011-E/094-I-11	58.598	121.378	24.0					33.1
2	LOT	B-057-I/094-O-15	59.960	122.984	16.4					
5	LOT	B-25-60-30-122-30	60.402	122.574	17.8	5.5		12.8		
7	LOT	L-63-61-00-124-15	60.877	124.465	19.6					
1	FBP	A-018-J/094-O-11	59.677	123.216	17.6	22.8				
2	FBP	A-037-B/094-I-08	58.277	120.203	12.9			8.6	12.6	17.2
3	FBP	A-049-J/094-O-11	59.702	123.228	23.6					
5	FBP	A-077-B/094-O-14	59.810	123.203	19.7	24.9				
6	FBP	A-081-A/094-I-03	58.069	121.003	12.4		8.2			
7	FBP	A-083-E/094-I-03	58.152	121.403	18.5		12.4			
9	FBP	B-004-H/094-I-03	58.085	121.047	13.5		8.8			
10	FBP	B-022-K/094-I-10	58.685	120.772	21.6			11.4		
12	FBP	B-039-C-094-I-02	58.027	120.859	14.8		10.1			
13	FBP	B-041-G-094-I-03	58.119	121.134	13.5	6.1	8.8	11.3	18.4	
14	FBP	B-049-J/094-O-11	59.702	123.234	14.8	21.3				
15	FBP	B-052-K-094-O-11	59.71	123.272	16.8	22.4				
16	FBP	B-055-B/094-O-15	59.794	122.684	18.6					
17	FBP	B-058-B/094-O-14	59.794	123.222	20.1	26.7				
18	FBP	B-088-D-094-I-02	58.069	120.972	28.7		19.3			
19	FBP	B-099-D-094-I-02	58.077	120.984	24.7					
21	FBP	C-009-C-094-I-02	58.006	120.859	15.8		11.1			
22	FBP	C-018-J/094-O-11	59.681	123.222	20.7					
23	FBP	C-026-G/094-O-14	59.856	123.197	18.5	19.9				
25	FBP	C-028-C-094-I-02	58.023	120.847	16.3		11.1			
26	FBP	C-054-G-094-I-03	58.131	121.172	14.7		9.6			
27	FBP	C-056-B/094-I-13	58.798	121.697	10.7			8.6	12.0	17.0
28	FBP	C-084-F-094-I-03	58.156	121.297	16		10.5			
29	FBP	D-006-H-094-I-03	58.09	121.066	14.5					
31	FBP	D-024-D-094-I-02	58.023	120.916	20.8		14.0			
32	FBP	D-026-H-094-I-03	58.106	121.066	17.9		11.7			
33	FBP	D-030-H-094-I-03	58.106	121.116	18.7		12.3			
34	FBP	D-042-D-094-I-02	58.04	120.891	21.4		14.6			
35	FBP	D-055-G/094-O-14	59.881	123.178	26.8	31.2				
36	FBP	D-070-D-094-I-02	58.056	120.991	28.4		18.8			
37	FBP	D-086-K/094-I-08	58.490	120.316	23.6					

Table 8.  $S_{Hmin}$  magnitudes at formation tops in the Liard Basin

LOT = Leak Off Test    FBP = Fracture Breakdown Pressure     = No information available

$S_{Hmin}$  magnitude maps were not made for the tops of the Kotcho and Jean Marie Formations because of lack of data points.

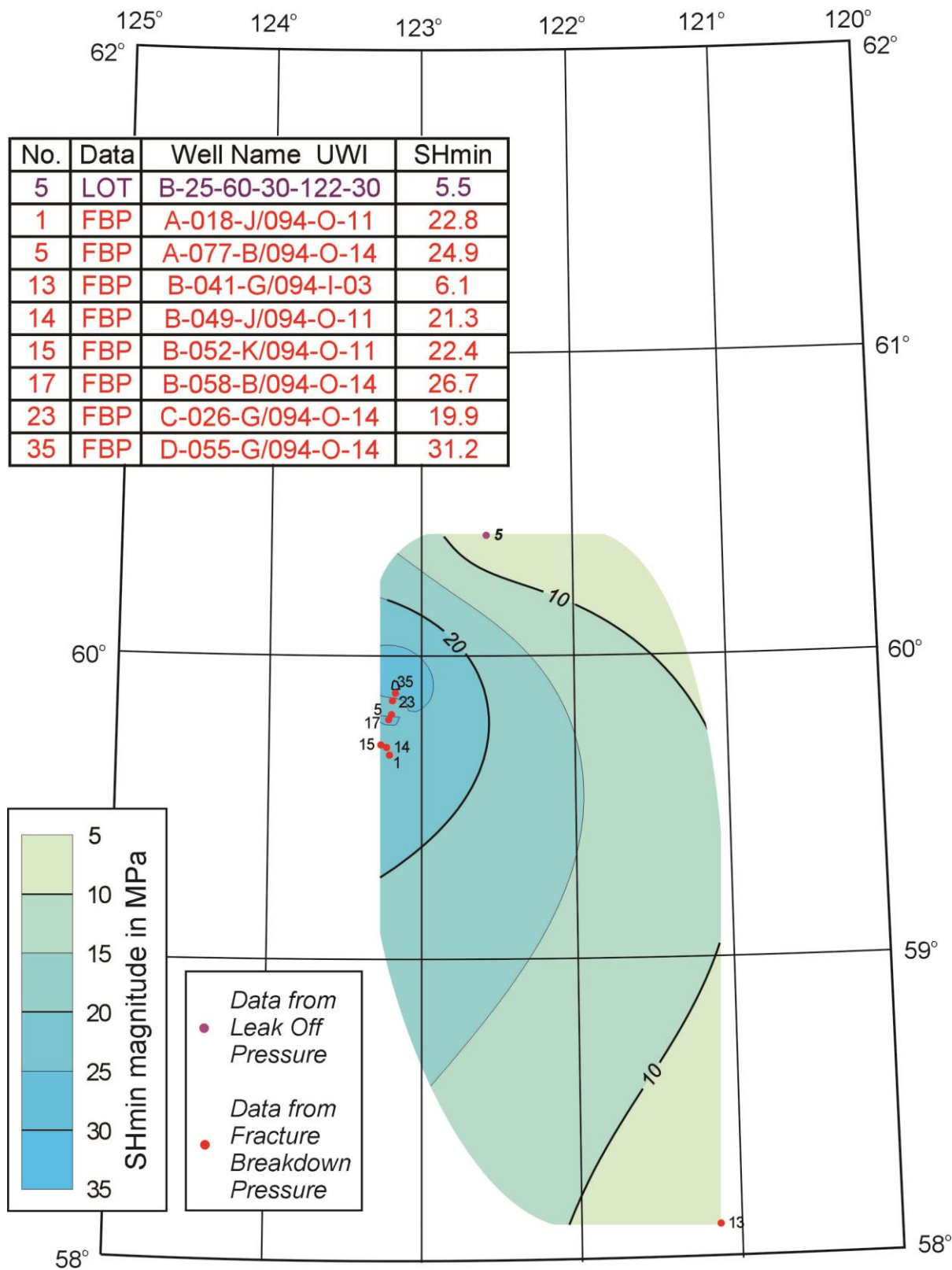


Fig. 35. Magnitudes of  $S_{Hmin}$  at the top of the Scatter Formation

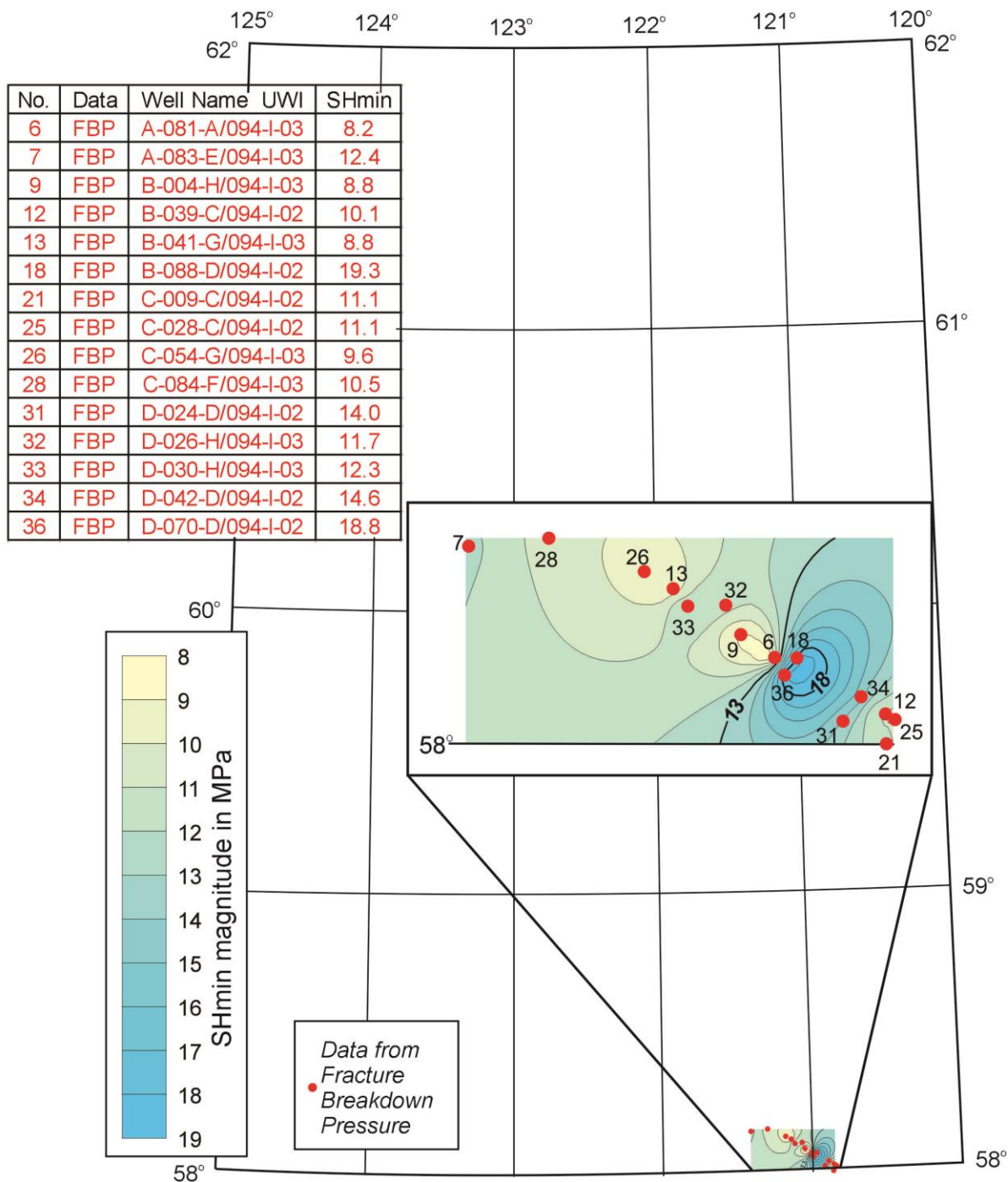


Fig. 36. Magnitudes of  $S_{Hmin}$  at the top of the Montney Formation. All the wells with data are concentrated in 094-I-02 and 094-I-03.

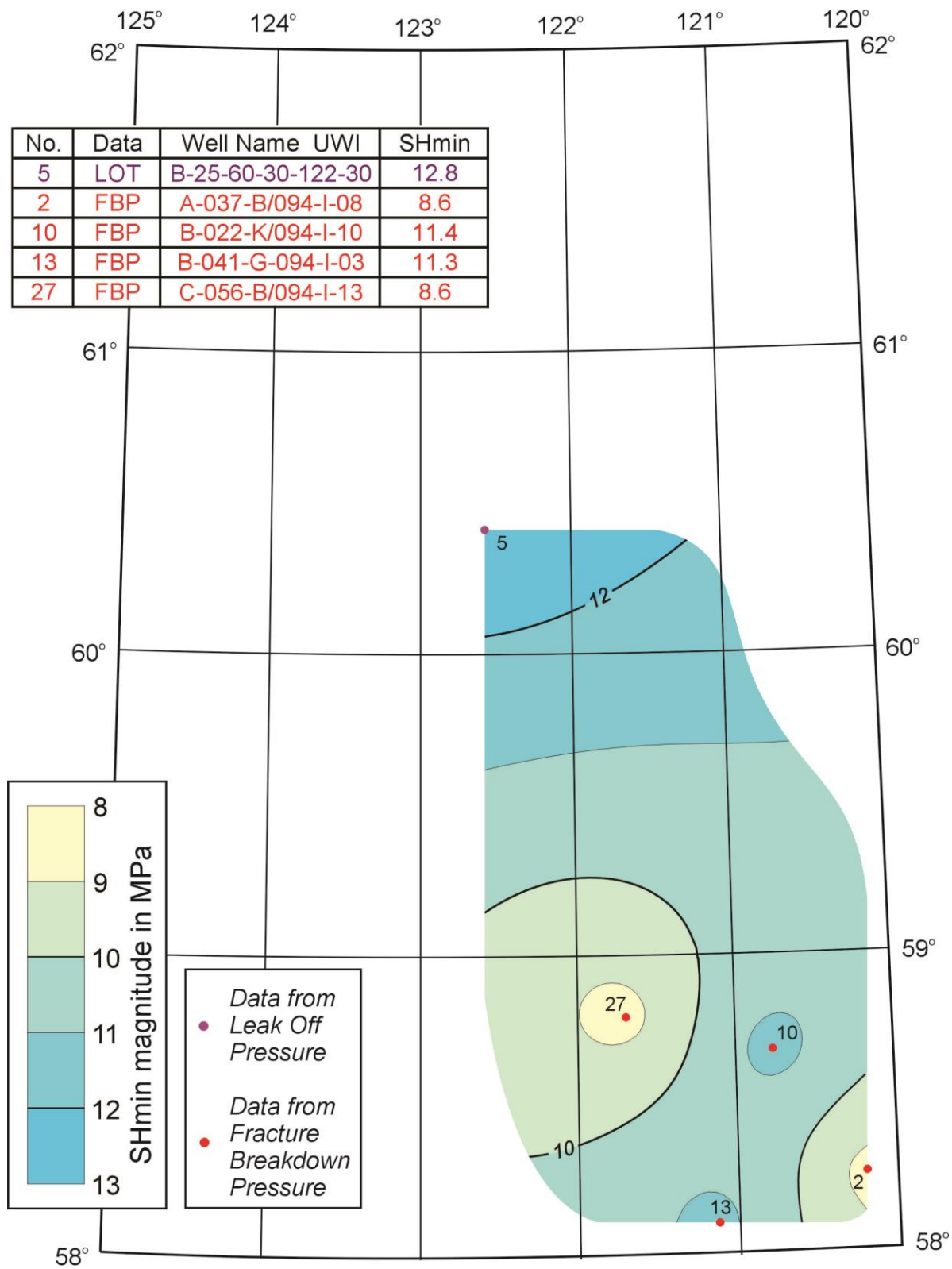


Fig. 37. Magnitudes of  $S_{Hmin}$  at the top of the Banff Formation.

### 13. ESTIMATING THE LARGER HORIZONTAL STRESS, $S_{Hmax}$

One of the continuing challenges of subsurface geomechanics is determining the magnitude of  $S_{Hmax}$ . This parameter can assist in assessing borehole stability, as well as in designing scenarios for optimal hydrocarbon recovery. Currently, there is no technique for directly measuring  $S_{Hmax}$  in oil wells, so we are obliged to estimate its magnitude. Three approaches are used today.

1. The Algebraic Method where:

$$S_{Hmax} = 3 S_{Hmin} - Pr - Po$$

in which Pr is the fracture reopening pressure and Po is the pore pressure (Bredehoeft et al., 1967). Ervine and Bell (1987) simplified this equation to:

$$S_{Hmax} = 2(\text{Leak-off Pressure}) - Po$$

and applied it to well data from the Venture Field on the Scotian Shelf.

2. The Inclined Well Method that employs leak-off pressures from differently inclined wells (Aadnoy, 1990).

3. The Breakout Geometry Simulation Method that fits observed spalling failure to a failure criterion and known parameter values.

The Algebraic Method can certainly be applied to the stress data gathered in this investigation. As noted earlier, the lack of micro-frac and mini-frac closure pressures meant that no adjustments could be made to leak-off pressures or fracture breakdown pressures. Accordingly, the original gradients of both were combined and mapped as  $S_{Hmin}$ . Thus, Ervine and Bell's (1987) simplification of Bredehoeft et al.'s (1976) equation can be applied to the stress data gathered in the Liard Basin.

The Inclined Well Method, however, is not suitable. It requires a population of leak-off pressures from several closely spaced and differently inclined wells that penetrate rocks that share a common stress regime. Such drilling configurations are not found in the Liard Basin.

Breakout Geometry Simulation was pioneered by Moos and Zoback (1990), developed by Tan et al. (1993) and Peska and Zoback (1995) and subsequently elaborated and programmed by Zhou (1997). Zhou (1997) programmed the routines with finite element modelling. In 1998, Azer Mustaqeem, working with Sigma H Consultants Ltd, developed user friendly simulation routines employing EXCEL. At the same time, Sigma H Consultants elaborated Zhou's Mohr-Coulomb simulation routine so

that it employed a three cycle failure routine, since breakouts were being observed that were deeper than single cycle failure simulations could model.

Four simulation models have been used in this study. Breakout failure has been modelled using the Mohr-Coulomb failure criterion, the Drucker-Prager failure criterion, the extended Drucker-Prager failure criteria developed by Zhou (1997), and a 3-cycle Mohr-Coulomb failure simulation developed by Sigma H Consultants Ltd. Failure around a breakout interval in a well was modelled with as many of the relevant parameters specified as accurately as possible. Iterations were run with various values of  $S_{Hmax}$  until a good match with the observed borehole geometry was achieved. At that stage, the  $S_{Hmax}$  magnitude was inferred.

It should be emphasised that breakout geometry simulation techniques can only model rock failure around boreholes. Failure need not necessarily lead to spalling. Thus, the rock around a borehole can fail by fracturing but, unless small pieces become dislodged and break away from the borehole wall, a breakout will not develop. It is believed that breakout intervals need time to fail and laterally extend themselves and, also, that drill pipe abrasion on borehole walls plays a role in assisting spalling. Most wells exhibit few, if any, breakouts in the lower parts of a drilled interval, where the “open hole” time has been the least. On the other hand, in the majority of wells, breakouts are most prominent and extend deepest in the upper part of a drilled interval, where the “open hole” time has been the greatest. Such breakout distributions are seen in wells in the Liard Basin, and they have been observed also in wells in many other areas. Accordingly, breakout geometry simulations have been applied only to deeply incised breakouts that occur near the tops of drilled intervals. These breakouts are most likely to exhibit complete, or near complete, failure.

We also have to consider the data sources for the breakout failure simulations. Breakout intervals were selected on the following bases: 1) the breakout interval should be near the top of a drilled interval, 2) the breakout interval should be reasonably evenly caved, in other words, it should not exhibit highly variable caving across its length, 3) The selected breakout interval should be that which has caved the most, so that complete, or near complete, failure is likely. Of the 51 wells analysed for breakouts (Fig. 38), only 27 of the studied wells provided suitable breakouts (Fig. 39; Table 9).

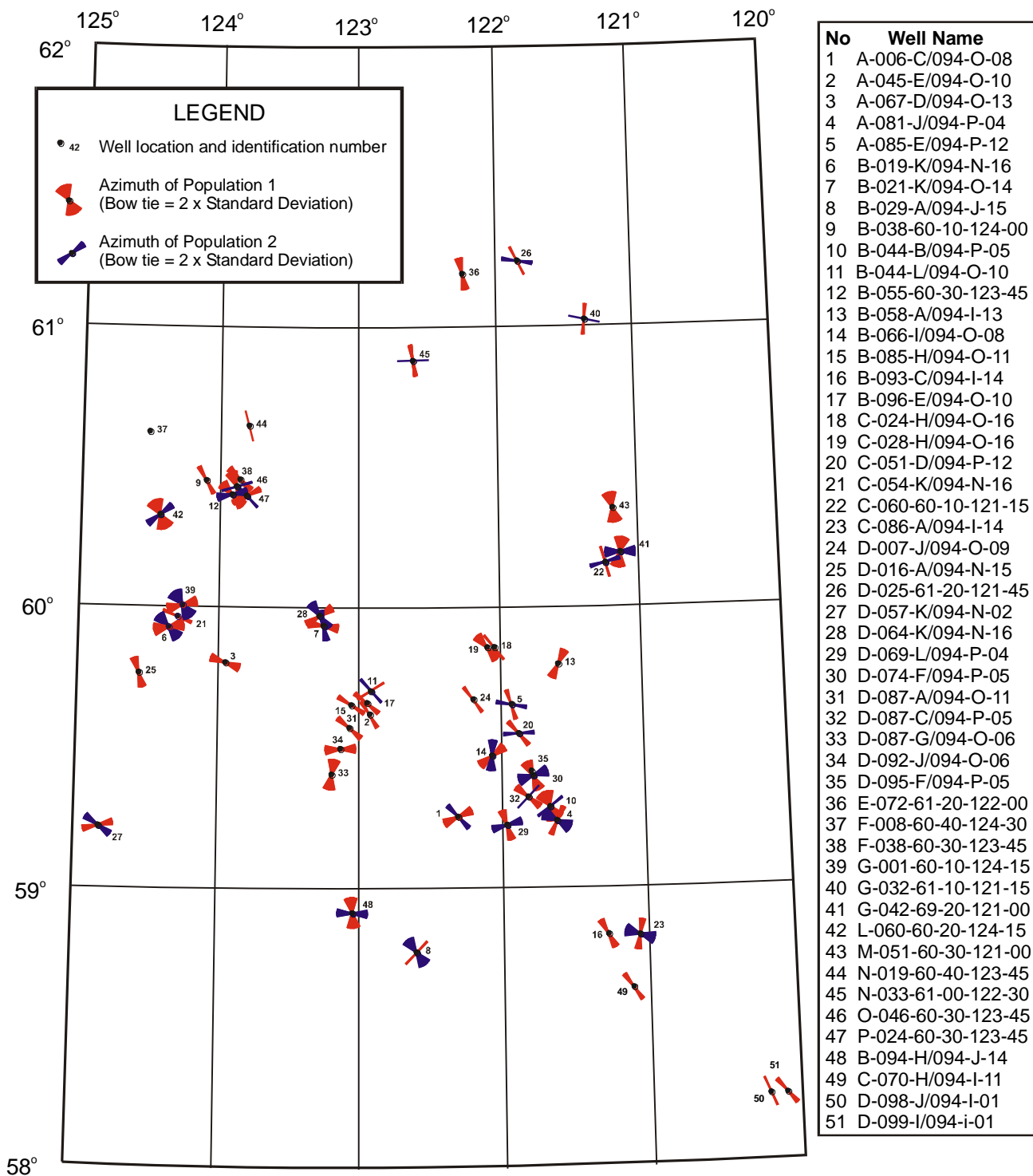


Fig. 38. Wells analysed for breakouts showing the mean azimuths of the major and minor breakout populations



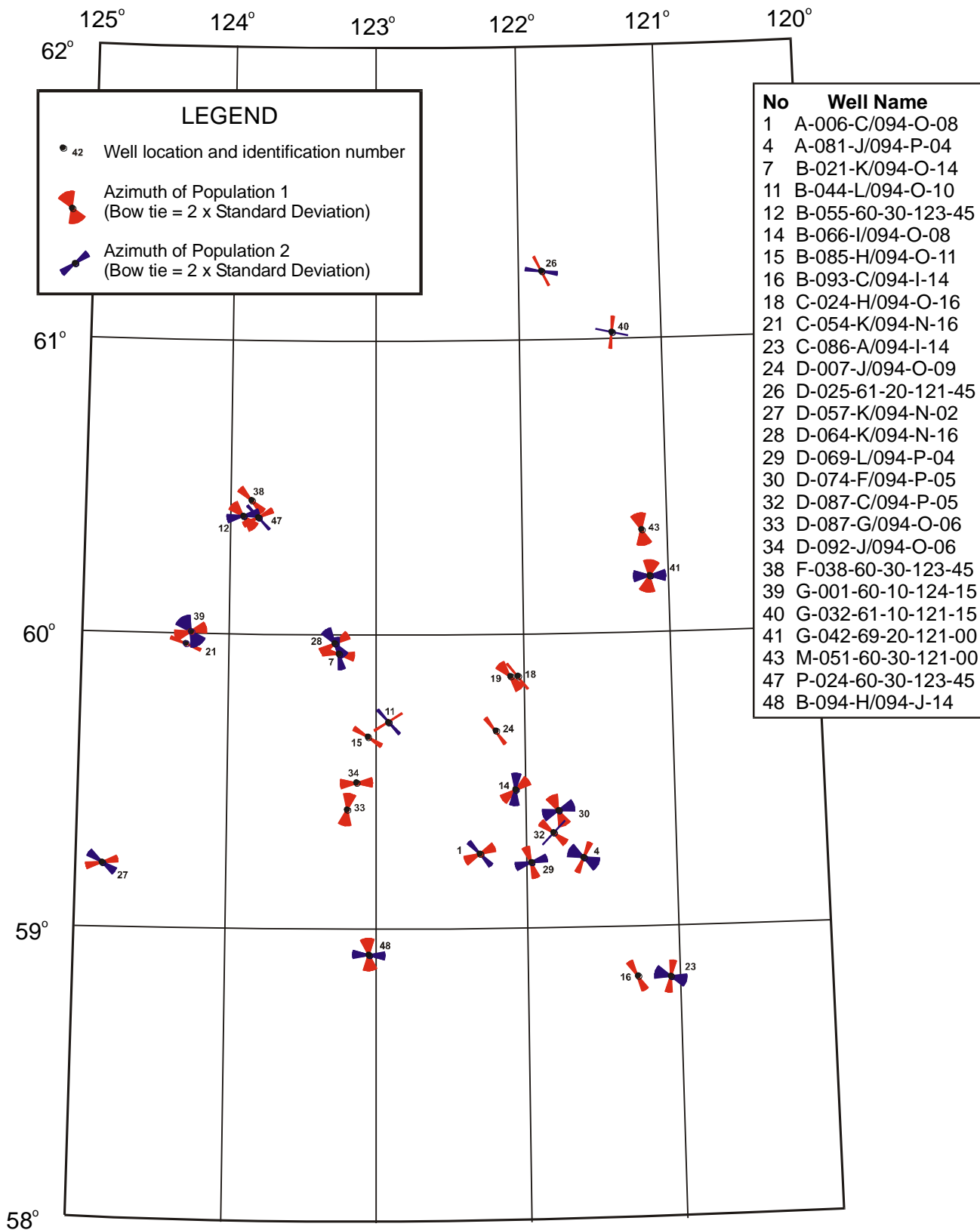


Fig. 39. Wells with breakouts that were selected for failure simulations aimed at estimating  $S_{Hmax}$  magnitudes.

Map Number	Well Name UWI	Latitude	Longitude	Top of Breakout (m KB)	Base of Breakout (m KB)	Thickness of Breakout (m)	Stratigraphic Unit containing simulated Breakout	Geological Era	Main Rock Type in Breakout interval
1	A-006-C/094-O-08	59.252	122.316	1445	1491	46	Fort Simpson	Paleozoic	Shale
4	A-081-J/094-P-04	59.235	121.628	2110	2121	11	Muskwa	Paleozoic	Shale
7	B-021-K/094-O-14	59.935	123.259	352	382	30	Sikanni	Mesozoic	Sandstone
11	B-044-L/094-O-10	59.702	122.924	254	266	12	Mesozoic	Mesozoic	Clastics
12	B-055-60-30-123-45	60.402	123.918	767	789	22	Mississippian	Paleozoic	Limestone
14	B-066-I/094-O-08	59.469	122.073	979	1012	33	Banff	Paleozoic	Shale
15	B-085-H/094-O-11	59.652	123.061	250	286	36	Fort St John	Mesozoic	Clastics
16	B-093-C/094-I-14	58.827	121.286	293	381	88	pre-Bullhead	Mesozoic	Clastics
18	C-024-H/094-O-16	59.856	122.047	426	442	16	Mesozoic	Mesozoic	Clastics
19	C-028-H/094-O-16	59.856	122.097	2250	2266	16	Hay River	Paleozoic	Shale
21	C-054-K/094-N-16	59.965	124.297	3182	3198	16	Pre-Banff	Paleozoic	Limestone?
23	C-086-A/094-I-14	58.823	121.072	363	393	30	Mesozoic	Mesozoic	Clastics
24	D-007-J/094-O-09	59.671	122.200	2369	2379	10	Redknife	Paleozoic	Limestone
26	D-025-61-20-121-45	61.235	121.840	794	817	23	Fort Simpson	Paleozoic	Shale
27	D-057-K/094-N-02	59.213	124.825	765	785	20	Pre-Stone	Paleozoic	?Shale
28	D-064-K/094-N-16	59.973	124.291	1654	1684	30	Mississippian	Paleozoic	Limestone
29	D-069-L/094-P-04	59.221	121.975	1595	1635	40	Fort Simpson	Paleozoic	Shale
30	D-074-F/094-P-05	59.396	121.788	290	305	15	Mesozoic	Mesozoic	Clastics
32	D-087-C/094-P-05	59.321	121.825	2001	2067	66	Fort Simpson	Paleozoic	Shale
33	D-087-G/094-O-06	59.404	123.200	300	441	141	Scatter	Mesozoic	Clastics
34	D-092-J/094-O-06	59.496	123.138	822	847	25	Mesozoic	Mesozoic	Clastics
38	F-038-60-30-123-45	60.456	123.863	976	985	9	Mattson	Paleozoic	Sandstone
39	G-001-60-10-124-15	60.006	124.262	1246	1264	18	Mattson	Paleozoic	Sandstone
40	G-032-61-10-121-15	61.023	121.355	1082	1106	24	Fort Simpson	Paleozoic	Shale
41	G-042-60-20-121-00	60.190	121.137	972	986	14	Banff	Paleozoic	Shale
43	M-051-60-30-121-00	60.348	121.184	944	964	20	Kotcho	Paleozoic	Limestone
47	P-024-60-30-123-45	60.398	123.816	352	372	20	Garbutt	Mesozoic	Shale
48	B-094-H/094-J-14	59.652	123.048	303	318	15	Mesozoic	Mesozoic	Clastics

Table 9. Breakout intervals selected for failure simulations in order to estimate  $S_{Hmax}$  magnitudes.

The breakout geometry was well documented in every case. The caliper extension records, 1 & 3 and 2 & 4, were logged in each well by four-arm dipmeter tools and the measurements are available at 1 metre intervals in inches. The mean long and short axes of each breakout were calculated from the digital record.

Detailed  $S_V$  gradient and magnitude profiles were available for 10 of the wells. These provided the  $S_V$  magnitudes for the median depths of the breakout intervals. For the remaining 18 of the wells,  $S_V$  magnitudes for breakout intervals were estimated by reference to the well locations as plotted on maps of the  $S_V$  gradients at 500 metres depth and 1000 metres depth (Figs 40, 41). No  $S_{Hmin}$  data were available for any of the 28 wells, so all the  $S_{Hmin}$  magnitudes used in the simulation modelling were inferred from well location sites on the map contouring the gradients of leak-off pressures and fracture breakdown pressures (Fig. 42).

Pore pressures and drilling mud weight data were not available for most of the wells that supplied suitable breakouts. As is discussed later in this report, there is good evidence that all the formations in the Liard Basin are normally pressured, so both of these parameters were assigned gradients of 10 kPa/m and their magnitudes were calculated for the median depths of the breakout intervals that were being simulated.

The coefficient of friction plays a minor role in modelling breakout failure. It was assigned a value of 0.6 for each simulation. Poisson's Ratio also has little effect on  $S_{Hmax}$  magnitudes and was set at 0.2.

No cohesive strengths have been measured for any subsurface rocks in the Liard Basin. Clearly cohesive strength will increase with burial, but it is also a function of rock type. The latter factor could not be considered here, but the effect of depth could be allowed for. The values selected here reflect Sigma H Consultants experience and also the degree of spalling of the selected breakouts. For the Mesozoic breakouts, cohesive strengths ranged from 2.0 to 3.0 MPa. Figure 43 illustrates the relationship between the chosen cohesive strengths and the burial depths of the Paleozoic breakout intervals. There appears to be little distinction between the cohesive strengths applied to Paleozoic clastics and to Paleozoic carbonates. It should be noted, however, that the calcareous shale of the Banff Formation is assigned clastic status.

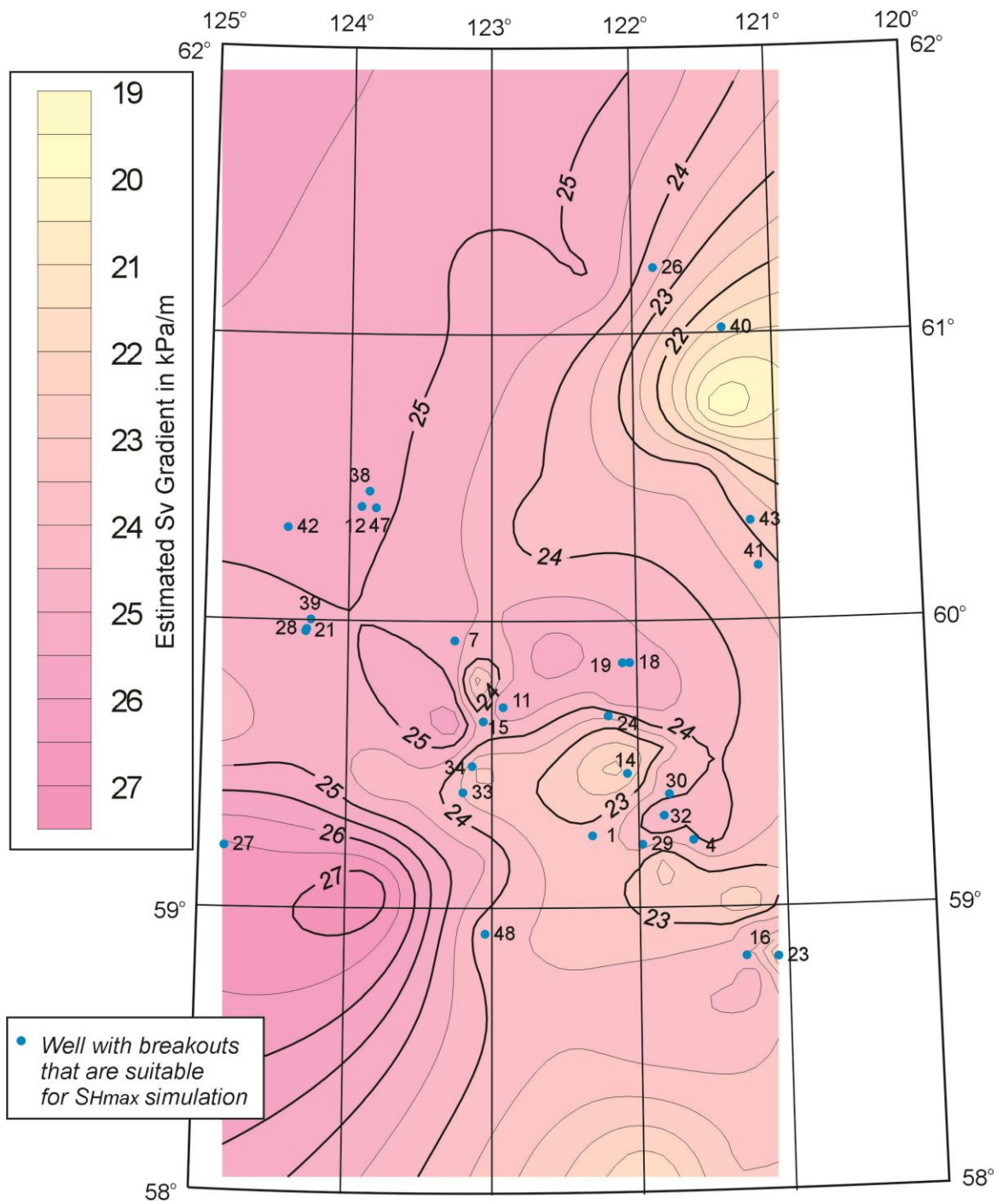


Fig. 40. Wells in the Liard Basin that exhibit breakouts that are suitable for determining  $S_{Hmax}$  magnitudes via numerical simulation.  $S_V$  gradients are contoured at 500 metres depth.  $S_V$  gradients are inferred from this map.

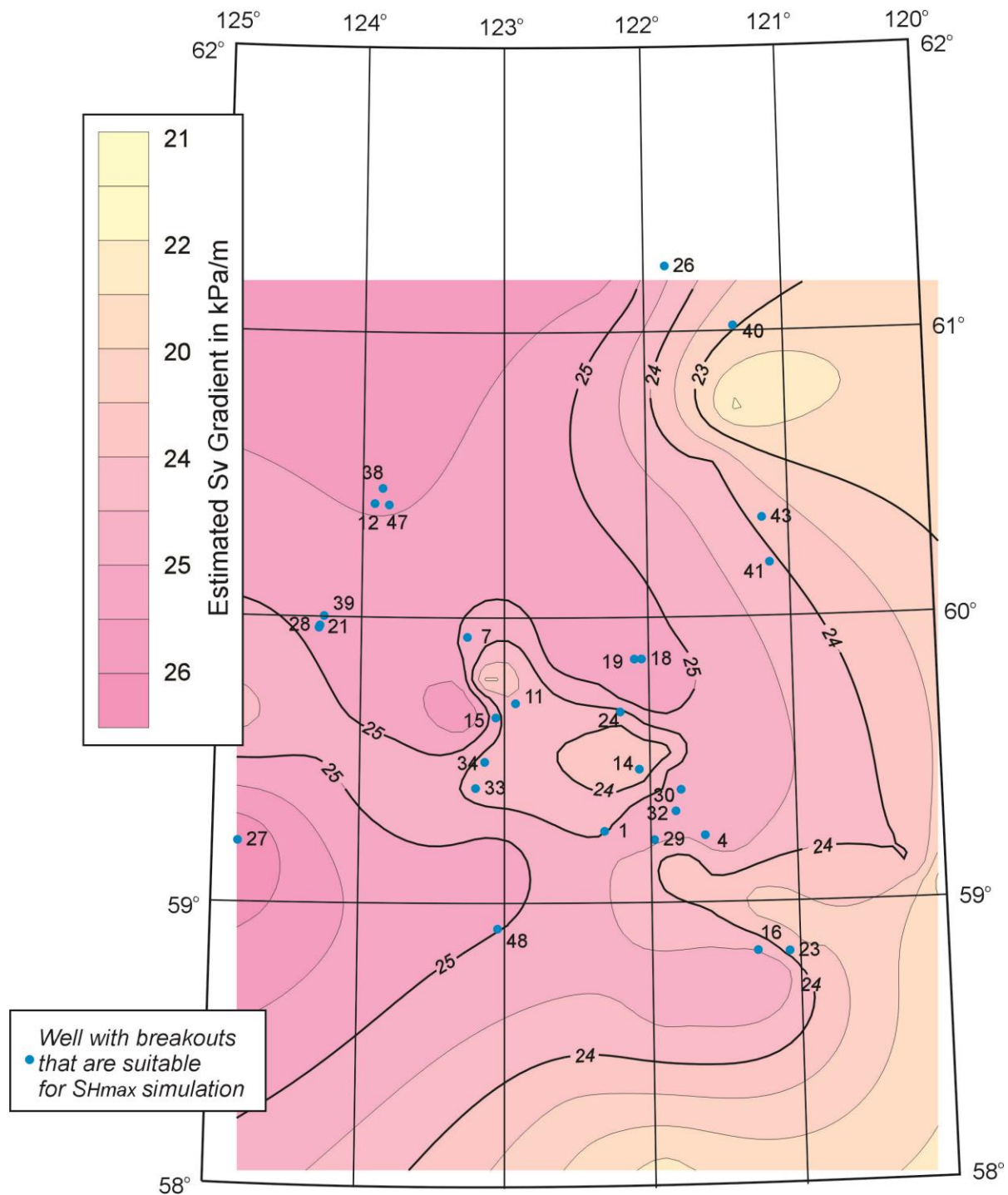


Fig. 41. The map shows wells in the Liard Basin that exhibit breakouts suitable for estimating  $S_{Hmax}$  magnitudes by modelling.  $S_v$  gradients are contoured at 1000 metres depth. This map was used to estimate gradients for wells lacking  $S_v$  gradient data

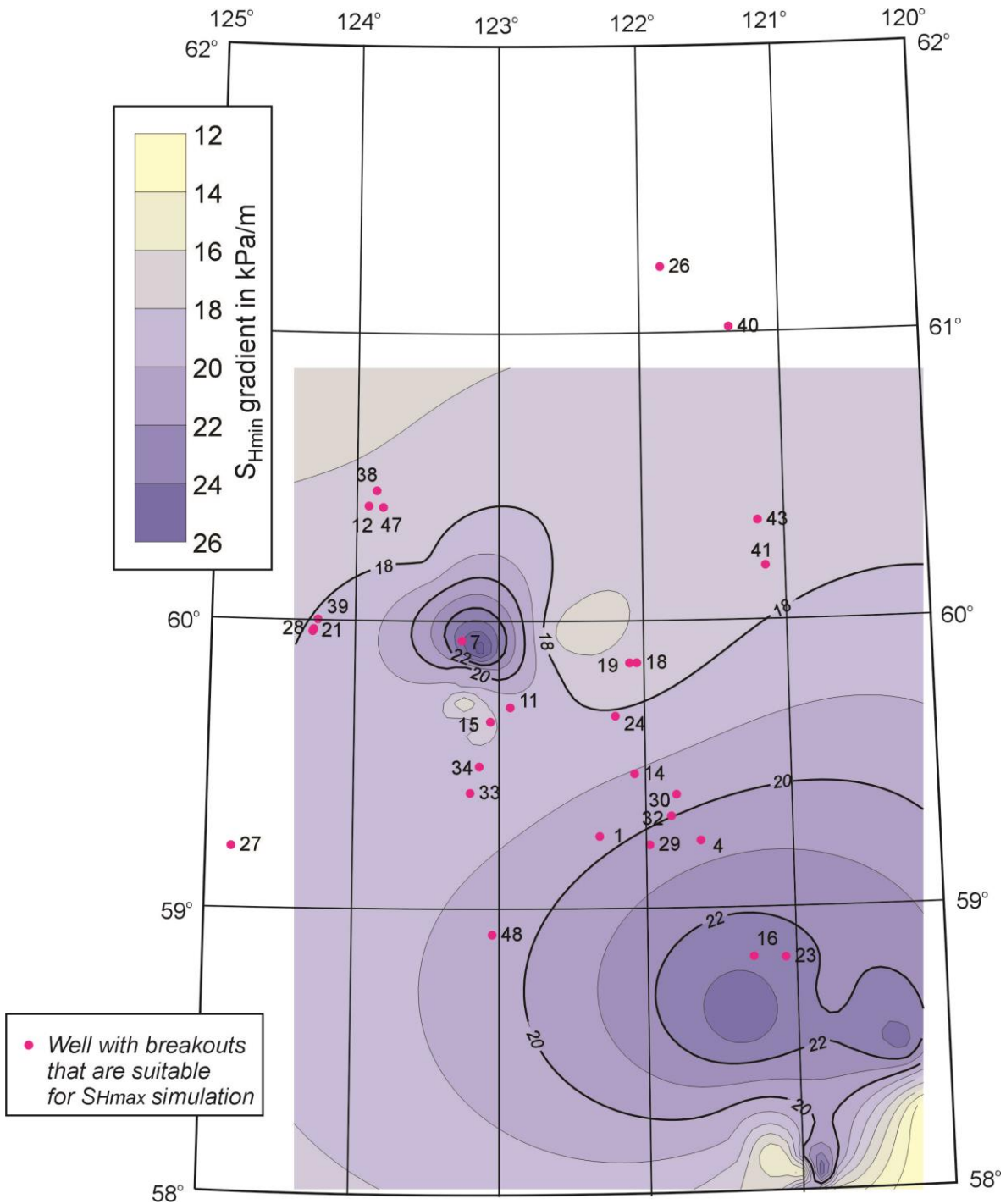


Fig. 42. The map shows wells in the Liard Basin that exhibit breakouts suitable for estimating  $S_{Hmax}$  magnitudes by modelling.  $S_{Hmin}$  gradients are contoured at 1000 metres depth. This map was used to estimate gradients for wells with simulated breakouts

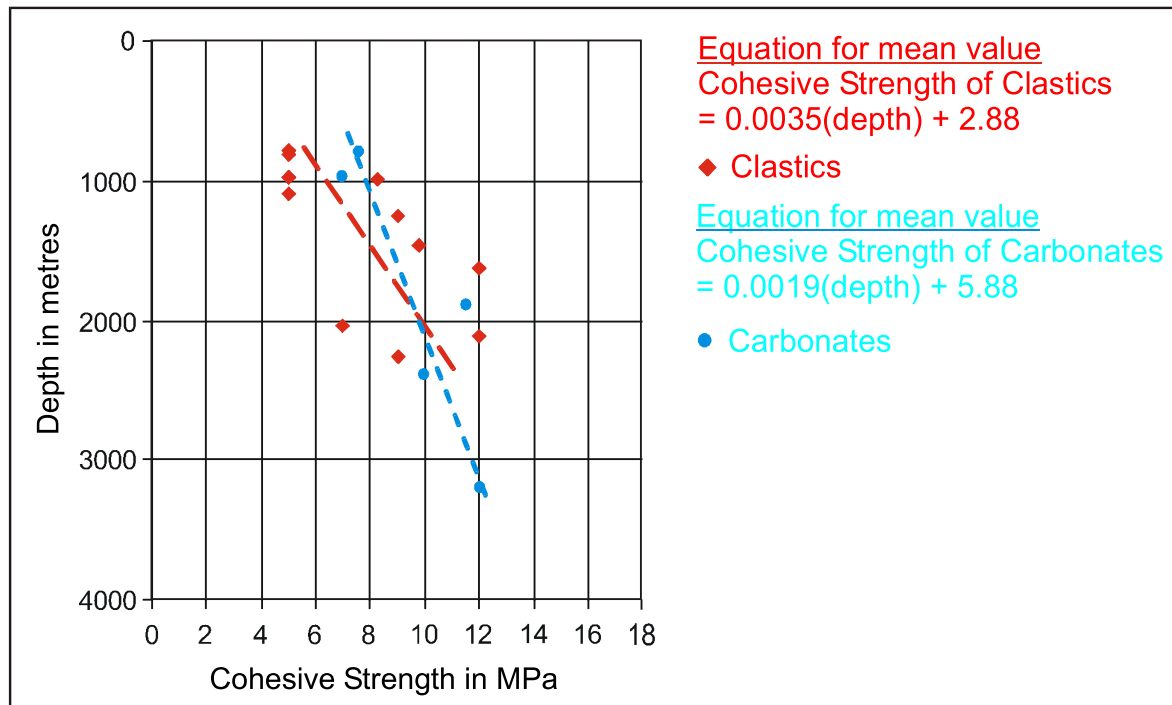


Fig. 43. Cohesive strengths plotted against depth that were assigned to breakout intervals in Paleozoic rocks and used in successful simulations to determine  $S_{Hmax}$

Four failure simulation models were available for this study. These were: Mohr-Coulomb, Drucker-Prager, Extended Drucker-Prager and 3 cycle Mohr Coulomb. In each simulation, the lowest magnitude of  $S_{Hmax}$  that satisfied the geometry of the breakout interval was selected as the likely value. Hence, the inferred  $S_{Hmax}$  magnitudes are conservative; the breakout geometries would allow for approximately 0.5 MPa additional lateral stress.

Provided that the selected breakout interval was not deeply spalled, and could be modelled satisfactorily by any or all of the three single simulation routines, the 3 cycle Mohr Coulomb failure simulation was not applied. The 3 cycle failure simulation was used when none of the other simulation routines generated the observed depth of spalling. The results are listed in Table 10 and are discussed in the Commentary Texts in Appendix 3.

Figure 44 plots and contours the  $S_{Hmax}$  gradients obtained from the numerical simulations that were completed for breakouts in 27 wells. Quite a similar configuration was obtained when gradients derived from  $S_{Hmax}$  magnitudes obtained with the simple equation  $S_{Hmax} = 2(S_{Hmin}) - P_O$  were contoured.

Table 10 lists the  $S_{Hmax}$  gradients derived from these equation-based magnitudes and they are plotted and contoured on Figure 45.

Map Number	Well Name UWI	Breakout number	SHmin gradient (kPa/m)	SV gradient (kPa/m)	Top of Breakout (m KB)	Base of Breakout (m KB)	Median depth of Breakout (m KB)	Drill Bit size (in)	Extension of Callipers 1 & 3 (in)	Extension of Callipers 2 & 4 (in)	SV (MPa)	SHmin (MPa)	Pore Pressure (MPa)	Mud Weight (MPa)	Coef. of Friction	Cohesive Strength (MPa)	Poisson's Ratio	SHmax simulation Mohr Coulomb	SHmax simulation Drucker-Prager	SHmax simulation Mod. Strain Energy	SHmax simulation 3 Cycle Mohr Coul.	SHmax gradient (kPa/m)	2SHmin - Po	25Hmin - Po gradient (kPa/m)
1	A-006-C/094-O-08	4	19.7	24.9	1445	1491	1468	8.5	8.54	9.74	36.6	28.9	14.7	14.7	0.6	9.8	0.2	42.8	62.2	54.1	SHmax simulation	29.2	43.1	29.4
4	A-081-J/094-P-04	3	20.6	24.4	2110	2121	2115.5	8.5	9.31	11.33	51.6	43.6	21.2	21.2	0.6	12.0	0.2	70.9	98.8	87.6	SHmax simulation	33.5	66.0	31.2
7	B-021-K/094-O-14	2	23.8	24.6	352	382	367	8.5	9.72	11.78	9.0	8.7	3.7	3.7	0.6	2.0	0.2	12.5	18.8	17.2	SHmax simulation	34.1	13.7	37.3
11	B-044-L/094-O-10	3	18.8	24.6	254	266	260	6.25	8.15	7.06	6.4	4.9	2.6	2.6	0.6	2.0	0.2	8.6	12.2	10.8	SHmax simulation	33.1	7.2	27.7
12	B-055-60-30-123-45	2	17.4	25.3	767	789	778	11	14.98	11.38	19.7	13.5	7.8	7.8	0.6	7.6	0.2	26.3	31.9	29.6	SHmax simulation	27.0	19.2	24.7
14	B-066-I/094-O-08	1	19.1	24.2	979	1012	995.5	8.5	12.42	9.50	23.5	19.0	10.0	10.0	0.6	8.3	0.2	41.0	48.0	46.0	SHmax simulation	31.5	31.6	28.1
15	B-085-H/094-O-11	part of 1	17.9	24.7	250	286	268	8.5	8.08	10.72	6.3	4.8	2.7	2.7	0.6	2.0	0.2	7.7	10.3	9.1	SHmax simulation	8.9	33.2	6.9
16	B-093-C/094-I-14	3	22.7	23.6	293	381	337	16	19.77	16.42	7.7	7.6	3.4	3.4	0.6	2.8	0.2	9.6	13.1	11.7	SHmax simulation	10.1	30.0	11.8
18	C-024-H/094-O-16	KS? 6	17.5	24.7	426	442	434	7.875	10.26	7.79	10.7	7.6	4.3	4.3	0.6	3.0	0.2	15.6	18.5	16.6	SHmax simulation	12.2	28.1	25.1
19	C-028-H/094-O-16	8	17.4	24.7	2250	2266	2258	8.5	8.58	13.02	55.8	39.3	22.6	22.6	0.6	9.0	0.2	64.7	83.4	78.1	SHmax simulation	58.5	25.9	56.0
21	C-054-K/094-N-16	3	18.1	24.7	3182	3198	3190	8.5	8.08	10.42	78.8	57.7	31.9	31.9	0.6	12.0	0.2	84.8	124.0	107.6	SHmax simulation	26.6	83.5	26.2
23	C-086-A/094-I-14	2	22.5	22.4	363	393	378	8	9.09	7.66	8.5	8.5	3.8	3.8	0.6	3.0	0.2	12.4	16.3	14.9	SHmax simulation	32.8	13.2	34.9
24	D-007-J/094-O-09	2	18.1	24.1	2369	2379	2374	9	8.93	11.06	57.2	43.0	23.7	23.7	0.6	10.0	0.2	69.0	95.6	84.4	SHmax simulation	29.1	62.3	26.2
26	D-025-61-20-121-45	1	17.0	25.5	794	817	805.5	8.5	12.18	14.21	20.5	13.7	8.1	8.1	0.6	5.0	0.2	23.5	35.6	30.3	SHmax simulation	29.2	19.3	24.0
27	D-057-K/094-N-02	part of 4	18.3	26.5	765	785	775	12.25	14.53	12.72	20.5	14.2	7.8	7.8	0.6	5.0	0.2	21.9	33.5	28.3	SHmax simulation	28.3	20.6	26.6
28	D-064-K/094-N-16	4	18.1	24.7	1654	1684	1669	12.25	12.13	17.71	41.2	30.2	16.7	16.7	0.6	10.0	0.2	53.0	65.3	65.6	SHmax simulation	50.4	30.2	43.7
29	D-069-L/094-P-04	2 to 3	20.3	24.7	1595	1635	1615	8.5	12.65	9.83	40.3	32.8	16.2	16.2	0.6	7.12	0.2	50.9	61.7	70.5	SHmax simulation	46.3	28.7	49.4
30	D-074-F/094-P-05	part of 1	19.7	24.4	290	305	297.5	8.5	14.15	8.61	7.3	5.9	3.0	3.0	0.6	2.0	0.2	10.3	13.1	11.4	SHmax simulation	10.2	34.3	8.8
32	D-087-C/094-P-05	1	20.0	24.6	2001	2067	2034	8.5	7.79	14.90	50.6	40.7	20.3	20.3	0.6	7.0	0.2	63.4	82.5	72.5	SHmax simulation	58.7	28.9	61.1
33	D-087-G/094-O-06	1	18.5	23.5	300	441	370.5	7.875	7.49	10.50	8.6	6.9	3.7	3.7	0.6	3.25	0.2	13.6	17.2	16.1	SHmax simulation	10.6	28.6	10.1
34	D-092-J/094-O-06	4	18.3	24.7	822	847	834.5	8.5	14.50	8.06	19.9	15.3	8.3	8.3	0.6	2.8	0.2	24.1	32.2	27.4	SHmax simulation	22.9	27.4	22.3
38	F-038-60-30-123-45	3	17.3	25.4	976	985	980.5	12	14.19	12.08	25.1	17.0	9.8	9.8	0.6	5.0	0.2	27.1	42.4	35.4	SHmax simulation	27.6	24.2	24.7
39	G-001-60-10-124-15	4	18.1	24.8	1246	1264	1255	12.25	15.27	12.23	31.1	22.7	12.5	12.5	0.6	9.0	0.2	40.4	56.3	50.5	SHmax simulation	33.3	26.5	32.9
40	G-032-61-10-121-15	1	17.2	23.9	1082	1106	1094	8.5	8.65	13.24	26.1	18.8	10.9	10.9	0.6	5.0	0.2	32.8	41.5	38.9	SHmax simulation	30.6	28.0	26.7
41	G-042-60-20-121-00	1	17.8	24.7	972	986	979	8.5	11.57	9.07	24.2	17.4	9.8	9.8	0.6	4.5	0.2	29.7	38.6	36.1	SHmax simulation	27.0	27.6	25.0
43	M-051-60-30-121-00	4	17.6	24.6	944	964	954	8.5	8.56	10.92	23.5	16.8	9.5	9.5	0.6	4.5	0.2	29.3	37.5	35.6	SHmax simulation	26.5	27.8	24.1
47	P-024-60-30-123-45	5	17.5	25.1	352	372	362	8.5	12.48	9.41	9.1	6.3	3.6	3.6	0.6	2.5	0.2	12.8	15.1	14.1	SHmax simulation	10.5	29.0	9.0
48	B-094-H/094-J-14	2	19.5	23.9	303	318	310.5	12.25	13.55	11.84	7.4	6.1	3.1	3.1	0.6	3.0	0.2	10.2	13.9	12.0	SHmax simulation	32.9	9.1	29.3

Table 10 Details of breakouts selected for failure simulation and the other parameters required for  $S_{Hmax}$  magnitude estimation. **Vertical stresses in red were determined from density logs.** *Values in italics indicate failure to simulate the breakout.* **Bold values indicate successful simulations.**



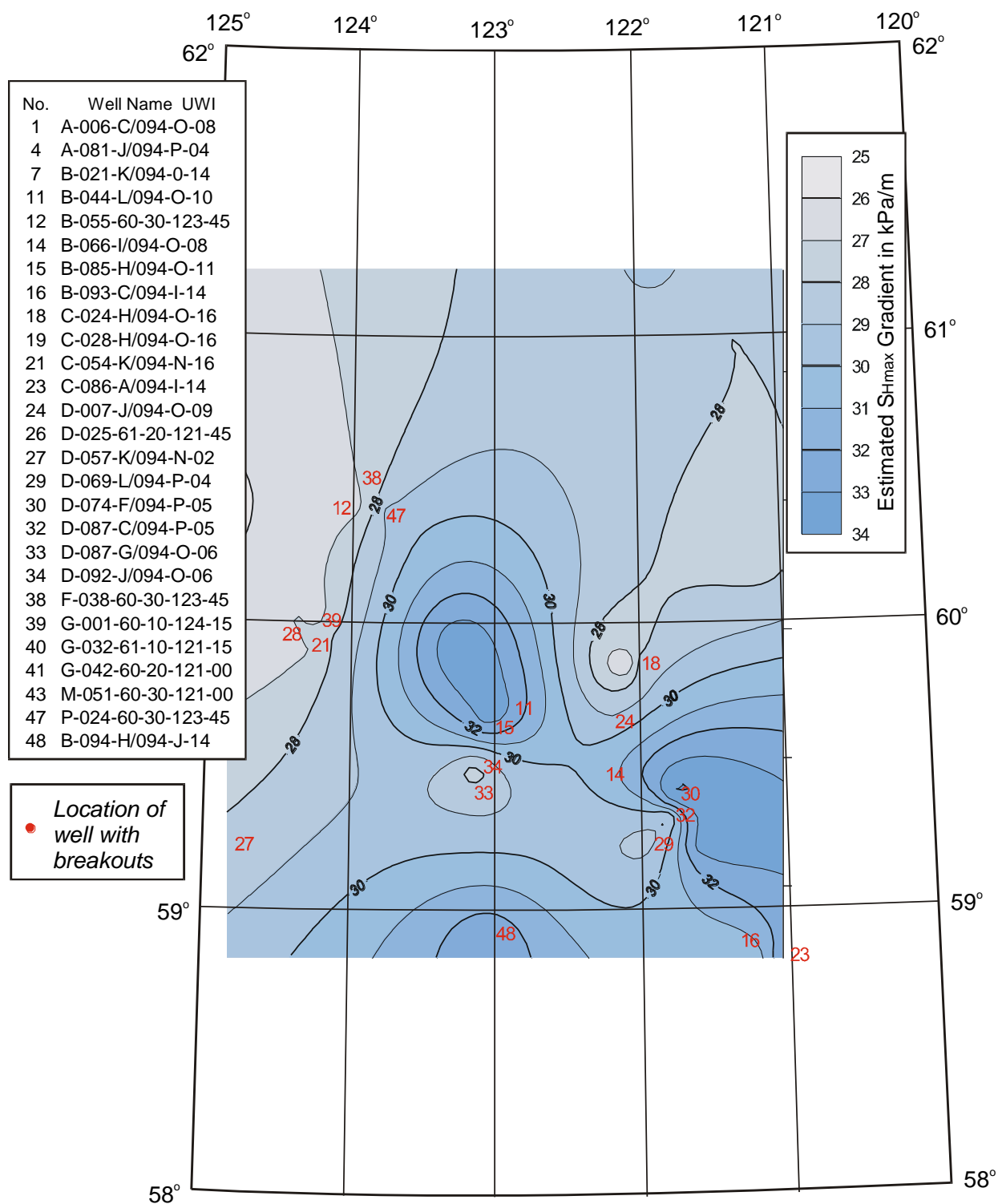


Fig. 44. Contour map of estimated  $S_{Hmax}$  gradients that were derived from  $S_{Hmax}$  magnitudes inferred from modelling breakout failure in 27 wells in the Liard Basin.

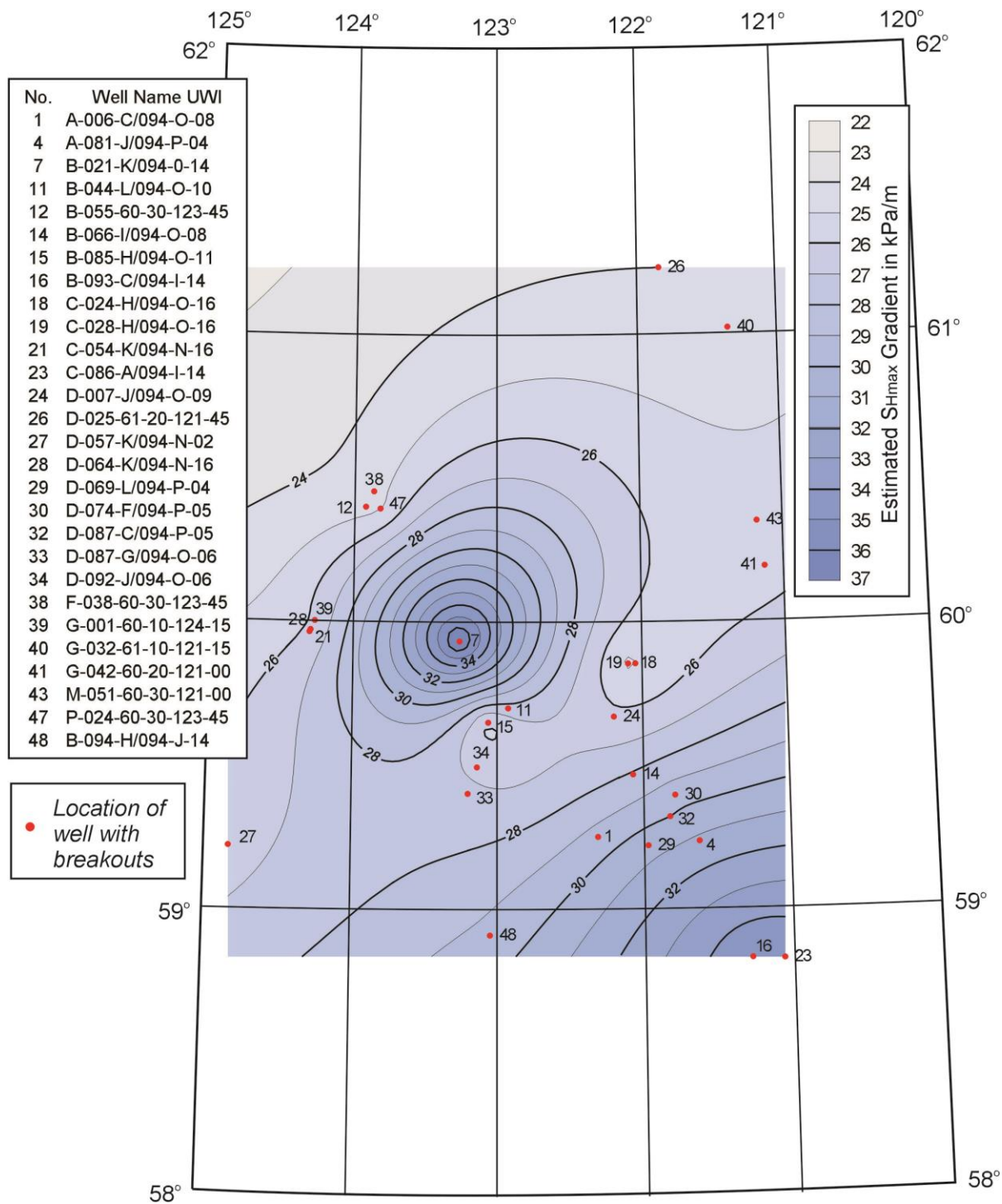


Fig. 45. Contour map of estimated  $S_{Hmax}$  gradients that were derived from  $S_{Hmax}$  magnitudes calculated from the equation  $S_{Hmax} = 2(S_{Hmin}) - P_o$ .

All the relevant breakout failure simulations are reproduced in the Appendix, and are discussed in the associated commentary texts. Where single cycle simulations modelled breakout spalling satisfactorily, the Mohr-Coulomb routine succeeded in generating the breakout geometry with the smallest  $S_{Hmax}$  magnitude. Such simulations were interpreted as providing reliable results. The next smallest  $S_{Hmax}$  magnitudes were provided by the Modified Strain Energy Criterion, while the Drucker Prager Criterion routinely calculated the highest values of  $S_{Hmax}$  for breakout simulation.

Formation tops reported for the 27 wells where breakout failure was simulated are listed in Table 11. Many stratigraphic horizons are not represented in enough wells to support meaningful contour maps of  $S_{Hmax}$  magnitudes. Seven stratigraphic horizons were selected and their  $S_{Hmax}$  magnitudes are listed in Table 12.

Five wells provide  $S_{Hmax}$  magnitudes at the top of the Scatter Formation (Fig. 46). A bull's eye is contoured around well B-021-K/094-O-14, probably due to downfaulting.

The  $S_{Hmax}$  magnitudes at the top of the Bluesky Formation are recorded in only five wells. They suggest a northwestward increase in magnitude (Fig. 47).

Nine top Mattson Formation data points are clustered on the west side of the basin, and display the bull's eye around well B-021-K/094-O-14 (Fig. 48).

A northwestward increase in  $S_{Hmax}$  magnitude is suggested by the 12 top Debolt wells (Fig. 49).

The top of the Banff Formation provides the best areal coverage for  $S_{Hmax}$  mapping. At this horizon, 13 wells neatly document a westward increase in stress magnitude (Fig. 50).

Although 12 wells provide  $S_{Hmax}$  magnitudes for the top of the Kotcho Formation, they are located on the east side of the Liard Basin, where their contours suggest an eastward increase in magnitude (Fig. 51).

The deepest horizon at which the  $S_{Hmax}$  magnitude is mapped is the top of the Jean Marie Formation. At this horizon, 10 wells provide data along narrow north south strip and suggest a southward increase in  $S_{Hmax}$  magnitudes (Fig. 52).

Map Number	Well Name UWI	Shmax gradient (kPa/m)	Sikanni	Scatter	Bluesky	Fantasque	Mattson	Mississippian	Debolt	Banff	Kotcho	Jean Marie	Fort Simpson	Slave Point	Keg River
1	A-006-C/094-O-08	29.2							482.8	767.1	1112.5		1408.7		
4	A-081-J/094-P-04	33.5							668.0	847.0	1199.0	1583.0	1614.0		
7	B-021-K/094-O-14	34.1	345.3	1038.7	1291.7	1506.6	1620.2		2248.7						
11	B-044-L/094-O-10	33.1													
12	B-055-60-30-123-45	27.0													
14	B-066-I/094-O-08	31.6			624.0				634.0	843.0	1223.0	1844.0	1891.0		
15	B-085-H/094-O-11	33.2					958.5		1356.3						
16	B-093-C/094-I-14	30.0								773.0	1076.5	1426.5	1448.5		2210.0
18	C-024-H/094-O-16	28.1													
19	C-028-H/094-O-16	25.9						376.4							
21	C-054-K/094-N-16	26.6				465.1	643.1	1292.3		2804.9					
23	C-086-A/094-I-14	32.8			542.0				568.0	732.5	1039.2	1376.2	1395.6	1874.0	
24	D-007-J/094-O-09	29.1						460.2							
26	D-025-61-20-121-45	29.2													
27	D-057-K/094-N-02	28.3													
28	D-064-K/094-N-16	30.2				426.7	607.4	1232.9							
29	D-069-L/094-P-04	28.7			520.0				538.0	735.0	1092.0	1575.0			
30	D-074-F/094-P-05	34.3							701.0	887.0	1253.0	1670.0			
32	D-087-C/094-P-05	28.9							612.8	775.6	1130.0	1477.8	1623.0	2313.6	
33	D-087-G/094-O-06	28.6		385.2	578.5		623.0		1010.1						
34	D-092-J/094-O-06	27.4				852.8	975.3		1611.7						
38	F-038-60-30-123-45	27.6													
39	G-001-60-10-124-15	26.5				434.0	637.0								
40	G-032-61-10-121-15	28.0									189.0	620.6	634.0		
41	G-042-60-20-121-00	27.6		541.0						619.7	1041.8	1530.2	1545.3	2055.9	2210.4
43	M-051-60-30-121-00	27.8		423.1						513.6	885.1	1399.0	1415.2	1912.3	
47	P-024-60-30-123-45	29.0		76.2		425.2	533.4								
48	B-094-H/094-J-14	32.9							605.0	961.0	133.4			2028.0	2331.6

Table 11. Formation tops for wells for which failure simulations of breakthroughs were conducted.

Map Number	Well Name UWI	SHmax gradient (kPa/m)	Scatter SHmax (MPa)	Bluesky SHmax (MPa)	Mattson SHmax (MPa)	Debolt SHmax (MPa)	Banff SHmax (MPa)	Kotcho SHmax (MPa)	Jean Marie SHmax (MPa)
1	A-006-C/094-O-08	29.2				14.1	22.4	32.4	
4	A-081-J/094-P-04	33.5				22.4	28.4	40.2	53.1
7	B-021-K/094-O-14	34.1	35.4	44.0	55.2	76.6			
11	B-044-L/094-O-10	33.1			13.0				
12	B-055-60-30-123-45	27.0							
14	B-066-I/094-O-08	31.6		19.7		20.1	26.7	38.7	58.3
15	B-085-H/094-O-11	33.2			31.8	45.0			
16	B-093-C/094-I-14	30.0					23.2	32.3	42.8
18	C-024-H/094-O-16	28.1							
19	C-028-H/094-O-16	25.9							
21	C-054-K/094-N-16	26.6			17.1		74.6		
23	C-086-A/094-I-14	32.8		17.8		18.6	24.0	34.1	45.1
24	D-007-J/094-O-09	29.1							
26	D-025-61-20-121-45	29.2							
27	D-057-K/094-N-02	28.3							
28	D-064-K/094-N-16	30.2			18.3				
29	D-069-L/094-P-04	28.7		14.9		15.4	21.1	31.3	45.2
30	D-074-F/094-P-05	34.3				24.0	30.4	43.0	57.3
32	D-087-C/094-P-05	28.9				17.7	22.4	32.6	42.6
33	D-087-G/094-O-06	28.6	11.0	16.6	17.8	28.9			
34	D-092-J/094-O-06	27.4			26.8	44.2			
38	F-038-60-30-123-45	27.6					39.5		
39	G-001-60-10-124-15	26.5			16.9				
40	G-032-61-10-121-15	28.0						5.3	17.4
41	G-042-60-20-121-00	27.6	14.9				17.1	28.7	42.2
43	M-051-60-30-121-00	27.8	11.8				14.3	24.6	38.9
47	P-024-60-30-123-45	29.0	2.2		15.5				
48	B-094-H/094-J-14	32.9				19.9	31.6	4.4	

Table 12. Estimated  $S_{Hmax}$  magnitudes at selected formation tops in wells in the Liard Basin. The  $S_{Hmax}$  magnitudes were determined from gradients obtained by breakout failure simulation.

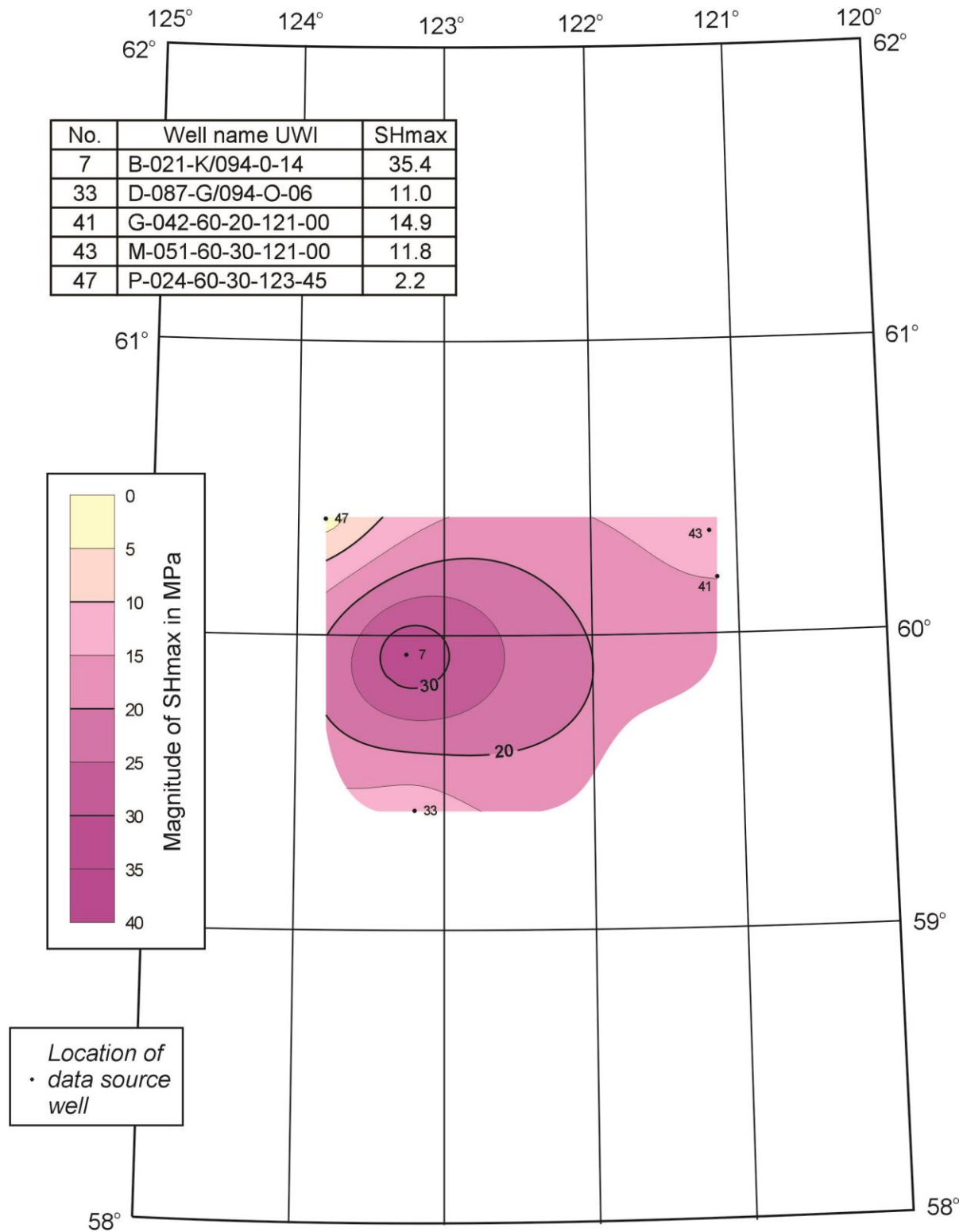


Fig. 46.  $S_{Hmax}$  magnitudes in MPa at the top of the Scatter Formation in the Liard Basin.

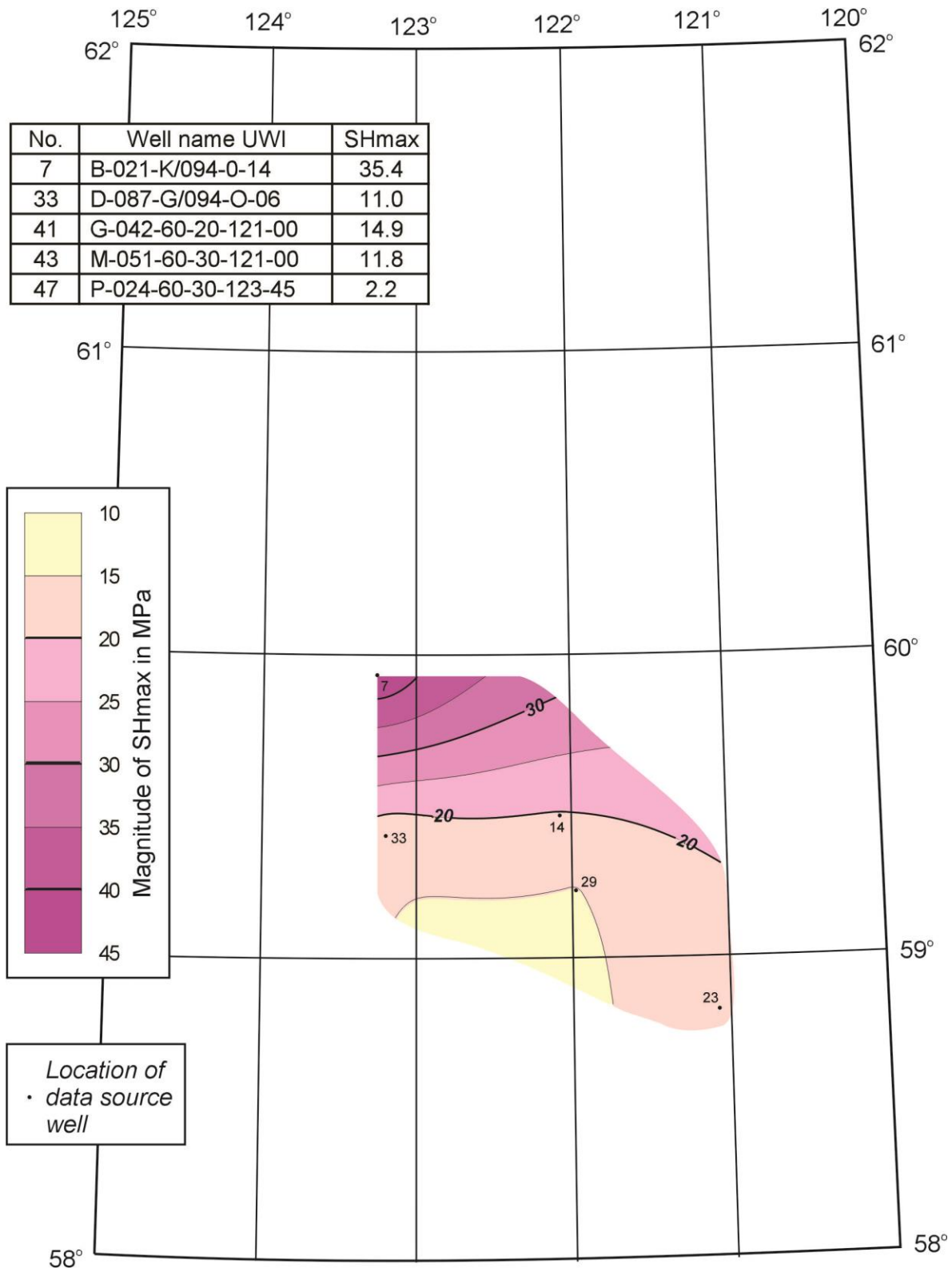


Fig. 47.  $S_{Hmax}$  magnitudes in MPa at the top of the Bluesky Formation in the Liard Basin.

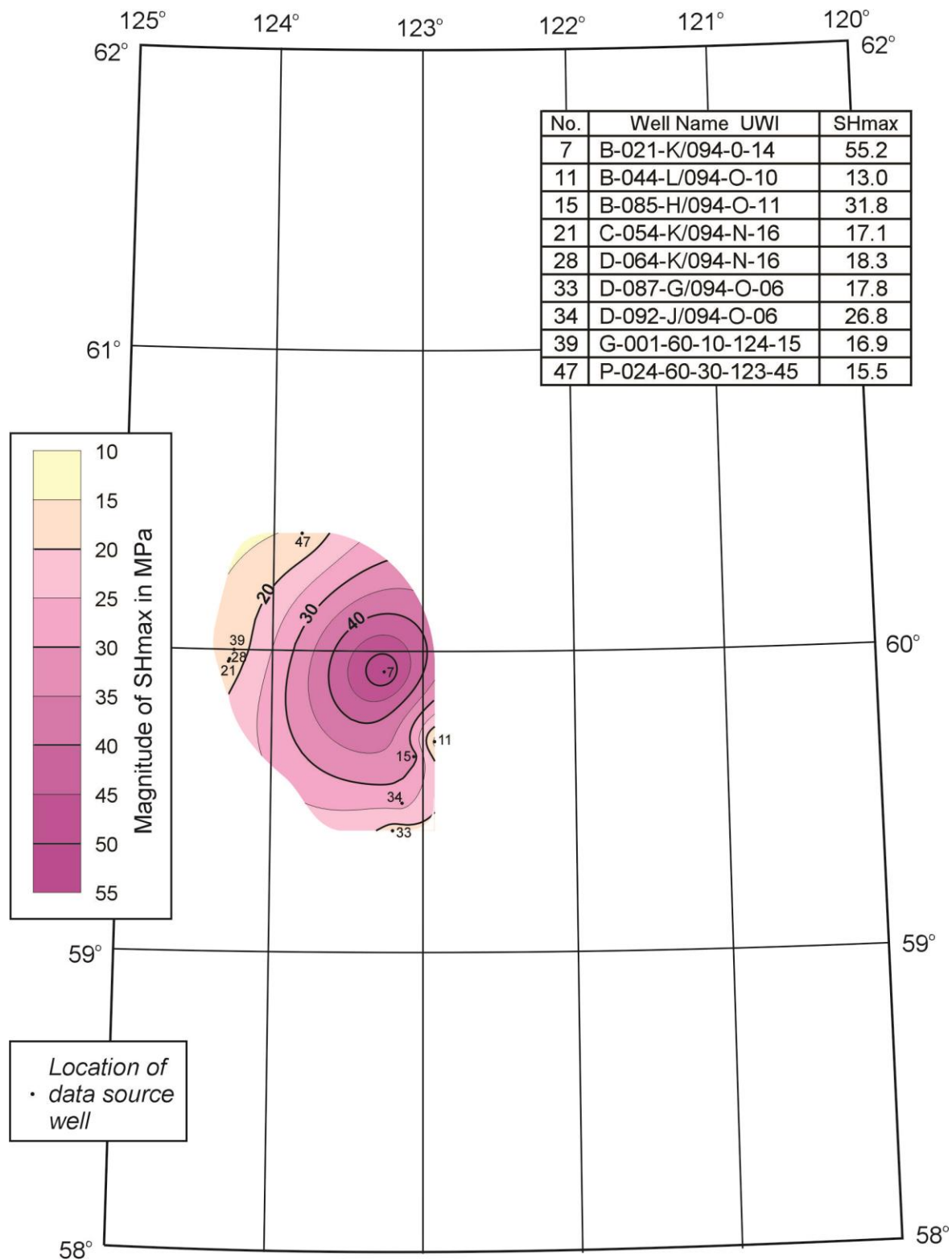


Fig. 48.  $S_{Hmax}$  magnitudes in MPa at the top of the Mattson Formation in the Liard Basin.



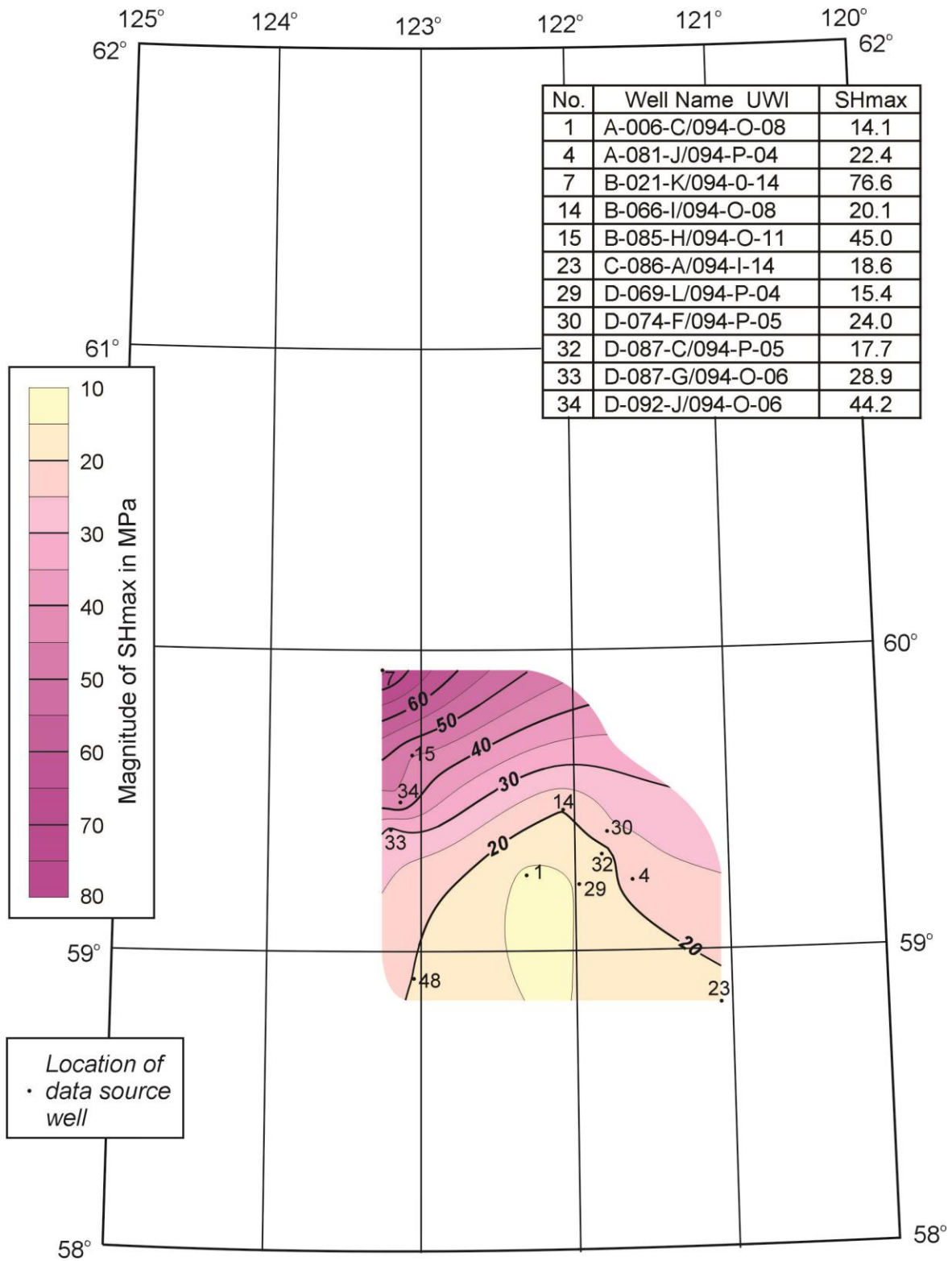


Fig. 49.  $S_{Hmax}$  magnitudes in MPa at the top of the Debolt Formation in the Liard Basin.

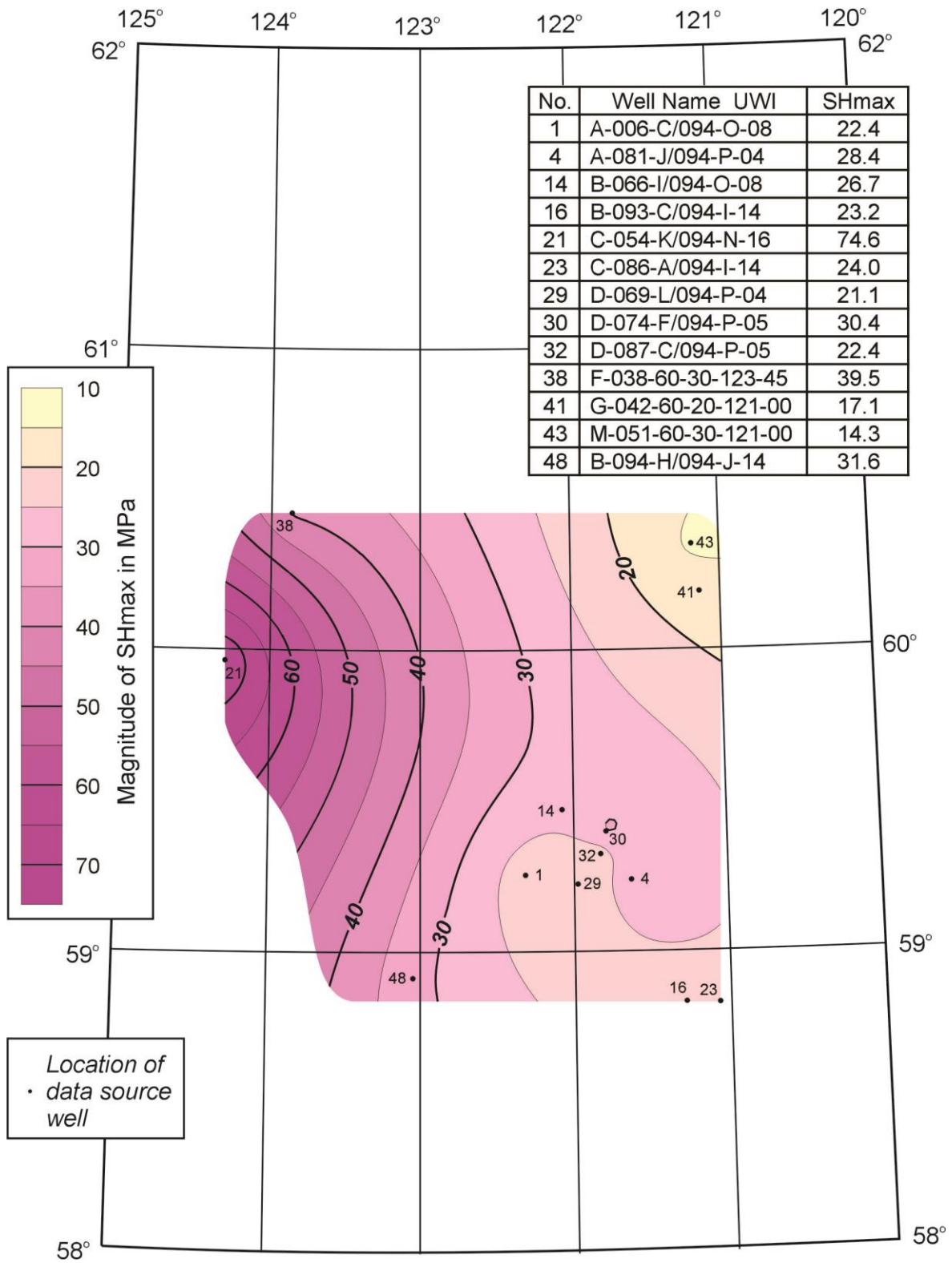


Fig. 50.  $S_{Hmax}$  magnitudes in MPa at the top of the Banff Formation in the Liard Basin.

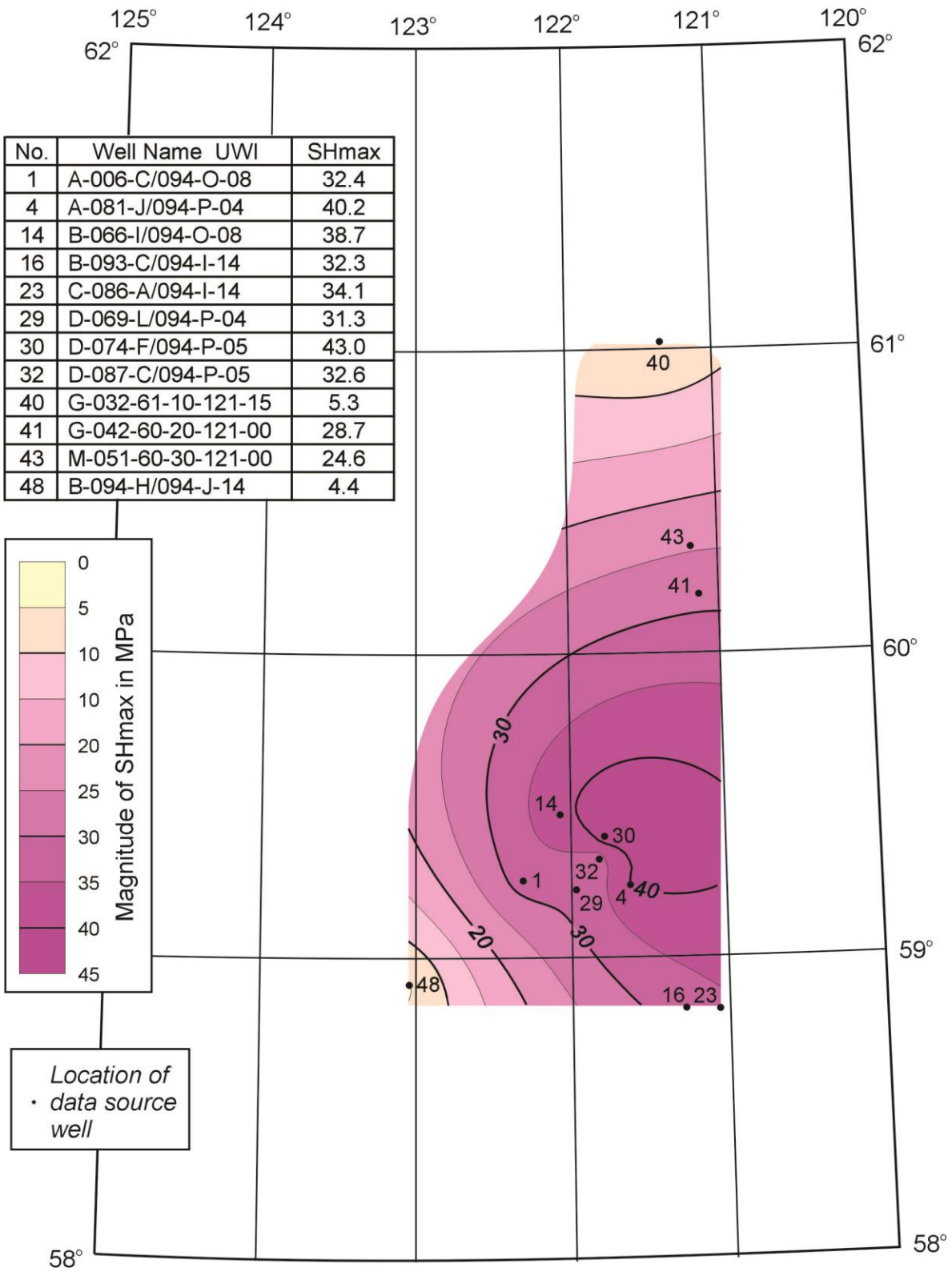


Fig. 51.  $S_{Hmax}$  magnitudes in MPa at the top of the Kotcho Formation in the Liard Basin.

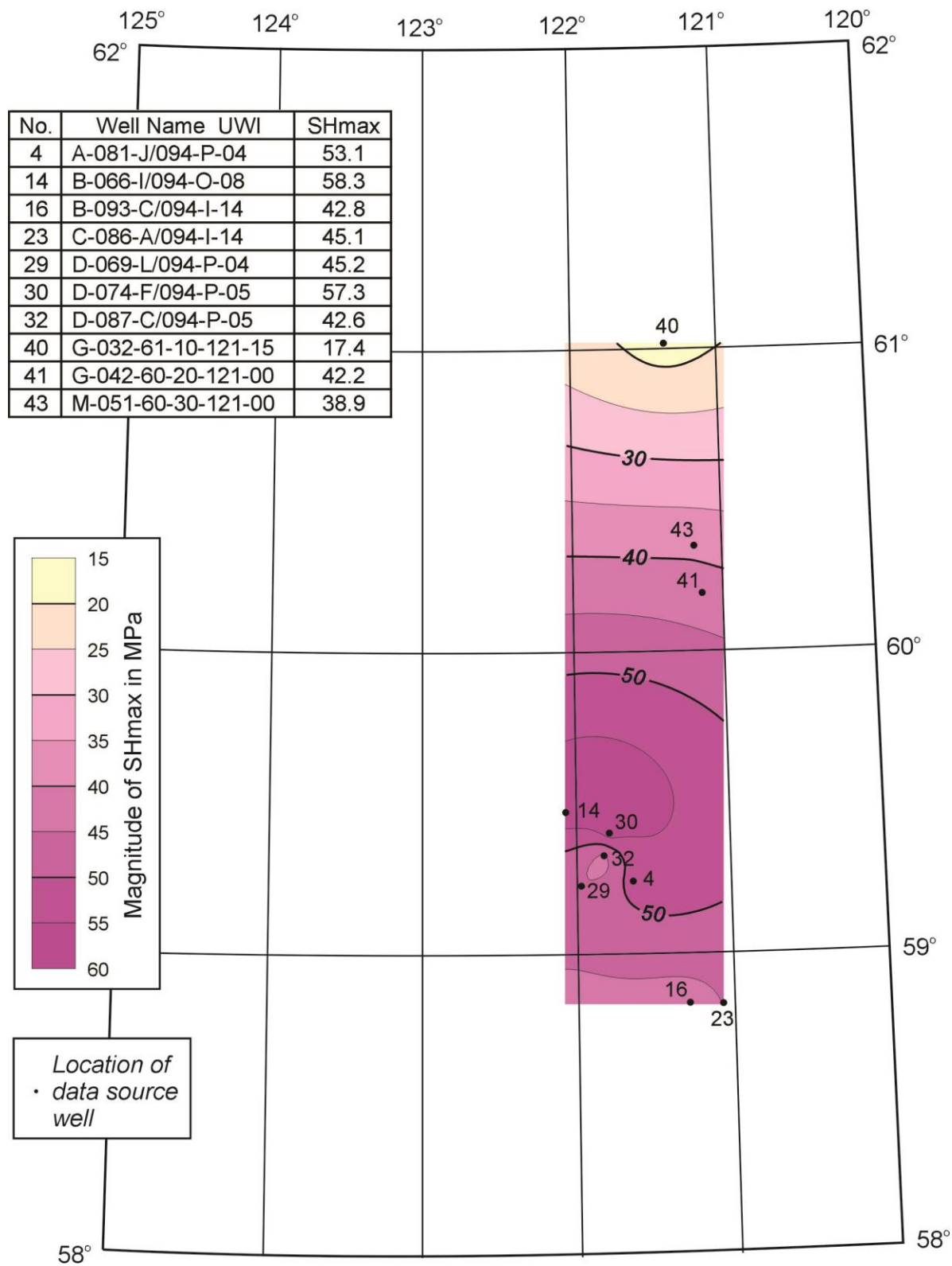


Fig. 52.  $S_{Hmax}$  magnitudes in MPa at the top of the Jean Marie Formation in the Liard Basin.

## 14. ESTIMATING AND MAPPING EFFECTIVE STRESS

Effective stresses in buried rock masses are calculated by subtracting the pore fluid pressure from the vertical or horizontal stress at a common depth.

Effective Vertical Stress:  $S_V - P_o$     Effective Horizontal Stress:  $S_{Hmin} - P_o$

Their accuracy will be dependent on the precision of the relevant stress magnitudes and of the pore fluid pressures. In this study, vertical stress magnitudes,  $S_V$ , have been determined with reasonable accuracy, in wells where suitable density logs were available. The smaller horizontal stress,  $S_{Hmin}$ , is far less well constrained, being equated with leak-off test pressures and fracture breakdown pressures that were obtained from a limited number of wells that were less than ideally located within the Liard Basin.

In terms of pore pressure, the only data available come from the mudweights used for drilling and drill stem tests. These show no indications of significant overpressuring in any of the wells. For example, in well F-38-60-30-123-45 in the Northwest Territories, a mudweight of 8.6 lbs/gallon, which is equivalent to water with a density of  $1.03 \text{ g/cm}^3$  (i.e. sea water), was used to drill at a depth of 4668 metres. At shallower depths, heavier muds (up to 11.9 lbs/gallon =  $1.4 \text{ g/cm}^3$ ) were used in this well, but this was to achieve faster drilling, not to counter elevated pore pressures. In well D-25-61-20-121-45 mudweights range from 1.03 to  $1.13 \text{ g/cm}^3$ , in well E-72-61-20-122-00 they range from 1.01- $1.16 \text{ g/cm}^3$ , and in well L-20-61-00-123-30 from 1.03 to  $1.20 \text{ g/cm}^3$ .

Drill stem tests tell the same story, with reported fluid pressures from these and other wells in the Yukon and Northwest Territories ranging from  $1.03$  to  $1.17 \text{ g/cm}^3$ . With salt water reported as being recovered from several drill stem tests, it can be assumed that pore fluid pressures within rocks in the Liard Basin are likely to be approximately equivalent to the weight of a column of sea water. Therefore, it is assumed that the pore pressures in the Liard Basin will have a gradient of  $10.3 \text{ kPa/m}$ .

Effective vertical stresses at 250, 500 and 1000 metres depth are listed in Table 13. Maps contouring their values at these depths are presented in Figures 53, 54, and 55. The geometric configurations of these maps are essentially identical with those for vertical stresses at the same depths; what differs are the magnitudes of the compression.

Mapping effective horizontal stress magnitudes relies on  $S_{Hmin}$  gradients (Table 14). Therefore the contour configurations of the maps at 250 metres depth (Fig. 56), 500 metres depth (Fig. 57) and 1000 metres depth (Fig. 58) will be the same. Again, the differences lie in the magnitudes of the values.

The effective stress interpretations presented herein refer to rocks buried at 1000 metres or less, although many of the horizontal effective stress gradients are based on deeper fracture pressure measurements. Most of the earthquakes in the Liard Basin have epicentres that are much deeper than 1000 metres. Yet, since effective stress is a measure of rock strength, it is interesting to plot seismic activity and see how it might relate to effective stress magnitudes. Since the horizontal effective stresses are of lesser magnitude than the vertical effective stresses, they define rock weakness. The horizontal effective stress magnitude maps (Figs. 56-58) suffer from lack of data and, at this stage, it is not possible to assess how deep the mapped magnitude differences might extend. Despite these provisos, it is interesting to observe that, since 1985, earthquakes of magnitude 2 and 3 have largely occurred beneath rocks that are subject to relatively low horizontal effective stresses (Fig. 59). If this pattern of weakness extends to depth, it could account for the locations of subsurface failure that led to the observed seismicity.

In the case of the vertical effective stresses, their magnitudes are higher than the horizontal effective stresses. Where they are low, the rock column will be better supported by its contained fluids and will be easier to deform by horizontal slippage, or thrusting. In the central part of the study area, around latitude  $59^{\circ} 30'$  and longitude  $122^{\circ} 25'$ , a number of magnitude 2 and 3 earthquakes are clustered within a low magnitude "trough" (Fig. 60). Yet, paradoxically, the most active seismic region, centred on latitude  $61^{\circ} 50'$  and longitude  $124^{\circ} 20'$ , is located where the vertical effective stress appears to be highest. Admittedly, this high magnitude is based only on data from one well. It may be that, tectonically, there is a structural need for subsurface faulting to occur here. The greater vertical effective stresses in this area could have led to larger seismic disruptions occurring here than elsewhere. In other words, the rocks are harder to fracture here and so this occurs less often but with more force when it does. It will be worth assessing such speculations in light of first motion studies of these earthquakes.

No.	Well Name UWI	Latitude	Longitude	Sv-Po at 250 m (MPa)	Sv-Po at 500m (MPa)	Sv-Po at 1000m (MPa)
1	A015J094I14	58.927	121.178	3.4	7.1	
2	A039B094N08	59.277	124.228	3.9	8.0	29.1
3	A064H094O16	59.885	122.041	3.4	7.2	14.8
4	A067D094O13	59.802	123.953	3.4		
5	A085E094P12	59.652	121.928	3.4	7.0	14.7
6	A088F094P12	59.652	121.841	3.5	7.1	14.6
7	B015B094I14	58.760	121.184	3.4	7.1	14.8
8	B043K094O05	59.452	123.784	3.3	6.9	14.3
9	B044B094P05	59.285	121.672	3.3	6.9	14.6
10	B044L094O10	59.702	122.922	3.6	7.5	
11	B058A094I13	58.794	121.597	3.2	6.8	14.4
12	B058H094O15	59.877	122.597	3.6	7.6	15.2
13	B066I094O08	59.469	122.072	2.8	5.9	13.3
14	B072J094O01	59.727	123.147	3.2	6.6	14.4
15	B085H094O11	59.652	123.059	3.3	6.9	14.2
16	B086F094P04	59.152	121.822	2.9	6.0	13.3
17	B093C094I14	58.827	121.284	3.0	6.5	14.2
18	B094G094O09	59.660	122.172	3.2	6.5	13.9
19	C040C094P12	59.531	121.872	2.9	6.0	13.5
20	C051B094O14	59.798	123.134	3.0	6.2	12.8
21	C086A094I14	58.823	121.072	2.7	5.7	13.3
22	D008I094P04	59.173	121.591	3.5	7.2	15.0
23	D016A094N15	59.765	124.566	3.5	7.3	14.5
24	D035F094I14	58.865	121.303	3.3	6.9	
25	D035F094P05	59.365	121.803	3.2	6.8	14.3
26	D051A094O08	59.298	122.003	3.4	6.9	14.8
27	D057K094N02	59.215	124.828	4.0	8.2	16.2
28	D060I094O09	59.715	122.116	3.5	7.3	15.1
29	D067A094O11	59.556	123.078	3.1	6.6	
30	D069L094P04	59.223	121.978	3.3	6.8	14.4
31	D071I094P04	59.231	121.503	3.4	7.0	14.7
32	D077J094O08	59.481	122.203	2.8	5.8	13.2
33	D082K094I14	58.990	121.266	2.7	5.8	12.9
34	D087A094O11	59.573	123.078	3.4	7.1	
35	D087C094P05	59.323	121.828	3.5	7.2	14.7
36	D087G094O06	59.406	123.203	3.2	6.6	14.0
37	D092J094O06	59.498	123.141	3.0	6.4	13.9
38	D098F094N10	59.665	124.841	3.1	6.9	13.9
39	D099H094I14	58.915	121.103	3.2	6.9	
40	D099K094P05	59.498	121.853	3.4	6.8	14.4
41	D31603012230	60.335	122.621	3.1	6.7	
42	E72612012200	61.190	122.246	3.6	7.4	15.3
43	F38603012345	60.456	123.863	3.7	7.5	15.3
44	H45605012115	60.740	121.379	2.5	4.6	11.6
45	J15612012300	61.244	123.043	3.6	7.3	
46	J66620012145	61.927	121.949	3.4	7.4	
47	L20610012330	60.994	123.559	3.7	7.5	15.4
48	L49603012230	60.477	122.652	3.3	6.9	
49	M05602012245	60.248	122.777	3.3	6.9	
50	M73604012115	60.548	121.496	3.2	6.5	13.7
51	N44620012345	61.898	123.895	4.2	8.7	
52	A077D094I04	58.060	121.953	2.4	5.4	12.0
53	B084D094I03	58.069	121.422	3.0	6.3	
54	C012A094J07	58.265	122.522	3.0	6.3	13.0
55	A018E094I12	58.594	121.966	3.2	6.8	14.3
56	B094H094J14	58.910	123.047	3.0	6.6	
57	A056G094P01	59.127	120.191	2.4	6.0	13.7
58	B028B094O11	59.519	123.222	3.4	7.1	14.4
59	A087G094P10	59.652	120.703	3.4		
60	D034B094P14	59.781	121.166	3.2	6.8	
61	A064B094O14	59.802	123.166	3.4	7.1	14.4
62	C075D094I08	58.315	120.434	3.2	6.7	
63	B076G094P10	59.644	120.697	3.3		
64	D095A094P01	59.081	120.053	2.2	4.8	12.0

Table 13. Effective vertical stresses for wells in the Liard Basin.

Map No.	Data source	Well Name UWI	Latitude	Longitude	Gradient (kPa/m)	SHmin - Po at 250 m (MPa)	SHmin - Po at 500 m (MPa)	SHmin - Po at 1000 m (MPa)
1	LOT	D-011-E/094-I-11	58.598	121.378	24.0	3.4	6.9	13.7
2	LOT	B-057-I/094-O-15	59.960	122.984	16.4	1.5	3.1	6.1
3	LOT	B-25-60-30-122-30	60.402	122.574	17.8	1.9	3.8	7.5
4	LOT	L-63-61-00-124-15	60.877	124.465	21.6	2.8	4.7	9.3
5	FBP	A-018-J/094-O-11	59.677	123.216	17.6	1.8	3.7	7.3
6	FBP	A-037-B/094-I-08	58.277	120.203	12.9	0.7	1.3	2.6
7	FBP	A-049-J/094-O-11	59.702	123.228	23.6	3.3	6.7	13.3
8	FBP	A-077-B/094-O-14	59.810	123.203	19.7	2.3	4.7	9.4
9	FBP	A-081-A/094-I-03	58.069	121.003	12.4	0.5	1.1	2.1
10	FBP	A-083-E/094-I-03	58.152	121.403	18.5	2.1	4.1	8.2
11	FBP	B-004-H/094-I-03	58.085	121.047	13.5	0.8	1.6	3.2
12	FBP	B-022-K/094-I-10	58.685	120.772	21.6	2.8	5.7	11.3
13	FBP	B-039-C-094-I-02	58.027	120.859	14.8	1.1	2.3	4.5
14	FBP	B-041-G-094-I-03	58.119	121.134	13.5	0.8	1.6	3.2
15	FBP	B-049-J/094-O-11	59.702	123.234	14.8	1.1	2.2	4.5
16	FBP	B-052-K-094-O-11	59.71	123.272	16.8	1.6	3.3	6.5
17	FBP	B-055-B/094-O-15	59.794	122.684	18.6	2.1	4.2	8.3
18	FBP	B-058-B/094-O-14	59.794	123.222	20.1	2.5	4.9	9.8
19	FBP	B-088-D-094-I-02	58.069	120.972	28.7	4.6	9.2	18.4
20	FBP	B-099-D-094-I-02	58.077	120.984	24.7	3.6	7.2	14.4
21	FBP	C-009-C-094-I-02	58.006	120.859	15.8	1.4	2.8	5.5
22	FBP	C-018-J/094-O-11	59.681	123.222	20.7	2.6	5.2	10.4
23	FBP	C-026-G/094-O-14	59.856	123.197	18.5	2.0	4.1	8.2
24	FBP	C-028-C-094-I-02	58.023	120.847	16.3	1.5	3.0	6.0
25	FBP	C-054-G-094-I-03	58.131	121.172	14.7	1.1	2.2	4.4
26	FBP	C-084-F-094-I-03	58.156	121.297	16	1.4	2.9	5.7
27	FBP	D-006-H-094-I-03	58.09	121.066	14.5	1.1	2.1	4.2
28	FBP	D-024-D-094-I-02	58.023	120.916	20.8	2.6	5.3	10.5
29	FBP	D-026-H-094-I-03	58.106	121.066	17.9	1.9	3.8	7.6
30	FBP	D-030-H-094-I-03	58.106	121.116	18.7	2.1	4.2	8.4
31	FBP	D-042-D-094-I-02	58.04	120.891	21.4	2.8	5.6	11.1
32	FBP	D-055-G/094-O-14	59.881	123.178	26.8	4.1	8.3	16.5
33	FBP	D-070-D-094-I-02	58.056	120.991	28.4	4.5	9.1	18.1
34	FBP	D-086-K/094-I-08	58.490	120.316	23.6	3.3	6.6	13.3

Table 14. Effective horizontal stresses for wells in the Liard Basin.  
(LOT = Leak-off test pressure, FBP = Fracture breakdown pressure)



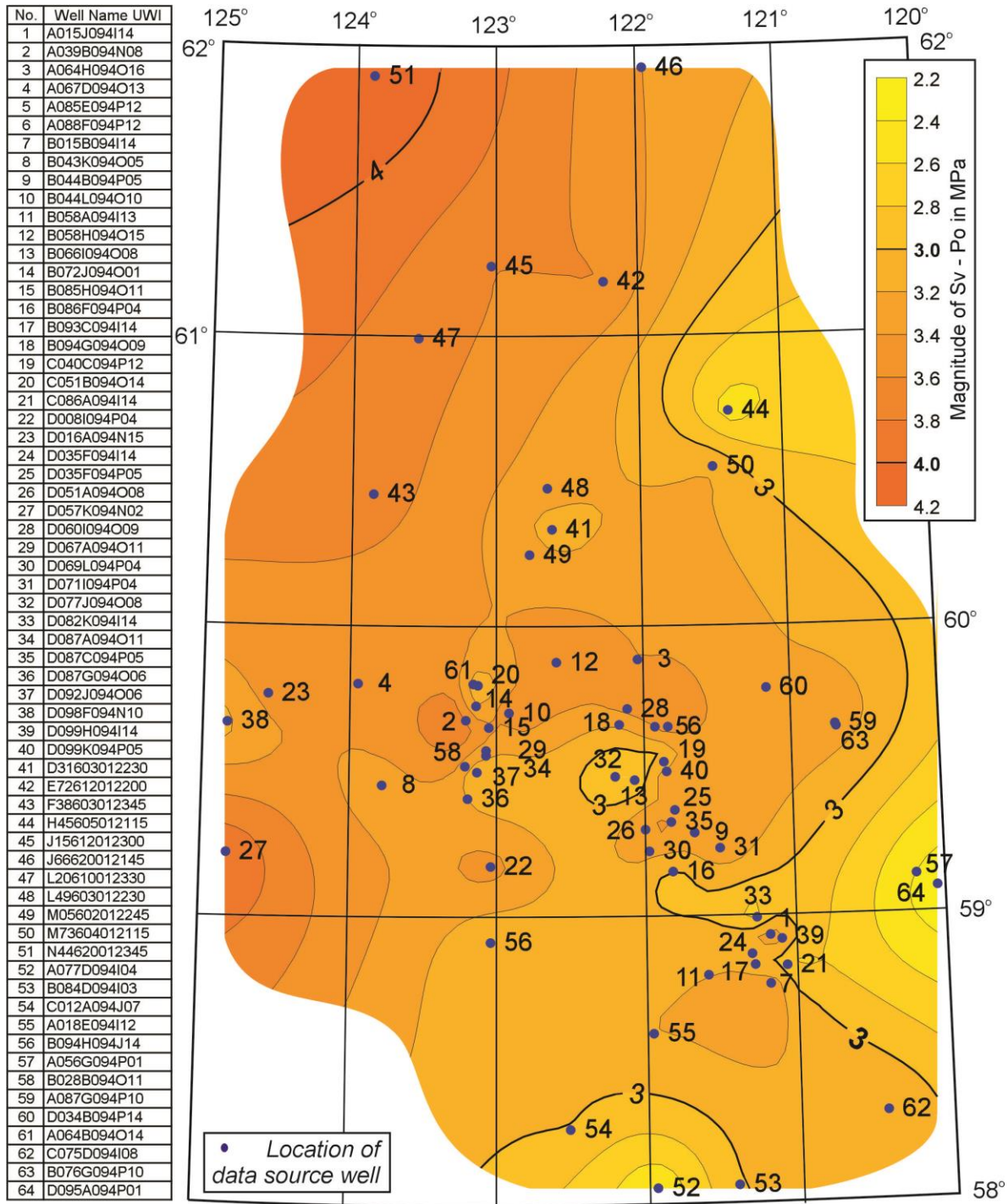


Fig. 53. Effective vertical stress at 250 m depth in the Liard Basin.

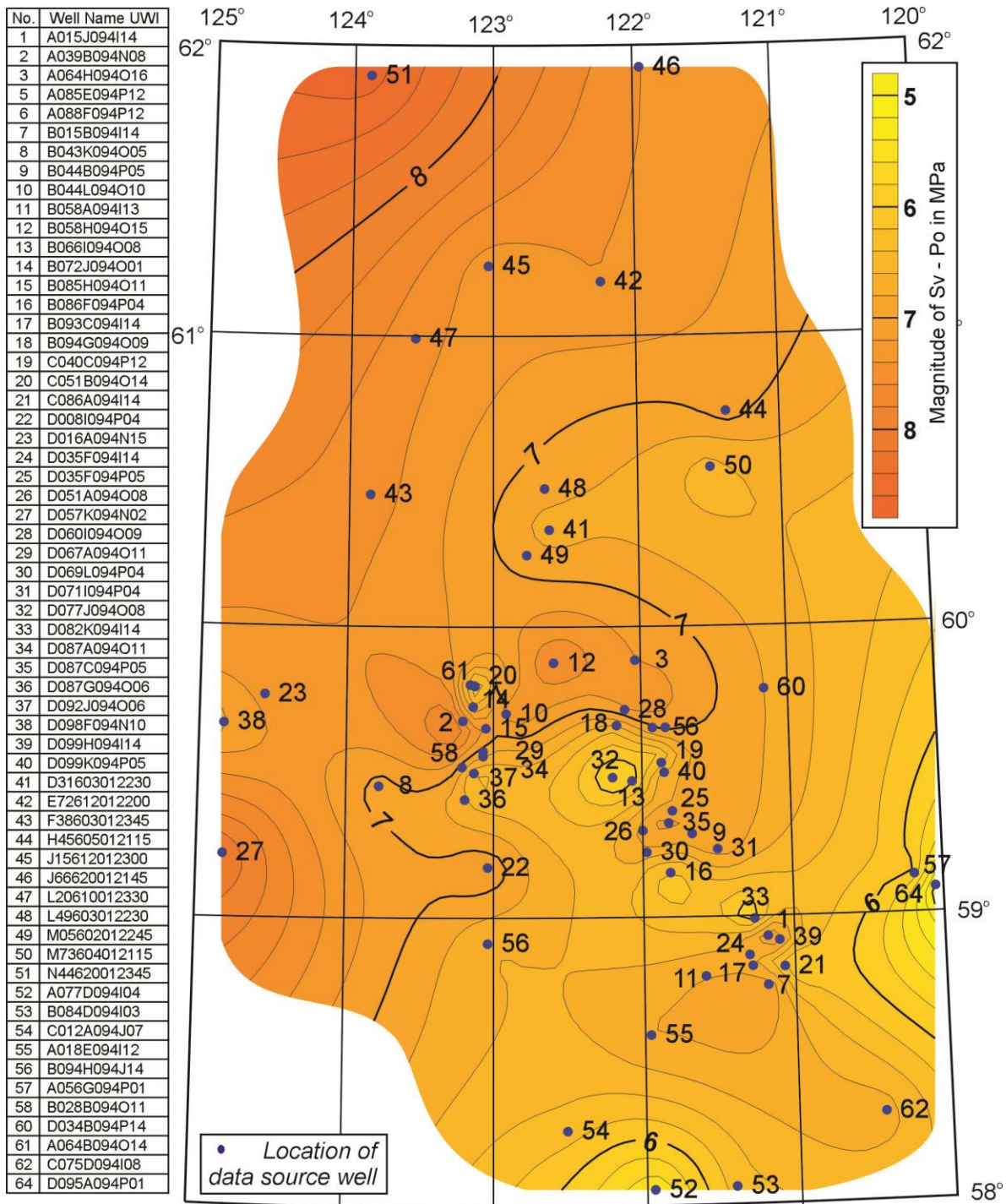


Fig. 54. Effective vertical stress at 500 m depth in the Liard Basin.

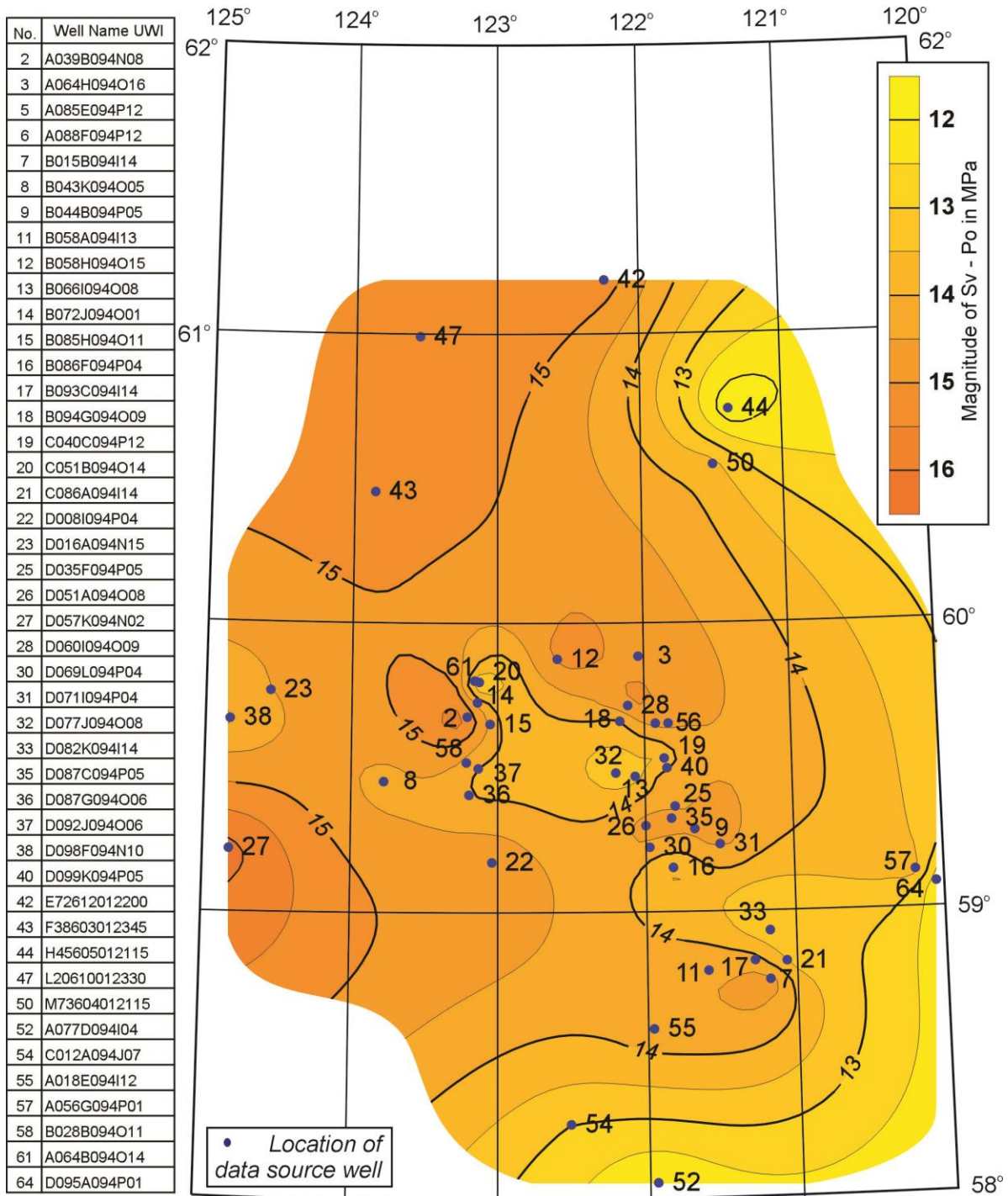


Fig. 55. Effective vertical stress at 1000 m depth in the Liard Basin.

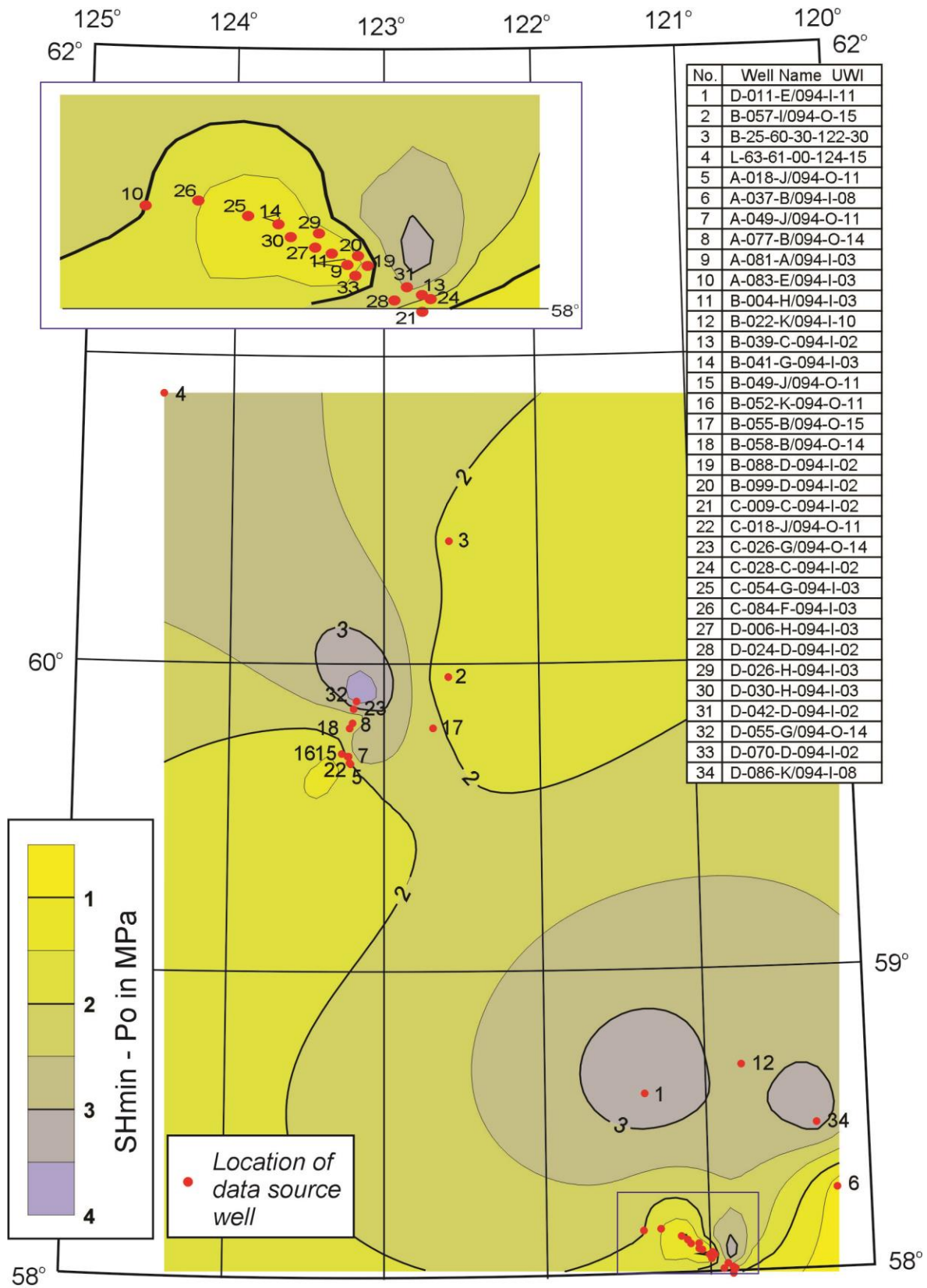


Fig. 56. Effective horizontal stress at 250 m depth in the Liard Basin. See inset (top left) for location of boxed wells.

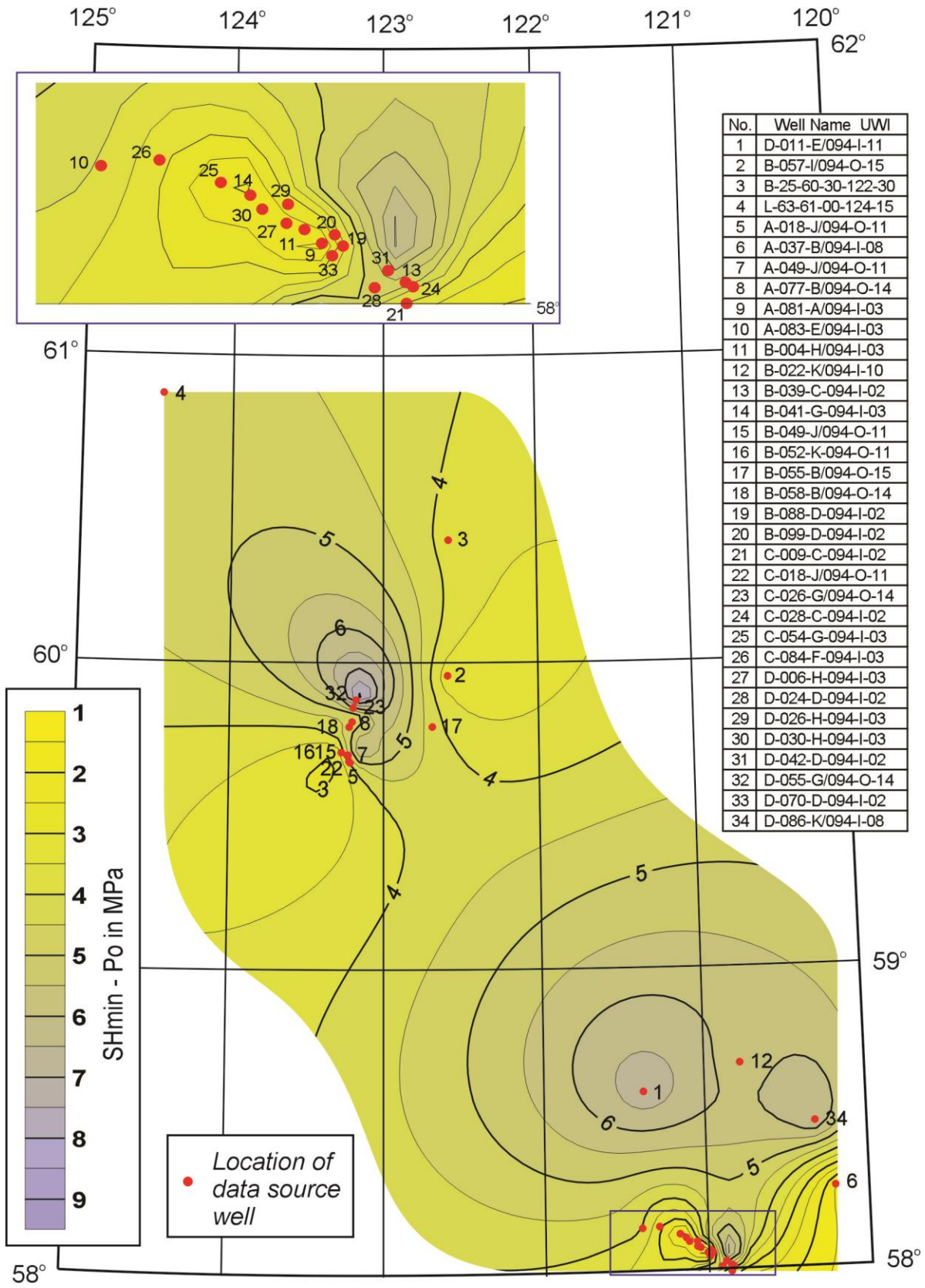


Fig. 57. Effective horizontal stress at 500 m depth in the Liard Basin.  
See inset (top left) for boxed wells.

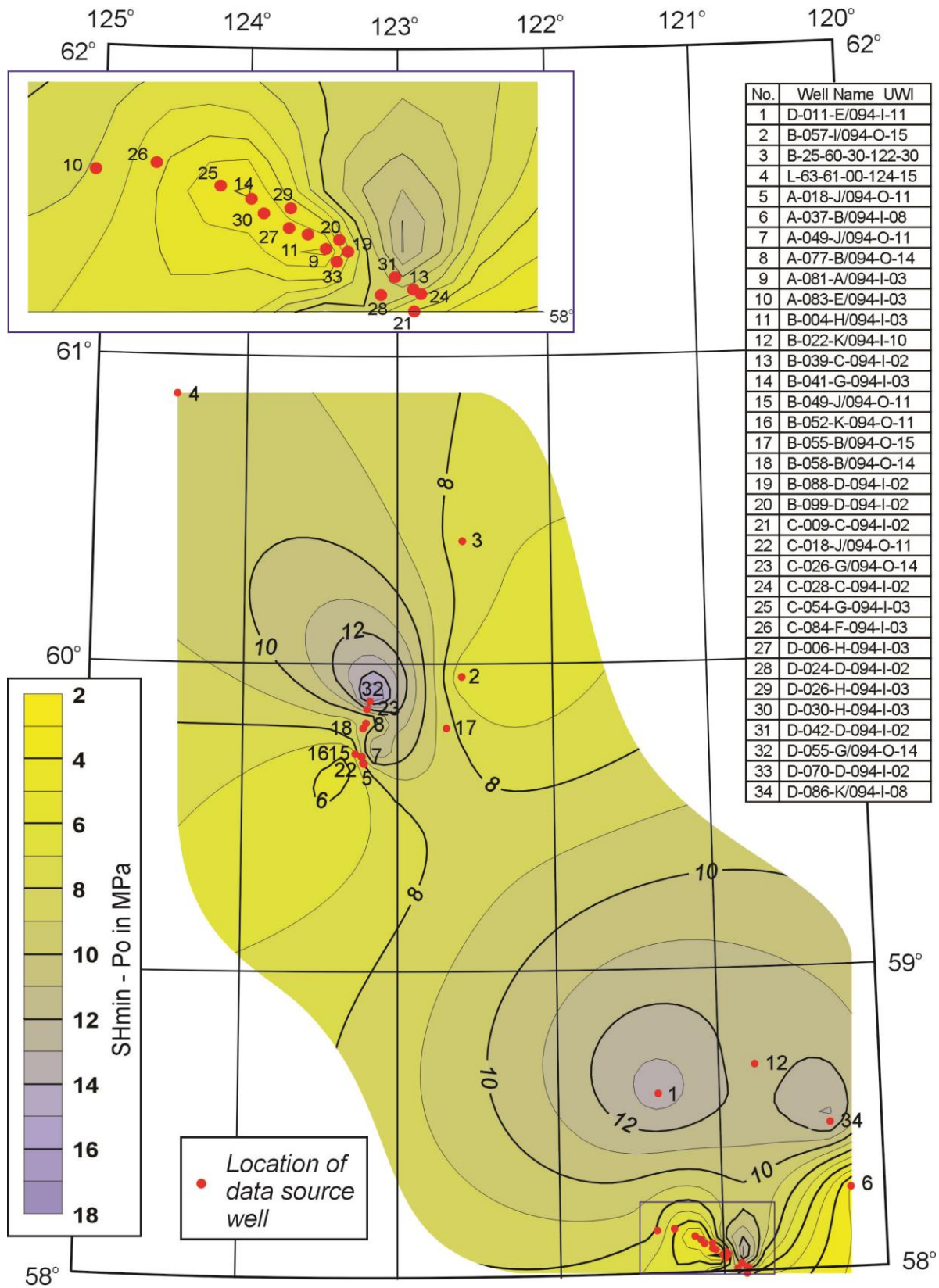


Fig. 58. Effective horizontal stress at 1000 m depth in the Liard Basin.

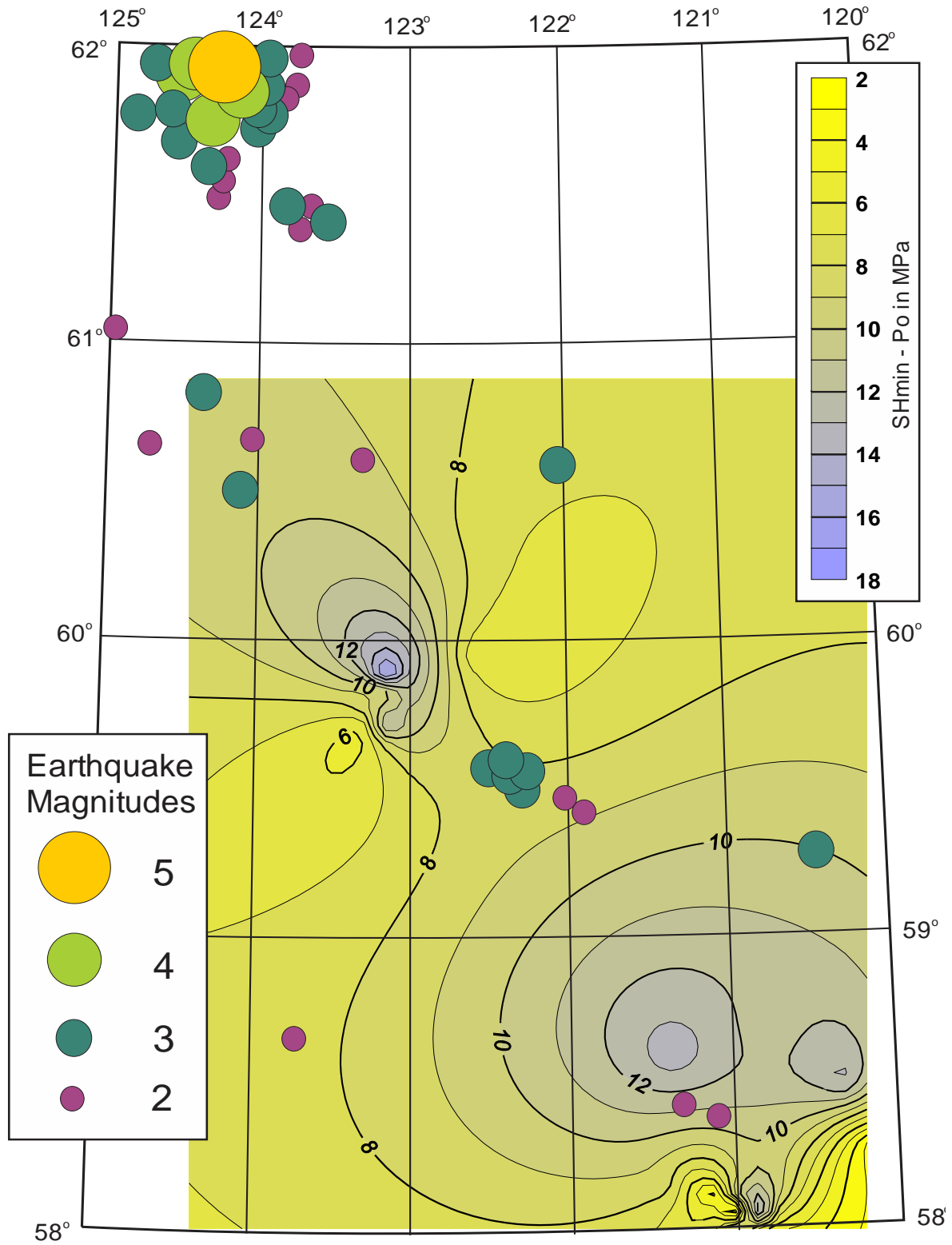


Fig. 59. Post-1985 earthquakes in the Liard Basin, superimposed on horizontal effective stress magnitudes at 1000 metres depth.

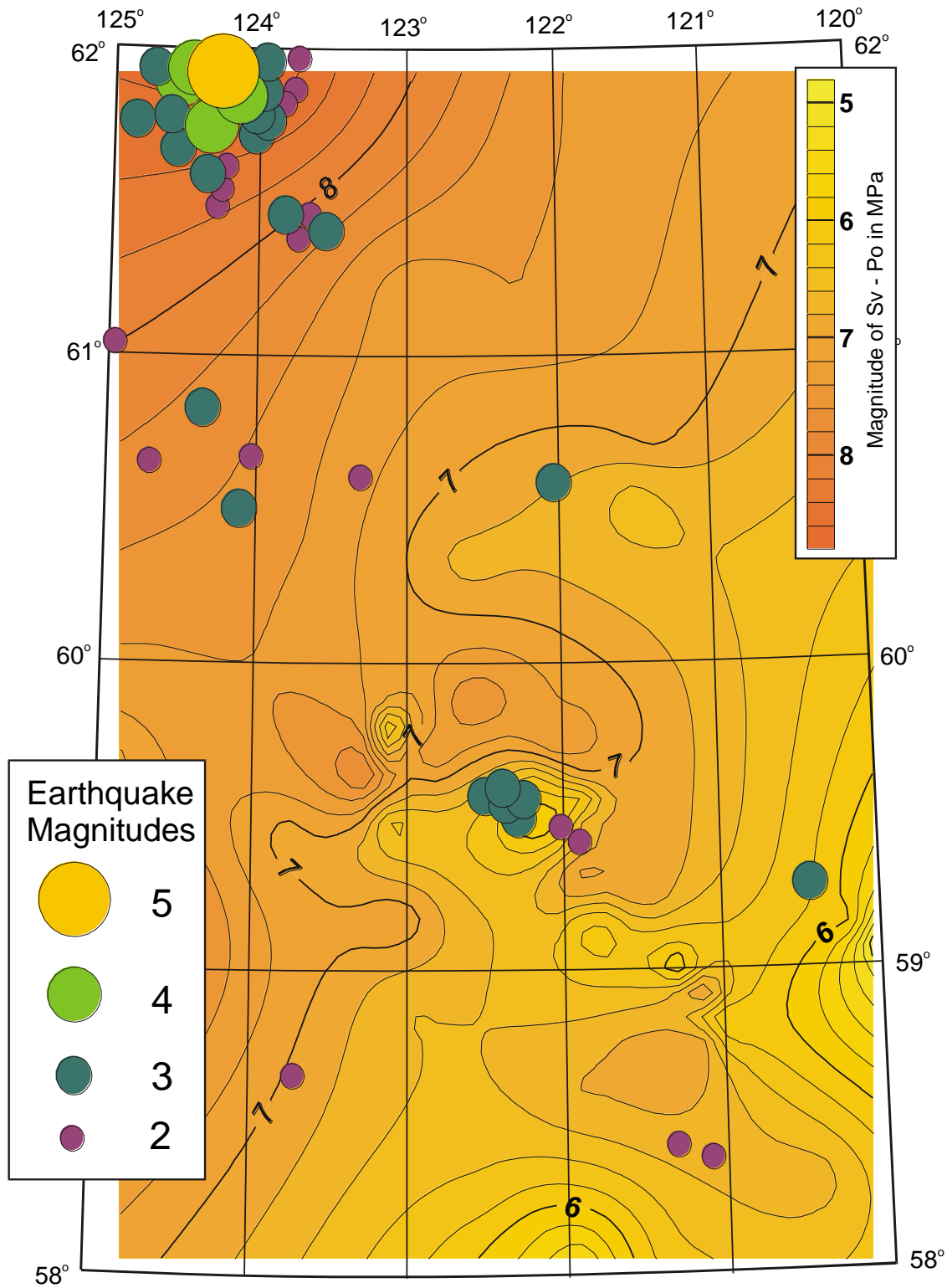


Fig. 60. Post-1985 earthquakes in the Liard Basin, superimposed on the vertical effective stress magnitudes at 500 metres depth.



## 15. TRANS-BASINAL RELATIONSHIPS

Two cross sections have been constructed to illustrate how the *in situ* stresses and pore pressure vary with depth and between wells (Figs 61, 62). Also shown is a limited amount of stratigraphic correlation, based on the formation tops listed on scout tickets. Table 14 lists all the formation tops that have been recognised by the operators and those that are represented in several adjacent wells are shown on the cross sections. Faults are not shown since such structural detail was not available to the investigator.

Formation tops	Wells in Figure 51						Wells in Figure 52				
	H-45-60-50-121-15	M-05-60-20-122-45	B-058-H/094-O-15	B-086-F/094-P-04	B-058-A/094-I-13	B-084-D/094-I-03	D-098-F/094-N-10	B-043-K/094-O-05	D-087-G/094-O-06	D-035-F/094-P-05	A-087-G/094-P-10
Sikanni	143.3	211.2						791.0			
Scatter		419.4						1330.0	385.2		
Garbutt		466.0						1601.0	537.0		
Bluesky		570.3			618.0				578.5		
Liard							399.3				
Toad							650.1				
Grayling							1174.3				
Montney						725.0					
Belloy						846.5		2418.0		670.5	
Fantasque							1473.0	2431.0			
Mattson		576.1					1538.9		623.0		
Stoddart											
Debolt			430.5	551.7	640.0	856.0		2750.0	1010.1	678.0	
Shunda			624.0	621.5							
Banff	280.4		1240.5	740.3	825.0	1084.5				831.0	409.5
Exshaw	390.4			1068.0						1204.5	723.0
Kotcho	400.5		1271.5	1074.1	1112.0	1389.0				1218.5	727.5
Tetcho	680.3		1556.3	1200.9	1210.0					1410.0	894.0
Trout River	759.0		1608.0	1236.8	1280.0					1501.0	968.0
Kakisa	819.0		1689.5	1291.7	1307.0					1540.0	986.0
Redknife	831.2			1303.3	1324.0					1555.0	1043.0
Jean Marie	968.3			1422.1	1461.0	1690.0				1736.0	1203.0
Fort Simpson	985.1		1706.0	1511.7	1493.0	1719.0				1806.0	
Muskwa			2611.0	2088.4							
Slave Point	1492.0		2710.5								
Keg River	1609.3		2762.0								
Chinchaga			2912.5	2359.6							
TD	1702.0	579.1	2950.0	2432.5	1525.0	1735.0	3755.7	2795.0	1219.5	1863.0	2192.0

Table 15. Formation tops for wells in the cross-sections in Figures 61 and 62.

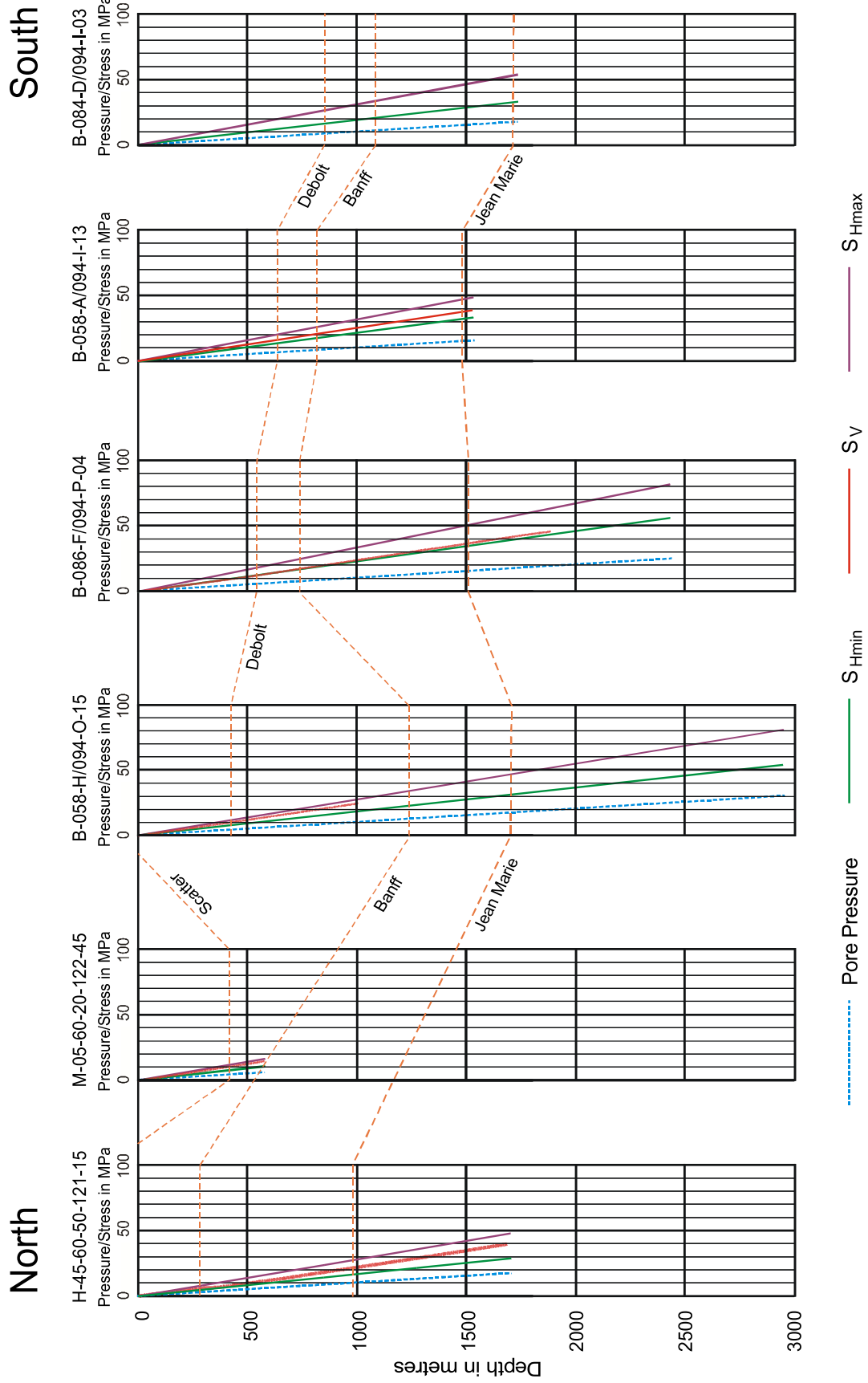
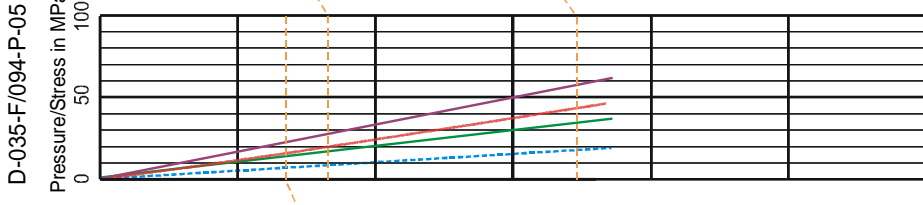
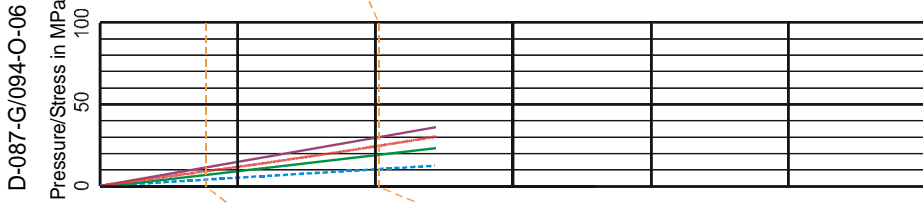
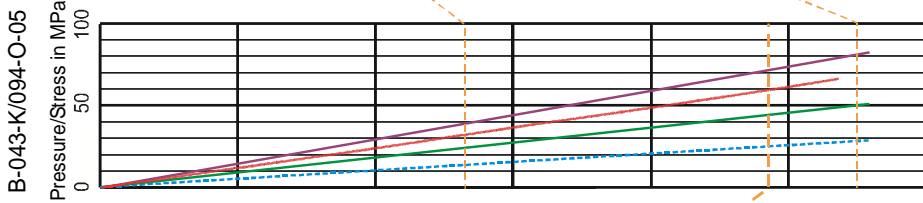
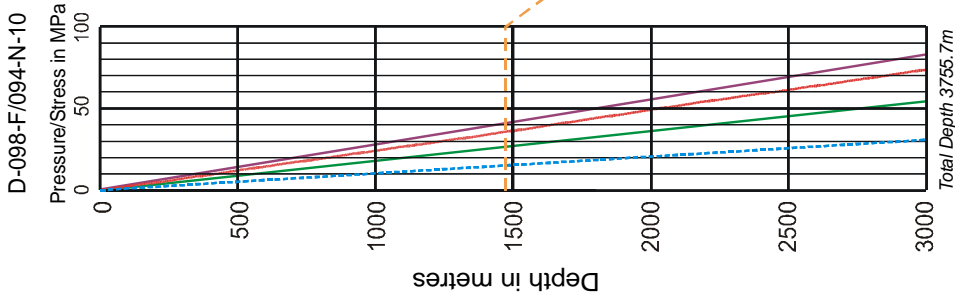


Fig. 61. North-South cross-section of stress magnitude and pore pressure profiles across the Liard Basin. From left to right, well numbers are: 44, 49, 12, 16, 11 and 53. Their locations are shown on Figure 18.

West



East

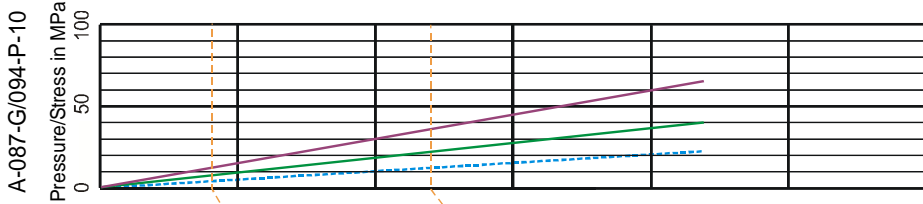


Fig. 62. West-East cross-section of stress magnitude and pore pressure profiles across the Liard Basin. From left to right, well numbers are: 38, 8, 36, 25 and 59 Their locations are shown on Figure 18.

## 16. OVERVIEW AND CONCLUSIONS

This investigation has brought to light a body of data concerning *in situ* stress in the Liard Basin. This is the first study of the stress regime of this basin and, while the results should stimulate and encourage further work, at this time the results cannot be claimed to be highly focussed. The chief reason for this is the lack of drilling information in many parts of the basin, where it is essentially unexplored.

Furthermore, most of the exploration wells in the Northwest Territories and Yukon were drilled several decades ago before modern drilling and logging techniques had been developed. Running leak-off tests was not required and, if they were run, the results were rarely reported.

There is a reasonable geographic spread of wells in which density logs were run, so mapping the vertical stress magnitudes has generated maps that cover most of the basin. This has meant that vertical stresses ( $S_V$ ) and effective vertical stresses can be well mapped. Unfortunately, much less information was available for mapping the smaller horizontal stress ( $S_{Hmin}$ ) and effective horizontal stresses. There were no closure pressure measurements of *in situ* stress and few leak-off test pressures. Locally, hydraulic fracturing supplied a number of fracture breakdown pressures but these were largely concentrated in two areas. As a result the  $S_{Hmin}$  maps do not offer good basinwide coverage.

Nevertheless, the  $S_{Hmin}$  and  $S_V$  maps were the sources for the stress magnitude information that was used in the breakout failure simulations aimed at estimating magnitudes of the larger horizontal stress,  $S_{Hmax}$ . Other modelling parameters also had to be estimated but, despite this, it is believed that the  $S_{Hmax}$  magnitudes derived from the various breakout failure routines provide sensible values. Breakouts from 27 wells were modelled. To the writer's knowledge, this is the first time that enough breakout failure simulations have been run so that  $S_{Hmax}$  gradients could be mapped across a large part of a sedimentary basin.

The effective stress maps mimic those of the stress magnitudes because there were insufficient data to customise pore pressure profiles for individual wells. There is, however, enough drill stem test data and mudweight information to demonstrate that significant overpressuring is not present in the basin.

An attempt was made to relate the geographic configurations of effective stress magnitudes to recent seismicity. There is some apparent correspondence, but this is an endeavour that requires much more information than is available today, but which may provide interesting insights in the future.

As noted in the section on vertical stress ( $S_V$ ), its areal variation in magnitude may reflect both paleogeomorphology and paleotectonics. Different amounts of recent

burial can give rise to lateral variations in  $S_V$  magnitude and one should not discount the effects of recently eroded topography or the removal of Pleistocene ice sheet loads. In this regard, it will be interesting to compare the  $S_V$  magnitude maps at specific horizons with maps of organic maturation. Laramide crustal shortening in the west may also have compressed the rocks and led to increased rock density and hence greater vertical stress magnitudes along the western margin of the basin.

In summary, this investigation has maximised the information available concerning the stress regime of the Liard Basin. These studies have shown that  $S_{H_{max}} > S_V > S_{H_{min}}$  in all wells where this can be demonstrated, so that the stress regime in Liard Basin appears to be quite similar quantitatively to that of the Western Canada Sedimentary Basin to the south.

## **17. ACKNOWLEDGEMENTS**

Sigma H Consultants is grateful to Dr. Larry Lane for his great assistance in providing data for this investigation and for arranging for the digitisation of the uncomputed dipmeter logs. Technical help from Mr. C. Overton is also acknowledged. Breakout analysis was performed with the PFAS software developed by ITC in Norway. Dr. G.S. Stockmal provided a thorough critical review and Ms. Sarah Saad conducted an in-depth editorial review of the text, tables, figures and appendices. Her close attention to detail led to a much improved final product.

## 18. REFERENCES

Aadnoy, B. S., 1990. Inversion technique to determine the in-situ stress field from fracturing data; *Journal of Petroleum Science and Engineering*, v. 6, no. 4, p. 127-141.

Bell, J. S., 1990. The stress regime of the Scotian Shelf, offshore eastern Canada to 6 kilometers depth and implications for rock mechanics and hydrocarbon migration; *in* *Rock at Great Depth*, (ed.) V. Maury and D. Fourmaintraux,; A.A. Balkema, Rotterdam, Netherlands, v. 3., p. 1243-1265.

Bell, J. S. and Babcock, E. A., 1986. The stress regime of the Western Canadian Basin and implications for hydrocarbon production. *Bulletin of Canadian Petroleum Geology*, v. 34, p. 364-378.

Bell, J. S., Caillet, G. and Adams, J., 1992. Attempts to detect open fractures and non-sealing faults with dipmeter logs; *in* *Geological Applications of Wireline Logs II*, (ed.) A.C. Hurst, C.M. Griffiths, and P.F. Worthington; Geological Society of London, special Publication No. 66, p. 211-220.

Bredehoeft, J. D., Wolff, R. G., Keys, W. S., and Schuter, E., 1976. Hydraulic fracturing to determine the regional *in situ* stress field, Piceance Basin, Colorado. *Geological Society of America Bulletin*, v. 87, no.2, p. 250-258.

David, C. and Darot, M., 1989. Permeability and conductivity of sandstones; *in* *Proceedings, symposium on Rock at Great Depth*, (ed.) V. Maury and D. Fourmaintraux; A.A.Balkema, Rotterdam, p. 203-209.

Enever, J.R., Pattison, C.I., McWatters, R.H., and Clark, I.H., 1994. The relationship between in-situ stress and reservoir permeability as a component in developing an exploration strategy for coalbed methane in Australia; *in* *EUROCK '94, SPE-ISRMRock Mechanics in Petroleum Engineering*, Balkema, Rotterdam, Netherlands, p. 163-171.

Ervine, W. B. and Bell, J. S., 1987. Subsurface *in situ* stress magnitudes from oil-well drilling records: an example from the Venture area, offshore eastern Canada; *Canadian Journal of Earth Sciences*, v. 24, no. 9, p. 1748-1759.

Gronseth, J.M. and Kry, P.R., 1983. Instantaneous Shut-in Pressure and its relationship to the minimum in-situ stress; *in* *Hydraulic Fracturing Stress Measurements*, M.D. Zoback and B.C. Haimson (eds.) National Academy Press, Washington, December 2-5, 1981, p. 55-63.

Gronseth, J.M. and Kry, P.R., 1987. *In situ* stresses and the Norman Wells expansion project; Paper 87-38-57, 38<sup>th</sup> Annual Meeting of the Petroleum Society of CIM, Calgary, Alberta, June 7-10, 9 p.

Haimson, B.C. and Fairhurst, C., 1970. In-situ stress determination at great depth by means of hydraulic fracturing; *in* Rock mechanics, theory and practice. Proceedings, 11th Symposium on Rock Mechanics, W. Somerton (eds.) American Institute of Mining Engineers, New York, NY, p. 559-584.

Heffer, K.J. and Lean, J.C., 1993. Earth stress orientation - a control on, and guide to, flooding directionality in a majority of reservoirs; *in* Reservoir Characterization III, (ed.) W. Linville; Pennwell Books, Tulsa, p. 799-822.

Hoek, E. and Brown, E. T., 1980. Underground excavations in rock; Institute of Mining and Metallurgy, London, UK, 527 p.

ITC a.s., 1998. PFAS User Manual. 65p.

Jaeger, J.C. and Cook, N.G.W., 1976. Fundamentals of rock mechanics; London, UK, Chapman and Hall, 585 p. (second edition)

Kry, P.R. and Gronseth, J.M., 1982 *In-situ* stresses and hydraulic fracturing in the Deep Basin; Paper 88-33-21, 33rd Annual Technical Meeting, Petroleum Society of CIMM, Calgary, June 6-9, 1982.

Mardia, K.V., 1972. The statistics of directional data. Academic Press. London. 357 p.

Mastin, L., 1988. Effect of borehole deviation on breakout orientations; Journal of Geophysical Research, v. 93, no. B8, p. 9187-9195.

McGarr, A. and Gay, N. C., 1978. State of stress in the Earth's crust; Annual Review of Earth and Planetary Sciences, v. 6, p. 405-436.

McLellan, P. J., 1988. In-situ stress prediction and measurement by hydraulic Fracturing, Wapiti, Alberta; Journal of Canadian Petroleum Technology, v. 27, no. 2, p. 85-95.

Moos, D. and Zoback, M. D., 1990. Utilization of observations of well bore failure to constrain the orientation and magnitude of crustal stresses: Application to continental, deep sea drilling project, and ocean drilling program boreholes; Journal of Geophysical Research, v. 95, no. B6, p. 9305-9325.

Nolte, K. G., 1988a. Principles for fracture design based on pressure analysis. SPE Production Engineering, v. 3, no. 1, p. 22-30.

- Nolte, K. G., 1988b. Application of fracture design based on pressure analysis. SPE Production Engineering, v. 3, no. 1, p. 31-42.
- Peska, P. and Zoback, M. D., 1995. Observations of borehole breakouts and tensile wall-fractures in deviated boreholes: A technique to constrain *in situ* stress and rock strength; in Proceedings of the 35<sup>th</sup> U.S. Symposium on Rock Mechanics, J. J. K Daeman and R. A. Schultz (Eds.), Balkema, Rotterdam, p. 319-325.
- Plumb, R. A. and Hickman, S. H., 1985. Stress-induced borehole elongation: A comparison between the four-arm dipmeter and the borehole televiewer in the Auburn geothermal well. Journal of Geophysical Research, v. 90, no. B7, p.5513-5521.
- Salz, L. B., 1977. Relationship between fracture propagation pressure and pore pressure; SPE Paper 6870, presented at 1977 Society of Petroleum Engineers' Annual Technical Conference and Exhibition, Denver, USA., October 9-12, 1977.
- Schneider, T., 1985. Bohrlochrandausbreuche in norddeutschen bohrungen und ihm beziehung zum regionalen spannungsfeldbeobachtung und theorie. Diploma thesis, University of Karlsruhe, Germany.
- Sparks, D.P., McLendon, T.H., Saulsberry, J.L., and Lambert, S.W., 1995. The effects of stress on coalbed reservoir performance, Black Warrior Basin, U.S.A; SPE Paper 30734 in Proceedings of the Society of Petroleum Engineers Annual Technical Conference and Exhibition, 22-25 October 1995, Dallas, USA, p. 339-351.
- Tan, C. P., Willoughby, D. R., Zhou, S., and Hillis R. R., 1993. An analytical method for determining horizontal stress bounds from wellbore data; International Journal of Rock Mechanics and Mining Sciences and Geomechanics Abstracts, v. 30. no. 7, p. 1103-1109.
- Zhou, S., 1997. A method of estimating horizontal principal stress magnitudes from stress-induced wellbore breakouts and leak-off tests and its application to petroleum engineering. Petroleum Geoscience, v. 3, no 1, p. 57-64.



## 19. APPENDIX NOTES

Appendix 1 contains the breakout statistics and commentaries for the complete suite of wells studied.

Appendix 2 contains graphic plots of the overburden gradients and vertical stress magnitudes calculated from density logs that were used to generate maps. Tables of these overburden gradients and vertical stress magnitudes are available in digital format.

Appendix 3 contains graphic plots of the breakout failure simulations that were run in order to estimate magnitudes of  $S_{Hmax}$ , the larger horizontal stress. Also included for each well are tables of the parameters used in the numerical modeling and commentary texts. All of this material is also available in digital format.

## Appendix 1: Breakout Statistics and Commentaries

### Well: A-006-C/094-O-08 Breakouts identified by PFAS

Magnetic Declination 31.2

Breakout Interval		Length (m)	Measured azimuth (degrees)	Standard Deviation (degrees)	Corrected Azimuth (degrees)
Top (mKB)	Base (mKB)				
1352	1364	12	9.9	3.4	41.1
1369	1375	6	7.4	1.5	38.6
1439	1441	2	35.2	2.4	66.4
1445	1491	46	44.5	3.4	75.7
2197	2219	22	110.4	2.1	141.6
2391	2396	5	90.1	2.5	121.3
2456	2475	19	25.4	1.7	56.6

Total thickness of Breakouts (m)	90.0
Breakouts associated with washouts (m)	22.0
Washouts (m)	30.0
Key Seats (m)	0.0
Undergauge hole (m)	0.0
In gauge hole (m)	370.0
Undetermined intervals (m)	892.0
Thickness of logged interval (m)	1404.0

Mean Azimuth of all breakouts (degrees)	71.2
<b>Mean azimuth of SHmax from all breakouts</b>	<b>161.2</b>
Standard Deviation (degrees)	34.4
Mean Azimuth of Pop 1 breakouts (degrees)	64.3
<b>Mean azimuth of Pop 1 SHmax (degrees)</b>	<b>154.3</b>
Standard Deviation (degrees)	15.8
Mean Azimuth of Pop 2 breakouts (degrees)	137.8
<b>Mean azimuth of Pop 2 SHmax (degrees)</b>	<b>47.8</b>
Standard Deviation (degrees)	7.9

#### ANALYTICAL PARAMETERS

Interval	1348-2750 m
Bit size	8.5 in
Minimum smaller hole axis diameter	7.5 in
Maximum smaller hole axis diameter	9.5 in
Minimum axes diameter difference	0.5 in
Maximum vertical deviation of well	10°
Azimuth tolerance within breakout	5°
Maximum tool rotation within breakout	5°
Minimum length of breakout	2 m

Well: A-006-C/094-O-08

The dipmeter record for this well is poor, making it difficult to determine how to interpret the breakout axes. There are two populations with long axes at high angles to each other.

Population 1 consists of 5 breakouts with a net thickness of 90 metres and exhibits a mean azimuth of  $64.3^\circ \pm 15.8^\circ$ . Population 2 consists of 2 breakouts with a net thickness of 27 metres and mean azimuth of  $137.8^\circ \pm 7.9^\circ$ . It is present in the lower part of the logged interval.

Four of the breakouts in Population 1 occur at the top of the logged interval.

It is possible that the caving there is due to collapse of drilling induced fractures possibly associated with a leak off test, although there is no documentation of such a procedure in the drilling history of this well.

However, for this reason, the regional stress axes are provisionally interpreted as aligned with Population 2, and also because this is the predominant orientation for  $S_{Hmin}$  and  $S_{Hmax}$  in the Liard Basin. Future work may indicate that stress trajectories have been locally deflected by faults.

**Well: A-045-E/094-O-10 Breakouts identified by PFAS**

Magnetic Declination 31.3

Breakout Interval		Length (m)	Measured azimuth (degrees)	Standard Deviation (degrees)	Corrected Azimuth (degrees)
Top (mKB)	Base (mKB)				
236	243	7	115.4	2.8	146.7
250	286	36	120.5	5.6	151.8
515	560	45	118.8	2.3	150.1
563	593	30	116.9	2.8	148.2
601	633	32	111.5	2.7	142.8
637	644	7	115.0	1.6	146.3
647	674	27	118.5	1.4	149.8
781	787	6	110.6	4.1	141.9
790	794	4	116.0	1.5	147.3
803	807	4	102.3	3.4	133.6
816	821	5	104.9	0.9	136.2
843	846	3	102.6	1.3	133.9
916	922	6	89.3	1.6	120.6

Total thickness of Breakouts (m)	204.0
Breakouts associated with washouts (m)	8.0
Washouts (m)	9.0
Key Seats (m)	0.0
Undergauge hole (m)	0.0
In gauge hole (m)	534.0
Undetermined intervals (m)	85.0
Thickness of logged interval (m)	840.0

Mean Azimuth of all breakouts (degrees)	146.9
<b>Mean azimuth of SHmax from all breakouts</b>	<b>56.9</b>
Standard Deviation (degrees)	6.2
Mean Azimuth of Pop 1 breakouts (degrees)	146.9
<b>Mean azimuth of Pop 1 SHmax (degrees)</b>	<b>56.9</b>
Standard Deviation (degrees)	6.2

**ANALYTICAL PARAMETERS**

Interval	149-1006 m
Bit size	8.5 in
Minimum smaller hole axis diameter	7.5 in
Maximum smaller hole axis diameter	9.5 in
Minimum axes diameter difference	0.5 in
Maximum vertical deviation of well	10°
Azimuth tolerance within breakout	5°
Maximum tool rotation within breakout	5°
Minimum length of breakout	2 m

Well: A-045-E-094-O-10

Well A-045-E-094-O-10 has 13 breakouts between 236 and 922 m KB. They all fall into one population with a mean azimuth of  $146.9^{\circ} \pm 6.2^{\circ}$  and a net thickness of 212 metres.

**Well: A-067-D/094-O-13 Breakouts identified by PFAS**

Magnetic Declination 31.6

Breakout Interval		Length (m)	Measured azimuth (degrees)	Standard Deviation (degrees)	Corrected Azimuth (degrees)
Top (mKB)	Base (mKB)				
233	239	6	82.3	3.5	113.9
313	321	8	81.7	3.3	113.3
348	357	9	45.5	2.0	77.1
360	361	1	44.7	0.1	76.3
363	364	1	44.1	0.8	75.7
383	394	11	68.2	1.4	99.8
399	452	53	78.0	3.0	109.6
455	482	27	87.4	5.5	119.0
485	486	1	94.7	0.4	126.3
492	499	7	99.0	1.9	130.6
525	553	28	77.7	3.6	109.3
585	591	6	80.2	1.3	111.8
596	600	4	83.5	0.5	115.1
607	613	6	82.4	0.9	114.0
618	620	2	94.4	1.2	126.0
644	645	1	80.9	0.4	112.5
646	651	5	77.2	2.8	108.8
655	656	1	77.1	0.7	108.7
671	672	1	95.0	0.3	126.6
691	692	1	81.6	0.0	113.2
700	728	28	64.2	5.9	95.8
736	743	7	69.7	2.1	101.3
745	753	8	71.4	2.1	103.0
776	804	28	69.0	2.1	100.6
816	819	3	71.3	2.6	102.9
824	850	26	67.5	4.0	99.1
894	901	7	61.1	1.9	92.7
904	905	1	59.1	1.1	90.7
910	912	2	60.4	3.5	92.0
915	916	1	60.7	1.9	92.3
919	921	2	62.8	1.4	94.4
924	931	7	64.2	4.0	95.8
934	935	1	52.7	1.4	84.3
938	939	1	58.7	1.9	90.3
970	978	8	76.6	2.6	108.2
981	992	11	68.0	1.2	99.6
1031	1061	30	70.6	2.6	102.2
1064	1074	10	67.8	2.6	99.4
1077	1079	2	65.4	0.8	97.0
1082	1104	22	70.5	4.3	102.1
1107	1114	7	72.3	3.2	103.9
1117	1124	7	76.2	1.7	107.8
1129	1138	9	71.7	2.1	103.3
1141	1153	12	72.4	1.6	104.0
1156	1160	4	80.1	2.8	111.7

1163	1183	20	80.0	3.5	111.6
1186	1210	24	78.8	2.2	110.4
1212	1224	12	78.8	2.6	110.4
1233	1241	8	79.4	1.3	111.0
3502	3505	3	63.0	6.8	94.6
3579	3583	4	56.2	3.6	87.8
3664	3695	31	68.9	5.0	100.5
3712	3718	6	63.9	6.3	95.5
3725	3744	19	64.7	5.2	96.3
3751	3767	16	70.2	9.8	101.8
3782	3820	38	72.5	3.0	104.1
3824	3916	92	67.4	4.8	99.0
3931	3952	21	101.2	4.0	132.8
3954	4000	46	99.5	3.1	131.1
4005	4007	2	95.5	0.8	127.1
4015	4018	3	95.7	2.0	127.3
4058	4071	13	98.0	2.5	129.6
4094	4103	9	134.6	3.0	166.2
4195	4208	13	89.5	6.5	121.1
4241	4247	6	147.6	1.9	179.2
4457	4459	2	87.6	1.1	119.2
4542	4555	13	128.3	3.0	159.9
5203	5233	30	90.6	5.8	122.2
5264	5271	7	113.3	2.4	144.9

Total thickness of Breakouts (m)	227.0
Breakouts associated with washouts (m)	634.0
Washouts (m)	362.0
Key Seats (m)	1.0
Undergauge hole (m)	0.0
In gauge hole (m)	1091.0
Undetermined intervals (m)	2845.0
Thickness of logged interval (m)	5160.0

Mean Azimuth of all breakouts (degrees)	108.5
<b>Mean azimuth of SHmax from all breakouts</b>	<b>18.5</b>
Standard Deviation (degrees)	14.9
Mean Azimuth of Pop 1 breakouts (degrees)	108.5
<b>Mean azimuth of Pop 1 SHmax (degrees)</b>	<b>18.5</b>
Standard Deviation (degrees)	14.9

#### ANALYTICAL PARAMETERS

Interval	200-3400 m
Bit size	17.5 in
Minimum smaller hole axis diameter	16.5 in
Maximum smaller hole axis diameter	18.5 in
Minimum axes diameter difference	0.5 in
Maximum vertical deviation of well	10°
Azimuth tolerance within breakout	5°
Maximum tool rotation within breakout	5°

Minimum length of breakout	1 m
Interval	3400-5376 m
Bit size	7.75 in
Minimum smaller hole axis diameter	6.75 in
Maximum smaller hole axis diameter	8.75 in
Minimum axes diameter difference	0.5 in
Maximum vertical deviation of well	10°
Azimuth tolerance within breakout	5°
Maximum tool rotation within breakout	5°
Minimum length of breakout	1 m

Well: A-067-D/094-O-13

Well A-067-D/094-O-13 exhibits consistent breakout orientations throughout the logged interval. The mean azimuth calculates at 108.5° with a small standard deviation of 14.9°.

Dipmeter logs are available from 216 to 1250 m KB (Mesozoic section) and from 3414 to 5377 m KB (Paleozoic section). Mesozoic breakouts exhibit a mean azimuth of 105.5° +/- 8.5°. Paleozoic breakouts exhibit a mean azimuth of 113.3° +/- 20.0°. There are 49 breakouts in the logged Mesozoic section with a net thickness of 487 metres. The logged Paleozoic section contains 20 breakouts with a net thickness of 374 metres.



**Well: A-081-J/094-P-04 Breakouts identified by PFAS**

Magnetic Declination 26.4

Breakout Interval		Length (m)	Measured azimuth (degrees)	Standard Deviation (degrees)	Corrected Azimuth (degrees)
Top (mKB)	Base (mKB)				
2045	2047	2	5.5	1.3	31.9
2048	2057	9	2.5	2.5	28.9
2110	2121	11	178.2	1.6	204.6
2121	2152	31	176.8	1.7	203.2
2260	2263	3	94.4	2.6	120.8
2279	2283	4	52.6	1.9	79.0
2295	2301	6	152.3	2.8	178.7
2306	2310	4	115.4	0.8	141.8
2315	2318	3	98.6	1.1	125.0

Total thickness of Breakouts (m)	20.0
Breakouts associated with washouts (m)	53.0
Washouts (m)	97.0
Key Seats (m)	0.0
Undergauge hole (m)	2.0
In gauge hole (m)	297.0
Undetermined intervals (m)	46.0
Thickness of logged interval (m)	515.0

Mean Azimuth of all breakouts (degrees)	21.3
<b>Mean azimuth of SHmax from all breakouts</b>	<b>111.3</b>
Standard Deviation (degrees)	26.6
Mean Azimuth of Pop 1 breakouts (degrees)	22.4
<b>Mean azimuth of Pop 1 SHmax (degrees)</b>	<b>112.4</b>
Standard Deviation (degrees)	8.1
Mean Azimuth of Pop 2 breakouts (degrees)	118.2
<b>Mean azimuth of Pop 2 SHmax (degrees)</b>	<b>28.2</b>
Standard Deviation (degrees)	25.5

ANALYTICAL PARAMETERS

Interval	2044-2560m
Bit size	8.5 in
Minimum smaller hole axis diameter	7.5 in
Maximum smaller hole axis diameter	9.5 in
Minimum axes diameter difference	0.5 in
Maximum vertical deviation of well	10°
Azimuth tolerance within breakout	5°
Maximum tool rotation within breakout	5°
Minimum length of breakout	2 m

Well: A-081-J/094-P-04

Well A-081-J/094-P-04 has breakouts above 2350 m KB. Orientations are consistent for the upper four breakouts but variable for the five that are deeper. Whether either Population 1 or Population 2 are giving accurate axes for  $S_{Hmin}$  is questionable, but Population 1 is provisionally mapped as representing  $S_{Hmin}$ , despite the fact that Population 2 with a mean azimuth of  $118.2^\circ \pm 25.5^\circ$  is more closely aligned with the mean breakout axes of neighbouring wells B-044-B/094-P-05 and D-087-A/094-O-11.

Population 1 yields a mean azimuth of  $22.4^\circ \pm 8.1^\circ$  from a net thickness of breakouts of 59 metres, whereas Population 2 only consists of 14 net metres.

**Well: A-085-E/094-P-12 Breakouts identified by PFAS**

Magnetic Declination 30

Breakout Interval		Length (m)	Measured azimuth (degrees)	Standard Deviation (degrees)	Corrected Azimuth (degrees)
Top (mKB)	Base (mKB)				
2048	2071	23	66.5	2.2	96.5
2076	2084	8	77.8	2.1	107.8
2086	2092	6	76.7	2.0	106.7
2110	2117	7	124.0	2.1	154.0
2121	2124	3	122.1	1.5	152.1
2142	2147	5	135.3	1.9	165.3
2155	2159	4	133.7	4.0	163.7
2163	2190	27	132.1	4.2	162.1
2201	2207	6	134.9	0.5	164.9
2230	2237	7	134.2	2.6	164.2
2240	2245	5	137.1	3.4	167.1
2253	2259	6	116.0	1.1	146.0

Total thickness of Breakouts (m)	0.0
Breakouts associated with washouts (m)	107.0
Washouts (m)	12.0
Key Seats (m)	0.0
Undergauge hole (m)	0.0
In gauge hole (m)	253.0
Undetermined intervals (m)	136.0
Thickness of logged interval (m)	508.0

Mean Azimuth of all breakouts (degrees)	54.7
<b>Mean azimuth of SHmax from all breakouts</b>	<b>144.7</b>
Standard Deviation (degrees)	31.1
Mean Azimuth of Pop 1 breakouts (degrees)	160.7
<b>Mean azimuth of Pop 1 SHmax (degrees)</b>	<b>70.7</b>
Standard Deviation (degrees)	5.9
Mean Azimuth of Pop 2 breakouts (degrees)	100.6
<b>Mean azimuth of Pop 2 SHmax (degrees)</b>	<b>10.6</b>
Standard Deviation (degrees)	5.3

ANALYTICAL PARAMETERS

Interval	2050-2300 m
Bit size	8.5 in
Minimum smaller hole axis diameter	7.5 in
Maximum smaller hole axis diameter	9.5 in
Minimum axes diameter difference	0.5 in
Maximum vertical deviation of well	10°
Azimuth tolerance within breakout	5°
Maximum tool rotation within breakout	5°
Minimum length of breakout	2 m
Interval	2300-2557 m
Bit size	6.0 in
Minimum smaller hole axis diameter	5.0 in

Maximum smaller hole axis diameter	6.0 in
Minimum axes diameter difference	0.5 in
Maximum vertical deviation of well	10°
Azimuth tolerance within breakout	5°
Maximum tool rotation within breakout	5°
Minimum length of breakout	2 m

Well: A-085-E/094-P-12

The  $S_{Hmin}$  axis for Population 1 at well A-085-E/094-P-12 is aligned at  $160.7^\circ \pm 5.9^\circ$  according to a cluster of breakouts between depths of 2110 and 2259 metres KB. Nine breakouts in this population cover a net thickness of 70 metres.

Higher in the well are three breakouts amounting to a net thickness of 37 metres with a mean azimuth of  $100.6^\circ \pm 5.3^\circ$  for Population 2. Combining the two populations gives a mean azimuth of  $144.7^\circ$ , but with a standard deviation of  $31.1^\circ$ , which is unreasonably high, so the Population 1 azimuth is preferred. Moreover, it is derived from a deeply caved zone as the graphic log indicates.

**Well: B-019-K/094-N-16 Breakouts identified by PFAS**

Magnetic Declination 32.1

Breakout Interval		Length (m)	Measured azimuth (degrees)	Standard Deviation (degrees)	Corrected Azimuth (degrees)
Top (mKB)	Base (mKB)				
865	885	20	52.5	1.9	84.6
899	912	13	51.9	2.1	84.0
912	943	31	63.8	6.9	95.9
975	981	6	72.8	1.6	104.9
1001	1011	10	46.2	1.8	78.3
1015	1017	2	43.7	0.3	75.8
1020	1021	1	40.2	1.5	72.3
1095	1107	12	33.9	2.2	66.0
1115	1151	36	19.6	3.1	51.7
1238	1277	39	55.8	2.0	87.9
1450	1453	3	53.3	1.3	85.4
1503	1513	10	63.9	2.0	96.0
1670	1675	5	70.6	1.8	102.7
2026	2030	4	113.8	2.4	145.9
2046	2052	6	108.2	1.1	140.3
2094	2100	6	172.2	1.2	204.3
2107	2113	6	135.2	3.4	167.3
2157	2164	7	102.6	3.5	134.7
2166	2171	5	98.9	5.4	131.0
2211	2214	3	110.6	2.0	142.7
2215	2218	3	20.0	0.9	52.1
2230	2234	4	102.0	1.7	134.1
2255	2257	2	117.6	1.3	149.7
2272	2274	2	115.8	1.3	147.9
2279	2281	2	113.5	0.4	145.6
2282	2285	3	109.2	1.6	141.3
2286	2293	7	108.7	2.3	140.8
2298	2302	4	104.0	2.1	136.1
2329	2336	7	25.0	3.0	57.1
2340	2345	5	18.0	1.3	50.1
2363	2367	4	114.3	1.4	146.4
2400	2413	13	177.2	2.0	209.3
2429	2436	7	10.5	2.2	42.6
2451	2452	1	7.7	1.6	39.8
2464	2489	25	19.5	2.6	51.6
2502	2507	5	27.7	3.2	59.8
2540	2547	7	124.0	1.3	156.1
2611	2649	38	77.6	8.5	109.7
2664	2668	4	13.2	2.2	45.3
2691	2694	3	15.8	3.2	47.9
2722	2728	6	115.7	2.9	147.8
2756	2764	8	91.8	2.7	123.9
2786	2820	34	91.3	5.7	123.4
2821	2838	17	95.0	2.7	127.1
2854	2861	7	109.6	3.2	141.7

2881	2886	5	105.3	1.2	137.4
------	------	---	-------	-----	-------

Total thickness of Breakouts (m)	269.0
Breakouts associated with washouts (m)	179.0
Washouts (m)	155.0
Key Seats (m)	205.0
Undergauge hole (m)	5.0
In gauge hole (m)	771.0
Undetermined intervals (m)	464.0
Thickness of logged interval (m)	2048.0

Mean Azimuth of all breakouts (degrees)	95.7
<b>Mean azimuth of SHmax from all breakouts</b>	<b>5.7</b>
Standard Deviation (degrees)	38.2
Mean Azimuth of Pop 1 breakouts (degrees)	78.9
<b>Mean azimuth of Pop 1 SHmax (degrees)</b>	<b>168.9</b>
Standard Deviation (degrees)	22.6
Mean Azimuth of Pop 2 breakouts (degrees)	138.3
<b>Mean azimuth of Pop 2 SHmax (degrees)</b>	<b>48.3</b>
Standard Deviation (degrees)	23.3

#### ANALYTICAL PARAMETERS

Interval	853-2889m
Bit size	12.25 in
Minimum smaller hole axis diameter	11.25 in
Maximum smaller hole axis diameter	13.25 in
Minimum axes diameter difference	0.5 in
Maximum vertical deviation of well	10°
Azimuth tolerance within breakout	5°
Maximum tool rotation within breakout	5°
Minimum length of breakout	2 m

Much of Population 1 could be interpreted as key seating  
Log below 2889m needs to be redigitised.

#### Well: B-019-K/094-N-16

In well B-019-K/094-N-16, 448 net metres of breakouts were identified between depths of 865 and 2886 m KB. Long axis orientation was quite variable and the two populations identified could have been grouped differently. Population 1 consists of 23 breakouts with a net thickness of 286 metres and has a mean azimuth of  $78.9^{\circ} \pm 22.6^{\circ}$ . Population 2 consists of 23 breakouts with a net thickness of 162 metres and has a mean azimuth of  $138.3^{\circ} \pm 23.3^{\circ}$ . Many of the breakouts in Population 1 occur in the upper part of the logged section and could possibly be due to key seat caving rather than stress-induced borehole breakout effects. Because of this, the provisional interpretation of the orientation of  $S_{Hmin}$  at this well is interpreted as being aligned with Population 2 at  $138.3^{\circ} \pm 23.3^{\circ}$ .

**Well: B-021-K/094-O-14 Breakouts identified by PFAS**

Magnetic Declination 31.3

Breakout Interval		Length (m)	Measured azimuth (degrees)	Standard Deviation (degrees)	Corrected Azimuth (degrees)
Top (mKB)	Base (mKB)				
329	347	18	71.3	2.2	102.6
348	349	1	67.6	0.0	98.9
352	382	30	68.4	2.8	99.7
382	403	21	68.0	2.5	99.3
540	574	34	46.9	3.3	78.2
684	693	9	142.1	1.0	173.4
707	738	31	151.0	2.1	182.3
816	1012	196	68.7	3.9	100.0
1125	1131	6	82.8	2.8	114.1
1160	1169	9	84.6	0.6	115.9
1264	1301	37	30.9	5.2	62.2
1350	1352	2	66.6	1.1	97.9
1356	1359	3	54.0	2.1	85.3
1401	1409	8	68.9	2.9	100.2
1466	1493	27	150.4	2.8	181.7
1825	1827	2	101.6	3.2	132.9
1864	1871	7	109.6	8.2	140.9
1899	1903	4	102.3	2.3	133.6
1932	1934	2	102.9	2.0	134.2
1947	1948	1	103.0	3.2	134.3
1960	1964	4	116.3	8.0	147.6
2001	2003	2	105.9	1.2	137.2
2018	2035	17	88.9	6.6	120.2
2044	2051	7	90.7	2.7	122.0
2055	2076	21	89.0	5.7	120.3
2128	2133	5	94.5	4.2	125.8
2210	2213	3	108.0	4.8	139.3
2215	2217	2	128.8	5.0	160.1

Total thickness of Breakouts (m)	434.0
Breakouts associated with washouts (m)	75.0
Washouts (m)	13.0
Key Seats (m)	8.0
Undergauge hole (m)	0.0
In gauge hole (m)	1228.0
Undetermined intervals (m)	251.0
Thickness of logged interval (m)	2009.0

Mean Azimuth of all breakouts (degrees)	102.6
<b>Mean azimuth of SHmax from all breakouts</b>	<b>12.6</b>
Standard Deviation (degrees)	29.0
Mean Azimuth of Pop 1 breakouts (degrees)	98.3
<b>Mean azimuth of Pop 1 SHmax (degrees)</b>	<b>8.3</b>

Standard Deviation (degrees)	14.8
Mean Azimuth of Pop 2 breakouts (degrees)	169.6
<b>Mean azimuth of Pop 2 SHmax (degrees)</b>	<b>79.6</b>
Standard Deviation (degrees)	12.0

#### ANALYTICAL PARAMETERS

Interval	274-2298 m
Bit size	8.5 in
Minimum smaller hole axis diameter	7.5 in
Maximum smaller hole axis diameter	9.5 in
Minimum axes diameter difference	0.5 in
Maximum vertical deviation of well	10°
Azimuth tolerance within breakout	5°
Maximum tool rotation within breakout	5°
Minimum length of breakout	2 m

#### Well: B-021-K/094-O-14

In the upper 1500 metres of this well, 432 net metres of breakouts in Mesozoic age rocks exhibit significant vertical extent and extensive caving accompanied by variable orientations. Their mean azimuth is  $96.5^{\circ} \pm 28.4^{\circ}$ . In contrast, in the 77 net metres of breakouts within the Paleozoic section below 1507 metres KB, they are shorter in vertical extent and exhibit much more directional consistency. Their mean azimuth is  $139.6^{\circ} \pm 10.3^{\circ}$ .

This raises the question as to how much emphasis to place on the statistically determined populations. Population 1 contains 412 net metres of breakouts with a mean azimuth of  $98.3^{\circ} \pm 14.8^{\circ}$ . Population 2 contains 97 net metres of breakouts with a mean azimuth of  $169.6^{\circ} \pm 12.0^{\circ}$ .

Provisionally, the  $S_{Hmin}$  axis at this well is interpreted as being best documented by the deepest breakouts and assigned their azimuth of  $139.6^{\circ} \pm 10.3^{\circ}$ . However, there is a nearby fault zone which could be influencing stress trajectories locally.



**Well: B-029-A/094-J-15 Breakouts identified by PFAS**

Magnetic Declination 28.7

Breakout Interval		Length (m)	Measured azimuth (degrees)	Standard Deviation (degrees)	Corrected Azimuth (degrees)
Top (mKB)	Base (mKB)				
1628	1635	7	113.2	1.6	141.9
1650	1652	2	81.3	1.4	110.0
1658	1662	4	121.3	3.3	150.0
1837	1839	2	8.6	0.6	37.3
1843	1852	9	13.6	3.6	42.3
1855	1858	3	15.5	1.5	44.2
1860	1868	8	13.4	3.3	42.1
1869	1870	1	15.9	2.1	44.6
1878	1879	1	173.6	1.0	202.3
1892	1893	1	170.5	2.4	199.2

Total thickness of Breakouts (m)	14.0
Breakouts associated with washouts (m)	24.0
Washouts (m)	160.0
Key Seats (m)	0.0
Undergauge hole (m)	8.0
In gauge hole (m)	616.0
Undetermined intervals (m)	230.0
Thickness of logged interval (m)	1052.0

Mean Azimuth of all breakouts (degrees)	122.5
<b>Mean azimuth of SHmax from all breakouts</b>	<b>32.5</b>
Standard Deviation (degrees)	40.6
Mean Azimuth of Pop 1 breakouts (degrees)	42.2
<b>Mean azimuth of Pop 1 SHmax (degrees)</b>	<b>132.2</b>
Standard Deviation (degrees)	1.7
Mean Azimuth of Pop 2 breakouts (degrees)	144.7
<b>Mean azimuth of Pop 2 SHmax (degrees)</b>	<b>54.7</b>
Standard Deviation (degrees)	23.1

**ANALYTICAL PARAMETERS**

Interval	1087-2142 m
Bit size	8.4
Minimum smaller hole axis diameter	7.4 in
Maximum smaller hole axis diameter	9.4 in
Minimum axes diameter difference	0.5 in
Maximum vertical deviation of well	10°
Azimuth tolerance within breakout	5°
Maximum tool rotation within breakout	5°
Minimum length of breakout	2 m

Well: B-029-A/094-J-15

Well B-029-A/094-J-15 does not exhibit much breakout caving. The most consistently oriented breakouts occur between 1837 and 1870 metres KB and these 23 net metres constitute Population 1. Their mean azimuth is  $42.2^{\circ} \pm 1.7^{\circ}$ . This is provisionally interpreted as the  $S_{Hmin}$  axis at the well site. It may reflect stress deflection by local faulting, in which case the Population 2 mean breakout azimuth of  $144.7^{\circ}$  would be more representative of the regional stress trajectories.

**Well: B-038-60-10-124-00 Breakouts identified by PFAS**

Magnetic Declination 31.6

Breakout Interval		Length (m)	Measured azimuth (degrees)	Standard Deviation (degrees)	Corrected Azimuth (degrees)
Top (mKB)	Base (mKB)				
3775	3787	12	117.2	4.8	148.8
3792	3796	4	129.1	5.0	160.7
3802	3807	5	110.1	3.6	141.7
3810	3816	6	109.8	5.1	141.4
3831	3833	2	118.8	4.1	150.4

Total thickness of Breakouts (m)	29.0
Breakouts associated with washouts (m)	0.0
Washouts (m)	0.0
Key Seats (m)	0.0
Undergauge hole (m)	0.0
In gauge hole (m)	576.0
Undetermined intervals (m)	4.0
Thickness of logged interval (m)	609.0

Mean Azimuth of all breakouts (degrees)	147.8
<b>Mean azimuth of SHmax from all breakouts</b>	<b>57.8</b>
Standard Deviation (degrees)	6.2
Mean Azimuth of Pop 1 breakouts (degrees)	147.8
<b>Mean azimuth of Pop 1 SHmax (degrees)</b>	<b>57.8</b>
Standard Deviation (degrees)	6.2

ANALYTICAL PARAMETERS

Interval	3285-3898m
Bit size	8.5 in
Minimum smaller hole axis diameter	7.5 in
Maximum smaller hole axis diameter	9.5 in
Minimum axes diameter difference	0.5 in
Maximum vertical deviation of well	10°
Azimuth tolerance within breakout	5°
Maximum tool rotation within breakout	5°
Minimum length of breakout	2m

Well: B-038-60-10-124-00

Well B-038-60-10-124-00 exhibits 29 net metres of breakouts between depths of 3775 and 3833 metres KB. They fall into a single population with a mean azimuth of  $147.8^{\circ} \pm 6.2^{\circ}$ . This is interpreted as the  $S_{Hmin}$  axis at the well site.

**Well: B-044-B/094-P-05 Breakouts identified by PFAS**

Magnetic Declination 30

Breakout Interval		Length (m)	Measured azimuth (degrees)	Standard Deviation (degrees)	Corrected Azimuth (degrees)
Top (mKB)	Base (mKB)				
1528	1532	4	13.1	1.2	43.1
1592	1599	7	95.6	2.0	125.6
1601	1604	3	93.8	1.0	123.8
1713	1714	1	18.6	0.2	48.6
1722	1730	8	20.6	1.9	50.6
1732	1749	17	23.2	1.1	53.2
1751	1796	45	22.0	2.3	52.0
1798	1799	1	12.9	0.3	42.9
1801	1802	1	13.5	0.3	43.5
1804	1814	10	19.7	5.8	49.7
1835	1837	2	33.9	1.1	63.9
1859	1873	14	146.1	3.1	176.1
1875	1887	12	161.0	2.4	191.0
1901	1908	7	79.5	1.5	109.5
1910	1911	1	82.4	0.1	112.4
1919	1922	3	92.4	1.8	122.4
1923	1924	1	96.4	0.2	126.4
1925	1926	1	98.3	1.4	128.3
1927	1928	1	101.4	1.4	131.4
1929	1930	1	101.5	1.7	131.5
1931	1932	1	97.7	1.0	127.7
1945	1949	4	101.0	1.4	131.0

Total thickness of Breakouts (m)	138.0
Breakouts associated with washouts (m)	7.0
Washouts (m)	1.0
Key Seats (m)	0.0
Undergauge hole (m)	1.0
In gauge hole (m)	409.0
Undetermined intervals (m)	117.0
Thickness of logged interval (m)	673.0

Mean Azimuth of all breakouts (degrees)	48.3
<b>Mean azimuth of SHmax from all breakouts</b>	<b>138.3</b>
Standard Deviation (degrees)	36.9
Mean Azimuth of Pop 1 breakouts (degrees)	149.1
<b>Mean azimuth of Pop 1 SHmax (degrees)</b>	<b>59.1</b>
Standard Deviation (degrees)	34.9
Mean Azimuth of Pop 2 breakouts (degrees)	51.5
<b>Mean azimuth of Pop 2 SHmax (degrees)</b>	<b>141.5</b>
Standard Deviation (degrees)	3.1

ANALYTICAL PARAMETERS

Interval	1521-2199 m
Bit size	8.5 in
Minimum smaller hole axis diameter	7.5 in
Maximum smaller hole axis diameter	9.5 in
Minimum axes diameter difference	0.5 in
Maximum vertical deviation of well	10°
Azimuth tolerance within breakout	5°
Maximum tool rotation within breakout	5°
Minimum length of breakout	2 m

Well: B-044-B/094-P-05

In well B-044-B/094-P-05, the breakouts fall into two populations. For the purpose of determining the axis of  $S_{Hmin}$ , the smaller population with 56 net metres of breakouts is used. The rationale is that this population is predominantly composed of the deeper breakouts that are more likely to reflect regional  $S_{Hmin}$  trajectories.

**Well: B-044-L/094-O-10 Breakouts identified by PFAS**

Magnetic Declination 31.3

Breakout Interval		Length (m)	Measured azimuth (degrees)	Standard Deviation (degrees)	Corrected Azimuth (degrees)
Top (mKB)	Base (mKB)				
238	241	3	34.0	1.0	65.3
244	252	8	26.7	3.9	58.0
254	266	12	25.1	1.5	56.4
267	270	3	26.6	1.2	57.9
343	395	52	24.8	3.9	56.1
410	414	4	104.3	3.5	135.6
415	417	2	111.1	4.6	142.4

Total thickness of Breakouts (m)	81.0
Breakouts associated with washouts (m)	3.0
Washouts (m)	0.0
Key Seats (m)	0.0
Undergauge hole (m)	1.0
In gauge hole (m)	354.0
Undetermined intervals (m)	60.0
Thickness of logged interval (m)	499.0

Mean Azimuth of all breakouts (degrees)	57.4
<b>Mean azimuth of SHmax from all breakouts</b>	<b>147.4</b>
Standard Deviation (degrees)	15.8
Mean Azimuth of Pop 1 breakouts (degrees)	56.7
<b>Mean azimuth of Pop 1 SHmax (degrees)</b>	<b>146.7</b>
Standard Deviation (degrees)	1.8
Mean Azimuth of Pop 2 breakouts (degrees)	137.9
<b>Mean azimuth of Pop 2 SHmax (degrees)</b>	<b>47.9</b>
Standard Deviation (degrees)	3.2

ANALYTICAL PARAMETERS

Interval	162-682 m
Bit size	6.25 in
Minimum smaller hole axis diameter	5.25 in
Maximum smaller hole axis diameter	7.25 in
Minimum axes diameter difference	0.5 in
Maximum vertical deviation of well	10°
Azimuth tolerance within breakout	5°
Maximum tool rotation within breakout	5°
Minimum length of breakout	2 m

Well: B-044-L/094-O-10

In well B-044-L/094-O-10, the breakouts above 400 metres KB fall into a coherent population of 78 net metres that exhibit a mean azimuth of  $56.7^{\circ} \pm 1.8^{\circ}$ . Below 400 metres KB, there are two short breakout intervals with a mean azimuth of  $137.9^{\circ} \pm 3.2^{\circ}$ .

The larger population contains breakouts that are approximately  $90^{\circ}$  different in orientation from the major breakout populations of three wells to the immediate south. The anomalous breakout orientations between 238 and 395 metres in well B-044-L/094-O-10 could be due to stress deflection caused by a nearby fault zone.

**Well: B-055-60-30-123-45 Breakouts identified by PFAS**

Magnetic Declination 32.1

Breakout Interval		Length (m)	Measured azimuth (degrees)	Standard Deviation (degrees)	Corrected Azimuth (degrees)
Top (mKB)	Base (mKB)				
758	762	4	112.5	0.4	144.6
911	914	3	89.8	2.0	121.9
956	968	12	93.6	1.1	125.7
969	971	2	91.5	0.3	123.6
973	1041	68	99.3	4.5	131.4
1043	1072	29	111.2	2.6	143.3
1074	1078	4	118.5	1.1	150.6
1085	1114	29	111.8	4.5	143.9
1117	1124	7	93.7	2.8	125.8
1130	1133	3	93.5	2.8	125.6
1144	1156	12	85.8	2.8	117.9
1160	1175	15	82.9	1.6	115.0
1186	1235	49	85.2	2.5	117.3
1242	1252	10	92.2	1.4	124.3
1263	1304	41	83.3	6.0	115.4
1308	1319	11	87.2	1.9	119.3
1339	1346	7	76.0	0.6	108.1
1396	1443	47	32.7	3.5	64.8
1445	1454	9	47.3	1.9	79.4
1465	1467	2	125.1	1.5	157.2
1476	1493	17	109.1	5.6	141.2
1495	1500	5	110.5	3.5	142.6
1503	1509	6	113.1	3.2	145.2
1549	1555	6	125.9	1.3	158.0
1556	1571	15	121.2	1.8	153.3
1573	1580	7	112.9	1.9	145.0
1603	1608	5	64.1	1.8	96.2
1611	1645	34	63.0	5.8	95.1
1648	1652	4	64.4	2.2	96.5
1653	1688	35	70.0	2.6	102.1
1787	1791	4	75.6	3.0	107.7
1845	1848	3	25.1	1.2	57.2
1853	1861	8	22.7	2.6	54.8
1868	1900	32	32.1	3.0	64.2
1934	1936	2	43.1	0.7	75.2
1937	1941	4	54.1	1.5	86.2
1949	1963	14	37.4	2.8	69.5
1996	1998	2	141.0	0.4	173.1
2034	2036	2	136.2	1.3	168.3
2037	2052	15	133.6	3.6	165.7
2056	2058	2	131.4	2.2	163.5
2066	2072	6	132.5	3.6	164.6
2097	2099	2	143.7	0.4	175.8
2116	2118	2	158.1	1.3	190.2
2128	2131	3	82.9	1.5	115.0



2153	2155	2	87.7	1.2	119.8
2156	2166	10	90.1	3.3	122.2
2181	2182	1	94.1	3.8	126.2
2185	2188	3	97.7	4.7	129.8
2250	2254	4	101.6	5.3	133.7
2263	2265	2	105.4	6.0	137.5
2270	2291	21	48.0	3.9	80.1
2306	2315	9	51.6	2.1	83.7
2317	2336	19	57.9	5.4	90.0
2350	2353	3	98.2	0.8	130.3
2397	2413	16	147.3	2.6	179.4
2511	2515	4	39.5	2.9	71.6
2519	2538	19	43.1	1.5	75.2
2542	2552	10	46.1	1.9	78.2
2565	2601	36	55.7	2.0	87.8
2601	2602	1	55.8	2.0	87.9
2602	2612	10	62.2	2.1	94.3
2661	2667	6	98.3	3.9	130.4
2673	2683	10	103.1	2.0	135.2
2686	2715	29	118.9	3.1	151.0
2813	2826	13	130.2	5.3	162.3

Total thickness of Breakouts (m)	650.0
Breakouts associated with washouts (m)	177.0
Washouts (m)	73.0
Key Seats (m)	0.0
Undergauge hole (m)	13.0
In gauge hole (m)	1176.0
Undetermined intervals (m)	901.0
Thickness of logged interval (m)	2990.0

Mean Azimuth of all breakouts (degrees)	113.9
<b>Mean azimuth of SHmax from all breakouts</b>	<b>23.9</b>
Standard Deviation (degrees)	33.6
Mean Azimuth of Pop 1 breakouts (degrees)	135.4
<b>Mean azimuth of Pop 1 SHmax (degrees)</b>	<b>45.4</b>
Standard Deviation (degrees)	18.2
Mean Azimuth of Pop 2 breakouts (degrees)	80.9
<b>Mean azimuth of Pop 2 SHmax (degrees)</b>	<b>170.9</b>
Standard Deviation (degrees)	13.8

#### ANALYTICAL PARAMETERS

Interval	742-2500m
Bit size	11.0 in
Minimum smaller hole axis diameter	10.0 in
Maximum smaller hole axis diameter	9.0 in
Minimum axes diameter difference	0.5 in
Maximum vertical deviation of well	10°
Azimuth tolerance within breakout	5°
Maximum tool rotation within breakout	5°
Minimum length of breakout	2m

Interval	2500-3578m
Bit size	8.5 in
Minimum smaller hole axis diameter	7.5 in
Maximum smaller hole axis diameter	9.5 in
Minimum axes diameter difference	0.5 in
Maximum vertical deviation of well	10°
Azimuth tolerance within breakout	5°
Maximum tool rotation within breakout	5°
Minimum length of breakout	2m

Well: B-055-60-30-123-45

Well B-055-60-30-123-45 exhibits 827 net metres of breakouts between depths of 758 and 2826 metres KB. They are divided into two populations that do not differ greatly in their mean azimuths. The lower part of the logged section, below 2826 metres KB, is free of breakouts.

Population 1 contains the greatest net thickness, with 488 metres of breakouts and it includes the majority of the most deeply caved breakouts. It is interpreted as representing the regional alignment of  $S_{Hmin}$  at  $135.4^{\circ} \pm 18.2^{\circ}$ .

**Well: B-058-A/094-I-13 Breakouts identified by PFAS**

Magnetic Declination 25.2

Breakout Interval		Length (m)	Measured azimuth (degrees)	Standard Deviation (degrees)	Corrected Azimuth (degrees)
Top (mKB)	Base (mKB)				
1343	1345	2	3.8	2.1	29.0
1347	1355	8	7.7	2.5	32.9
1363	1365	2	3.7	2.2	28.9
1368	1371	3	173.5	1.5	18.7
1376	1378	2	132.5	1.1	157.7
1398	1407	9	171.6	2.6	16.8

Total thickness of Breakouts (m)	26.0
Breakouts associated with washouts (m)	0.0
Washouts (m)	0.0
Key Seats (m)	0.0
Undergauge hole (m)	0.0
In gauge hole (m)	141.0
Undetermined intervals (m)	54.0
Thickness of logged interval (m)	221.0

Mean Azimuth of all breakouts (degrees)	22.0
<b>Mean azimuth of SHmax from all breakouts</b>	<b>112.0</b>
Standard Deviation (degrees)	13.7
Mean Azimuth of Pop 1 breakouts (degrees)	22.0
<b>Mean azimuth of Pop 1 SHmax (degrees)</b>	<b>112.0</b>
Standard Deviation (degrees)	13.7

ANALYTICAL PARAMETERS

Interval	1300-1521 m
Bit size	8.5 in
Minimum smaller hole axis diameter	7.5 in
Maximum smaller hole axis diameter	9.5 in
Minimum axes diameter difference	0.5 in
Maximum vertical deviation of well	10°
Azimuth tolerance within breakout	5°
Maximum tool rotation within breakout	5°
Minimum length of breakout	2 m

Well: B-058-A/094-I-13

Well B-058-A/094-I-13 only has a short section logged with a four-arm dipmeter tool. Six breakouts amounting to 26 net metres are identified between depths of 1343 and 1407 metres KB. They all fall into a single population with a mean azimuth of 22.0° +/- 13.7°.

Regionally, this is an anomalous axis for  $S_{Hmin}$  and it could indicate deflection by a nearby fault zone. Alternatively, the caliper pads may have been mislabelled during logging. This is always a possibility when assessing anomalous orientations, but it is prudent to suspect and, if possible, investigate a geomechanical cause, such as a lateral change in rock mechanical properties that might characterise a fault zone.

**Well: B-066-I/094-O-08 Breakouts identified by PFAS**

Magnetic Declination 29.4

Breakout Interval		Length (m)	Measured azimuth (degrees)	Standard Deviation (degrees)	Corrected Azimuth (degrees)
Top (mKB)	Base (mKB)				
979	1012	33	68.5	1.7	97.9
1016	1026	10	58.7	1.4	88.1
1048	1083	35	38.4	4.1	67.8
1171	1205	34	31.6	1.6	61.0
1264	1287	23	20.4	2.2	49.8
1287	1292	5	23.4	0.7	52.8
1292	1339	47	27.4	2.7	56.8
1339	1362	23	33.0	0.9	62.4
1362	1385	23	34.8	2.0	64.2
1478	1488	10	20.6	2.4	50.0
1540	1556	16	8.7	2.2	38.1
1559	1583	24	3.2	3.0	32.6
1638	1640	2	31.7	1.3	61.1
1686	1726	40	5.7	4.7	35.1
1730	1752	22	5.9	2.7	35.3
1754	1787	33	16.9	4.8	46.3
1788	1824	36	25.4	4.2	54.8
1923	1955	32	148.2	7.1	177.6
1959	1968	9	125.7	1.3	155.1
1970	1974	4	124.2	1.6	153.6
1994	1996	2	21.6	0.8	51.0
1997	2000	3	24.4	1.5	53.8
2001	2003	2	24.1	0.4	53.5
2007	2010	3	23.2	0.5	52.6
2012	2014	2	23.4	1.2	52.8
2015	2097	82	14.2	8.0	43.6
2098	2123	25	4.0	2.3	33.4
2125	2145	20	6.7	2.9	36.1
2146	2181	35	176.9	4.1	206.3
2183	2207	24	168.9	2.2	198.3
2213	2222	9	160.1	0.9	189.5
2226	2233	7	153.2	3.3	182.6
2234	2260	26	146.5	2.3	175.9
2261	2264	3	142.7	0.6	172.1
2267	2284	17	142.6	1.4	172.0

Total thickness of Breakouts (m)	479.0
Breakouts associated with washouts (m)	242.0
Washouts (m)	95.0
Key Seats (m)	0.0
Undergauge hole (m)	0.0
In gauge hole (m)	641.0
Undetermined intervals (m)	267.0
Thickness of logged interval (m)	1724.0

Mean Azimuth of all breakouts (degrees)	41.2
<b>Mean azimuth of SHmax from all breakouts</b>	<b>131.2</b>
Standard Deviation (degrees)	26.0
Mean Azimuth of Pop 1 breakouts (degrees)	50.6
<b>Mean azimuth of Pop 1 SHmax (degrees)</b>	<b>140.6</b>
Standard Deviation (degrees)	16.9
Mean Azimuth of Pop 2 breakouts (degrees)	4.8
<b>Mean azimuth of Pop 2 SHmax (degrees)</b>	<b>94.8</b>
Standard Deviation (degrees)	15.6

#### ANALYTICAL PARAMETERS

Interval	894-2625 m
Bit size	8.5 in
Minimum smaller hole axis diameter	7.5 in
Maximum smaller hole axis diameter	9.5 in
Minimum axes diameter difference	0.5 in
Maximum vertical deviation of well	10°
Azimuth tolerance within breakout	5°
Maximum tool rotation within breakout	5°
Minimum length of breakout	2 m

Population 1: 508 metres

Population 2: 166 metres

#### Well: B-066-I/094-O-08

Well B-066-I/094-O-08 is extensively broken-out between the depth of 979 and 2284 metres KB. In the upper part of the logged section, most of the breakouts fall into Population 1 consisting of 555 net metres with a mean azimuth of  $50.6^{\circ} \pm 16.9^{\circ}$ . Population 2 breakouts amount to 166 net metres and are largely concentrated in the lower part of the logged section. Their mean azimuth is  $4.8^{\circ} \pm 15.6^{\circ}$ .

Because their abundance cannot be ignored, the mean azimuth of Population 1 of  $50.6^{\circ} \pm 16.9^{\circ}$  is interpreted as the axis of  $S_{Hmin}$  at the well site. Regionally, this is an anomalous axis for  $S_{Hmin}$  and it may indicate deflection by a nearby fault zone. Alternatively, the caliper pads may have been mislabelled during logging. This is always a possibility when assessing anomalous orientations, but it is prudent to suspect a geomechanical cause, such as a lateral change in rock mechanical properties that might be associated with a fault zone.

**Well: B-085-H/094-O-11 Breakouts identified by PFAS**

Magnetic Declination 31.5

Breakout Interval		Length (m)	Measured azimuth (degrees)	Standard Deviation (degrees)	Corrected Azimuth (degrees)
Top (mKB)	Base (mKB)				
205	421	216	85.5	3.8	117.0
537	538	1	82.1	2.0	113.6
655	696	41	101.2	1.4	132.7
702	703	1	99.2	0.3	130.7
828	836	8	99.7	1.3	131.2
839	867	28	100.3	3.5	131.8
884	887	3	99.0	1.8	130.5
889	893	4	101.1	3.1	132.6
897	913	16	99.4	1.6	130.9

Total thickness of Breakouts (m)	271.0
Breakouts associated with washouts (m)	47.0
Washouts (m)	4.0
Key Seats (m)	2.0
Undergauge hole (m)	24.0
In gauge hole (m)	830.0
Undetermined intervals (m)	91.0
Thickness of logged interval (m)	1269.0

Mean Azimuth of all breakouts (degrees)	121.6
<b>Mean azimuth of SHmax from all breakouts</b>	<b>31.6</b>
Standard Deviation (degrees)	7.0
Mean Azimuth of Pop 1 breakouts (degrees)	121.6
<b>Mean azimuth of Pop 1 SHmax (degrees)</b>	<b>31.6</b>
Standard Deviation (degrees)	7.0

ANALYTICAL PARAMETERS

Interval	189-1459m
Bit size	8.75 in
Minimum smaller hole axis diameter	7.75 in
Maximum smaller hole axis diameter	9.75 in
Minimum axes diameter difference	0.5 in
Maximum vertical deviation of well	10°
Azimuth tolerance within breakout	5°
Maximum tool rotation within breakout	5°
Minimum length of breakout	2 m

Population 1: 508 metres

Population 2: 166 metres

Well: B-085-H/094-O-11

This well exhibits breakouts with a very consistent orientation that fall into a single population with a mean azimuth of  $121.6^{\circ} \pm 7.0^{\circ}$ . This is interpreted as the axis of  $S_{Hmin}$ .

**Well: B-093-C/094-I-14 Breakouts identified by PFAS**

Magnetic Declination 29

Breakout Interval		Length (m)	Measured azimuth (degrees)	Standard Deviation (degrees)	Corrected Azimuth (degrees)
Top (mKB)	Base (mKB)				
293	381	88	112.9	10.5	141.9
383	465	82	119.2	7.5	148.2
466	470	4	126.1	0.4	155.1
471	495	24	127.4	2.3	156.4
496	500	4	132.8	1.5	161.8
501	550	49	142.9	4.9	171.9
570	579	9	141.5	3.8	170.5
871	883	12	116.4	2.0	145.4
887	891	4	122.0	3.2	151.0
896	900	4	126.4	0.5	155.4
949	951	2	123.1	0.7	152.1
976	979	3	147.9	1.9	176.9
993	994	1	151.7	0.8	180.7
1030	1031	1	126.5	1.0	155.5

Total thickness of Breakouts (m)	206.0
Breakouts associated with washouts (m)	81.0
Washouts (m)	12.0
Key Seats (m)	35.0
Undergauge hole (m)	3.0
In gauge hole (m)	504.0
Undetermined intervals (m)	1322.0
Thickness of logged interval (m)	2163.0

Mean Azimuth of all breakouts (degrees)	152.2
<b>Mean azimuth of SHmax from all breakouts</b>	<b>62.2</b>
Standard Deviation (degrees)	11.5
Mean Azimuth of Pop 1 breakouts (degrees)	152.2
<b>Mean azimuth of Pop 1 SHmax (degrees)</b>	<b>62.2</b>
Standard Deviation (degrees)	11.5

**ANALYTICAL PARAMETERS**

Interval	187-2359 m
Bit size	16.0 in
Minimum smaller hole axis diameter	15.0 in
Maximum smaller hole axis diameter	17.0 in
Minimum axes diameter difference	0.5 in
Maximum vertical deviation of well	10°
Azimuth tolerance within breakout	5°
Maximum tool rotation within breakout	5°
Minimum length of breakout	2 m

**Well: B-093-C/094-I-14**

This well exhibits breakouts with similar orientations that fall into a single population with a mean azimuth of 152.2° +/- 11.5°. This is interpreted as the axis of S<sub>Hmin</sub>.

**Well: B-094-H/094-J-14 Breakouts identified by PFAS**

Magnetic Declination 30.6

Breakout Interval		Length (m)	Measured azimuth (degrees)	Standard Deviation (degrees)	Corrected Azimuth (degrees)
Top (mKB)	Base (mKB)				
259	262	3	103.6	2.7	134.2
303	318	15	66.8	2.4	97.4
326	330	4	66.8	2.5	97.4
336	340	4	56.3	1.1	86.9
447	451	4	134.1	2.3	164.7
519	521	2	47.4	1.2	78.0
530	533	3	38.2	1.2	68.8
728	731	3	174.2	2.1	204.8
744	745	1	169.5	2.2	200.1
861	863	2	173.3	0.3	203.9
866	868	2	164.2	3.4	194.8
887	920	33	145.9	4.5	176.5
921	930	9	159.9	2.3	190.5
935	959	24	141.9	3.4	172.5
960	963	3	154.1	2.6	184.7
965	1008	43	146.1	6.3	176.7
1008	1015	7	139.7	4.2	170.3
1022	1024	2	126.8	2.1	157.4
1025	1027	2	125.9	2.0	156.5
1032	1034	2	136.3	2.2	166.9
1048	1070	22	105.2	5.6	135.8
1073	1109	36	106.3	3.5	136.9
1274	1276	2	101.0	0.9	131.6
1277	1288	11	108.2	5.1	138.8
1335	1387	52	126.9	2.8	157.5
1398	1412	14	123.6	1.4	154.2
1451	1454	3	129.8	3.6	160.4
1457	1462	5	112.8	3.1	143.4
1479	1490	11	129.8	2.2	160.4
1500	1507	7	135.8	2.0	166.4
1507	1518	11	137.1	1.8	167.7
1518	1537	19	143.9	3.4	174.5
1539	1541	2	138.3	2.7	168.9
1546	1550	4	118.4	2.1	149.0
1589	1596	7	125.1	2.0	155.7
1597	1627	30	123.8	2.1	154.4
1628	1666	38	123.3	2.6	153.9
1669	1678	9	137.4	1.4	168.0
1680	1683	3	144.3	0.9	174.9
1693	1697	4	164.9	0.9	195.5
1700	1704	4	174.0	1.1	204.6
1706	1711	5	173.0	1.1	203.6
1712	1766	54	169.3	2.3	199.9



1767	1772	5	176.6	2.1	207.2
1774	1779	5	157.3	1.3	187.9
1782	1785	3	164.8	0.8	195.4
1788	1795	7	162.0	3.7	192.6
1796	1798	2	160.1	2.4	190.7
1801	1803	2	168.4	1.0	199.0
1807	1822	15	175.4	4.7	206.0
1822	1823	1	2.8	1.2	33.4
1825	1862	37	173.9	2.0	204.5
1863	1864	1	169.2	0.5	199.8
1864	1875	11	173.6	2.6	204.2
1939	1944	5	158.5	1.0	189.1
1945	1950	5	160.3	0.7	190.9
1953	1972	19	163.9	2.8	194.5
1972	1986	14	165.4	4.0	196.0
2001	2002	1	130.7	0.8	161.3
2004	2012	8	114.2	4.7	144.8
2374	2376	2	119.2	3.1	149.8
2385	2387	2	117.7	2.5	148.3

Total thickness of Breakouts (m)	326.0
Breakouts associated with washouts (m)	340.0
Washouts (m)	141.0
Key Seats (m)	6.0
Undergauge hole (m)	80.0
In gauge hole (m)	1107.0
Undetermined intervals (m)	230.0
Thickness of logged interval (m)	2230.0

Mean Azimuth of all breakouts (degrees)	172.2
<b>Mean azimuth of all BOs SHmax (degrees)</b>	<b>82.2</b>
Standard Deviation (degrees)	26.5
Mean Azimuth of Pop 1 breakouts (degrees)	172.7
<b>Mean azimuth of Pop 1 SHmax (degrees)</b>	<b>82.7</b>
Standard Deviation (degrees)	23.1
Mean Azimuth of Pop 2 breakouts (degrees)	90.7
<b>Mean azimuth of Pop 1 SHmax (degrees)</b>	<b>0.7</b>
Standard Deviation (degrees)	13.4

#### ANALYTICAL PARAMETERS

Interval	249-594m
Bit size	12.0
Minimum smaller hole axis diameter	11.0 in
Maximum smaller hole axis diameter	13.0 in
Minimum axes diameter difference	0.5 in
Maximum vertical deviation of well	10°
Azimuth tolerance within breakout	5°
Maximum tool rotation within breakout	5°
Minimum length of breakout	2 m

Interval	594-2482m
----------	-----------

Bit size	8.75 in
Minimum smaller hole axis diameter	7.75in
Maximum smaller hole axis diameter	9.75 in
Minimum axes diameter difference	0.5 in
Maximum vertical deviation of well	10°
Azimuth tolerance within breakout	5°
Maximum tool rotation within breakout	5°
Minimum length of breakout	2 m

Population 1: 403 metres

Population 2: 158 metres

#### Well: B-094-H/094-J-14

Well B-094-H/094-J-14 is heavily broken out, especially between the depths of 800 and 2100 metres KB. Of the 666 net metres of breakouts in this logged section, 637 fall into a single population that exhibits a mean azimuth of  $172.7^\circ \pm 23.1^\circ$ . This azimuth is interpreted to represent  $S_{Hmin}$  at this location.

**Well: B-096-E/094-O-10 Breakouts identified by PFAS**

Magnetic Declination 31.3

Breakout Interval		Length (m)	Measured azimuth (degrees)	Standard Deviation (degrees)	Corrected Azimuth (degrees)
Top (mKB)	Base (mKB)				
510	514	4	96.9	7.0	128.2

Total thickness of Breakouts (m)	4.0
Breakouts associated with washouts (m)	0.0
Washouts (m)	0.0
Key Seats (m)	0.0
Undergauge hole (m)	2215.0
In gauge hole (m)	325.0
Undetermined intervals (m)	21.0
Thickness of logged interval (m)	2565.0

Mean Azimuth of all breakouts (degrees)	128.2
<b>Mean azimuth of SHmax from all breakouts</b>	<b>38.2</b>
Standard Deviation (degrees)	7.0

ANALYTICAL PARAMETERS

Interval	456-3022m
Bit size	7.88 in
Minimum smaller hole axis diameter	6.88 in
Maximum smaller hole axis diameter	8.88 in
Minimum axes diameter difference	0.5 in
Maximum vertical deviation of well	10°
Azimuth tolerance within breakout	5°
Maximum tool rotation within breakout	5°
Minimum length of breakout	3m

Dipmeter data were only available for 456-808 m and 2890-3020 m  
The section from 2890 to 3020 m contains no breakouts.

Well: B-096-E/094-O-10

Well B-096-E/094-O-10 exhibits a single breakout with an azimuth of 128.2° +/- 7.0°. This azimuth is interpreted to represent S<sub>Hmin</sub> at this location.

**Well: C-024-H/094-O-16 Breakouts identified by PFAS**

Magnetic Declination 31.5

Breakout Interval		Length (m)	Measured azimuth (degrees)	Standard Deviation (degrees)	Corrected Azimuth (degrees)
Top (mKB)	Base (mKB)				
557	590	33	107.0	2.6	138.5
856	860	4	112.8	0.6	144.3

Total thickness of Breakouts (m)	37.0
Breakouts associated with washouts (m)	0.0
Washouts (m)	0.0
Key Seats (m)	69.0
Undergauge hole (m)	0.0
In gauge hole (m)	616.0
Undetermined intervals (m)	39.0
Thickness of logged interval (m)	761.0

Mean Azimuth of all breakouts (degrees)	139.1
<b>Mean azimuth of SHmax from all breakouts</b>	<b>49.1</b>
Standard Deviation (degrees)	1.8

ANALYTICAL PARAMETERS

Interval	355-1125 m
Bit size	7.88 in
Minimum smaller hole axis diameter	6.88 in
Maximum smaller hole axis diameter	8.88 in
Minimum axes diameter difference	0.5 in
Maximum vertical deviation of well	10°
Azimuth tolerance within breakout	5°
Maximum tool rotation within breakout	5°
Minimum length of breakout	3m

Well: C-024-H/094-O-16

Well C-024-H/094-O-16 exhibits only two breakouts amounting to 37 net metres. Their mean azimuth is 139.1° +/- 1.8° and is interpreted to represent  $S_{Hmin}$  at this location.

**Well: C-028-H/094-O-16 Breakouts identified by PFAS**

Magnetic Declination 31

Breakout Interval		Length (m)	Measured azimuth (degrees)	Standard Deviation (degrees)	Corrected Azimuth (degrees)
Top (mKB)	Base (mKB)				
2127	2129	2	121.9	0.0	152.9
2132	2134	2	114.6	1.5	145.6
2137	2140	3	113.7	0.9	144.7
2151	2153	2	89.6	0.3	120.6
2157	2159	2	98.8	0.2	129.8
2172	2174	2	53.0	0.3	84.0
2236	2248	12	103.0	3.7	134.0
2254	2258	4	78.1	1.1	109.1
2566	2578	12	123.0	2.1	154.0
2587	2597	10	121.5	1.4	152.5

Total thickness of Breakouts (m)	33.0
Breakouts associated with washouts (m)	18.0
Washouts (m)	12.0
Key Seats (m)	25.0
Undergauge hole (m)	0.0
In gauge hole (m)	264.0
Undetermined intervals (m)	153.0
Thickness of logged interval (m)	505.0

Mean Azimuth of all breakouts (degrees)	138.0
<b>Mean azimuth of SHmax from all breakouts</b>	<b>48.0</b>
Standard Deviation (degrees)	17.9

ANALYTICAL PARAMETERS

Interval	2102-2615 m
Bit size	8.75 in
Minimum smaller hole axis diameter	7.75 in
Maximum smaller hole axis diameter	9.75 in
Minimum axes diameter difference	0.5 in
Maximum vertical deviation of well	10°
Azimuth tolerance within breakout	5°
Maximum tool rotation within breakout	5°
Minimum length of breakout	3m

Well: C-028-H/094-O-16

Well C-028-H/094-O-16 exhibits ten breakouts amounting to 51 net metres between depths of 2127 and 2597 metres. They fall into a single population with a mean azimuth of 138.0° +/- 17.9°, which is interpreted to represent  $S_{Hmin}$  at this location.

**Well: C-051-D/094-P-12 Breakouts identified by PFAS**

Magnetic Declination 31.2

Breakout Interval		Length (m)	Measured azimuth (degrees)	Standard Deviation (degrees)	Corrected Azimuth (degrees)
Top (mKB)	Base (mKB)				
1092	1104	12	124.9	4.1	156.1
1121	1129	8	118.0	1.7	149.2
1135	1139	4	119.9	2.5	151.1
1142	1152	10	109.1	2.1	140.3
1255	1263	8	70.0	1.4	101.2
1331	1332	1	66.3	1.6	97.5
1384	1392	8	101.9	2.9	133.1
1393	1463	70	105.4	3.9	136.6
1483	1515	32	52.1	7.0	83.3
1523	1560	37	59.6	7.1	90.8

Total thickness of Breakouts (m)	103.0
Breakouts associated with washouts (m)	87.0
Washouts (m)	186.0
Key Seats (m)	2.0
Undergauge hole (m)	0.0
In gauge hole (m)	275.0
Undetermined intervals (m)	530.0
Thickness of logged interval (m)	1183.0

Mean Azimuth of all breakouts (degrees)	120.6
<b>Mean azimuth of SHmax from all breakouts</b>	<b>30.6</b>
Standard Deviation (degrees)	27.8
Mean Azimuth of Pop 1 breakouts (degrees)	140.1
<b>Mean azimuth of Pop 1 SHmax (degrees)</b>	<b>50.1</b>
Standard Deviation (degrees)	7.0
Mean Azimuth of Pop 2 breakouts (degrees)	88.8
<b>Mean azimuth of Pop 2 SHmax (degrees)</b>	<b>178.8</b>
Standard Deviation (degrees)	5.6

ANALYTICAL PARAMETERS

Interval	1066-2266m
Bit size	8.5 in
Minimum smaller hole axis diameter	7.5 in
Maximum smaller hole axis diameter	9.5 in
Minimum axes diameter difference	0.5 in
Maximum vertical deviation of well	10°
Azimuth tolerance within breakout	5°
Maximum tool rotation within breakout	5°
Minimum length of breakout	3m

Well: C-051-D/094-P-12

Well C-051-D/094-P-12 exhibits ten breakouts amounting to 190 net metres between depths of 1092 and 1560 metres. They fall into two populations, the larger of which has a mean azimuth of  $140.1^\circ \pm 7.0^\circ$ , which is interpreted to represent  $S_{Hmin}$  at this location.

**Well C-054-K/094-N-16 Breakouts identified by PFAS**

Magnetic Declination 31.6

Breakout Interval		Length (m)	Measured azimuth (degrees)	Standard Deviation (degrees)	Corrected Azimuth (degrees)
Top (mKB)	Base (mKB)				
3167	3174	7	78.4	1.6	110.0
3176	3179	3	73.3	3.1	104.9
3182	3198	16	77.9	3.5	109.5
3302	3346	44	80.2	3.9	111.8
3348	3350	2	73.9	1.1	105.5
3363	3369	6	93.7	2.5	125.3

Total thickness of Breakouts (m)	78.0
Breakouts associated with washouts (m)	0.0
Washouts (m)	0.0
Key Seats (m)	0.0
Undergauge hole (m)	33.0
In gauge hole (m)	980.0
Undetermined intervals (m)	80.0
Thickness of logged interval (m)	1171.0

Mean Azimuth of all breakouts (degrees)	111.8
<b>Mean azimuth of SHmax from all breakouts</b>	<b>21.8</b>
Standard Deviation (degrees)	4.3
Mean Azimuth of Pop 1 breakouts (degrees)	111.8
<b>Mean azimuth of Pop 1 SHmax (degrees)</b>	<b>21.8</b>
Standard Deviation (degrees)	4.3

ANALYTICAL PARAMETERS

Interval	3157-4340m
Bit size	8.5 in
Minimum smaller hole axis diameter	7.5 in
Maximum smaller hole axis diameter	9.5 in
Minimum axes diameter difference	0.5 in
Maximum vertical deviation of well	10°
Azimuth tolerance within breakout	5°
Maximum tool rotation within breakout	5°
Minimum length of breakout	3m

Well: C-054-K/094-N-16

Well C-054-K/094-N-16 exhibits six breakouts amounting to 78 net metres between depths of 3167 and 3369 metres. They are all similarly aligned and fall into a single population, which has a mean azimuth of  $111.8^{\circ} \pm 4.3^{\circ}$ . This is interpreted as the  $S_{Hmin}$  axis at this location.

**Well: C-060-60-10-121-15 Breakouts identified by PFAS**

Magnetic Declination 32.0

Breakout Interval		Length (m)	Measured azimuth (degrees)	Standard Deviation (degrees)	Corrected Azimuth (degrees)
Top (mKB)	Base (mKB)				
1505	1511	6	135.7	1.5	167.7
1522	1524	2	133.7	1.2	165.7
1529	1530	1	50.4	0.3	82.4
1535	1536	1	38.4	0.6	70.4
1583	1584	1	131.9	0.6	163.9
1959	1982	23	131.9	2.7	163.9

Total thickness of Breakouts (m)	23.0
Breakouts associated with washouts (m)	11.0
Washouts (m)	3.0
Key Seats (m)	0.0
Undergauge hole (m)	3.0
In gauge hole (m)	113.0
Undetermined intervals (m)	487.0
Thickness of logged interval (m)	640.0

Mean Azimuth of all breakouts (degrees)	164.6
<b>Mean azimuth of SHmax from all breakouts</b>	<b>74.6</b>
Standard Deviation (degrees)	14.3
Mean Azimuth of Pop 1 breakouts (degrees)	164.7
<b>Mean azimuth of Pop 1 SHmax (degrees)</b>	<b>74.7</b>
Standard Deviation (degrees)	1.5
Mean Azimuth of Pop 2 breakouts (degrees)	76.4
<b>Mean azimuth of Pop 2 SHmax (degrees)</b>	<b>166.4</b>
Standard Deviation (degrees)	6.0

ANALYTICAL PARAMETERS

Interval	1494-2226m
Bit size	8.75 in
Minimum smaller hole axis diameter	7.75 in
Maximum smaller hole axis diameter	9.75 in
Minimum axes diameter difference	0.5 in
Maximum vertical deviation of well	10°
Azimuth tolerance within breakout	5°
Maximum tool rotation within breakout	5°
Minimum length of breakout	2m

Well: C-060-60-10-121-15

Well C-060-60-10-121-15 exhibits six breakouts amounting to 34 net metres between depths of 1505 and 1982 metres. The dipmeter coverage is broken into three short sections, so the sample is not necessarily representative. Two populations were recognised with the larger containing four breakouts amounting to 32 net metres. This population has a mean azimuth of 164.7° +/- 1.5° and is interpreted as the S<sub>Hmin</sub> axis at this location.



**Well: C-086-A/094-I-14 Breakouts identified by PFAS**

Magnetic Declination 29.0

Breakout Interval		Length (m)	Measured azimuth (degrees)	Standard Deviation (degrees)	Corrected Azimuth (degrees)
Top (mKB)	Base (mKB)				
322	334	12	177.4	3.4	206.4
363	393	30	60.9	3.0	89.9
408	419	11	38.6	2.6	67.6
442	449	7	173.2	3.0	202.2
451	474	23	170.3	3.9	199.3
490	499	9	170.1	3.8	199.1
762	768	6	87.8	1.7	116.8
847	851	4	138.0	1.8	167.0
863	937	74	150.0	3.5	179.0
1011	1029	18	151.8	3.2	180.8
1136	1144	8	167.1	1.8	196.1
1298	1303	5	167.3	1.4	196.3
1315	1317	2	158.8	3.0	187.8
1320	1327	7	162.7	2.3	191.7
1336	1339	3	163.3	2.9	192.3
1341	1350	9	167.7	2.5	196.7
1397	1410	13	93.4	4.7	122.4
1417	1450	33	98.4	4.1	127.4
1617	1624	7	177.8	1.2	206.8

Total thickness of Breakouts (m)	174.0
Breakouts associated with washouts (m)	107.0
Washouts (m)	24.0
Key Seats (m)	0.0
Undergauge hole (m)	3.0
In gauge hole (m)	847.0
Undetermined intervals (m)	526.0
Thickness of logged interval (m)	1681.0

Mean Azimuth of all breakouts (degrees)	3.1
<b>Mean azimuth of SHmax from all breakouts</b>	<b>93.1</b>
Standard Deviation (degrees)	38.9
Mean Azimuth of Pop 1 breakouts (degrees)	8.8
<b>Mean azimuth of Pop 1 SHmax (degrees)</b>	<b>98.8</b>
Standard Deviation (degrees)	11.0
Mean Azimuth of Pop 2 breakouts (degrees)	108.1
<b>Mean azimuth of Pop 2 SHmax (degrees)</b>	<b>18.1</b>
Standard Deviation (degrees)	22.3

ANALYTICAL PARAMETERS

Interval	317-1876m
Bit size	8.0 in
Minimum smaller hole axis diameter	7.0 in
Maximum smaller hole axis diameter	9.0 in
Minimum axes diameter difference	0.5 in
Maximum vertical deviation of well	10°

Azimuth tolerance within breakout	5°
Maximum tool rotation within breakout	5°
Minimum length of breakout	2m
Interval	1876-2000m
Bit size	6.0 in
Minimum smaller hole axis diameter	5.0 in
Maximum smaller hole axis diameter	7.0 in
Minimum axes diameter difference	0.5 in
Maximum vertical deviation of well	10°
Azimuth tolerance within breakout	5°
Maximum tool rotation within breakout	5°
Minimum length of breakout	2m

Well: C-086-A/094-I-14

Well C-086-A/094-I-14 exhibits 19 breakouts amounting to 281 net metres.

Two populations are recognised. Population 1 consists of 188 net metres of breakouts with a mean azimuth of  $8.8^\circ \pm 11.0^\circ$ . Population 2 consists of 93 net metres of breakouts with a mean azimuth of  $108.1^\circ \pm 22.3^\circ$ . Population 1 is interpreted as defining the  $S_{Hmin}$  axis at this location.

**Well: D-007-J/094-O-09 Breakouts identified by PFAS**

Magnetic Declination 31.3

Breakout Interval		Length (m)	Measured azimuth (degrees)	Standard Deviation (degrees)	Corrected Azimuth (degrees)
Top (mKB)	Base (mKB)				
2342	2344	2	124.0	1.7	155.3
2369	2379	10	110.1	2.5	141.4

Total thickness of Breakouts (m)	10.0
Breakouts associated with washouts (m)	2.0
Washouts (m)	12.0
Key Seats (m)	0.0
Undergauge hole (m)	6.0
In gauge hole (m)	292.0
Undetermined intervals (m)	24.0
Thickness of logged interval (m)	346.0

Mean Azimuth of all breakouts (degrees)	143.7
<b>Mean azimuth of SHmax from all breakouts</b>	<b>53.7</b>
Standard Deviation (degrees)	5.2
Mean Azimuth of Pop 1 breakouts (degrees)	143.7
<b>Mean azimuth of Pop 1 SHmax (degrees)</b>	<b>53.7</b>
Standard Deviation (degrees)	5.2

ANALYTICAL PARAMETERS

Interval	2341-2438m
Bit size	8.75 in
Minimum smaller hole axis diameter	7.75 in
Maximum smaller hole axis diameter	9.75 in
Minimum axes diameter difference	0.5 in
Maximum vertical deviation of well	10°
Azimuth tolerance within breakout	5°
Maximum tool rotation within breakout	5°
Minimum length of breakout	2m

Interval	2438-2694m
Bit size	6.0 in
Minimum smaller hole axis diameter	5.0 in
Maximum smaller hole axis diameter	7.0 in
Minimum axes diameter difference	0.5 in
Maximum vertical deviation of well	10°
Azimuth tolerance within breakout	5°
Maximum tool rotation within breakout	5°
Minimum length of breakout	2m

Well: D-007-J/094-O-09

Well D-007-J/094-O-09 exhibits two breakouts amounting to 12 net metres. Their mean azimuth is 143.7° +/- 5.2° and is interpreted to represent S<sub>Hmin</sub> at this location.

**Well: D-016-A/094-N-15 Breakouts identified by PFAS**

Magnetic Declination 28.8

Breakout Interval		Length (m)	Measured azimuth (degrees)	Standard Deviation (degrees)	Corrected Azimuth (degrees)
Top (mKB)	Base (mKB)				
3275	3287	12	103.4	3.3	132.2
3294	3299	5	95.4	2.7	124.2
3425	3432	7	92.1	2.1	120.9
3511	3522	11	137.2	1.0	166.0
3525	3561	36	139.8	2.2	168.6
3568	3573	5	131.2	1.8	160.0
3663	3750	87	146.9	7.1	175.7
3782	3831	49	133.4	5.3	162.2
3840	3877	37	116.6	3.1	145.4
3946	3961	15	134.3	2.1	163.1
3972	3981	9	114.2	7.1	143.0
4104	4114	10	149.2	5.6	178.0
4145	4191	46	132.8	10.7	161.6
4213	4215	2	131.2	6.9	160.0

Total thickness of Breakouts (m)	319.0
Breakouts associated with washouts (m)	12.0
Washouts (m)	25.0
Key Seats (m)	0.0
Undergauge hole (m)	2.0
In gauge hole (m)	606.0
Undetermined intervals (m)	199.0
Thickness of logged interval (m)	1163.0

Mean Azimuth of all breakouts (degrees)	162.7
<b>Mean azimuth of SHmax from all breakouts</b>	<b>72.7</b>
Standard Deviation (degrees)	13.7
Mean Azimuth of Pop 1 breakouts (degrees)	162.7
<b>Mean azimuth of Pop 1 SHmax (degrees)</b>	<b>72.7</b>
Standard Deviation (degrees)	13.7

ANALYTICAL PARAMETERS

Interval	3173-4336m
Bit size	8.5 in
Minimum smaller hole axis diameter	7.5 in
Maximum smaller hole axis diameter	9.5 in
Minimum axes diameter difference	0.5 in
Maximum vertical deviation of well	10°
Azimuth tolerance within breakout	5°
Maximum tool rotation within breakout	5°
Minimum length of breakout	2m

Muddled digitisation: Plot P1Az as AZIM, AZIM as Hazi and Hazi as RB

Well: D-016-A/094-N-15

Well D-016-A/094-N-15 exhibits 14 breakouts amounting to 331 net metres between depths of 3275 and 4215 m KB. Their mean azimuth is  $162.7^\circ \pm 13.7^\circ$  and this orientation is interpreted to represent the  $S_{Hmin}$  axis at this location.

**Well: D-025-61-20-121-45 Breakouts identified by PFAS**

Magnetic Declination 33.4

Breakout Interval		Length (m)	Measured azimuth (degrees)	Standard Deviation (degrees)	Corrected Azimuth (degrees)
Top (mKB)	Base (mKB)				
794	817	23	120.7	2.2	154.1
899	903	4	64.3	5.5	97.7

Total thickness of Breakouts (m)	4.0
Breakouts associated with washouts (m)	23.0
Washouts (m)	6.0
Key Seats (m)	0.0
Undergauge hole (m)	0.0
In gauge hole (m)	213.0
Undetermined intervals (m)	7.0
Thickness of logged interval (m)	253.0

Mean Azimuth of all breakouts (degrees)	149.2
<b>Mean azimuth of SHmax from all breakouts</b>	<b>59.2</b>
Standard Deviation (degrees)	18.8
Mean Azimuth of Pop 1 breakouts (degrees)	154.1
<b>Mean azimuth of Pop 1 SHmax (degrees)</b>	<b>64.1</b>
Standard Deviation (degrees)	2.2
Mean Azimuth of Pop 2 breakouts (degrees)	97.7
<b>Mean azimuth of Pop 2 SHmax (degrees)</b>	<b>7.7</b>
Standard Deviation (degrees)	5.5

ANALYTICAL PARAMETERS

Interval	791-1045m
Bit size	8.5 in
Minimum smaller hole axis diameter	7.5 in
Maximum smaller hole axis diameter	9.5 in
Minimum axes diameter difference	0.5 in
Maximum vertical deviation of well	10°
Azimuth tolerance within breakout	5°
Maximum tool rotation within breakout	5°
Minimum length of breakout	2m

Well: D-025-61-20-121-45

Well D-025-61-20-121-45 exhibits two breakouts amounting to 27 net metres. The longer breakout of 23 metres has a mean azimuth of  $154.1^{\circ} \pm 2.2^{\circ}$  and this orientation is interpreted to represent the  $S_{Hmin}$  axis at this location.

**Well: D-057-K/094-N-02 Breakouts identified by PFAS**

Magnetic Declination 31.3

Breakout Interval		Length (m)	Measured azimuth (degrees)	Standard Deviation (degrees)	Corrected Azimuth (degrees)
Top (mKB)	Base (mKB)				
323	327	4	27.3	2.0	58.6
686	692	6	25.7	1.3	57.0
727	743	16	116.2	6.8	147.5
753	793	40	98.5	6.4	129.8
817	823	6	84.6	1.2	115.9
882	894	12	77.0	2.0	108.3
920	923	3	30.9	2.6	62.2
931	933	2	19.3	0.4	50.6
1204	1268	64	31.0	3.7	62.3
1269	1280	11	41.0	2.5	72.3
1281	1319	38	40.2	4.6	71.5
1333	1420	87	49.8	5.3	81.1
1425	1452	27	63.5	6.9	94.8
1463	1468	5	37.1	1.6	68.4
1472	1479	7	59.6	1.0	90.9
1483	1493	10	68.7	2.6	100.0
1506	1518	12	48.5	3.5	79.8
1521	1529	8	54.8	2.0	86.1
1537	1551	14	100.0	2.5	131.3
1559	1576	17	81.4	2.0	112.7
1602	1618	16	43.4	2.9	74.7
1620	1664	44	38.6	4.4	69.9
1701	1705	4	30.2	1.2	61.5

Total thickness of Breakouts (m)	306.0
Breakouts associated with washouts (m)	147.0
Washouts (m)	101.0
Key Seats (m)	12.0
Undergauge hole (m)	70.0
In gauge hole (m)	1890.0
Undetermined intervals (m)	371.0
Thickness of logged interval (m)	2897.0

Mean Azimuth of all breakouts (degrees)	83.5
<b>Mean azimuth of SHmax from all breakouts</b>	<b>173.5</b>
Standard Deviation (degrees)	24.5
Mean Azimuth of Pop 1 breakouts (degrees)	74.9
<b>Mean azimuth of Pop 1 SHmax (degrees)</b>	<b>164.9</b>
Standard Deviation (degrees)	10.9
Mean Azimuth of Pop 2 breakouts (degrees)	126.6
<b>Mean azimuth of Pop 2 SHmax (degrees)</b>	<b>36.6</b>
Standard Deviation (degrees)	12.3

ANALYTICAL PARAMETERS

Interval	155-1078m
Bit size	12.25 in
Minimum smaller hole axis diameter	11.25 in
Maximum smaller hole axis diameter	13.25 in
Minimum axes diameter difference	0.5 in
Maximum vertical deviation of well	10°
Azimuth tolerance within breakout	5°
Maximum tool rotation within breakout	5°
Minimum length of breakout	3 m
Interval	1078-3049m
Bit size	8.5 in
Minimum smaller hole axis diameter	7.5 in
Maximum smaller hole axis diameter	9.5 in
Minimum axes diameter difference	0.5 in
Maximum vertical deviation of well	10°
Azimuth tolerance within breakout	5°
Maximum tool rotation within breakout	5°
Minimum length of breakout	3 m

Well: D-057-K/094-N-02

Well D-057-K/094-N-02 exhibits 23 breakouts between the depths of 323 and 1705 m KB amounting to 453 net metres. Population 1 consists of 348 net metres of breakouts and has a mean azimuth of  $74.9^{\circ} \pm 10.9^{\circ}$ . Population 2 consists of 105 net metres of breakouts and has a mean azimuth of  $126.6^{\circ} \pm 12.3^{\circ}$ . The mean azimuth of Population 1 is interpreted to represent the  $S_{Hmin}$  axis at this location, thus  $S_{Hmin}$  is interpreted to be aligned at  $74.9^{\circ} \pm 10.9^{\circ}$ .



**Well: D-064-K/094-N-16 Breakouts identified by PFAS**

Magnetic Declination 32.1

Breakout Interval		Length (m)	Measured azimuth (degrees)	Standard Deviation (degrees)	Corrected Azimuth (degrees)
Top (mKB)	Base (mKB)				
1220	1231	11	87.5	1.3	119.6
1264	1269	5	170.3	1.7	202.4
1405	1416	11	111.7	6.0	143.8
1654	1684	30	28.9	3.4	61.0
1707	1728	21	28.7	3.2	60.8
1765	1775	10	100.8	1.9	132.9
1779	1782	3	96.4	0.7	128.5
1857	1940	83	34.0	2.9	66.1
1942	1949	7	45.5	1.7	77.6
1952	1955	3	41.9	3.8	74.0
1984	1986	2	29.7	1.5	61.8
2003	2023	20	17.3	2.9	49.4
2033	2050	17	141.2	1.6	173.3
2071	2074	3	20.5	0.5	52.6
2089	2116	27	19.6	4.9	51.7
2120	2136	16	29.5	1.5	61.6
2137	2143	6	29.1	2.0	61.2
2179	2220	41	178.8	2.9	210.9
2221	2360	139	8.4	4.0	40.5
2471	2492	21	24.3	1.8	56.4
2493	2503	10	18.8	3.5	50.9
2550	2555	5	49.7	1.5	81.8
2882	2937	55	39.5	2.6	71.6
2939	2958	19	49.7	2.2	81.8
2966	2970	4	96.6	0.9	128.7
2997	3011	14	116.3	1.7	148.4
3105	3124	19	32.2	1.2	64.3
3270	3280	10	120.9	1.8	153.0
3292	3310	18	106.5	2.6	138.6
3389	3394	5	106.4	2.4	138.5
4009	4010	1	119.9	1.6	152.0
4019	4021	2	95.9	1.8	128.0
4031	4033	2	125.4	0.3	157.5
4045	4049	4	120.3	2.8	152.4

Total thickness of Breakouts (m)	531.0
Breakouts associated with washouts (m)	113.0
Washouts (m)	384.0
Key Seats (m)	2.0
Undergauge hole (m)	4.0
In gauge hole (m)	1178.0
Undetermined intervals (m)	834.0
Thickness of logged interval (m)	3046.0

Mean Azimuth of all breakouts (degrees)	55.1
<b>Mean azimuth of SHmax from all breakouts</b>	<b>145.1</b>
Standard Deviation (degrees)	30.1
Mean Azimuth of Pop 1 breakouts (degrees)	55.3
<b>Mean azimuth of Pop 1 SHmax (degrees)</b>	<b>145.3</b>
Standard Deviation (degrees)	14.3
Mean Azimuth of Pop 2 breakouts (degrees)	145.7
<b>Mean azimuth of Pop 2 SHmax (degrees)</b>	<b>55.7</b>
Standard Deviation (degrees)	18.7

#### ANALYTICAL PARAMETERS

Interval	3173-4336m
Bit size	8.5 in
Minimum smaller hole axis diameter	7.5 in
Maximum smaller hole axis diameter	9.5 in
Minimum axes diameter difference	0.5 in
Maximum vertical deviation of well	10°
Azimuth tolerance within breakout	5°
Maximum tool rotation within breakout	5°
Minimum length of breakout	2m

#### Well: D-064-K/094-N-16

Well D-064-K/094-N-16 exhibits 34 breakouts amounting to 644 net metres between depths of 1220 and 4049 m KB. They fall into two populations. Population 1 contains 527 metres of breakouts with a mean azimuth of  $55.3^{\circ} \pm 14.3^{\circ}$ . Population 2 contains 117 metres of breakouts with a mean azimuth of  $145.7^{\circ} \pm 18.7^{\circ}$ .

Population 1 with a mean azimuth of  $55.3^{\circ} \pm 14.3^{\circ}$  is interpreted to represent the  $S_{Hmin}$  axis at this location. This anomalous orientation, that is approximately  $90^{\circ}$  different from the regional trend, is believed to be due to stress trajectory deflection by a nearby fault zone.

**Well: D-069-L/094-P-04 Breakouts identified by PFAS**

Magnetic Declination 28.8

Breakout Interval		Length (m)	Mean azimuth (degrees)	Standard Deviation (degrees)	Corrected Azimuth (degrees)
Top (mKB)	Base (mKB)				
1580	1586	6	122.0	1.5	150.8
1595	1598	3	119.5	0.4	148.3
1625	1635	10	57.6	3.0	86.4
1655	1676	21	136.3	1.8	165.1
1677	1713	36	132.1	2.1	160.9
1716	1732	16	131.9	2.2	160.7
1735	1788	53	130.2	8.0	159.0
1790	1825	35	130.2	1.5	159.0
1827	1850	23	129.1	2.1	157.9
1861	1870	9	31.5	1.8	60.3
1952	1971	19	179.7	1.9	208.5

Total thickness of Breakouts (m)	76.0
Breakouts associated with washouts (m)	155.0
Washouts (m)	135.0
Key Seats (m)	0.0
Undergauge hole (m)	0.0
In gauge hole (m)	81.0
Undetermined intervals (m)	126.0
Thickness of logged interval (m)	573.0

Mean Azimuth of all breakouts (degrees)	162.3
<b>Mean azimuth of SHmax from all breakouts</b>	<b>72.3</b>
Standard Deviation (degrees)	22.1
Mean Azimuth of Pop 1 breakouts (degrees)	162.5
<b>Mean azimuth of Pop 1 SHmax (degrees)</b>	<b>72.5</b>
Standard Deviation (degrees)	13.3
Mean Azimuth of Pop 2 breakouts (degrees)	74.1
<b>Mean azimuth of Pop 2 SHmax (degrees)</b>	<b>164.1</b>
Standard Deviation (degrees)	13.2

ANALYTICAL PARAMETERS

Interval	1078-3049m
Bit size	8.5 in
Minimum smaller hole axis diameter	7.5 in
Maximum smaller hole axis diameter	9.5 in
Minimum axes diameter difference	0.5 in
Maximum vertical deviation of well	10°
Azimuth tolerance within breakout	5°
Maximum tool rotation within breakout	5°
Minimum length of breakout	3 m

Well: D-069-L/094-P-04

Well D-069-L/094-P-04 exhibits 11 breakouts amounting to 231 net metres. Except for two short breakouts, of 10 and 9 metres length, all of the breakouts fall into one population with a mean azimuth of  $162.5^{\circ} \pm 13.3^{\circ}$ . This orientation is interpreted to represent the  $S_{Hmin}$  axis at this location.

**Well: D-074-F/094-P-05 Breakouts identified by PFAS**

Magnetic Declination 30.3

Breakout Interval		Length (m)	Measured azimuth (degrees)	Standard Deviation (degrees)	Corrected Azimuth (degrees)
Top (mKB)	Base (mKB)				
292	340	48	58.7	4.5	89.0
348	378	30	55.6	3.6	85.9
416	507	91	109.8	2.9	140.1
520	579	59	127.9	3.3	158.2
664	675	11	36.7	2.8	67.0
691	695	4	62.0	3.3	92.3
771	775	4	120.1	2.2	150.4
782	786	4	136.6	2.1	166.9
887	895	8	26.7	2.8	57.0
899	906	7	29.3	2.1	59.6
907	918	11	30.4	1.8	60.7
922	935	13	33.1	7.3	63.4
1033	1043	10	46.2	3.8	76.5
1094	1126	32	15.0	3.4	45.3
1128	1142	14	20.8	1.4	51.1
1145	1151	6	23.2	1.1	53.5
1307	1322	15	100.2	2.0	130.5
1323	1335	12	113.1	3.6	143.4
1352	1361	9	129.9	3.5	160.2
1365	1375	10	131.1	4.5	161.4
1398	1401	3	98.7	3.7	129.0
1471	1474	3	49.6	0.6	79.9
1541	1543	2	50.2	2.7	80.5
1546	1551	5	45.2	1.6	75.5
1561	1569	8	112.7	1.9	143.0
1570	1572	2	119.5	1.4	149.8
1576	1579	3	112.1	1.5	142.4
1596	1603	7	103.3	3.2	133.6
1706	1716	10	12.0	6.4	42.3
1724	1727	3	167.5	1.4	197.8
1762	1788	26	155.3	3.0	185.6
1797	1820	23	167.8	4.4	198.1
1824	1831	7	171.0	2.8	201.3
1900	1923	23	144.6	4.8	174.9
1936	1940	4	126.9	0.7	157.2
2015	2033	18	51.0	4.8	81.3
2100	2103	3	146.2	3.6	176.5

Total thickness of Breakouts (m)	303.0
Breakouts associated with washouts (m)	245.0
Washouts (m)	315.0
Key Seats (m)	10.0
Undergauge hole (m)	9.0
In gauge hole (m)	442.0
Undetermined intervals (m)	671.0

Thickness of logged interval (m) 1995.0

Mean Azimuth of all breakouts (degrees)	141.7
<b>Mean azimuth of SHmax from all breakouts</b>	<b>51.7</b>
Standard Deviation (degrees)	57.1
Mean Azimuth of Pop 1 breakouts (degrees)	156.3
<b>Mean azimuth of Pop 1 SHmax (degrees)</b>	<b>66.3</b>
Standard Deviation (degrees)	21.0
Mean Azimuth of Pop 2 breakouts (degrees)	72.2
<b>Mean azimuth of Pop 2 SHmax (degrees)</b>	<b>162.2</b>
Standard Deviation (degrees)	20.5

#### ANALYTICAL PARAMETERS

Interval	234-2240m
Bit size	8.5 in
Minimum smaller hole axis diameter	7.5 in
Maximum smaller hole axis diameter	9.5 in
Minimum axes diameter difference	0.5 in
Maximum vertical deviation of well	10°
Azimuth tolerance within breakout	5°
Maximum tool rotation within breakout	5°
Minimum length of breakout	2 m

#### Well: D-074-F/094-P-05

Well D-074-F/094-P-05 exhibits 37 breakouts amounting to 548 net metres between the depths of 292 and 2103 m KB. These breakouts fall into two populations: Population 1 contains 316 metres of breakouts with a mean azimuth of 156.3° +/- 21.0°. Population 2 contains 232 metres of breakouts with a mean azimuth of 72.2° +/- 20.5°.

The azimuth of Population 1 is interpreted to represent the S<sub>Hmin</sub> axis at this location.

**Well: D-087-A/094-P-11 Breakouts identified by PFAS**

Magnetic Declination 31.3

Breakout Interval		Length (m)	Measured azimuth (degrees)	Standard Deviation (degrees)	Corrected Azimuth (degrees)
Top (mKB)	Base (mKB)				
284	285	1	106.4	4.5	137.7
286	288	2	114.0	3.5	145.3
293	295	2	102.8	3.2	134.1
409	415	6	90.5	4.0	121.8

Total thickness of Breakouts (m)	8.0
Breakouts associated with washouts (m)	3.0
Washouts (m)	0.0
Key Seats (m)	0.0
Undergauge hole (m)	0.0
In gauge hole (m)	505.0
Undetermined intervals (m)	20.0
Thickness of logged interval (m)	536.0

Mean Azimuth of all breakouts (degrees)	129.6
<b>Mean azimuth of SHmax from all breakouts</b>	<b>39.6</b>
Standard Deviation (degrees)	9.4
Mean Azimuth of Pop 1 breakouts (degrees)	129.6
<b>Mean azimuth of Pop 1 SHmax (degrees)</b>	<b>39.6</b>
Standard Deviation (degrees)	9.4

ANALYTICAL PARAMETERS

Interval	283-823m
Bit size	7.75 in
Minimum smaller hole axis diameter	6.75 in
Maximum smaller hole axis diameter	8.75 in
Minimum axes diameter difference	0.5 in
Maximum vertical deviation of well	10°
Azimuth tolerance within breakout	5°
Maximum tool rotation within breakout	5°
Minimum length of breakout	2m

Well: D-087-A/094-P-11

Well D-087-A/094-P-11 exhibits four breakouts amounting to 11 net metres between depths of 284 and 415 m KB. Their mean azimuth is  $129.6^{\circ} \pm 9.4^{\circ}$  and is interpreted to represent  $S_{Hmin}$  at this location.

**Well: D-087-C/094-P-05 Breakouts identified by PFAS**

Magnetic Declination 29.4

Breakout Interval		Length (m)	Measured azimuth (degrees)	Standard Deviation (degrees)	Corrected Azimuth (degrees)
Top (mKB)	Base (mKB)				
2001	2067	66	14.4	3.6	43.8
2101	2112	11	109.0	4.0	138.4
2134	2146	12	85.6	1.4	115.0
2152	2178	26	81.6	2.1	111.0
2194	2197	3	10.4	1.9	39.8
2298	2306	8	107.7	2.2	137.1

Total thickness of Breakouts (m)	126.0
Breakouts associated with washouts (m)	0.0
Washouts (m)	25.0
Key Seats (m)	0.0
Undergauge hole (m)	0.0
In gauge hole (m)	313.0
Undetermined intervals (m)	74.0
Thickness of logged interval (m)	538.0

Mean Azimuth of all breakouts (degrees)	66.6
<b>Mean azimuth of SHmax from all breakouts</b>	<b>156.6</b>
Standard Deviation (degrees)	47.4
Mean Azimuth of Pop 1 breakouts (degrees)	130.6
<b>Mean azimuth of Pop 1 SHmax (degrees)</b>	<b>40.6</b>
Standard Deviation (degrees)	12.3
Mean Azimuth of Pop 2 breakouts (degrees)	43.7
<b>Mean azimuth of Pop 2 SHmax (degrees)</b>	<b>133.7</b>
Standard Deviation (degrees)	0.8

ANALYTICAL PARAMETERS

Interval	1993-2532m
Bit size	8.5 in
Minimum smaller hole axis diameter	7.5 in
Maximum smaller hole axis diameter	9.5 in
Minimum axes diameter difference	0.5 in
Maximum vertical deviation of well	10°
Azimuth tolerance within breakout	5°
Maximum tool rotation within breakout	5°
Minimum length of breakout	2m



Well: D-087-C/094-P-05

Well D-087-C/094-P-05 exhibits six breakouts amounting to 126 net metres between depths of 2001 and 2306 m KB which fall into two populations. Population 1 consists of 57 net metres of breakouts with a mean azimuth of  $130.6^{\circ} \pm 12.3^{\circ}$ . Population 2 consists of 69 net metres of breakouts with a mean azimuth of  $43.7^{\circ} \pm 0.8^{\circ}$ .

Provisionally, the former population is interpreted as aligned with  $S_{Hmin}$ . This is because these breakouts are mostly deeper than those in the latter population and are aligned with the regional trend. Also, the latter population is dominated by a 66 metre long breakout immediately below the casing shoe, which could have resulted from the collapse of a drilling induced fracture.

**Well: D-087-G/094-O-06 Breakouts identified by PFAS**

Magnetic Declination 30.5

Breakout Interval		Length (m)	Measured azimuth (degrees)	Standard Deviation (degrees)	Corrected Azimuth (degrees)
Top (mKB)	Base (mKB)				
299	441	142	168.0	8.1	198.5
451	492	41	152.3	5.1	182.8
537	556	19	110.0	3.2	140.5
556	560	4	108.0	2.8	138.5
560	578	18	111.1	3.8	141.6

Total thickness of Breakouts (m)	220.0
Breakouts associated with washouts (m)	4.0
Washouts (m)	13.0
Key Seats (m)	0.0
Undergauge hole (m)	0.0
In gauge hole (m)	561.0
Undetermined intervals (m)	121.0
Thickness of logged interval (m)	919.0

Mean Azimuth of all breakouts (degrees)	8.4
<b>Mean azimuth of SHmax from all breakouts</b>	<b>98.4</b>
Standard Deviation (degrees)	21.3
Mean Azimuth of Pop 1 breakouts (degrees)	8.4
<b>Mean azimuth of Pop 1 SHmax (degrees)</b>	<b>98.4</b>
Standard Deviation (degrees)	21.3

ANALYTICAL PARAMETERS

Interval	300-1219m
Bit size	7.75 in
Minimum smaller hole axis diameter	6.75 in
Maximum smaller hole axis diameter	8.75 in
Minimum axes diameter difference	0.5 in
Maximum vertical deviation of well	10°
Azimuth tolerance within breakout	5°
Maximum tool rotation within breakout	5°
Minimum length of breakout	2m

Well: D-087-G/094-O-06

Well D-87-G/094-O-06 exhibits five breakouts amounting to 224 net metres. Their mean azimuth is  $8.4^{\circ} \pm 21.3^{\circ}$  and is interpreted to represent  $S_{Hmin}$  at this location. No breakouts were identified below 600 metres depth because the well's vertical deviation exceeded  $10^{\circ}$ .

**Well: D-092-J/094-O-06 Breakouts identified by PFAS**

Magnetic Declination 30.3

Breakout Interval		Length (m)	Measured azimuth (degrees)	Standard Deviation (degrees)	Corrected Azimuth (degrees)
Top (mKB)	Base (mKB)				
755	775	20	64.6	2.9	94.9
779	794	15	50.5	3.4	80.8
797	801	4	54.7	1.4	85.0
822	847	25	36.5	4.2	66.8
913	917	4	67.9	6.3	98.2
1052	1057	5	53.2	2.0	83.5
1107	1108	1	65.8	0.9	96.1
1353	1354	1	71.4	2.2	101.7
1416	1424	8	76.7	2.4	107.0
1486	1492	6	85.2	1.2	115.5

Total thickness of Breakouts (m)	70.0
Breakouts associated with washouts (m)	19.0
Washouts (m)	11.0
Key Seats (m)	0.0
Undergauge hole (m)	0.0
In gauge hole (m)	754.0
Undetermined intervals (m)	95.0
Thickness of logged interval (m)	949.0

Mean Azimuth of all breakouts (degrees)	86.1
<b>Mean azimuth of SHmax from all breakouts</b>	<b>176.1</b>
Standard Deviation (degrees)	15.5
Mean Azimuth of Pop 1 breakouts (degrees)	86.1
<b>Mean azimuth of Pop 1 SHmax (degrees)</b>	<b>176.1</b>
Standard Deviation (degrees)	15.5

ANALYTICAL PARAMETERS

Interval	754-1705m
Bit size	8.5 in
Minimum smaller hole axis diameter	7.5 in
Maximum smaller hole axis diameter	9.5 in
Minimum axes diameter difference	0.5 in
Maximum vertical deviation of well	10°
Azimuth tolerance within breakout	5°
Maximum tool rotation within breakout	5°
Minimum length of breakout	2m

Well: D-092-J/094-O-06

Well D-092-J/094-O-06 exhibits 10 breakouts amounting to 89 net metres between depths of 755 and 1492 m KB. Most of the breakouts are short but they exhibit consistently oriented long axes. Their mean azimuth is  $86.1^{\circ} \pm 15.5^{\circ}$  and is interpreted to represent  $S_{Hmin}$  at this location.

**Well: E-072-61-20-122-00 Breakouts identified by PFAS**

Magnetic Declination 33.4

Breakout Interval		Length (m)	Measured azimuth (degrees)	Standard Deviation (degrees)	Corrected Azimuth (degrees)
Top (mKB)	Base (mKB)				
219	229	10	161.7	3.2	195.1
277	319	42	130.2	5.0	163.6
401	431	30	147.5	4.2	180.9
449	450	1	146.1	2.1	179.5
504	514	10	126.4	3.1	159.8
520	551	31	118.7	2.6	152.1

Total thickness of Breakouts (m)	124.0
Breakouts associated with washouts (m)	0.0
Washouts (m)	49.0
Key Seats (m)	7.0
Undergauge hole (m)	4.0
In gauge hole (m)	637.0
Undetermined intervals (m)	163.0
Thickness of logged interval (m)	984.0

Mean Azimuth of all breakouts (degrees)	167.0
<b>Mean azimuth of SHmax from all breakouts</b>	<b>77.0</b>
Standard Deviation (degrees)	13.3
Mean Azimuth of Pop 1 breakouts (degrees)	167.0
<b>Mean azimuth of Pop 1 SHmax (degrees)</b>	<b>77.0</b>
Standard Deviation (degrees)	13.3

ANALYTICAL PARAMETERS

Interval	109-1094m
Bit size	7.75 in
Minimum smaller hole axis diameter	6.75 in
Maximum smaller hole axis diameter	8.75 in
Minimum axes diameter difference	0.5 in
Maximum vertical deviation of well	10°
Azimuth tolerance within breakout	5°
Maximum tool rotation within breakout	5°
Minimum length of breakout	2m

Well: E-072-61-20-122-00

Well E-072-61-20-122-00 exhibits six breakouts amounting to 124 net metres between depths of 219 and 551 m KB. Their mean azimuth is 167.0° +/- 13.3° and is interpreted to represent  $S_{Hmin}$  at this location.

**Well: F-008-60-40-124-30 Breakouts identified by PFAS**

Magnetic Declination

33.0

This well has been assigned the same dipmeter log as Well F-038-60-30-123-45

**Well: F-038-60-30-123-45 Breakouts identified by PFAS**

Magnetic Declination

32.3

Breakout Interval		Length (m)	Measured azimuth (degrees)	Standard Deviation (degrees)	Corrected Azimuth (degrees)
Top (mKB)	Base (mKB)				
960	970	10	119.7	3.4	152.0
970	975	5	119.8	1.6	152.1
976	985	9	124.5	1.9	156.8
999	1001	2	107.6	0.6	139.9
1041	1056	15	93.3	4.4	125.6
1060	1063	3	110.7	1.9	143.0
1163	1168	5	87.3	1.3	119.6
1219	1224	5	94.8	3.4	127.1
1246	1253	7	106.6	3.9	138.9
1286	1316	30	97.1	2.9	129.4
1332	1336	4	91.6	1.4	123.9
1351	1356	5	96.3	4.0	128.6
1370	1373	3	89.3	3.5	121.6
1375	1378	3	86.1	2.8	118.4
1401	1404	3	92.4	0.9	124.7
1424	1428	4	104.0	4.8	136.3

Total thickness of Breakouts (m)	101.0
Breakouts associated with washouts (m)	12.0
Washouts (m)	11.0
Key Seats (m)	6.0
Undergauge hole (m)	0.0
In gauge hole (m)	264.0
Undetermined intervals (m)	129.0
Thickness of logged interval (m)	523.0

Mean Azimuth of all breakouts (degrees)	133.8
<b>Mean azimuth of SHmax from all breakouts</b>	<b>43.8</b>
Standard Deviation (degrees)	11.6
Mean Azimuth of Pop 1 breakouts (degrees)	133.8
<b>Mean azimuth of Pop 1 SHmax (degrees)</b>	<b>43.8</b>
Standard Deviation (degrees)	11.6

ANALYTICAL PARAMETERS

Interval	908-1434m
Bit size	12.25 in
Minimum smaller hole axis diameter	11.25 in
Maximum smaller hole axis diameter	13.25 in
Minimum axes diameter difference	0.5 in
Maximum vertical deviation of well	10°
Azimuth tolerance within breakout	5°
Maximum tool rotation within breakout	5°
Minimum length of breakout	2m

Well: F-038-60-30-123-45

Well F-038-60-30-123-45 exhibits 16 breakouts amounting to 113 net metres. They are all reasonably consistent in their long axis orientations and have a mean azimuth of  $133.8^\circ \pm 11.6^\circ$ . This is interpreted as the axis of  $S_{Hmin}$  at this location.

**Well: G-001-60-10-124-15 Breakouts identified by PFAS**

Magnetic Declination 32.2

Breakout Interval		Length (m)	Measured azimuth (degrees)	Standard Deviation (degrees)	Corrected Azimuth (degrees)
Top (mKB)	Base (mKB)				
800	806	6	20.4	2.5	52.6
835	846	11	131.9	4.6	164.1
1104	1107	3	26.9	0.3	59.1
1240	1250	10	25.7	1.0	57.9
1255	1270	15	19.7	2.3	51.9
1289	1296	7	110.1	2.6	142.3
1477	1527	50	97.1	7.0	129.3
1582	1598	16	31.1	6.1	63.3
1800	1823	23	121.6	2.6	153.8
1949	1976	27	28.6	1.8	60.8
2107	2162	55	21.3	2.9	53.5
2228	2256	28	112.8	2.5	145.0
2328	2356	28	65.3	2.0	97.5
2418	2442	24	146.9	2.1	179.1
2444	2467	23	149.7	4.4	181.9
2581	2602	21	33.0	2.0	65.2
2602	2611	9	39.0	1.1	71.2
2645	2734	89	59.9	6.2	92.1
2737	2778	41	56.6	4.3	88.8
2799	2845	46	114.9	3.2	147.1
2922	2948	26	168.8	2.1	201.0
2949	3017	68	171.2	4.3	203.4
3064	3068	4	12.7	2.1	44.9
3135	3137	2	8.9	1.3	41.1
3175	3177	2	10.7	0.8	42.9
3326	3392	66	101.7	6.1	133.9
3392	3470	78	94.3	9.5	126.5
3487	3505	18	81.7	4.6	113.9
3539	3546	7	85.9	3.6	118.1
4337	4363	26	97.8	3.7	130.0
4380	4386	6	94.5	0.8	126.7
4407	4413	6	92.2	4.7	124.4

Total thickness of Breakouts (m)	200.0
Breakouts associated with washouts (m)	641.0
Washouts (m)	0.0
Key Seats (m)	0.0
Undergauge hole (m)	1.0
In gauge hole (m)	8.0
Undetermined intervals (m)	3235.0
Thickness of logged interval (m)	4085.0

Mean Azimuth of all breakouts (degrees)	114.5
<b>Mean azimuth of SHmax from all breakouts</b>	<b>24.5</b>
Standard Deviation (degrees)	49.9

Mean Azimuth of Pop 1 breakouts (degrees)	145.5
<b>Mean azimuth of Pop 1 SHmax (degrees)</b>	<b>55.5</b>
Standard Deviation (degrees)	30.0
Mean Azimuth of Pop 2 breakouts (degrees)	74.4
<b>Mean azimuth of Pop 2 SHmax (degrees)</b>	<b>164.4</b>
Standard Deviation (degrees)	18.5

#### ANALYTICAL PARAMETERS

Interval	366-3294m
Bit size	12.25 in
Minimum smaller hole axis diameter	11.25 in
Maximum smaller hole axis diameter	13.25 in
Minimum axes diameter difference	0.5 in
Maximum vertical deviation of well	10°
Azimuth tolerance within breakout	5°
Maximum tool rotation within breakout	5°
Minimum length of breakout	2m
Interval	3294-4452m
Bit size	8.5 in
Minimum smaller hole axis diameter	7.5 in
Maximum smaller hole axis diameter	9.5 in
Minimum axes diameter difference	0.5 in
Maximum vertical deviation of well	10°
Azimuth tolerance within breakout	5°
Maximum tool rotation within breakout	5°
Minimum length of breakout	2m

#### Well: G-001-60-10-124-15

Well G-001-60-10-124-15 exhibits 36 breakouts amounting to 841 net metres between depths of 800 and 4413 m KB. They fall into two populations. Population 1 contains 513 metres of breakouts with a mean azimuth of 145.5° +/- 30.0°. Population 2 contains 328 metres of breakouts with a mean azimuth of 74.4° +/- 18.5°.

Population 1 is interpreted as aligned with S<sub>Hmin</sub>.



**Well: G-032-61-10-121-15 Breakouts identified by PFAS**

Magnetic Declination 33.0

Breakout Interval		Length (m)	Measured azimuth (degrees)	Standard Deviation (degrees)	Corrected Azimuth (degrees)
Top (mKB)	Base (mKB)				
1082	1106	24	151.0	2.6	184.0
1107	1109	2	159.6	1.4	192.6
1112	1124	12	151.1	2.7	184.1
1125	1129	4	147.9	1.5	180.9
1130	1135	5	146.8	2.4	179.8
1138	1144	6	157.8	2.0	190.8
1147	1158	11	160.5	2.5	193.5
1191	1197	6	70.3	2.0	103.3

Total thickness of Breakouts (m)	45.0
Breakouts associated with washouts (m)	25.0
Washouts (m)	3.0
Key Seats (m)	0.0
Undergauge hole (m)	0.0
In gauge hole (m)	312.0
Undetermined intervals (m)	50.0
Thickness of logged interval (m)	435.0

Mean Azimuth of all breakouts (degrees)	5.3
<b>Mean azimuth of SHmax from all breakouts</b>	<b>95.3</b>
Standard Deviation (degrees)	18.2
Mean Azimuth of Pop 1 breakouts (degrees)	3.1
<b>Mean azimuth of Pop 1 SHmax (degrees)</b>	<b>93.1</b>
Standard Deviation (degrees)	4.5
Mean Azimuth of Pop 2 breakouts (degrees)	103.3
<b>Mean azimuth of Pop 2 SHmax (degrees)</b>	<b>13.3</b>
Standard Deviation (degrees)	0.0

ANALYTICAL PARAMETERS

Interval	109-1094m
Bit size	8.5 in
Minimum smaller hole axis diameter	7.5 in
Maximum smaller hole axis diameter	9.5 in
Minimum axes diameter difference	0.5 in
Maximum vertical deviation of well	10°
Azimuth tolerance within breakout	5°
Maximum tool rotation within breakout	5°
Minimum length of breakout	2m

Well: G-032-61-10-121-15

Well G-032-61-10-121-15 exhibits eight breakouts amounting to 70 net metres in thickness between 1082 and 1197 m KB. The upper seven breakouts constitute Population 1 with a mean azimuth of  $3.1^\circ \pm 4.5^\circ$ . The deepest breakout is only 6 metres in length and is assigned to Population 2. The mean azimuth is  $103.3^\circ$ . Population 1 is interpreted as aligned with  $S_{Hmin}$ .

Since this orientation is somewhat anomalous, it is likely that stresses have been deflected by a local fault zone.

**Well: G-042-60-20-121-00 Breakouts identified by PFAS**

Magnetic Declination 31.6

Breakout Interval		Length (m)	Measured azimuth (degrees)	Standard Deviation (degrees)	Corrected Azimuth (degrees)
Top (mKB)	Base (mKB)				
972	987	15	172.5	2.5	204.1
989	990	1	176.9	0.1	208.5
993	1019	26	174.3	2.7	205.9
1022	1026	4	163.1	1.0	194.7
1034	1036	2	62.7	1.2	94.3
1077	1080	3	48.4	0.5	80.0
1082	1085	3	47.6	1.3	79.2
1088	1091	3	50.2	1.0	81.8
1500	1502	2	8.8	0.9	40.4
1505	1515	10	104.2	1.5	135.8
1557	1563	6	78.7	1.1	110.3
1567	1574	7	60.5	2.4	92.1
1580	1586	6	61.0	1.8	92.6
1968	1972	4	149.8	1.2	181.4
1979	1989	10	123.0	3.1	154.6

Total thickness of Breakouts (m)	64.0
Breakouts associated with washouts (m)	38.0
Washouts (m)	493.0
Key Seats (m)	1.0
Undergauge hole (m)	10.0
In gauge hole (m)	275.0
Undetermined intervals (m)	562.0
Thickness of logged interval (m)	1443.0

Mean Azimuth of all breakouts (degrees)	25.7
<b>Mean azimuth of SHmax from all breakouts</b>	<b>115.7</b>
Standard Deviation (degrees)	50.9
Mean Azimuth of Pop 1 breakouts (degrees)	10.9
<b>Mean azimuth of Pop 1 SHmax (degrees)</b>	<b>100.9</b>
Standard Deviation (degrees)	27.7
Mean Azimuth of Pop 2 breakouts (degrees)	89.5
<b>Mean azimuth of Pop 2 SHmax (degrees)</b>	<b>179.5</b>
Standard Deviation (degrees)	18.2

**ANALYTICAL PARAMETERS**

Interval	971-2416m
Bit size	8.5 in
Minimum smaller hole axis diameter	7.5 in
Maximum smaller hole axis diameter	9.5 in
Minimum axes diameter difference	0.5 in
Maximum vertical deviation of well	10°
Azimuth tolerance within breakout	5°
Maximum tool rotation within breakout	5°
Minimum length of breakout	2m

Well: G-042-60-10-121-00

The dipmeter log coverage of well G-042-60-10-121-00 is somewhat broken up. However, 15 breakouts amounting to 102 net metres were identified between depths of 972 and 1989 m KB. They fall into two populations. Population 1 contains 69 metres of breakouts with a mean azimuth of  $10.9^\circ \pm 27.7^\circ$ . Population 2 consists of 33 metres of breakouts with a mean azimuth of  $89.5^\circ \pm 18.2^\circ$ .

Population 1 is interpreted as aligned with  $S_{Hmin}$ . It is a non-regional axis, but there may be some fault influence nearby that is responsible for deflecting stress trajectories.

**Well:L-060-60-20-124-15 Breakouts identified by PFAS**

Magnetic Declination 32.6

Breakout Interval		Length (m)	Measured azimuth (degrees)	Standard Deviation (degrees)	Corrected Azimuth (degrees)
Top (mKB)	Base (mKB)				
157	162	5	175.4	0.5	208.0
202	246	44	163.8	3.5	196.4
248	250	2	79.5	0.3	112.1
251	262	11	164.5	2.7	197.1
340	345	5	11.6	0.5	44.2
350	358	8	10.0	0.4	42.6
366	370	4	10.2	0.9	42.8
392	407	15	29.9	2.9	62.5
408	411	3	33.3	0.4	65.9
419	422	3	29.2	0.9	61.8
424	432	8	26.4	2.0	59.0
435	479	44	22.0	4.4	54.6
503	506	3	139.6	0.7	172.2
688	691	3	50.0	0.3	82.6
737	761	24	175.3	3.9	207.9
783	831	48	22.9	3.7	55.5
835	860	25	14.2	4.8	46.8
877	885	8	102.8	2.5	135.4
920	991	71	101.5	8.8	134.1
994	1047	53	111.4	7.9	144.0
1049	1056	7	111.3	2.9	143.9
1060	1077	17	109.8	4.2	142.4
1158	1161	3	85.5	0.5	118.1

Total thickness of Breakouts (m)	330.0
Breakouts associated with washouts (m)	84.0
Washouts (m)	3.0
Key Seats (m)	0.0
Undergauge hole (m)	12.0
In gauge hole (m)	847.0
Undetermined intervals (m)	200.0
Thickness of logged interval (m)	1476.0

Mean Azimuth of all breakouts (degrees)	28.7
<b>Mean azimuth of SHmax from all breakouts</b>	<b>118.7</b>
Standard Deviation (degrees)	56.5
Mean Azimuth of Pop 1 breakouts (degrees)	155.5
<b>Mean azimuth of Pop 1 SHmax (degrees)</b>	<b>65.5</b>
Standard Deviation (degrees)	31.7
Mean Azimuth of Pop 2 breakouts (degrees)	55.0
<b>Mean azimuth of Pop 2 SHmax (degrees)</b>	<b>145.0</b>
Standard Deviation (degrees)	11.0

ANALYTICAL PARAMETERS

Interval	157-1162m
Bit size	12.0 in
Minimum smaller hole axis diameter	11.0 in
Maximum smaller hole axis diameter	13.0 in
Minimum axes diameter difference	0.5 in
Maximum vertical deviation of well	10°
Azimuth tolerance within breakout	5°
Maximum tool rotation within breakout	5°
Minimum length of breakout	2m

Interval	1162-1634m
Bit size	8.5 in
Minimum smaller hole axis diameter	7.5 in
Maximum smaller hole axis diameter	9.5 in
Minimum axes diameter difference	0.5 in
Maximum vertical deviation of well	10°
Azimuth tolerance within breakout	5°
Maximum tool rotation within breakout	5°
Minimum length of breakout	2m

Well: L-060-60-20-124-15

Well L-060-60-20-124-15 exhibits 22 breakouts amounting to 414 net metres between depths of 157 and 1161 m KB. They fall into two populations. Population 1 contains 243 metres of breakouts with a mean azimuth of  $155.5^{\circ} \pm 31.7^{\circ}$ . Population 2 consists of 171 metres of breakouts with a mean azimuth of  $55.0^{\circ} \pm 11.0^{\circ}$ .

Population 1 is interpreted as aligned with  $S_{Hmin}$ .

**Well M-051-60-30-121-00 Breakouts identified by PFAS**

Magnetic Declination 32.1

Breakout Interval		Length (m)	Measured azimuth (degrees)	Standard Deviation (degrees)	Corrected Azimuth (degrees)
Top (mKB)	Base (mKB)				
848	861	13	175.6	1.4	207.7
926	933	7	174.5	2.4	206.6
936	943	7	158.1	3.2	190.2
944	986	42	148.0	3.0	180.1
1370	1388	18	92.6	3.7	124.7
1835	1870	35	122.6	2.2	154.7
1873	1876	3	117.4	1.1	149.5

Total thickness of Breakouts (m)	105.0
Breakouts associated with washouts (m)	20.0
Washouts (m)	19.0
Key Seats (m)	2.0
Undergauge hole (m)	7.0
In gauge hole (m)	193.0
Undetermined intervals (m)	842.0
Thickness of logged interval (m)	1188.0

Mean Azimuth of all breakouts (degrees)	170.2
<b>Mean azimuth of SHmax from all breakouts</b>	<b>80.2</b>
Standard Deviation (degrees)	26.2
Mean Azimuth of Pop 1 breakouts (degrees)	170.2
<b>Mean azimuth of Pop 1 SHmax (degrees)</b>	<b>80.2</b>
Standard Deviation (degrees)	26.2

ANALYTICAL PARAMETERS

Interval	848-203m
Bit size	8.5 in
Minimum smaller hole axis diameter	7.5 in
Maximum smaller hole axis diameter	9.5 in
Minimum axes diameter difference	0.5 in
Maximum vertical deviation of well	10°
Azimuth tolerance within breakout	5°
Maximum tool rotation within breakout	5°
Minimum length of breakout	2m

Well: M-051-60-30-121-00

The dipmeter log coverage of well M-051-60-30-121-00 is somewhat broken up. Nevertheless, seven breakouts amounting to 125 net metres were identified between depths of 848 and 1876 m KB. They fall into a single population with a mean azimuth of 170.2° +/- 26.2° that is interpreted as aligned with  $S_{Hmin}$ .

**Well N-019-60-40-123-45 Breakouts identified by PFAS**

Magnetic Declination 32.9

Breakout Interval		Length (m)	Measured azimuth (degrees)	Standard Deviation (degrees)	Corrected Azimuth (degrees)
Top (mKB)	Base (mKB)				
1414	1419	5	131.3	2.4	164.2

Total thickness of Breakouts (m)	0.0
Breakouts associated with washouts (m)	5.0
Washouts (m)	14.0
Key Seats (m)	0.0
Undergauge hole (m)	0.0
In gauge hole (m)	58.0
Undetermined intervals (m)	14.0
Thickness of logged interval (m)	91.0

Mean Azimuth of all breakouts (degrees)	164.2
<b>Mean azimuth of SHmax from all breakouts</b>	<b>74.2</b>
Standard Deviation (degrees)	0.0
Mean Azimuth of Pop 1 breakouts (degrees)	164.2
<b>Mean azimuth of Pop 1 SHmax (degrees)</b>	<b>74.2</b>
Standard Deviation (degrees)	0.0

ANALYTICAL PARAMETERS

Interval	1398-1501m
Bit size	8.5 in
Minimum smaller hole axis diameter	7.5 in
Maximum smaller hole axis diameter	9.5 in
Minimum axes diameter difference	0.5 in
Maximum vertical deviation of well	10°
Azimuth tolerance within breakout	5°
Maximum tool rotation within breakout	5°
Minimum length of breakout	2m

Well: N-019-60-40-123-45

Well N-019-60-40-123-45 has limited dipmeter coverage and only one breakout was identified with a mean azimuth of 164.2°. It is interpreted as aligned with  $S_{Hmin}$ .



**Well N-033-61-00-122-30 Breakouts identified by PFAS**

Magnetic Declination 33.0

Breakout Interval		Length (m)	Measured azimuth (degrees)	Standard Deviation (degrees)	Corrected Azimuth (degrees)
Top (mKB)	Base (mKB)				
1523	1527	4	53.4	2.1	86.4
1531	1536	5	132.9	10.2	165.9
1541	1563	22	134.1	6.1	167.1
1894	1896	2	158.4	2.0	191.4

Total thickness of Breakouts (m)	2.0
Breakouts associated with washouts (m)	31.0
Washouts (m)	33.0
Key Seats (m)	0.0
Undergauge hole (m)	26.0
In gauge hole (m)	271.0
Undetermined intervals (m)	44.0
Thickness of logged interval (m)	407.0

Mean Azimuth of all breakouts (degrees)	164.1
<b>Mean azimuth of SHmax from all breakouts</b>	<b>74.1</b>
Standard Deviation (degrees)	22.1
Mean Azimuth of Pop 1 breakouts (degrees)	168.4
<b>Mean azimuth of Pop 1 SHmax (degrees)</b>	<b>78.4</b>
Standard Deviation (degrees)	6.1
Mean Azimuth of Pop 2 breakouts (degrees)	86.4
<b>Mean azimuth of Pop 2 SHmax (degrees)</b>	<b>176.4</b>
Standard Deviation (degrees)	0.0

ANALYTICAL PARAMETERS

Interval	1498-1905m
Bit size	8.5 in
Minimum smaller hole axis diameter	7.5 in
Maximum smaller hole axis diameter	9.5 in
Minimum axes diameter difference	0.5 in
Maximum vertical deviation of well	10°
Azimuth tolerance within breakout	5°
Maximum tool rotation within breakout	5°
Minimum length of breakout	2m

Well: N-033-61-00-122-30

Well N-033-61-00-122-30 exhibits four breakouts amounting to 33 net metres between depths of 1523 and 1896 m KB. Two populations are recognised. Population 1 consists of three breakouts with 29 metres net thickness and a mean azimuth of 168.4° +/- 6.1°. It is interpreted as aligned with S<sub>Hmin</sub>.

**Well O-046-60-30-123-45 Breakouts identified by PFAS**

Magnetic Declination 32.7

Breakout Interval		Length (m)	Measured azimuth (degrees)	Standard Deviation (degrees)	Corrected Azimuth (degrees)
Top (mKB)	Base (mKB)				
950	953	3	171.1	1.2	203.8
1105	1108	3	122.4	2.9	155.1
1130	1133	3	115.1	2.0	147.8
1145	1151	6	116.3	1.4	149.0
1371	1374	3	41.5	1.8	74.2
1410	1414	4	38.2	1.0	70.9

Total thickness of Breakouts (m)	13.0
Breakouts associated with washouts (m)	9.0
Washouts (m)	0.0
Key Seats (m)	0.0
Undergauge hole (m)	14.0
In gauge hole (m)	1056.0
Undetermined intervals (m)	55.0
Thickness of logged interval (m)	1147.0

Mean Azimuth of all breakouts (degrees)	150.0
<b>Mean azimuth of SHmax from all breakouts</b>	<b>60.0</b>
Standard Deviation (degrees)	50.4
Mean Azimuth of Pop 1 breakouts (degrees)	158.0
<b>Mean azimuth of Pop 1 SHmax (degrees)</b>	<b>68.0</b>
Standard Deviation (degrees)	21.1
Mean Azimuth of Pop 2 breakouts (degrees)	72.3
<b>Mean azimuth of Pop 2 SHmax (degrees)</b>	<b>162.3</b>
Standard Deviation (degrees)	1.6

ANALYTICAL PARAMETERS

Interval	442-1590m
Bit size	12.0 in
Minimum smaller hole axis diameter	11.0 in
Maximum smaller hole axis diameter	13.0 in
Minimum axes diameter difference	0.5 in
Maximum vertical deviation of well	10°
Azimuth tolerance within breakout	5°
Maximum tool rotation within breakout	5°
Minimum length of breakout	2m

Well: O-046-60-30-123-45

Well O-046-60-30-123-45 exhibits six breakouts between 950 and 1414 m KB with a net thickness of 22 metres. Two populations are recognised. Population 1 consists of the upper four breakouts and has a mean azimuth of 158.0° +/- 21.1°. This orientation is interpreted to represent the S<sub>Hmin</sub> axis at the well site.

**Well:P-024-60-30-123-45 Breakouts identified by PFAS**

Magnetic Declination 32.4

Breakout Interval		Length (m)	Measured azimuth (degrees)	Standard Deviation (degrees)	Corrected Azimuth (degrees)
Top (mKB)	Base (mKB)				
191	208	17	44.1	3.0	76.5
256	283	27	31.1	1.5	63.5
286	316	30	29.5	4.1	61.9
319	321	2	29.3	0.5	61.7
322	350	28	29.1	2.5	61.5
352	372	20	32.3	2.3	64.7
372	413	41	40.1	3.3	72.5
511	540	29	32.1	3.4	64.5
630	637	7	20.8	2.1	53.2
681	721	40	16.4	1.2	48.8
854	858	4	23.3	0.4	55.7
998	1005	7	7.4	2.1	39.8
1327	1334	7	100.0	3.0	132.4
1453	1466	13	105.8	2.4	138.2
1535	1540	5	103.7	5.6	136.1
1620	1626	6	98.7	3.7	131.1

Total thickness of Breakouts (m)	184.0
Breakouts associated with washouts (m)	99.0
Washouts (m)	10.0
Key Seats (m)	44.0
Undergauge hole (m)	0.0
In gauge hole (m)	985.0
Undetermined intervals (m)	127.0
Thickness of logged interval (m)	1449.0

Mean Azimuth of all breakouts (degrees)	64.6
<b>Mean azimuth of SHmax from all breakouts</b>	<b>154.6</b>
Standard Deviation (degrees)	21.1
Mean Azimuth of Pop 1 breakouts (degrees)	62.3
<b>Mean azimuth of Pop 1 SHmax (degrees)</b>	<b>152.3</b>
Standard Deviation (degrees)	8.8
Mean Azimuth of Pop 2 breakouts (degrees)	135.2
<b>Mean azimuth of Pop 2 SHmax (degrees)</b>	<b>45.2</b>
Standard Deviation (degrees)	3.0

ANALYTICAL PARAMETERS

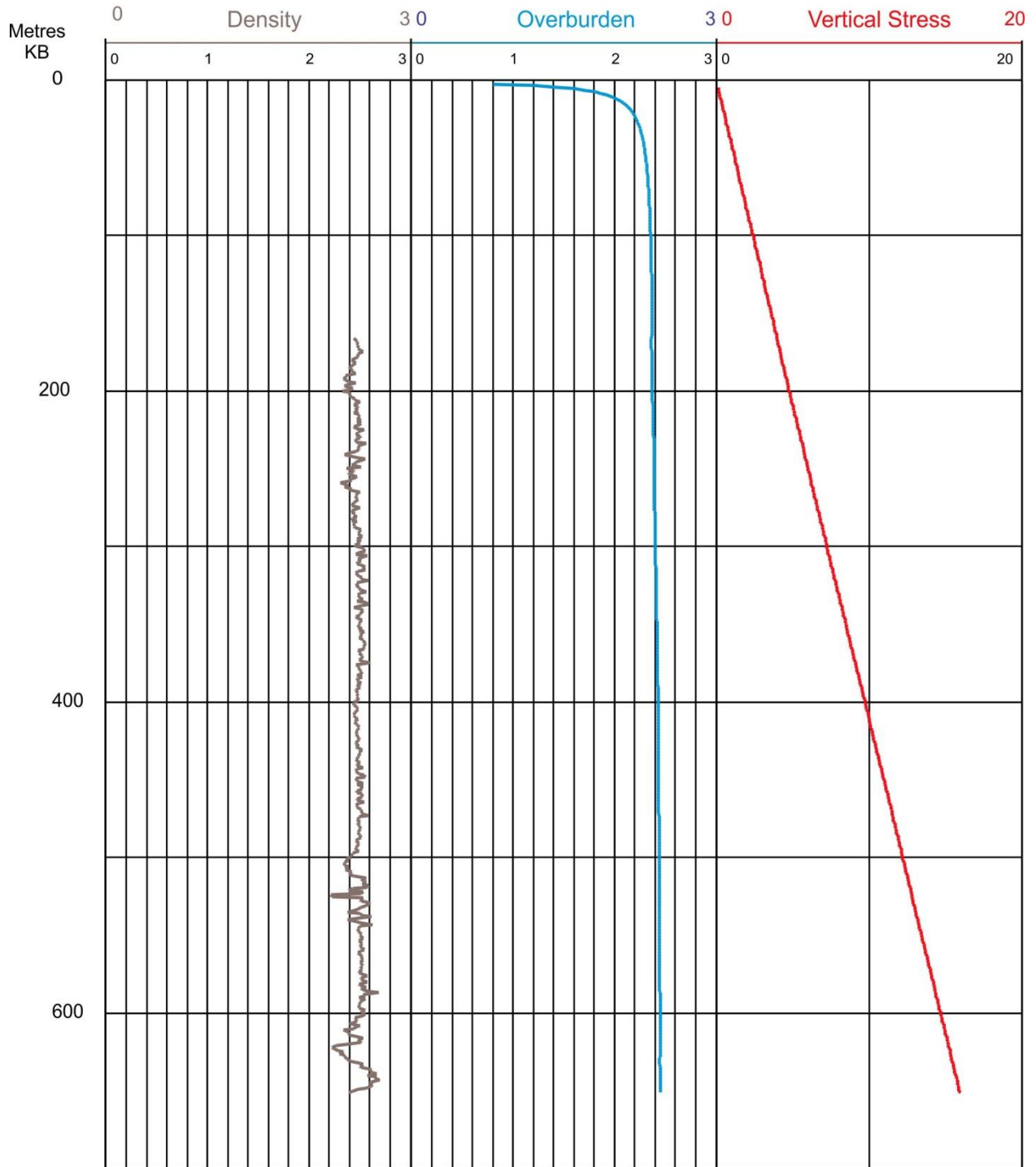
Interval	184-1640m
Bit size	8.5 in
Minimum smaller hole axis diameter	7.5 in
Maximum smaller hole axis diameter	9.5 in
Minimum axes diameter difference	0.5 in
Maximum vertical deviation of well	10°
Azimuth tolerance within breakout	5°
Maximum tool rotation within breakout	5°
Minimum length of breakout	2m

Well: P-024-60-30-123-45

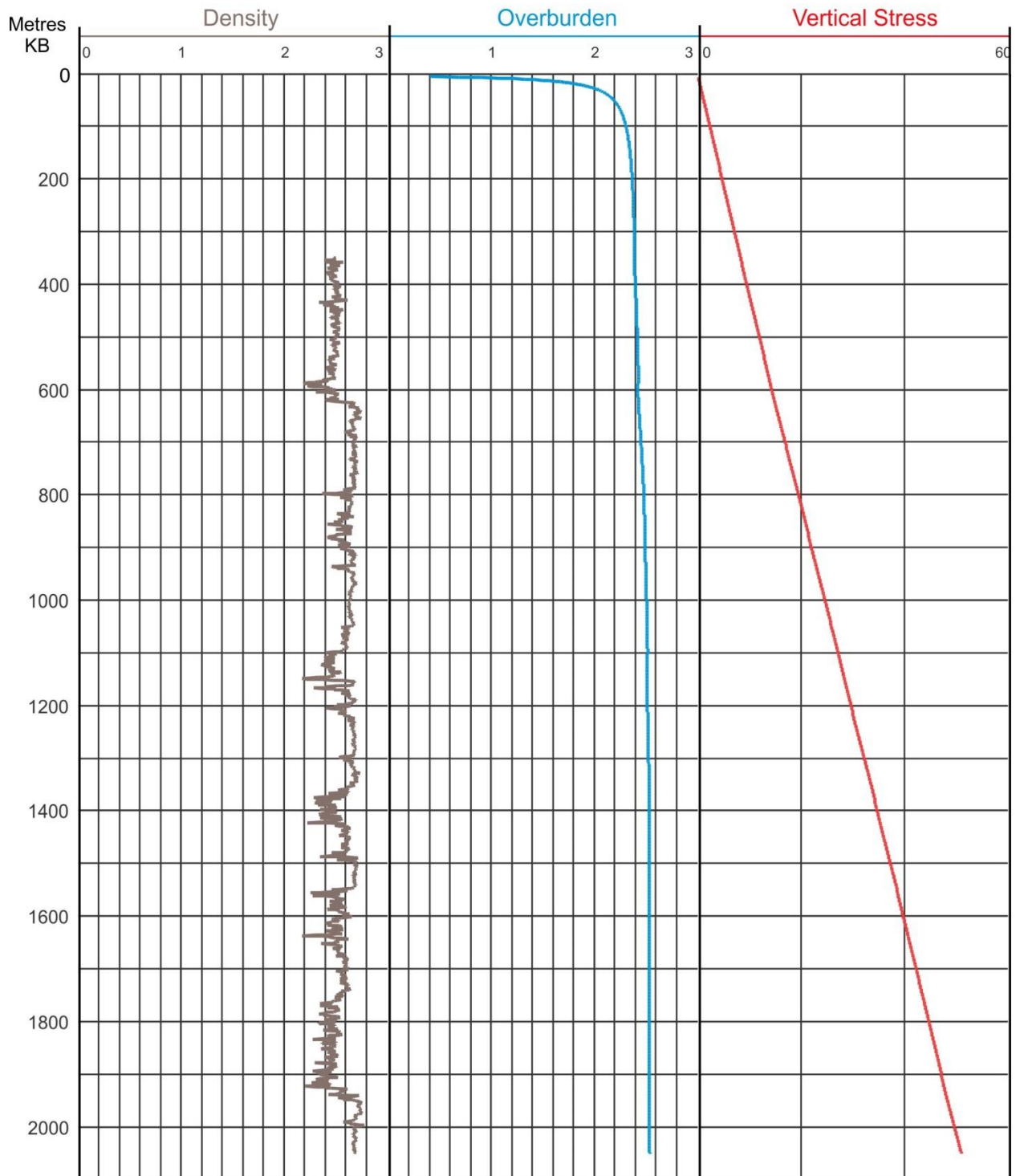
Well P-024-60-30-123-45 exhibits 16 breakouts with a net thickness of 283 metres between 191 and 1626 m KB. The breakouts fall into two populations. Population 1 is made up of the 12 uppermost breakouts above 1005 m KB and has a mean azimuth of  $62.3^{\circ} \pm 8.8^{\circ}$ . Population 2 consists of the four lowermost breakouts, a mere 31 m of net thickness and exhibits a mean azimuth of  $135.2^{\circ} \pm 3.0^{\circ}$ . Although, the latter orientation is well aligned with the regional trajectories for  $S_{Hmin}$ , it is more justified to interpret the  $S_{Hmin}$  axis as aligned with Population 1. There is faulting in the area that could well have affected stress trajectories.

## Appendix 2: Sv Graphic Plots

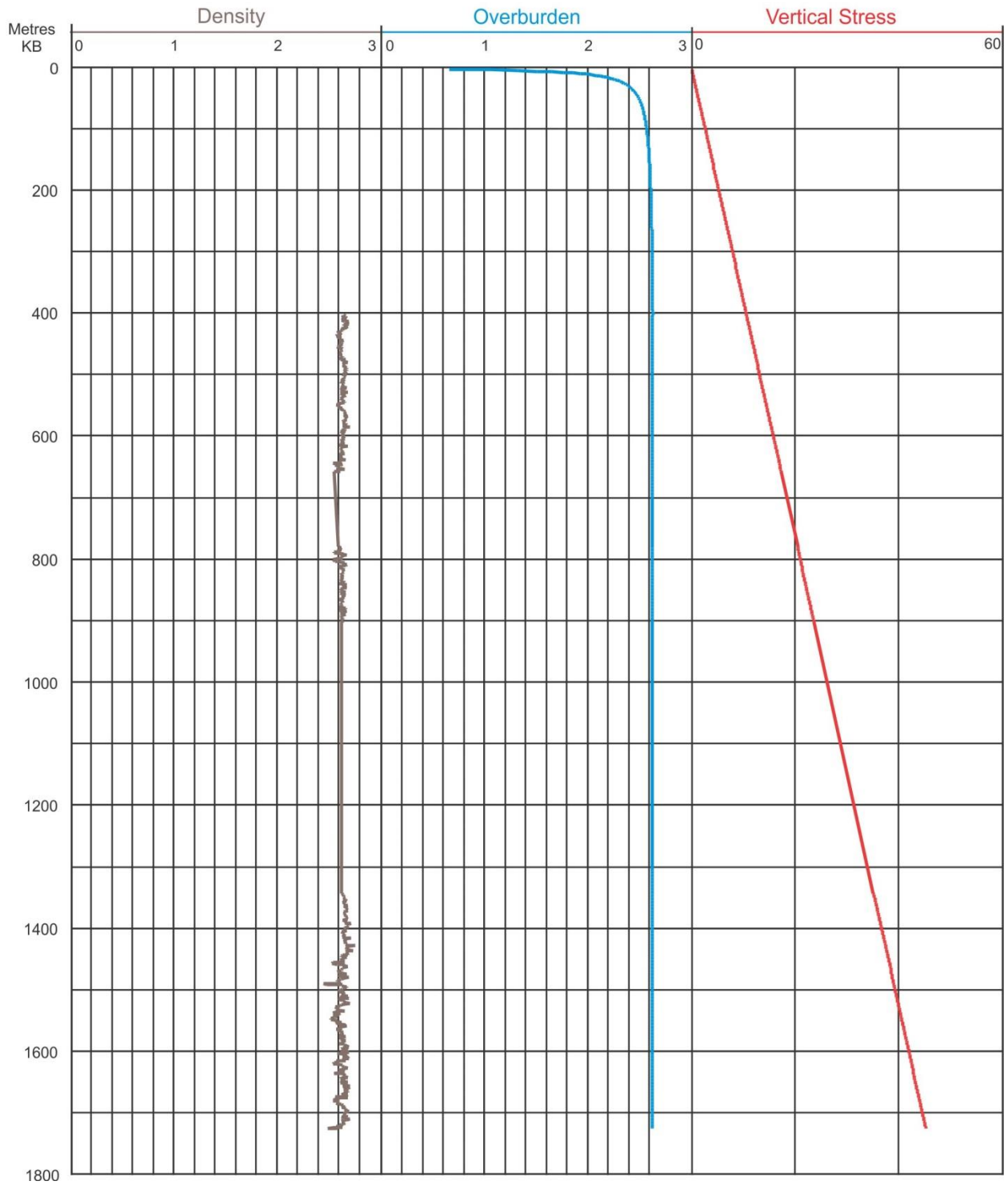
WELL : A-015-J/094-I-14



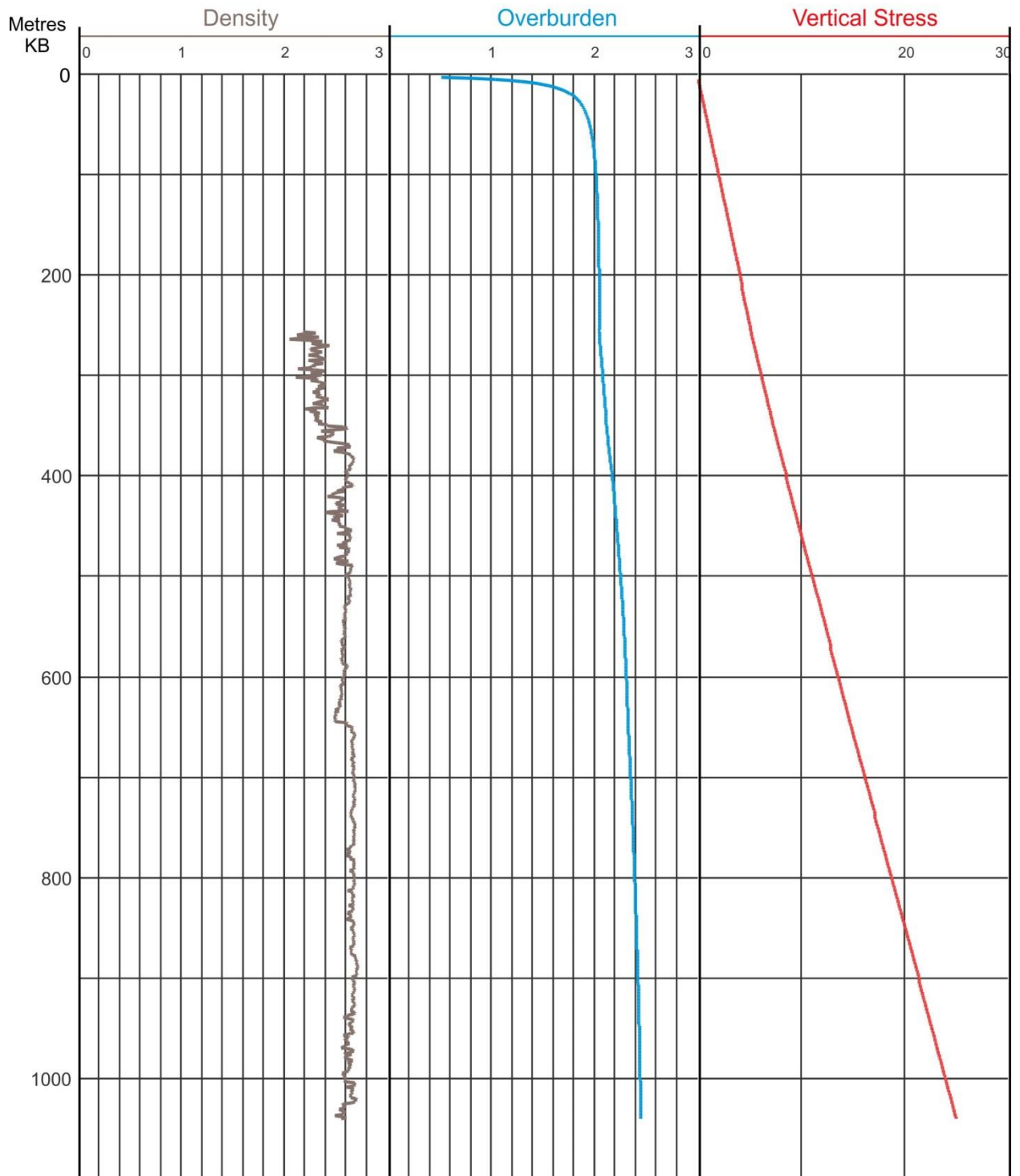
WELL : A-18-E/094-I-12



WELL: A-039-B/094-N-08

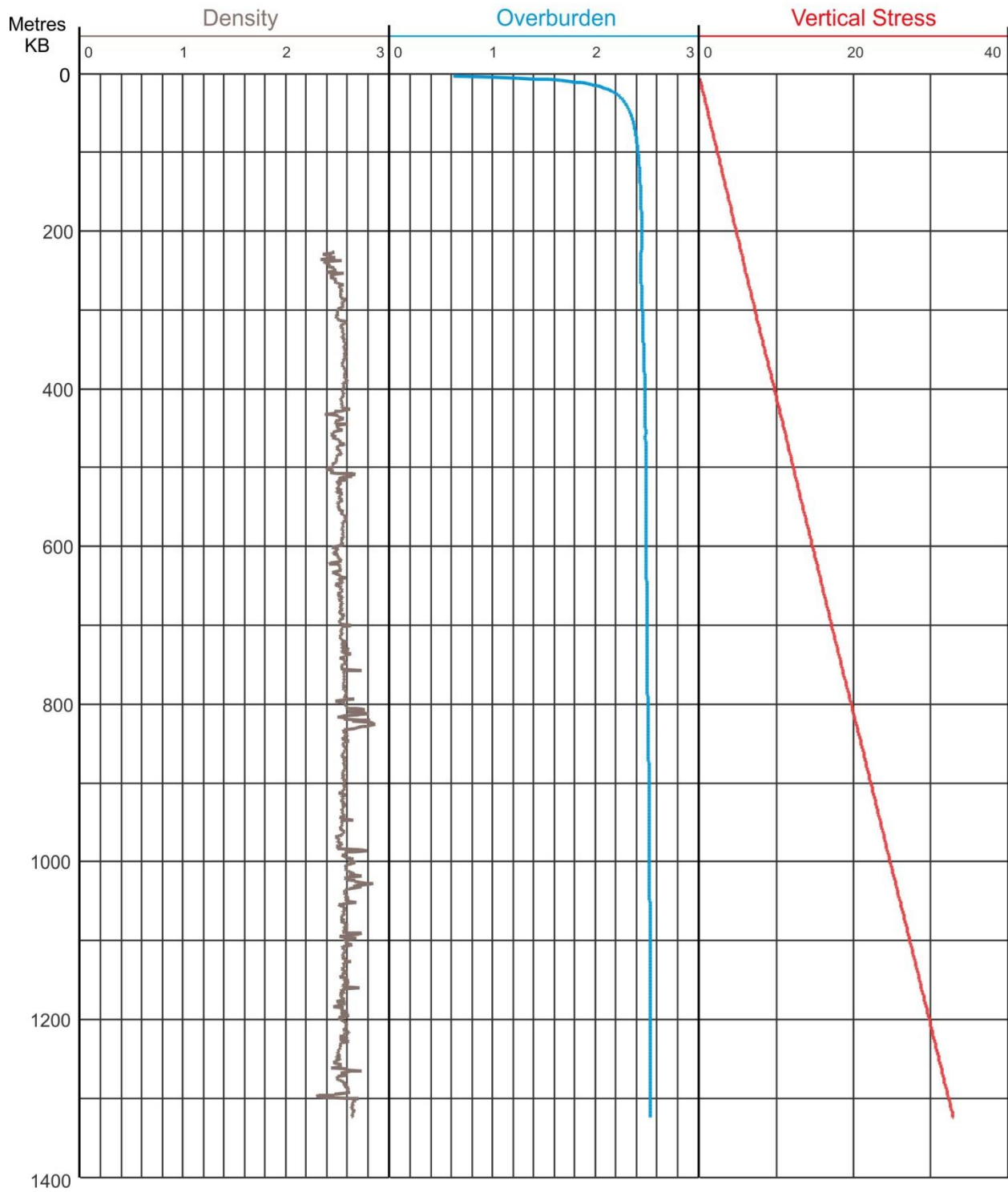


WELL: A-056-G/094-P-01

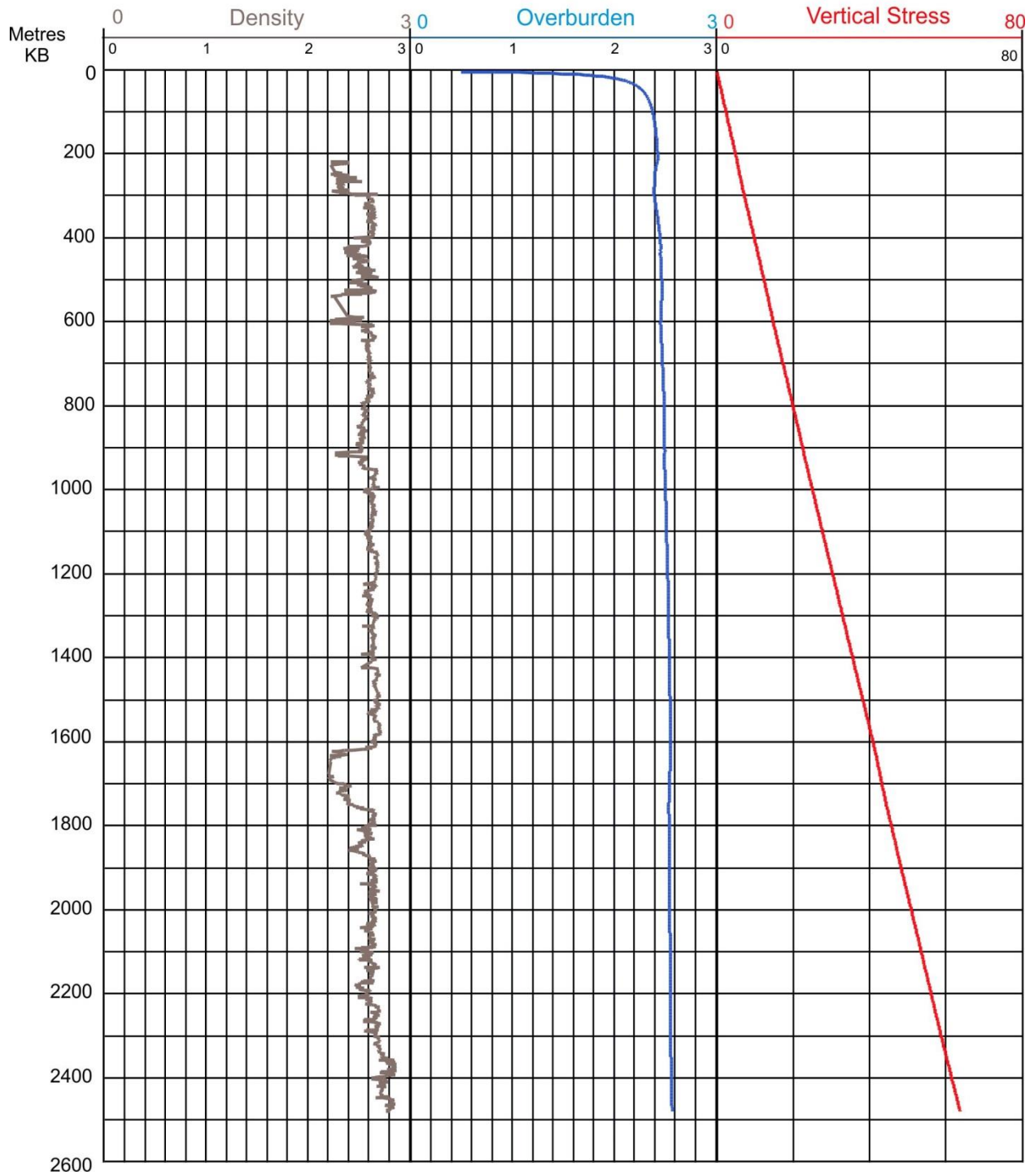




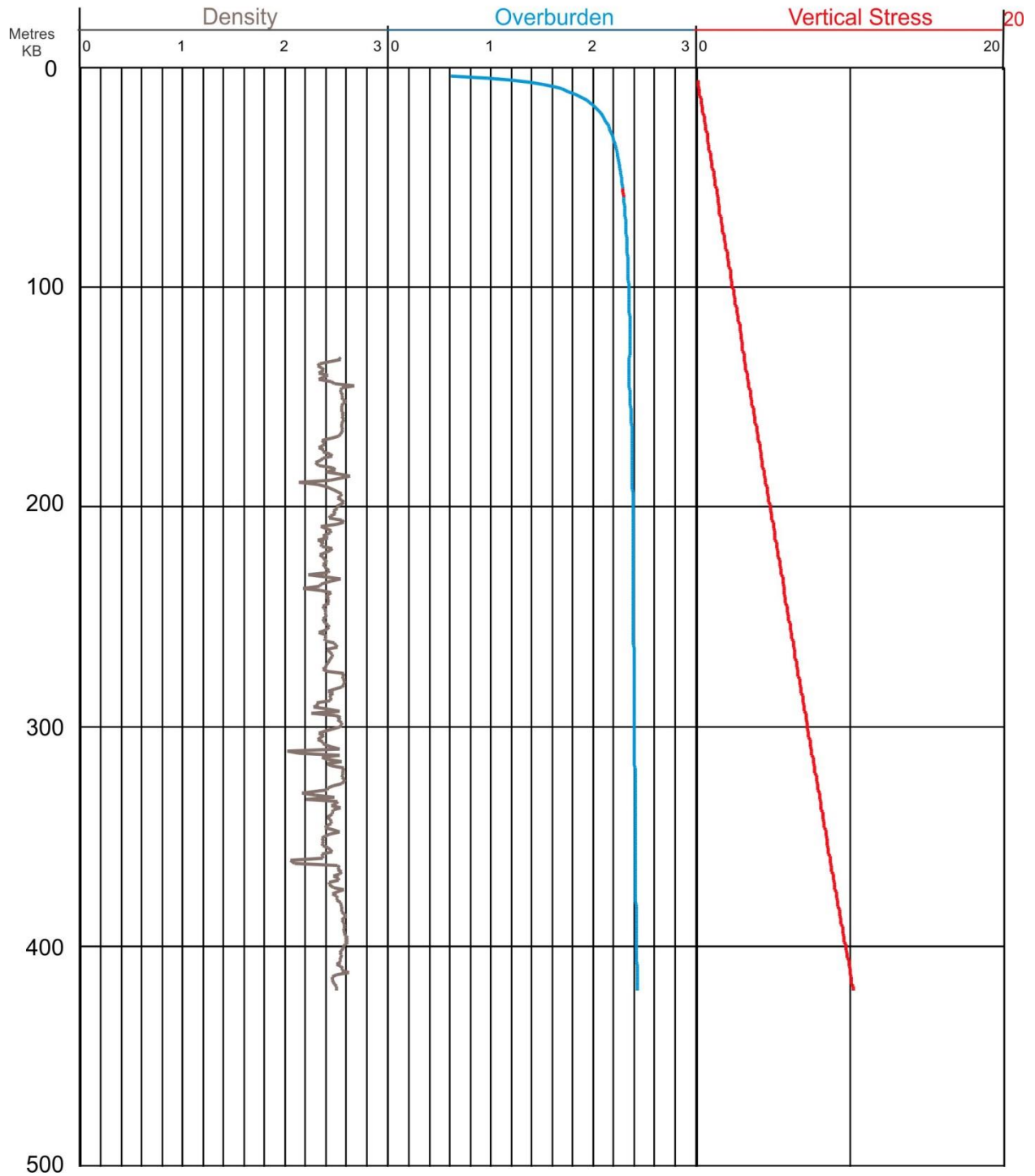
WELL: A-064-B/094-O-14



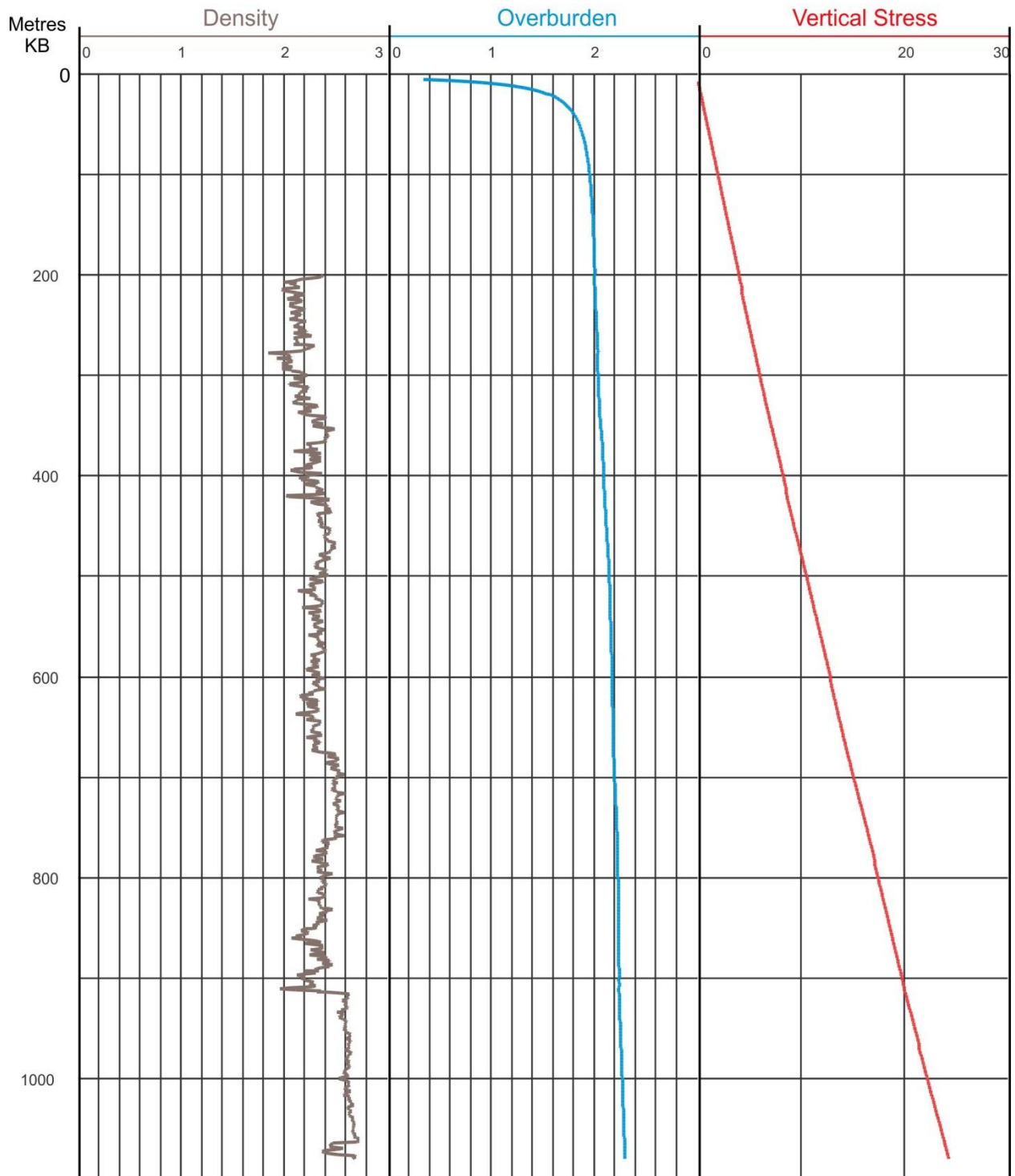
WELL : A-064-H/094-O-16



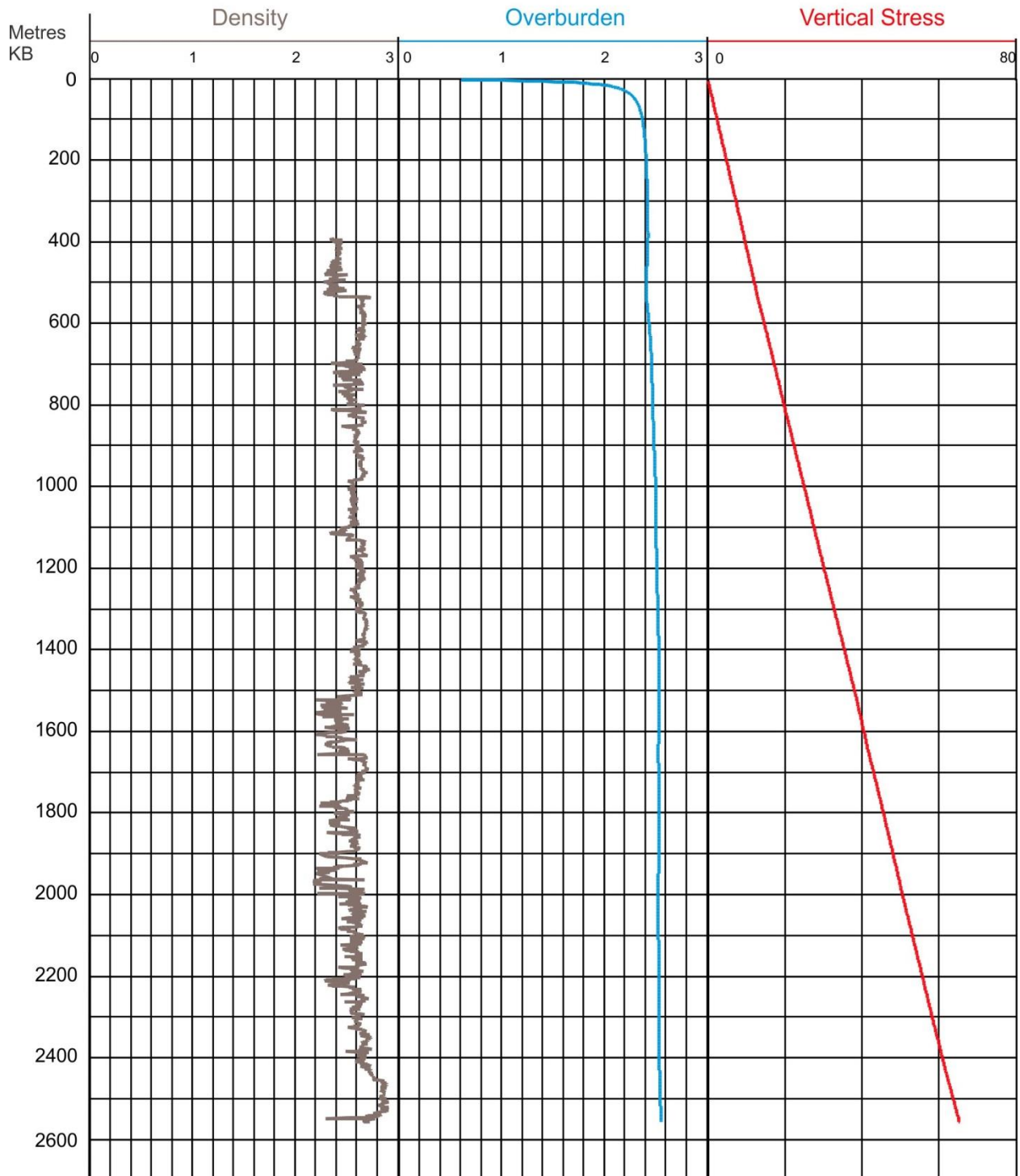
WELL: A-067-D/094-O-13



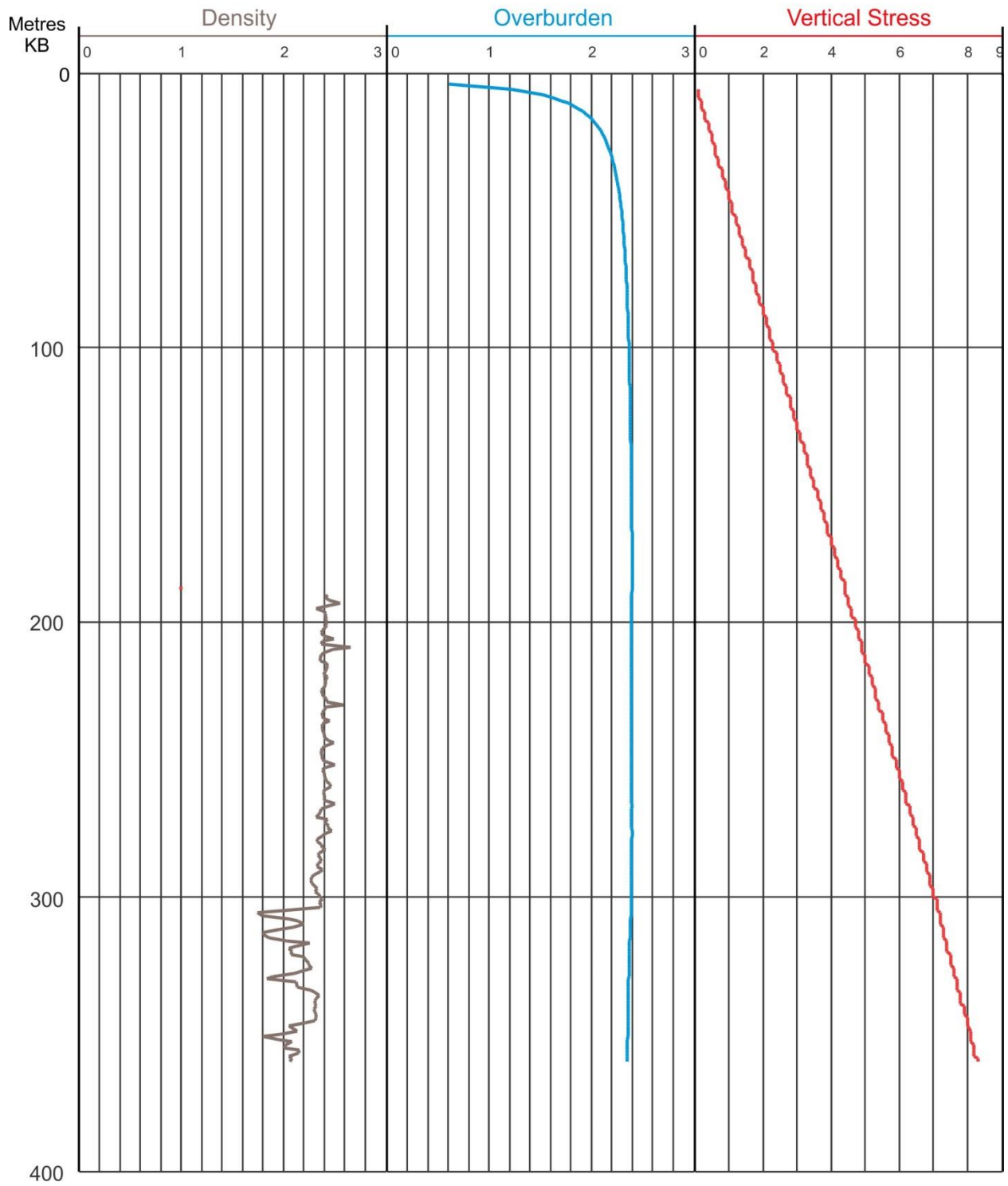
WELL: A-077-D/094-I-04



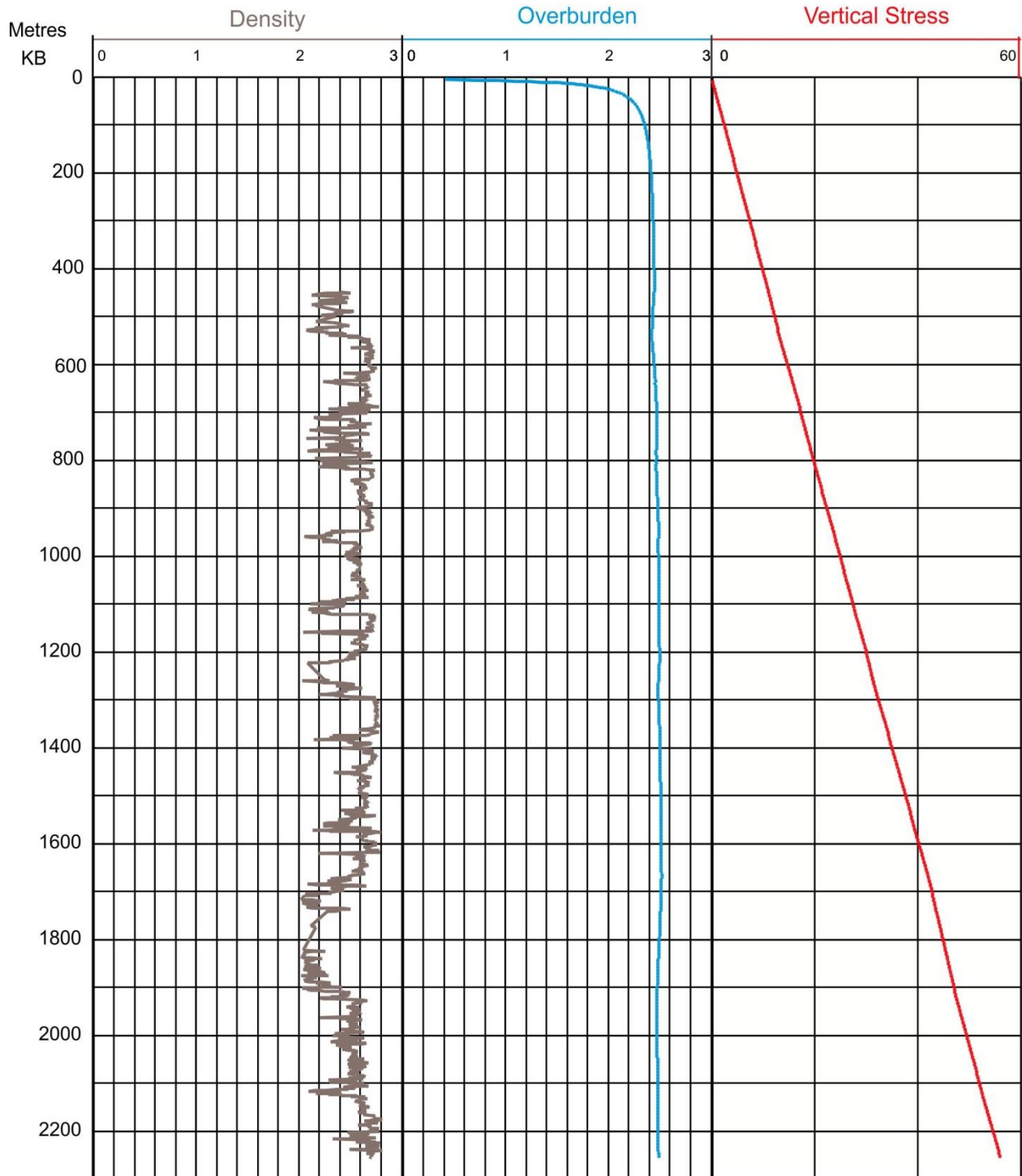
## WELL: A-085-E/094-P-12



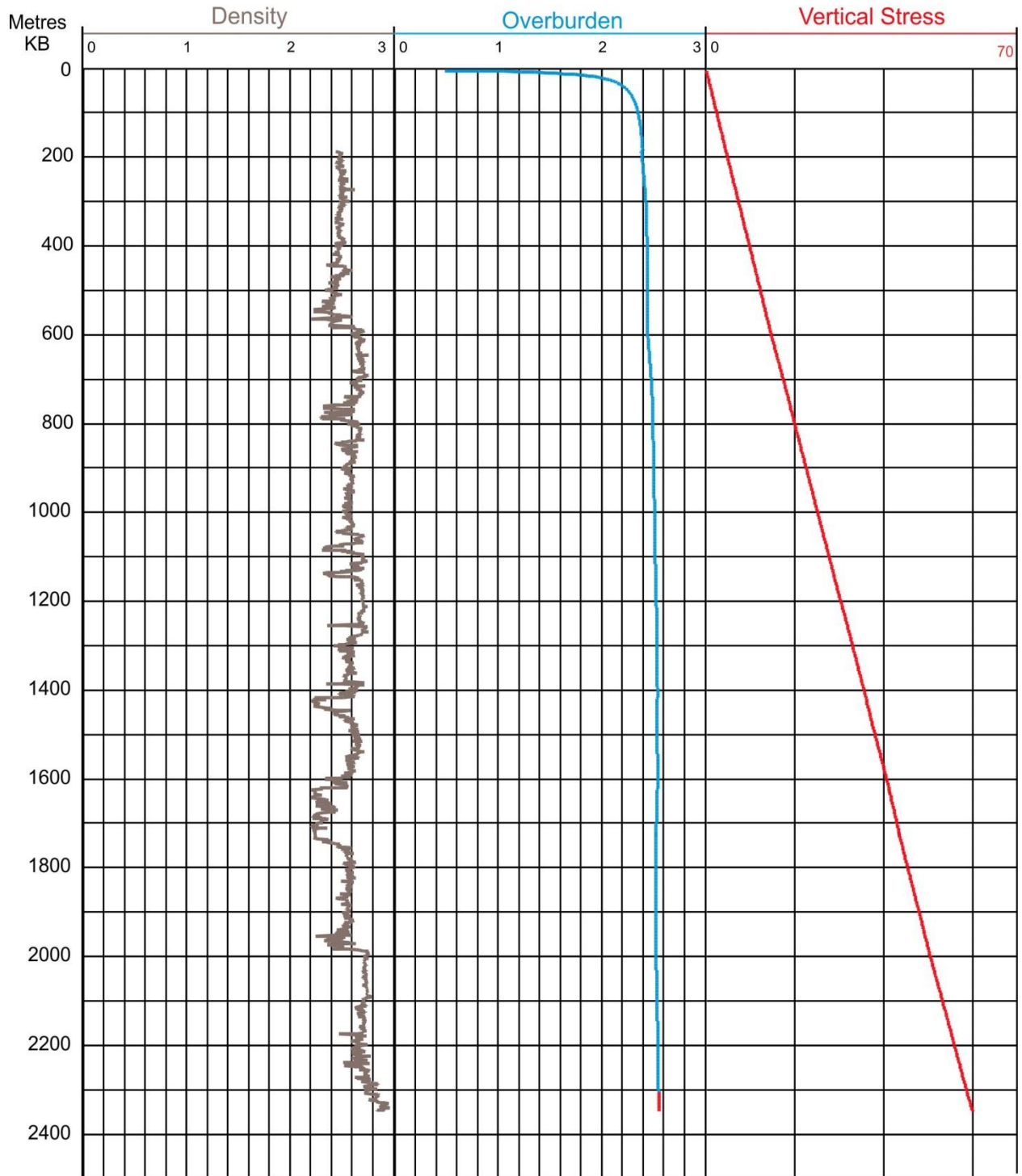
WELL: A-087-G/094-P-10



WELL: A-088-F/094-P-12

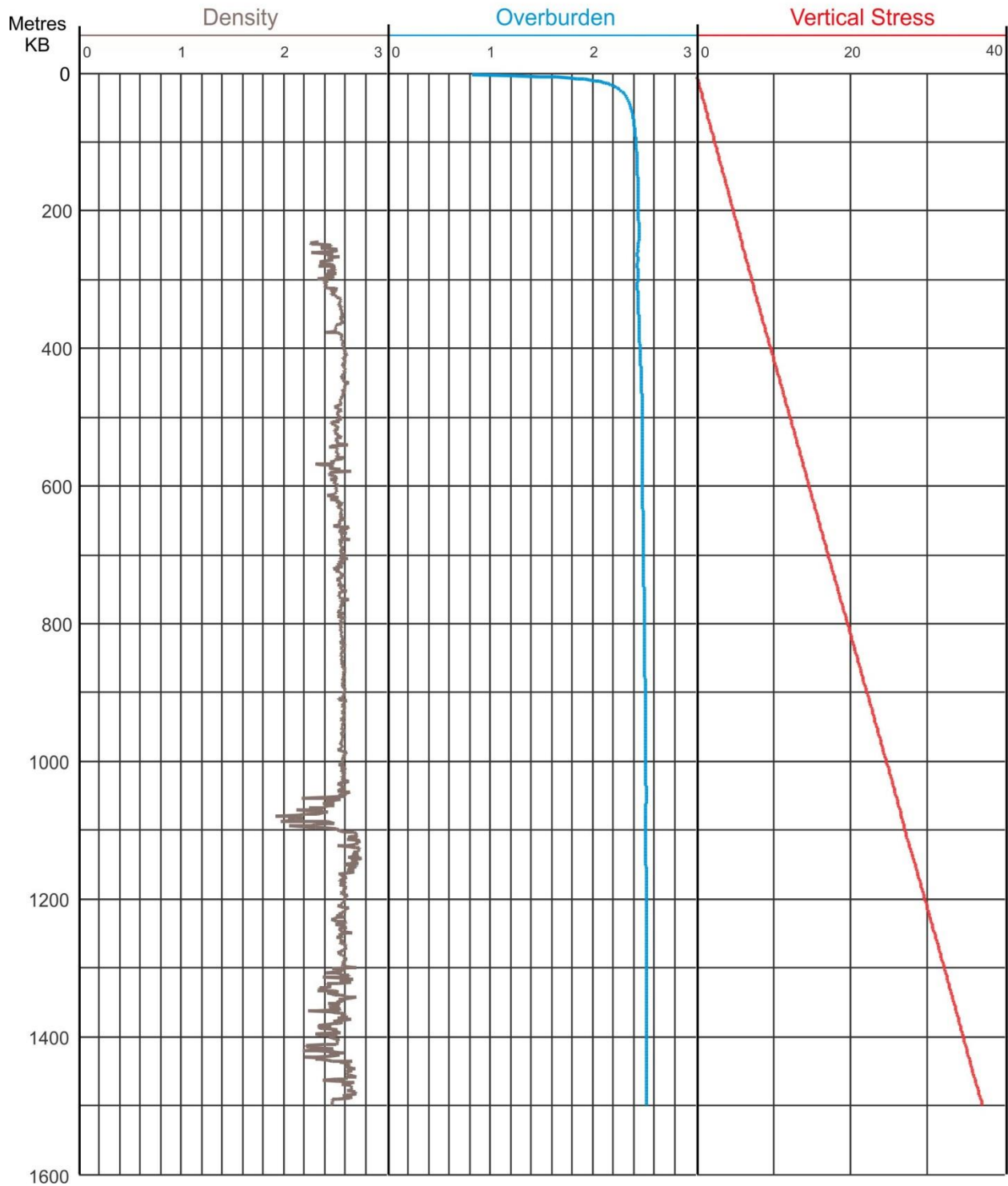


WELL: B-015-B/094-I-14

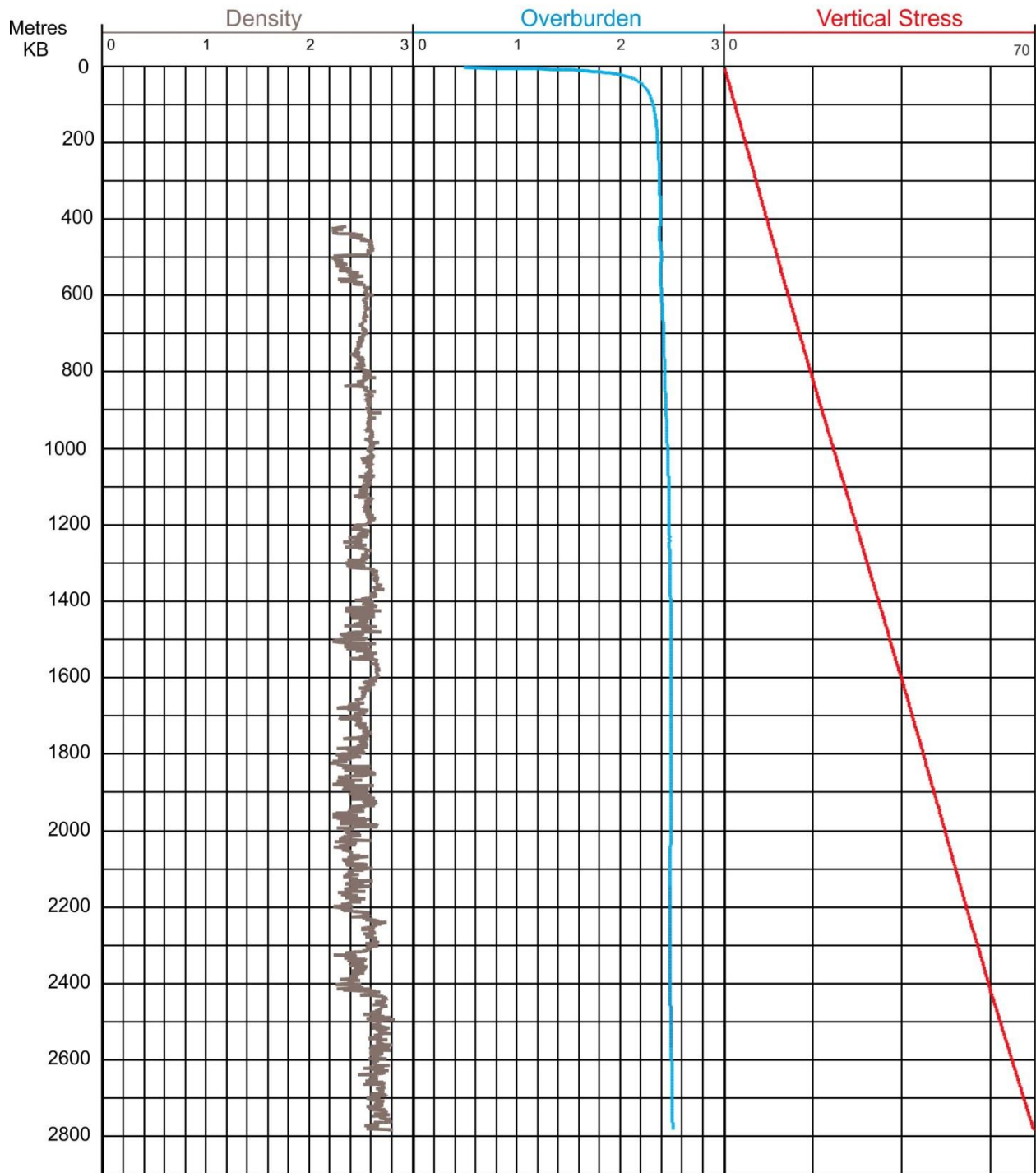




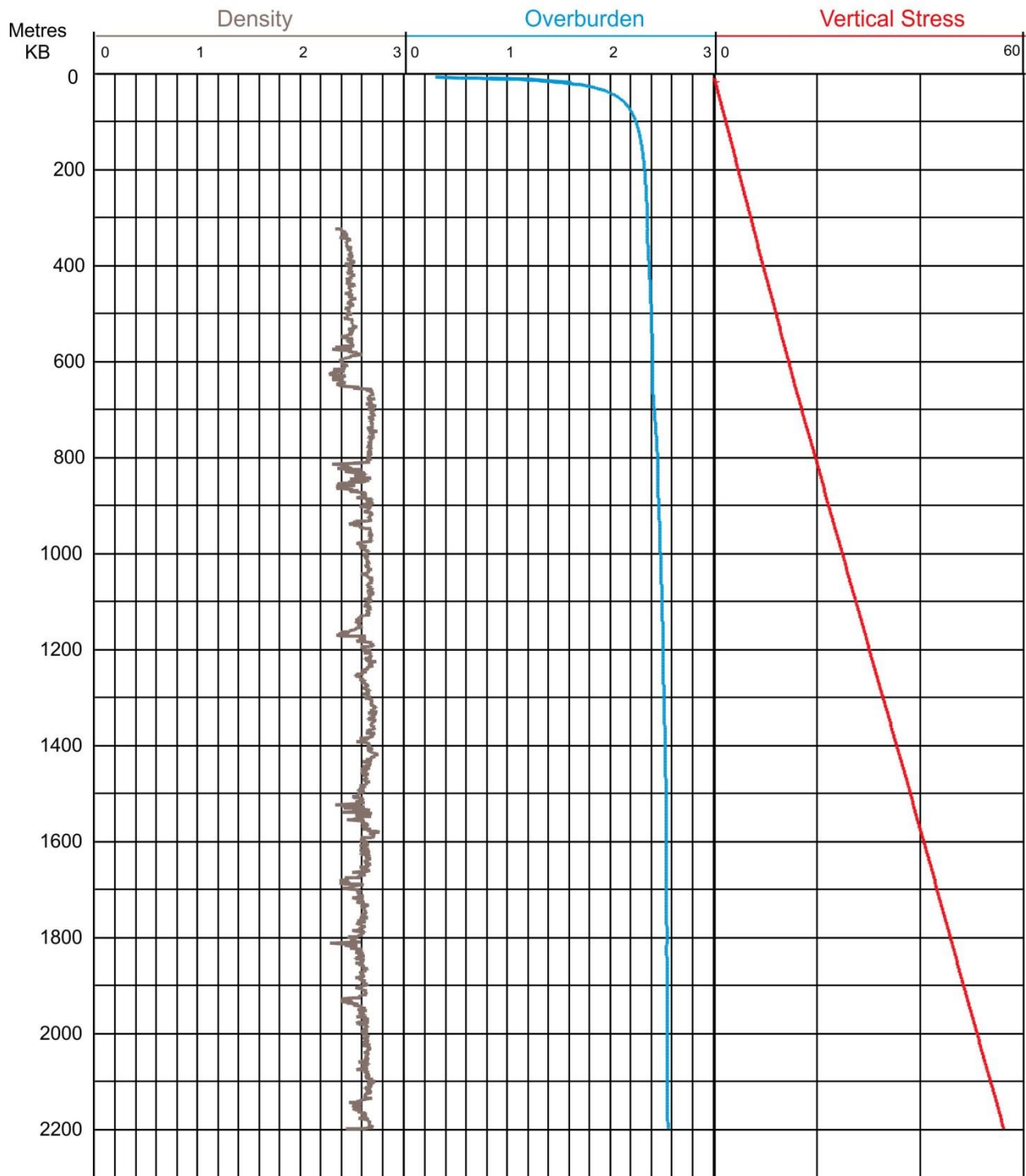
WELL: B-028-B/094-O-11



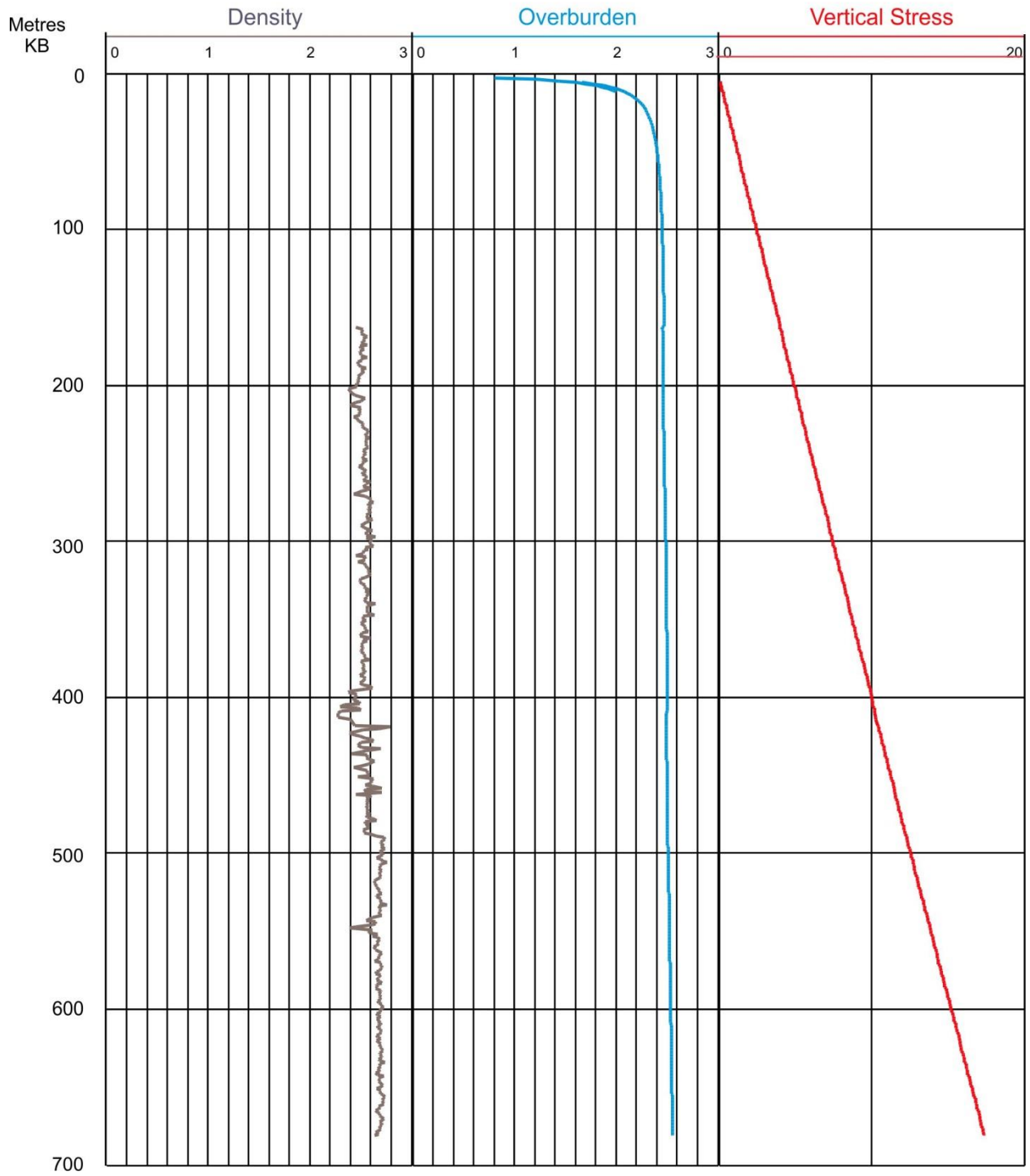
WELL: B-043-K/094-O-05



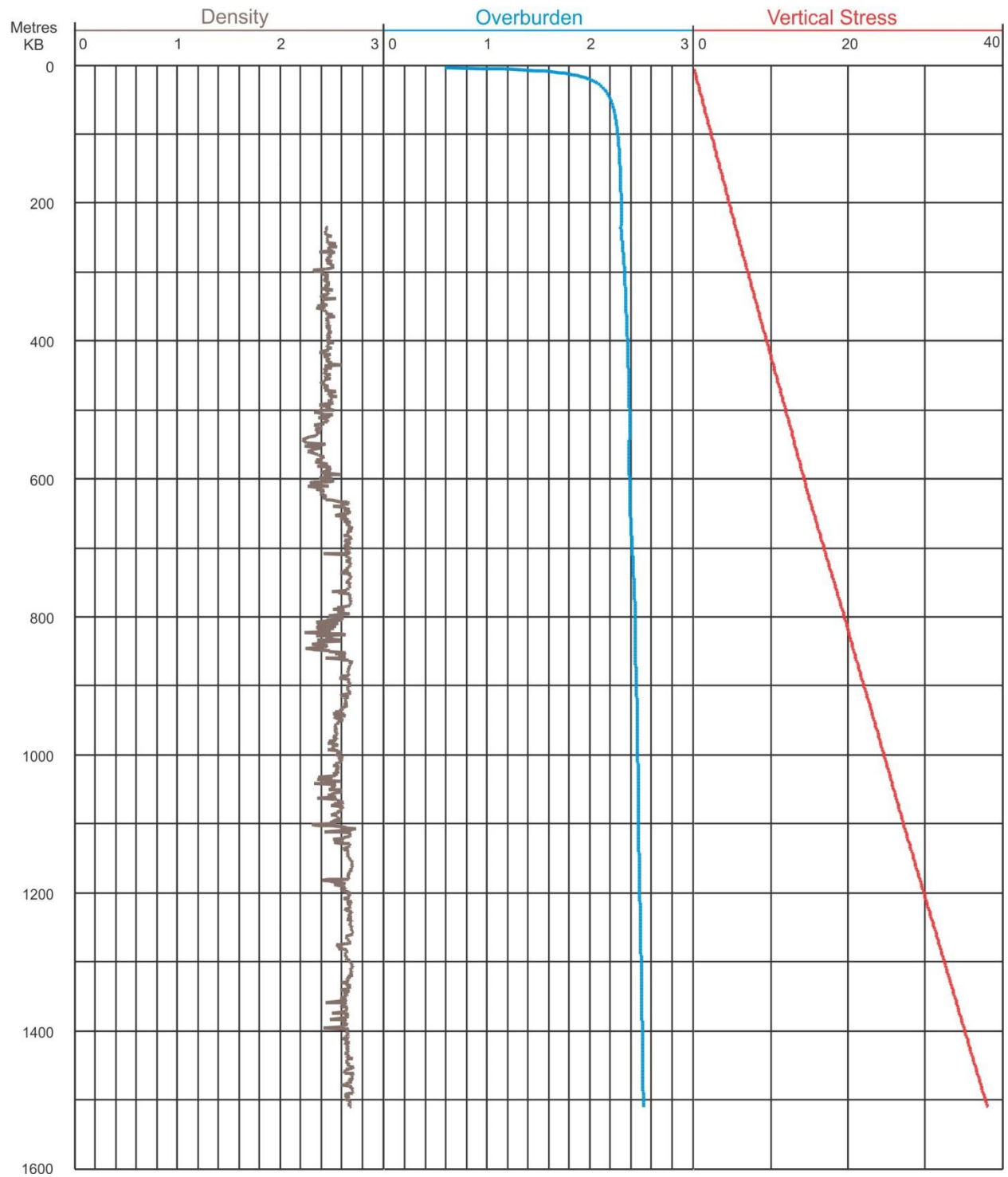
WELL: B-044-B/094-P-05



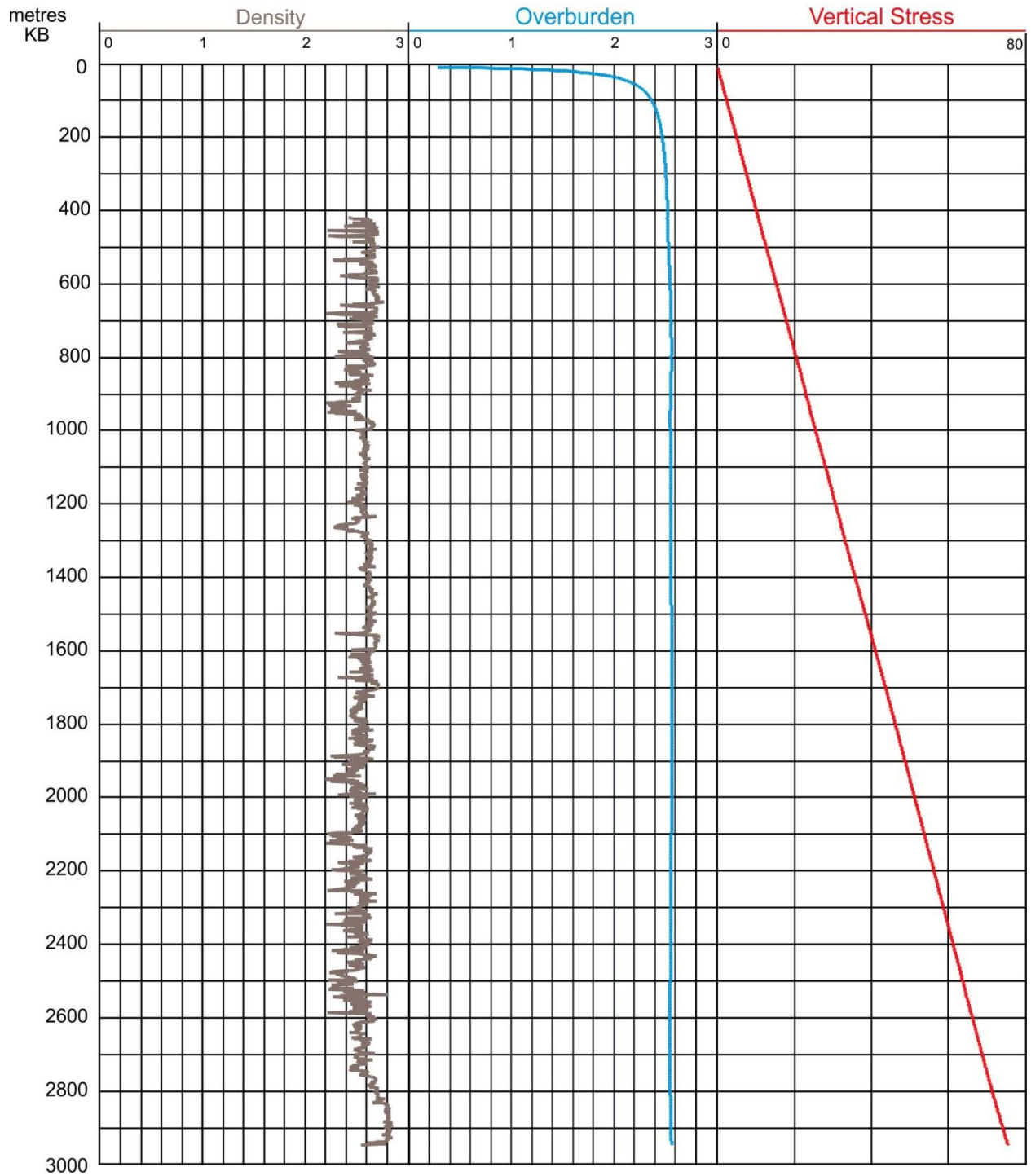
WELL: B-044-L/094-O-10



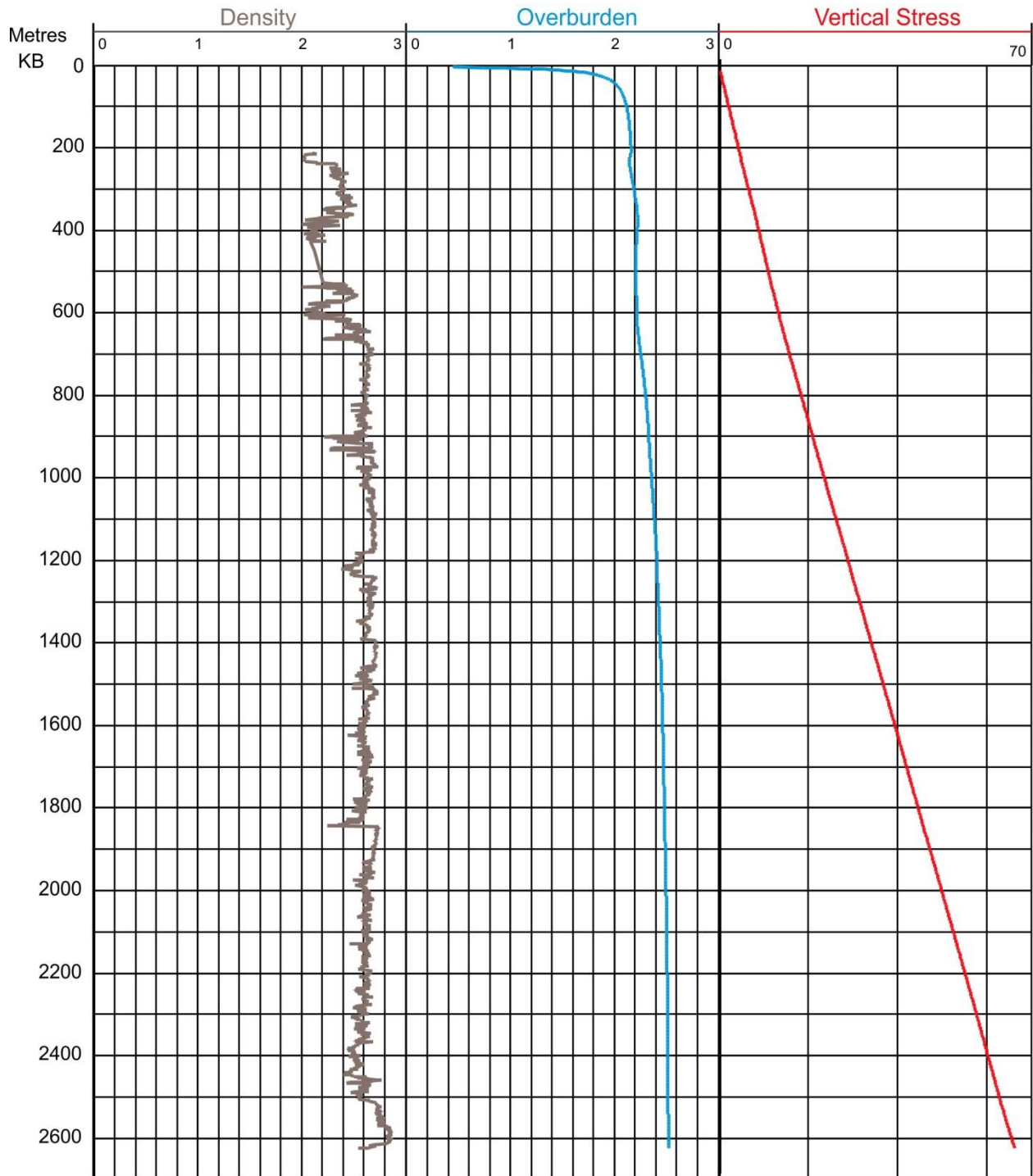
WELL: B-058-A/094-I-13



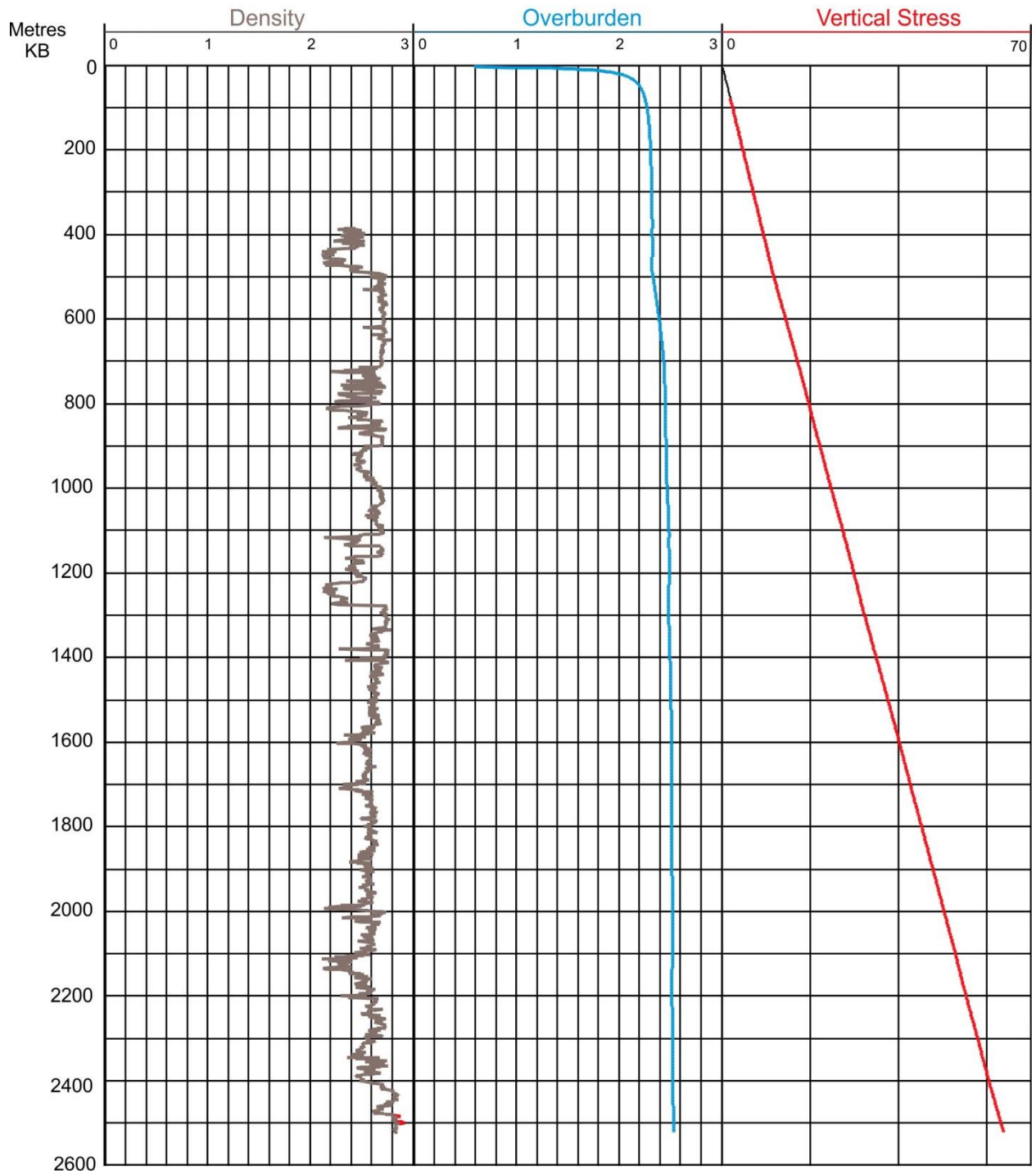
WELL: B-058-H/094-O-15



WELL: B-066-I/094-O-08

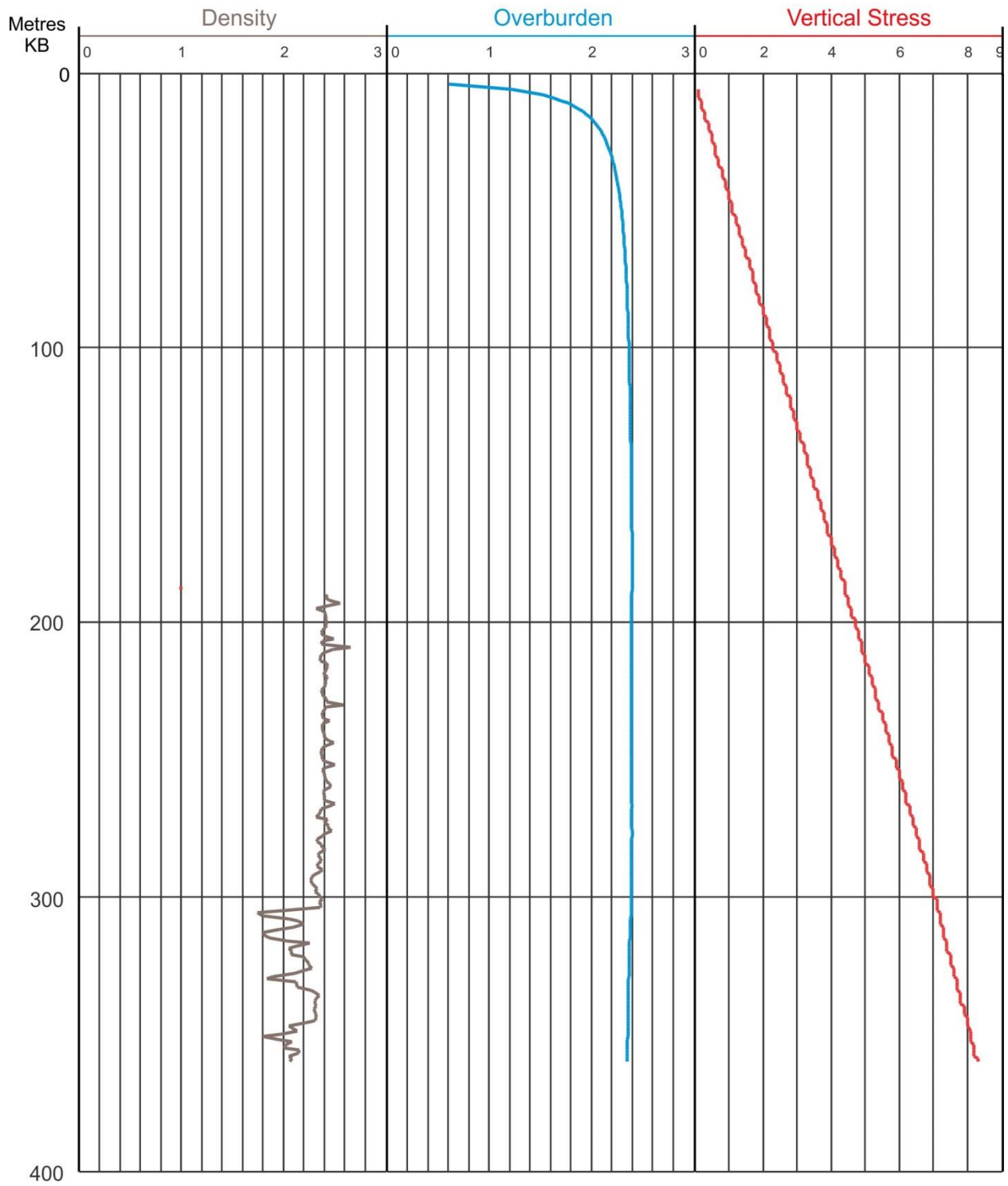


WELL: B-072-K/094-O-01

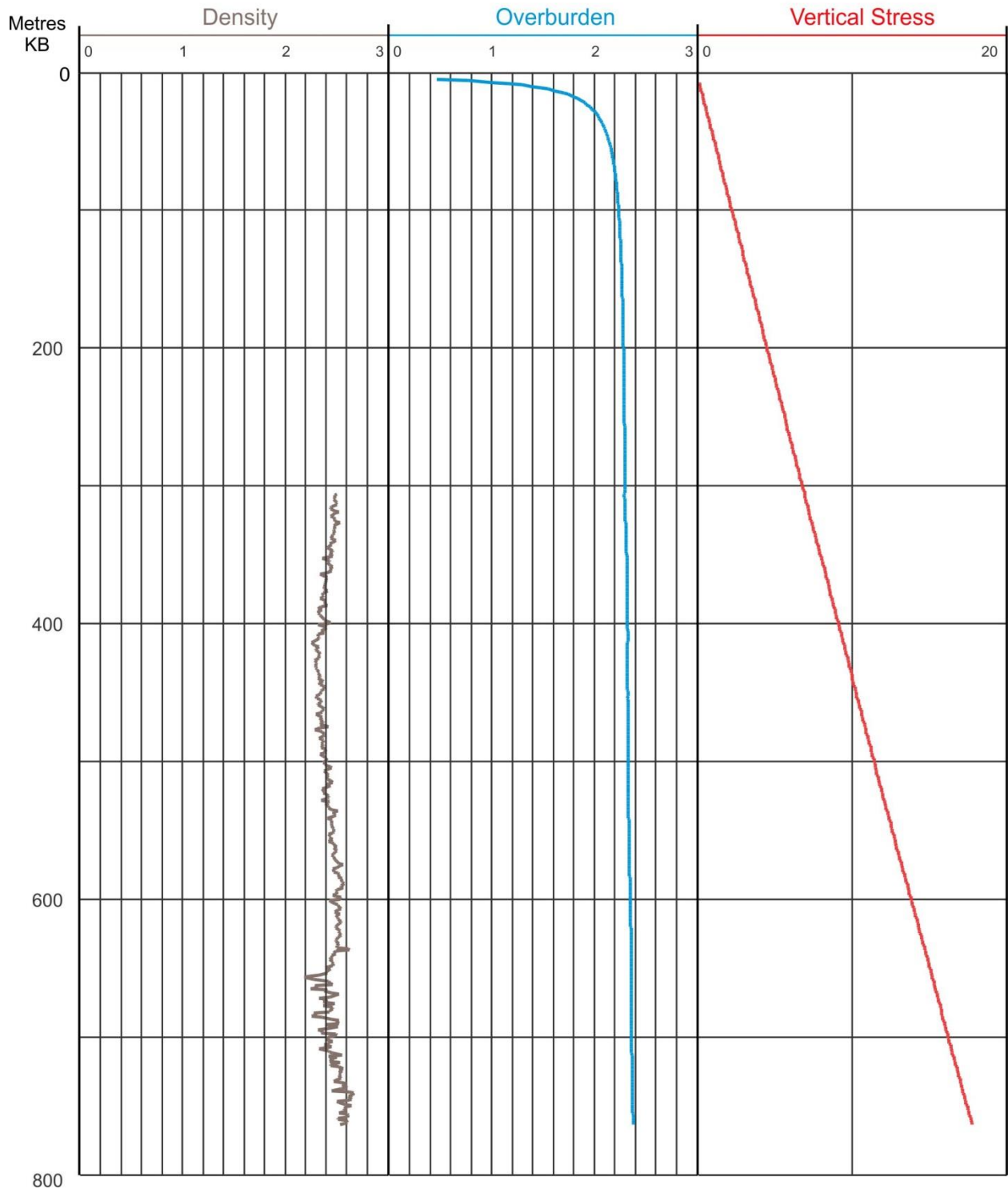




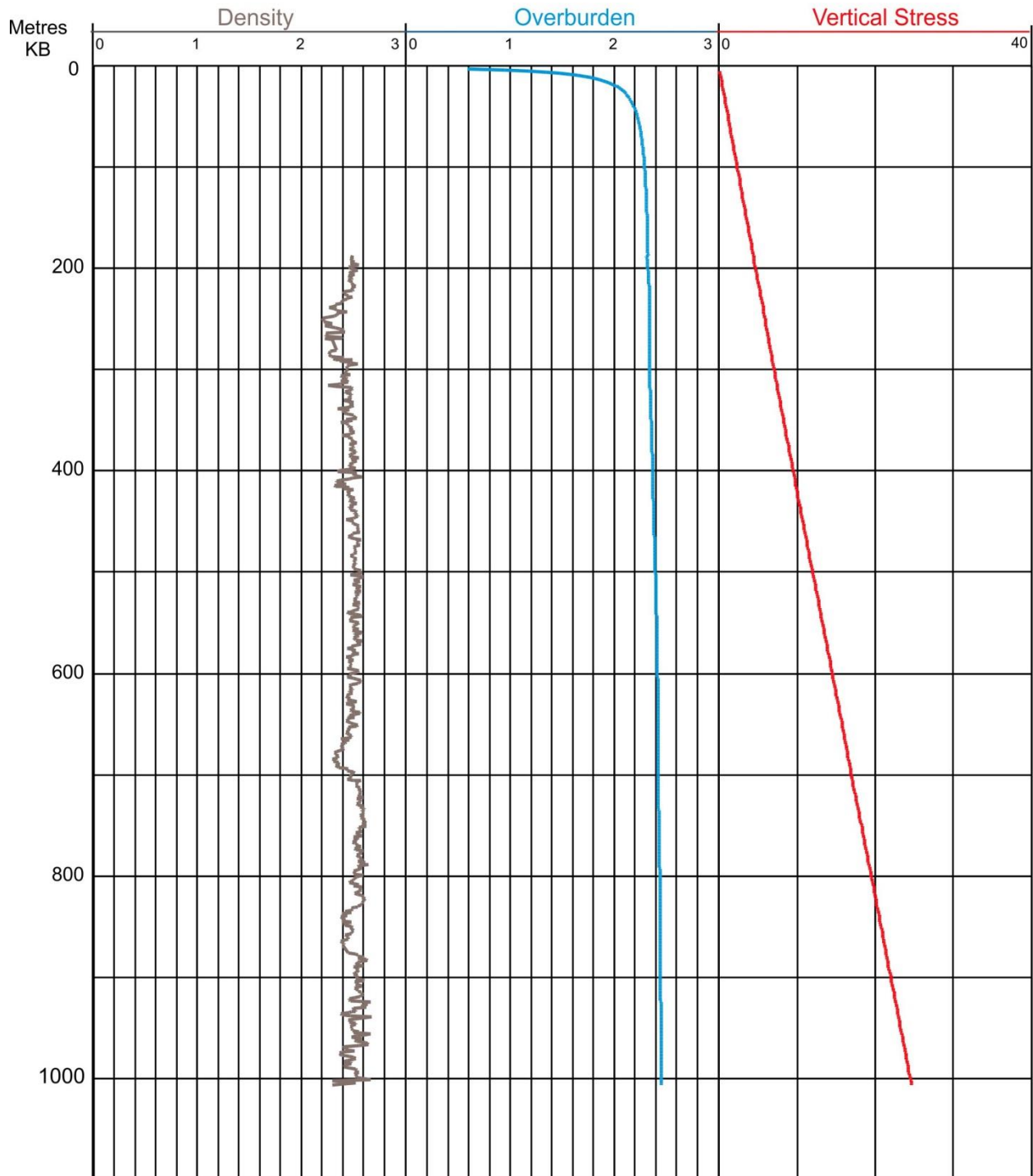
WELL: B-076-G/094-P-10



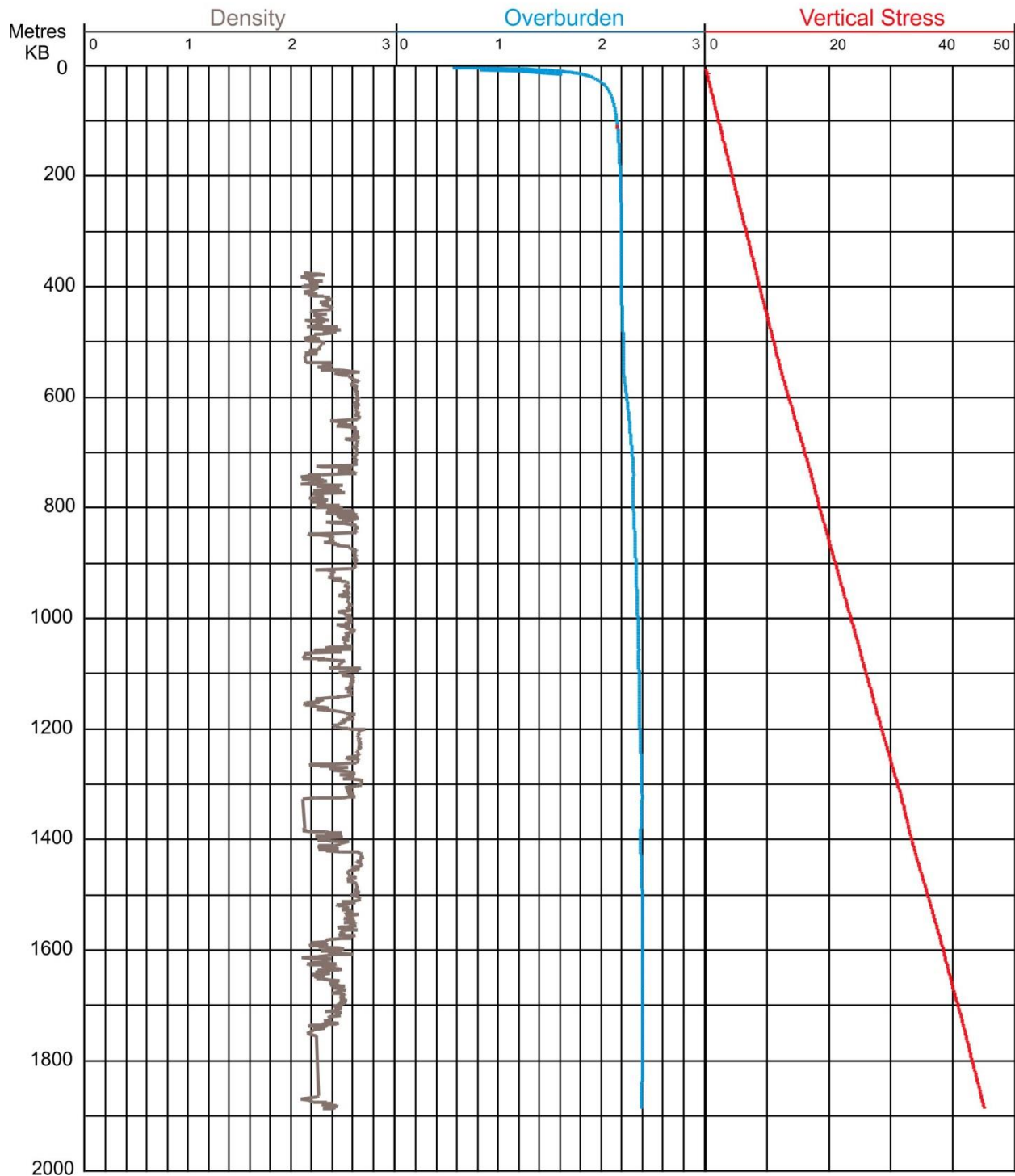
WELL: B-084-D/094-I03



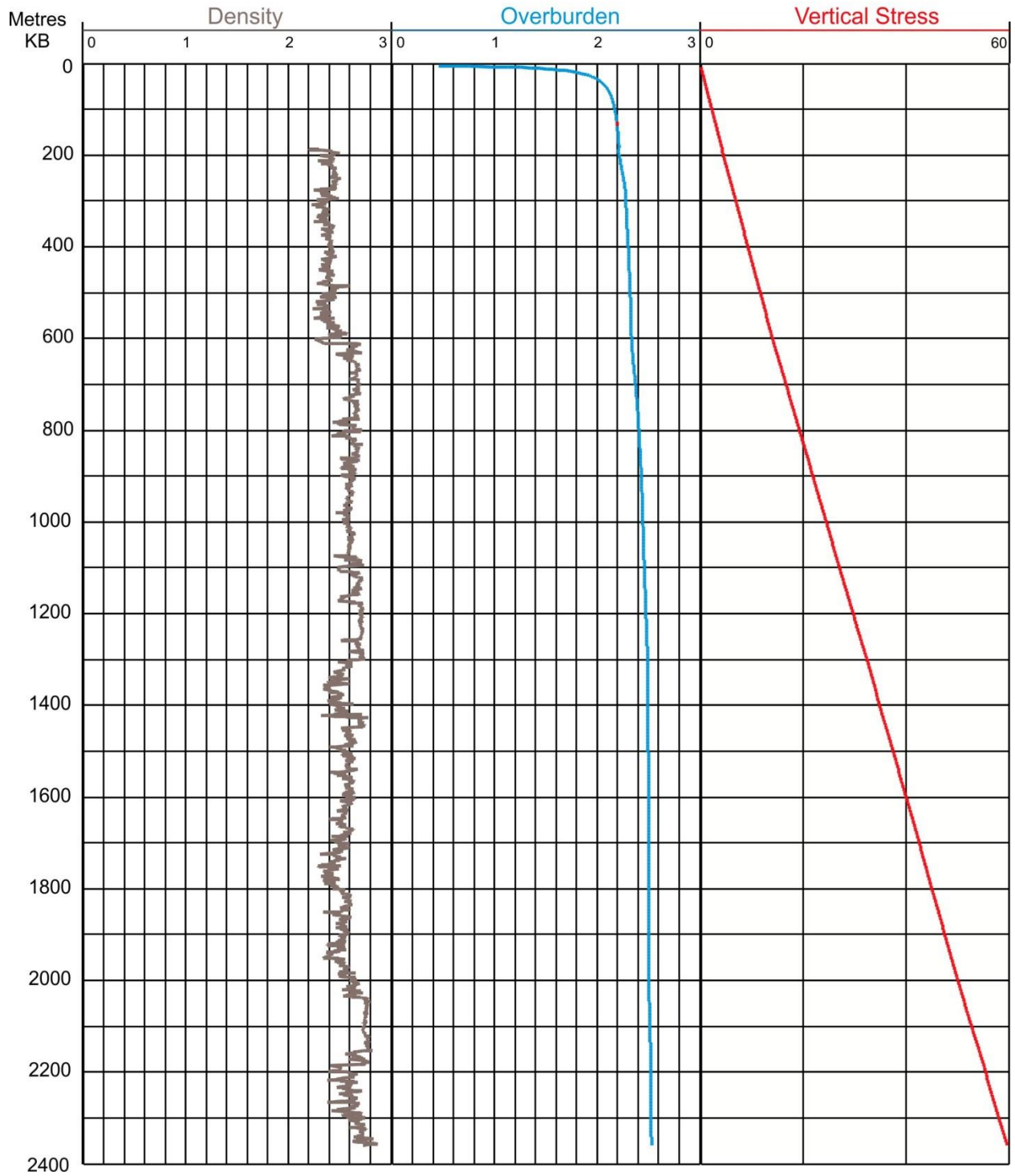
WELL: B-085-H/094-O-11



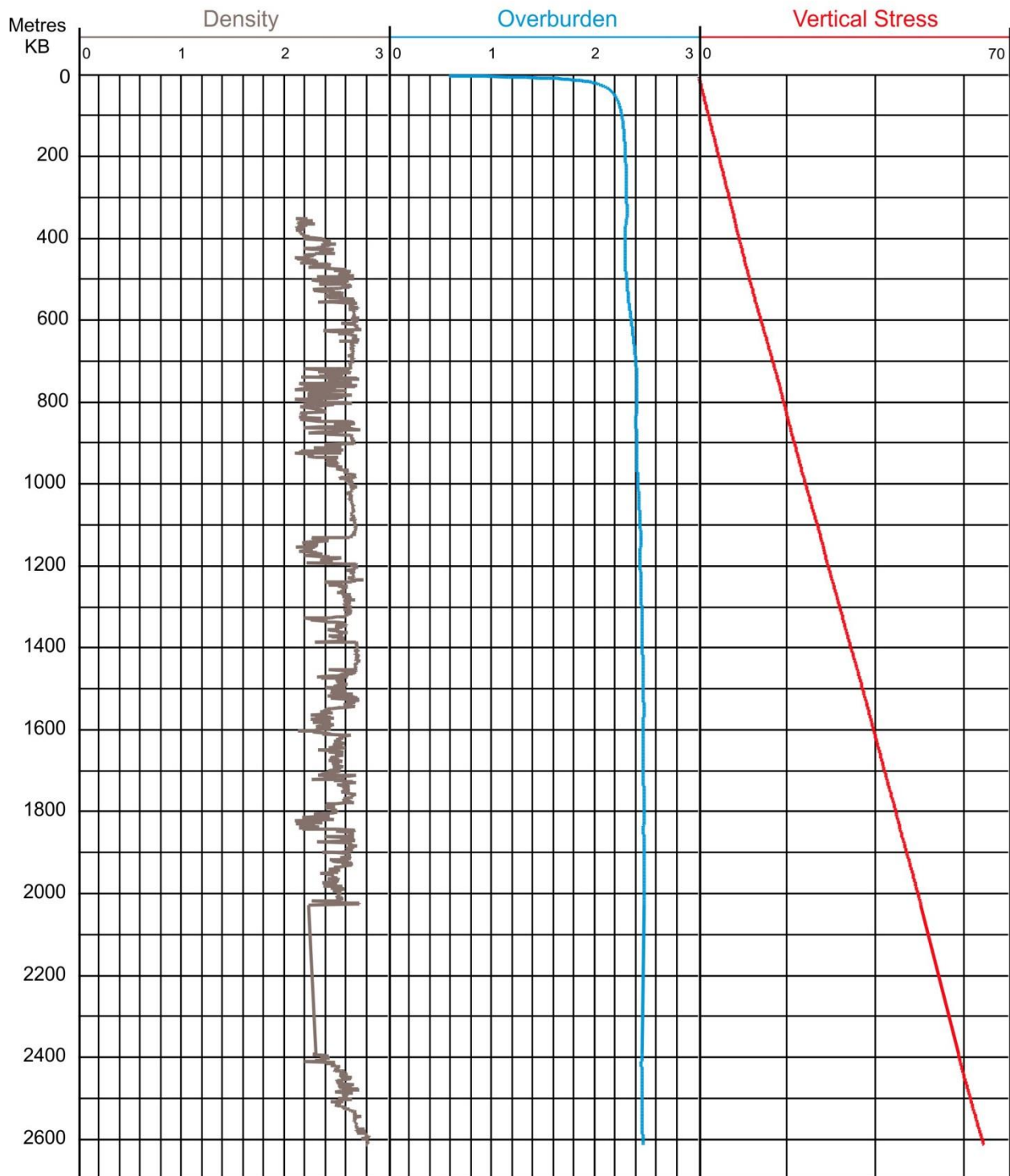
WELL: B-086-F/094-P-04



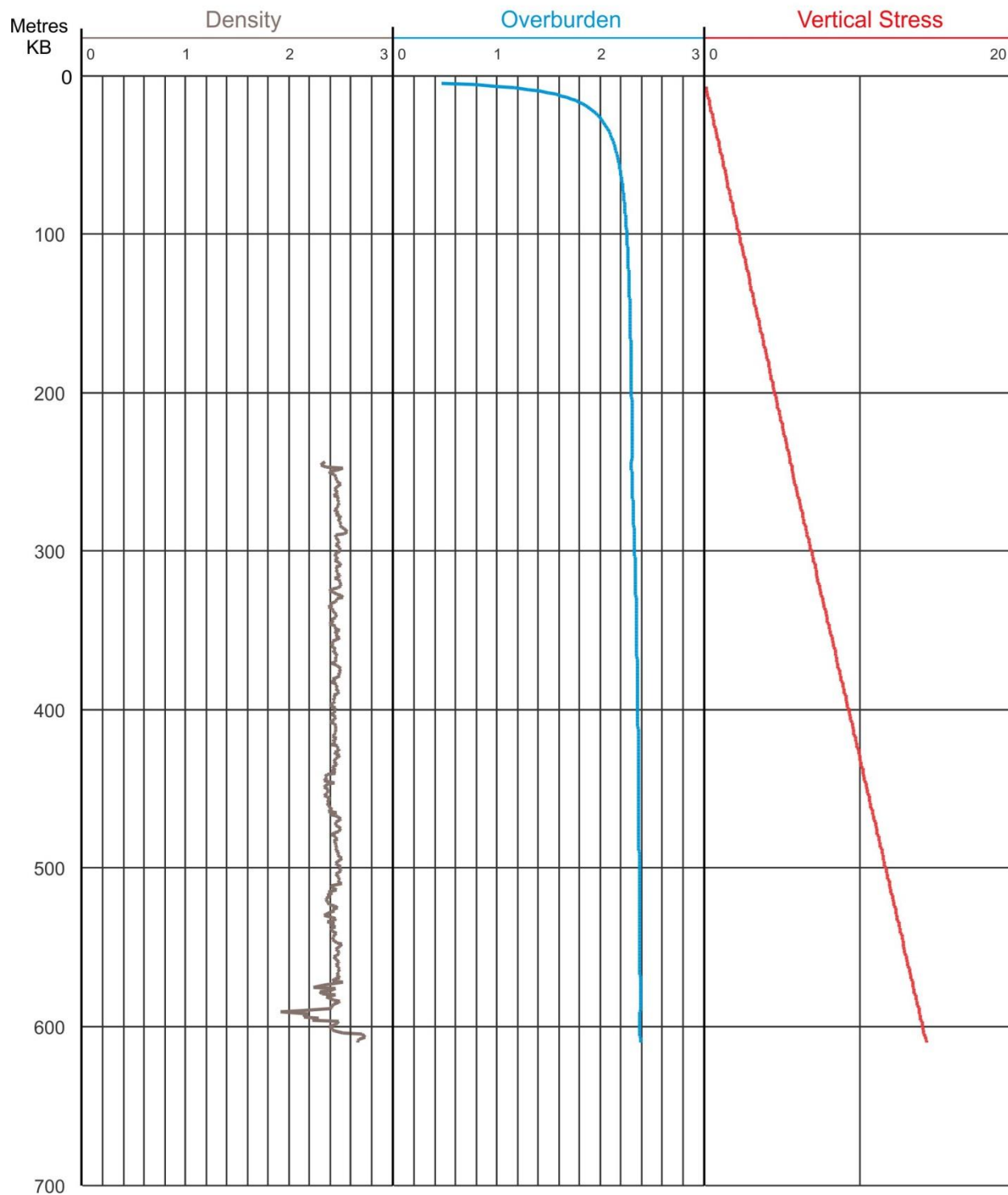
WELL: B-093-C/094-I-14



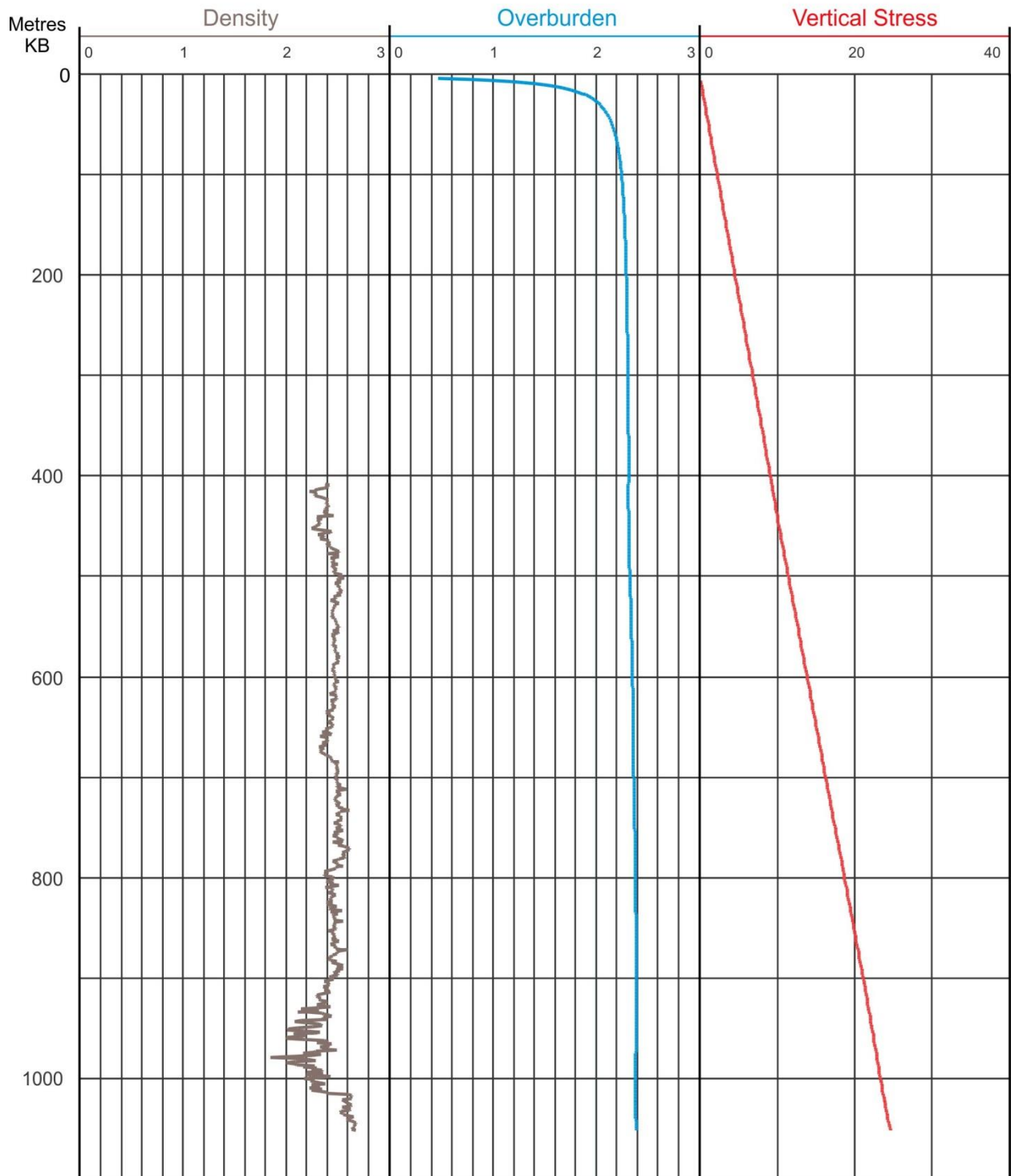
WELL: B-094-G/094-O-09



WELL: B-094-H/094-J-14

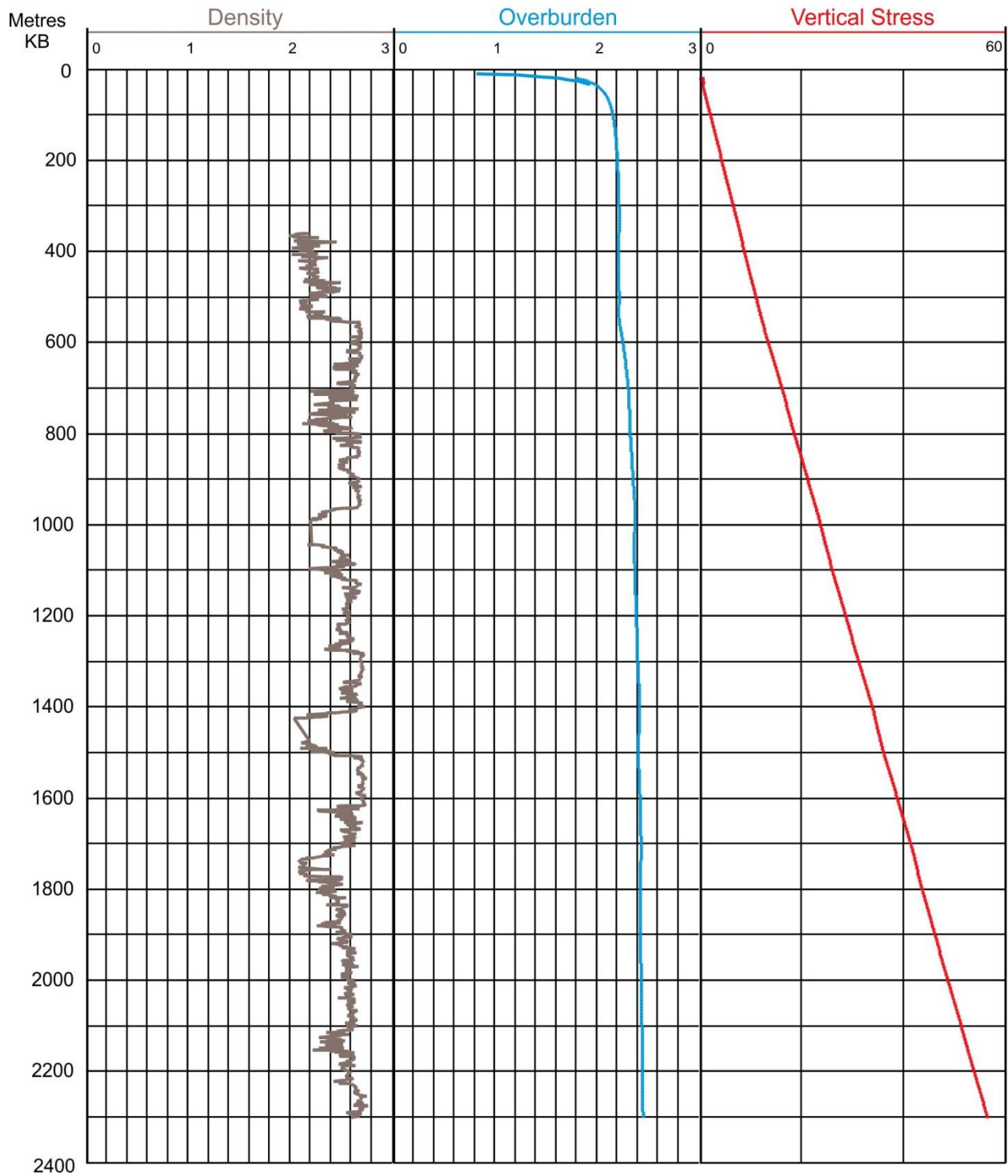


WELL: C-012-A/094-J-07

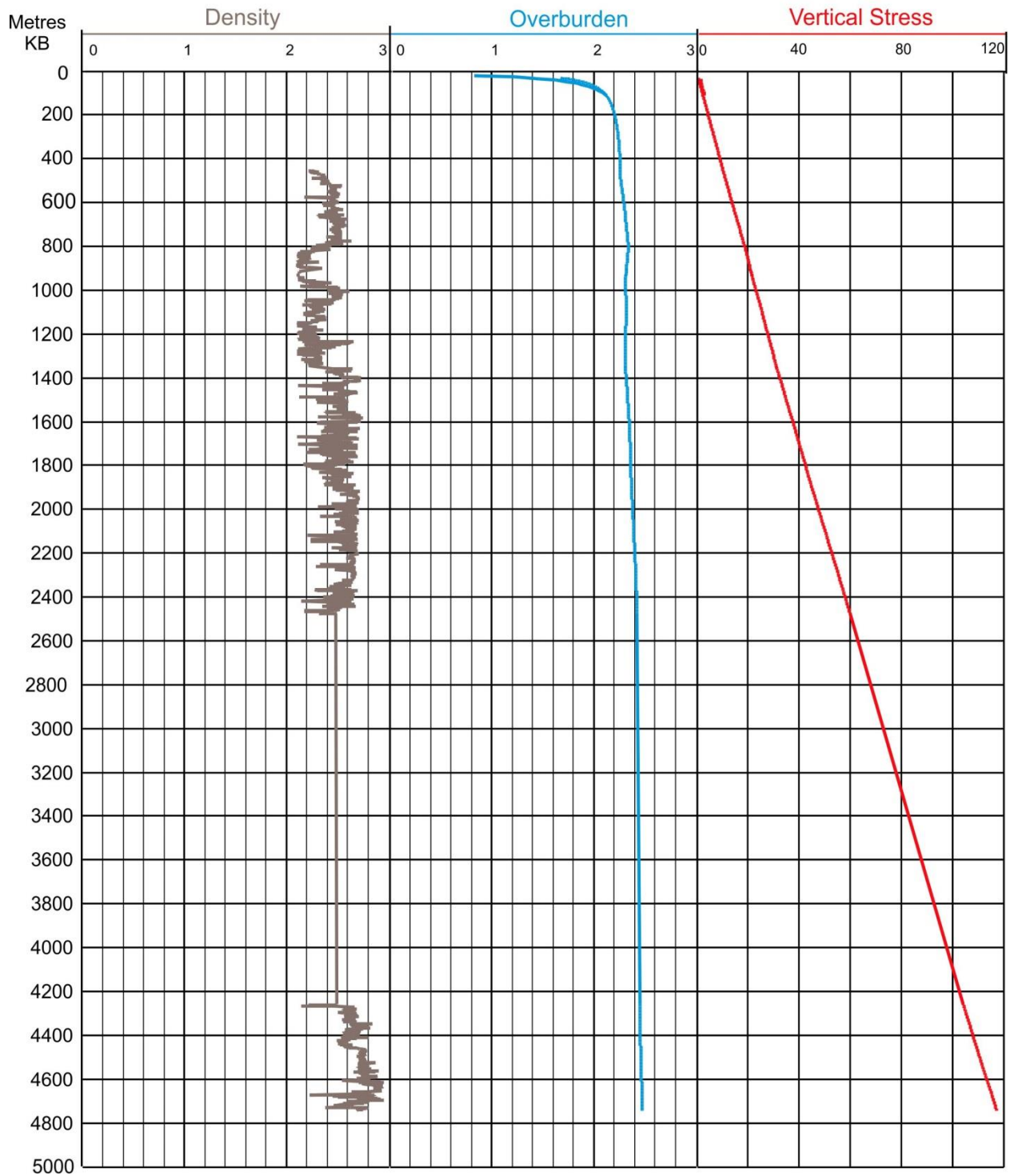




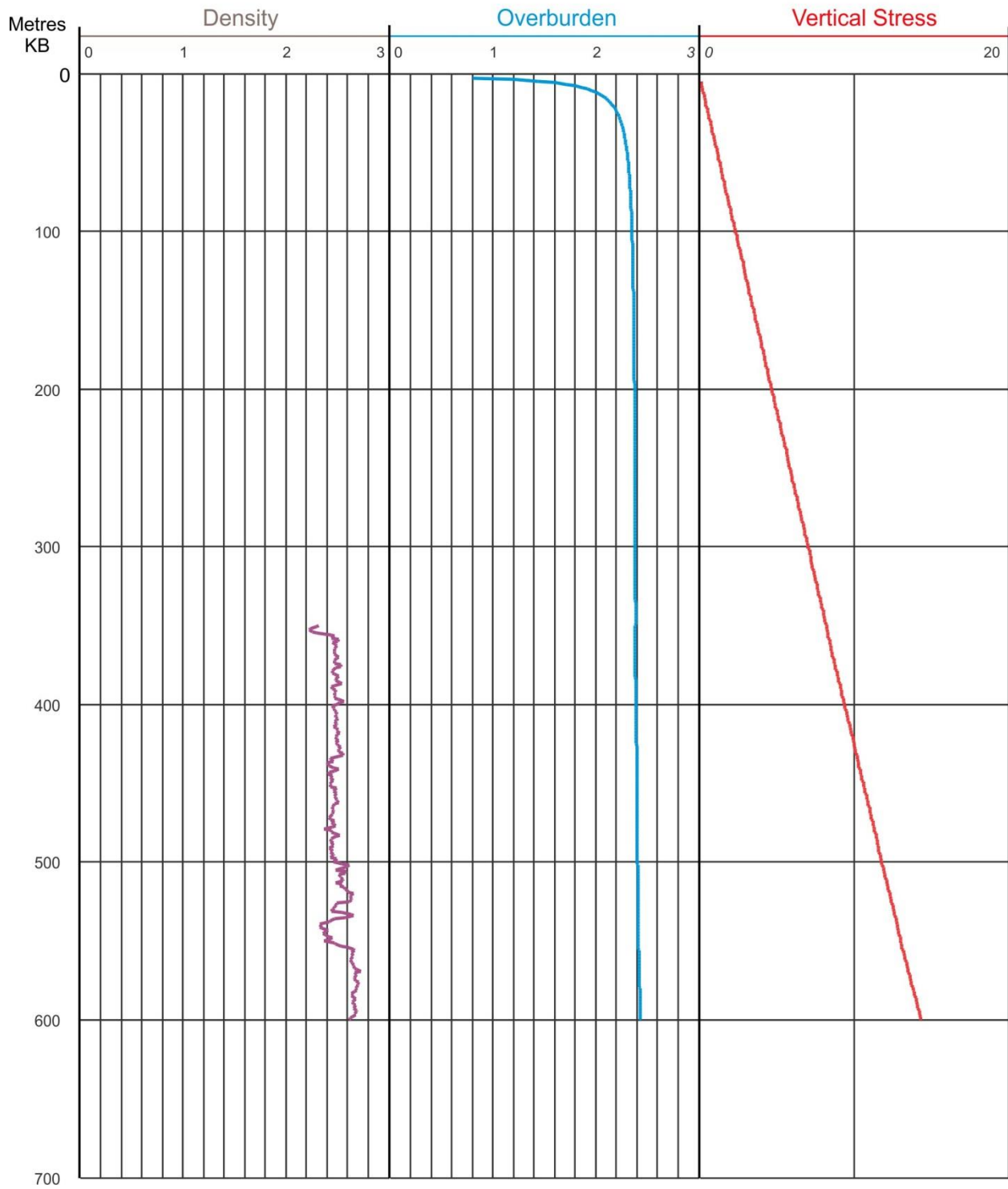
WELL: C-040-C/094-P-12



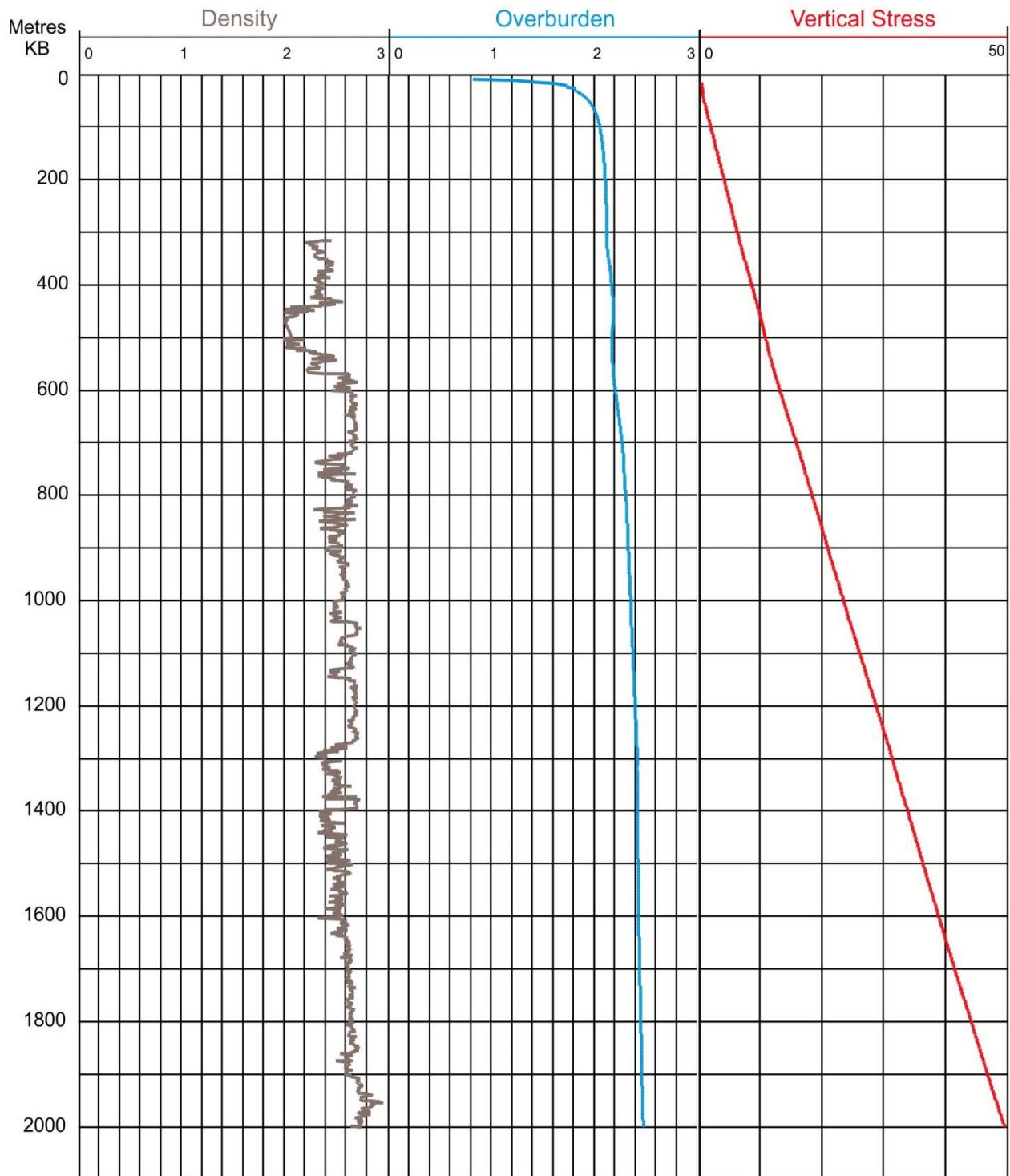
WELL: C-051-B/094-O-14



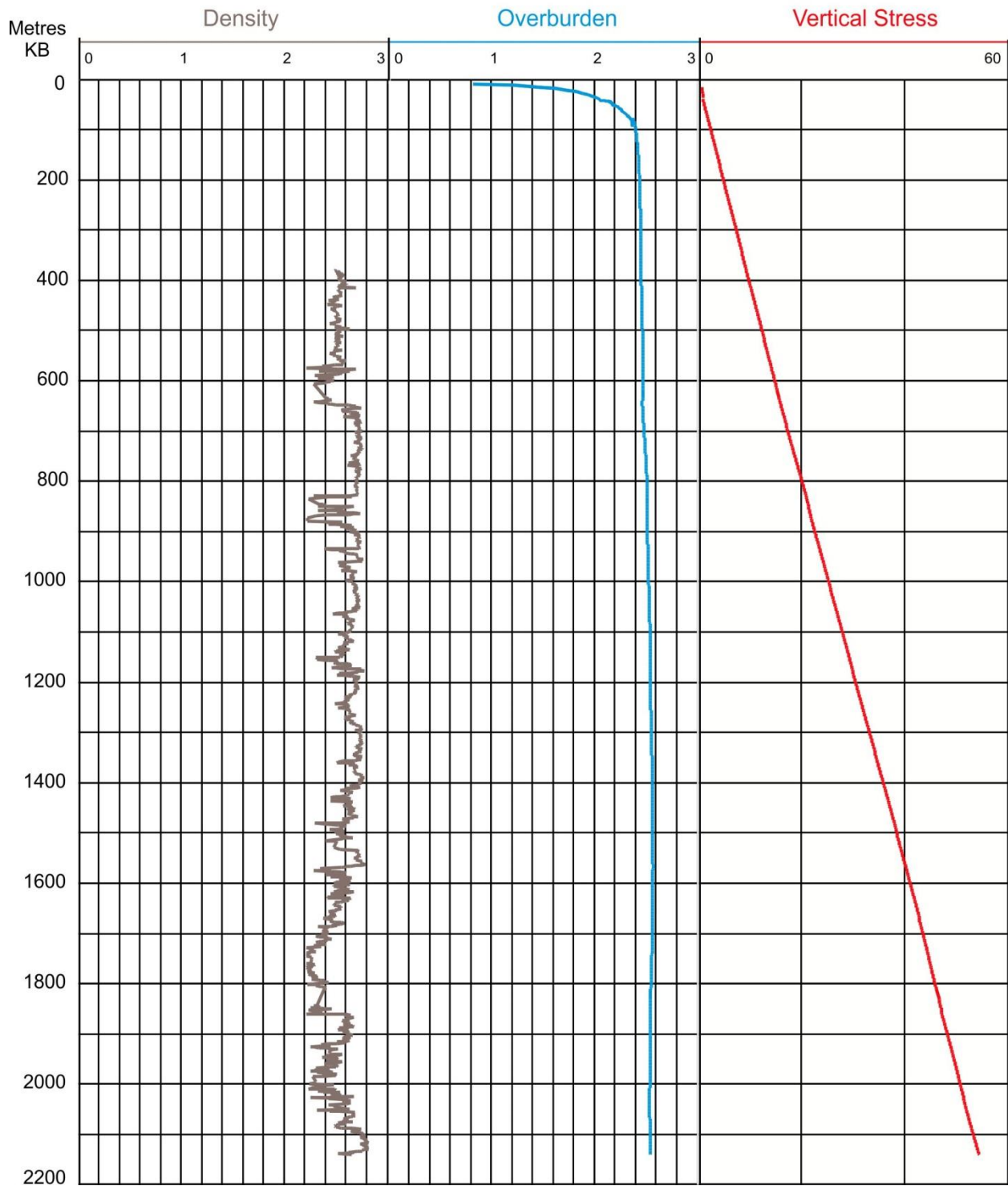
WELL: C-075-D/094-I-08



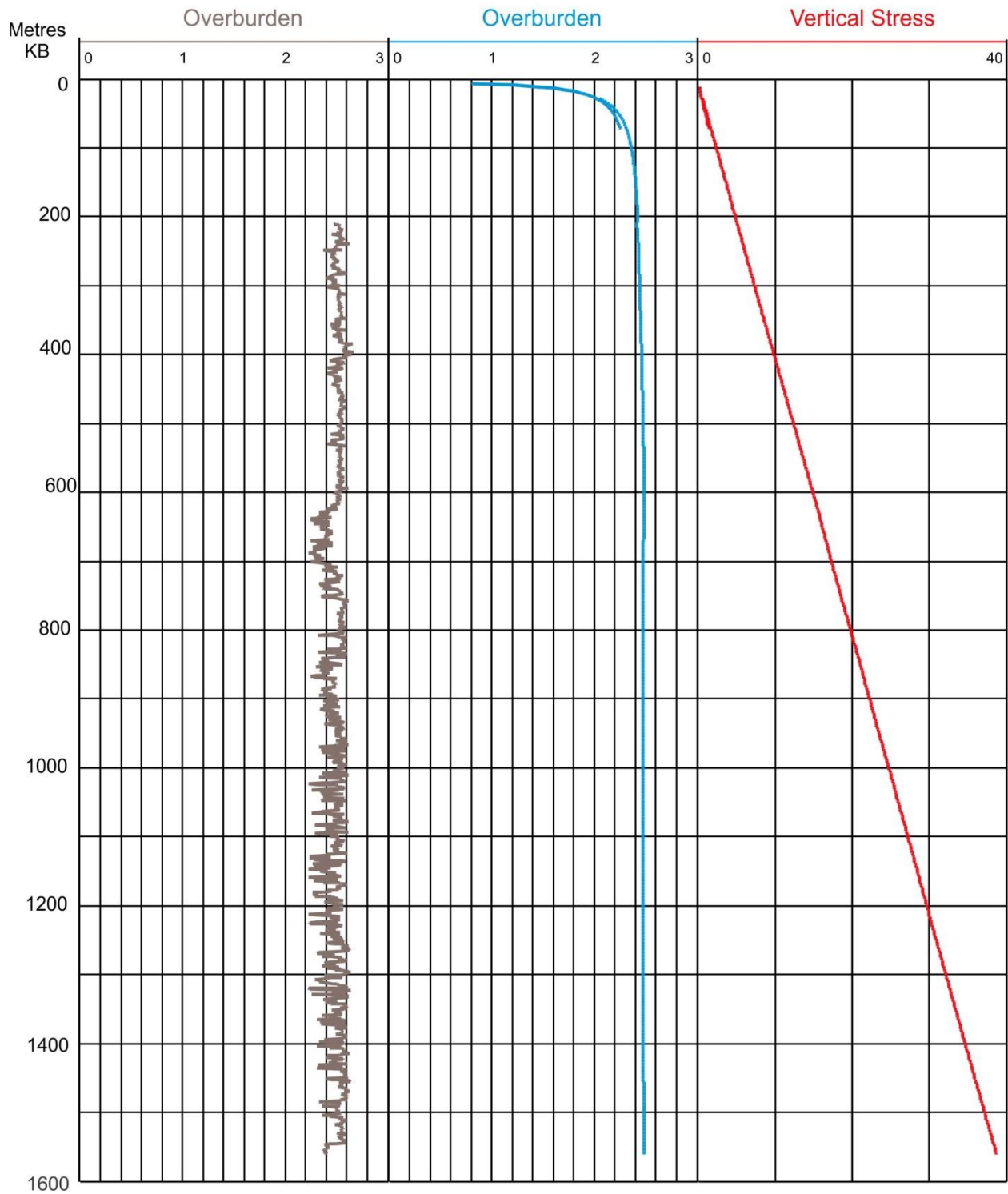
WELL: C-086-A/094-I-14



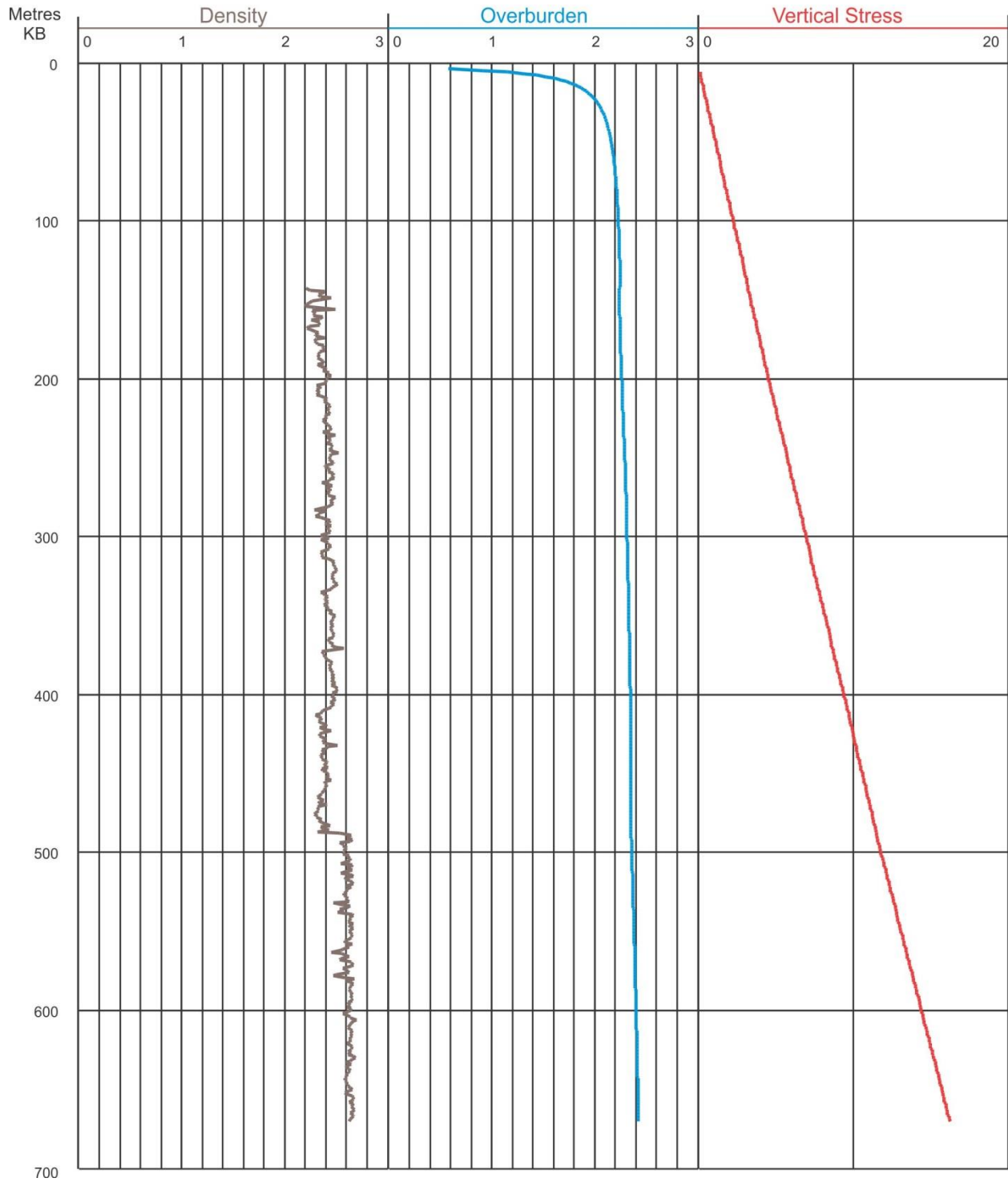
WELL : D-008-I/094-P-04



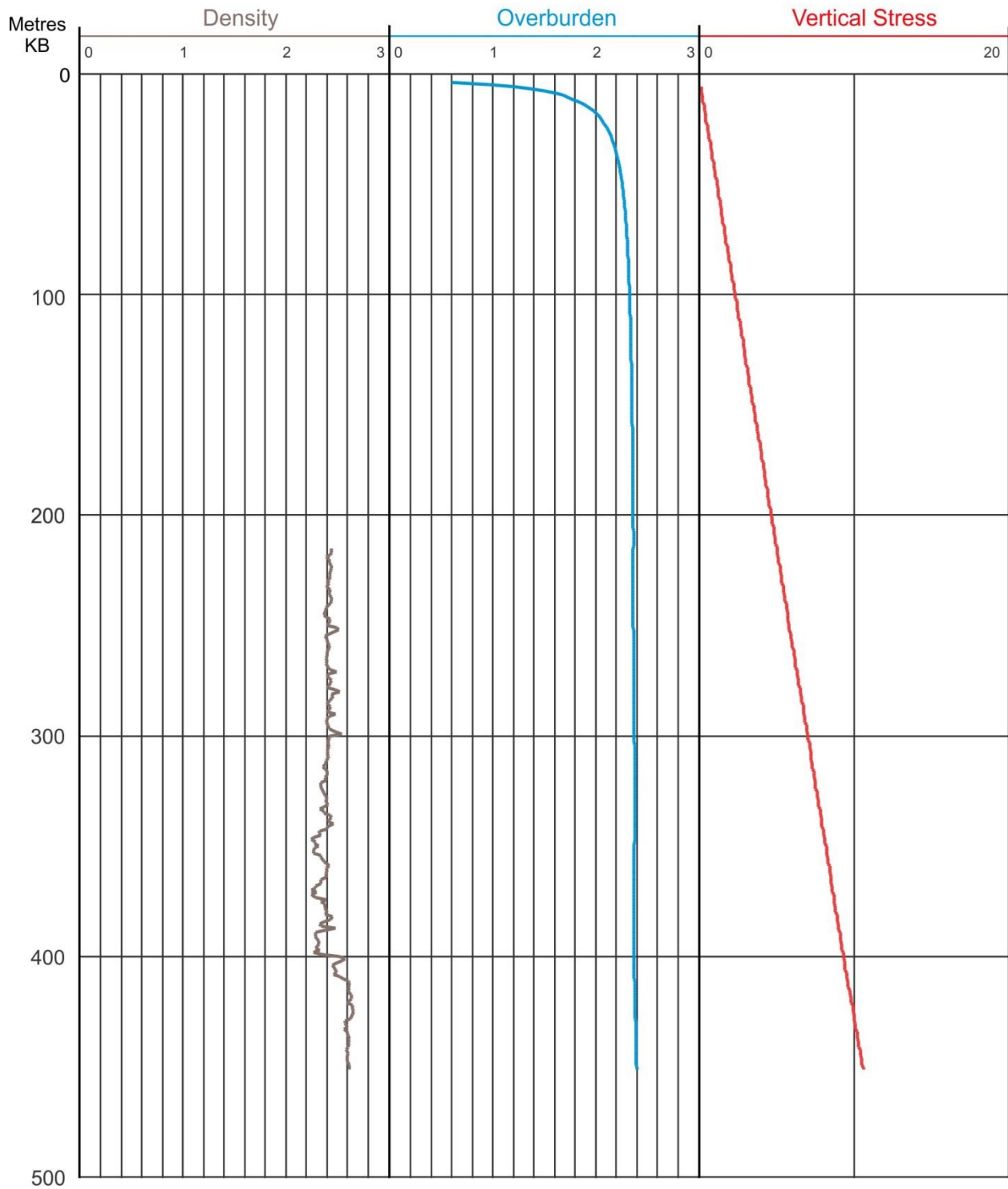
# WELL: D-016-A/094-N-15



WELL: D-31-60-30-122-30

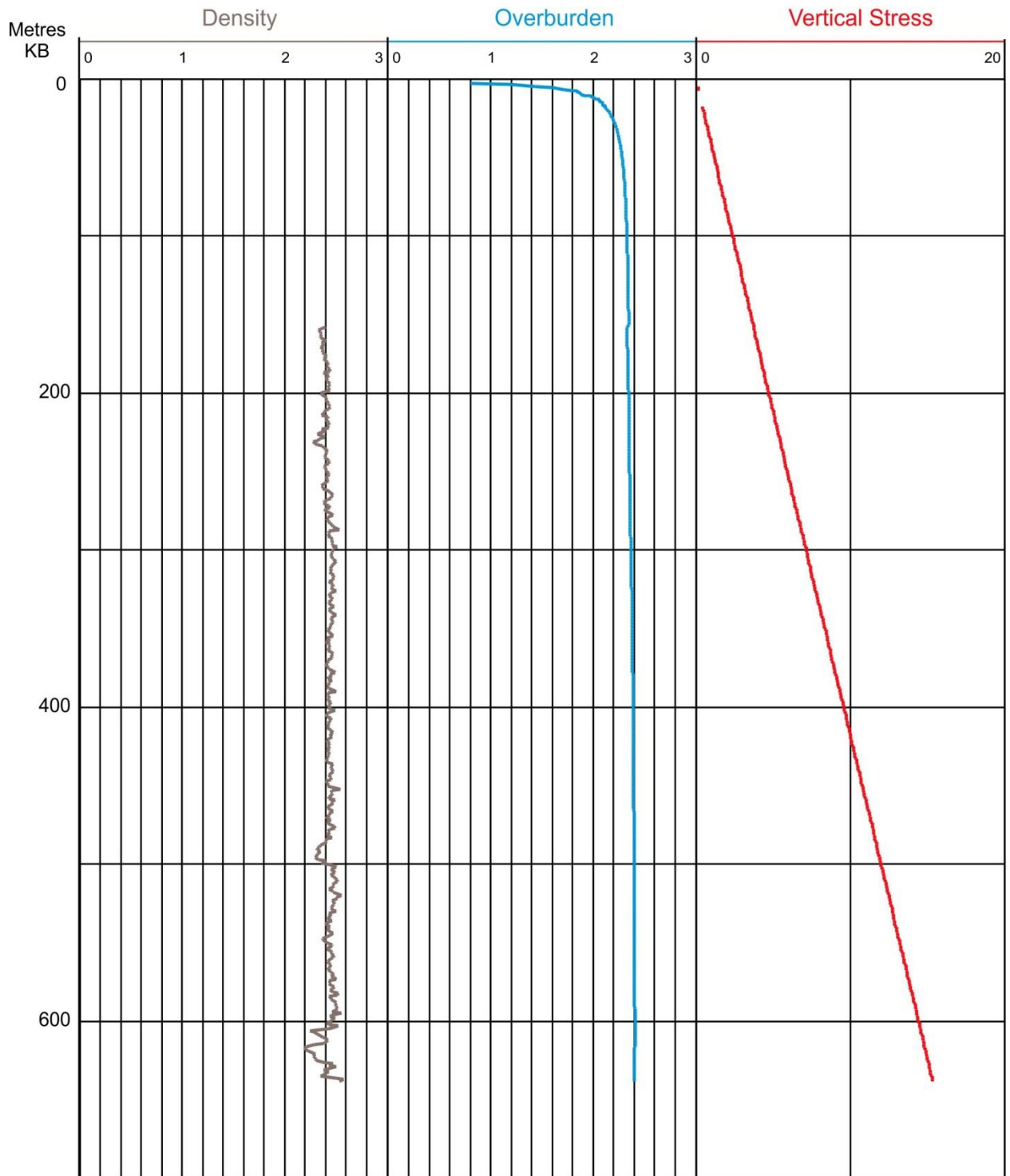


WELL: D-034-B/094-P-14

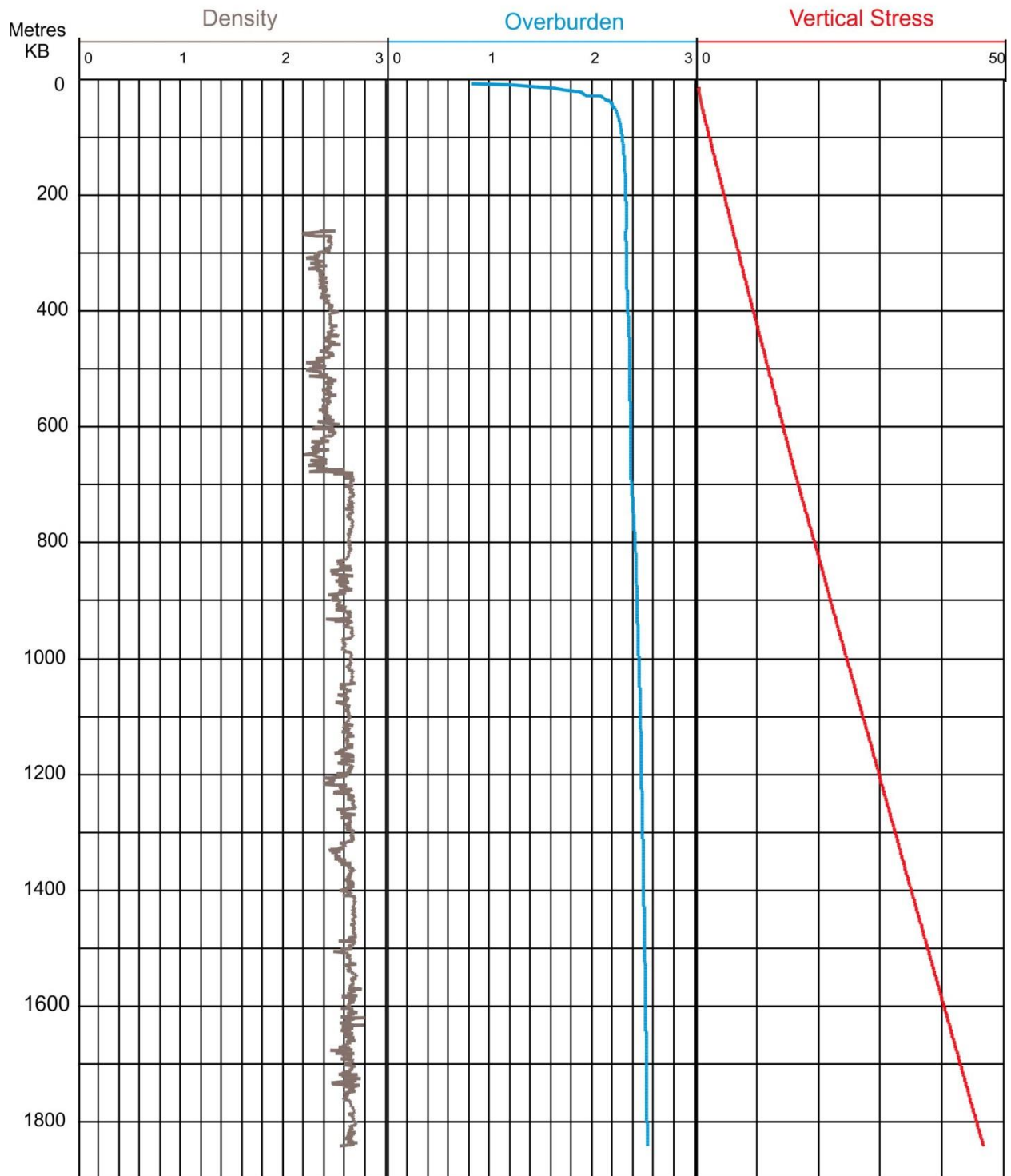




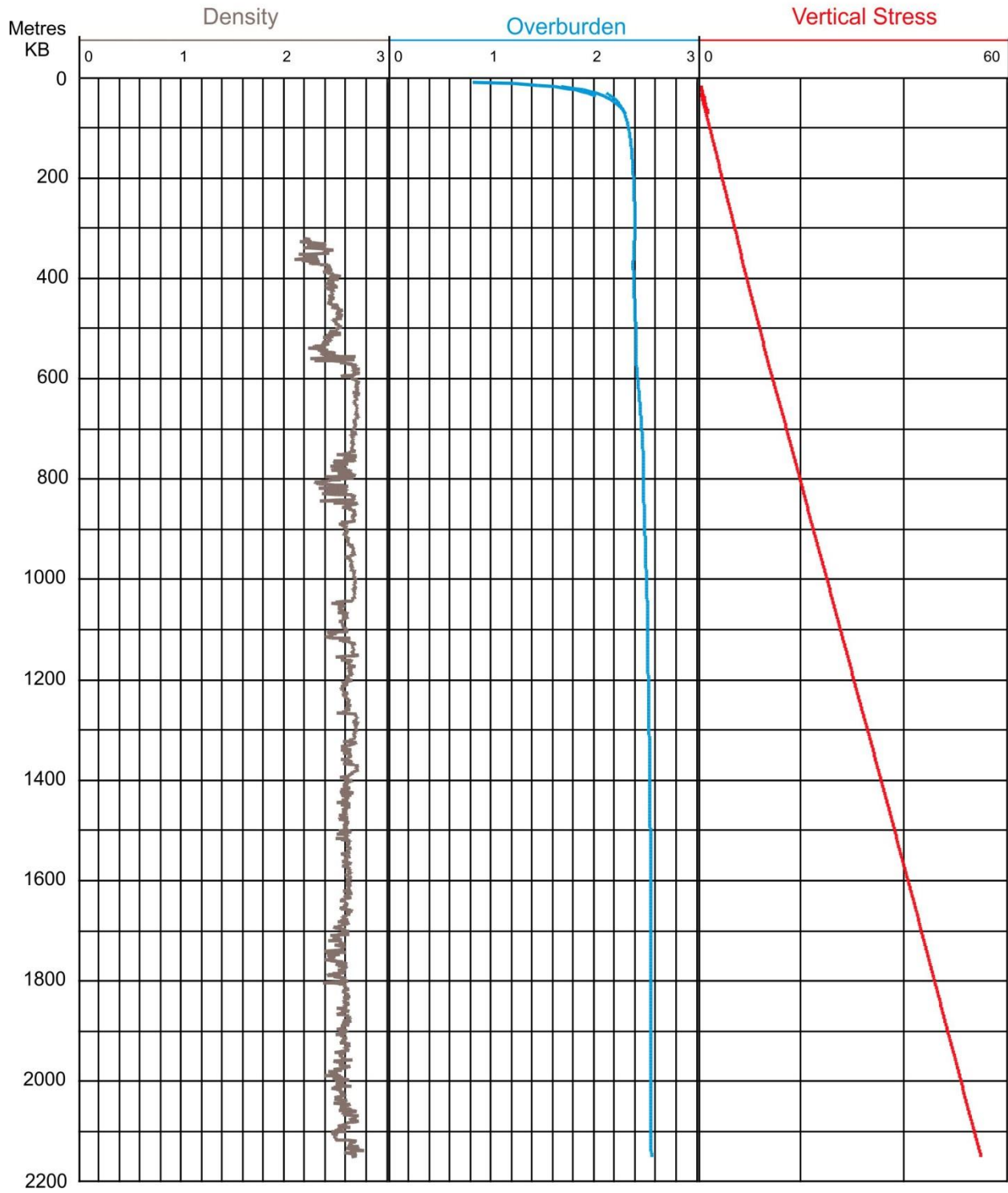
WELL: D-035-F/094-I-14



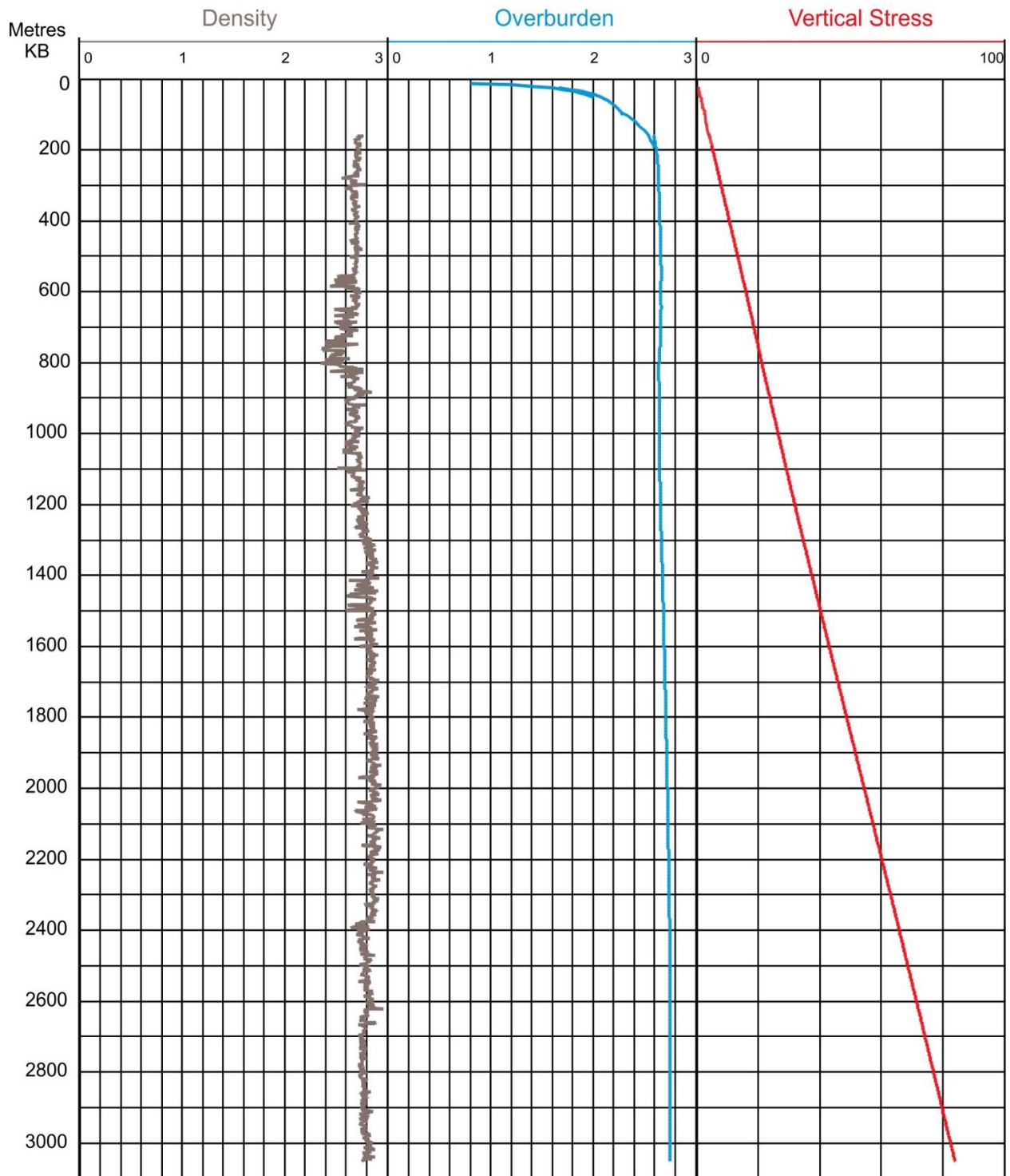
WELL: D-035-F/094-P-05



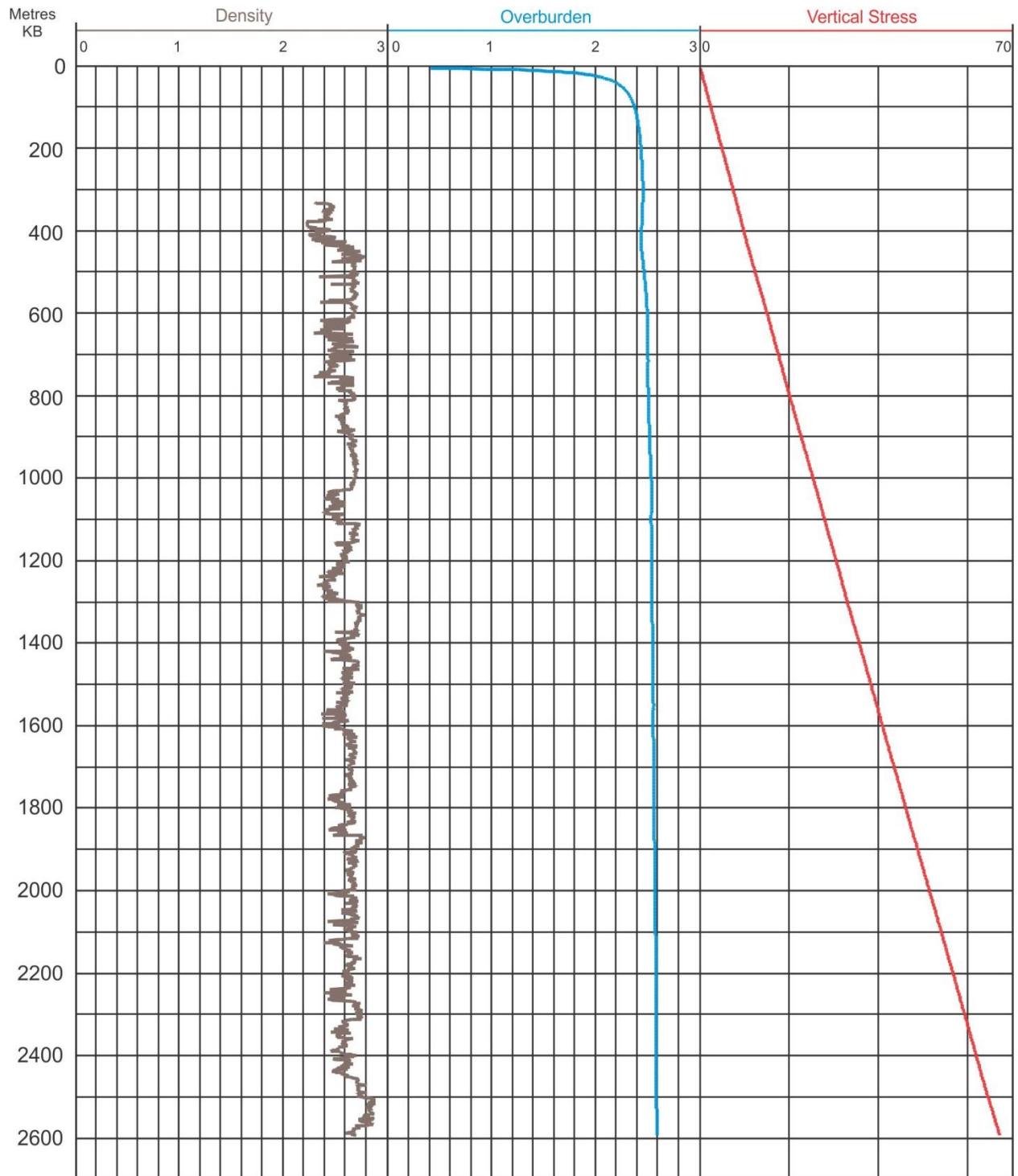
WELL: D-051-A/094-O-08



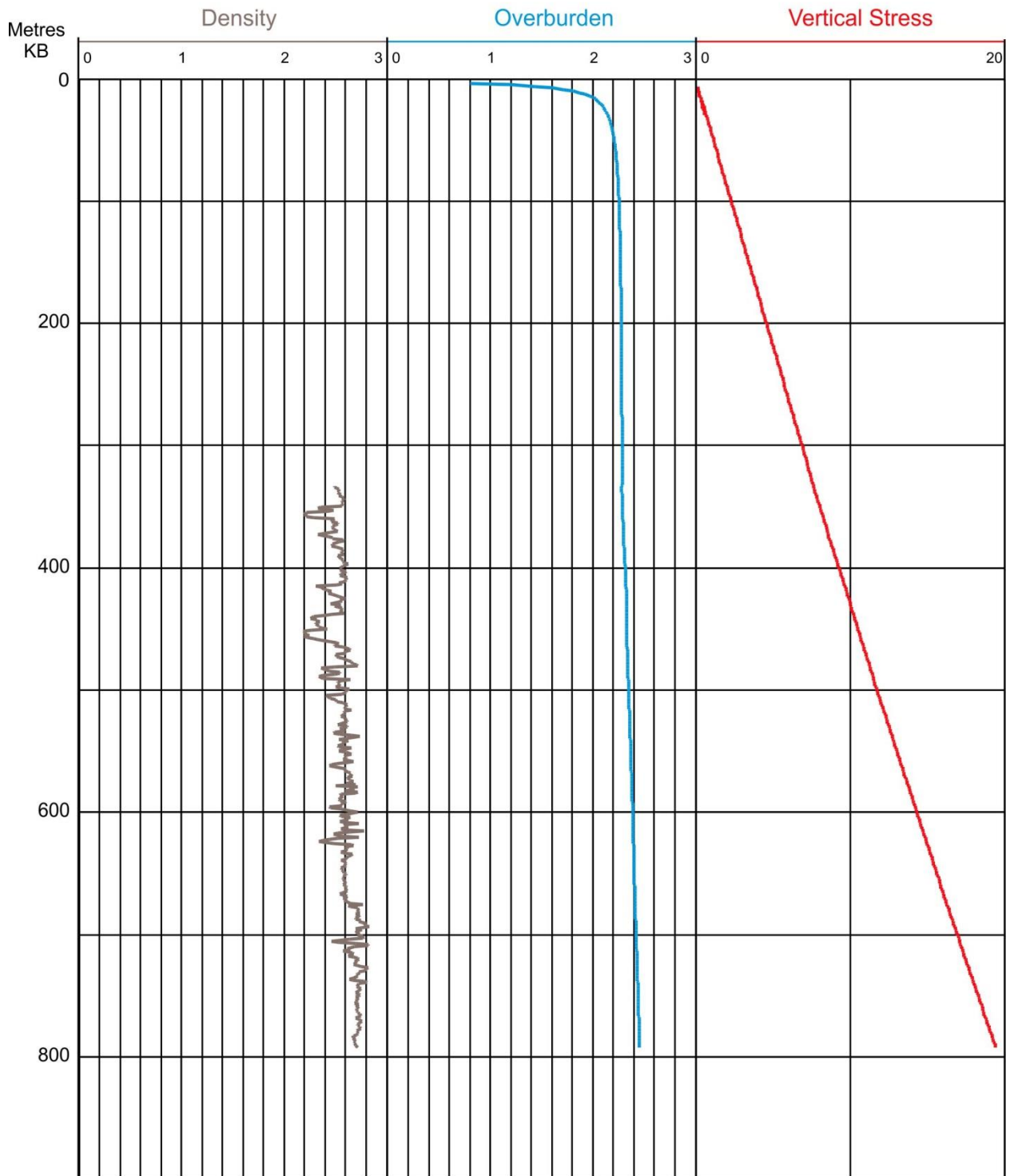
WELL: D-057-K/094-N-02



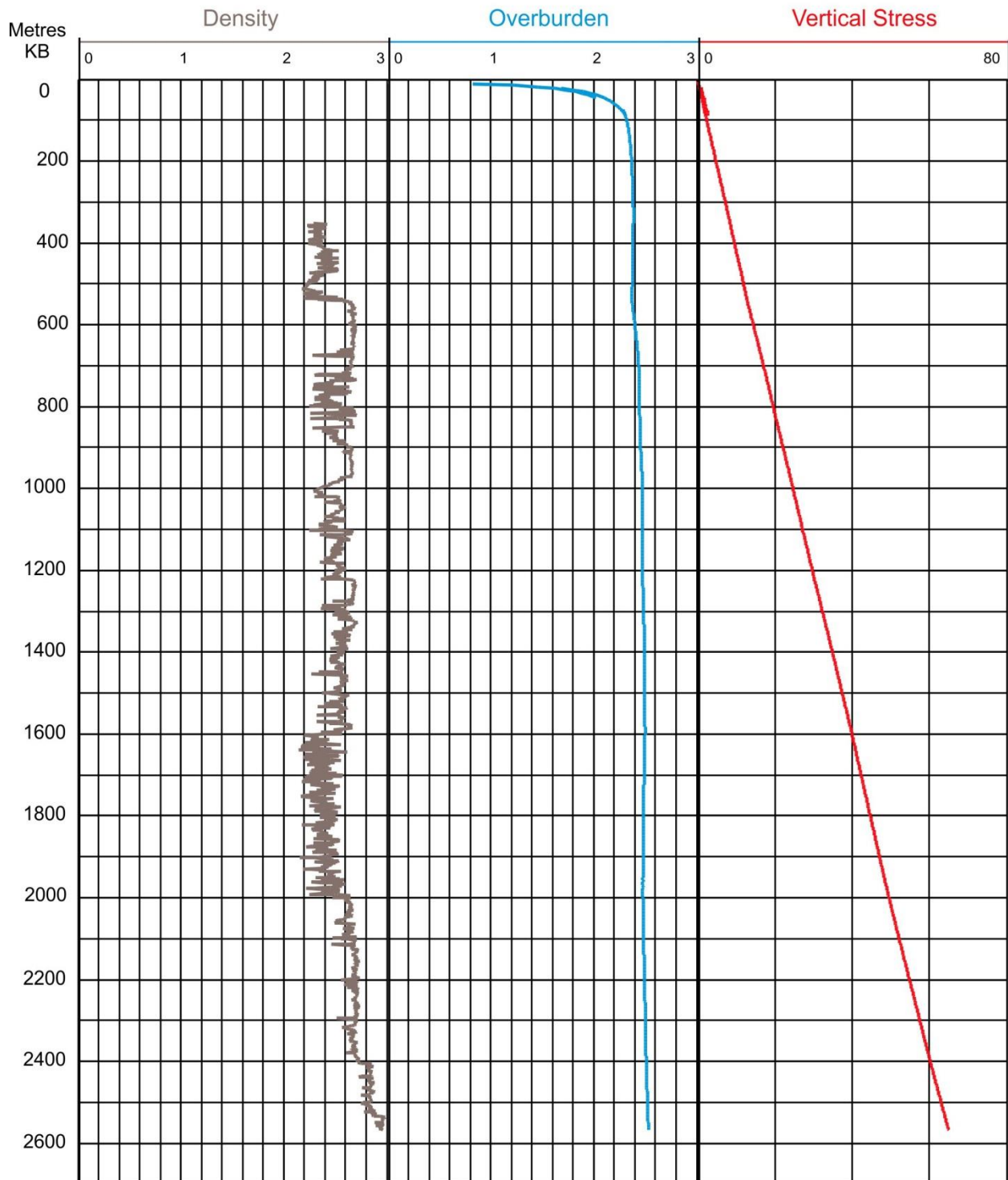
WELL: D-060-I/094-O-09



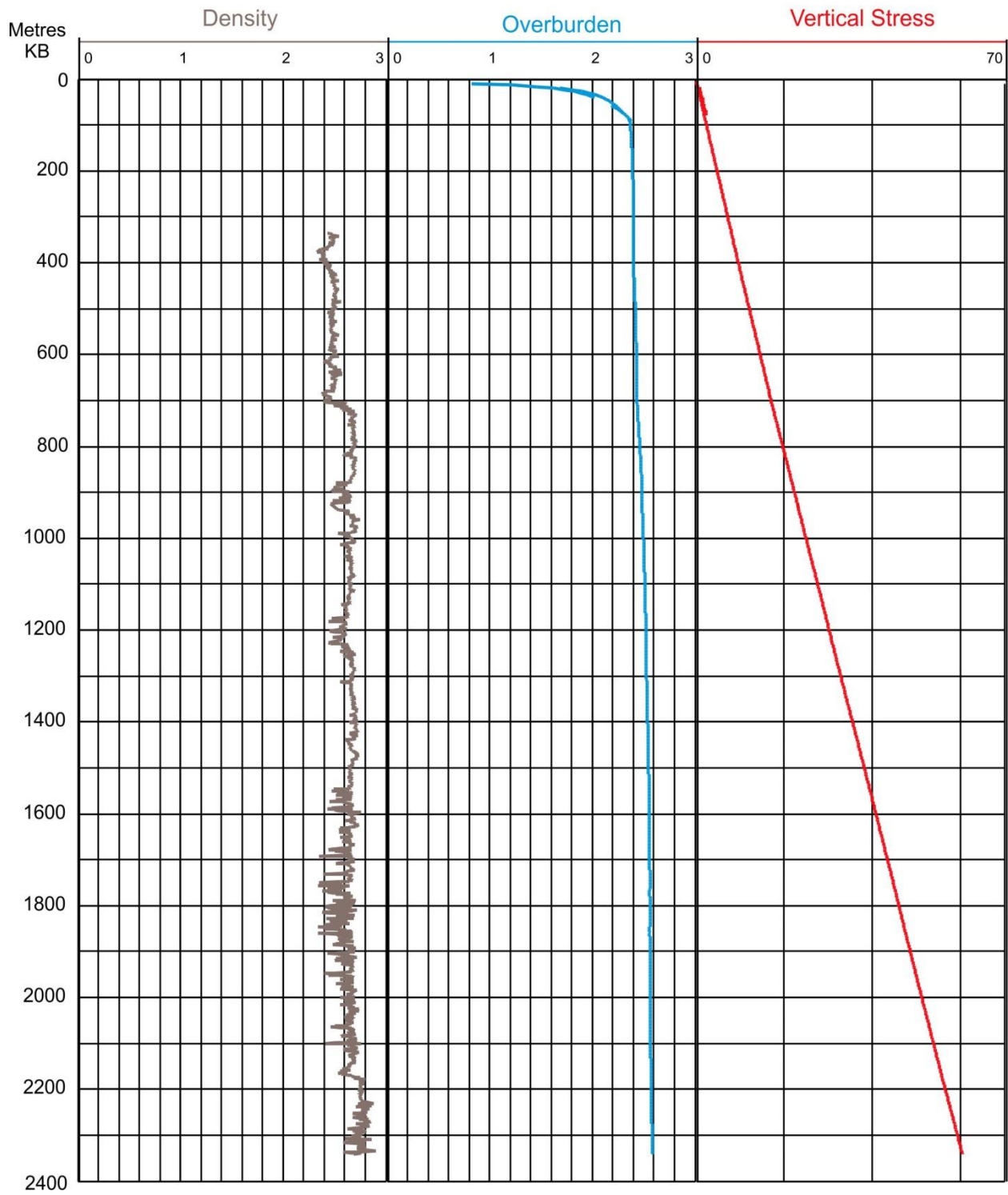
WELL: D-067-A/094-O-11



WELL : D-069-L/094-P-04

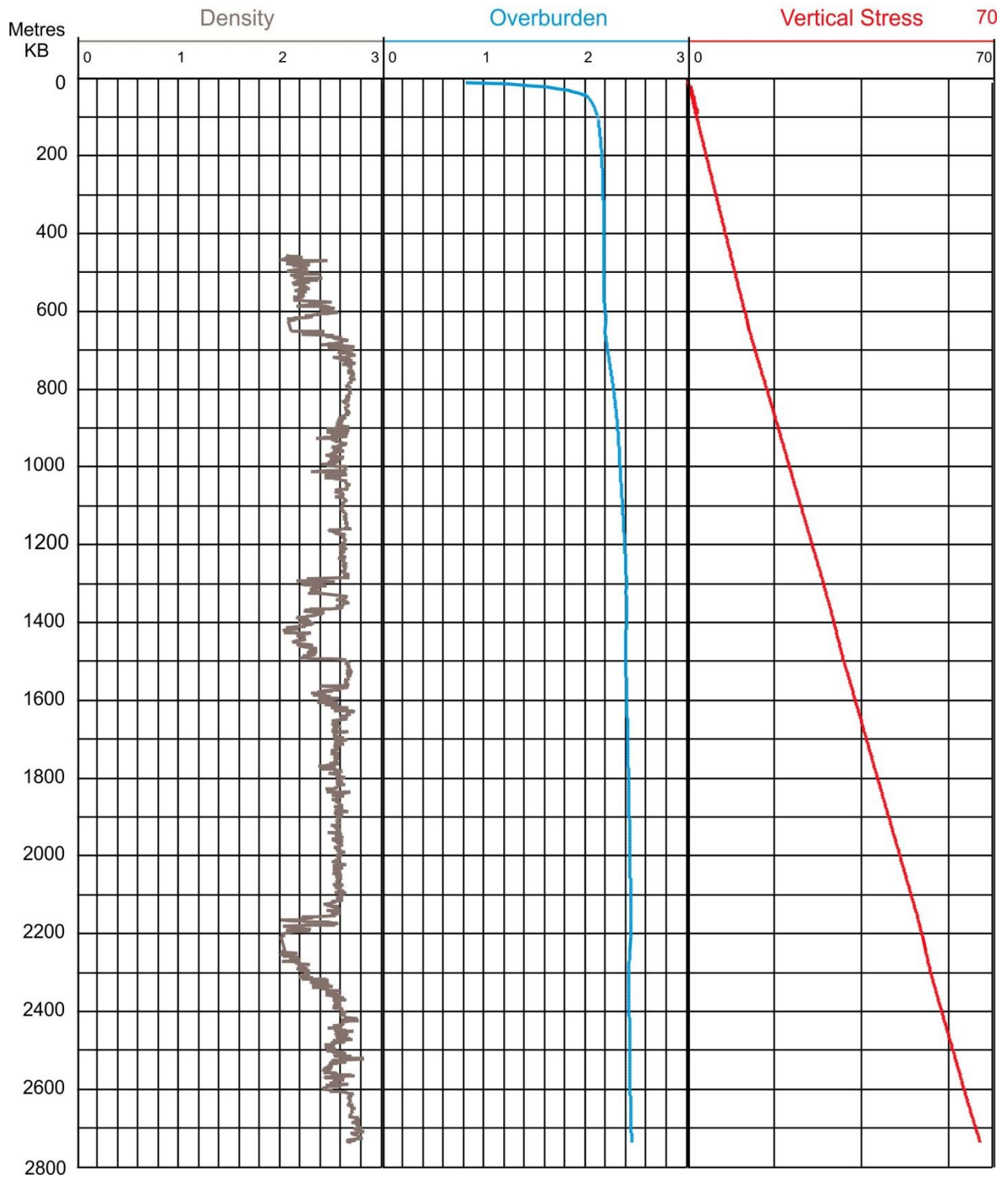


WELL: D-071-I/094-P-04

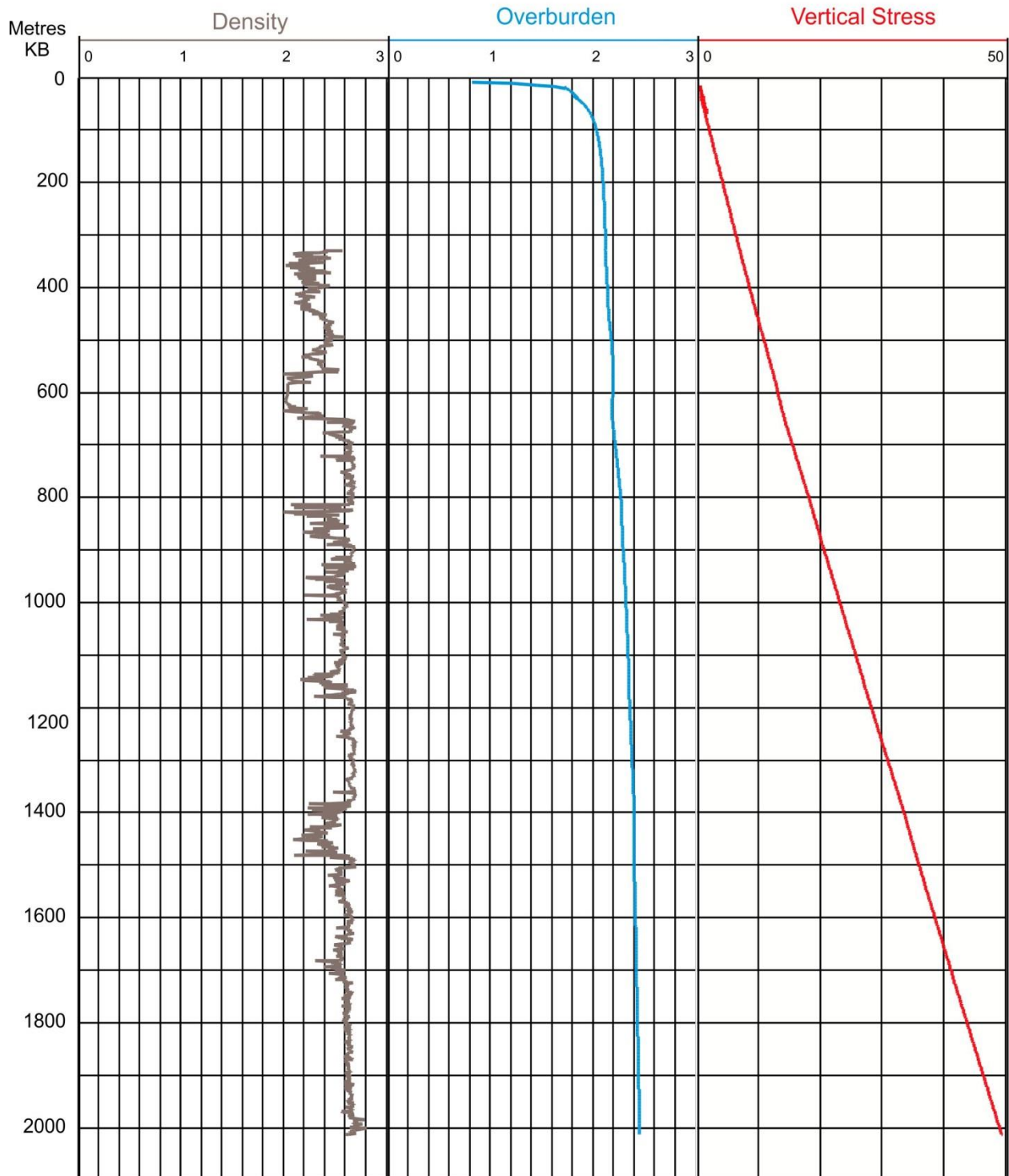




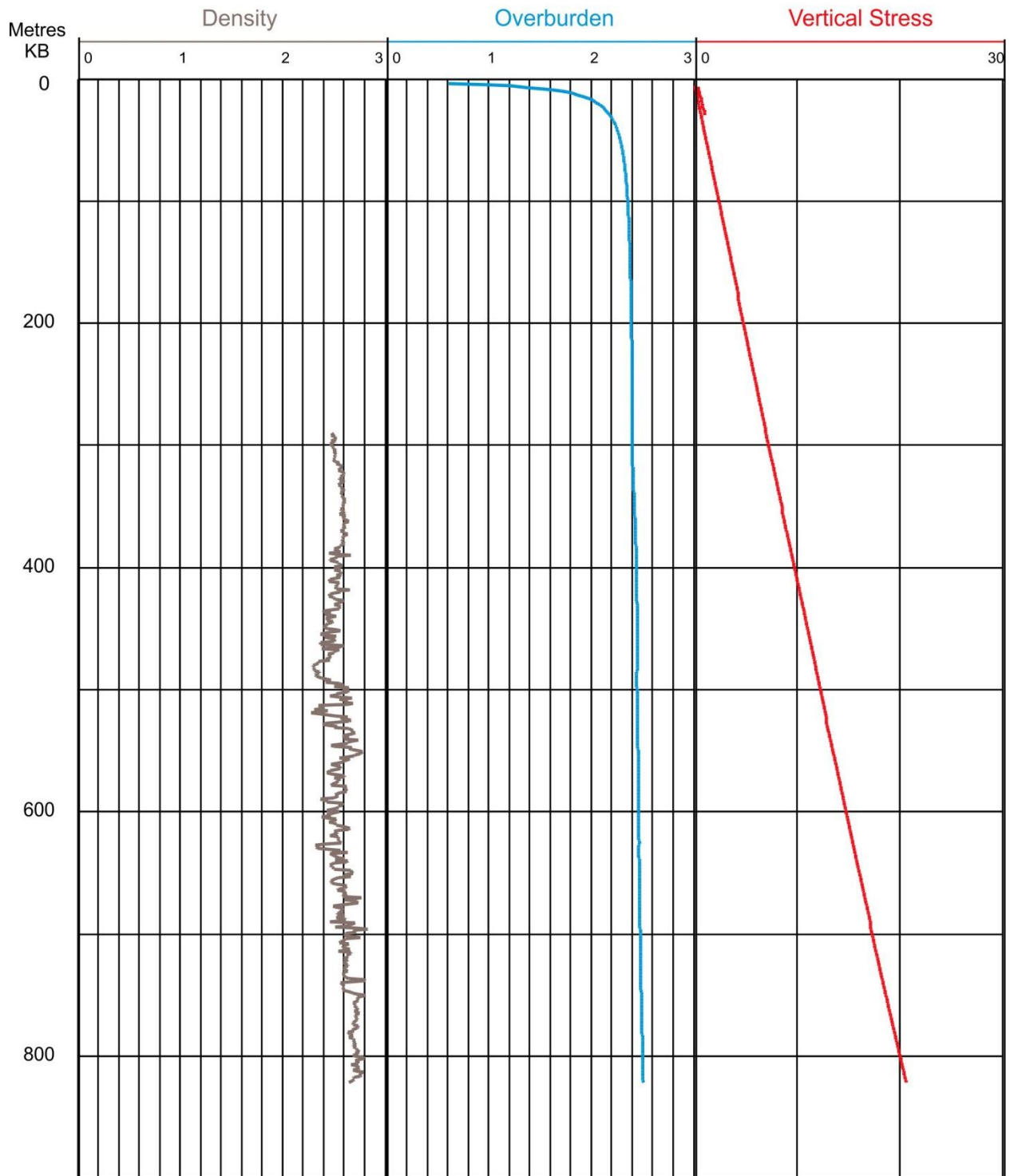
WELL: D-077-J/094-O-08



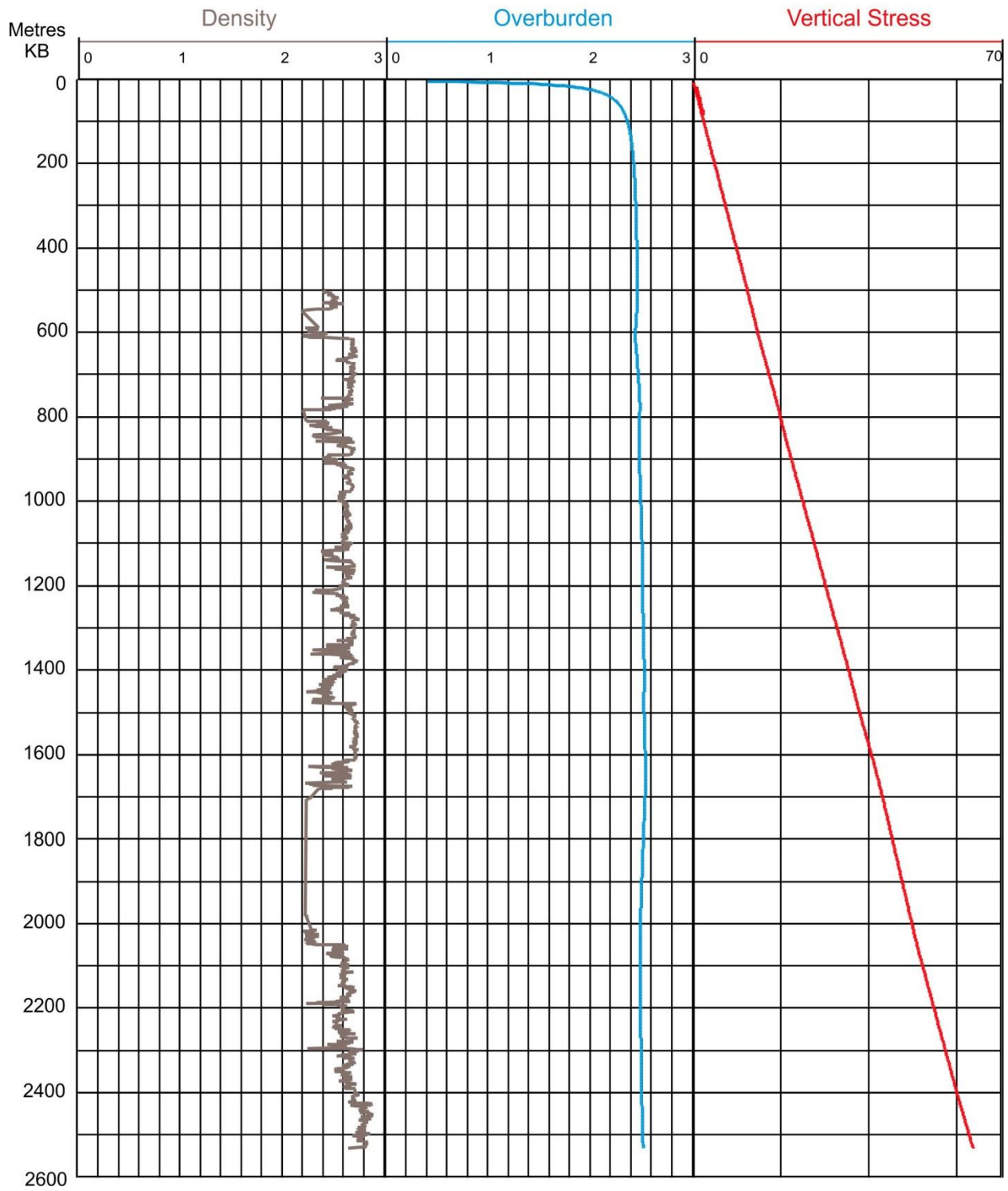
WELL: D-082-K/094-I-14



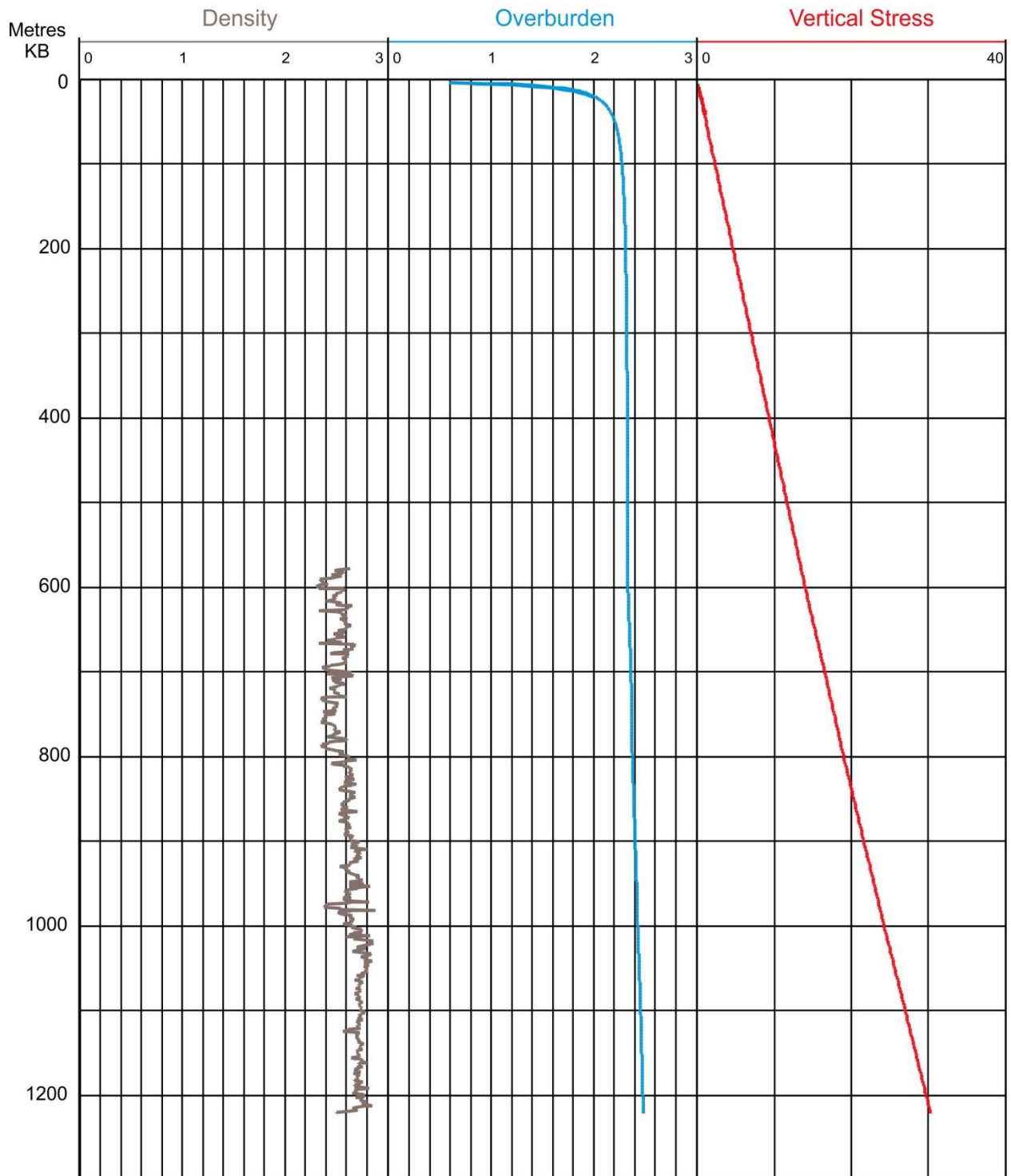
WELL: D-087-A/094-O-11



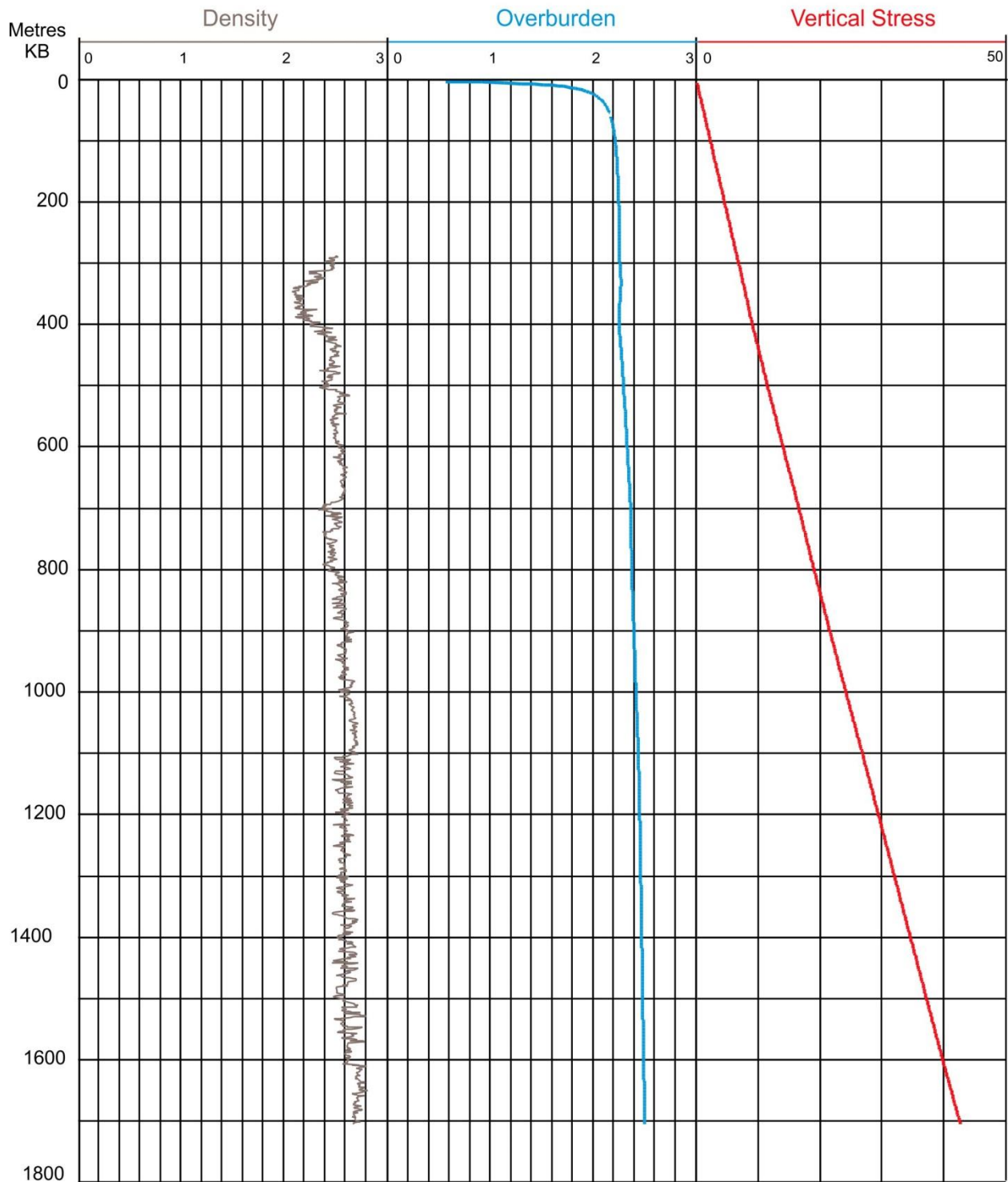
WELL: D-087-C/094-P-05



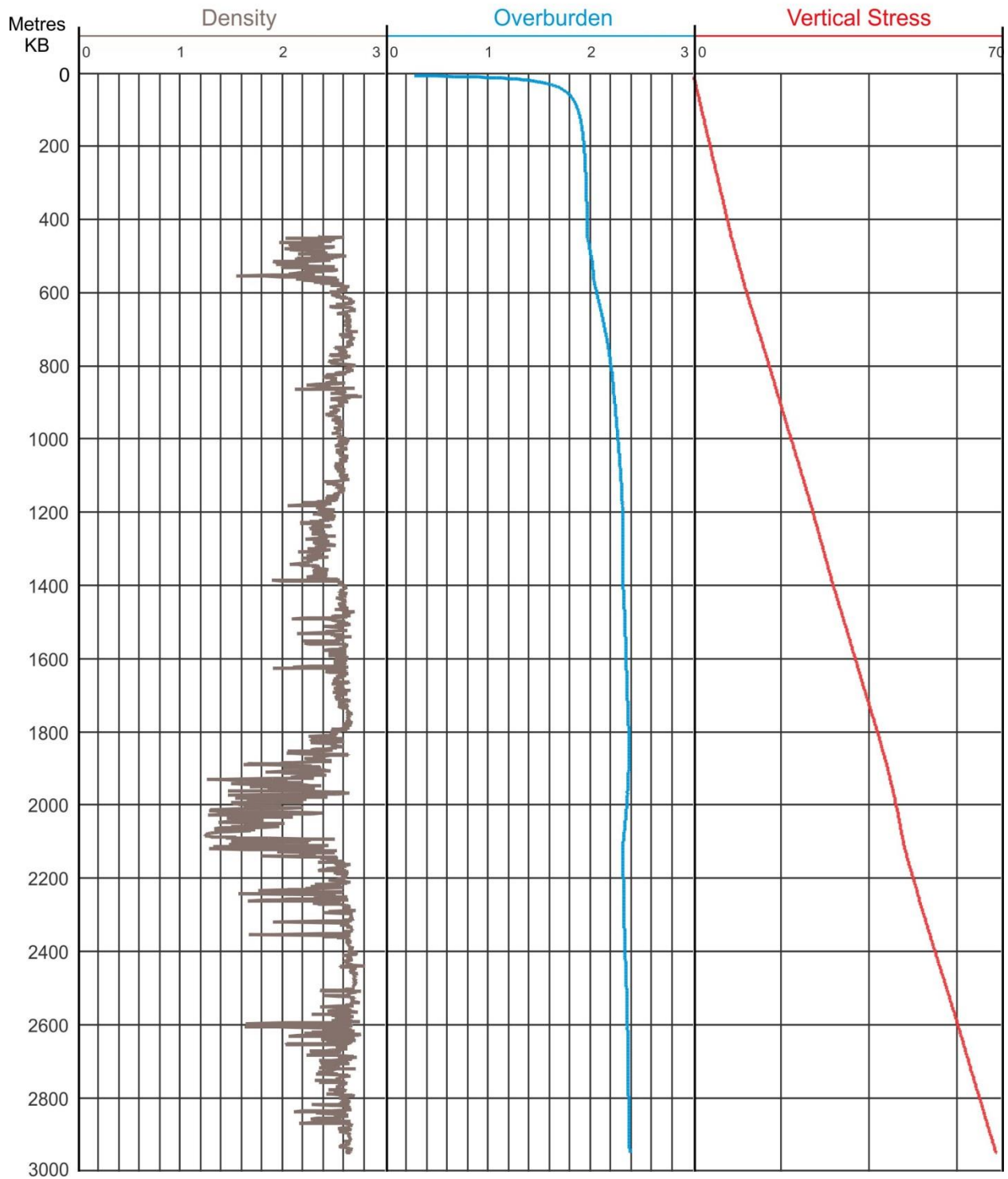
WELL: D-087-G/094-O-06



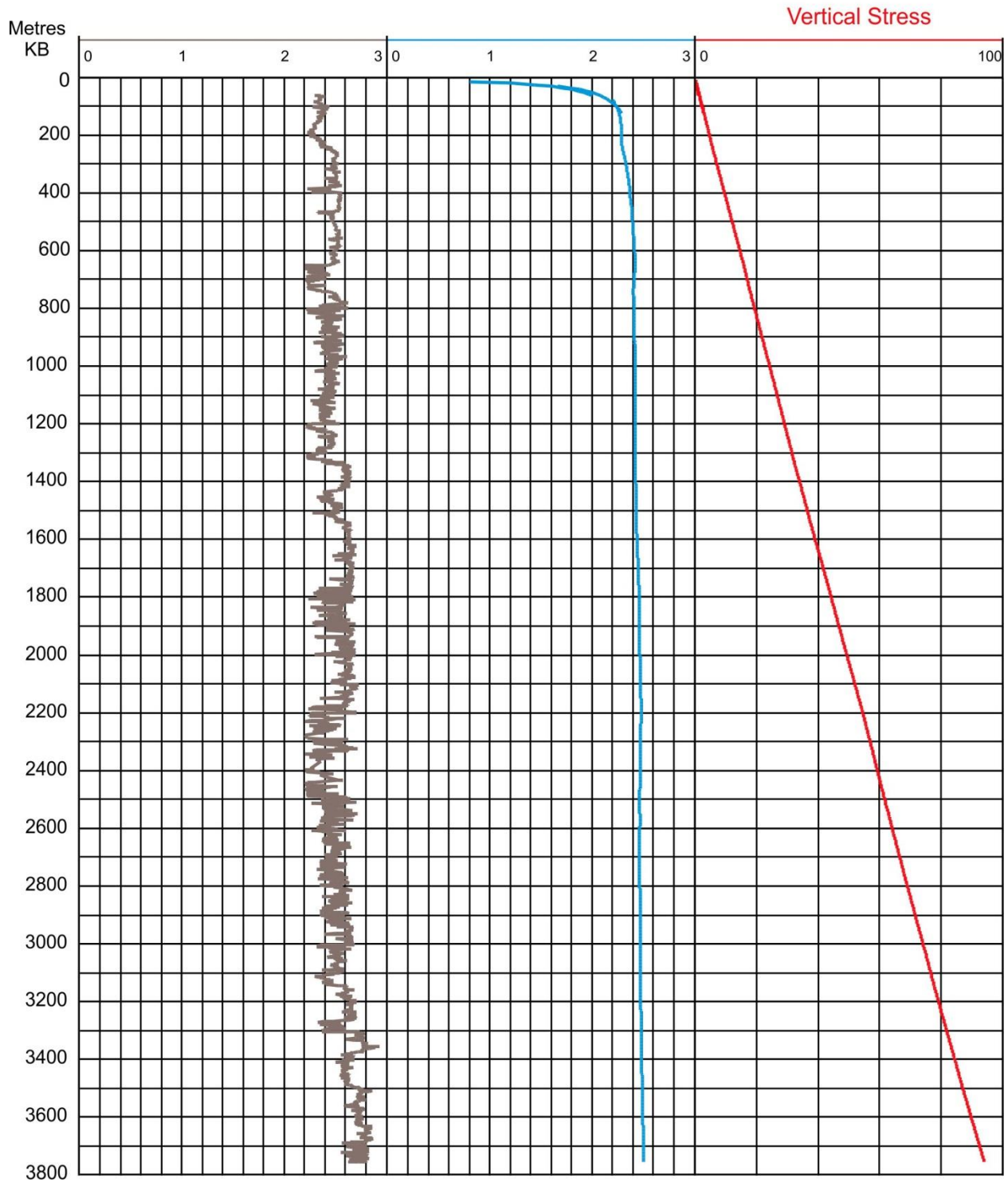
WELL: D-092-J/094-O-06



WELL : D-095-A/094-P-01

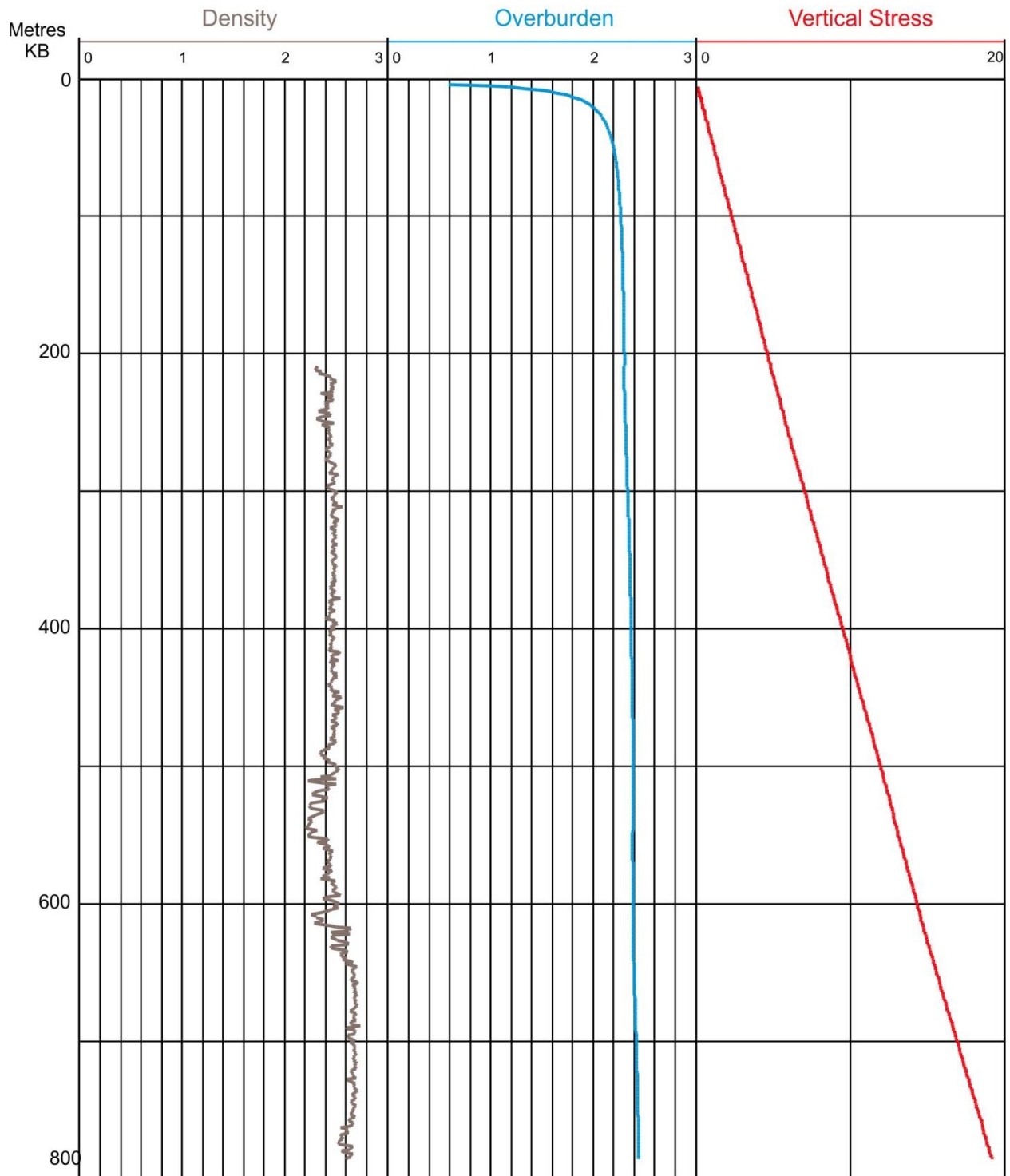


WELL: D-098-F/094-N-10

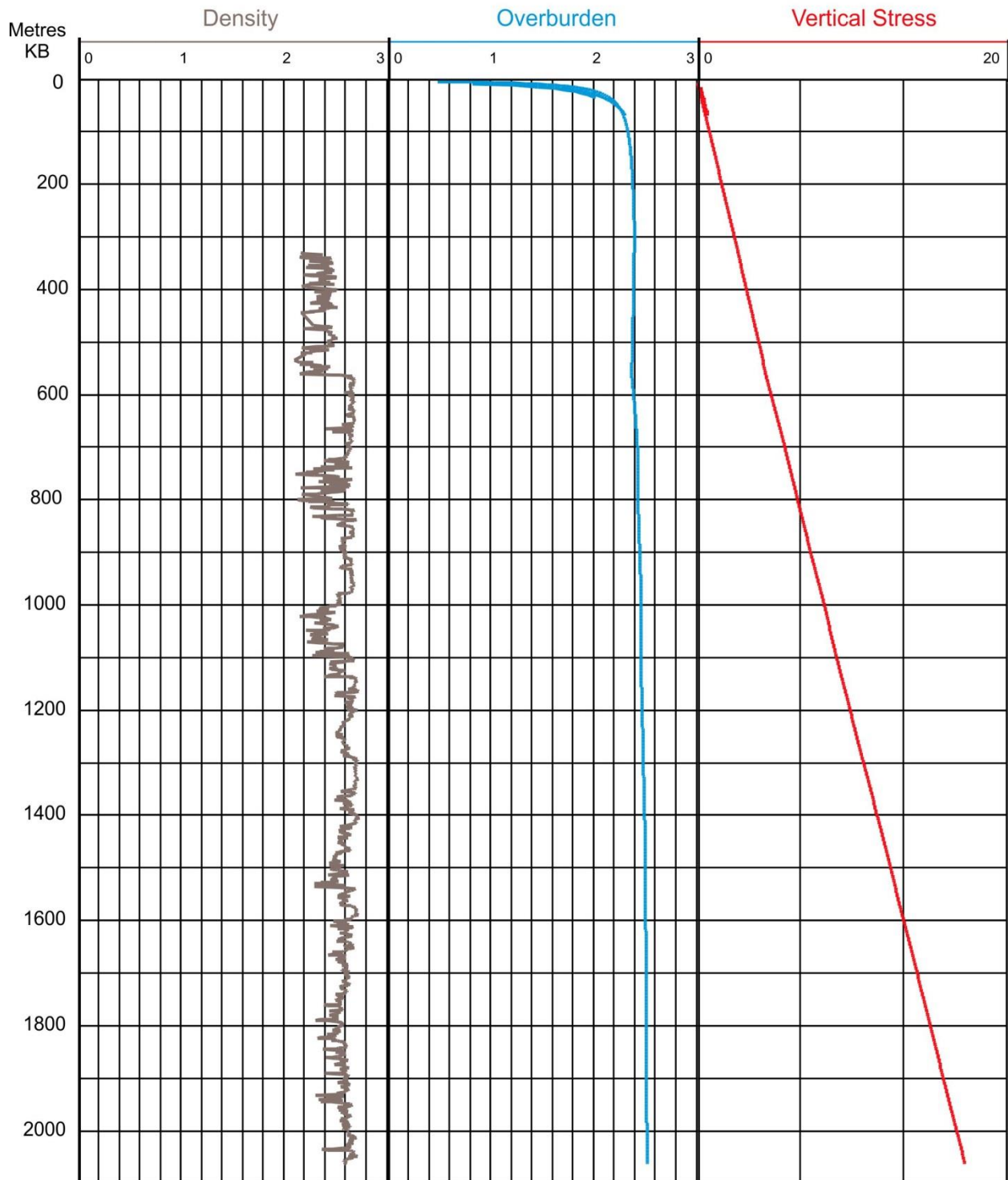




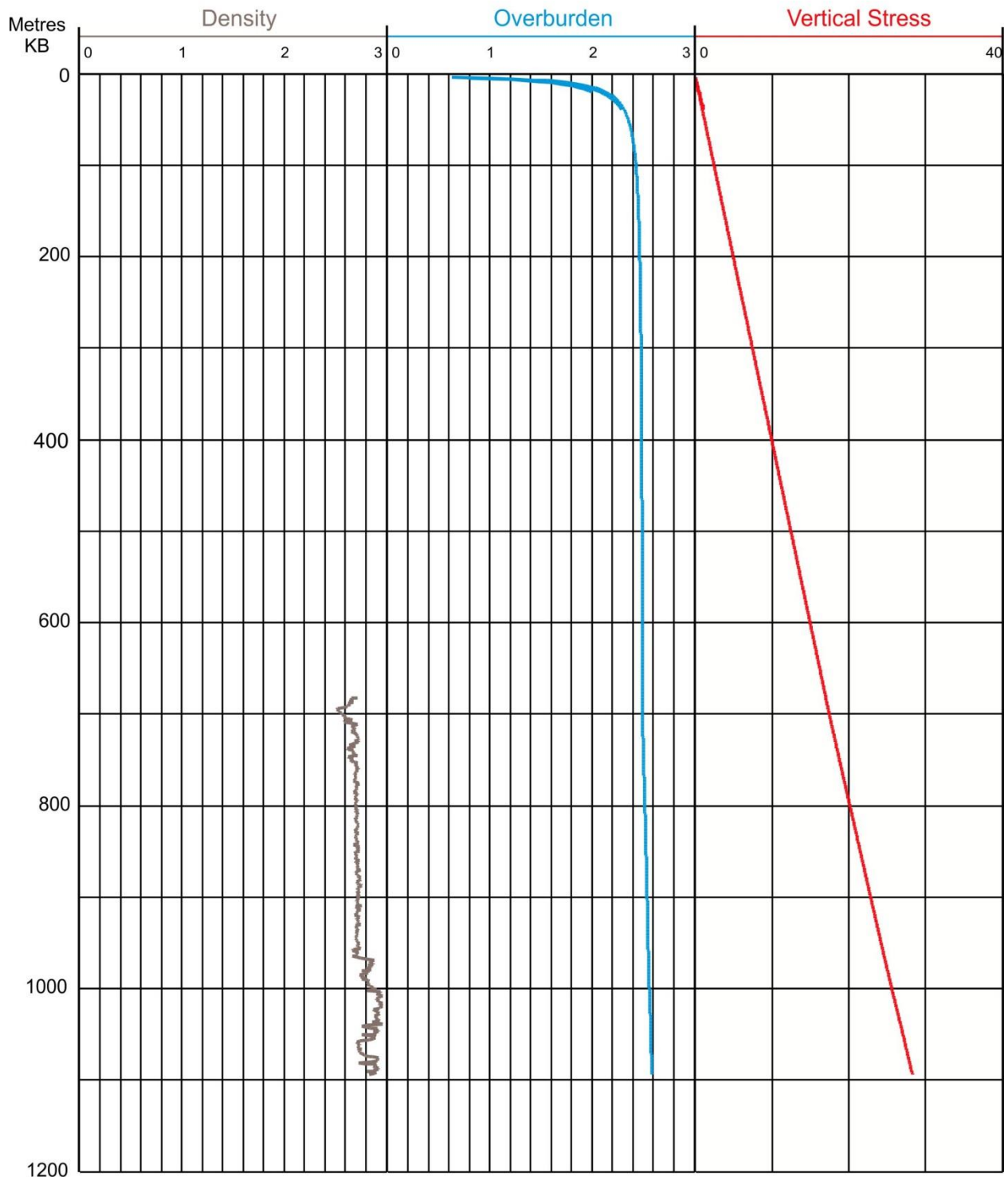
WELL: D-099-H/094-I-14



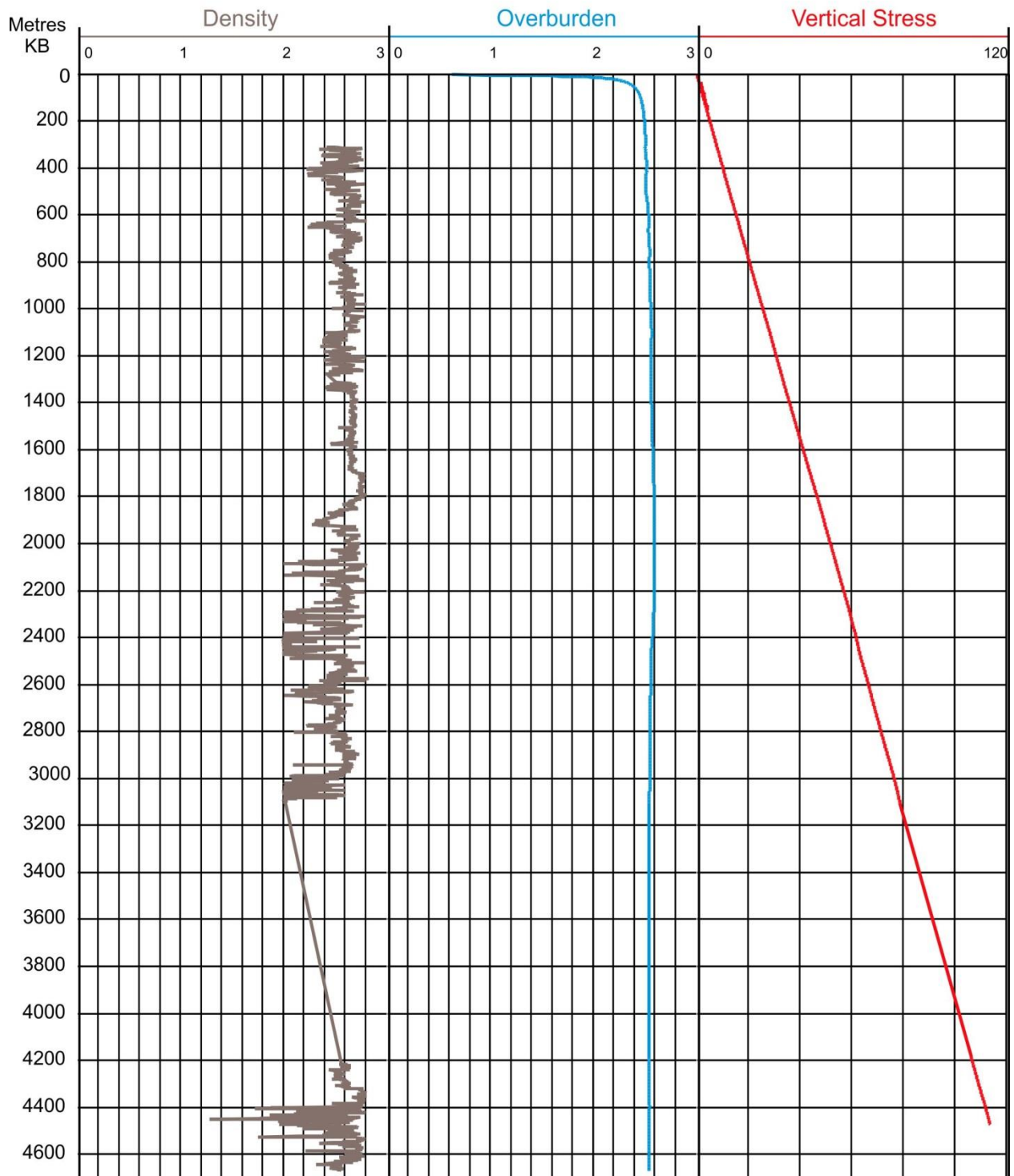
WELL: D-099-K/094-P-05



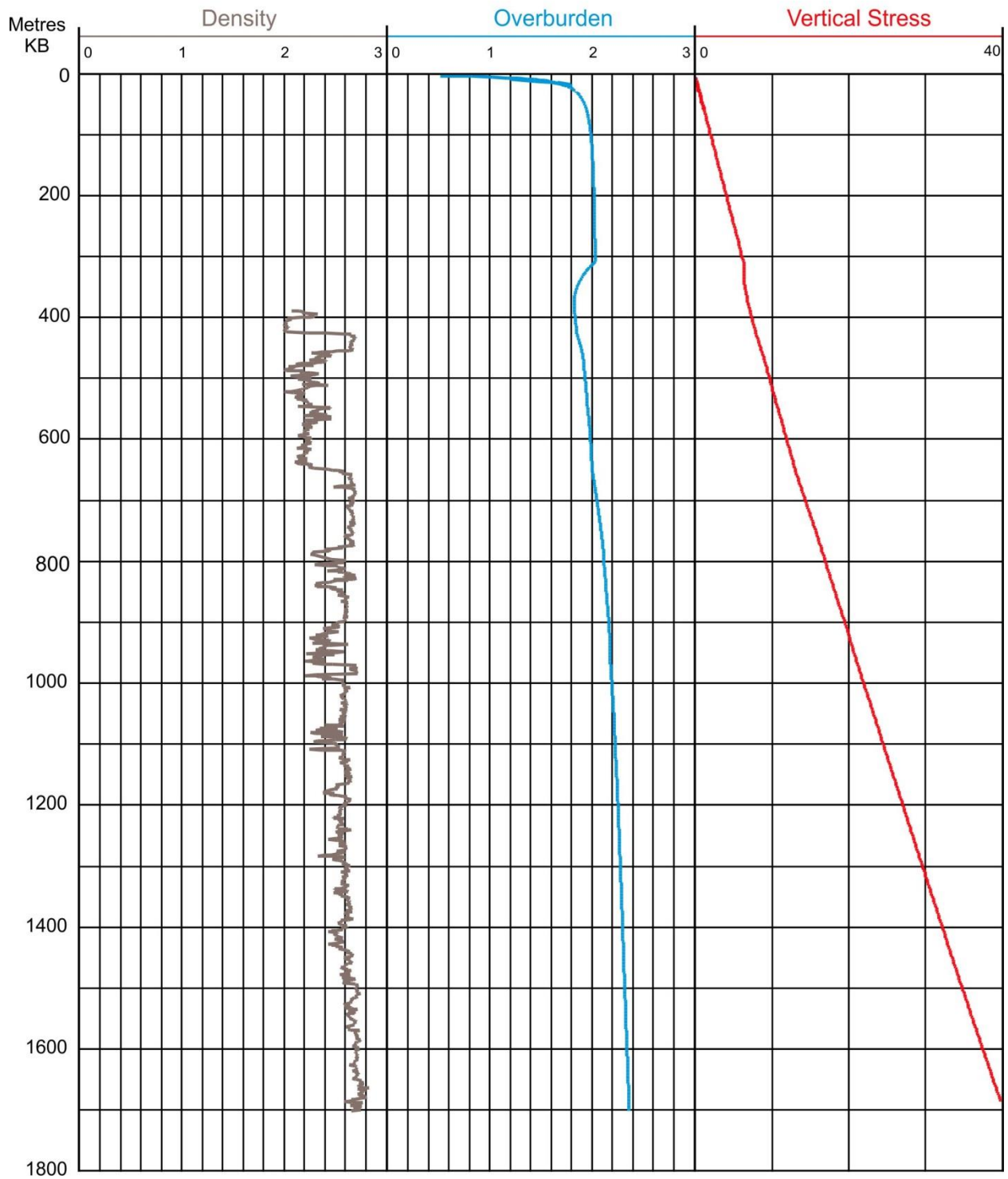
WELL: E-72-61-20-122-00



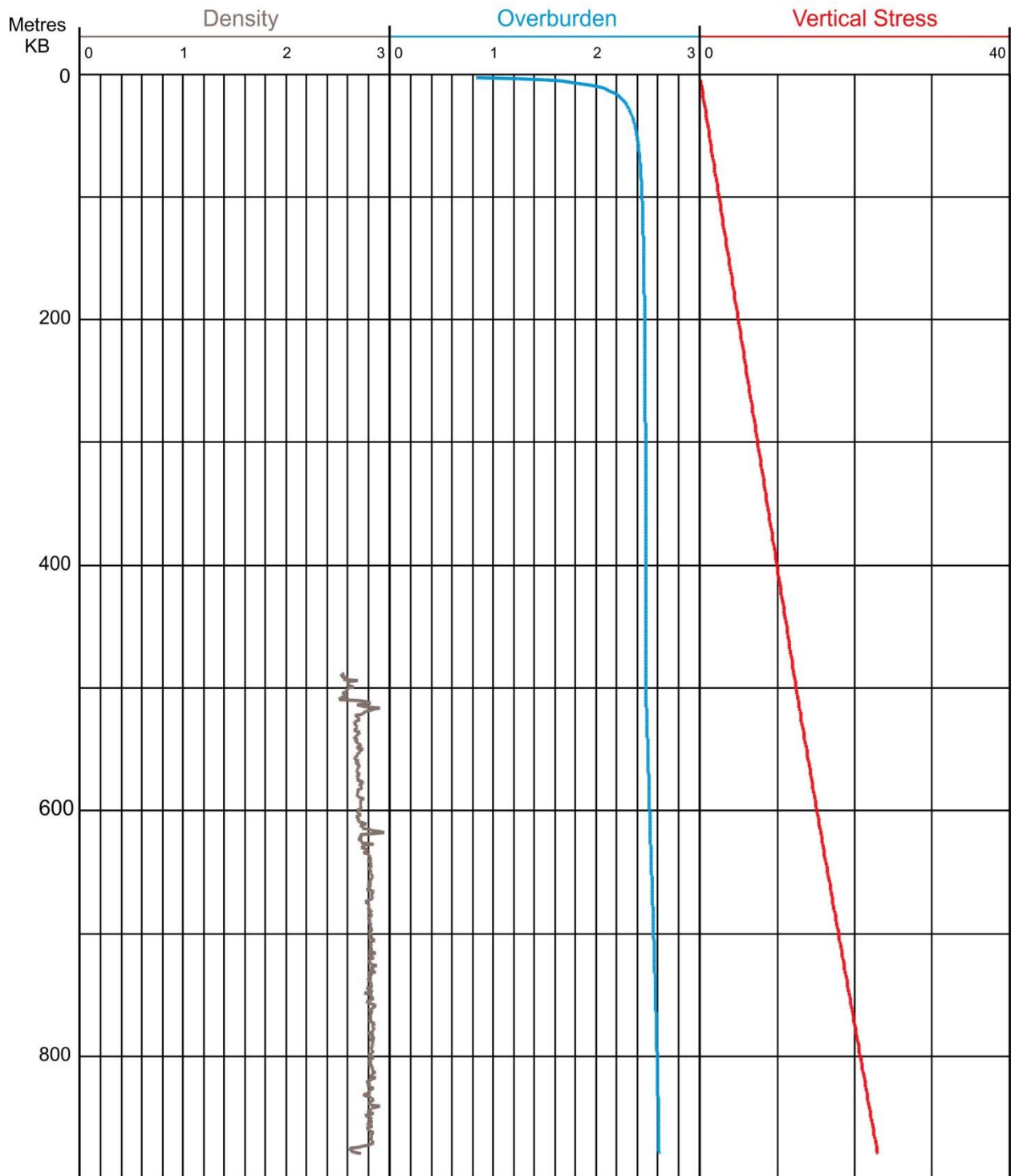
WELL: F-38-60-30-123-45



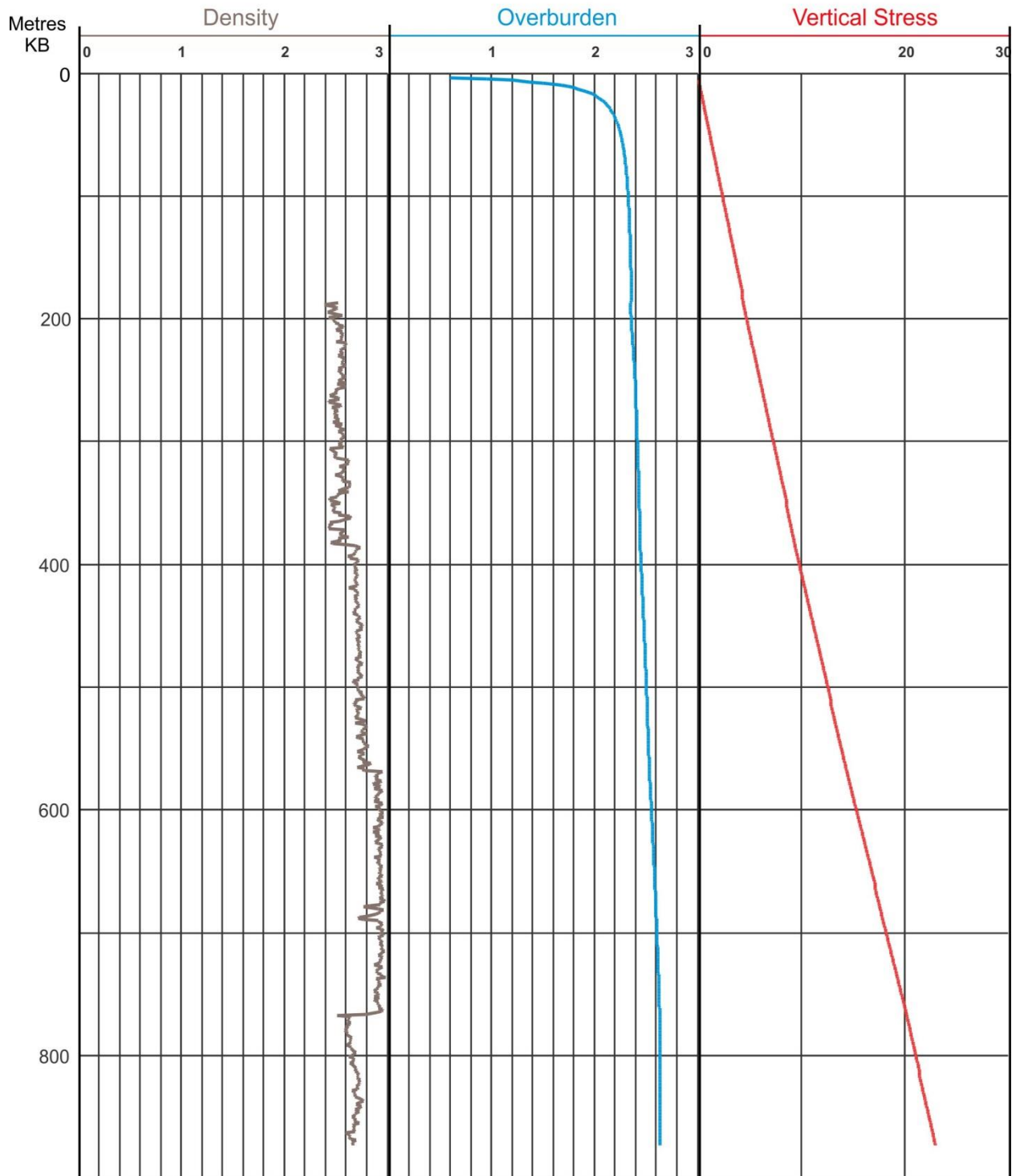
WELL: H-45-60-50-121-15



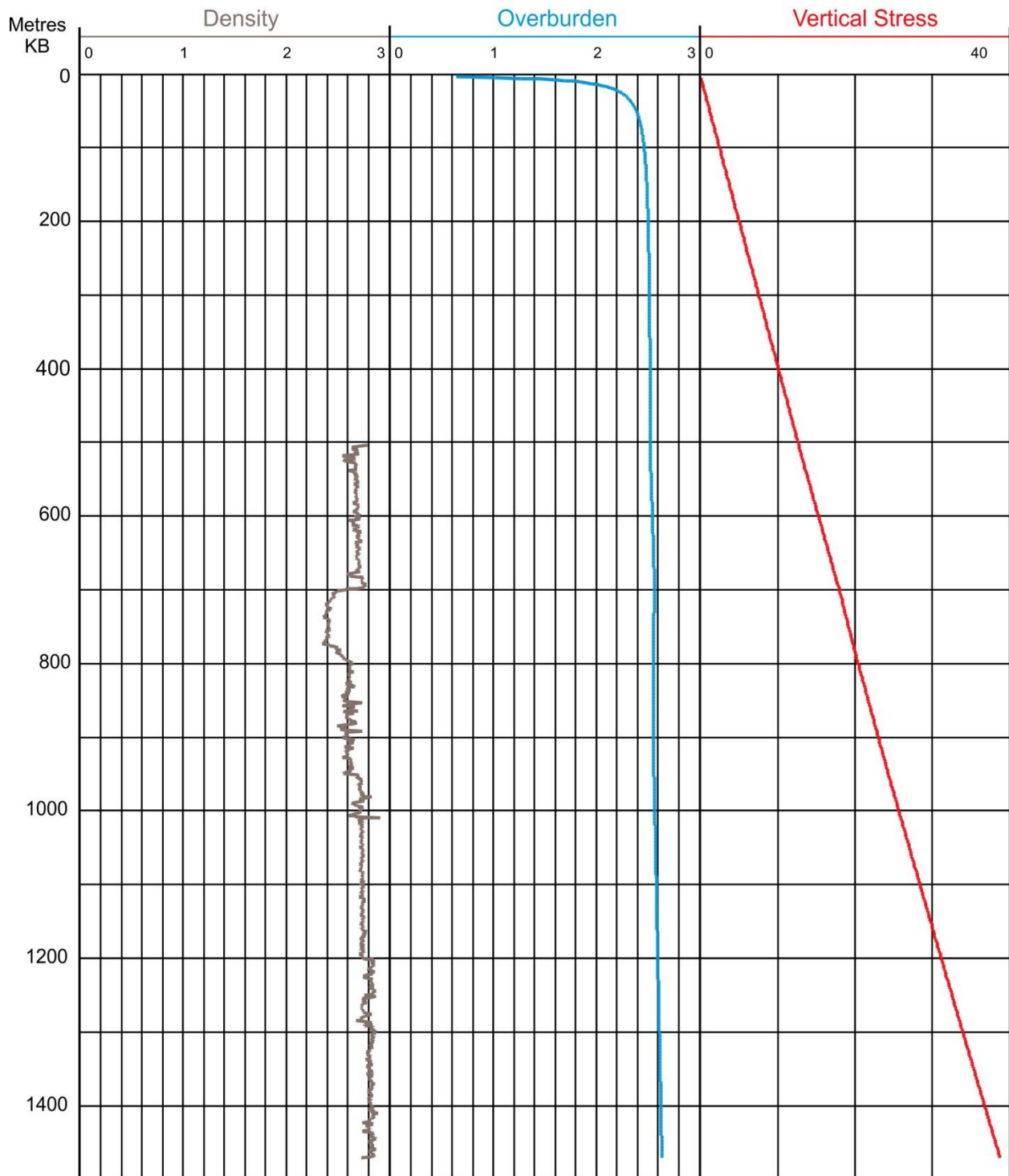
WELL: J-15-61-20-123-00



WELL: J-66-62-00-121-45

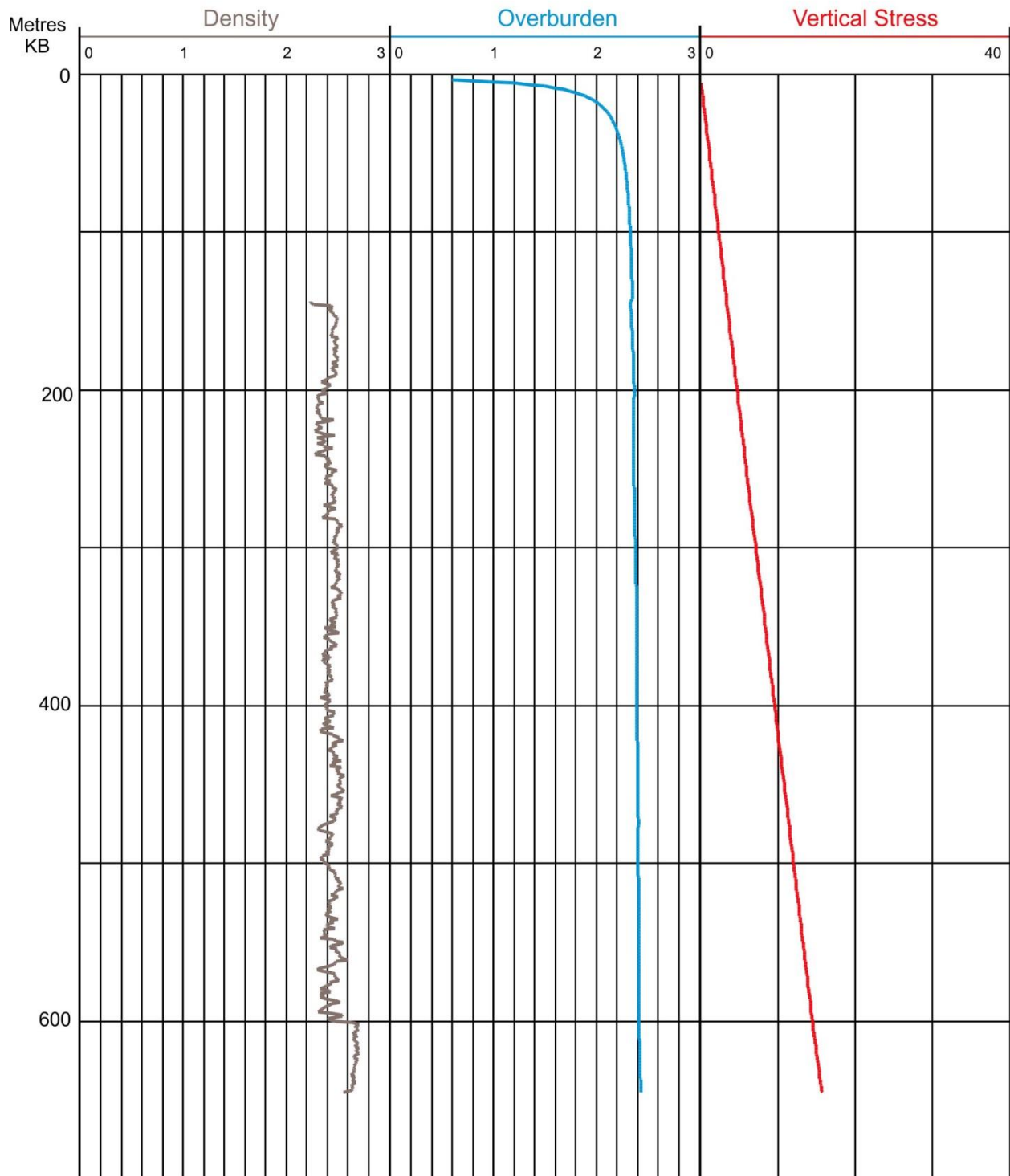


WELL: L-20-61-00-123-30

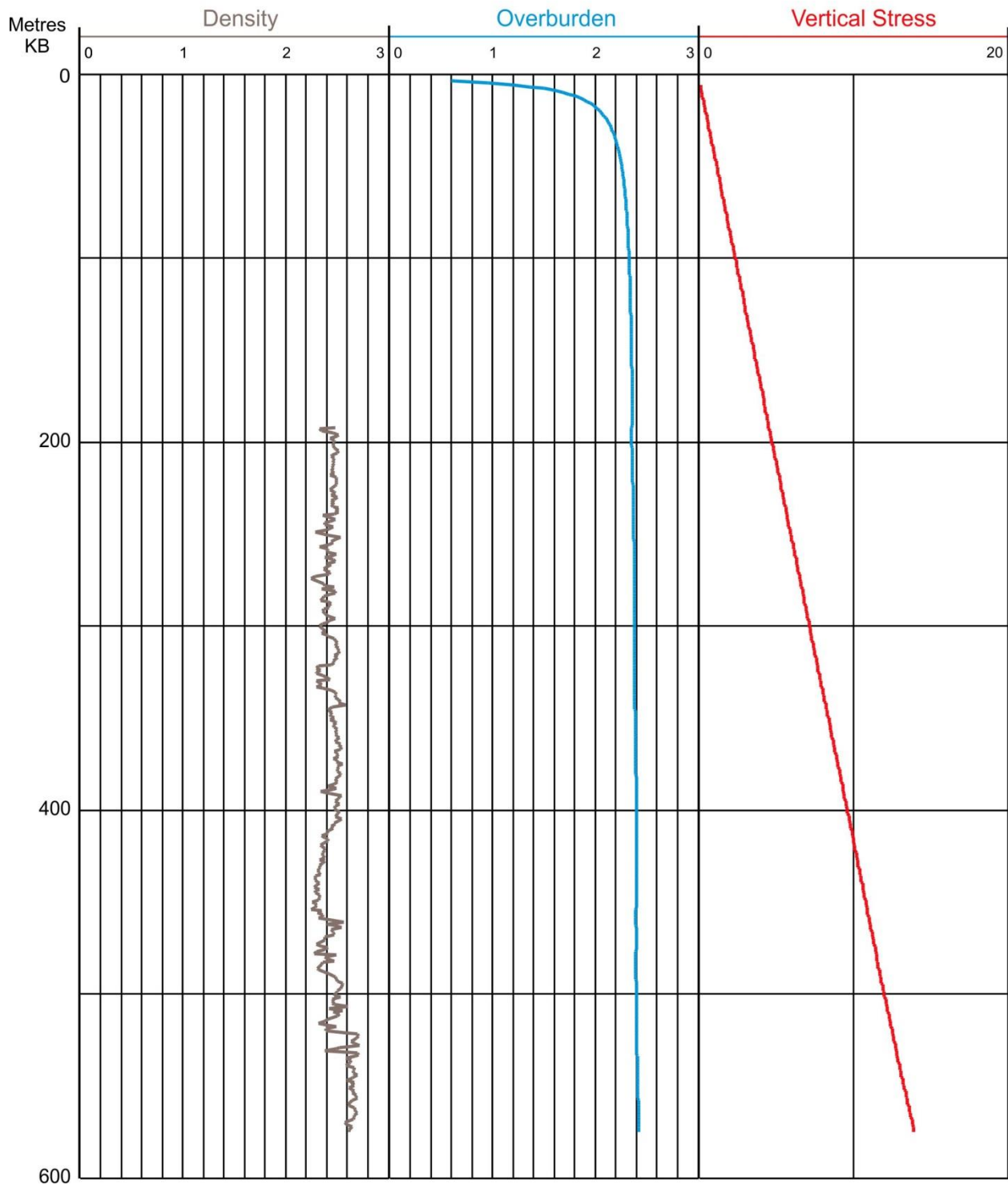




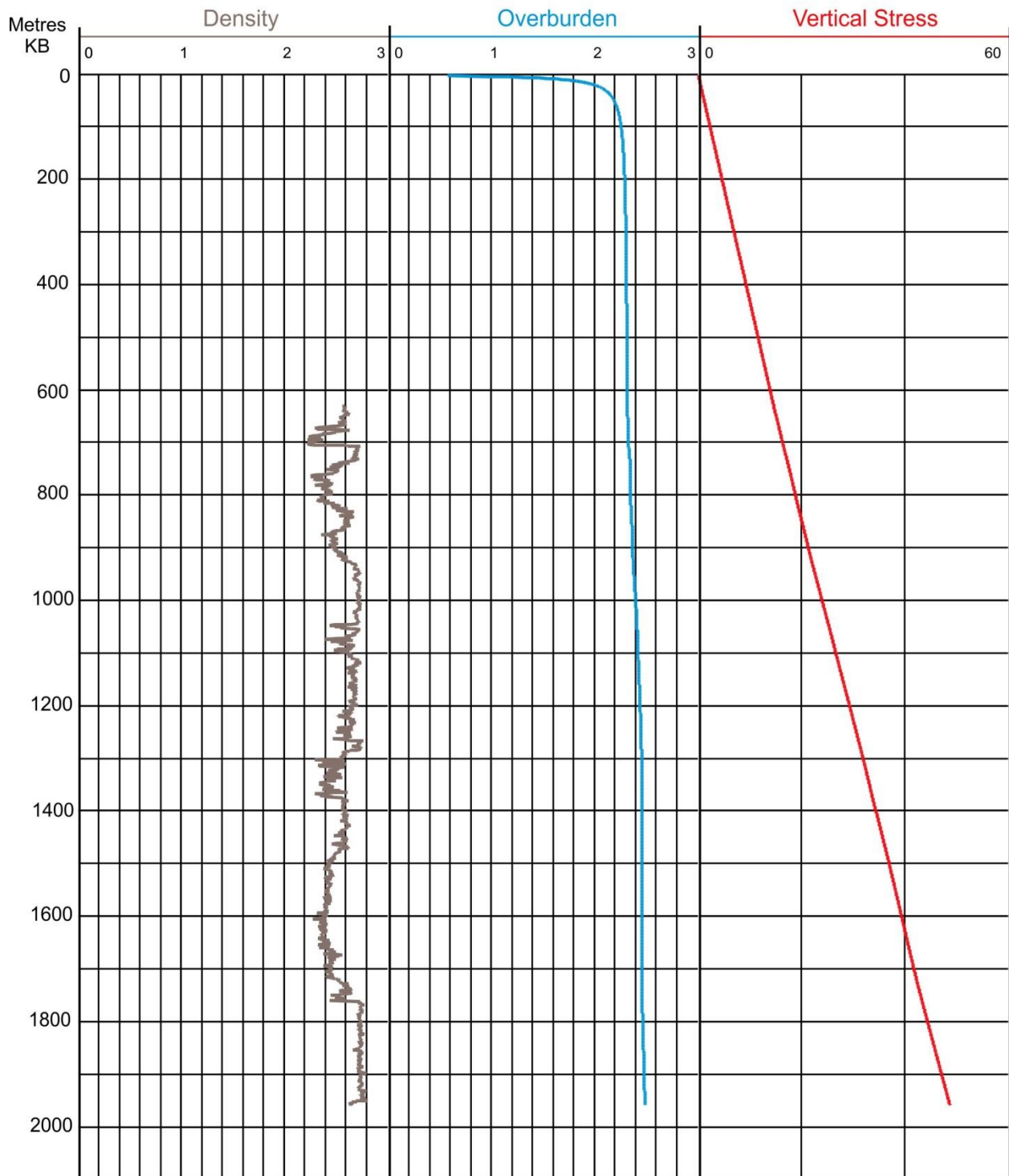
WELL: L-49-60-30-122-30



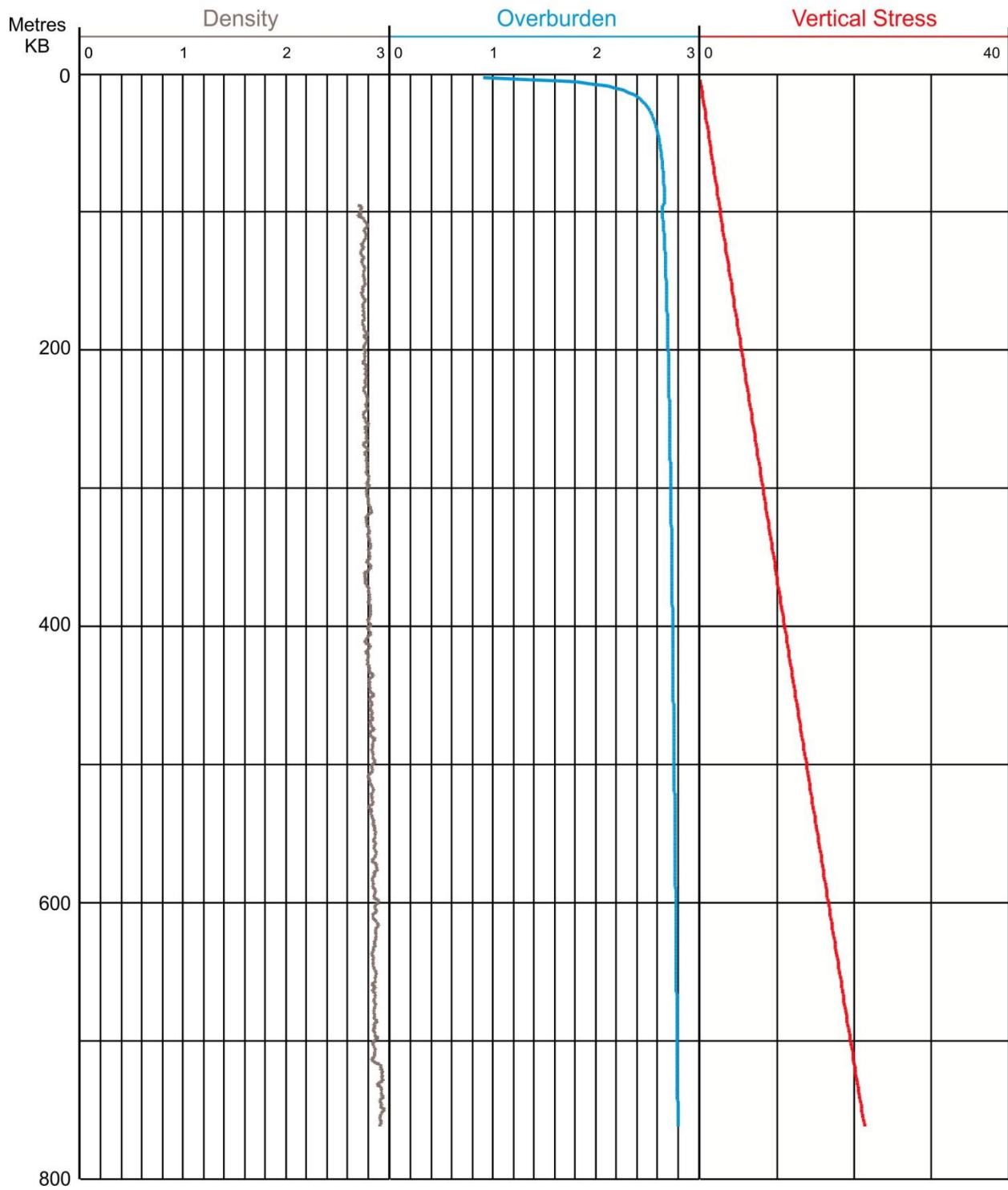
WELL: M-05-60-20-122-45



WELL: M-73-60-40-121-15



WELL: N-44-62-00-123-45



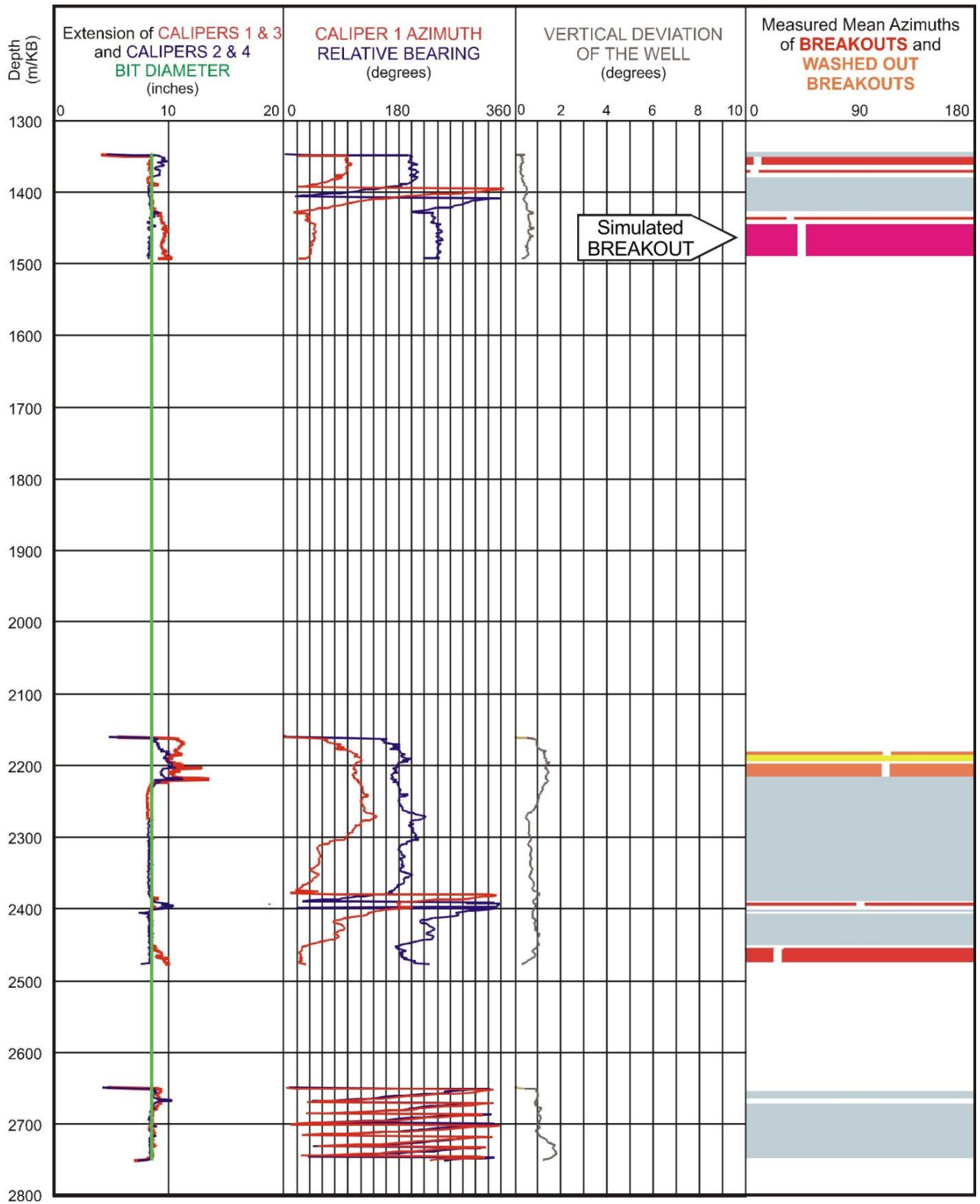
### Appendix 3: Breakout failure simulations aimed at establishing probable magnitudes of $S_{Hmax}$

#### $S_{Hmax}$ Simulation Commentary – A-006-C/094-O-08

Well: <b>A-006-C /094-O-08</b>	Failure Simulation Method				Formula
	Mohr Coulomb	Drucker Prager	Modified Strain Energy	3 Cycle Mohr Coulomb	2 SHmin - Po
Breakout Interval Top (m KB)	1445	1445	1445	1445	
Breakout Interval Base (m KB)	1491	1491	1491	1491	
Median Depth of Breakout (m KB)	1468	1468	1468	1468	
Calipers 1 and 3 extent (inches)	8.54	8.54	8.54	8.54	
Calipers 2 and 4 extent (inches)	9.74	9.74	9.74	9.74	
SHmax (MPa)	<b>42.8</b>	62.2	54.1		43.1
SHmax gradient (kPa/m)	29.2	42.4	36.9		29.4
SHmin (MPa)	28.9	28.9	28.9	28.9	
Sv (MPa)	36.6	36.6	36.6	36.6	
Pore pressure (MPa)	14.7	14.7	14.7	14.7	
Mudweight (MPa)	14.7	14.7	14.7	14.7	
u (Coefficient of Friction)	0.6	0.6	0.6	0.6	
Cohesive Strength of Rock (MPa)	9.8	9.8	9.8	9.8	
v (Poisson's Ratio)	0.2	0.2	0.2	0.2	
Diameter of Borehole (inches)	8.5	8.5	8.5	8.5	

The breakout interval between depths of 1445 and 1491 m KB was simulated satisfactorily by all three single cycle failure models. The lowest magnitude for  $S_{Hmax}$  was provided by simulating Mohr-Coulomb failure, so the interpreted magnitude at 1468 metres depth is **42.8 MPa**, resulting in an  $S_{Hmax}$  gradient of 29.2 kPa/m. This is close to the magnitude of 43.1 MPa suggested by the simplified equation:  $S_{Hmax} = 2 (S_{Hmin}) - Po$ .

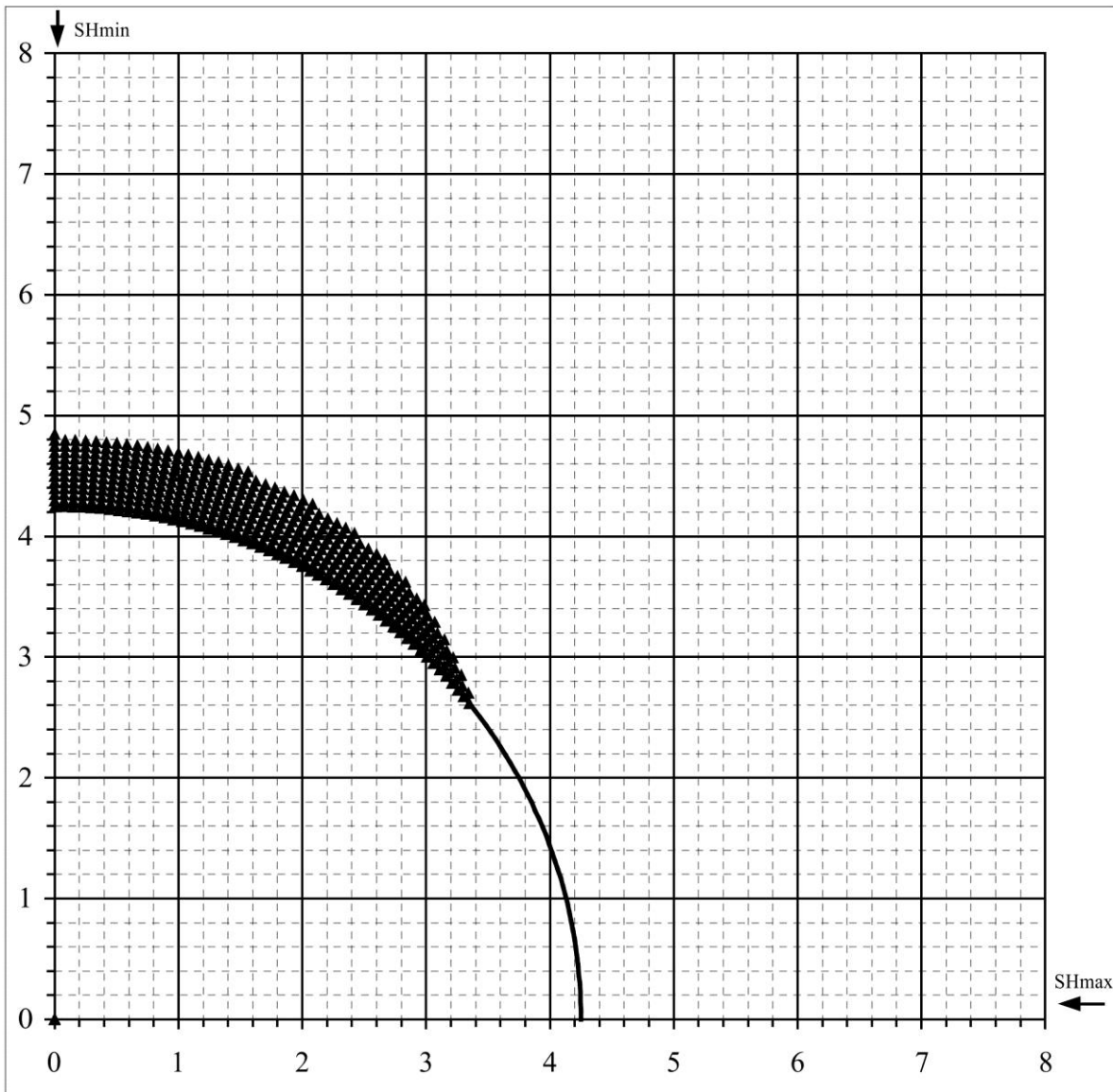
WELL : A-006-C/094-O-08      BREAKOUT ANALYSIS



A-006-C/094-O-08

### Mohr - Coulomb Failure Criterion

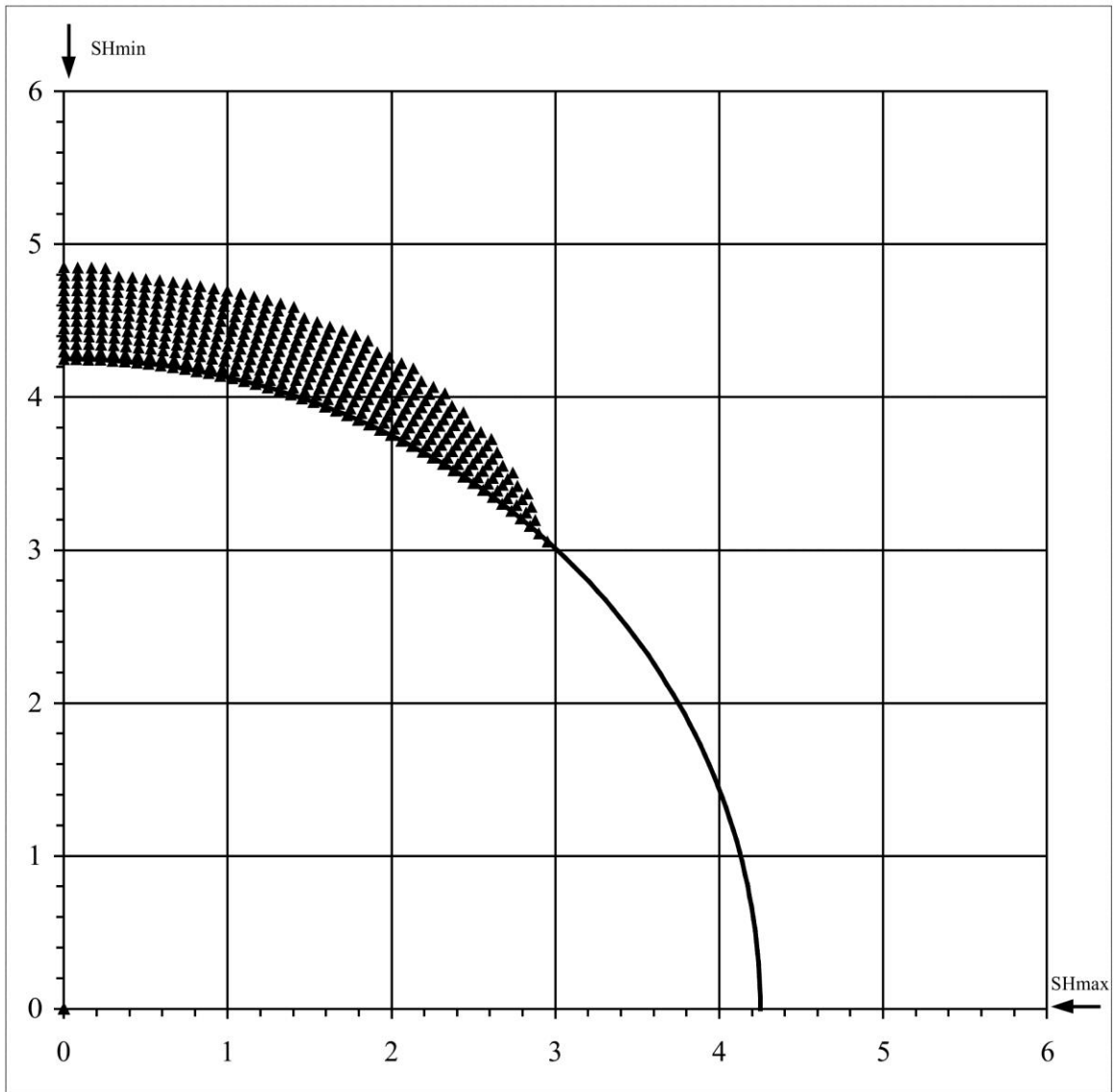
SHmax =	42.8 MPa	u (Coeff. of Friction) =	0.6
SHmin =	28.9 MPa	C (Cohesive Strength) =	9.84 MPa
Sv =	36.6 MPa	v (Poisson's Ratio) =	0.2
Po (Pore Pressure) =	14.7 MPa	Diameter of Borehole =	8.5 "
Pm (Mud Weight) =	14.7 MPa		
Sensitivity of Figure =	0.05 "	Angle of Max. Breakout =	90 deg
Depth of Max. Breakout =	0.6 "	Max caliper at 90 deg =	9.7 "
Validity of the results =	TRUE	Max caliper at 0 deg =	8 "



A-006-C/094-O-08

## Extended von-Mises Failure Criterion (Drucker-Prager Failure Criterion)

SHmax =	62.2 MPa	u (Coeff. of Friction) =	0.6
SHmin =	28.9 MPa	C (Cohesive Strength) =	9.8 MPa
Sv =	36.6 MPa	v (Poisson's Ratio) =	0.2
Po (Pore Pressure) =	14.7 MPa	Diameter of Borehole =	8.5 inches
Pm (Mud Weight) =	14.7 MPa	Depth of Max. Breakout =	0.6 inches
Sensitivity of Figure =	0.05 inches	Angle of Max. Breakout =	90 deg

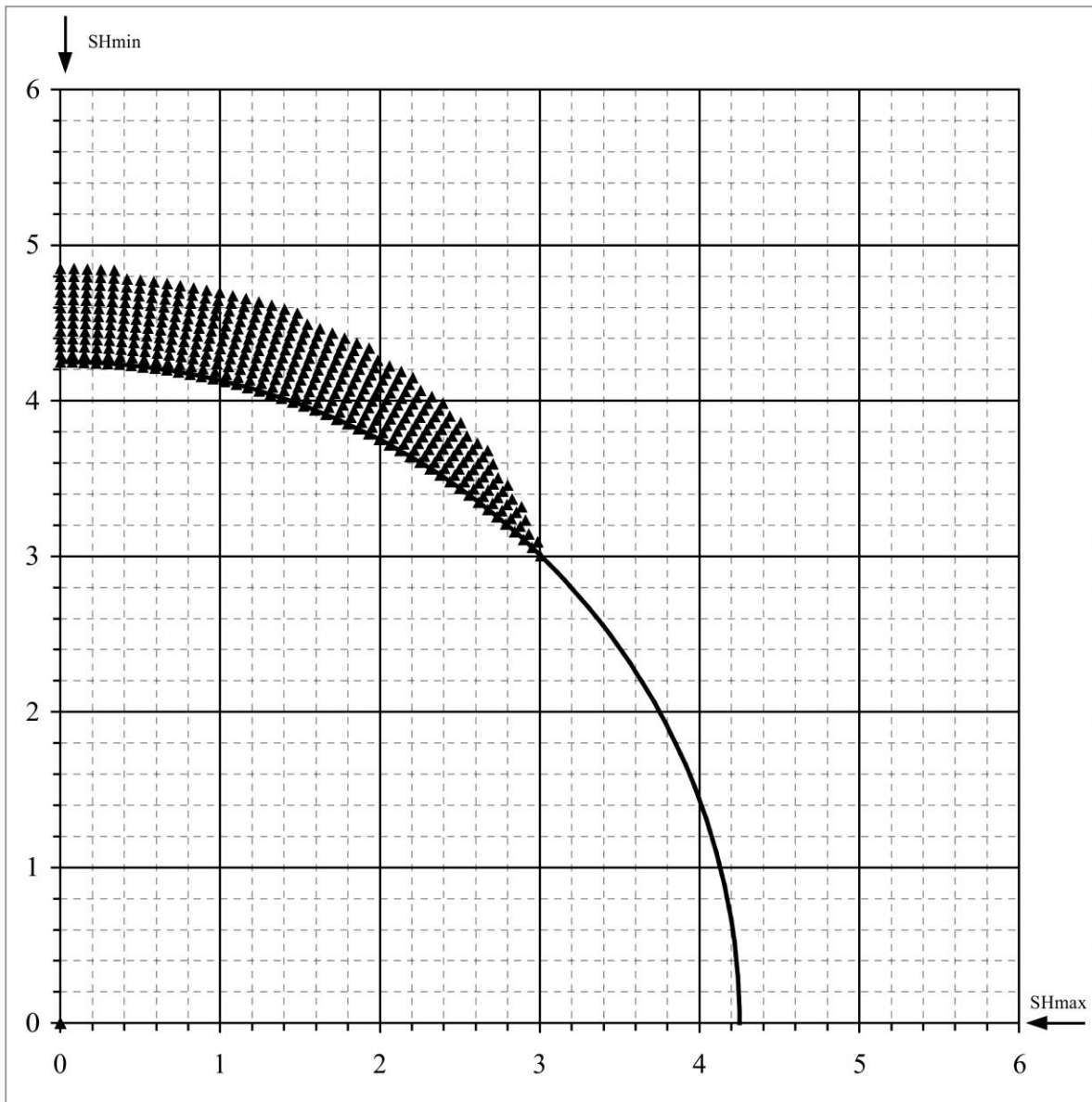




A-006-C/094-O-08

## Extended Drucker - Prager Failure Criterion (Modified Strain Energy Criterion)

SHmax =	54.1 MPa	u (Coeff. of Friction) =	0.6
SHmin =	28.9 MPa	C (Cohesive Strength) =	9.8 MPa
Sv =	36.6 MPa	v (Poisson's Ratio) =	0.2
Po (Pore Pressure) =	14.7 MPa	Diameter of Borehole =	8.5 inches
Pm (Mud Weight) =	14.7 MPa	Depth of Max. Breakout =	0.6 inches
Sensitivity of Figure =	0.05 inches	Angle of Max. Breakout =	90 deg



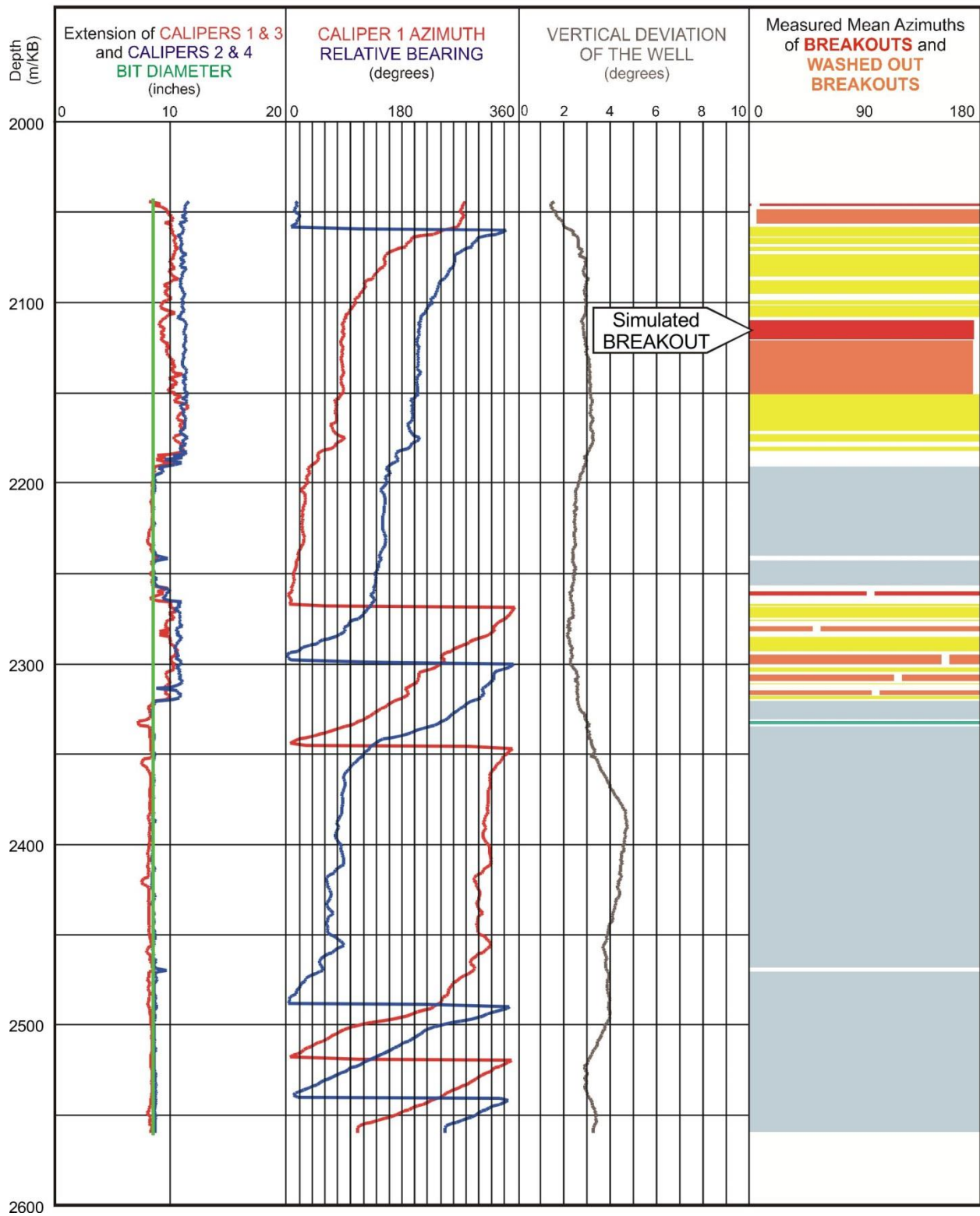
### $S_{Hmax}$ Simulation Commentary – A-081-J/094-P-04

Well: <b>A-081-J /094-P-04</b>	Failure Simulation Method				Formula
	Mohr Coulomb	Drucker Prager	Modified Strain Energy	3 Cycle Mohr Coulomb	2 SHmin - Po
Breakout Interval Top (m KB)	2110	2110	2110	2110	
Breakout Interval Base (m KB)	2121	2121	2121	2121	
Median Depth of Breakout (m KB)	2115.5	2115.5	2115.5	2115.5	
Calipers 1 and 3 extent (inches)	9.31	9.31	9.31	9.31	
Calipers 2 and 4 extent (inches)	11.33	11.33	11.33	11.33	
SHmax (MPa)	<b>70.9</b>	98.8	87.6		66.0
SHmax gradient (kPa/m)	33.5	46.7	41.4		31.2
SHmin (MPa)	43.6	43.6	43.6	43.6	
Sv (MPa)	51.6	51.6	51.6	51.6	
Pore pressure (MPa)	21.2	21.2	21.2	21.2	
Mudweight (MPa)	21.2	21.2	21.2	21.2	
u (Coefficient of Friction)	0.6	0.6	0.6	0.6	
Cohesive Strength of Rock (MPa)	12	12	12	12	
v (Poisson's Ratio)	0.2	0.2	0.2	0.2	
Diameter of Borehole (inches)	8.5	8.5	8.5	8.5	

The breakout interval between depths of 2110 and 2121 m KB was simulated satisfactorily by all three single cycle failure models, after the smaller axis of the borehole had been reset at 9.3 inches. All simulations failed when the smaller borehole axis was set at 8.5 inches.

This breakout interval has extended beyond the original well diameter of 8.5 inches so, in effect, it is a case of 2 cycle failure. As the borehole diameter widened in all directions, breakout failure developed and was only halted once the borehole had reached a minimum diameter of 9.3 inches. The lowest magnitude for  $S_{Hmax}$  was provided by simulating Mohr-Coulomb failure. At 2115.5 metres depth, the inferred  $S_{Hmax}$  magnitude is **70.9 MPa**, giving an  $S_{Hmax}$  gradient of 33.5 kPa/m. This is slightly greater than the  $S_{Hmax}$  magnitude of 66.0 MPa suggested by the equation:  $S_{Hmax} = 2(S_{Hmin}) - Po$ .

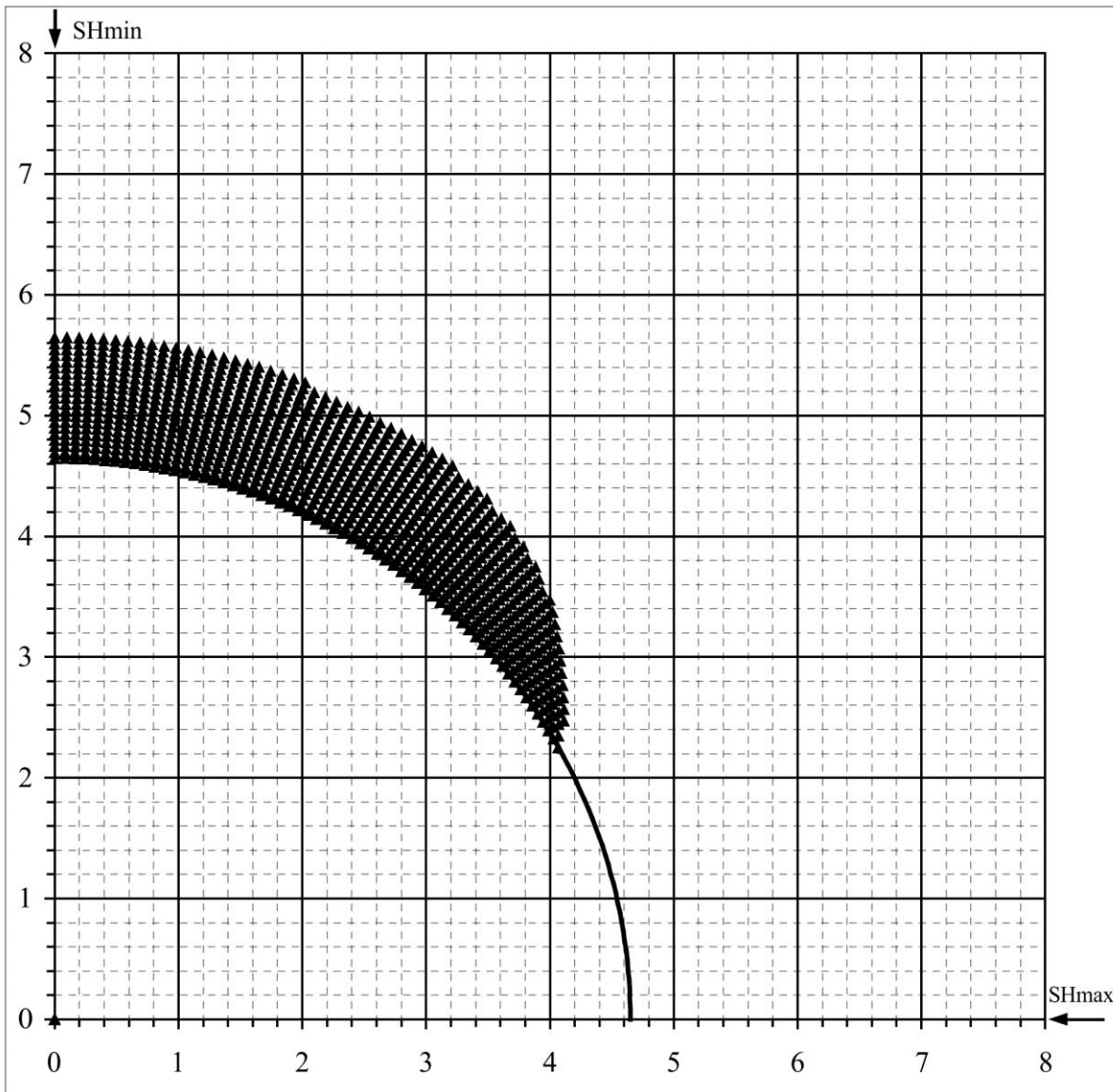
WELL : A-081-J/094-P-04 BREAKOUT ANALYSIS



A-081-J/094-P-04

### Mohr - Coulomb Failure Criterion

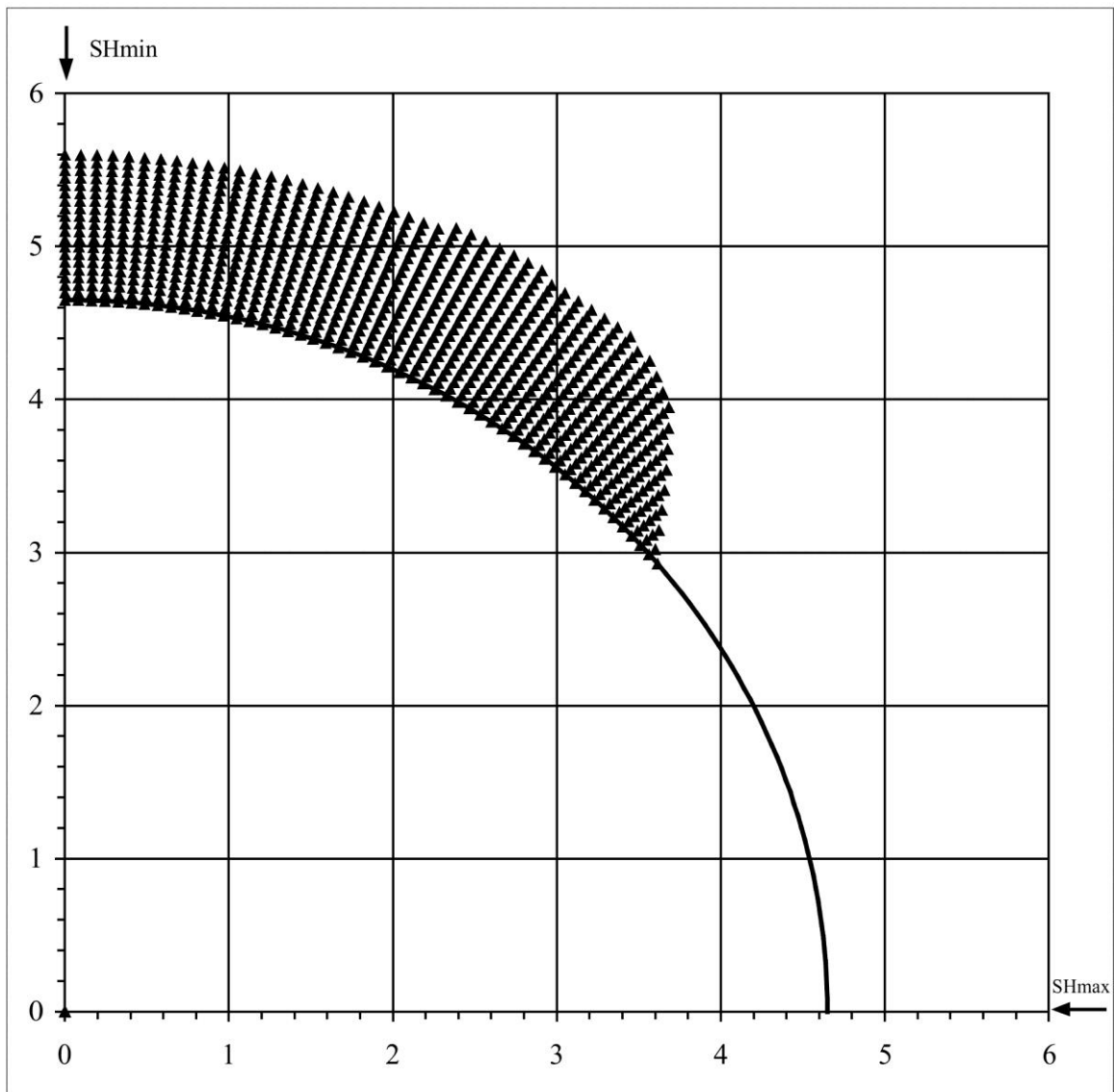
SHmax =	70.9 MPa	u (Coeff. of Friction) =	0.6
SHmin =	43.6 MPa	C (Cohesive Strength) =	12 MPa
Sv =	51.6 MPa	v (Poisson's Ratio) =	0.2
Po (Pore Pressure) =	21.2 MPa	Diameter of Borehole =	9.3 "
Pm (Mud Weight) =	21.2 MPa		
Sensitivity of Figure =	0.05 "	Angle of Max. Breakout =	76 deg
Depth of Max. Breakout =	1 "	Max caliper at 90 deg =	11.3 "
Validity of the results =	TRUE	Max caliper at 0 deg =	8 "



A-081-J/094-P-04

## Extended von-Mises Failure Criterion (Drucker-Prager Failure Criterion)

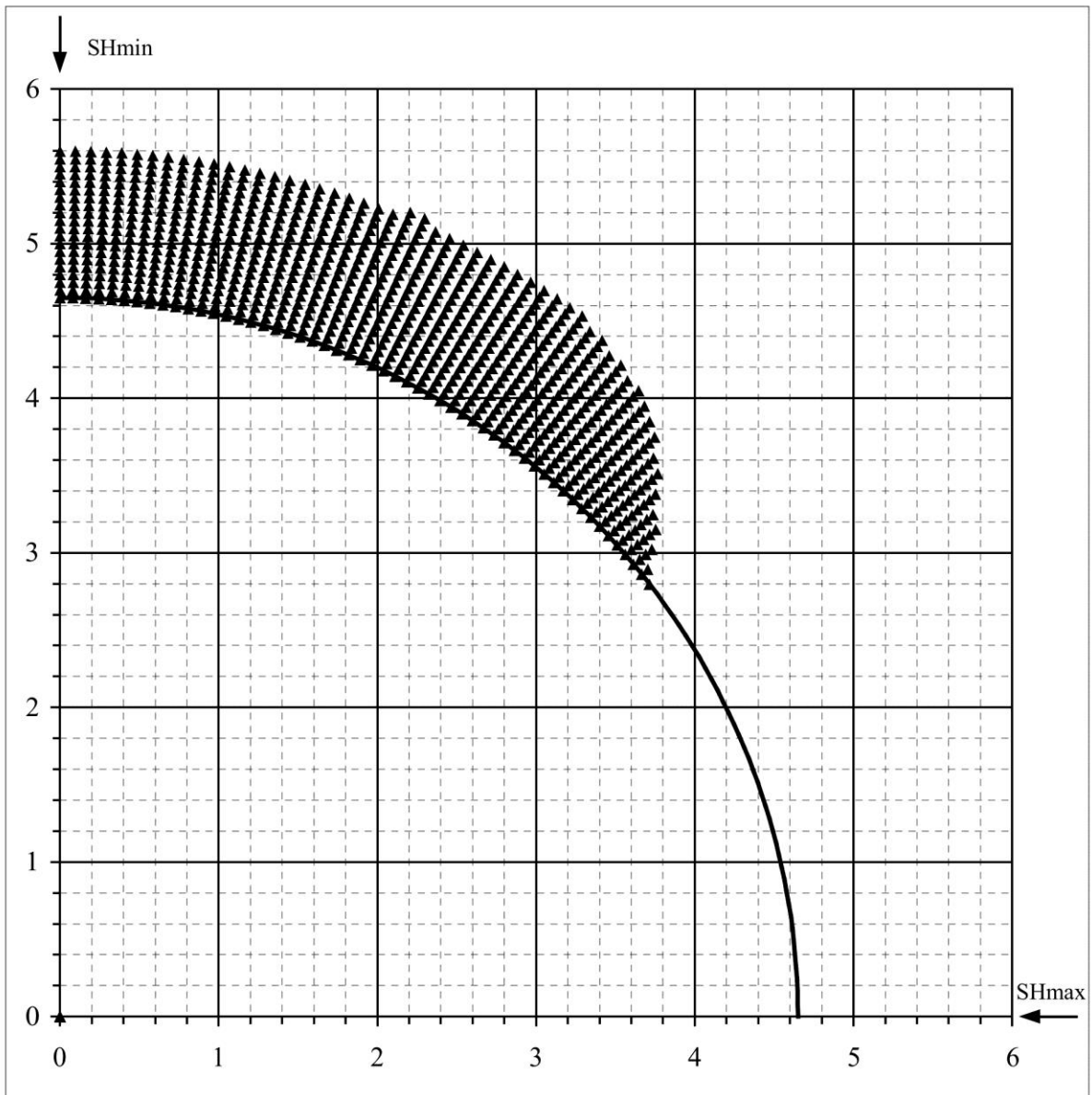
SHmax =	98.8 MPa	u (Coeff. of Friction)=	0.6
SHmin =	43.6 MPa	C (Cohesive Strength) =	12 MPa
Sv =	51.6 MPa	$\nu$ (Poisson's Ratio) =	0.2
Po (Pore Pressure) =	21.2 MPa	Diameter of Borehole =	9.3 inches
Pm (Mud Weight) =	21.2 MPa	Depth of Max. Breakout =	1 inches
Sensitivity of Figure =	0.05 inches	Angle of Max. Breakout =	62 deg



A-081-C/094-P-04

## Extended Drucker - Prager Failure Criterion (Modified Strain Energy Criterion)

SHmax =	87.6 MPa	u (Coeff. of Friction) =	0.6
SHmin =	43.6 MPa	C (Cohesive Strength) =	12 MPa
Sv =	51.6 MPa	v (Poisson's Ratio) =	0.2
Po (Pore Pressure) =	21.2 MPa	Diameter of Borehole =	9.3 inches
Pm (Mud Weight) =	21.2 MPa	Depth of Max. Breakout =	1 inches
Sensitivity of Figure =	0.05 inches	Angle of Max. Breakout =	67 deg



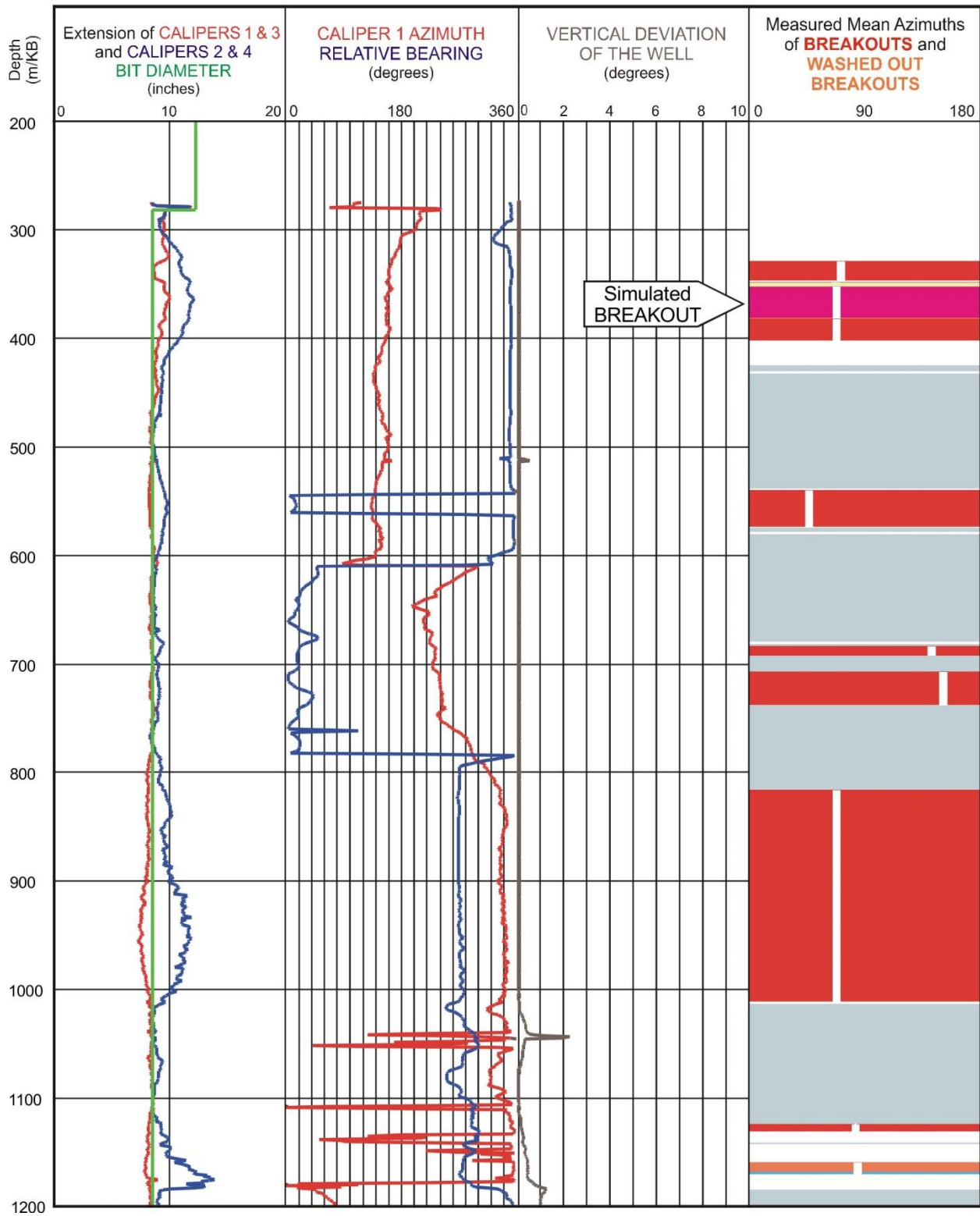
## $S_{Hmax}$ Simulation Commentary – B-021-K/094-O-14

Well: <b>B-021-K/094-O-14</b>	Failure Simulation Method				Formula
	Mohr Coulomb	Drucker Prager	Modified Strain Energy	3 Cycle Mohr Coulomb	2 SHmin - Po
Breakout Interval Top (m KB)	352	352	352	352	
Breakout Interval Base (m KB)	382	382	382	382	
Median Depth of Breakout (m KB)	367	367	367	367	
Calipers 1 and 3 extent (inches)	9.72	9.72	9.72	9.72	
Calipers 2 and 4 extent (inches)	11.78	11.78	11.78	11.78	
SHmax (MPa)	<b>12.5</b>	17.1	15.3		13.7
SHmax gradient (kPa/m)	34.1	46.6	41.7		37.3
SHmin (MPa)	8.7	8.7	8.7	8.7	
Sv (MPa)	9.0	9.0	9.0	9.0	
Pore pressure (MPa)	3.7	3.7	3.7	3.7	
Mudweight (MPa)	3.7	3.7	3.7	3.7	
u (Coefficient of Friction)	0.6	0.6	0.6	0.6	
Cohesive Strength of Rock (MPa)	2.0	2.0	2.0	2.0	
v (Poisson's Ratio)	0.2	0.2	0.2	0.2	
Diameter of Borehole (inches)	8.5	8.5	8.5	8.5	

The selected breakout interval occurs between the shallow depths of 352 and 382 m. Its mean maximum and minimum axes are 9.7 and 11.8 inches, respectively. All simulations failed when the smaller borehole axis was set at 8.5 inches, but the breakout was simulated satisfactorily by all three single cycle failure models, after the smaller axis of the borehole was reset at 9.7 inches.

This breakout interval has extended beyond the original well diameter of 8.5 inches so, in effect, it is a case of 2 cycle failure. It is believed that, as the borehole diameter widened in all directions, breakout failure developed and was only halted when the borehole had reached a minimum diameter of 9.7 inches. The lowest magnitude for  $S_{Hmax}$  was provided by simulating Mohr-Coulomb failure. At 367 metres depth, with the cohesive strength set at 2.0 MPa, the inferred  $S_{Hmax}$  magnitude was **12.5 MPa**, giving an  $S_{Hmax}$  gradient of 34.1 kPa/m. This is slightly less than the  $S_{Hmax}$  magnitude of 13.7 MPa suggested by the equation:  $S_{Hmax} = 2(S_{Hmin}) - Po$ .

WELL : B-021-K/094-O14 BREAKOUT ANALYSIS

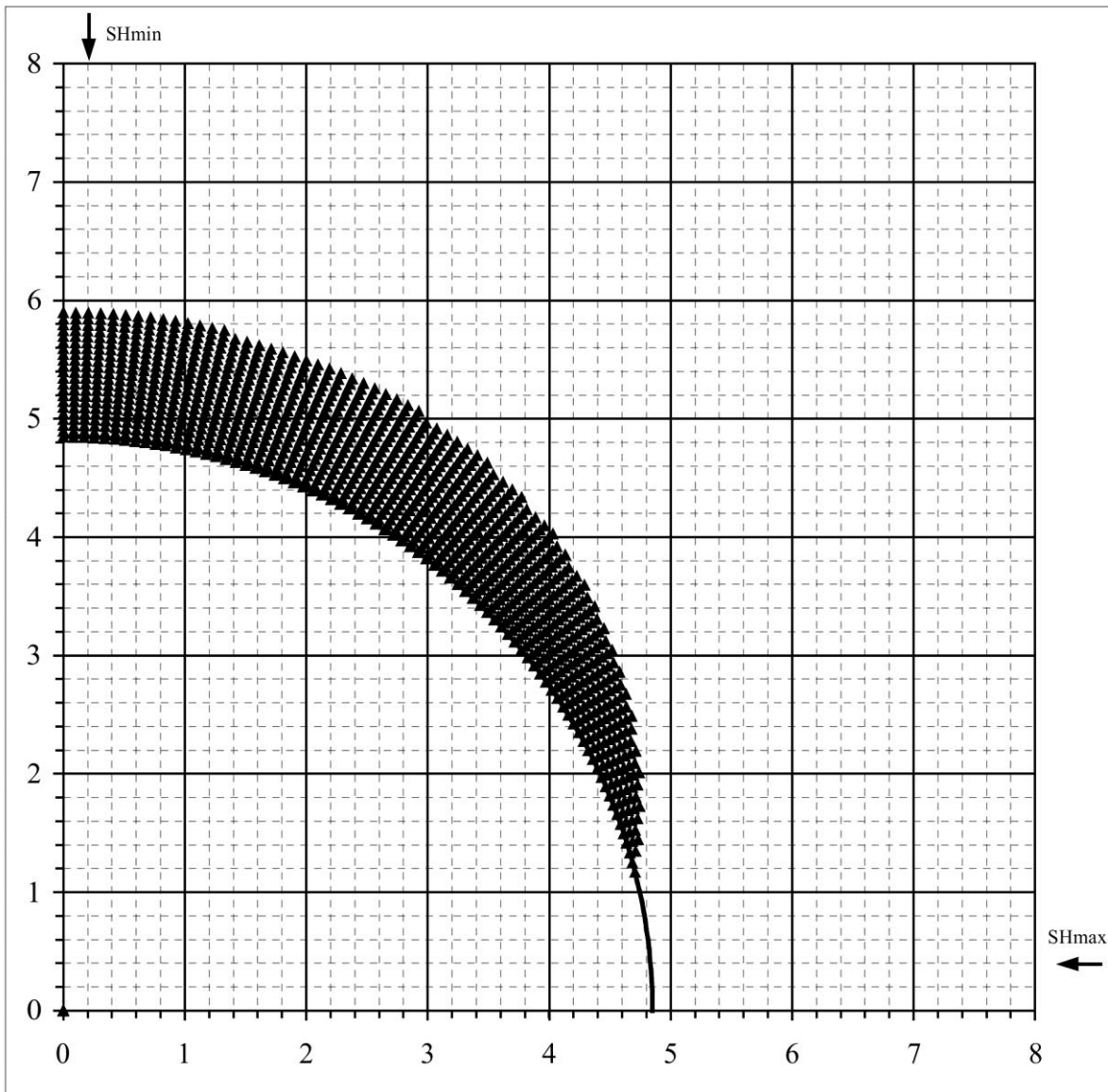




B-021-K/094-O-14

### Mohr - Coulomb Failure Criterion

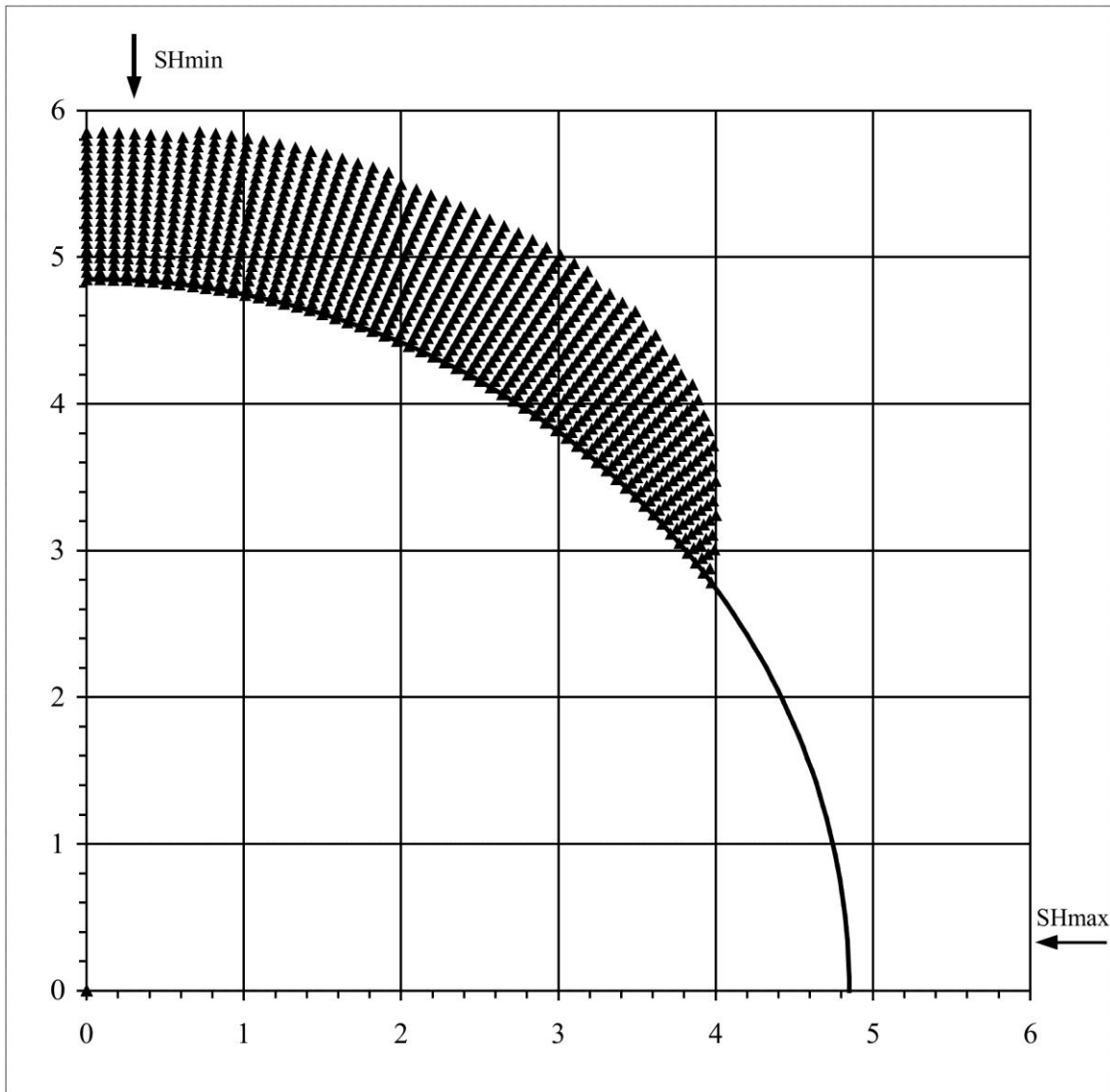
SHmax =	12.5 MPa	u (Coeff. of Friction) =	0.6
SHmin =	8.7 MPa	C (Cohesive Strength) =	2 MPa
Sv =	9 MPa	v (Poisson's Ratio) =	0.2
Po (Pore Pressure) =	3.7 MPa	Diameter of Borehole =	9.7 "
Pm (Mud Weight) =	3.7 MPa		
Sensitivity of Figure =	0.05 "	Angle of Max. Breakout =	90 deg
Depth of Max. Breakout =	1.05 "	Max caliper at 90 deg =	11.8 "
Validity of the results =	TRUE	Max caliper at 0 deg =	8.5 "



B-021-K/094-O-14

## Extended von-Mises Failure Criterion (Drucker-Prager Failure Criterion)

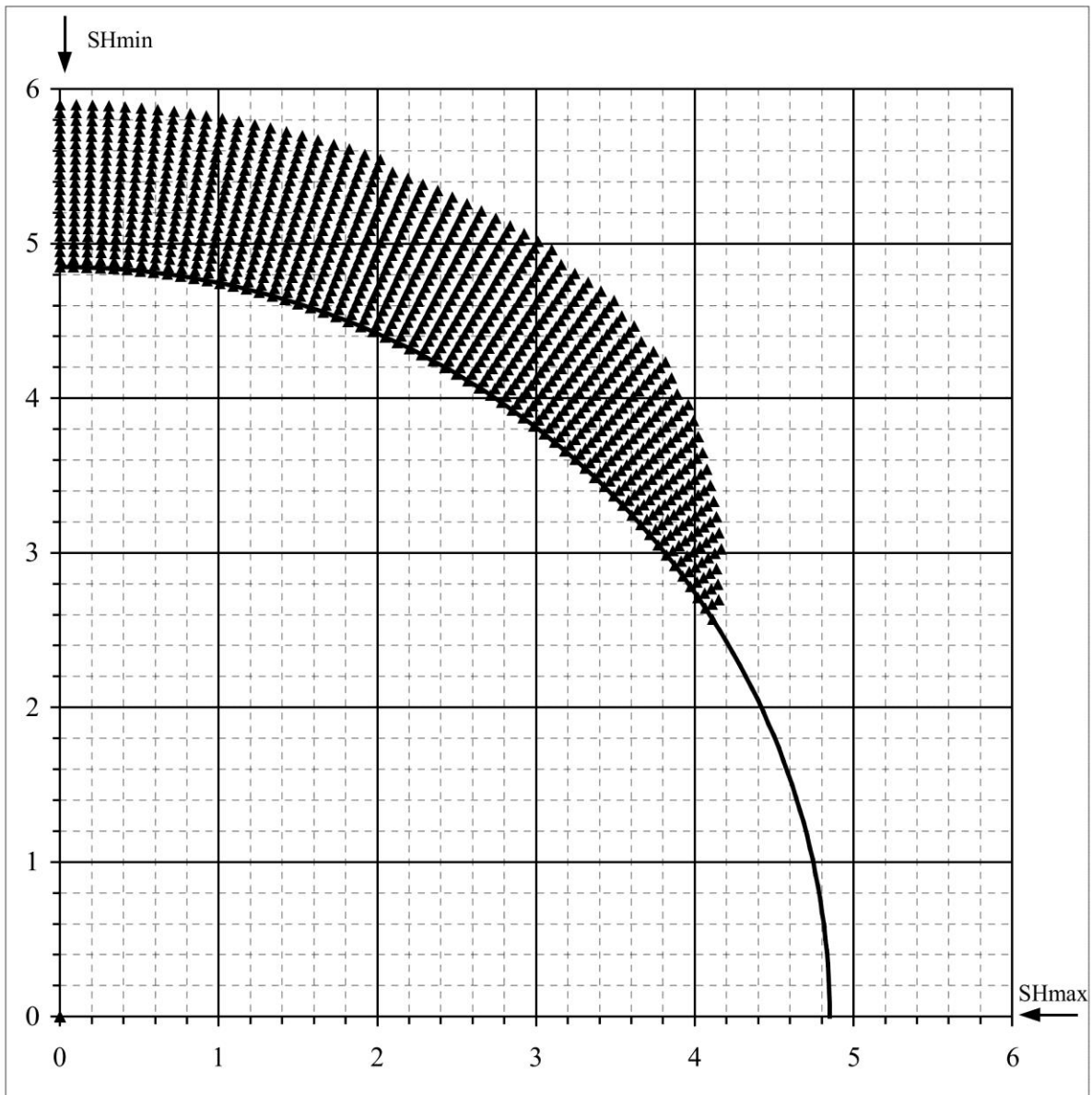
SHmax =	17.1 MPa	u (Coeff. of Friction) =	0.6
SHmin =	8.7 MPa	C (Cohesive Strength) =	2 MPa
Sv =	9 MPa	v (Poisson's Ratio) =	0.2
Po (Pore Pressure) =	3.7 MPa	Diameter of Borehole =	9.7 inches
Pm (Mud Weight) =	3.7 MPa	Depth of Max. Breakout =	1.05 inches
Sensitivity of Figure =	0.05 inches	Angle of Max. Breakout =	76 deg



B-021-K/094-O-14

## Extended Drucker - Prager Failure Criterion (Modified Strain Energy Criterion)

SHmax =	15.3 MPa	u (Coeff. of Friction) =	0.6
SHmin =	8.7 MPa	C (Cohesive Strength) =	2 MPa
Sv =	9 MPa	v (Poisson's Ratio) =	0.2
Po (Pore Pressure) =	3.7 MPa	Diameter of Borehole =	9.7 inches
Pm (Mud Weight) =	3.7 MPa	Depth of Max. Breakout =	1.05 inches
Sensitivity of Figure =	0.05 inches	Angle of Max. Breakout =	90 deg



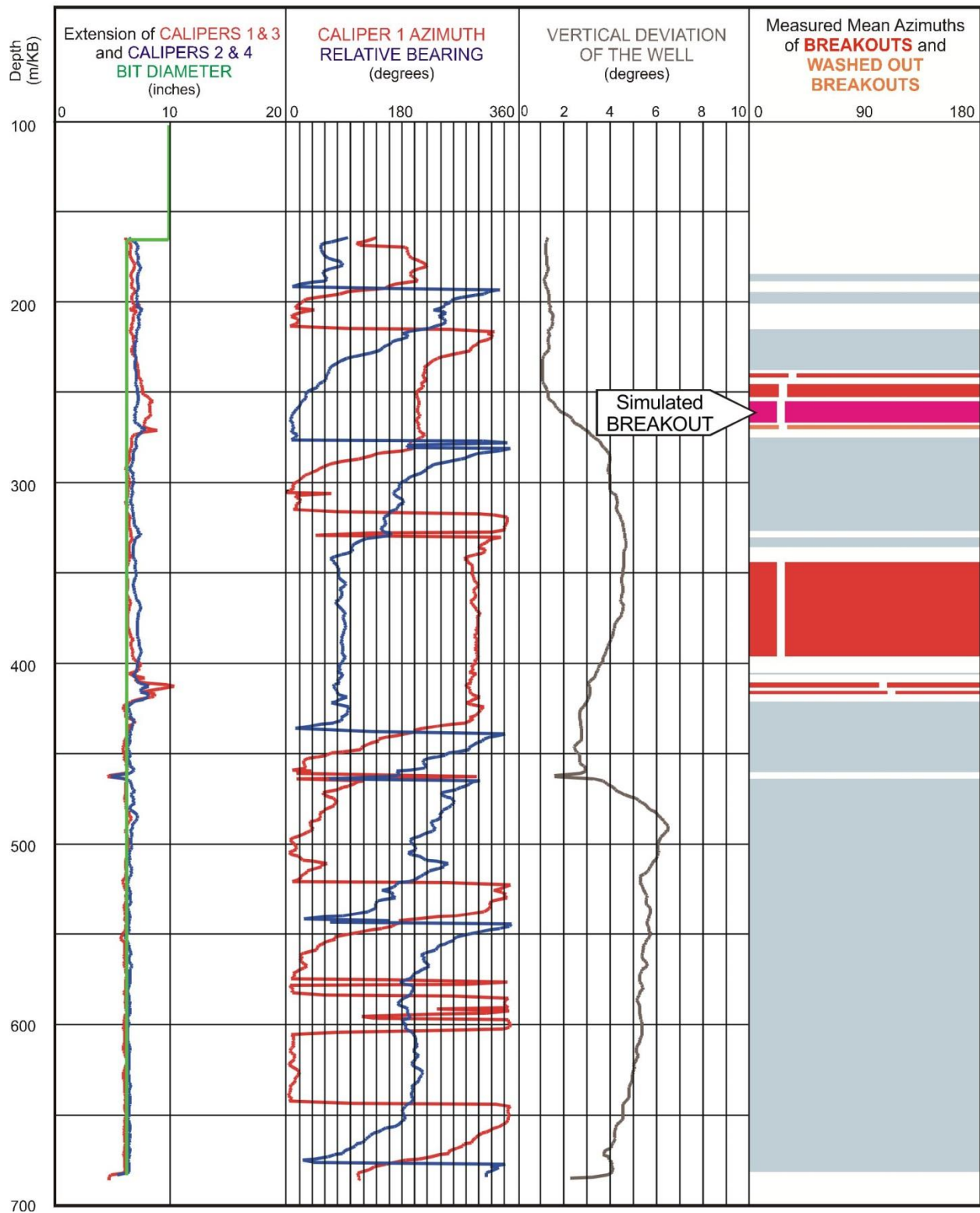
## $S_{Hmax}$ Simulation Commentary – B-044-L/094-O-10

Well: <b>B-044-L/094-O-10</b>	Failure Simulation Method				Formula
	Mohr Coulomb	Drucker Prager	Modified Strain Energy	3 Cycle Mohr Coulomb	$2 S_{Hmin} - P_o$
Breakout Interval Top (m KB)	254	254	254	254	
Breakout Interval Base (m KB)	266	266	266	266	
Median Depth of Breakout (m KB)	260	260	260	260	
Calipers 1 and 3 extent (inches)	8.15	8.15	8.15	8.15	
Calipers 2 and 4 extent (inches)	7.06	7.06	7.06	7.06	
SHmax (MPa)	<b>8.6</b>	12.2	10.8		7.2
SHmax gradient (kPa/m)	33.1	46.9	41.5		27.7
SHmin (MPa)	4.9	4.9	4.9	4.9	
Sv (MPa)	6.4	6.4	6.4	6.4	
Pore pressure (MPa)	2.6	2.6	2.6	2.6	
Mudweight (MPa)	2.6	2.6	2.6	2.6	
u (Coefficient of Friction)	0.6	0.6	0.6	0.6	
Cohesive Strength of Rock (MPa)	2	2	2	2	
v (Poisson's Ratio)	0.2	0.2	0.2	0.2	
Diameter of Borehole (inches)	6.25	6.25	6.25	6.25	

The selected breakout interval occurs between the shallow depths of 254 and 266 m. Its mean maximum and minimum axes are 8.15 and 7.06 inches, respectively. In this well, the  $S_v$  magnitude at 260 metres KB is well established from the density log. All simulations failed when the smaller borehole axis was set at 6.25 inches (drill bit diameter), but the breakout was simulated satisfactorily by all three single cycle failure models, after the smaller axis of the borehole was reset at 7.06 inches.

The lowest magnitude for  $S_{Hmax}$  was provided by simulating Mohr-Coulomb failure. At 260 metres depth, with the cohesive strength set at 2.0 MPa, the inferred  $S_{Hmax}$  magnitude was **8.6 MPa**, giving an  $S_{Hmax}$  gradient of 33.1 kPa/m. This is higher than the  $S_{Hmax}$  magnitude of 7.2 MPa suggested by the equation:  $S_{Hmax} = 2(S_{Hmin}) - P_o$ .

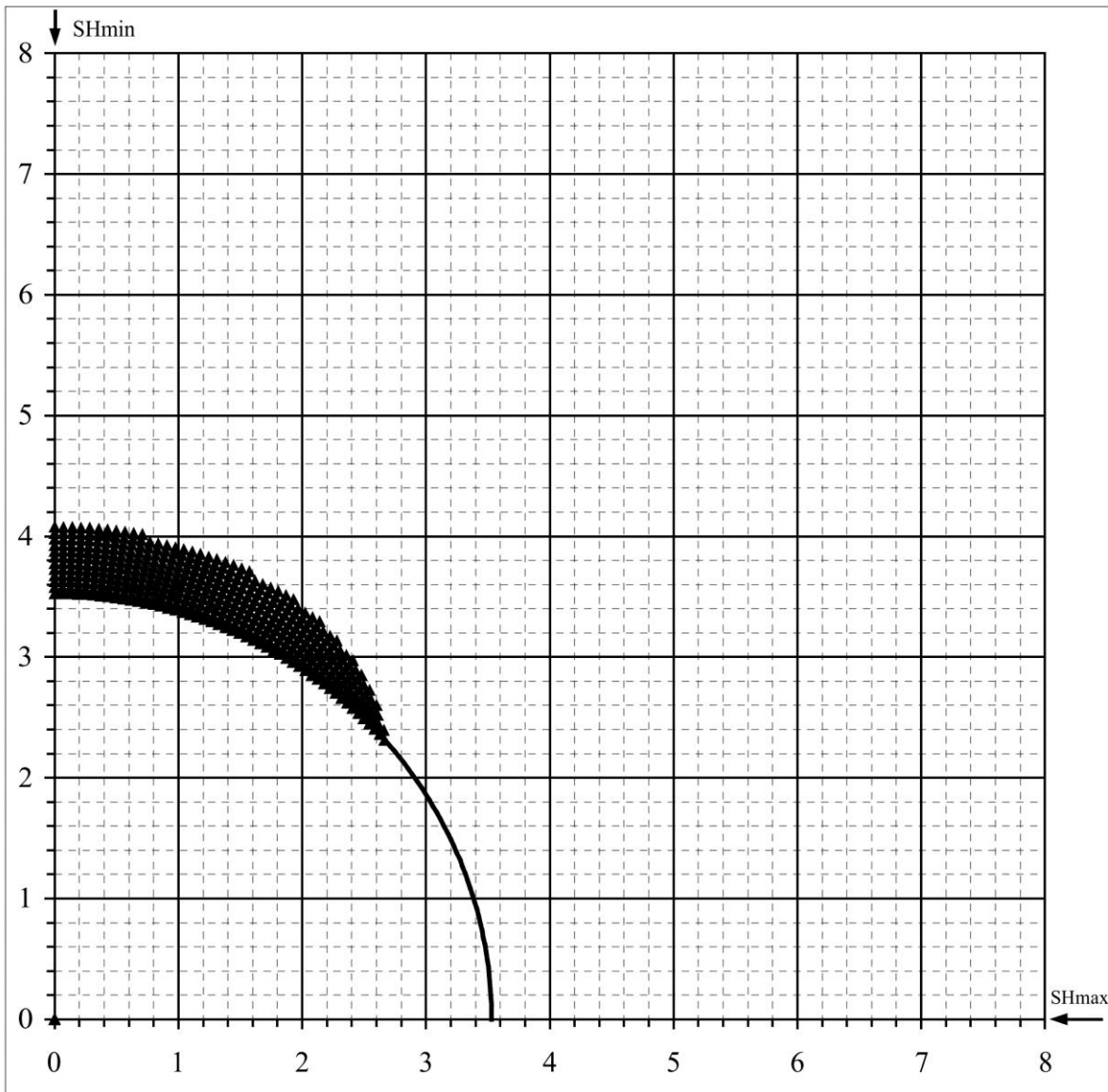
WELL : B-044-L/094-O-10 BREAKOUT ANALYSIS



B-044L/094-O-10

### Mohr - Coulomb Failure Criterion

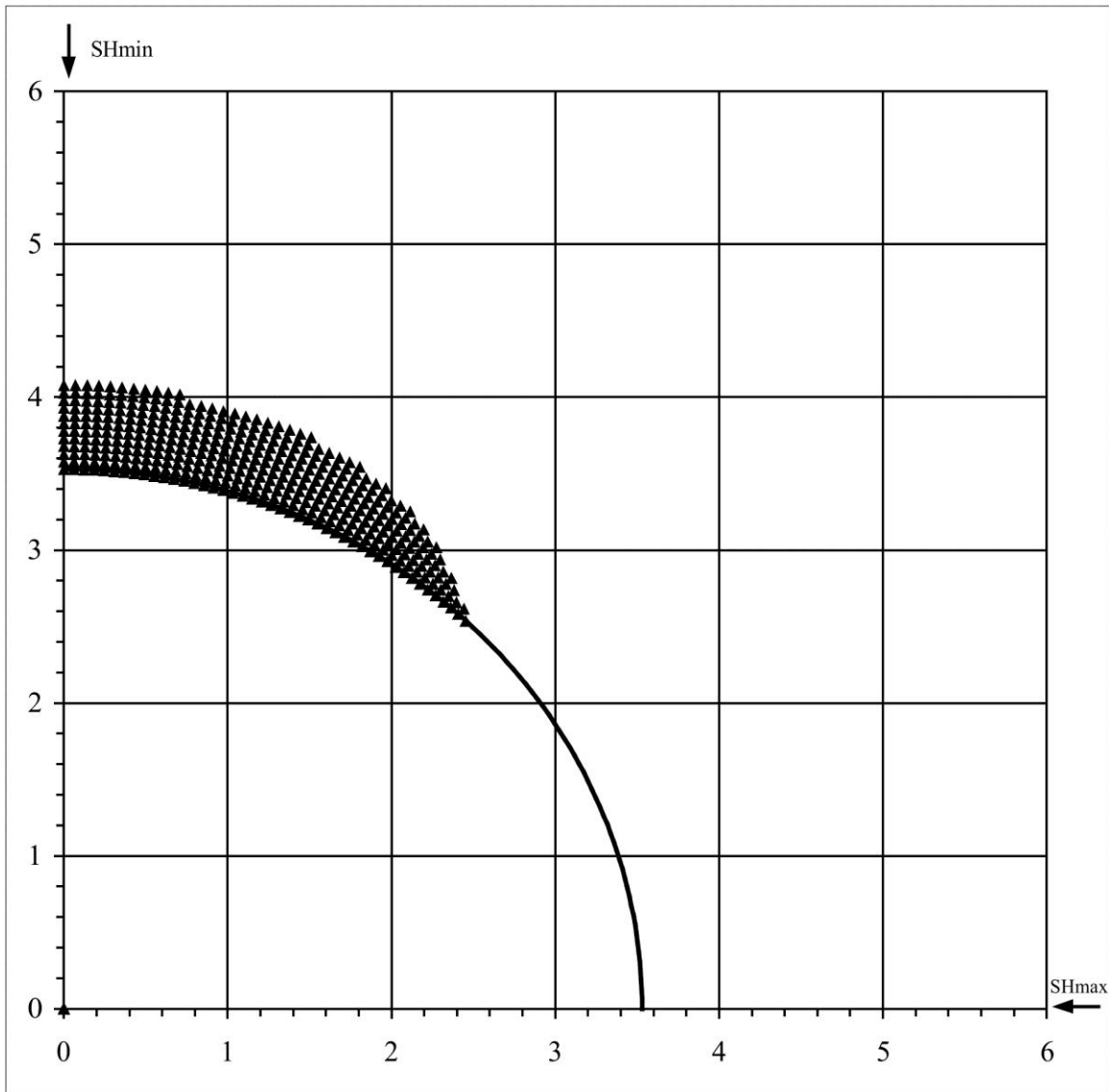
SHmax =	8.6 MPa	u (Coeff. of Friction) =	0.6
SHmin =	4.9 MPa	C (Cohesive Strength) =	2 MPa
Sv =	6.4 MPa	v (Poisson's Ratio) =	0.2
Po (Pore Pressure) =	2.6 MPa	Diameter of Borehole =	7.06 "
Pm (Mud Weight) =	2.6 MPa		
Sensitivity of Figure =	0.05 "	Angle of Max. Breakout =	90 deg
Depth of Max. Breakout =	0.55 "	Max caliper at 90 deg =	8.16 "
Validity of the results =	TRUE	Max caliper at 0 deg =	8 "



B-044-L/094-O-10

## Extended von-Mises Failure Criterion (Drucker-Prager Failure Criterion)

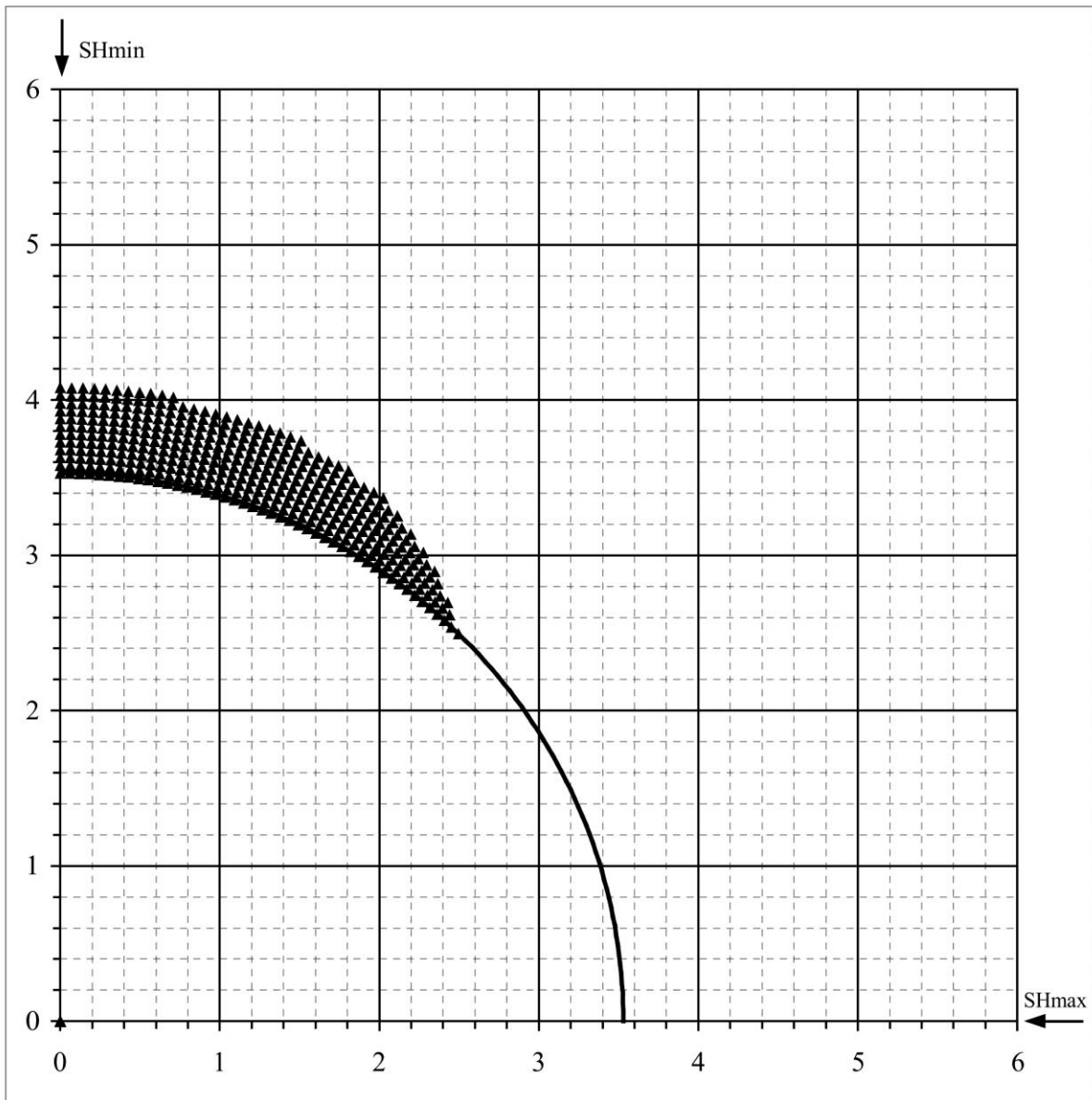
SHmax =	12.2 MPa	u (Coeff. of Friction) =	0.6
SHmin =	4.9 MPa	C (Cohesive Strength) =	2 MPa
Sv =	6.4 MPa	v (Poisson's Ratio) =	0.2
Po (Pore Pressure) =	2.6 MPa	Diameter of Borehole =	7.06 inches
Pm (Mud Weight) =	2.6 MPa	Depth of Max. Breakout =	0.55 inches
Sensitivity of Figure =	0.05 inches	Angle of Max. Breakout =	90 deg



B-044-L/094-O-16

## Extended Drucker - Prager Failure Criterion (Modified Strain Energy Criterion)

SHmax =	10.8 MPa	u (Coeff. of Friction) =	0.6
SHmin =	4.9 MPa	C (Cohesive Strength) =	2 MPa
Sv =	6.4 MPa	v (Poisson's Ratio) =	0.2
Po (Pore Pressure) =	2.6 MPa	Diameter of Borehole =	7.06 inches
Pm (Mud Weight) =	2.6 MPa	Depth of Max. Breakout =	0.55 inches
Sensitivity of Figure =	0.05 inches	Angle of Max. Breakout =	90 deg





## $S_{Hmax}$ Simulation Commentary – B-055-60-30-123-45

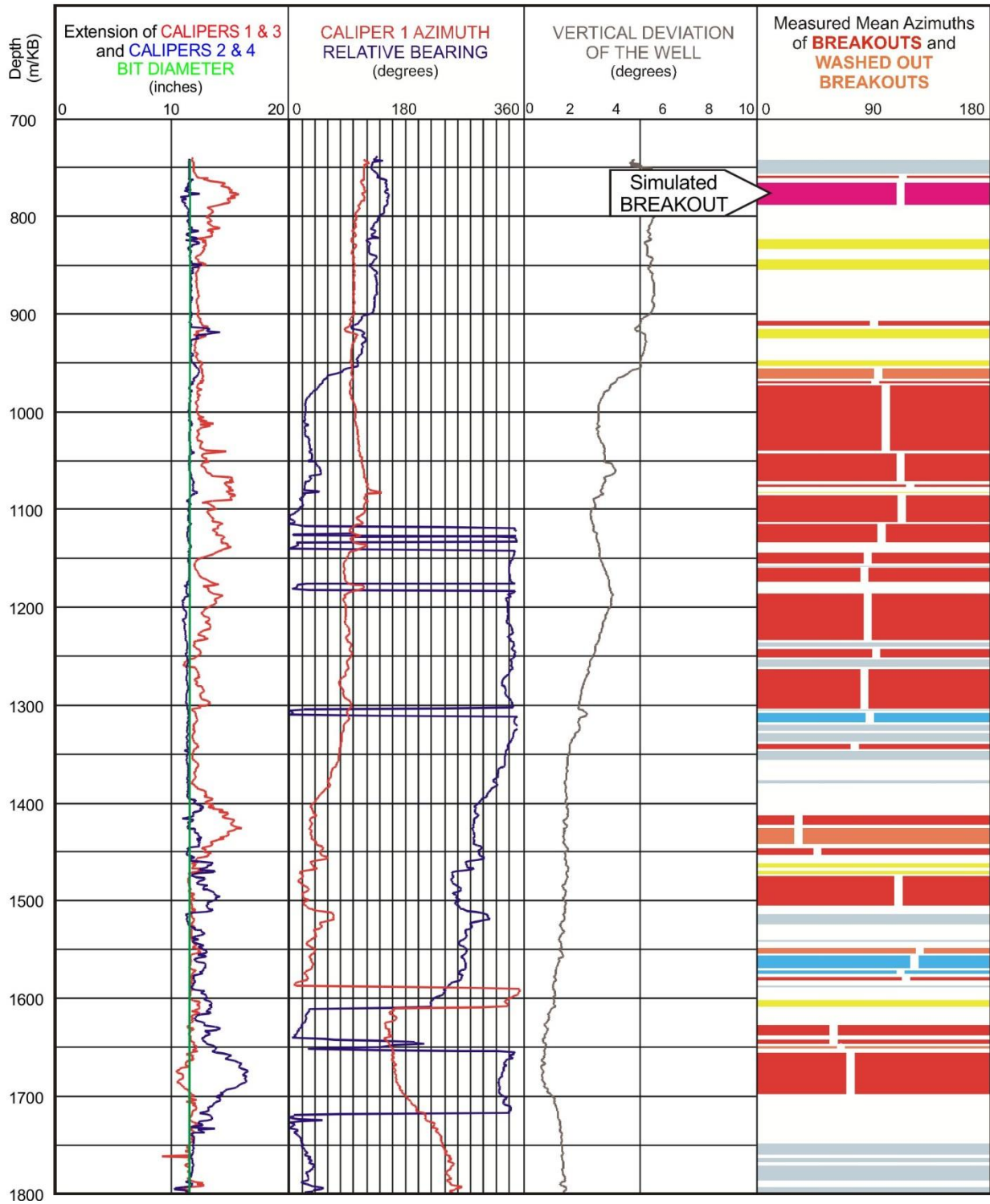
Well: B-055-60-30-123-45	Failure simulation Method				2SHmin-Po
	Mohr Coulomb	Drucker Prager	Modified Strain Energy	3 cycle Mohr Coulomb	
Breakout Interval Top (m KB)	767	767	767	767	
Breakout Interval Base (m KB)	789	789	789	789	
Median depth of Breakout (m KB)	778	778	778	778	
Calipers 1 and 3 extent (inches)	14.98	14.98	14.98	14.98	
Calipers 2 and 4 extent (inches)	11.38	11.38	11.38	11.38	
SHmax (MPa)	26.3*	31.9*	29.6*	<b>21.0</b>	19.2
SHmax gradient (kPa/m)	33.8	41.0	38.0	27.0	24.7
SHmin (MPa)	13.5	13.5	13.5	13.5	
Sv (MPa)	19.7	19.7	19.7	19.7	
Pore Pressure (MPa)	7.8	7.8	7.8	7.8	
Mudweight (MPa)	7.8	7.8	7.8	7.8	
u (Coefficient of Friction)	0.6	0.6	0.6	0.6	
Cohesive Strength of Rock (MPa)	5.0	5.0	7.6	5.0	
v (Poisson's Ratio)	0.2	0.2	0.2	0.2	
Bit size (inches)	11.0	11.0	11.0	11.0	

\* indicates that modelling could not simulate accurate breakout anisotropy

The selected breakout interval, 767-789 m, could not be simulated with any of the three single cycle methods, even when the cohesive strength was lowered to 1.0 MPa, which is a completely unreasonably low strength. Clearly this is a multi-cyclical breakout. The 3 cycle Mohr-Coulomb simulation modelled the breakout well with a cohesive strength of 5.0 MPa.

The resulting  $S_{Hmax}$  magnitude of **21.0 MPa** is slightly greater than 19.2 MPa, as suggested by the equation:  $S_{Hmax} = 2(S_{Hmin}) - Po$ .

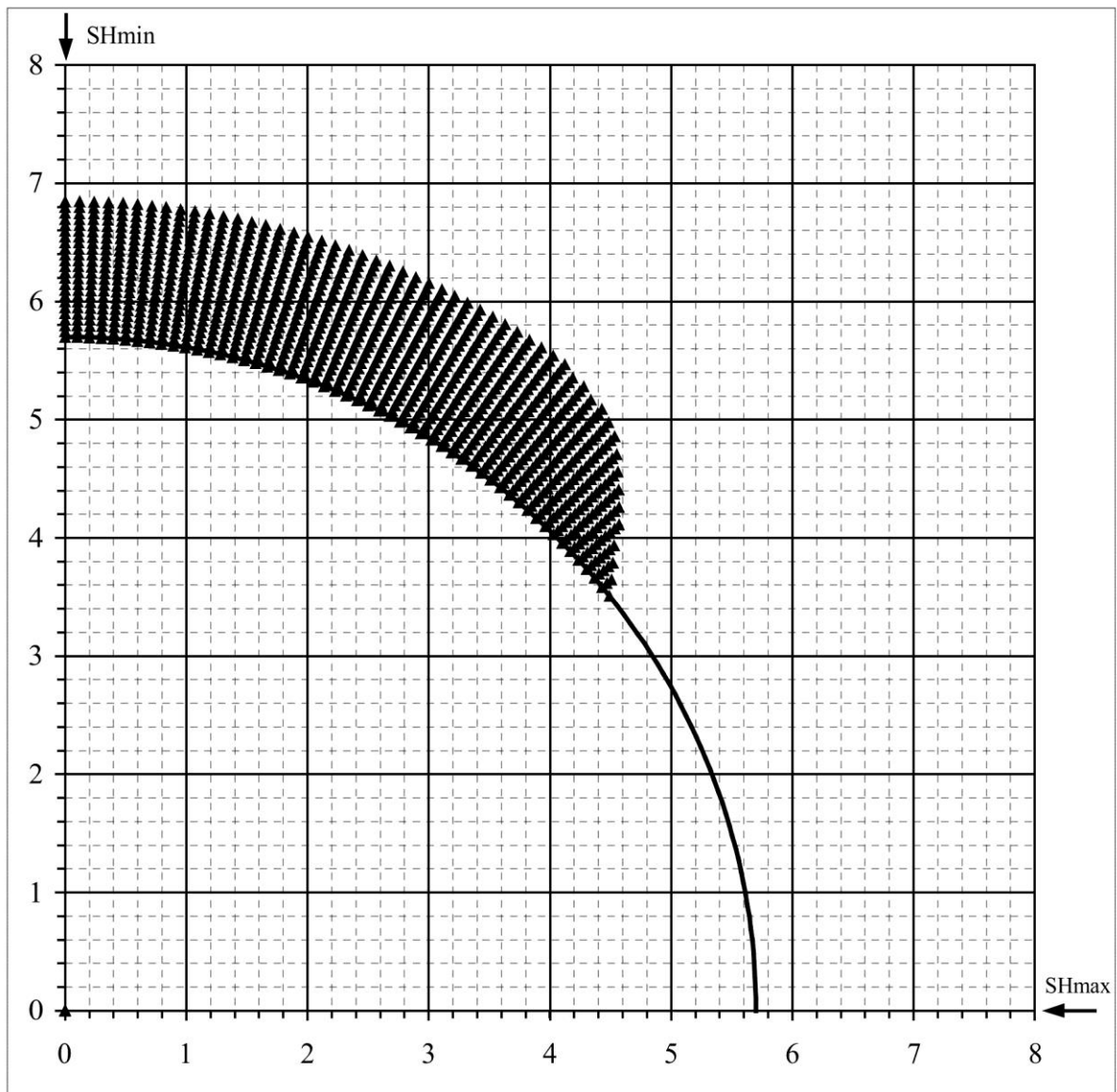
WELL : B-055-60-30-123-45 BREAKOUT ANALYSIS



B-055-60-30-123-45

## Mohr - Coulomb Failure Criterion

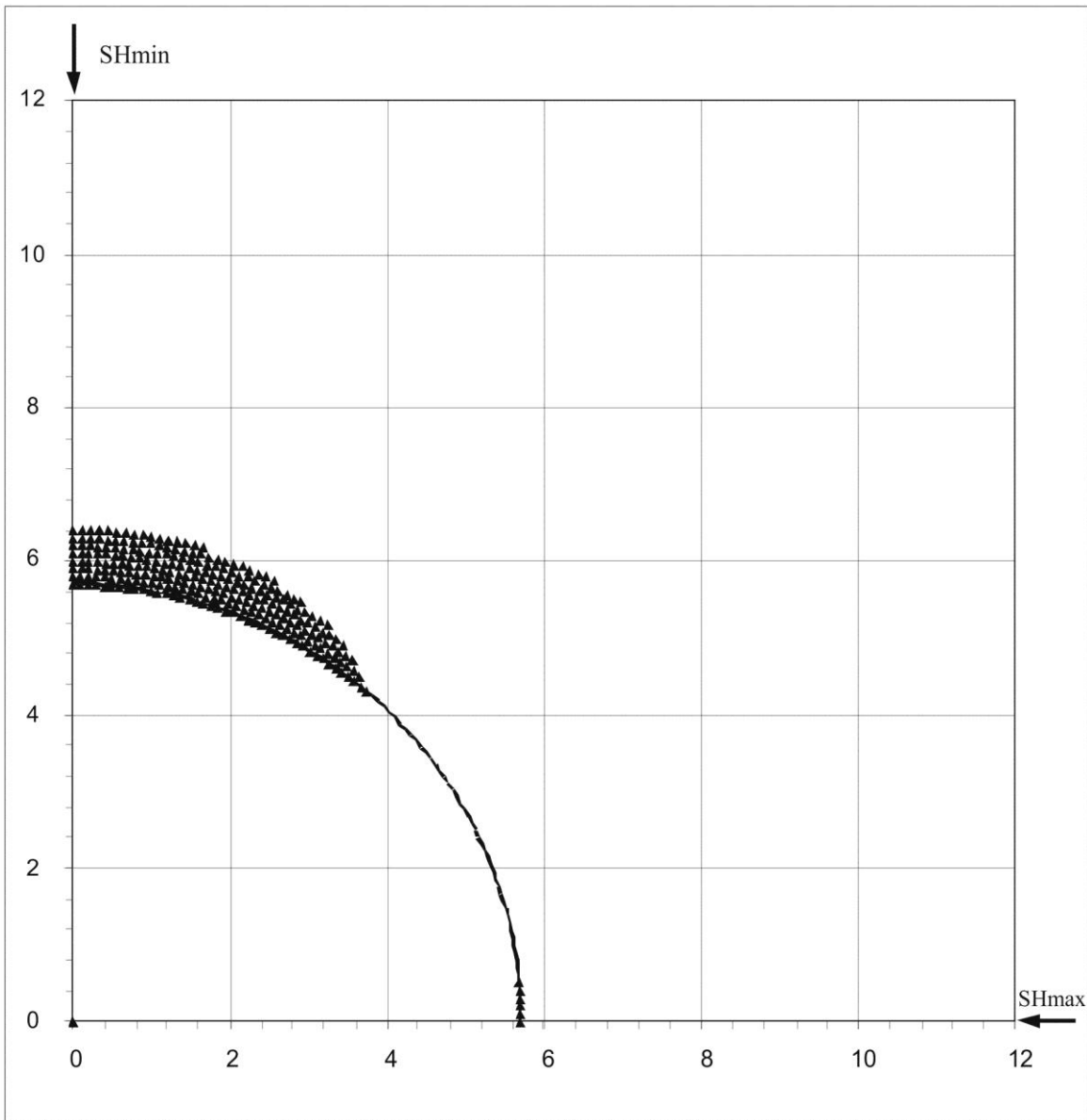
SHmax =	26.3 MPa	u (Coeff. of Friction) =	0.6
SHmin =	13.5 MPa	C (Cohesive Strength) =	5 MPa
Sv =	19.7 MPa	v (Poisson's Ratio) =	0.2
Po (Pore Pressure) =	7.8 MPa	Diameter of Borehole =	11.4 "
Pm (Mud Weight) =	7.8 MPa		
Sensitivity of Figure =	0.05 "	Angle of Max. Breakout =	66 deg
Depth of Max. Breakout =	1.15 "	Max caliper at 90 deg =	13.7 "
Validity of the results =	TRUE	Max caliper at 0 deg =	8 "



B-055-60-30-123-45

## Extended von-Mises Failure Criterion (Drucker-Prager Failure Criterion)

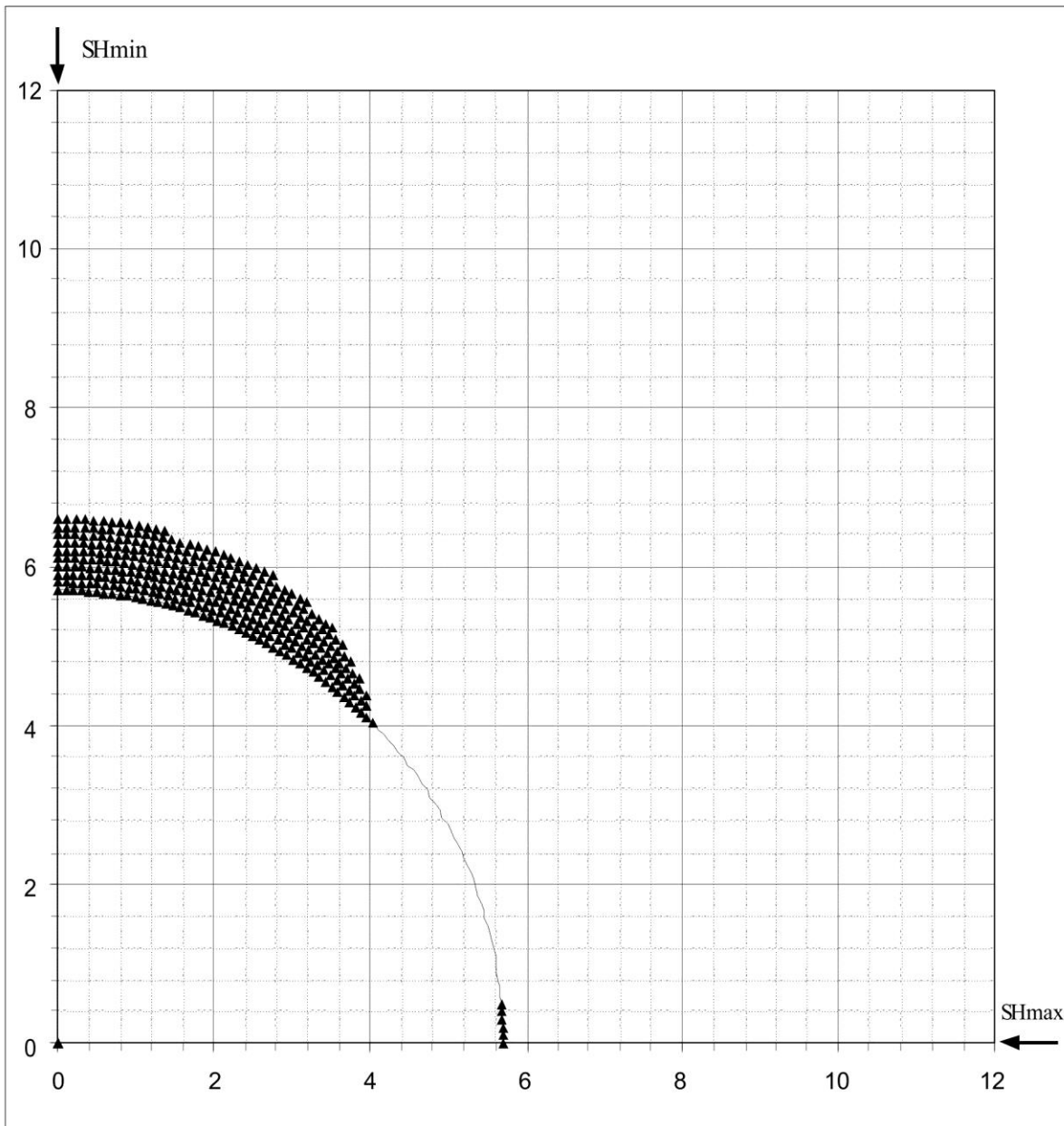
SHmax =	31.9 MPa	u (Coeff. of Friction)=	0.6
SHmin =	13.5 MPa	C (Cohesive Strength) =	5 MPa
Sv =	19.7 MPa	v (Poisson's Ratio) =	0.2
Po (Pore Pressure) =	7.8 MPa	Diameter of Borehole =	11.4 inches
Pm (Mud Weight) =	7.8 MPa	Depth of Max. Breakout =	0.75 inches
Sensitivity of Figure =	0.05 inches	Angle of Max. Breakout =	90 deg



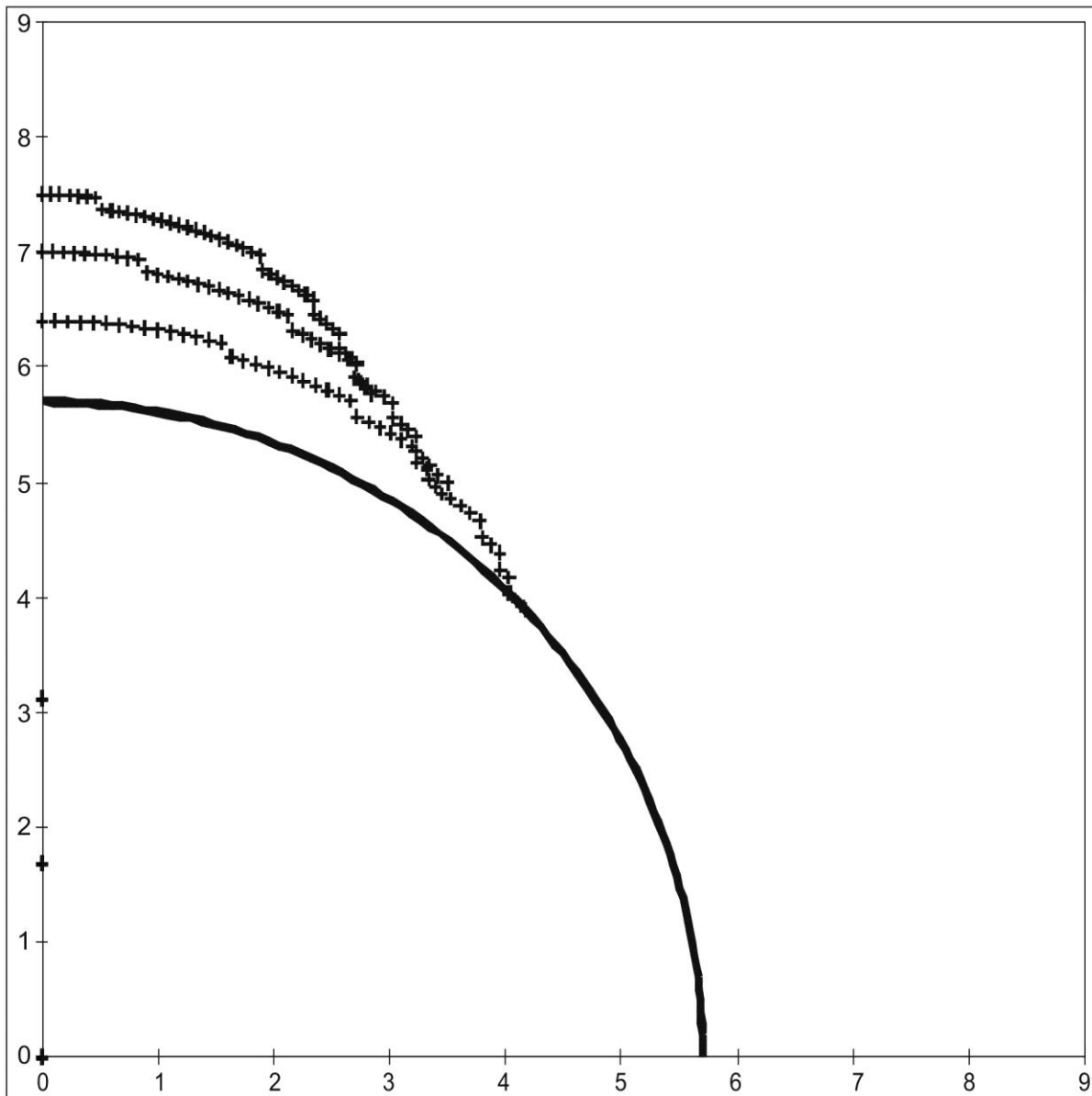
B-055-60-30-123-45

## Extended Drucker - Prager Failure Criterion (Modified Strain Energy Criterion)

SHmax =	29.6 MPa	u (Coeff. of Friction) =	0.6
SHmin =	13.5 MPa	C (Cohesive Strength) =	5 MPa
Sv =	19.7 MPa	v (Poisson's Ratio) =	0.2
Po (Pore Pressure) =	7.8 MPa	Diameter of Borehole =	11.4 inches
Pm (Mud Weight) =	7.8 MPa	Depth of Max. Breakout =	0.9 inches
Sensitivity of Figure =	0.05 inches	Angle of Max. Breakout =	88 deg



B-055-60-30-123-45					
3 Cycle Mohr - Coulomb Failure Criterion					
SHmax =	21 MPa	u (Coeff. of Friction) =	0.6		
SHmin =	13.5 MPa	C (Cohesive Strength) =	5 MPa		
Sv =	19.7 MPa	v (Poisson's Ratio)=	0.2		
Po (Pore Pressure) =	7.8 MPa	Diameter of Borehole =	11.4 "		
Pm (Mud Weight) =	7.8 MPa				
Sensitivity of Figure =	0.05 "				
Depth of Max. Breakout =	1.8 "	Max caliper at 90 deg =	15 "		
Validity of the results =	TRUE	Max caliper at 0 deg =	11.4 "		



## $S_{Hmax}$ Simulation Commentary – B-066-I/094-O-08

Well: <b>B-066-I/094-O-08</b>	Failure Simulation Method					Formula
	Mohr Coulomb # 1	Mohr Coulomb # 2	Drucker Prager	Modified Strain Energy	3 Cycle Mohr Coulomb	2 SHmin - Po
Breakout Interval Top (m KB)	979	979	979	979	979	
Breakout Interval Base (m KB)	1012	1012	1012	1012	1012	
Median Depth of Breakout (m KB)	995.5	995.5	995.5	995.5	995.5	
Calipers 1 and 3 extent (inches)	12.42	12.42	12.42	12.42	12.42	
Calipers 2 and 4 extent (inches)	9.50	9.50	9.50	9.50	9.50	
SHmax (MPa)	41.0*	27.0*	48.0*	46.0*	<b>31.5</b>	28.0
SHmax gradient (kPa/m)	41.2	27.1	48.2	46.2	31.6	28.1
SHmin (MPa)	19.0	19.0	19.0	19.0	19.0	
Sv (MPa)	23.5	23.5	23.5	23.5	23.5	
Pore pressure (MPa)	10.0	10.0	10.0	10.0	10.0	
Mudweight (MPa)	10.0	10.0	10.0	10.0	10.0	
u (Coefficient of Friction)	0.6	0.6	0.6	0.6	0.6	
Cohesive Strength of Rock (MPa)	8.3	3.0	8.3	8.3	8.3	
v (Poisson's Ratio)	0.2	0.2	0.2	0.2	0.2	
Bit size (inches)	8.5	8.5	8.5	8.5	8.5	

\* indicates that modelling could not simulate complete breakout anisotropy

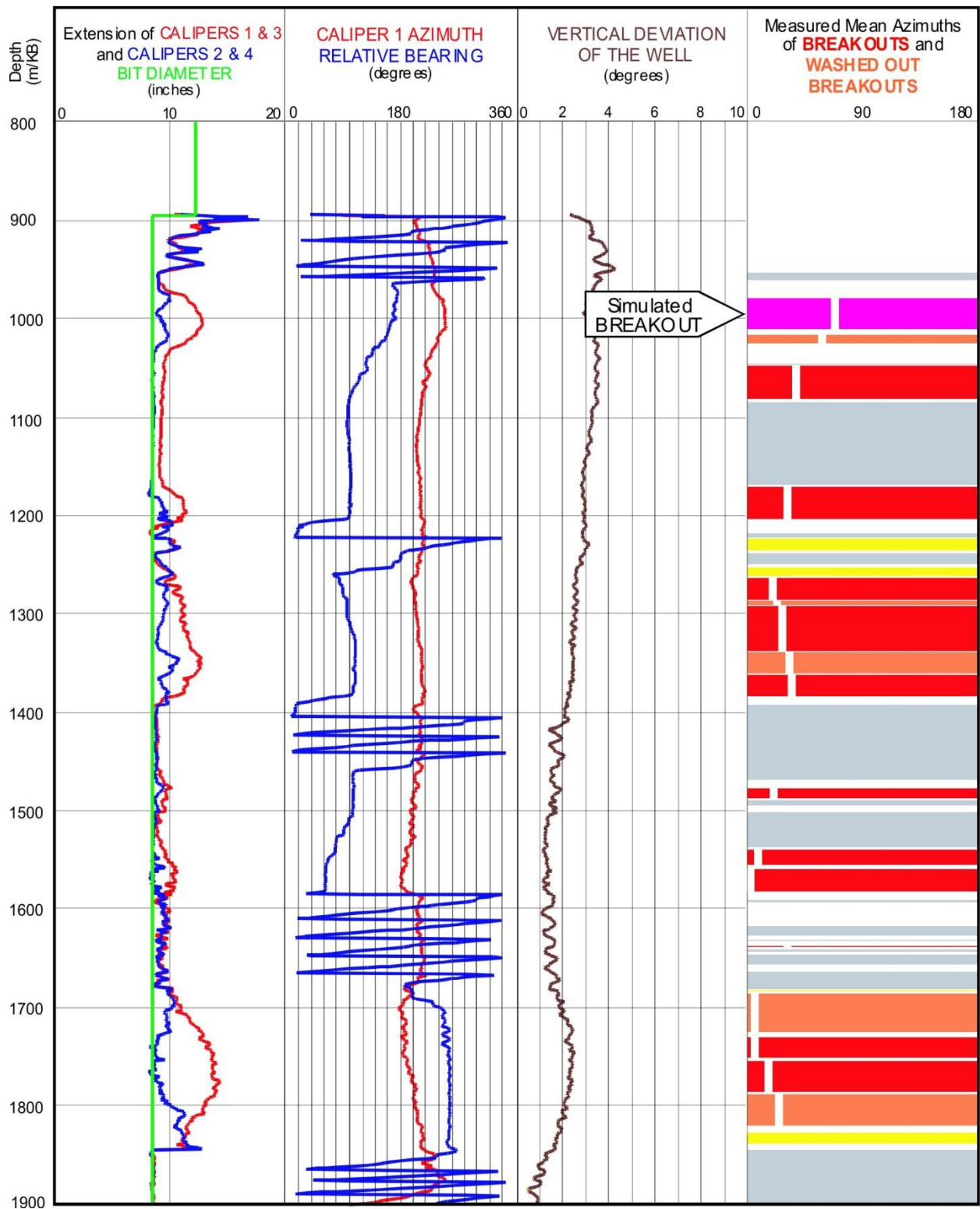
The selected breakout interval, 979-1012 m, could not be simulated with any of the three single cycle methods, even with Mohr-Coulomb when the cohesive strength was lowered from 8.3 to 3.0 MPa (Column # 2). Raising  $S_{Hmax}$  to unreasonably high magnitudes did not generate a sufficiently deep breakout. With Mohr-Coulomb, the deepest breakout that could be modeled extended only to 11.4 inches with  $S_{Hmax}$  set at 41 MPa. With the Drucker-Prager simulation 11.0 inches was reached at 48 MPa and, with the Modified Strain Energy simulation, 11.2 inches was reached at 46 MPa.

However, the 3 cycle Mohr-Coulomb simulation modelled the breakout completely with a cohesive strength of 8.3 MPa. The resulting  $S_{Hmax}$  magnitude of **31.5 MPa** is slightly greater than 28.0 MPa, as suggested by the equation:  

$$S_{Hmax} = 2(S_{Hmin}) - Po.$$

The  $S_v$  magnitude at 995.5 m in this well is established from the density log.

WELL : B-066-I/094-O-08 BREAKOUT ANALYSIS

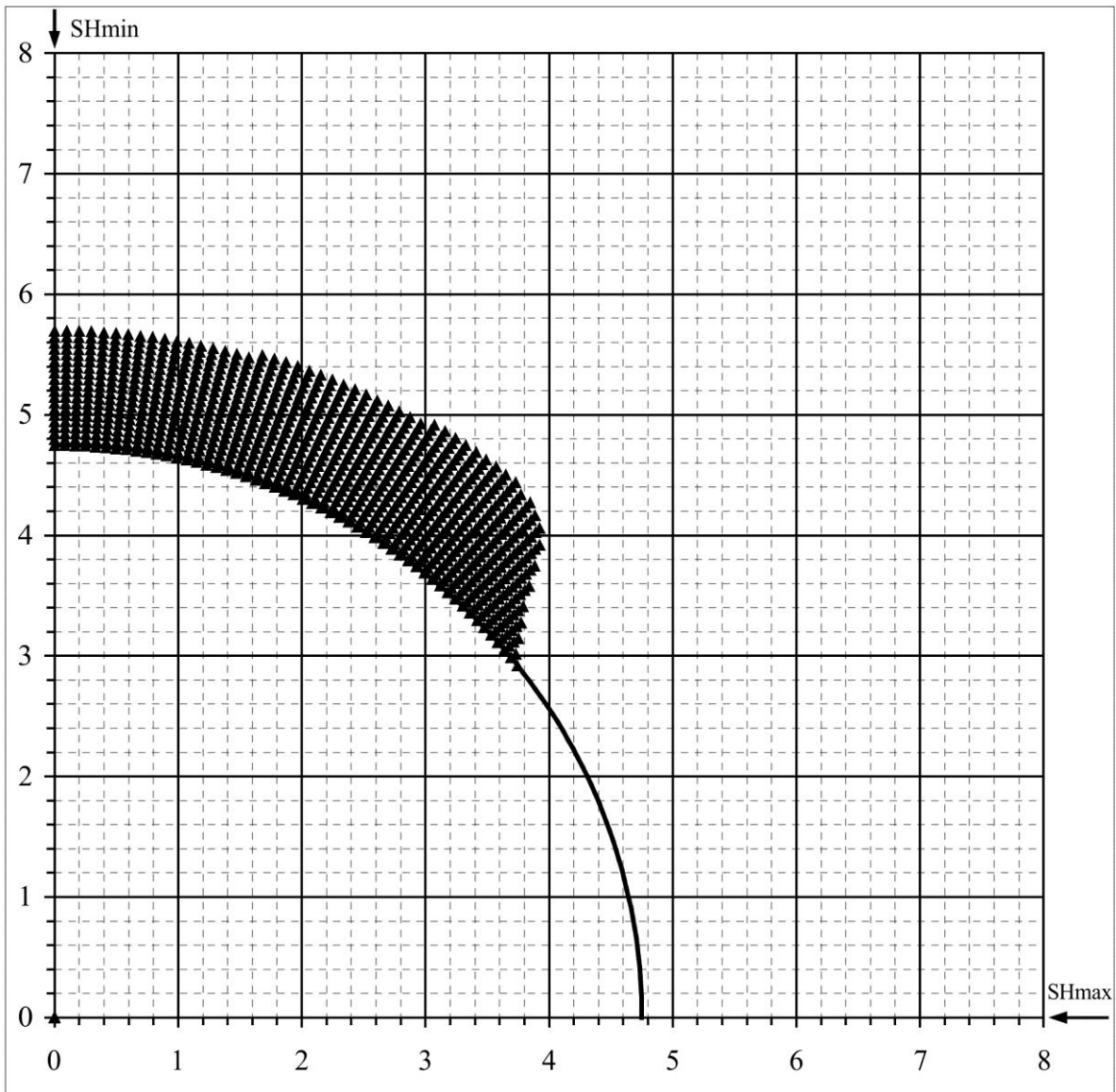




B-066-I/094-O-08

### Mohr - Coulomb Failure Criterion

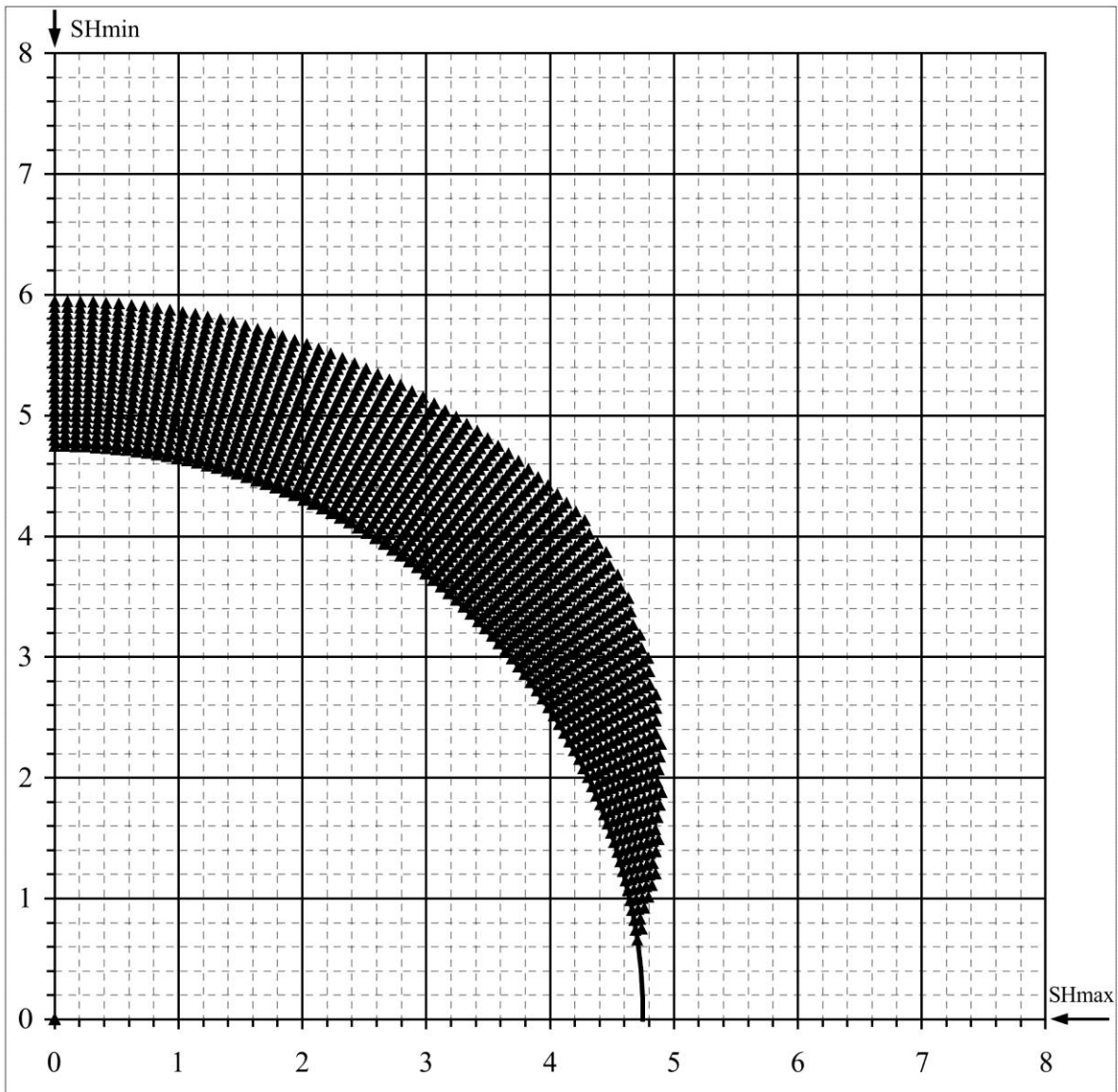
SHmax =	41 MPa	u (Coeff. of Friction) =	0.6
SHmin =	19 MPa	C (Cohesive Strength) =	8.3 MPa
Sv =	23.5 MPa	v (Poisson's Ratio) =	0.2
Po (Pore Pressure) =	10 MPa	Diameter of Borehole =	9.5 "
Pm (Mud Weight) =	10 MPa		
Sensitivity of Figure =	0.05 "	Angle of Max. Breakout =	54 deg
Depth of Max. Breakout =	1.05 "	Max caliper at 90 deg =	11.4 "
Validity of the results =	TRUE	Max caliper at 0 deg =	8 "



B-066-I/094-O-08

### Mohr - Coulomb Failure Criterion

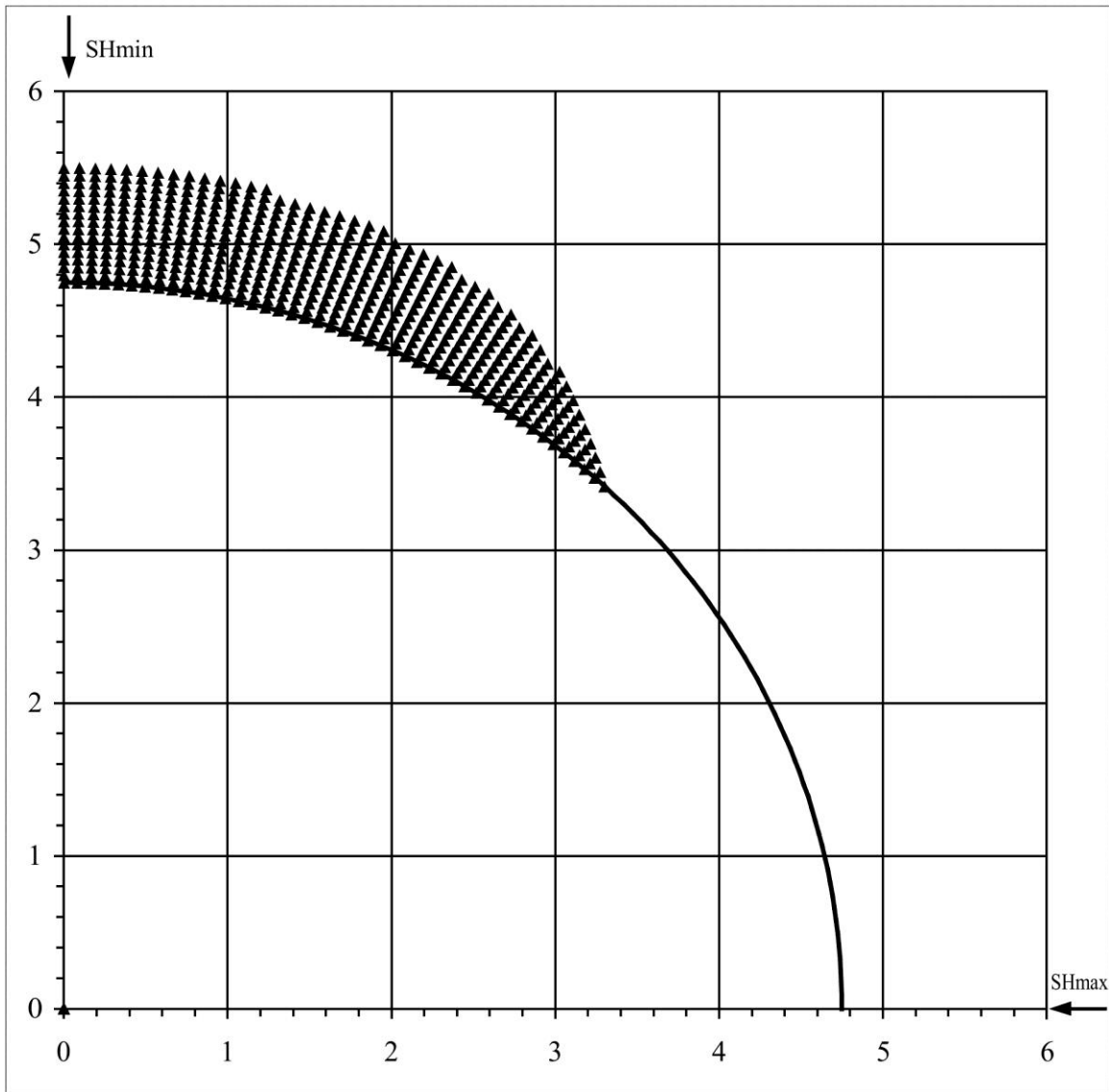
SHmax =	27 MPa	u (Coeff. of Friction) =	0.6
SHmin =	19 MPa	C (Cohesive Strength) =	3 MPa
Sv =	23.5 MPa	v (Poisson's Ratio) =	0.2
Po (Pore Pressure) =	10 MPa	Diameter of Borehole =	9.5 "
Pm (Mud Weight) =	10 MPa		
Sensitivity of Figure =	0.05 "	Angle of Max. Breakout =	64 deg
Depth of Max. Breakout =	1.2 "	Max caliper at 90 deg =	11.9 "
Validity of the results =	FALSE	Max caliper at 0 deg =	8 "



B-066-I/094-O-08

## Extended von-Mises Failure Criterion (Drucker-Prager Failure Criterion)

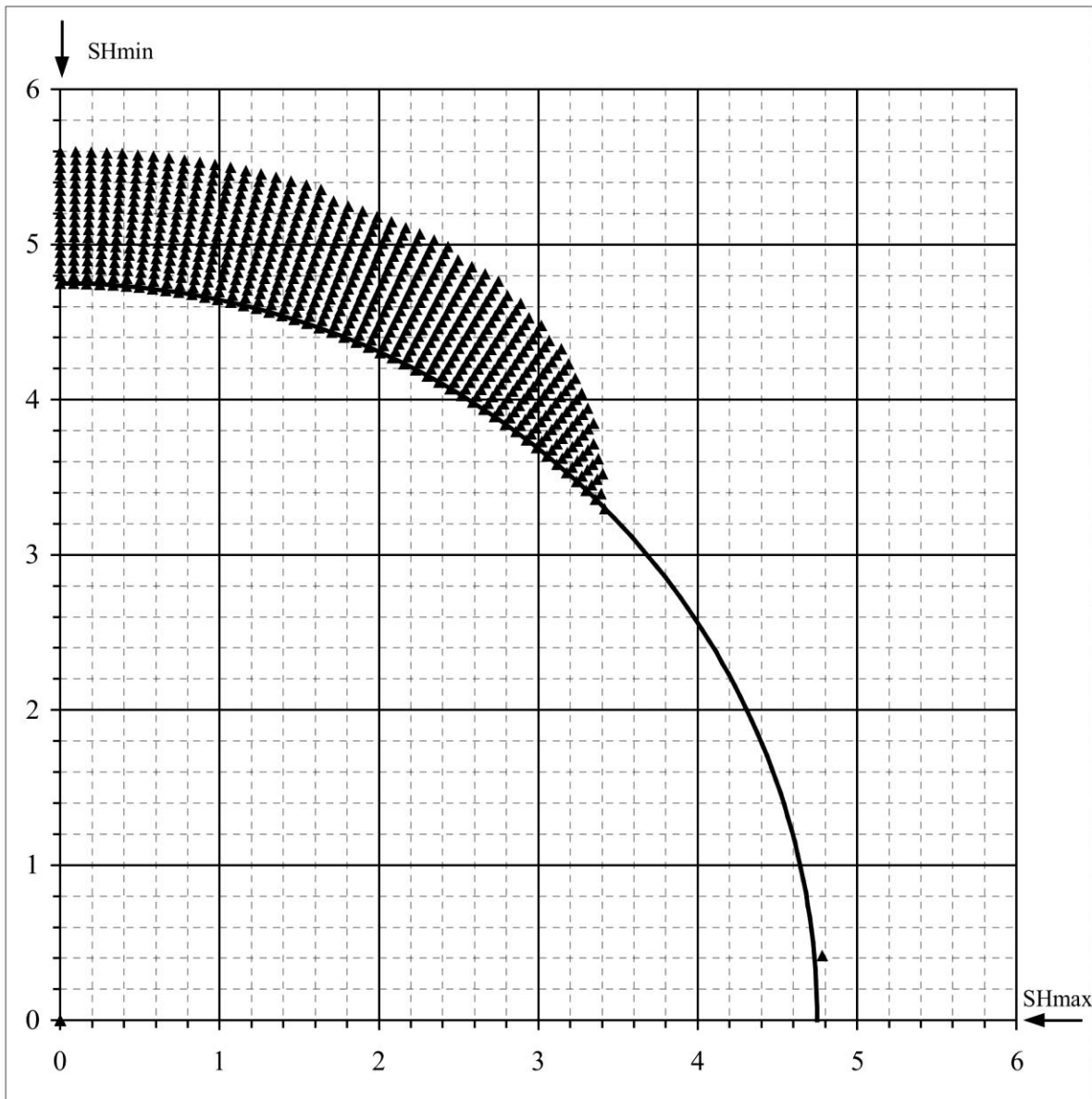
SHmax =	48 MPa	u (Coeff. of Friction) =	0.6
SHmin =	19 MPa	C (Cohesive Strength) =	8.3 MPa
Sv =	23.5 MPa	v (Poisson's Ratio) =	0.2
Po (Pore Pressure) =	10 MPa	Diameter of Borehole =	9.5 inches
Pm (Mud Weight) =	10 MPa	Depth of Max. Breakout =	0.75 inches
Sensitivity of Figure =	0.05 inches	Angle of Max. Breakout =	88 deg



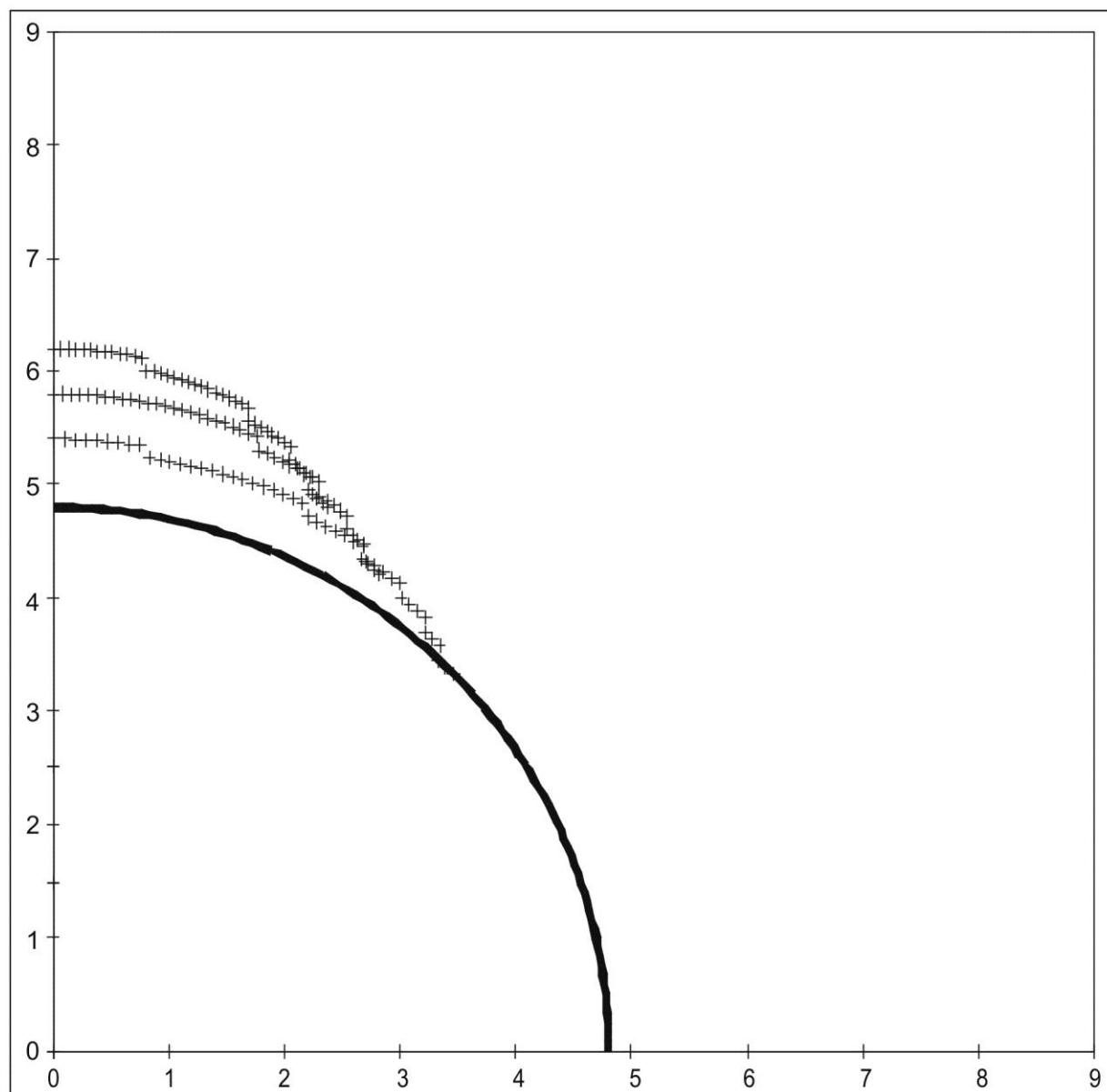
B-066-I/094-O-08

## Extended Drucker - Prager Failure Criterion (Modified Strain Energy Criterion)

SHmax =	46 MPa	u (Coeff. of Friction) =	0.6
SHmin =	19 MPa	C (Cohesive Strength) =	8.3 MPa
Sv =	23.5 MPa	v (Poisson's Ratio) =	0.2
Po (Pore Pressure) =	10 MPa	Diameter of Borehole =	9.5 inches
Pm (Mud Weight) =	10 MPa	Depth of Max. Breakout =	0.85 inches
Sensitivity of Figure =	0.05 inches	Angle of Max. Breakout =	89 deg



B-066-I-094-O-08					
<b>3 Cycle Mohr - Coulomb Failure Criterion</b>					
SHmax =	31.5	MPa	u (Coeff. of Friction) =	0.6	
SHmin =	19	MPa	C (Cohesive Strength) =	8.3	MPa
Sv =	23.5	MPa	v (Poisson's Ratio) =	0.2	
Po (Pore Pressure) =	10	MPa	Diameter of Borehole =	9.5	"
Pm (Mud Weight) =	10	MPa			
Sensitivity of Figure =	0.05	"			
Depth of Max. Breakout =	1.45	"	Max caliper at 90 deg =	12.4	"
Validity of the results =	TRUE		Max caliper at 0 deg =	9.5	"



## $S_{Hmax}$ Simulation Commentary – B-085-H/094-O-11

Well: B-085-H/094-O-11	Failure simulation Method				2SHmin-Po
	Mohr Coulomb	Drucker Prager	Modified Strain Energy	3 cycle Mohr Coulomb	
Breakout Interval Top (m KB)	250	250	250	250	
Breakout Interval Base (m KB)	286	286	286	286	
Median depth of Breakout (m KB)	268	268	268	268	
Calipers 1 and 3 extent (inches)	8.08	8.08	8.08	8.08	
Calipers 2 and 4 extent (inches)	10.72	10.72	10.72	10.72	
SHmax (MPa)	7.7*	10.3*	9.1*	<b>8.1</b>	6.9
SHmax gradient (kPa/m)	28.7	38.4	34.0	30.2	25.7
SHmin (MPa)	4.8	4.8	4.8	4.8	
Sv (MPa)	6.3	6.3	6.3	6.3	
Pore Pressure (MPa)	2.7	2.7	2.7	2.7	
Mudweight (MPa)	2.7	2.7	2.7	2.7	
u (Coefficient of Friction)	0.6	0.6	0.6	0.6	
Cohesive Strength of Rock (MPa)	1	1	1	2	
v (Poisson's Ratio)	0.2	0.2	0.2	0.2	
Bit size (inches)	8.75	8.75	8.75	8.75	

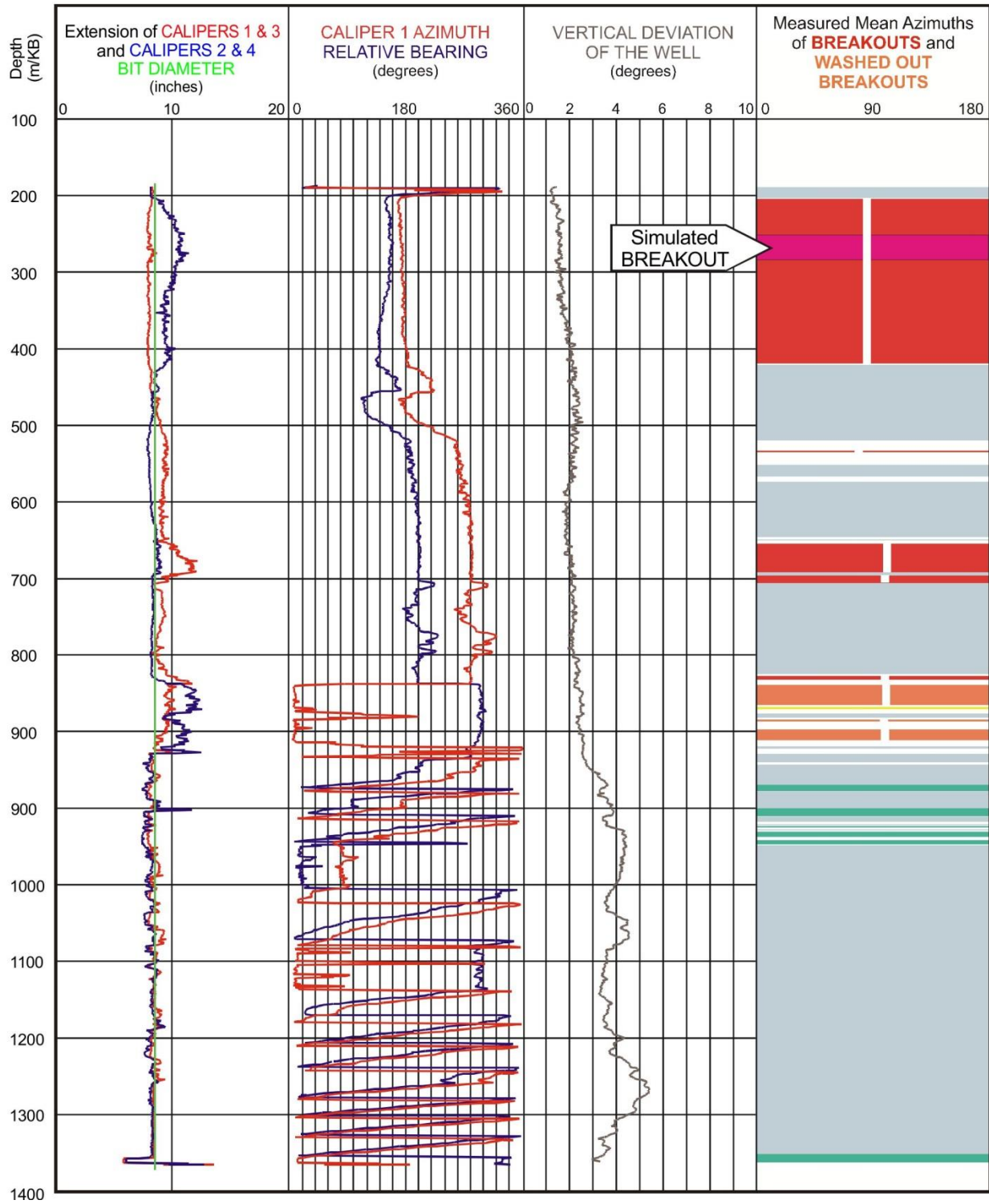
\* indicates that modelling could not simulate complete breakout anisotropy

The breakout interval that was selected for modelling, 250-286 m, is actually in the middle of a much longer breakout zone. It was selected because this was the part of the breakout that had exhibited the deepest spalling. It could not be simulated with any of the three single cycle methods, even when the cohesive strength was lowered from 2 to 1 MPa. Raising  $S_{Hmax}$  to high magnitudes did not generate sufficiently deep breakouts, the maximum being 10.3 inches generated by the Modified Strain Energy routine with an  $S_{Hmax}$  magnitude of 9.1 MPa.

The 3 cycle Mohr-Coulomb simulation modelled a breakout with long axis of 10.7 inches when the cohesive strength was set at 2 MPa. The resulting  $S_{Hmax}$  magnitude of **8.1 MPa** is slightly greater than 6.9 MPa, that was suggested by the equation:  $S_{Hmax} = 2(S_{Hmin}) - Po$ .

The  $S_v$  magnitude at 995.5 m in this well is established from the density log.

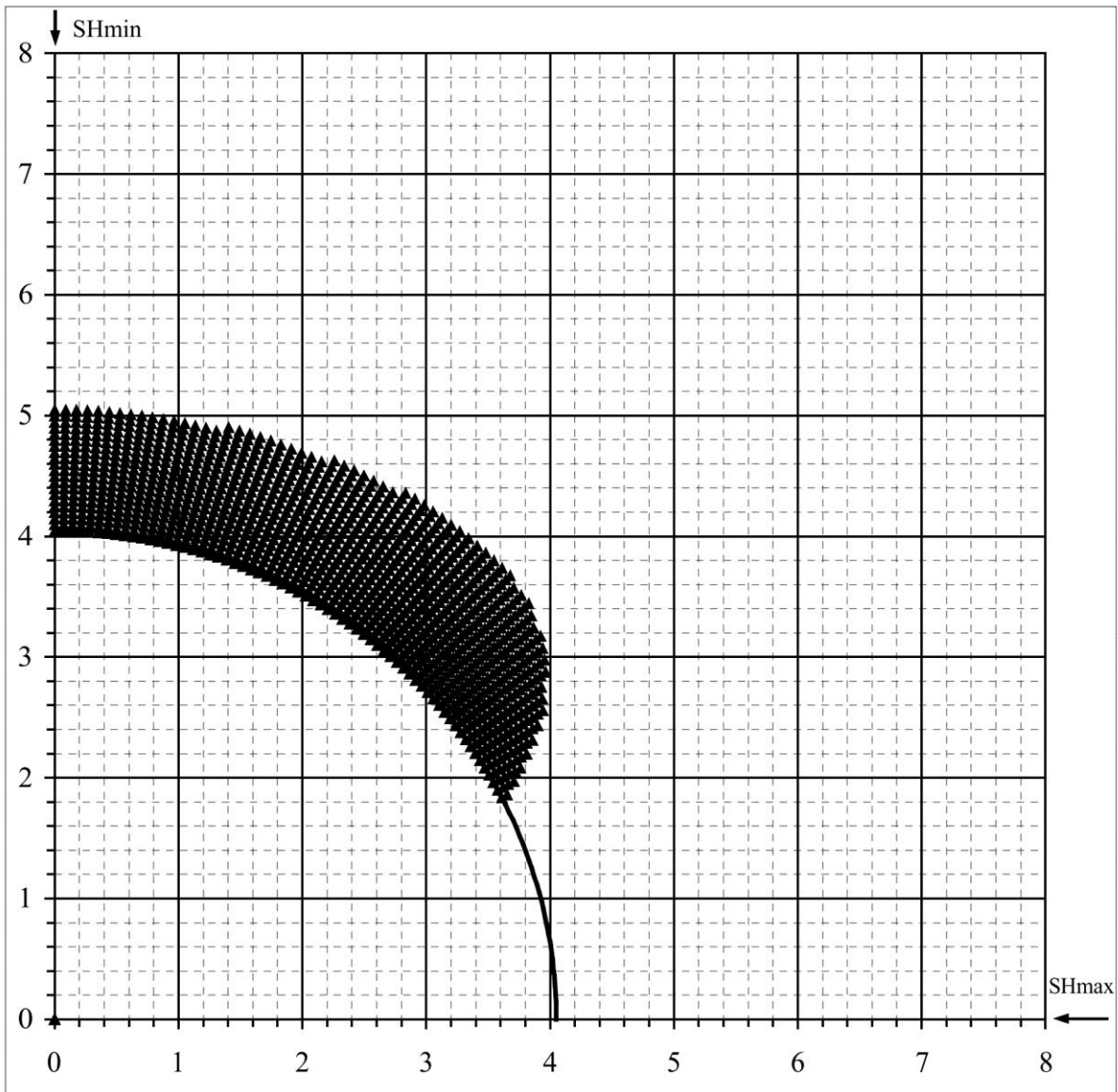
WELL : B-085-H/094-O-11 BREAKOUT ANALYSIS



B-085-H/094-O-11

### Mohr - Coulomb Failure Criterion

SHmax =	7.7 MPa	u (Coeff. of Friction) =	0.6
SHmin =	4.8 MPa	C (Cohesive Strength) =	1 MPa
Sv =	6.3 MPa	v (Poisson's Ratio) =	0.2
Po (Pore Pressure) =	2.7 MPa	Diameter of Borehole =	8.1 "
Pm (Mud Weight) =	2.7 MPa		
Sensitivity of Figure =	0.05 "	Angle of Max. Breakout =	51 deg
Depth of Max. Breakout =	1.15 "	Max caliper at 90 deg =	10.1 "
Validity of the results =	TRUE	Max caliper at 0 deg =	8 "

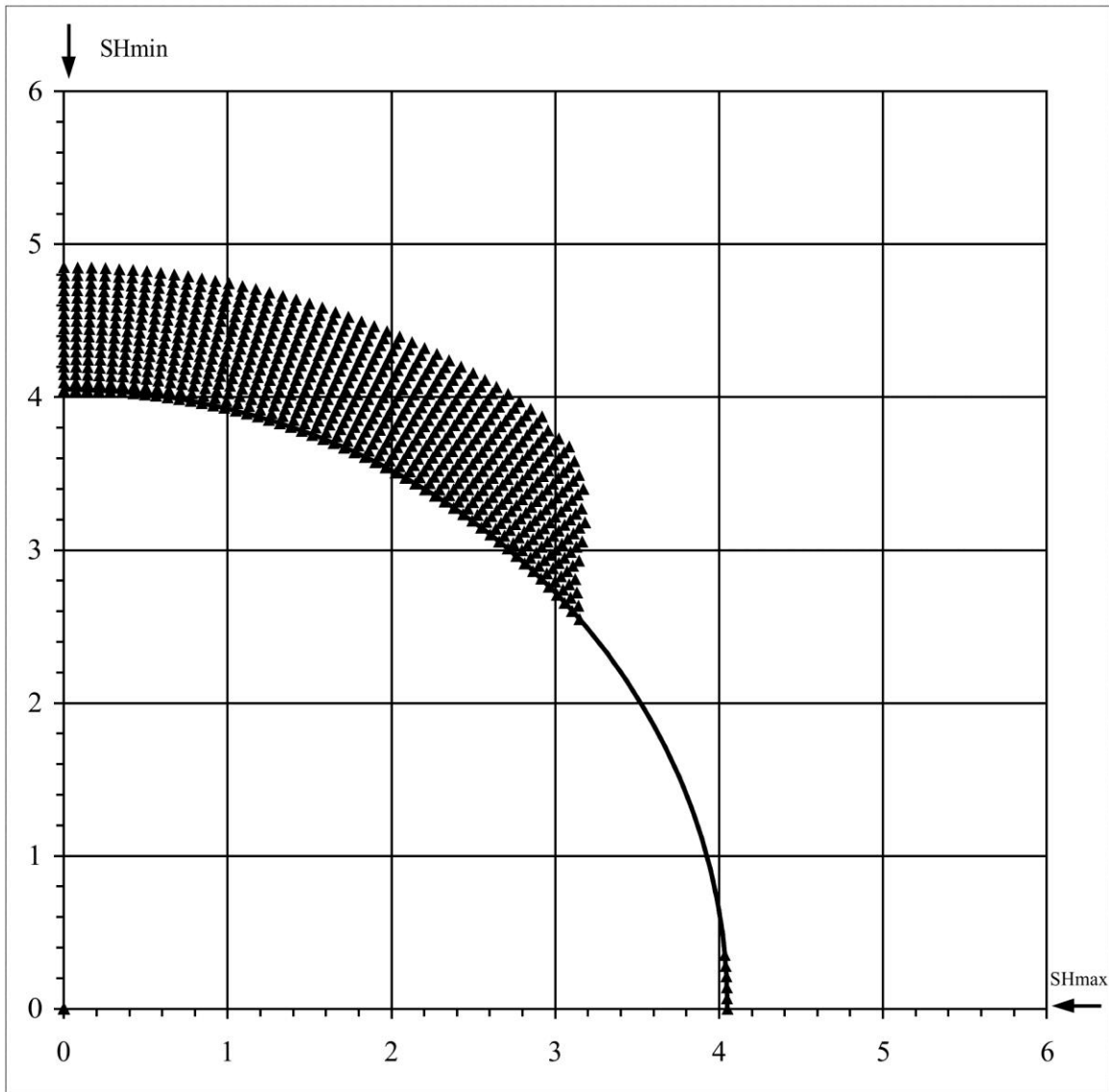




B-085-H/094-O-11

## Extended von-Mises Failure Criterion (Drucker-Prager Failure Criterion)

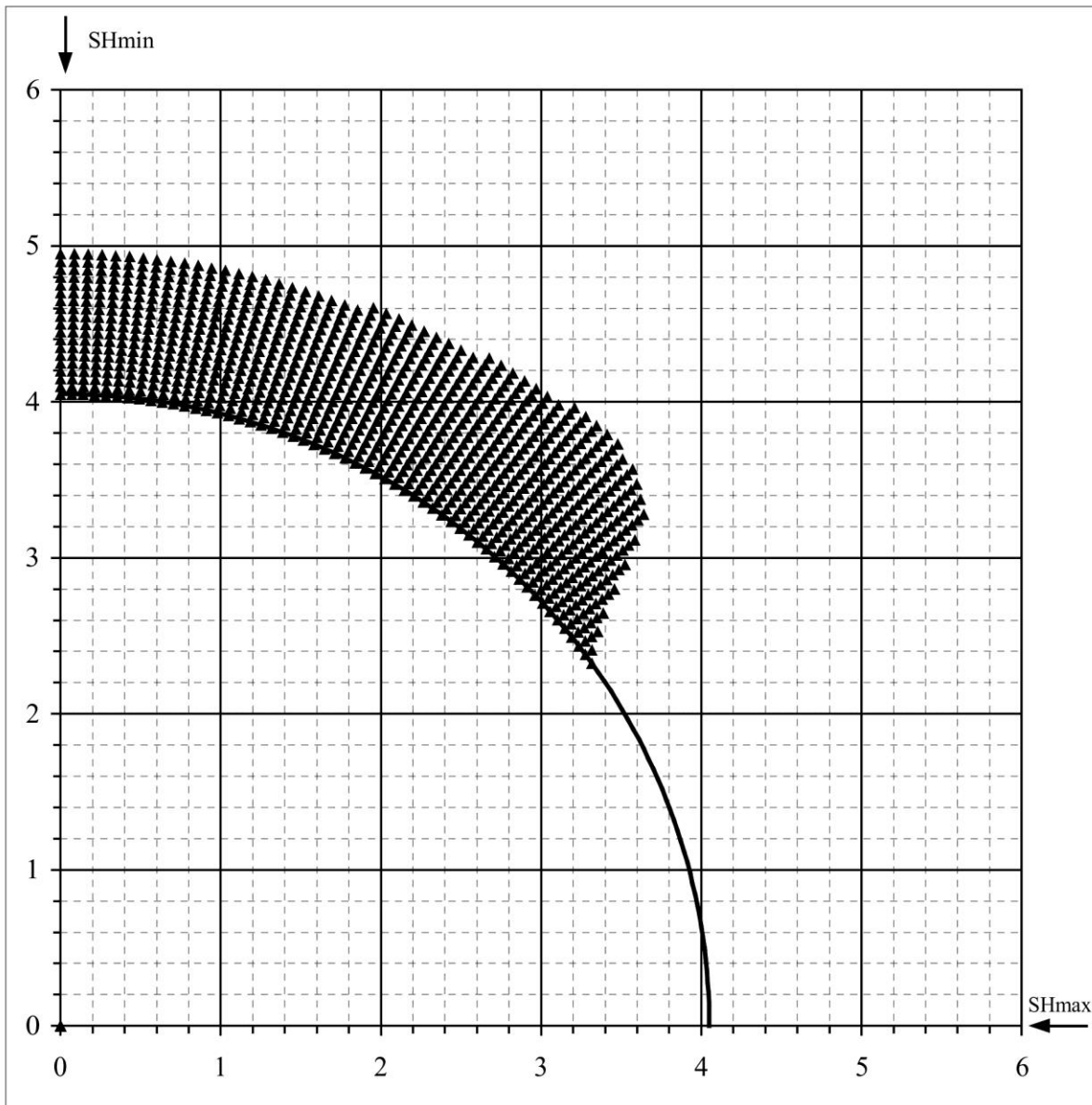
SHmax =	10.3 MPa	u (Coeff. of Friction) =	0.6
SHmin =	4.8 MPa	C (Cohesive Strength) =	1 MPa
Sv =	6.3 MPa	v (Poisson's Ratio) =	0.2
Po (Pore Pressure) =	2.7 MPa	Diameter of Borehole =	8.1 inches
Pm (Mud Weight) =	2.7 MPa	Depth of Max. Breakout =	0.8 inches
Sensitivity of Figure =	0.05 inches	Angle of Max. Breakout =	84 deg



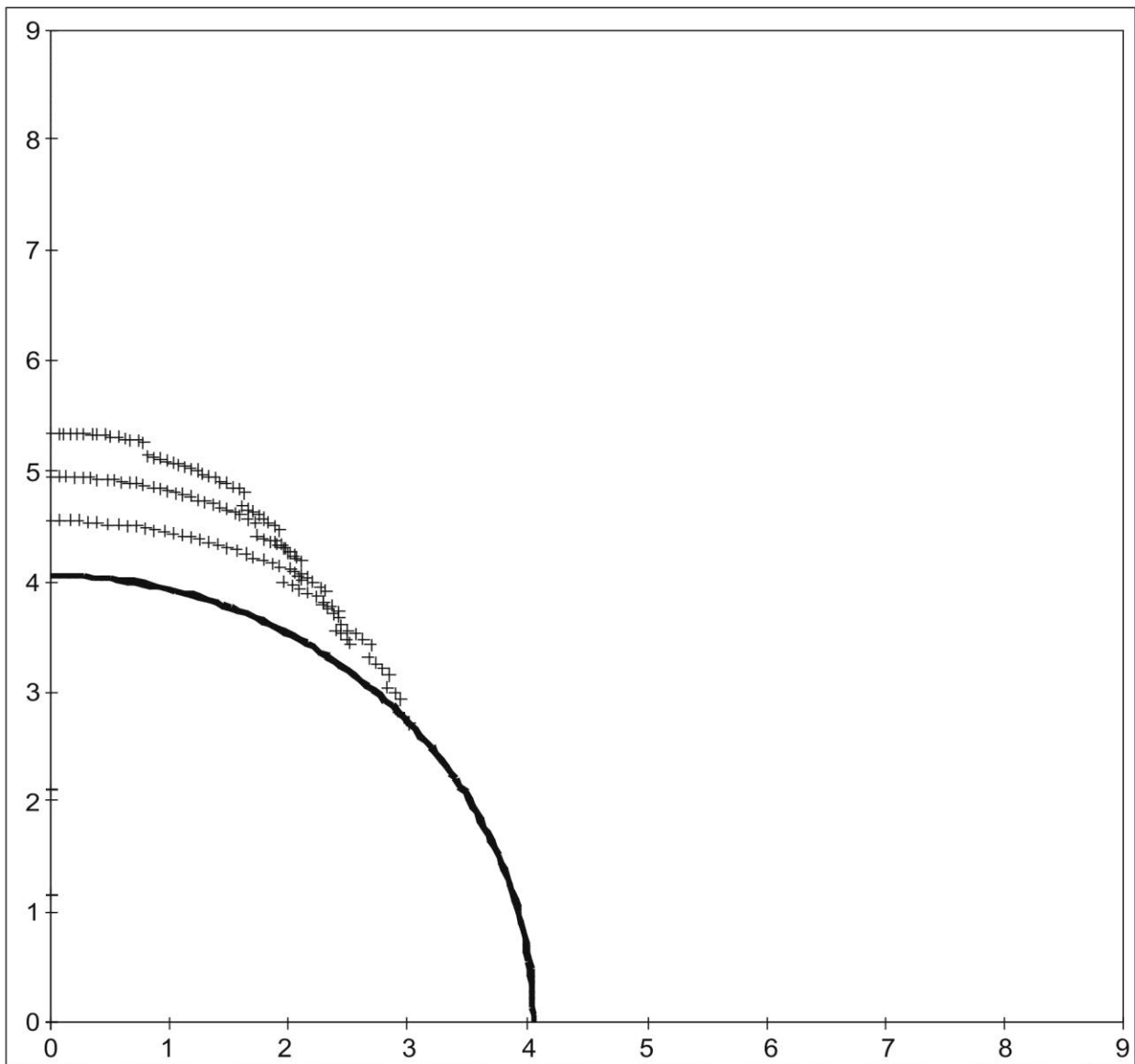
B-085-H/094-O-11

## Extended Drucker - Prager Failure Criterion (Modified Strain Energy Criterion)

SHmax =	9.1 MPa	u (Coeff. of Friction) =	0.6
SHmin =	4.8 MPa	C (Cohesive Strength) =	1 MPa
Sv =	6.3 MPa	v (Poisson's Ratio) =	0.2
Po (Pore Pressure) =	2.7 MPa	Diameter of Borehole =	8.1 inches
Pm (Mud Weight) =	2.7 MPa	Depth of Max. Breakout =	1.05 inches
Sensitivity of Figure =	0.05 inches	Angle of Max. Breakout =	49 deg



B-085-H/094-O-11					
3 Cycle Mohr - Coulomb Failure Criterion					
SHmax =	8.1	MPa	u (Coeff. of Friction) =	0.6	
SHmin =	4.8	MPa	C (Cohesive Strength) =	2	MPa
Sv =	6.3	MPa	v (Poisson's Ratio) =	0.2	
Po (Pore Pressure) =	2.7	MPa	Diameter of Borehole =	8.1	"
Pm (Mud Weight) =	2.7	MPa			
Sensitivity of Figure =	0.05	"			
Depth of Max. Breakout =	1.3	"	Max caliper at 90 deg =	10.7	"
Validity of the results =	TRUE		Max caliper at 0 deg =	8.1	"



## $S_{Hmax}$ Simulation Commentary – B-093-C/094-I-14

Well: B-093-C/094-I-14	Failure simulation Method				2SHmin-Po
	Mohr Coulomb	Drucker Prager	Modified Strain Energy	3 cycle Mohr Coulomb	
Breakout Interval Top (m KB)	293	293	293	293	
Breakout Interval Base (m KB)	381	381	381	381	
Median depth of Breakout (m KB)	337	337	337	337	
Calipers 1 and 3 extent (inches)	19.77	19.77	19.77	19.77	
Calipers 2 and 4 extent (inches)	16.42	16.42	16.42	16.42	
SHmax (MPa)	9.6*	13.1*	11.7*	<b>10.1</b>	11.8
SHmax gradient (kPa/m)	28.5	38.9	34.7	30.0	35.0
SHmin (MPa)	7.6	7.6	7.6	7.6	
Sv (MPa)	7.7	7.7	7.7	7.7	
Pore Pressure (MPa)	3.4	3.4	3.4	3.4	
Mudweight (MPa)	3.4	3.4	3.4	3.4	
u (Coefficient of Friction)	0.6	0.6	0.6	0.6	
Cohesive Strength of Rock (MPa)	2	2	2	3	
v (Poisson's Ratio)	0.2	0.2	0.2	0.2	
Bit size (inches)	16	16	16	16	

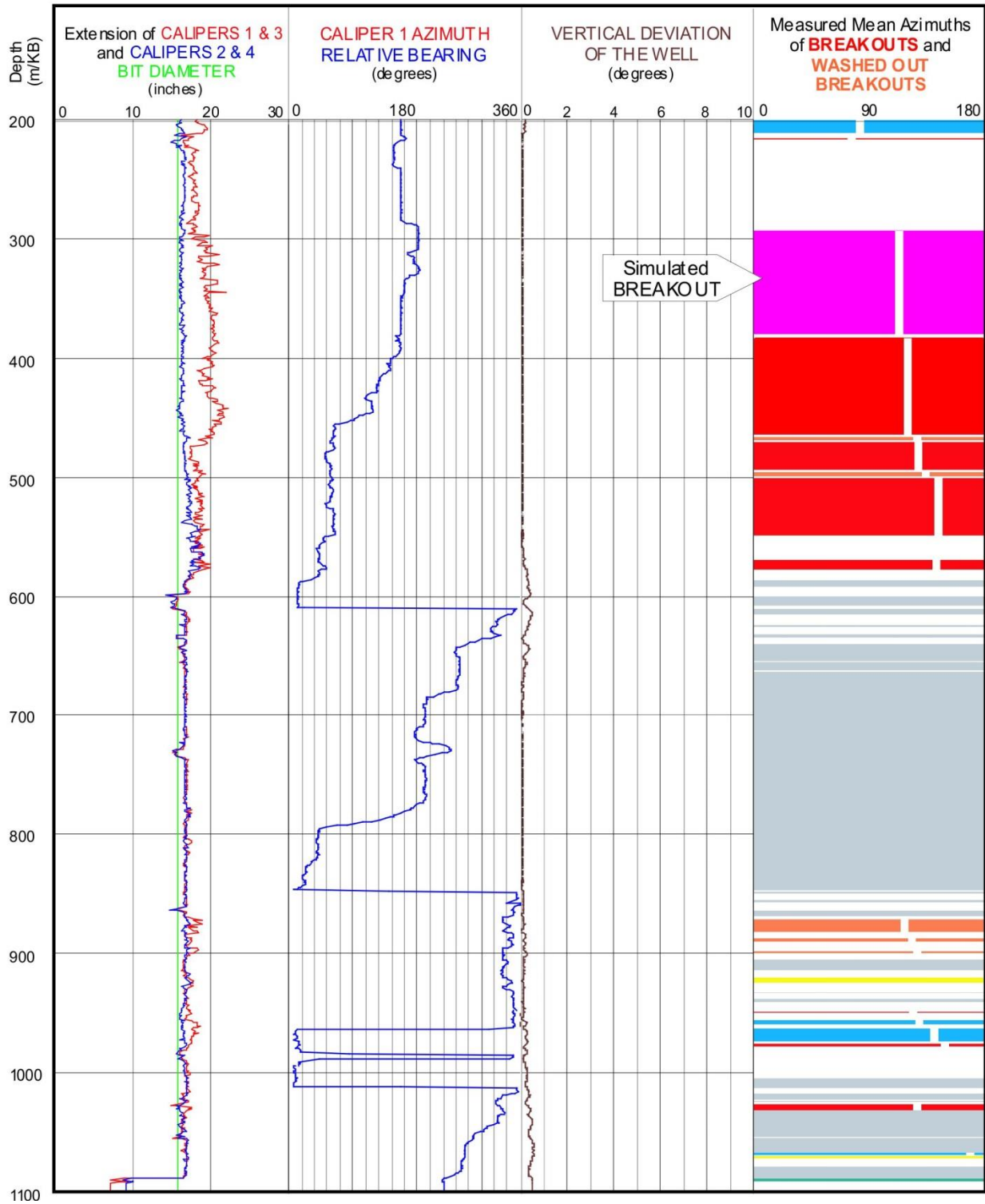
\* indicates that modelling could not simulate complete breakout anisotropy

The breakout interval that was selected for modelling runs from 293 m to-381 m. It could not be simulated with any of the three single cycle methods, even when the cohesive strength was lowered to 2 MPa. The simulations did not generate sufficiently deep breakouts, the maximum depth that was achieved was 18.7 inches, which was generated by all three single cycle methods.

The 3 cycle Mohr-Coulomb simulation modelled a breakout with long axis of 19.8 inches when the cohesive strength was set at 3 MPa. The resulting  $S_{Hmax}$  magnitude of **10.1 MPa** is lower than the 11.8 MPa magnitude suggested by the equation:  $S_{Hmax} = 2(S_{Hmin}) - Po$ .

The  $S_v$  magnitude at 337 m in this well is established from the density log.

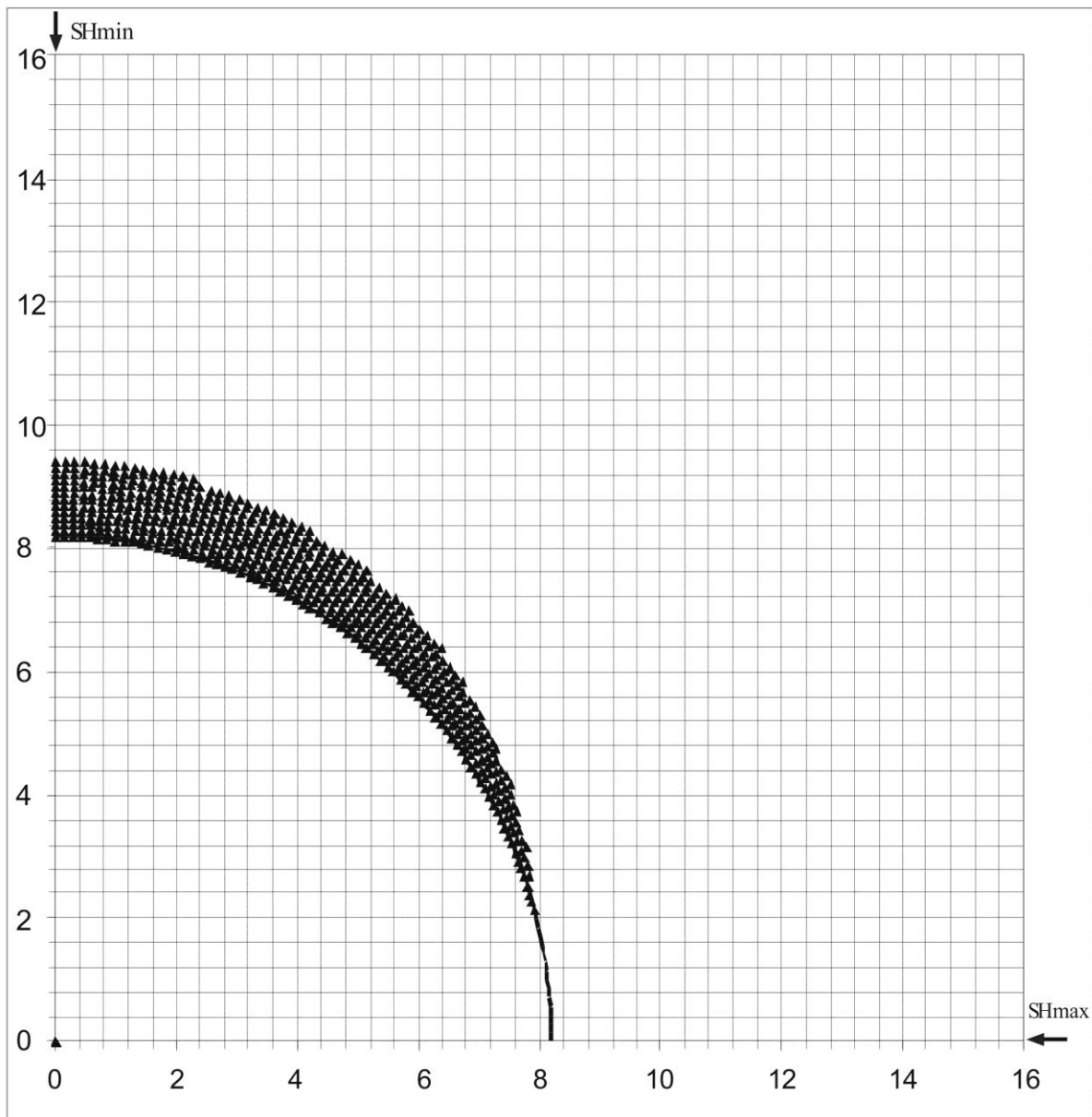
WELL : B-093-C-094-I-14      BREAKOUT ANALYSIS



B-093-C/094-I-14

## Mohr - Coulomb Failure Criterion

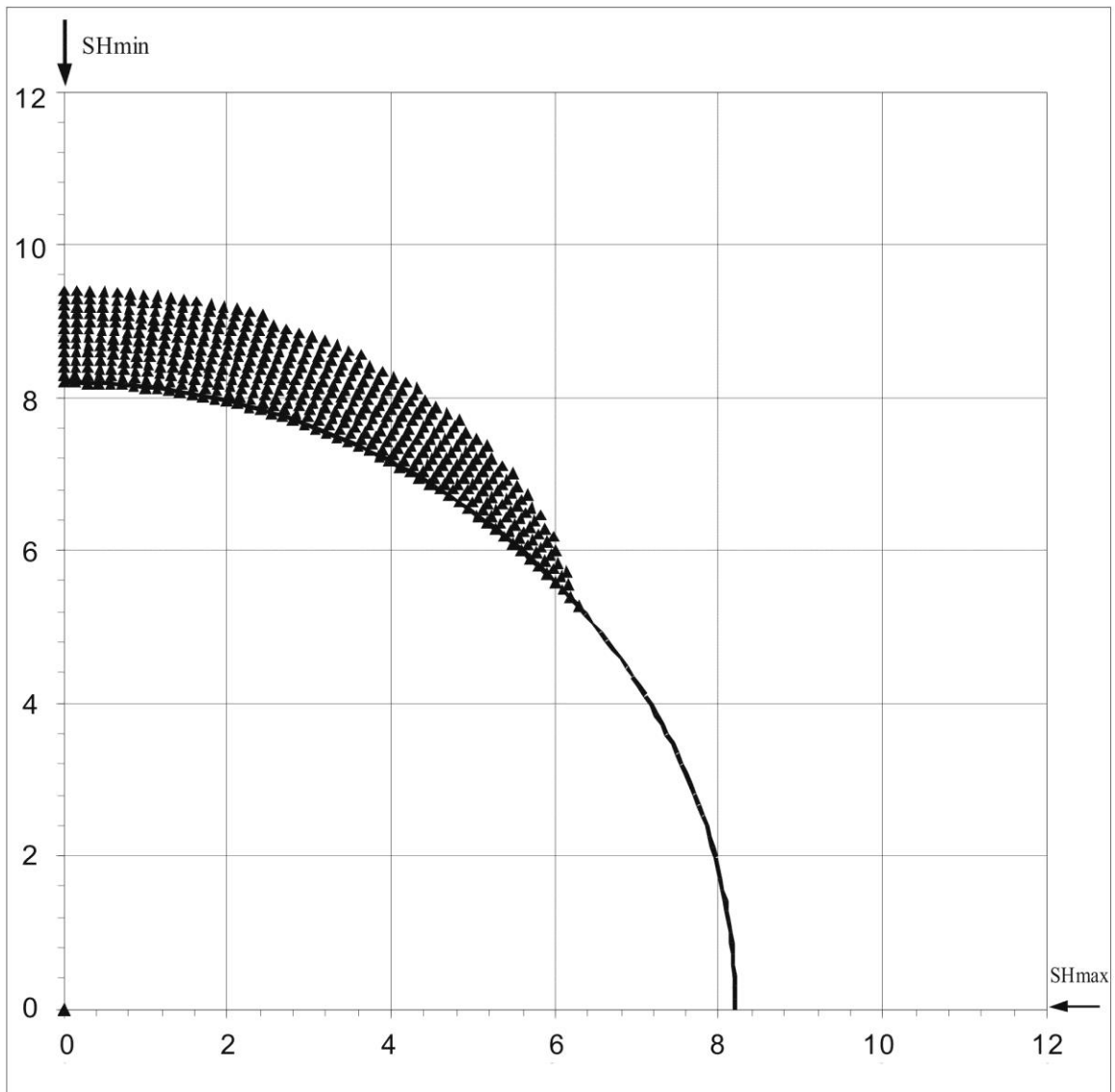
SHmax =	9.6 MPa	u (Coeff. of Friction) =	0.6
SHmin =	7.6 MPa	C (Cohesive Strength) =	2 MPa
Sv =	7.7 MPa	v (Poisson's Ratio) =	0.2
Po (Pore Pressure) =	3.4 MPa	Diameter of Borehole =	16.4 "
Pm (Mud Weight) =	3.4 MPa		
Sensitivity of Figure =	0.05 "	Angle of Max. Breakout =	90 deg
Depth of Max. Breakout =	1.15 "	Max caliper at 90 deg =	18.7 "
Validity of the results =	TRUE	Max caliper at 0 deg =	8 "



B-093-C/094-I-14

## Extended von-Mises Failure Criterion (Drucker-Prager Failure Criterion)

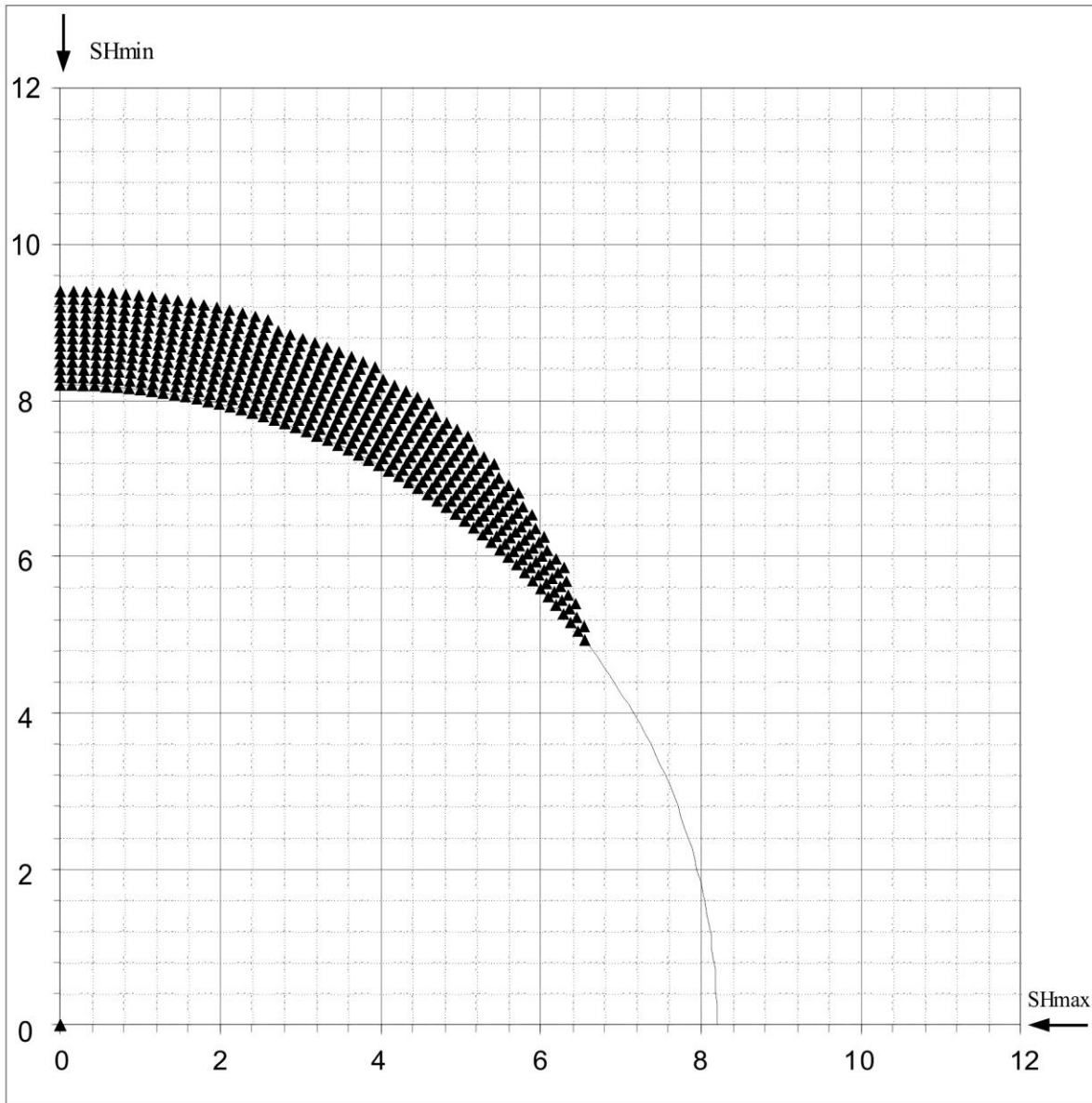
SHmax =	13.1 MPa	u (Coeff. of Friction)=	0.6
SHmin =	7.6 MPa	C (Cohesive Strength) =	2 MPa
Sv =	7.7 MPa	$\nu$ (Poisson's Ratio) =	0.2
Po (Pore Pressure) =	3.4 MPa	Diameter of Borehole =	16.4 inches
Pm (Mud Weight) =	3.4 MPa	Depth of Max. Breakout =	1.15 inches
Sensitivity of Figure =	0.05 inches	Angle of Max. Breakout =	90 deg



B-093-C/094-I-14

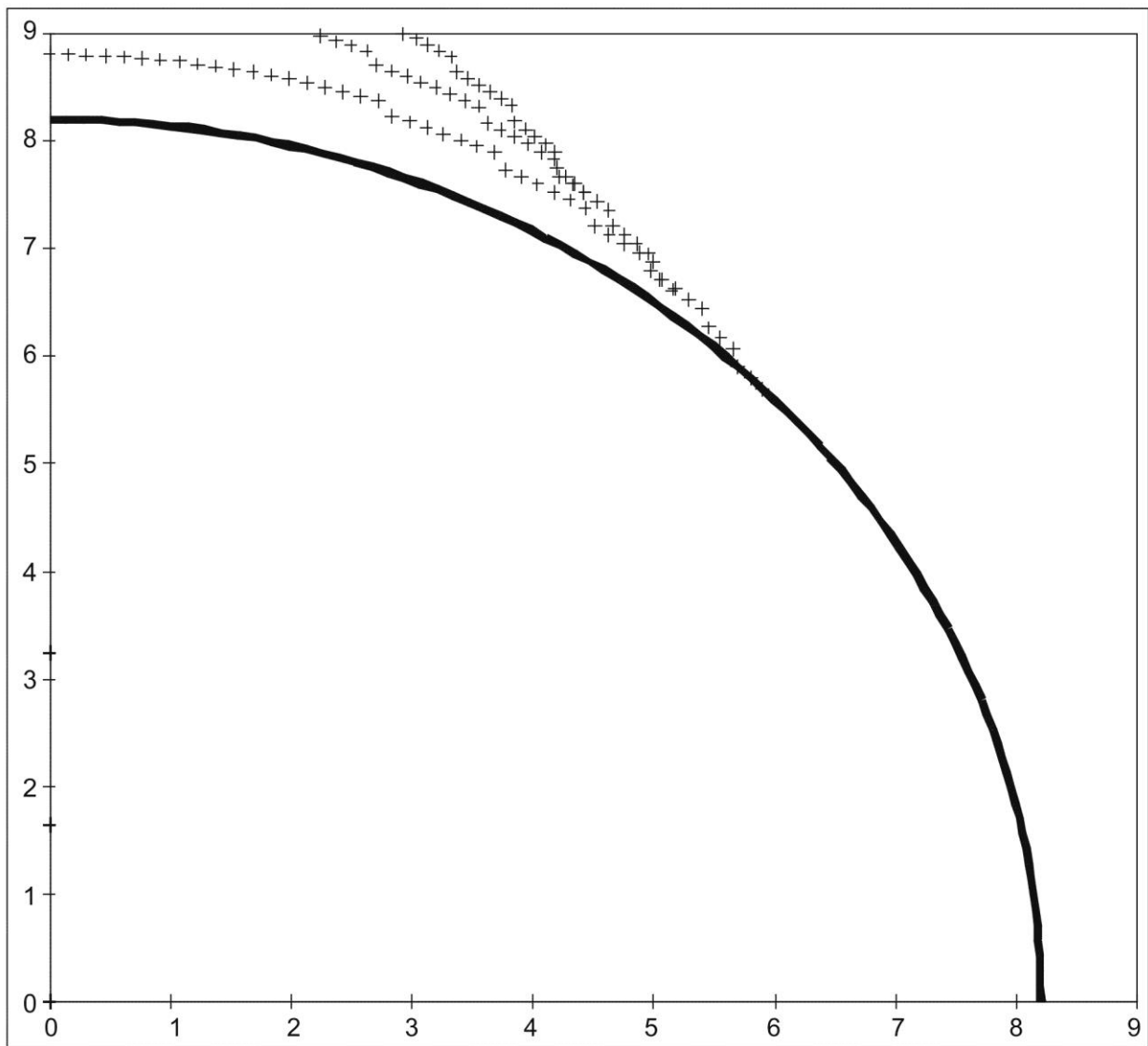
## Extended Drucker - Prager Failure Criterion (Modified Strain Energy Criterion)

SHmax =	11.7 MPa	u (Coeff. of Friction) =	0.6
SHmin =	7.6 MPa	C (Cohesive Strength) =	2 MPa
Sv =	7.7 MPa	v (Poisson's Ratio) =	0.2
Po (Pore Pressure) =	3.4 MPa	Diameter of Borehole =	16.4 inches
Pm (Mud Weight) =	3.4 MPa	Depth of Max. Breakout =	1.15 inches
Sensitivity of Figure =	0.05 inches	Angle of Max. Breakout =	90 deg





B-093-C/094-I-14					
3 Cycle Mohr - Coulomb Failure Criterion					
SHmax =	10.1	MPa	u (Coeff. of Friction) =	0.6	
SHmin =	7.6	MPa	C (Cohesive Strength) =	3	MPa
Sv =	7.7	MPa	v (Poisson's Ratio) =	0.2	
Po (Pore Pressure) =	3.4	MPa	Diameter of Borehole =	16.4	"
Pm (Mud Weight) =	3.4	MPa			
Sensitivity of Figure =	0.05	"			
Depth of Max. Breakout =	1.7	"	Max caliper at 90 deg =	19.8	"
Validity of the results =	TRUE		Max caliper at 0 deg =	16.4	"

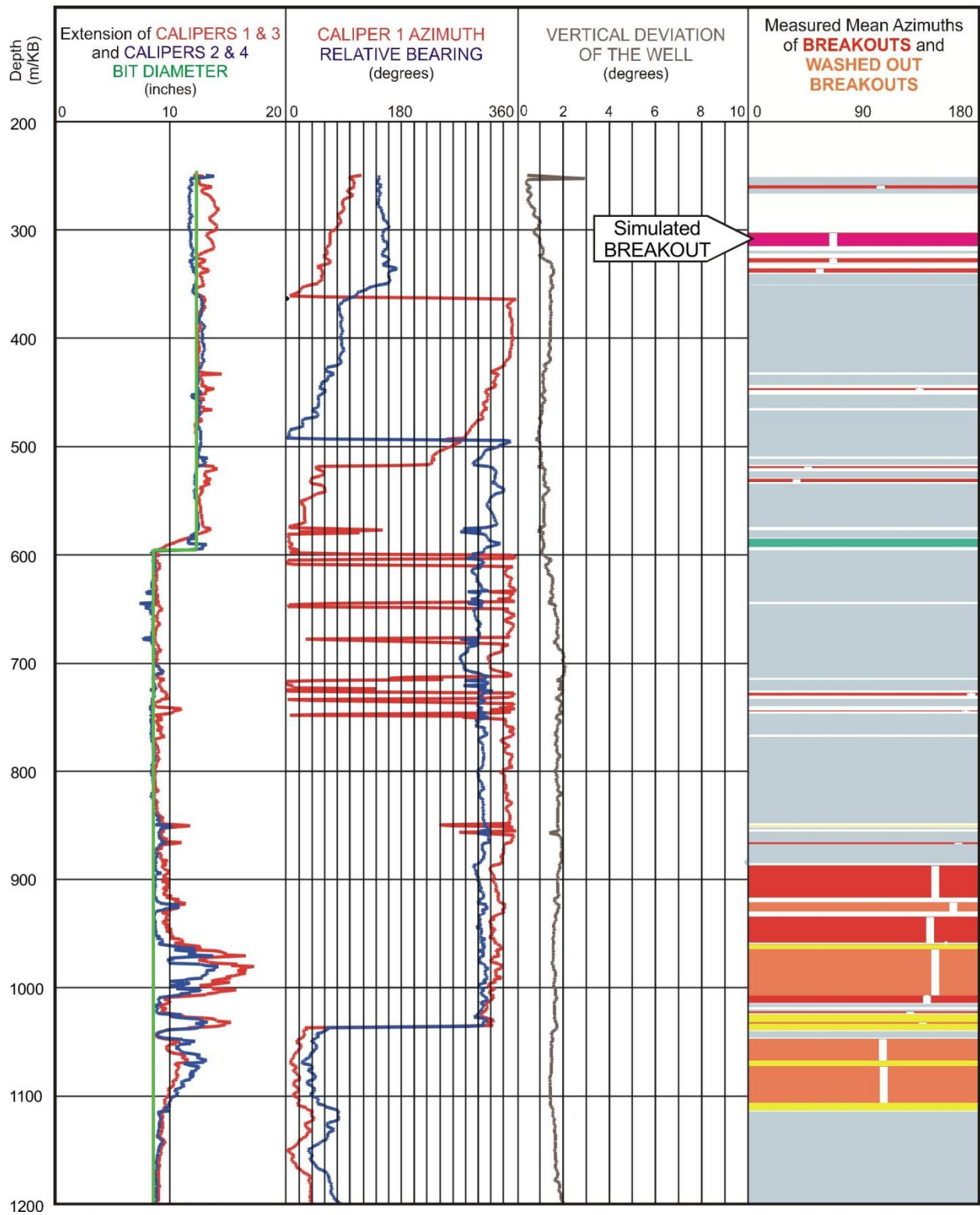


## $S_{Hmax}$ Simulation Commentary – B-094-H/094-J-14

Well: B-094-H/094-J-14	Failure simulation Method				2SHmin-Po
	Mohr Coulomb	Drucker Prager	Modified Strain Energy	3 cycle Mohr Coulomb	
Breakout Interval Top (m KB)	303	303	303	303	
Breakout Interval Base (m KB)	318	318	318	318	
Median depth of Breakout (m KB)	310.5	310.5	310.5	310.5	
Calipers 1 and 3 extent (inches)	13.55	13.55	13.55	13.55	
Calipers 2 and 4 extent (inches)	11.84	11.84	11.84	11.84	
SHmax (MPa)	<b>10.2</b>	13.9	12.0		9.1
SHmax gradient (kPa/m)	32.9	44.7	38.6		29.3
SHmin (MPa)	6.1	6.1	6.1	6.1	
Sv (MPa)	7.4	7.4	7.4	7.4	
Pore Pressure (MPa)	3.1	3.1	3.1	3.1	
Mudweight (MPa)	3.1	3.1	3.1	3.1	
u (Coefficient of Friction)	0.6	0.6	0.6	0.6	
Cohesive Strength of Rock (MPa)	3.0	3.0	3.0	3.0	
v (Poisson's Ratio)	0.2	0.2	0.2	0.2	
Bit size (inches)	12.25	8.5	8.5	8.5	

The breakout interval that was selected for modelling, 303-318 m, exhibits relatively shallow spalling. All the single cycle routines generated sufficiently deep breakouts, with the Mohr Coulomb routine requiring an  $S_{Hmax}$  magnitude of **10.2 MPa**, when the cohesive strength was set at 3 MPa, to generate a breakout with a long axis of 13.6 inches. This value was taken as a reliable estimate of  $S_{Hmax}$  and it compares well with the  $S_{Hmax}$  magnitude of 9.1 MPa, suggested by the equation:  $S_{Hmax} = 2(S_{Hmin}) - Po$ .

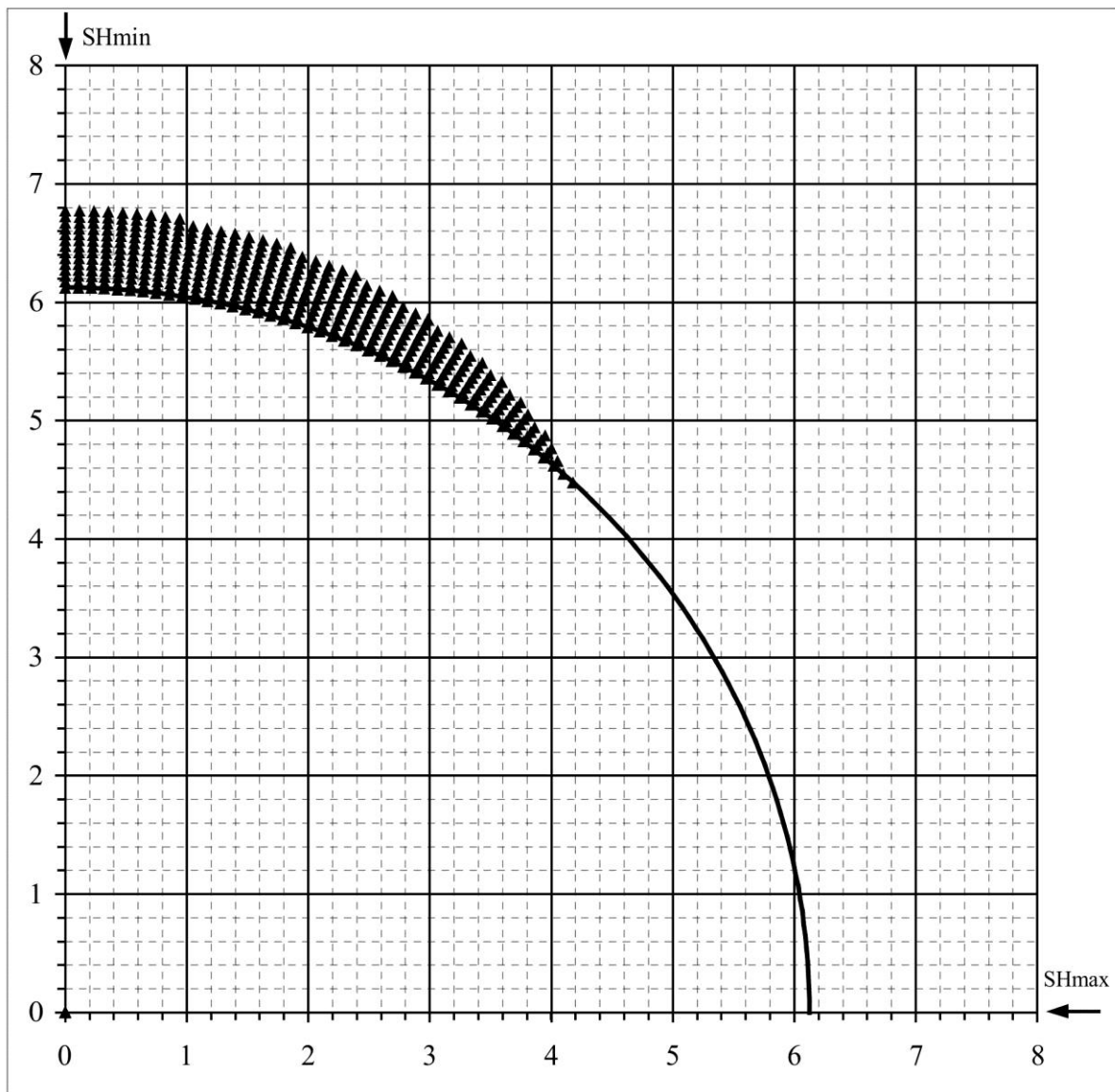
WELL : B-094-H/094-J-14 BREAKOUT ANALYSIS



B-094-H/094-J-14

## Mohr - Coulomb Failure Criterion

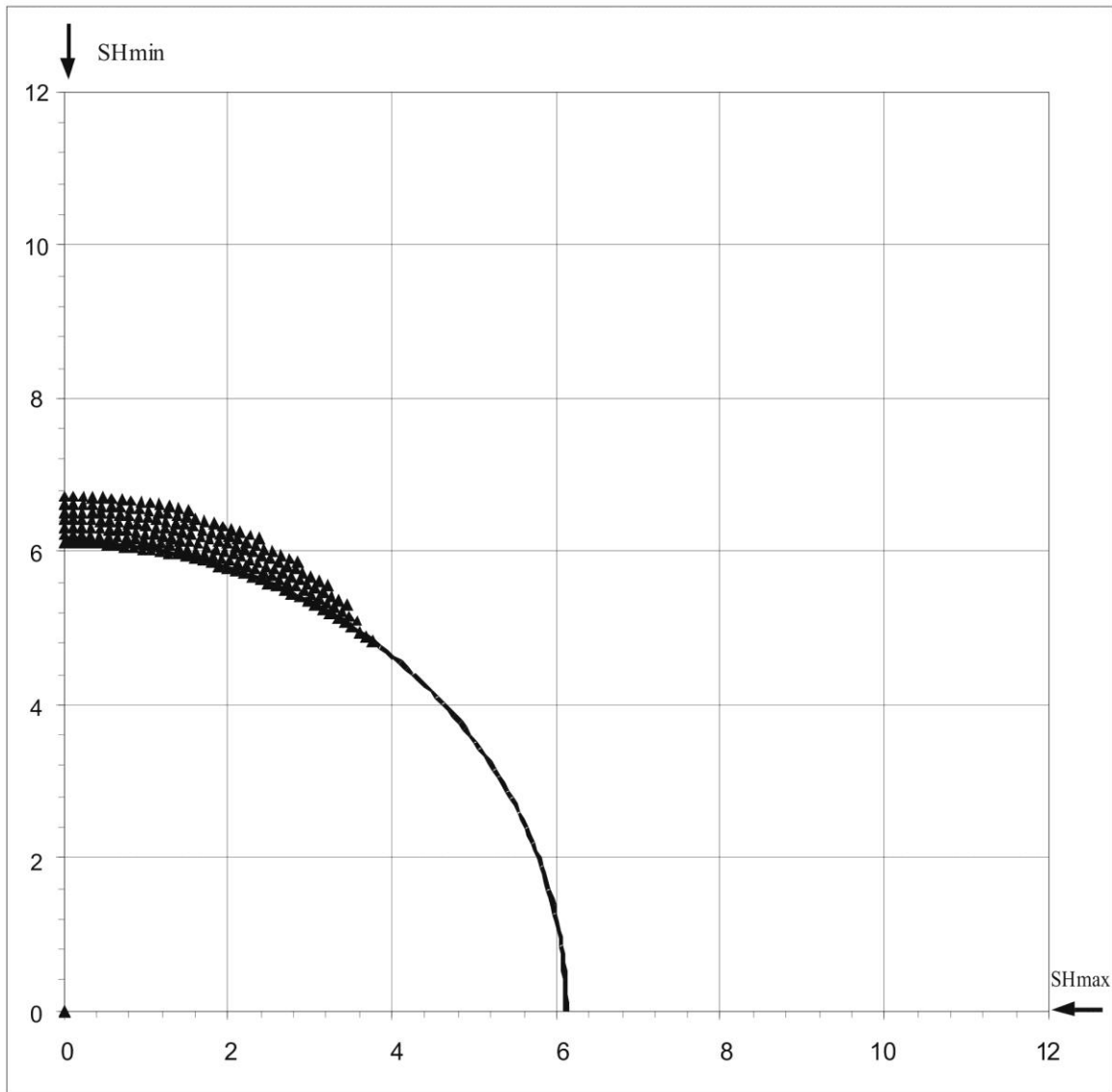
SHmax =	10.2 MPa	u (Coeff. of Friction) =	0.6
SHmin =	6.1 MPa	C (Cohesive Strength) =	3 MPa
Sv =	7.4 MPa	v (Poisson's Ratio) =	0.2
Po (Pore Pressure) =	3.1 MPa	Diameter of Borehole =	12.25 "
Pm (Mud Weight) =	3.1 MPa		
Sensitivity of Figure =	0.05 "	Angle of Max. Breakout =	89 deg
Depth of Max. Breakout =	0.65 "	Max caliper at 90 deg =	13.55 "
Validity of the results =	TRUE	Max caliper at 0 deg =	8 "



B-094-H/094-J-14

## Extended von-Mises Failure Criterion (Drucker-Prager Failure Criterion)

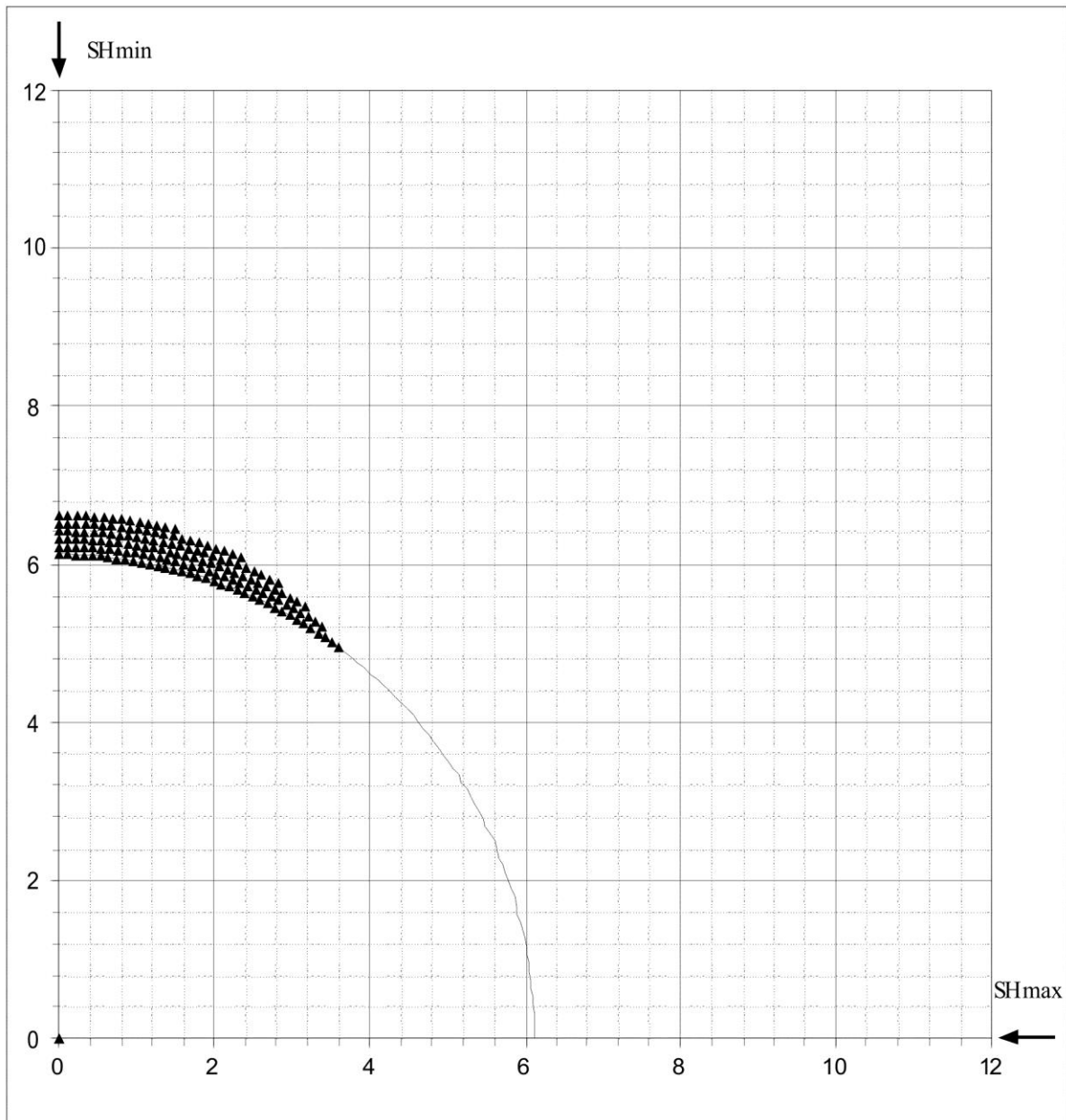
SHmax =	13.9 MPa	u (Coeff. of Friction) =	0.6
SHmin =	6.1 MPa	C (Cohesive Strength) =	3 MPa
Sv =	7.4 MPa	v (Poisson's Ratio) =	0.2
Po (Pore Pressure) =	3.1 MPa	Diameter of Borehole =	12.25 inches
Pm (Mud Weight) =	3.1 MPa	Depth of Max. Breakout =	0.65 inches
Sensitivity of Figure =	0.05 inches	Angle of Max. Breakout =	89 deg



B-094-H/094-J-14

## Extended Drucker - Prager Failure Criterion (Modified Strain Energy Criterion)

SHmax =	12 MPa	u (Coeff. of Friction) =	0.6
SHmin =	6.1 MPa	C (Cohesive Strength) =	3 MPa
Sv =	7.4 MPa	v (Poisson's Ratio) =	0.2
Po (Pore Pressure) =	3.1 MPa	Diameter of Borehole =	12.25 inches
Pm (Mud Weight) =	3.1 MPa	Depth of Max. Breakout =	0.55 inches
Sensitivity of Figure =	0.05 inches	Angle of Max. Breakout =	85 deg



**S<sub>Hmax</sub> Simulation Commentary – C-024-H/094-O-16**

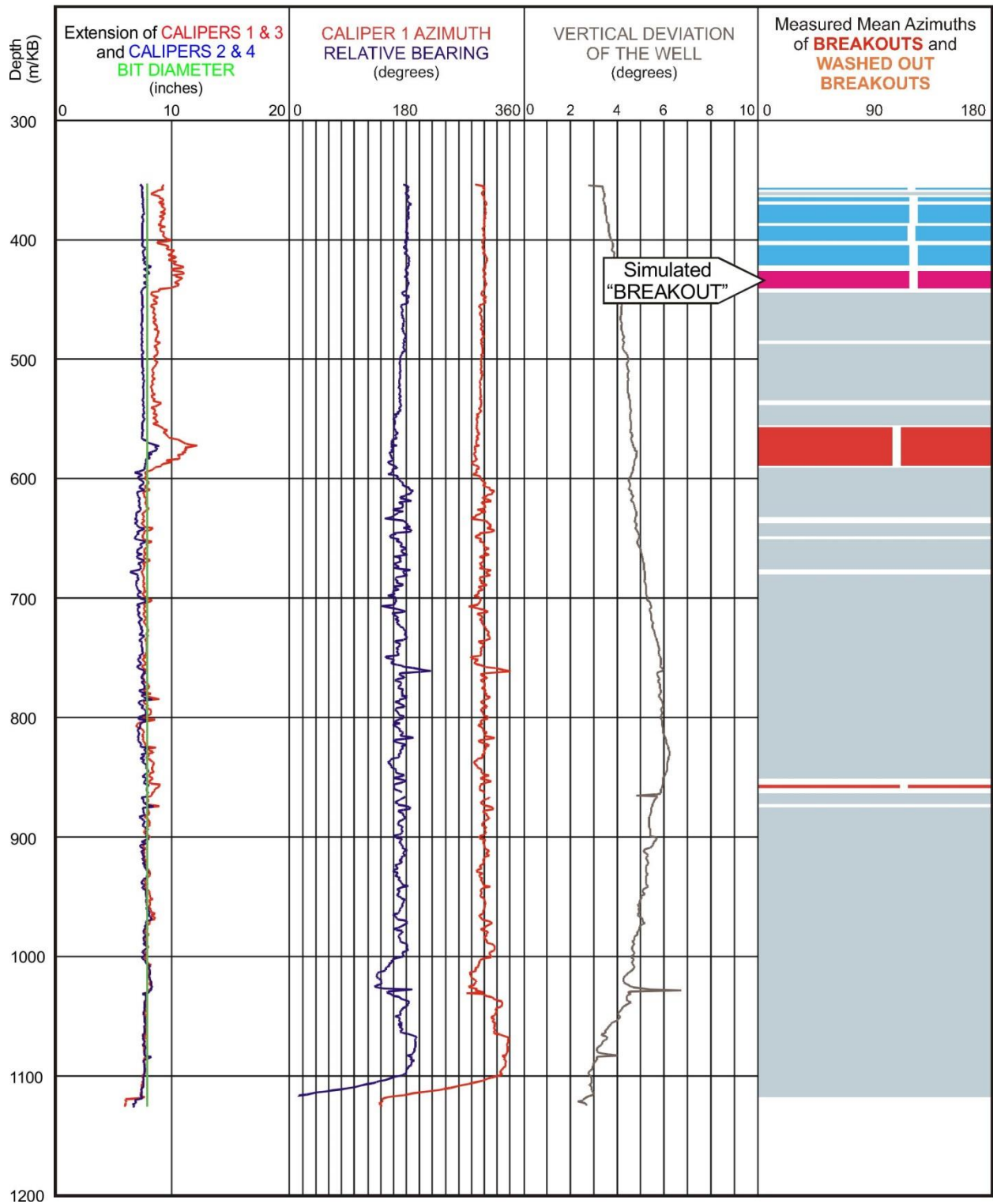
Well: <b>C-024-H/094-O-16</b>	Failure simulation Method				2SHmin-Po
	Mohr Coulomb	Drucker Prager	Modified Strain Energy	3 cycle Mohr Coulomb	
Breakout Interval Top (m KB)	426	426	426	426	
Breakout Interval Base (m KB)	444	444	444	444	
Median depth of Breakout (m KB)	435	435	435	435	
Calipers 1 and 3 extent (inches)	10.26	10.26	10.26	10.26	
Calipers 2 and 4 extent (inches)	7.79	7.79	7.79	7.79	
SHmax (MPa)	15.6*	18.5*	16.6*	<b>12.2</b>	10.9
SHmax gradient (kPa/m)	35.9	42.5	38.2	28.0	25.1
SHmin (MPa)	7.6	7.6	7.6	7.6	
Sv (MPa)	10.7	10.7	10.7	10.7	
Pore Pressure (MPa)	4.3	4.3	4.3	4.3	
Mudweight (MPa)	4.3	4.3	4.3	4.3	
u (Coefficient of Friction)	0.6	0.6	0.6	0.6	
Cohesive Strength of Rock (MPa)	3.0	3.0	3.0	3.0	
v (Poisson's Ratio)	0.2	0.2	0.2	0.2	
Bit size (inches)	7.875	7.875	7.875	7.875	

\* indicates that modelling could not simulate accurate breakout anisotropy

The interval selected for modelling runs from 426 m to 444 m. The PFAS software identifies this zone, as well as the section above it, as key seats. This is because the well's directional azimuth corresponds with the long axes of these lateral extensions of the borehole. In fact, key seats of the observed dimensions are unlikely features to form at the top of a vertically drilled interval, since they typically characterise highly inclined sections of wells. Furthermore, the long axes of the interpreted "keyseats" in well C-024-H/094-O-16 are essentially identical with the long axes of bona fide breakouts deeper in the well. Therefore, interval 426-444 m is most probably a genuine breakout and was judged suitable for simulation.

The breakout could not be simulated with any of the three single cycle methods, with the cohesive strength set at 3 MPa. The simulations did not generate sufficiently deep breakouts, the maximum depth that was achieved was 9.4 inches, with the Mohr Coulomb routine. On the other hand, the 3 Cycle Mohr-Coulomb simulation modelled a breakout with long axis of 10.2 inches when the cohesive strength was set at 3 MPa. The resulting  $S_{Hmax}$  magnitude of **12.2 MPa** is slightly higher than the 10.9 MPa magnitude suggested by the equation:  $S_{Hmax} = 2(S_{Hmin}) - P_o$ .

WELL : C-024-H/094-O-16 BREAKOUT ANALYSIS

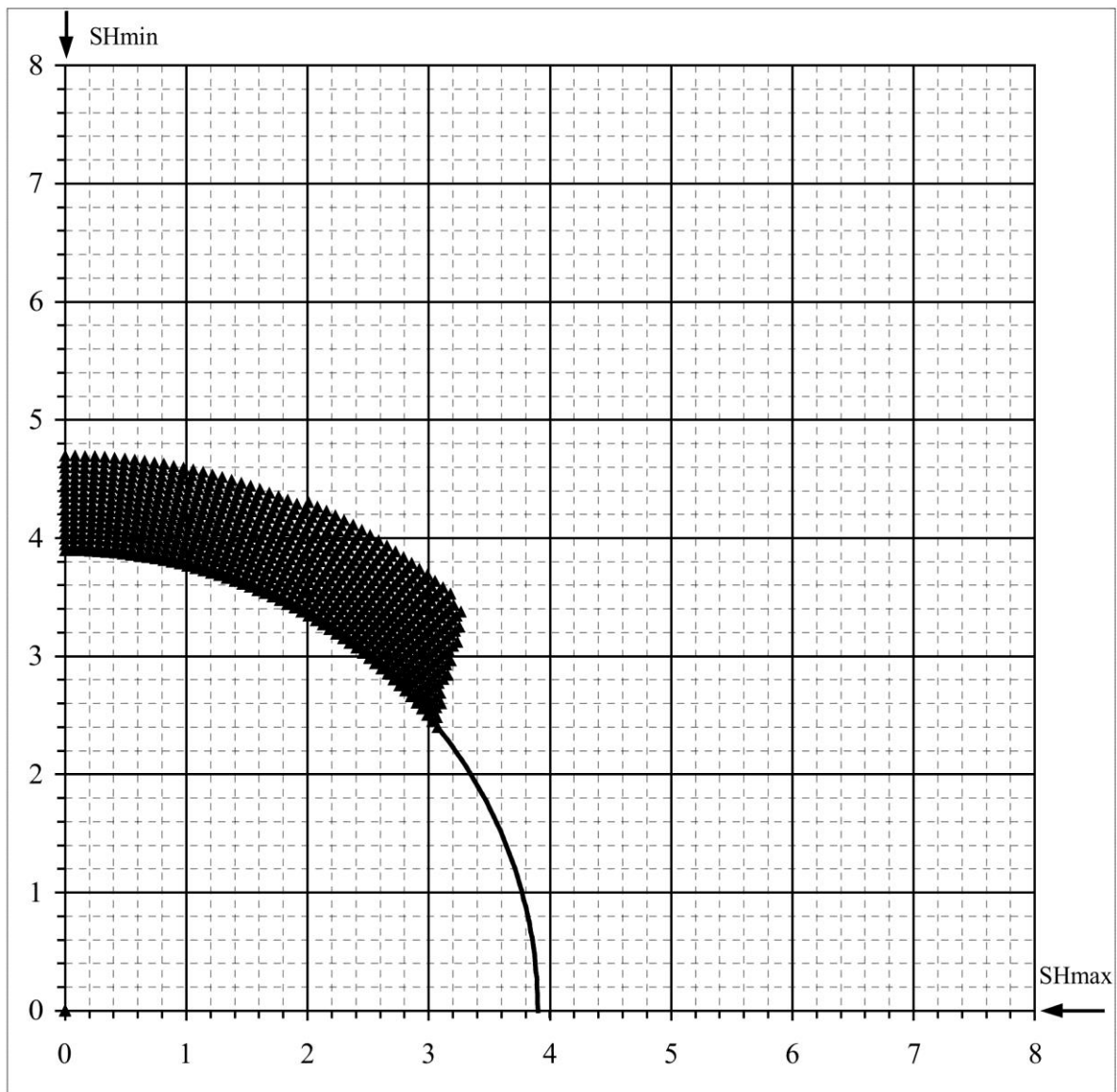




C-024-H/94-O-16

## Mohr - Coulomb Failure Criterion

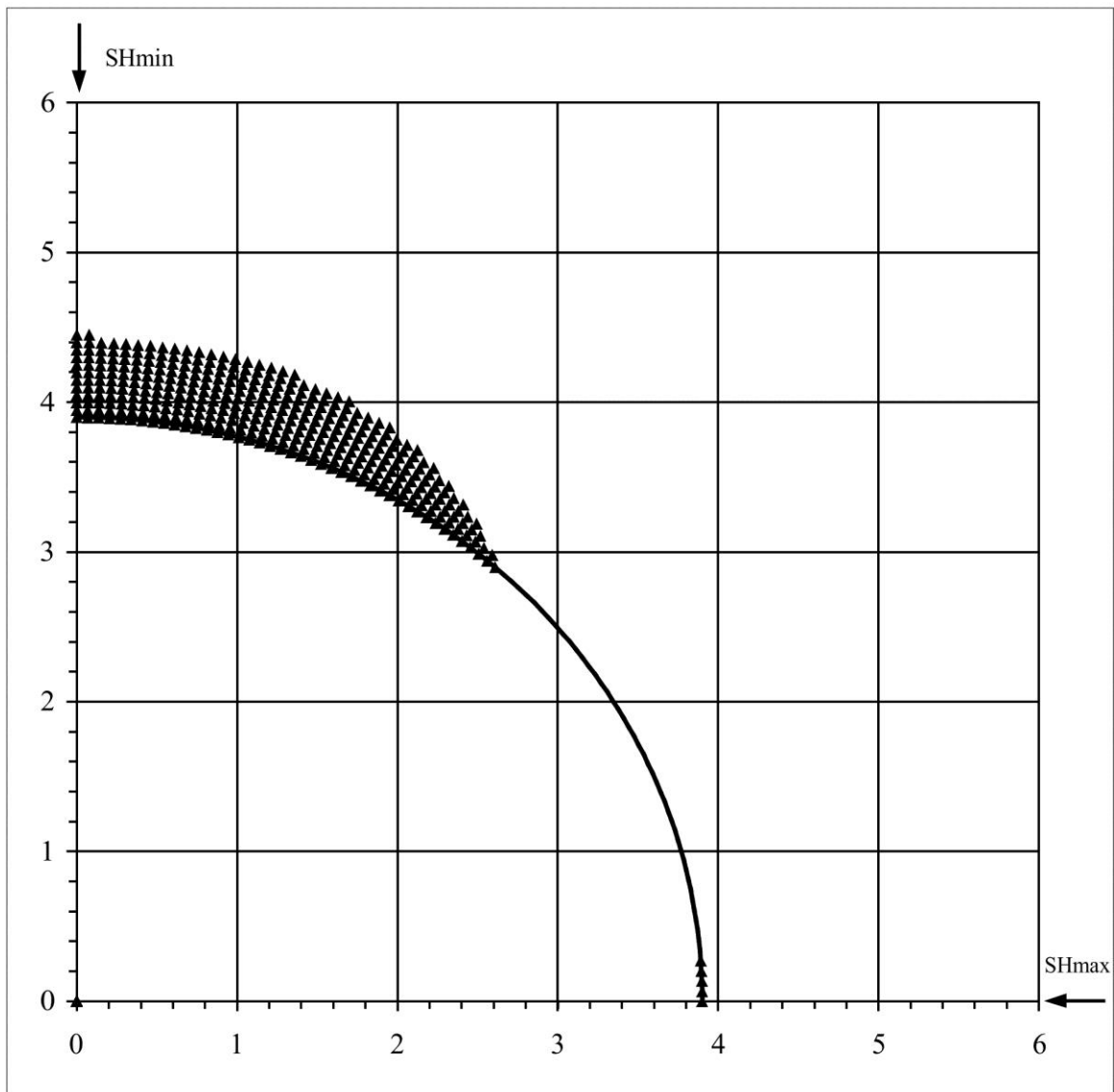
SHmax =	15.6 MPa	u (Coeff. of Friction) =	0.6
SHmin =	7.6 MPa	C (Cohesive Strength) =	3 MPa
Sv =	10.7 MPa	v (Poisson's Ratio) =	0.2
Po (Pore Pressure) =	4.3 MPa	Diameter of Borehole =	7.8 "
Pm (Mud Weight) =	4.3 MPa		
Sensitivity of Figure =	0.05 "	Angle of Max. Breakout =	55 deg
Depth of Max. Breakout =	0.85 "	Max caliper at 90 deg =	9.4 "
Validity of the results =	TRUE	Max caliper at 0 deg =	8 "



C-024H/094-O-16

## Extended von-Mises Failure Criterion (Drucker-Prager Failure Criterion)

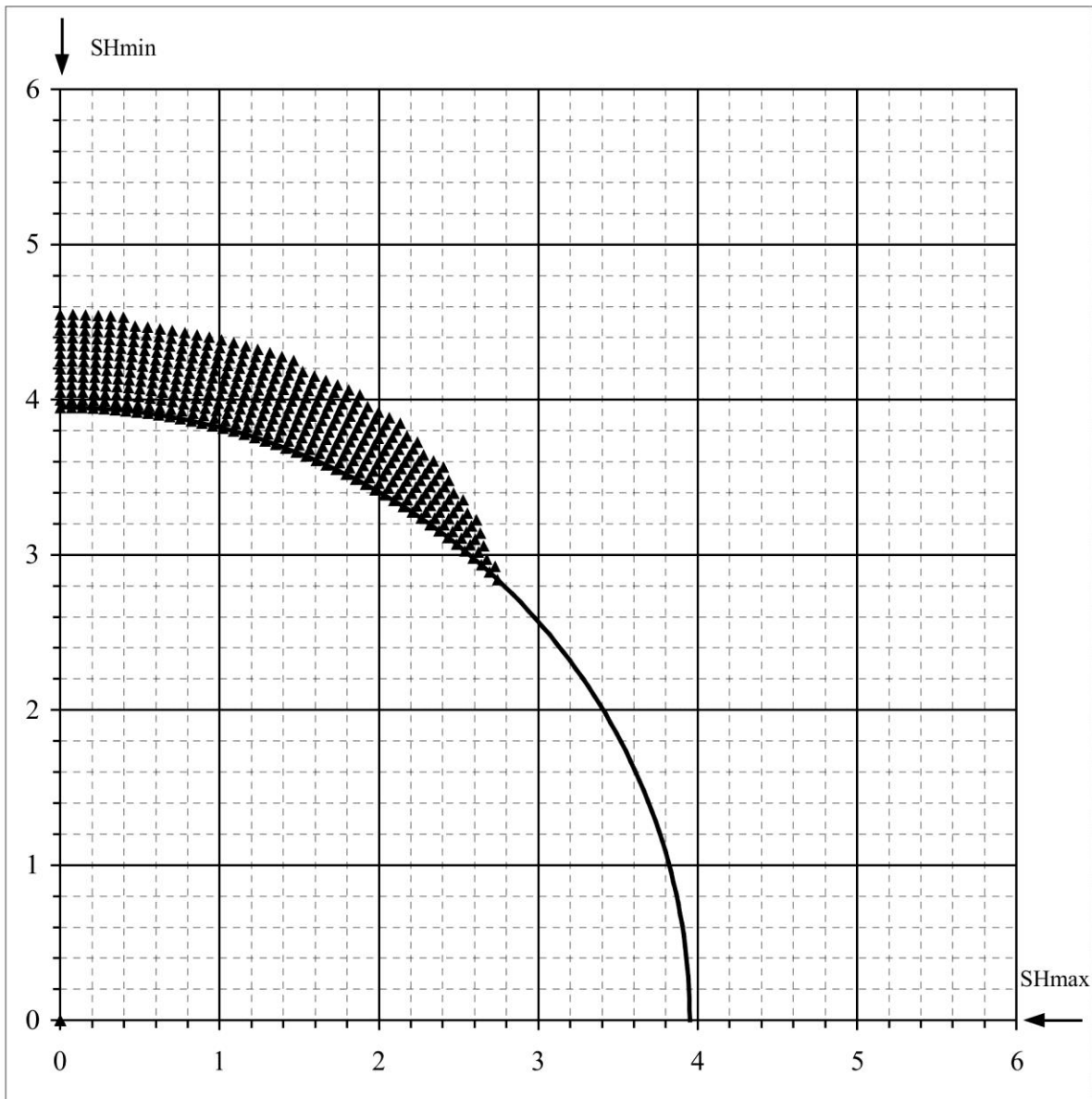
SHmax =	18.5 MPa	u (Coeff. of Friction) =	0.6
SHmin =	7.6 MPa	C (Cohesive Strength) =	3 MPa
Sv =	10.7 MPa	$\nu$ (Poisson's Ratio) =	0.2
Po (Pore Pressure) =	4.3 MPa	Diameter of Borehole =	7.8 inches
Pm (Mud Weight) =	4.3 MPa	Depth of Max. Breakout =	0.55 inches
Sensitivity of Figure =	0.05 inches	Angle of Max. Breakout =	90 deg



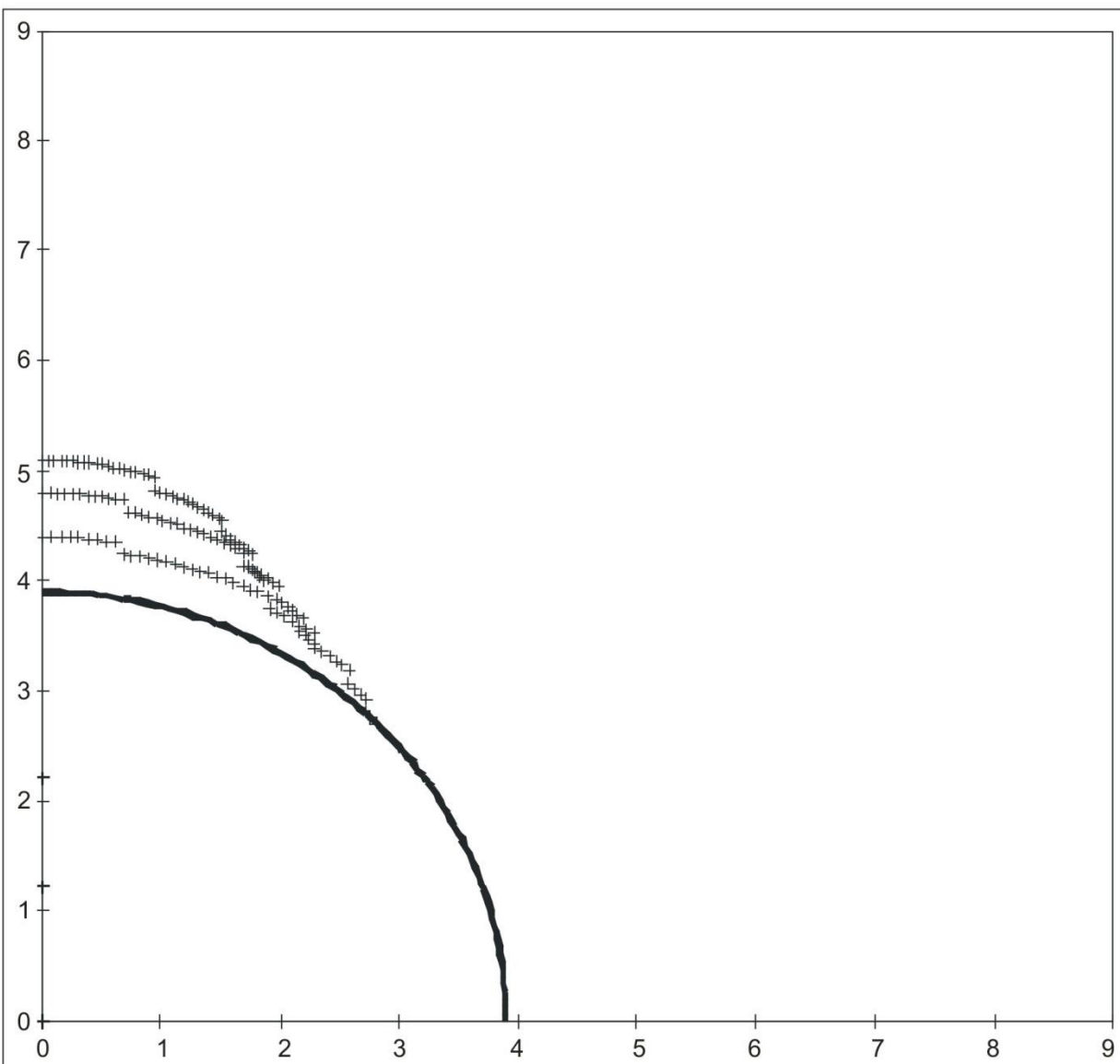
C-024-H/094-O-16

## Extended Drucker - Prager Failure Criterion (Modified Strain Energy Criterion)

SHmax =	16.6 MPa	u (Coeff. of Friction) =	0.6
SHmin =	7.6 MPa	C (Cohesive Strength) =	3 MPa
Sv =	10.7 MPa	v (Poisson's Ratio) =	0.2
Po (Pore Pressure) =	4.3 MPa	Radius of Borehole =	7.9 inches
Pm (Mud Weight) =	4.3 MPa	Depth of Max. Breakout =	0.6 inches
Sensitivity of Figure =	0.05 inches	Angle of Max. Breakout =	90 deg



C-024-H/094-O-16					
<b>3 Cycle Mohr - Coulomb Failure Criterion</b>					
SHmax =	12.2	MPa	u (Coeff. of Friction) =	0.6	
SHmin =	7.6	MPa	C (Cohesive Strength) =	3	MPa
Sv =	10.7	MPa	v (Poisson's Ratio) =	0.2	
Po (Pore Pressure) =	4.3	MPa	Diameter of Borehole =	7.8	"
Pm (Mud Weight) =	4.3	MPa			
Sensitivity of Figure =	0.05	"			
Depth of Max. Breakout =	1.2	"	Max caliper at 90 deg =	10.2	"
Validity of the results =	TRUE		Max caliper at 0 deg =	7.8	"



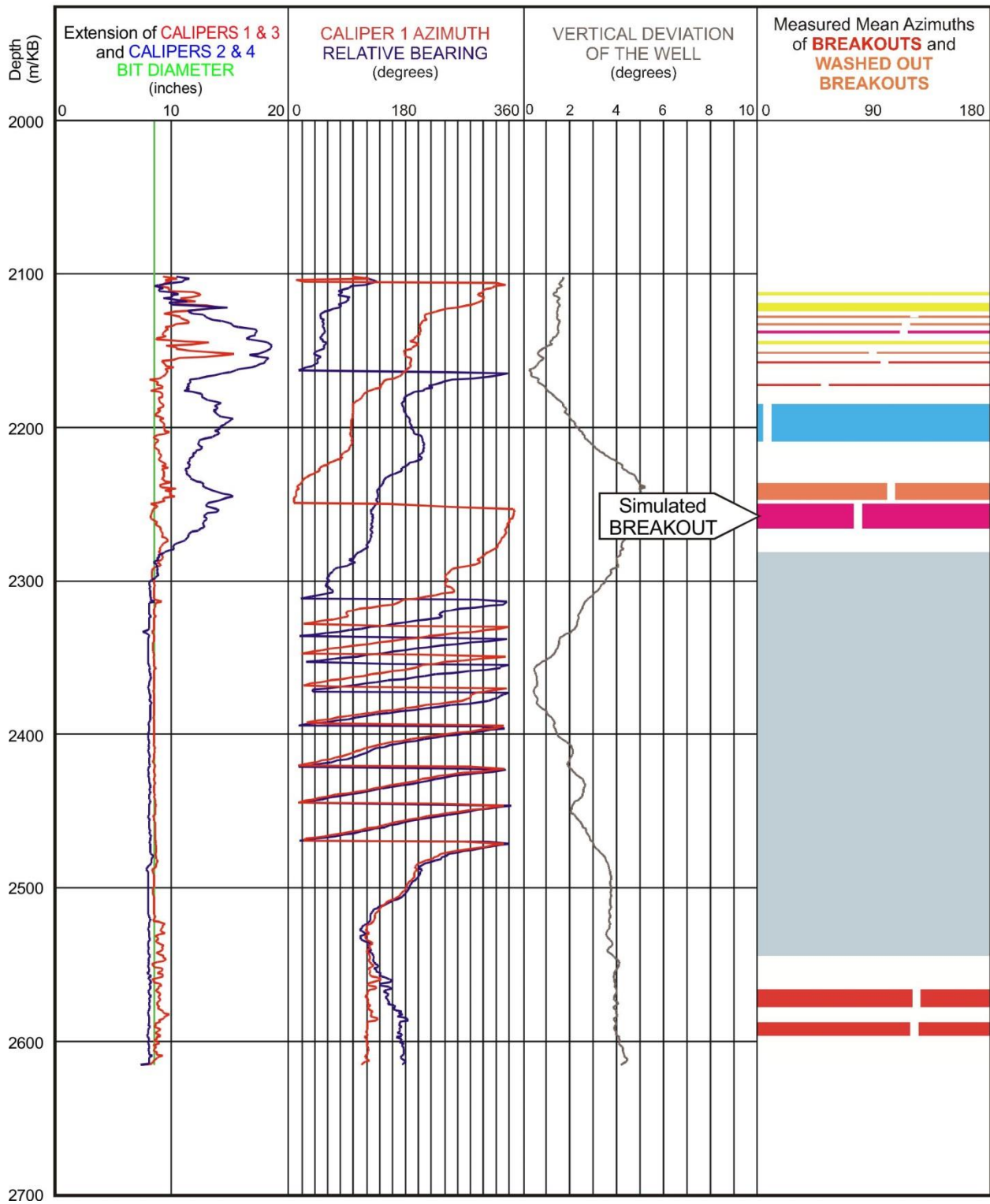
## $S_{Hmax}$ Simulation Commentary – C-028-H/094-O-16

Well: C-028-H/094-O-16	Failure simulation Method				2SHmin-Po
	Mohr Coulomb	Drucker Prager	Modified Strain Energy	3 cycle Mohr Coulomb	
Breakout Interval Top (m KB)	2250	2250	2250	2250	
Breakout Interval Base (m KB)	2266	2266	2266	2266	
Median depth of Breakout (m KB)	2258	2258	2258	2258	
Calipers 1 and 3 extent (inches)	8.58	8.58	8.58	8.58	
Calipers 2 and 4 extent (inches)	13.02	13.02	13.02	13.02	
SHmax (MPa)	64.7*	83.4*	78.1*	<b>58.5</b>	56.0
SHmax gradient (kPa/m)	28.7	36.9	34.6	25.9	24.8
SHmin (MPa)	39.3	39.3	39.3	39.3	
Sv (MPa)	55.8	55.8	55.8	55.8	
Pore Pressure (MPa)	22.6	22.6	22.6	22.6	
Mudweight (MPa)	22.6	22.6	22.6	22.6	
u (Coefficient of Friction)	0.6	0.6	0.6	0.6	
Cohesive Strength of Rock (MPa)	9.0	9.0	9.0	9.0	
v (Poisson's Ratio)	0.2	0.2	0.2	0.2	
Bit size (inches)	8.50	8.50	8.50	8.50	

\* indicates that modelling could not simulate accurate breakout anisotropy

The breakout could not be simulated with any of the three single cycle methods, with the cohesive strength set at 9 MPa. The single cycle simulations did not come close to generating sufficiently deep breakouts, but the 3 cycle Mohr-Coulomb simulation modelled a breakout with the appropriate depth of 13.0 inches with  $S_{Hmax}$  set at **58.5 MPa**. This is regarded as a satisfactory magnitude estimate of  $S_{Hmax}$  since it is close to the value of 56.0 MPa suggested by the equation  $S_{Hmax} = 2(S_{Hmin}) - Po$ .

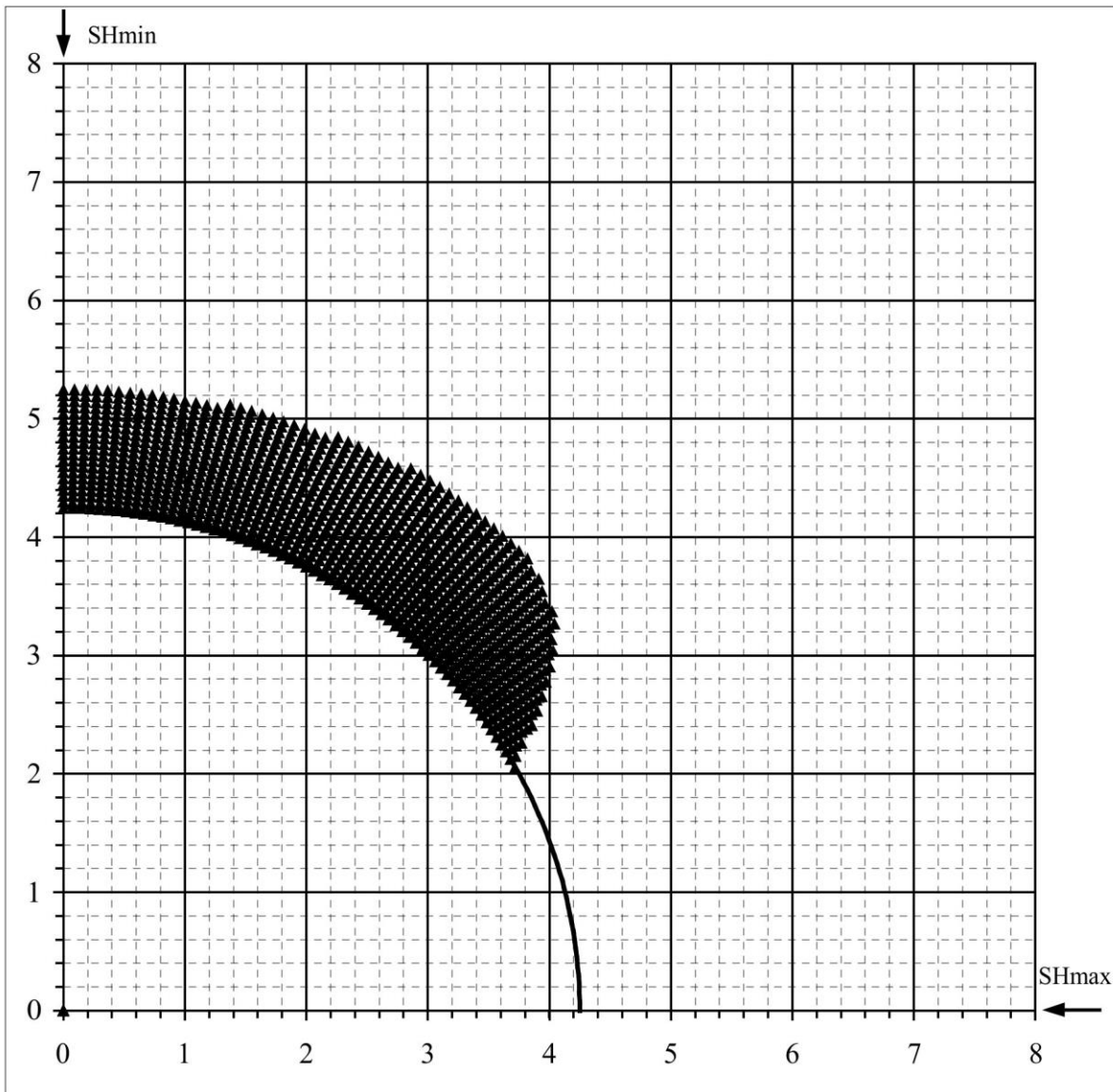
WELL : C-028-H/094-O-16 BREAKOUT ANALYSIS



C-028-H/094-O-16

### Mohr - Coulomb Failure Criterion

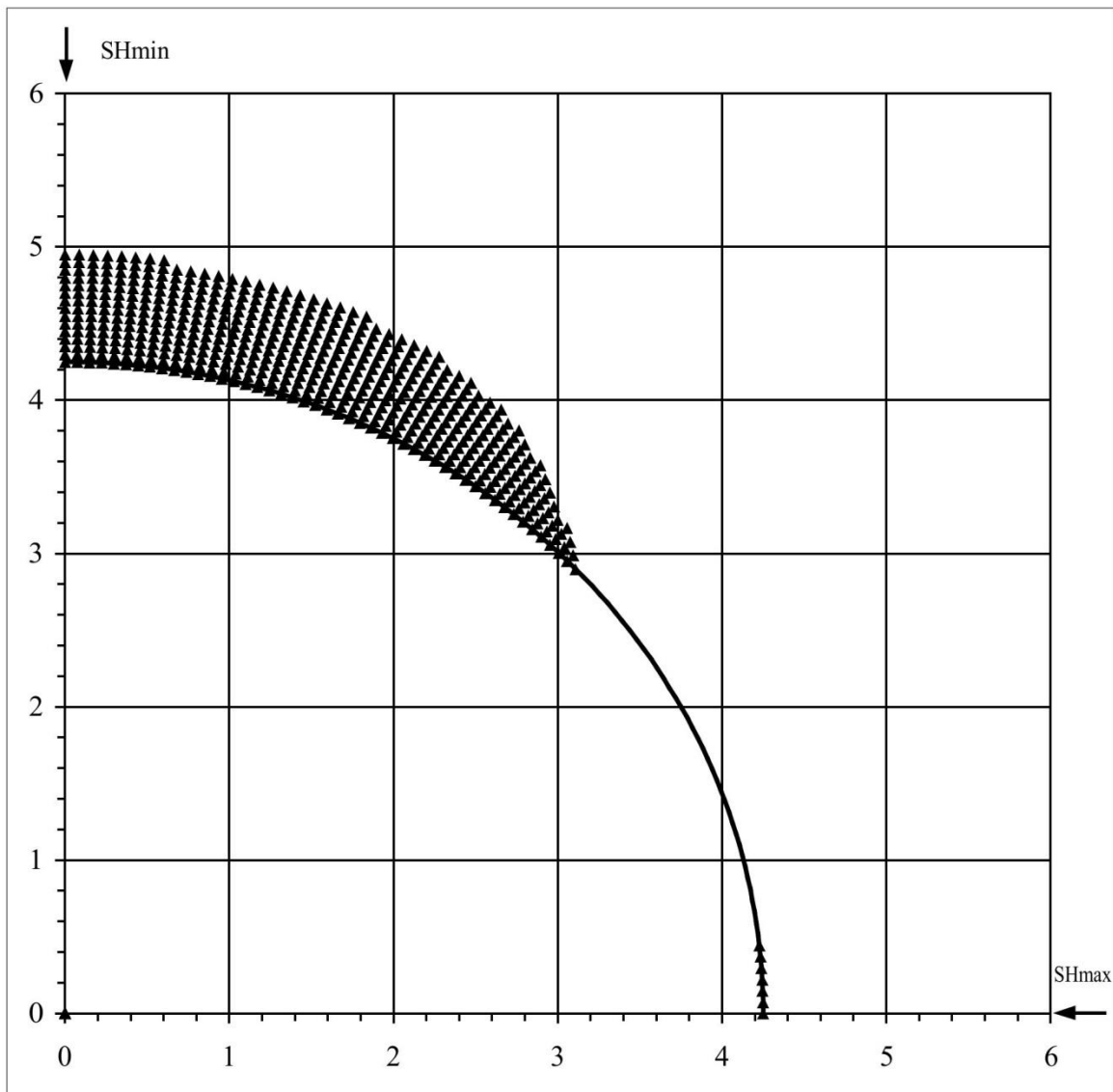
SHmax =	64.7 MPa	u (Coeff. of Friction) =	0.6
SHmin =	39.3 MPa	C (Cohesive Strength) =	9 MPa
Sv =	55.8 MPa	v (Poisson's Ratio) =	0.2
Po (Pore Pressure) =	22.6 MPa	Diameter of Borehole =	8.5 "
Pm (Mud Weight) =	22.6 MPa		
Sensitivity of Figure =	0.05 "	Angle of Max. Breakout =	51 deg
Depth of Max. Breakout =	1.15 "	Max caliper at 90 deg =	10.5 "
Validity of the results =	TRUE	Max caliper at 0 deg =	8 "



C-028-H/094-O-16

## Extended von-Mises Failure Criterion (Drucker-Prager Failure Criterion)

SHmax =	83.4 MPa	u (Coeff. of Friction) =	0.6
SHmin =	39.3 MPa	C (Cohesive Strength) =	9 MPa
Sv =	55.8 MPa	v (Poisson's Ratio) =	0.2
Po (Pore Pressure) =	22.6 MPa	Diameter of Borehole =	8.5 inches
Pm (Mud Weight) =	22.6 MPa	Depth of Max. Breakout =	0.7 inches
Sensitivity of Figure =	0.05 inches	Angle of Max. Breakout =	90 deg

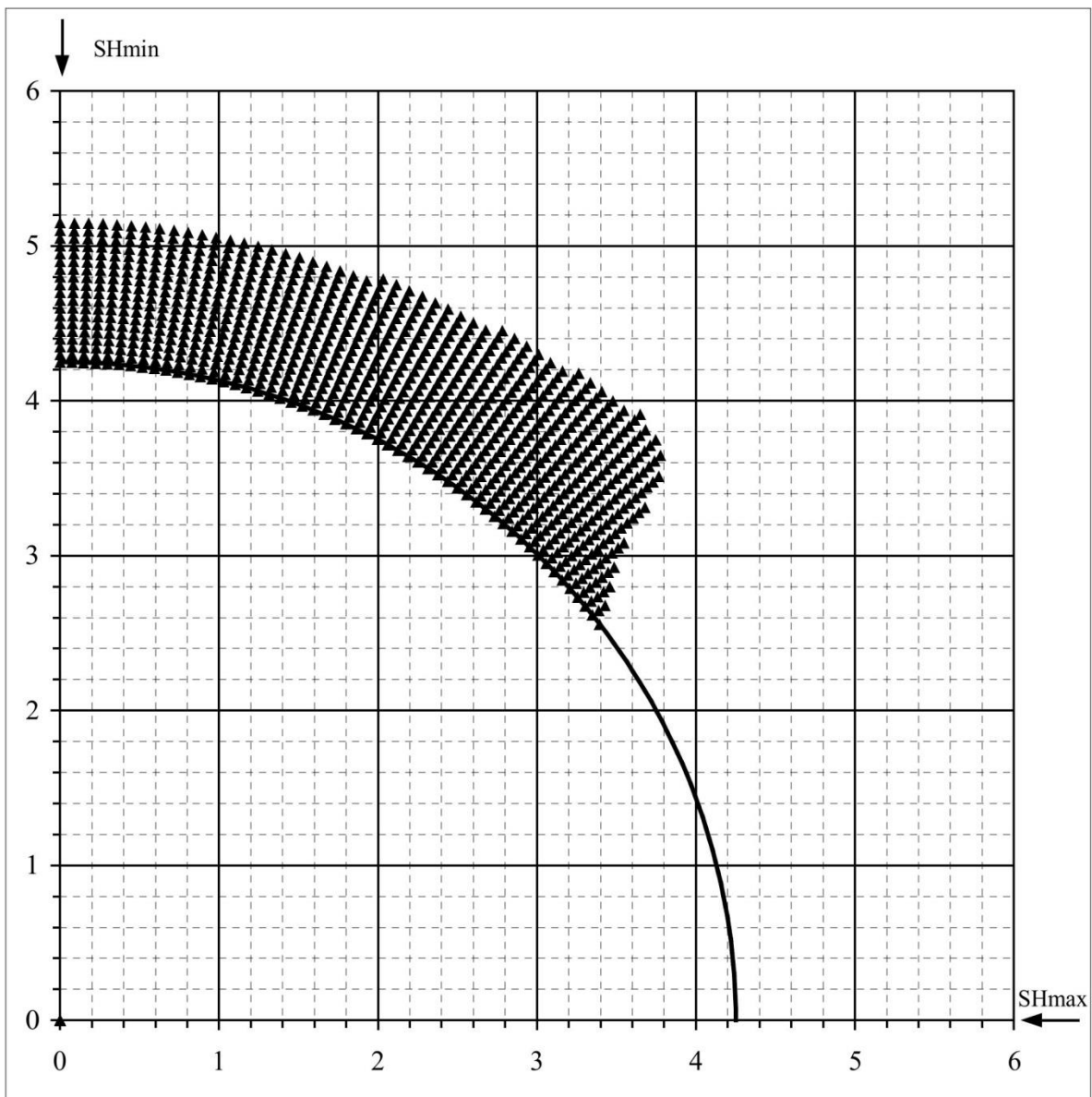




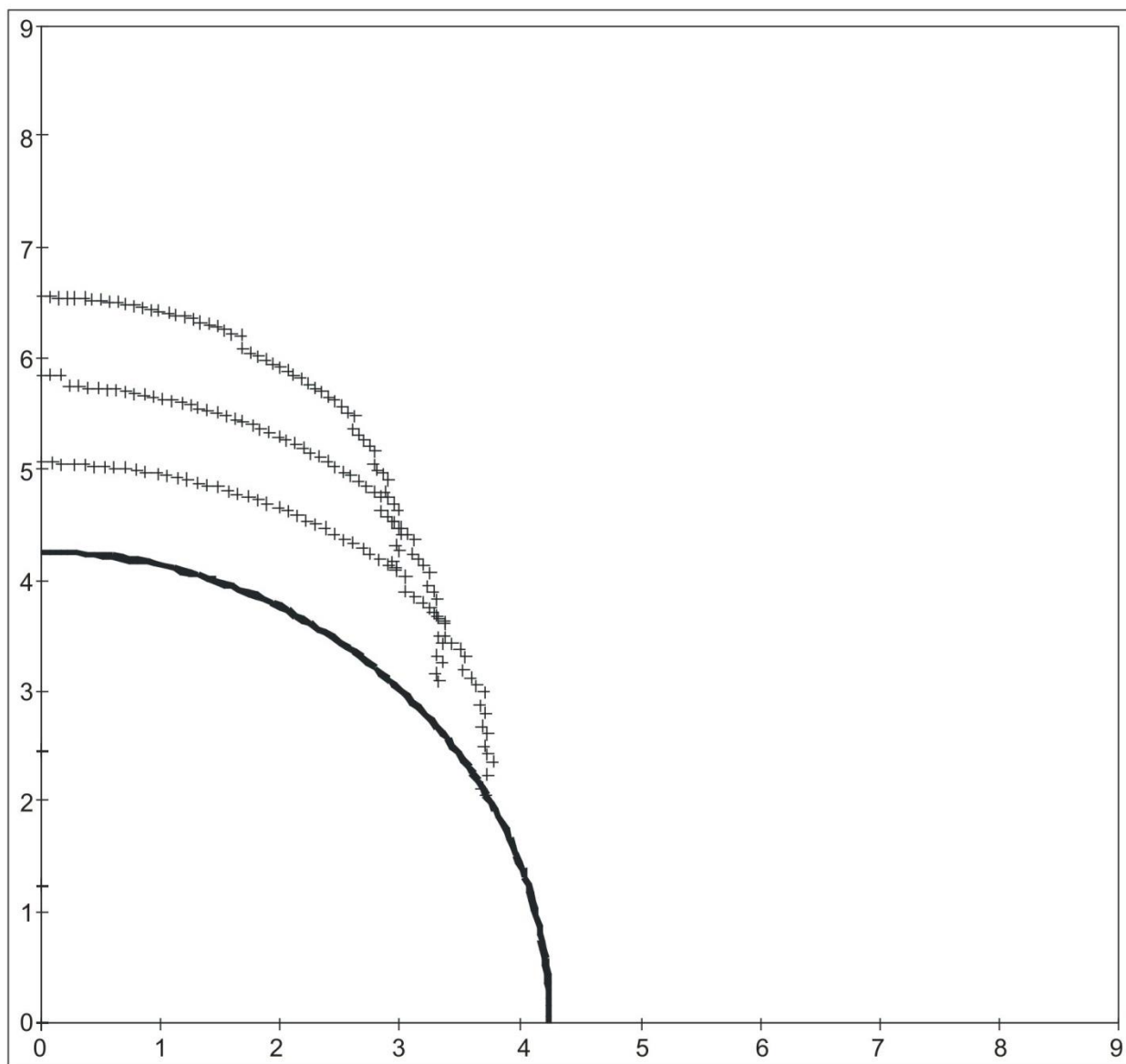
C-028-H/094-O-16

## Extended Drucker - Prager Failure Criterion (Modified Strain Energy Criterion)

SHmax =	78.1 MPa	u (Coeff. of Friction) =	0.6
SHmin =	39.3 MPa	C (Cohesive Strength) =	9 MPa
Sv =	55.8 MPa	v (Poisson's Ratio) =	0.2
Po (Pore Pressure) =	22.6 MPa	Radius of Borehole =	8.5 inches
Pm (Mud Weight) =	22.6 MPa	Depth of Max. Breakout =	1.1 inches
Sensitivity of Figure =	0.05 inches	Angle of Max. Breakout =	47 deg



C-028-H/094-O-16					
3 Cycle Mohr - Coulomb Failure Criterion					
SHmax =	58.5	MPa	u (Coeff. of Friction) =	0.6	
SHmin =	39.3	MPa	C (Cohesive Strength) =	9	MPa
Sv =	55.8	MPa	v (Poisson's Ratio) =	0.2	
Po (Pore Pressure) =	22	MPa	Diameter of Borehole =	8.5	"
Pm (Mud Weight) =	22.6	MPa			
Sensitivity of Figure =	0.05	"			
Depth of Max. Breakout =	2.25	"	Max caliper at 90 deg =	13	"
Validity of the results =	TRUE		Max caliper at 0 deg =	8.5	"



**SHmax Simulation Commentary – C-054-K/094-N-16**

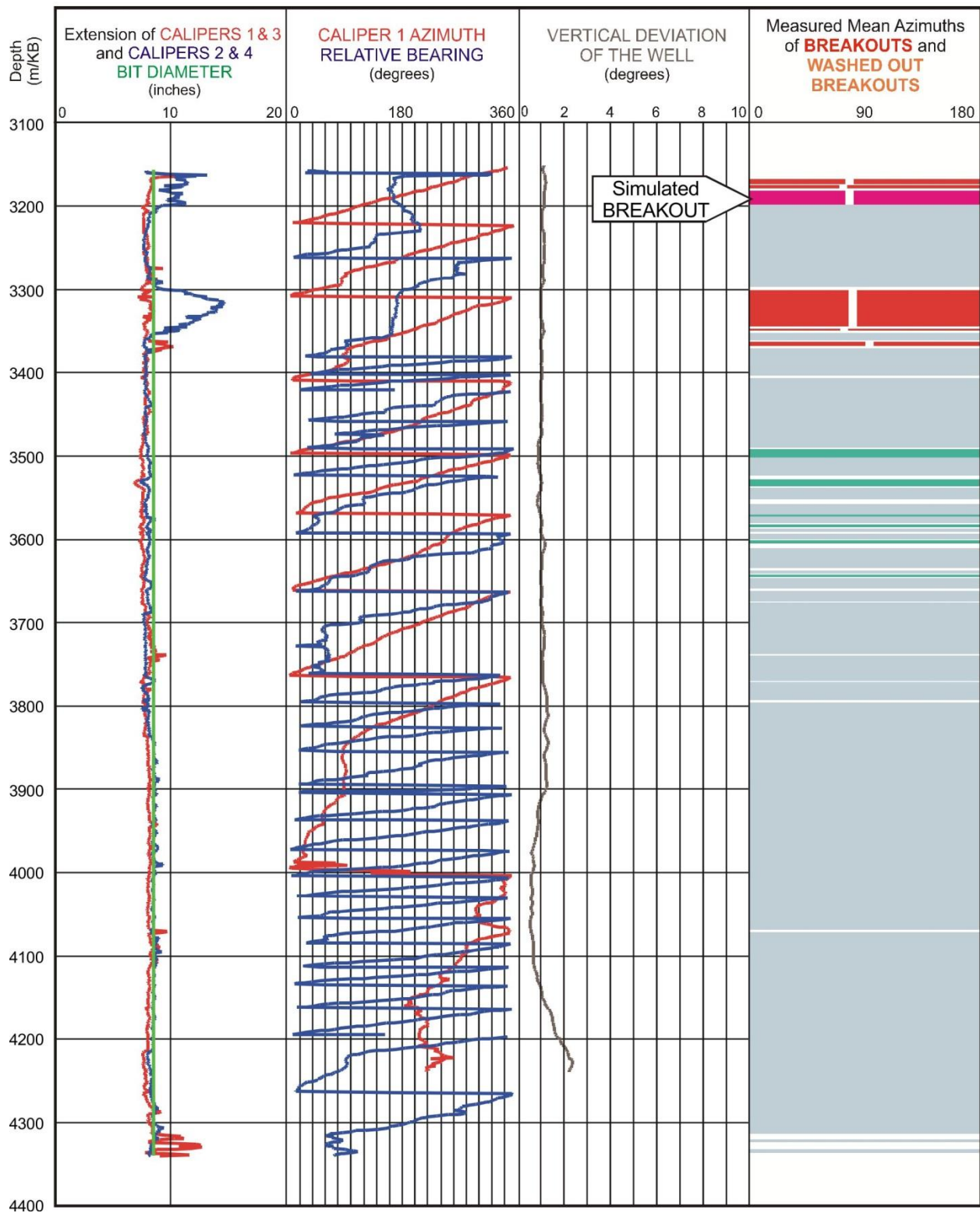
Well: <b>C-054-K/094-N-16</b>	Failure simulation Method				2SHmin-Po
	Mohr Coulomb	Drucker Prager	Modified Strain Energy	3 cycle Mohr Coulomb	
Breakout Interval Top (m KB)	3182	3182	3182	3182	
Breakout Interval Base (m KB)	3198	3198	3198	3198	
Median depth of Breakout (m KB)	3190	3190	3190	3190	
Calipers 1 and 3 extent (inches)	8.08	8.08	8.08	8.08	
Calipers 2 and 4 extent (inches)	10.42	10.42	10.42	10.42	
SHmax (MPa)	<b>84.8</b>	124.0*	107.6		83.5
SHmax gradient (kPa/m)	26.6	38.9	33.7		26.2
SHmin (MPa)	57.7	57.7	57.7	57.7	
Sv (MPa)	78.8	78.8	78.8	78.8	
Pore Pressure (MPa)	31.9	31.9	31.9	31.9	
Mudweight (MPa)	31.9	31.9	31.9	31.9	
u (Coefficient of Friction)	0.6	0.6	0.6	0.6	
Cohesive Strength of Rock (MPa)	12	12	12	12	
v (Poisson's Ratio)	0.2	0.2	0.2	0.2	
Bit size (inches)	8.5	8.5	8.5	8.5	

\* indicates that modelling could not simulate complete breakout anisotropy

The selected breakout in well C-054-K-/094-N-16 was satisfactorily modelled with the Mohr Coulomb and Modified Strain Energy routines. However, the Drucker-Prager failure criterion failed to generate a breakout deeper than 10.1 inches. The Mohr Coulomb failure simulation, with the cohesive strength set at 12 MPa, gave **84.8 MPa** as the  $S_{Hmax}$  magnitude, which is close to the value of 83.5 MPa suggested by  $2S_{Hmin} - P_o$ .

The  $S_{Hmax}$  magnitude at 3190 m in well C-054-K-/094-N-16 is interpreted to be 84.8 MPa.

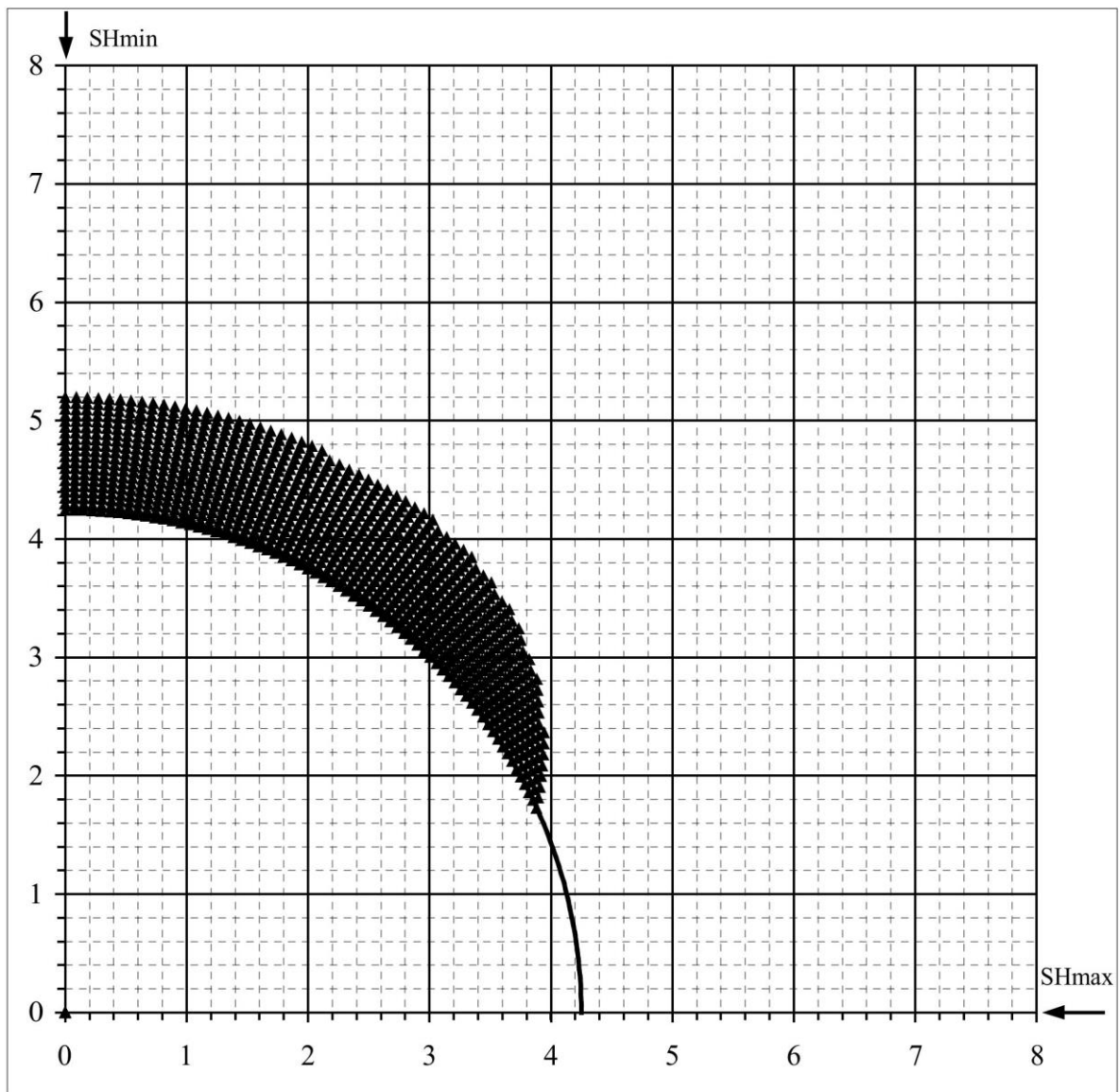
WELL : C-054-K/094-N-16 BREAKOUT ANALYSIS



C-054-K/094-N-16

## Mohr - Coulomb Failure Criterion

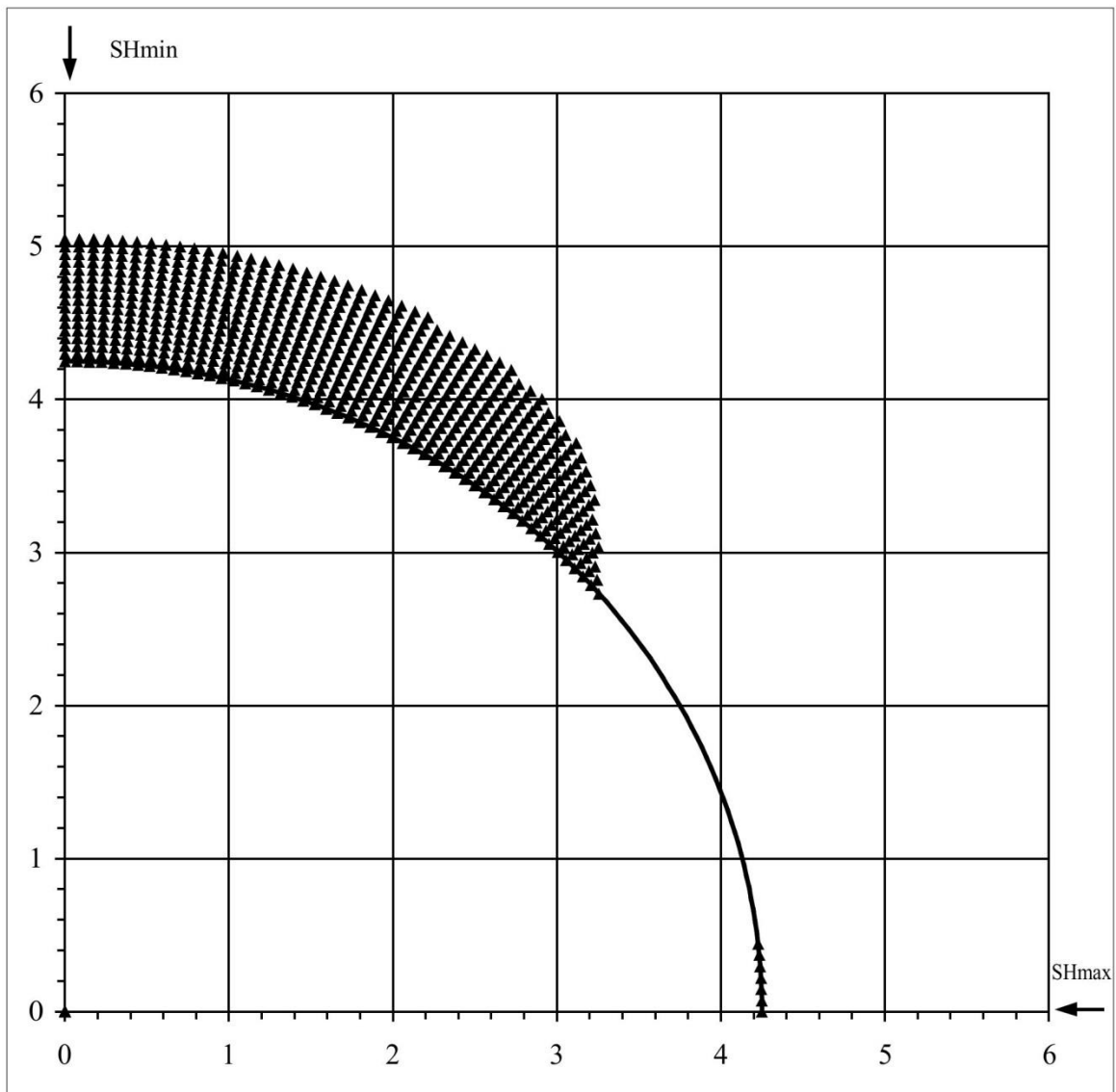
SHmax =	84.8 MPa	u (Coeff. of Friction) =	0.6
SHmin =	57.7 MPa	C (Cohesive Strength) =	12 MPa
Sv =	78.8 MPa	v (Poisson's Ratio) =	0.2
Po (Pore Pressure) =	31.9 MPa	Diameter of Borehole =	8.5 "
Pm (Mud Weight) =	31.9 MPa		
Sensitivity of Figure =	0.05 "	Angle of Max. Breakout =	74 deg
Depth of Max. Breakout =	0.95 "	Max caliper at 90 deg =	10.4 "
Validity of the results =	TRUE	Max caliper at 0 deg =	8 "



C-054-K/094-N-16

## Extended von-Mises Failure Criterion (Drucker-Prager Failure Criterion)

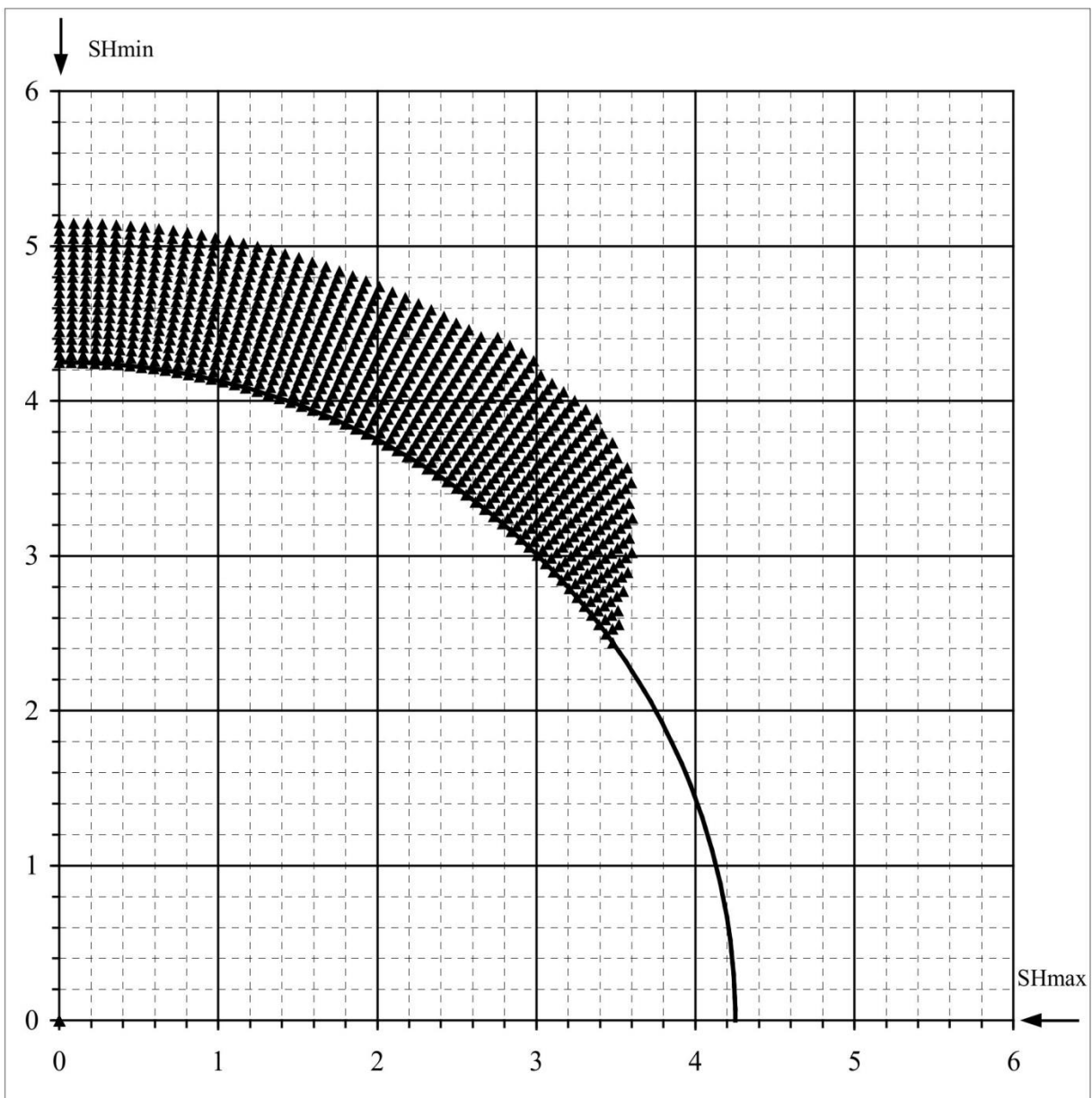
SHmax =	124 MPa	u (Coeff. of Friction) =	0.6
SHmin =	57.7 MPa	C (Cohesive Strength) =	12 MPa
Sv =	78.8 MPa	$\nu$ (Poisson's Ratio) =	0.2
Po (Pore Pressure) =	31.9 MPa	Diameter of Borehole =	8.5 inches
Pm (Mud Weight) =	31.9 MPa	Depth of Max. Breakout =	0.8 inches
Sensitivity of Figure =	0.05 inches	Angle of Max. Breakout =	74 deg



C-054-K/094-N-16

## Extended Drucker - Prager Failure Criterion (Modified Strain Energy Criterion)

SHmax =	107.6 MPa	u (Coeff. of Friction) =	0.6
SHmin =	57.7 MPa	C (Cohesive Strength) =	12 MPa
Sv =	78.8 MPa	v (Poisson's Ratio) =	0.2
Po (Pore Pressure) =	31.9 MPa	Radius of Borehole =	8.5 inches
Pm (Mud Weight) =	31.9 MPa	Depth of Max. Breakout =	0.95 inches
Sensitivity of Figure =	0.05 inches	Angle of Max. Breakout =	57 deg



## $S_{Hmax}$ Simulation Commentary – C-086-A/094-I-14

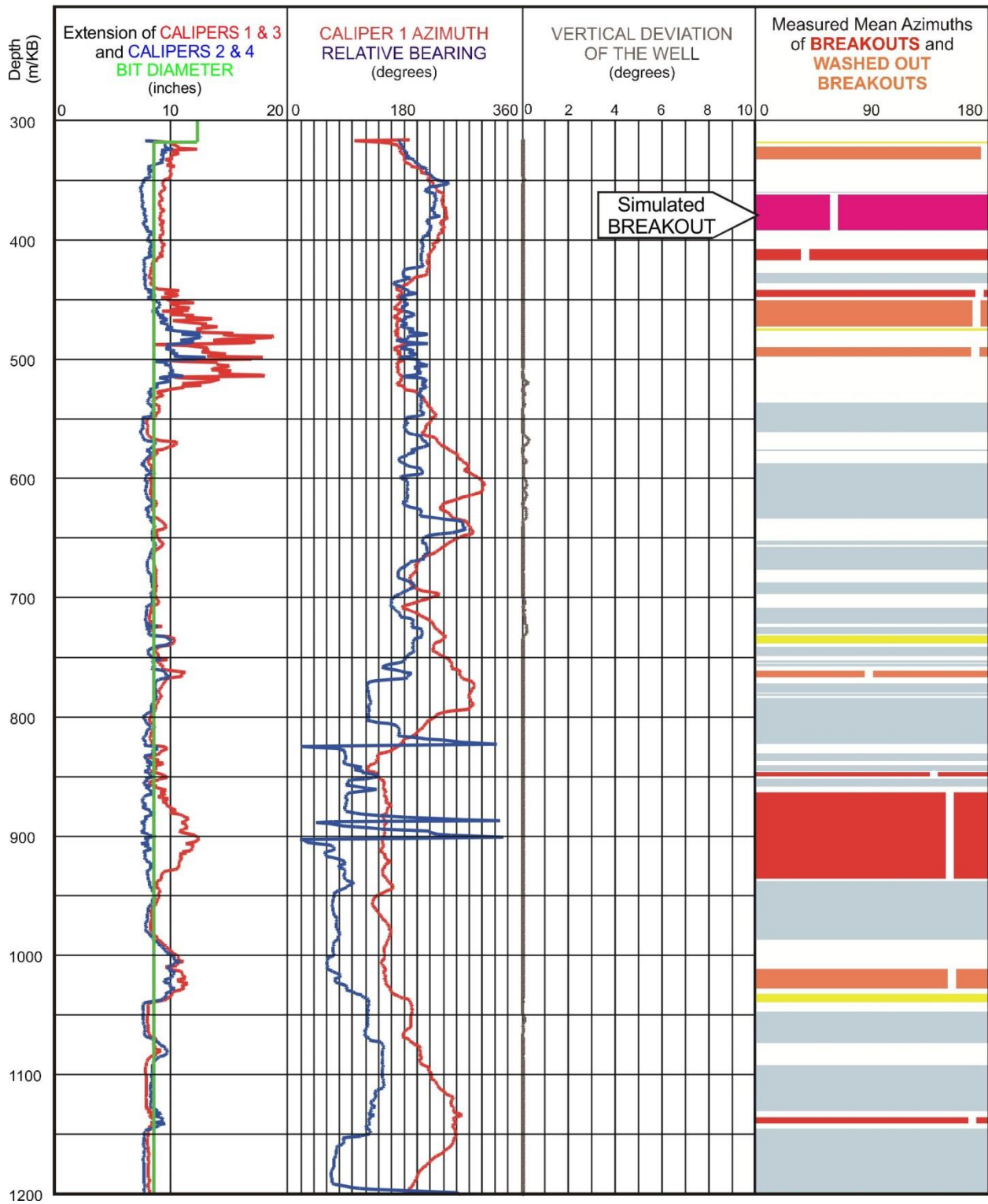
Well: C-086-A/094-I-14	Failure simulation Method				2SHmin-Po
	Mohr Coulomb	Drucker Prager	Modified Strain Energy	3 cycle Mohr Coulomb	
Breakout Interval Top (m KB)	363	363	363	363	
Breakout Interval Base (m KB)	393	393	393	393	
Median depth of Breakout (m KB)	378	378	378	378	
Calipers 1 and 3 extent (inches)	7.66	7.66	7.66	7.66	
Calipers 2 and 4 extent (inches)	9.09	9.09	9.09	9.09	
SHmax (MPa)	<b>12.4</b>	16.3	14.9		13.2
SHmax gradient (kPa/m)	32.8	43.1	39.4		34.9
SHmin (MPa)	8.5	8.5	8.5	8.5	
Sv (MPa)	8.5	8.5	8.5	8.5	
Pore Pressure (MPa)	3.8	3.8	3.8	3.8	
Mudweight (MPa)	3.8	3.8	3.8	3.8	
u (Coefficient of Friction)	0.6	0.6	0.6	0.6	
Cohesive Strength of Rock (MPa)	3.0	3.0	3.0	3.0	
v (Poisson's Ratio)	0.2	0.2	0.2	0.2	
Bit size (inches)	8.0	8.0	8.0	8.0	

The selected breakout in well C-086-A/094-I-14 was satisfactorily modelled with all three single cycle simulation routines.

The Mohr Coulomb failure simulation, with the cohesive strength set at 3 MPa, gave **12.4 MPa** as the  $S_{Hmax}$  magnitude, which is close to the value of 13.2 MPa suggested by the equation  $2S_{Hmin} - P_o$ .



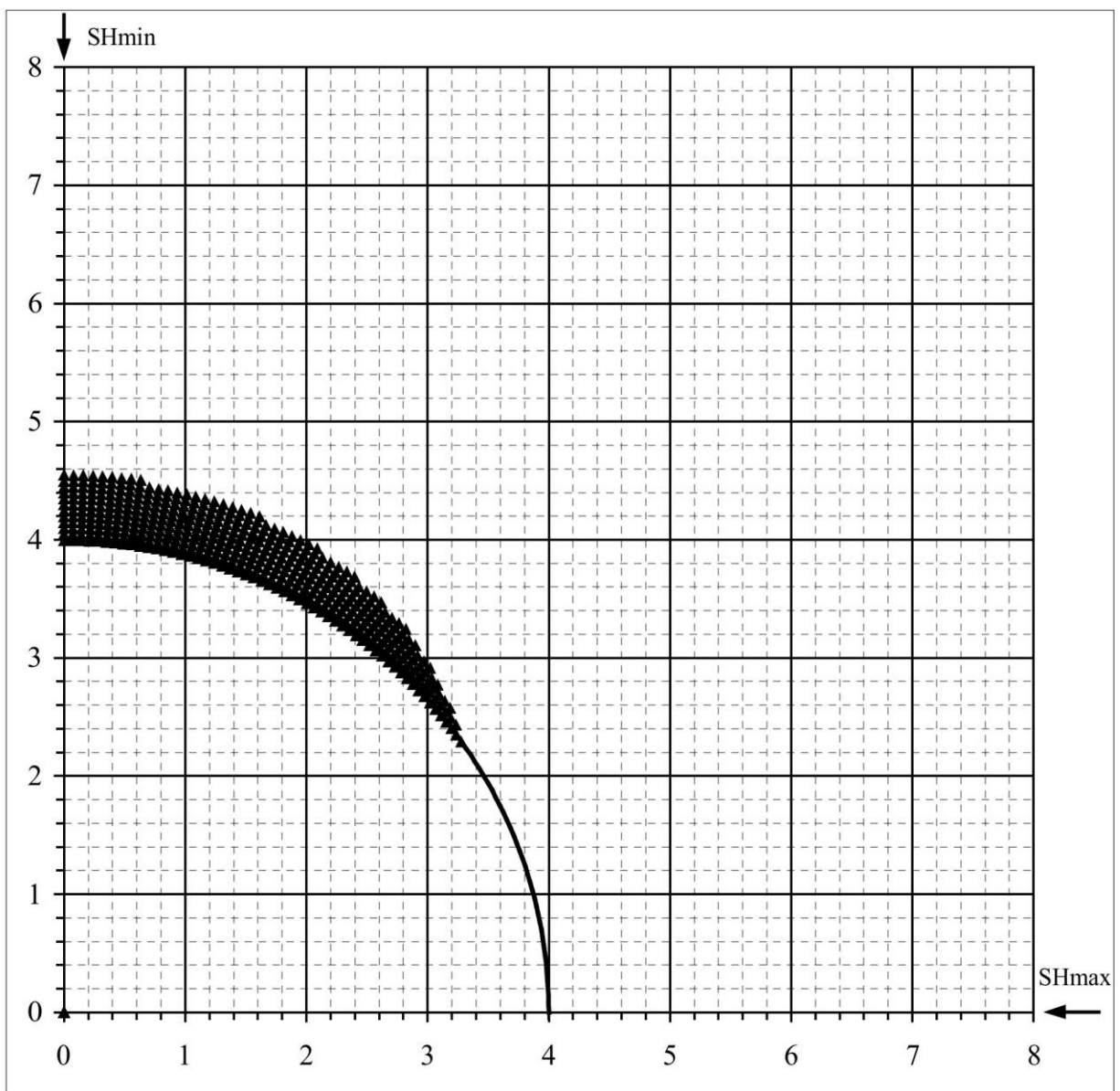
WELL : C-086-A/094-I-14 BREAKOUT ANALYSIS



C-086-A/094-I-14

## Mohr - Coulomb Failure Criterion

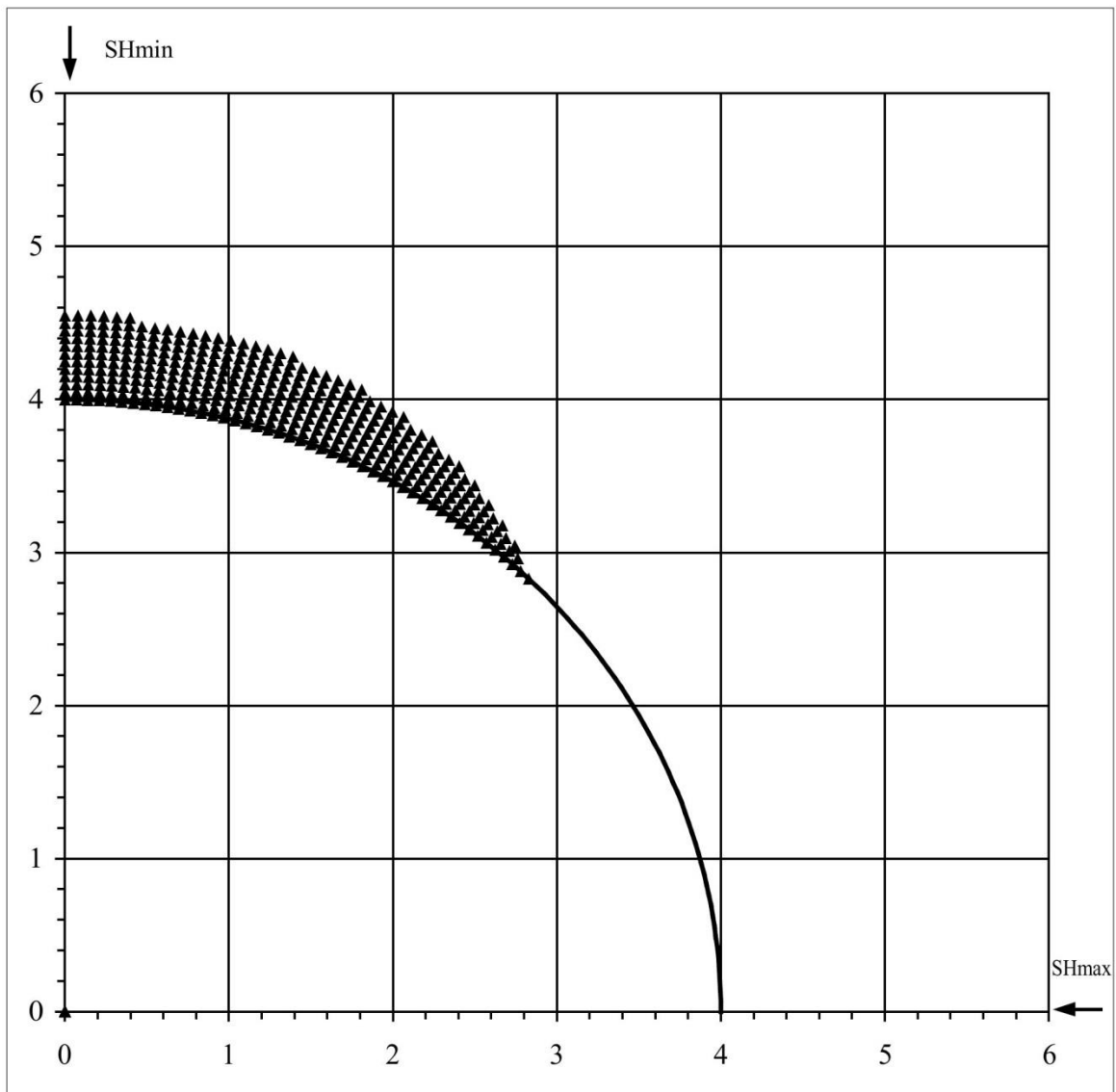
SHmax =	12.4 MPa	u (Coeff. of Friction) =	0.6
SHmin =	8.5 MPa	C (Cohesive Strength) =	3 MPa
Sv =	8.5 MPa	$\nu$ (Poisson's Ratio) =	0.2
Po (Pore Pressure) =	3.8 MPa	Diameter of Borehole =	8 "
Pm (Mud Weight) =	3.8 MPa		
Sensitivity of Figure =	0.05 "	Angle of Max. Breakout =	90 deg
Depth of Max. Breakout =	0.55 "	Max caliper at 90 deg =	9.1 "
Validity of the results =	TRUE	Max caliper at 0 deg =	8 "



C-086-A/094-I-14

## Extended von-Mises Failure Criterion (Drucker-Prager Failure Criterion)

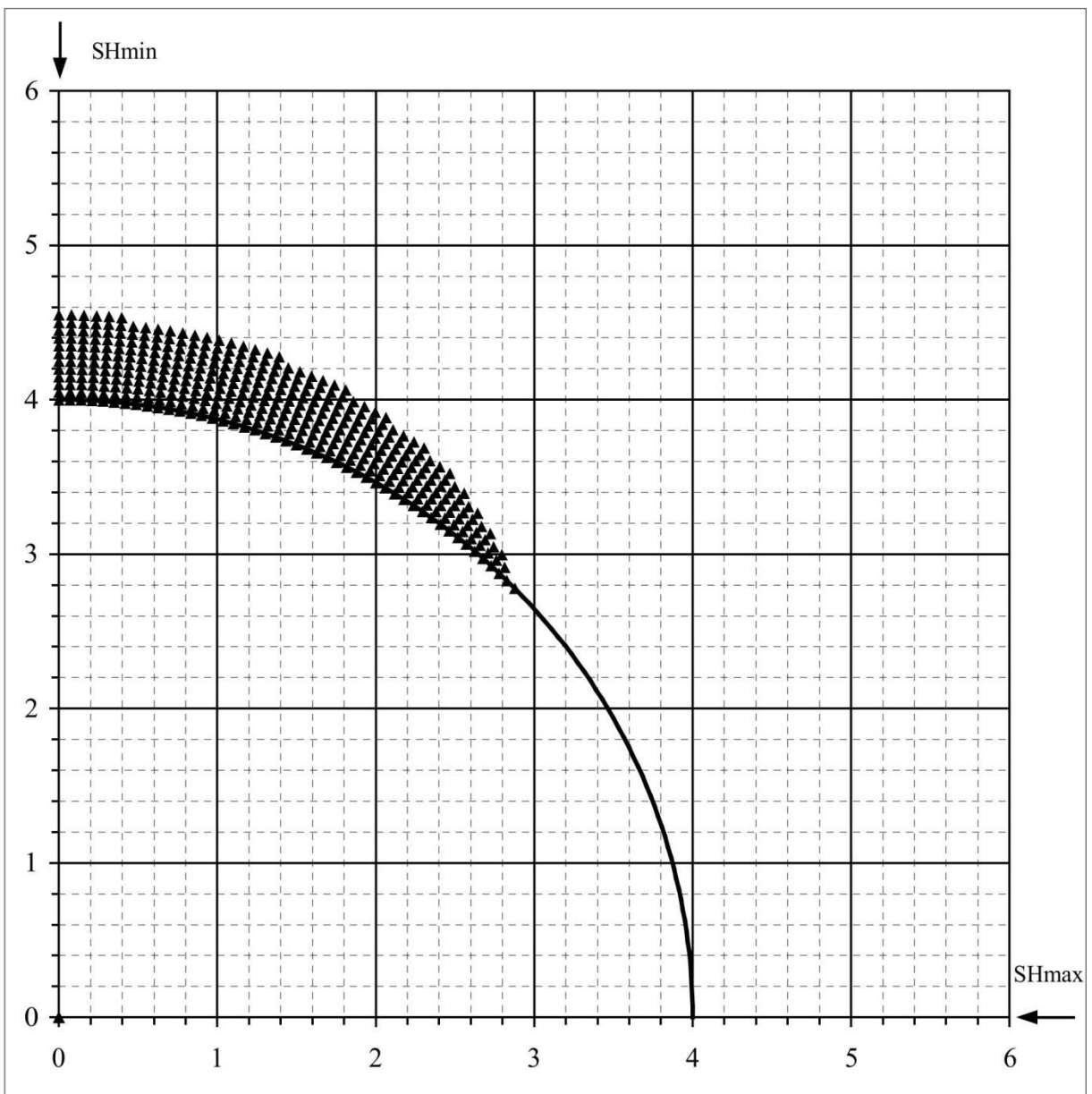
SHmax =	16.3 MPa	u (Coeff. of Friction) =	0.6
SHmin =	8.5 MPa	C (Cohesive Strength) =	3 MPa
Sv =	8.5 MPa	$\nu$ (Poisson's Ratio) =	0.2
Po (Pore Pressure) =	3.8 MPa	Diameter of Borehole =	8 inches
Pm (Mud Weight) =	3.8 MPa	Depth of Max. Breakout =	0.55 inches
Sensitivity of Figure =	0.05 inches	Angle of Max. Breakout =	90 deg



C-086-A/094-I-14

## Extended Drucker - Prager Failure Criterion (Modified Strain Energy Criterion)

SHmax =	14.9 MPa	u (Coeff. of Friction) =	0.6
SHmin =	8.5 MPa	C (Cohesive Strength) =	3 MPa
Sv =	8.5 MPa	v (Poisson's Ratio) =	0.2
Po (Pore Pressure) =	3.8 MPa	Radius of Borehole =	8 inches
Pm (Mud Weight) =	3.8 MPa	Depth of Max. Breakout =	0.55 inches
Sensitivity of Figure =	0.05 inches	Angle of Max. Breakout =	90 deg



## $S_{Hmax}$ Simulation Commentary – D-007-J/094-O-09

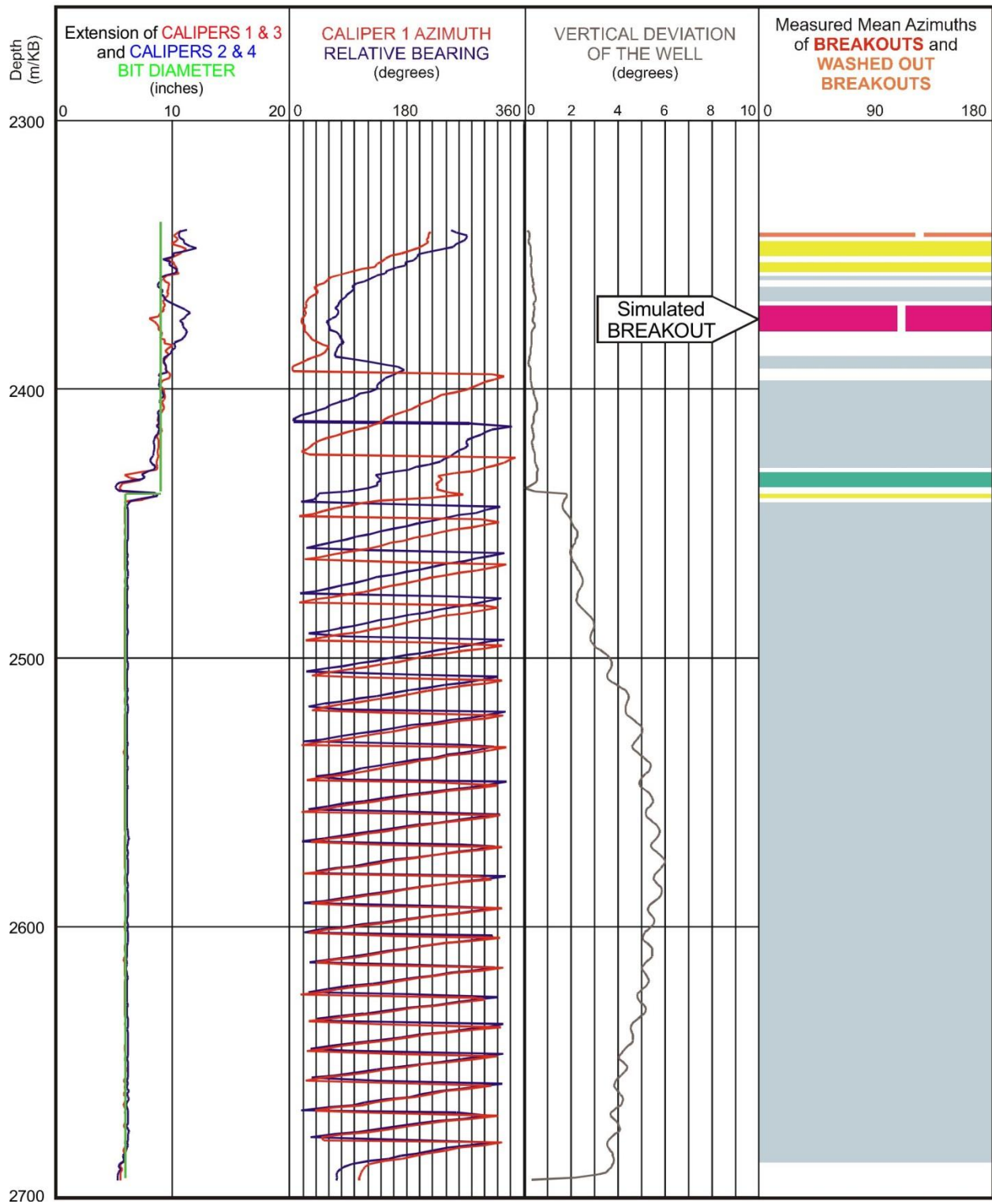
Well: D-007-J/094-O-09	Failure simulation Method				2SHmin-Po
	Mohr Coulomb	Drucker Prager	Modified Strain Energy	3 cycle Mohr Coulomb	
Breakout Interval Top (m KB)	2369	2369	2369	2369	
Breakout Interval Base (m KB)	2379	2379	2379	2379	
Median depth of Breakout (m KB)	2374	2374	2374	2374	
Calipers 1 and 3 extent (inches)	11.06	11.06	11.06	11.06	
Calipers 2 and 4 extent (inches)	8.93	8.93	8.93	8.93	
SHmax (MPa)	<b>69.0</b>	95.6*	84.4		62.3
SHmax gradient (kPa/m)	29.1	40.3	35.6		26.2
SHmin (MPa)	43.0	43.0	43.0	43.0	
Sv (MPa)	57.2	57.2	57.2	57.2	
Pore Pressure (MPa)	23.7	23.7	23.7	23.7	
Mudweight (MPa)	23.7	23.7	23.7	23.7	
u (Coefficient of Friction)	0.6	0.6	0.6	0.6	
Cohesive Strength of Rock (MPa)	10.0	10.0	10.0	10.0	
v (Poisson's Ratio)	0.2	0.2	0.2	0.2	
Bit size (inches)	9.0	9.0	9.0	9.0	

\* indicates that modelling could not simulate complete breakout anisotropy

The selected breakout in well D-007-J/094-O-09 was satisfactorily modelled with the Mohr Coulomb and Modified Strain Energy routines. However, the Drucker-Prager failure criterion failed to generate a breakout deeper than 10.7 inches. The Mohr Coulomb failure simulation, with the cohesive strength set at 10 MPa, gave **69.0 MPa** as the  $S_{Hmax}$  magnitude, which is slightly higher than the value of 62.3 MPa suggested by the equation  $2S_{Hmin} - Po$ .

The  $S_{Hmax}$  magnitude at 2374 m in well D-007-J/094-O-09 is interpreted to be 69.0 MPa.

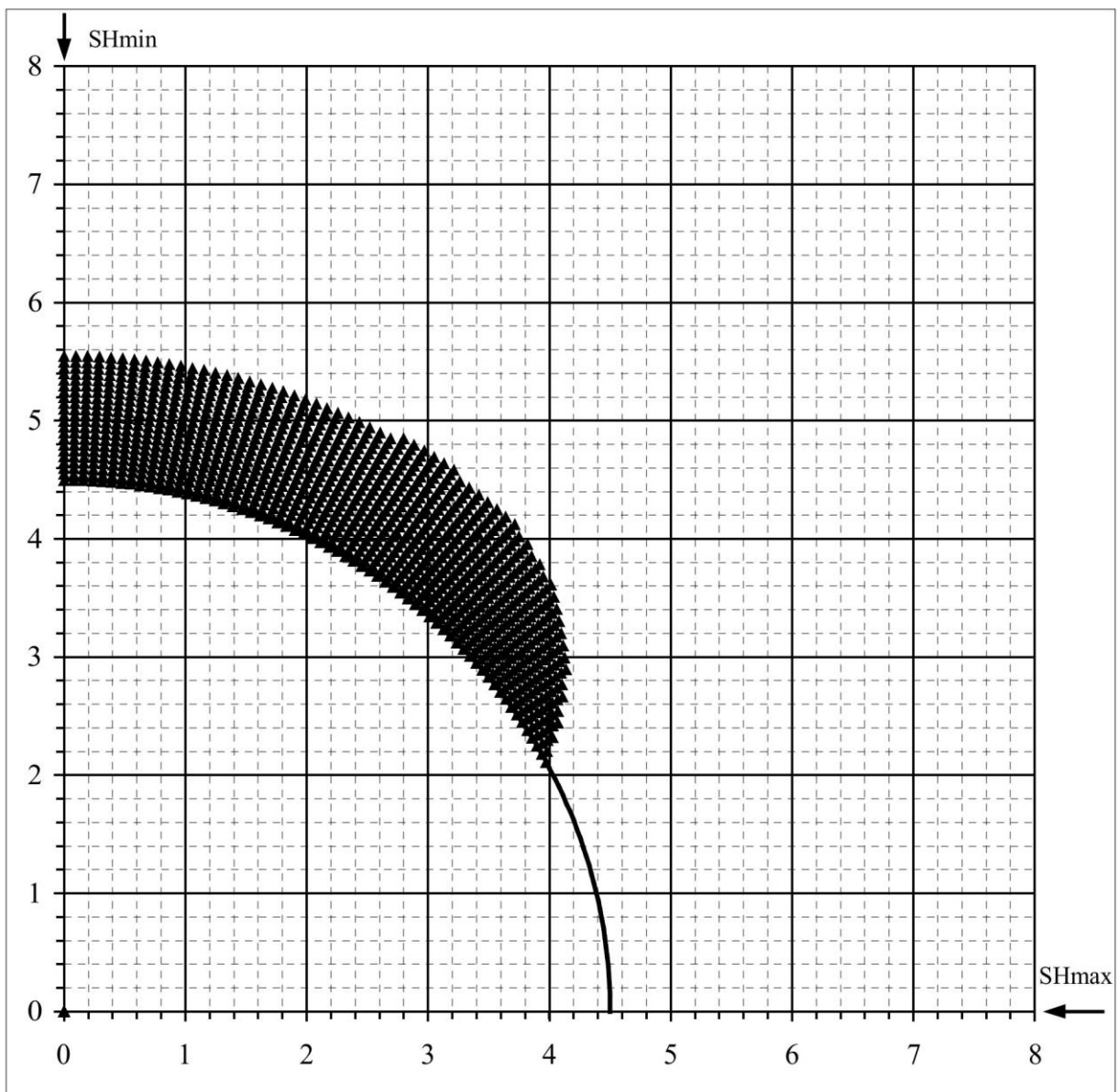
WELL : D-007-J/094-O-09 BREAKOUT ANALYSIS



D-007-J/094-O-09

## Mohr - Coulomb Failure Criterion

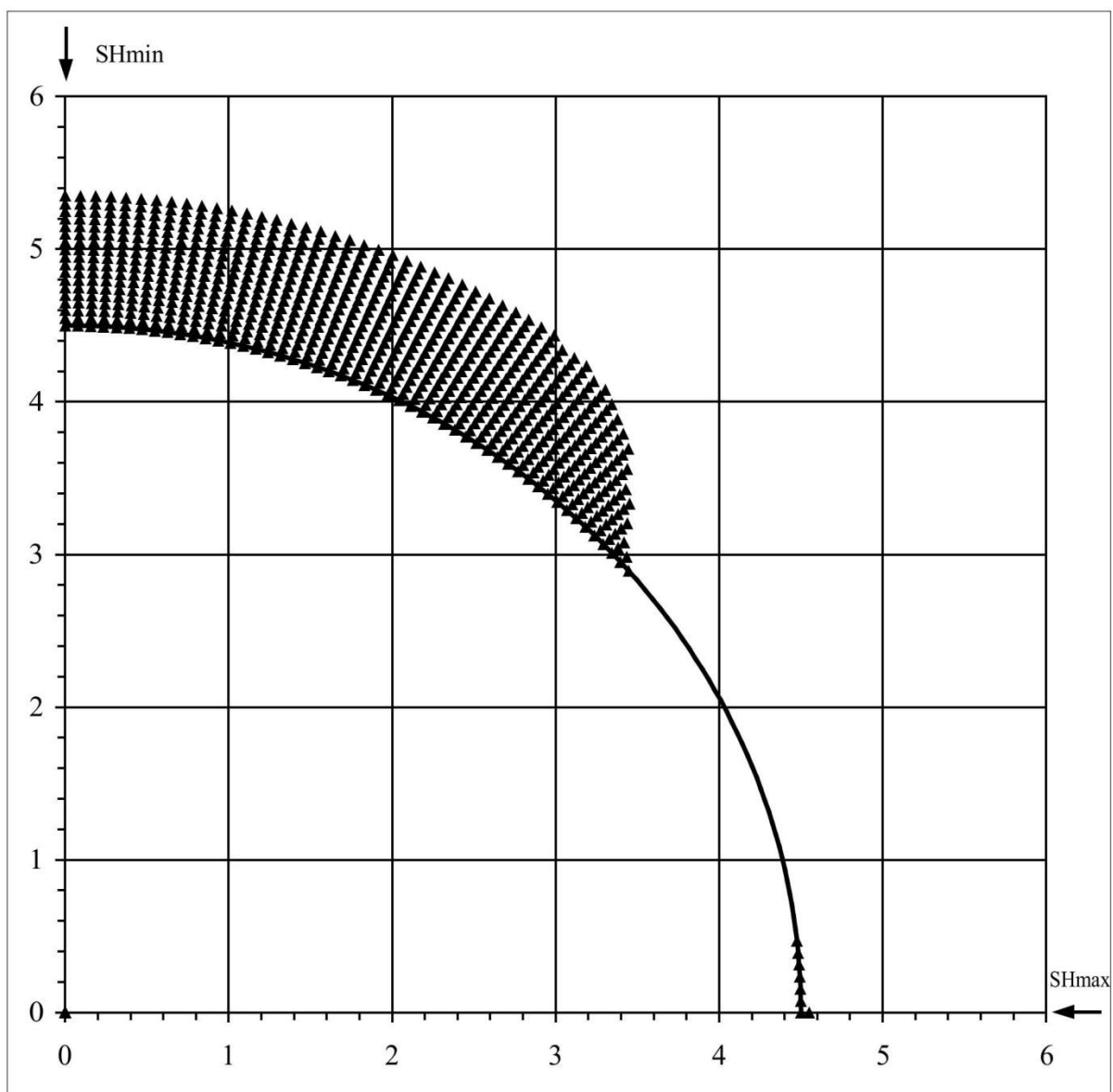
SHmax =	69 MPa	u (Coeff. of Friction) =	0.6
SHmin =	43 MPa	C (Cohesive Strength) =	10 MPa
Sv =	57.2 MPa	v (Poisson's Ratio) =	0.2
Po (Pore Pressure) =	23.7 MPa	Diameter of Borehole =	9 "
Pm (Mud Weight) =	23.7 MPa		
Sensitivity of Figure =	0.05 "	Angle of Max. Breakout =	57 deg
Depth of Max. Breakout =	1.1 "	Max caliper at 90 deg =	11.1 "
Validity of the results =	TRUE	Max caliper at 0 deg =	8 "



D-007-J/094-O-09

## Extended von-Mises Failure Criterion (Drucker-Prager Failure Criterion)

SHmax =	95.6 MPa	u (Coeff. of Friction) =	0.6
SHmin =	43 MPa	C (Cohesive Strength) =	10 MPa
Sv =	57.2 MPa	v (Poisson's Ratio) =	0.2
Po (Pore Pressure) =	23.7 MPa	Diameter of Borehole =	9 inches
Pm (Mud Weight) =	23.7 MPa	Depth of Max. Breakout =	0.85 inches
Sensitivity of Figure =	0.05 inches	Angle of Max. Breakout =	69 deg

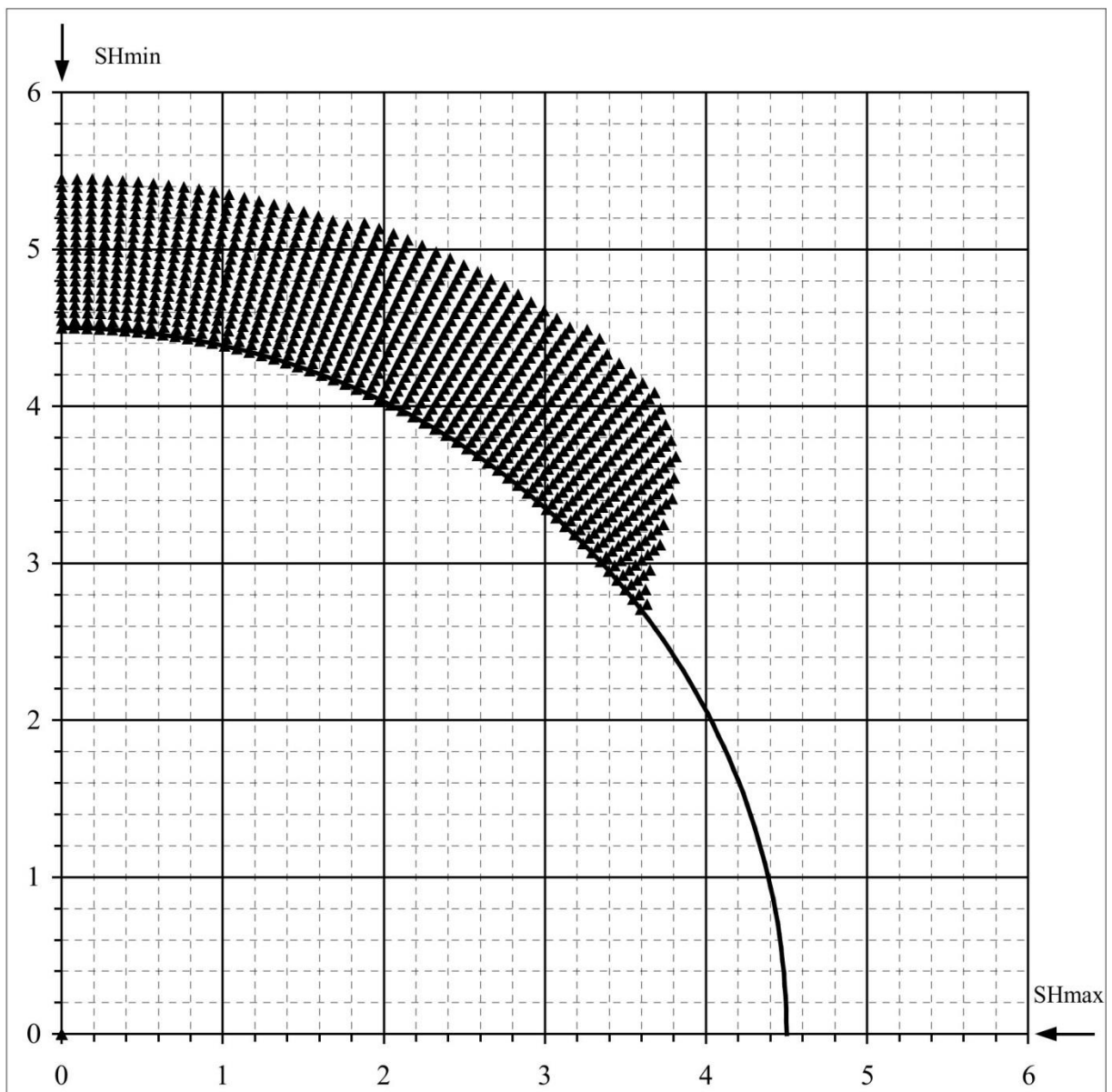




D-007-J/094-O-09

## Extended Drucker - Prager Failure Criterion (Modified Strain Energy Criterion)

SHmax =	84.4 MPa	u (Coeff. of Friction) =	0.6
SHmin =	43 MPa	C (Cohesive Strength) =	10 MPa
Sv =	57.2 MPa	v (Poisson's Ratio) =	0.2
Po (Pore Pressure) =	23.7 MPa	Radius of Borehole =	9 inches
Pm (Mud Weight) =	23.7 MPa	Depth of Max. Breakout =	1.05 inches
Sensitivity of Figure =	0.05 inches	Angle of Max. Breakout =	53 deg



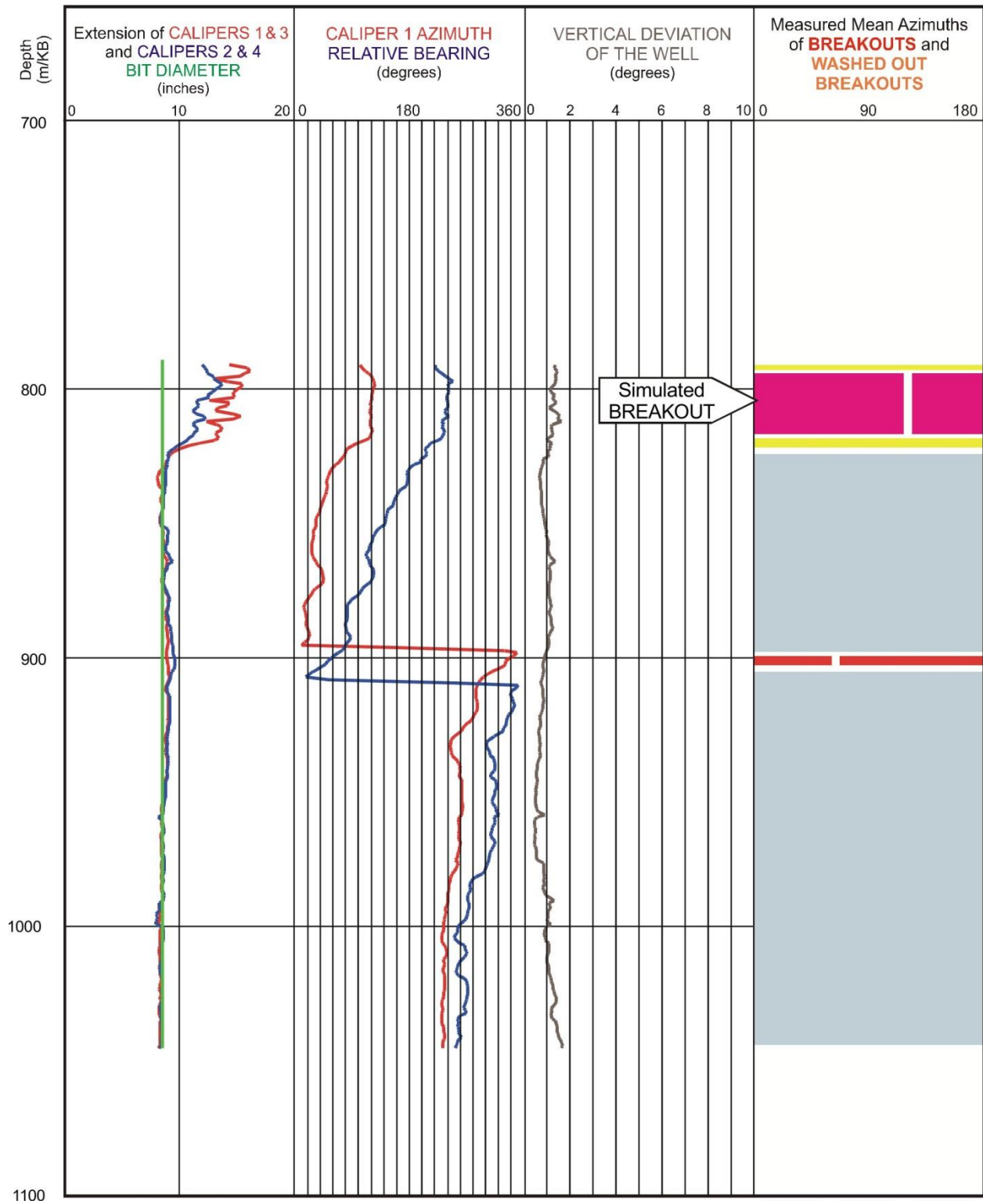
## $S_{Hmax}$ Simulation Commentary – D-25-61-20-121-45

Well: D-025-61-20-121-45	Failure simulation Method				2SHmin-Po
	Mohr Coulomb	Drucker Prager	Modified Strain Energy	3 cycle Mohr Coulomb	
Breakout Interval Top (m KB)	794	794	794	794	
Breakout Interval Base (m KB)	817	817	817	817	
Median depth of Breakout (m KB)	805.5	805.5	805.5	805.5	
Calipers 1 and 3 extent (inches)	12.18	12.18	12.18	12.18	
Calipers 2 and 4 extent (inches)	14.21	14.21	14.21	14.21	
SHmax (MPa)	<b>23.5</b>	35.6	30.3		19.3
SHmax gradient (kPa/m)	29.2	44.2	37.6		24.0
SHmin (MPa)	13.7	13.7	13.7	13.7	
Sv (MPa)	20.5	20.5	20.5	20.5	
Pore Pressure (MPa)	8.1	8.1	8.1	8.1	
Mudweight (MPa)	8.1	8.1	8.1	8.1	
u (Coefficient of Friction)	0.6	0.6	0.6	0.6	
Cohesive Strength of Rock (MPa)	5.0	5.0	5.0	5.0	
v (Poisson's Ratio)	0.2	0.2	0.2	0.2	
Bit size (inches)	8.5	8.5	8.5	8.5	

The selected breakout in well D-25-61-20-121-45 was satisfactorily modelled with all three single cycle simulation routines.

The lowest value for the  $S_{Hmax}$  magnitude was provided by the Mohr Coulomb failure simulation which, with the cohesive strength set at 5 MPa, gave **23.5 MPa** as the  $S_{Hmax}$  magnitude. This is slightly higher than the value of 19.3 MPa suggested by the equation  $2S_{Hmin} - Po$ , but is believed to be a good estimate of  $S_{Hmax}$ .

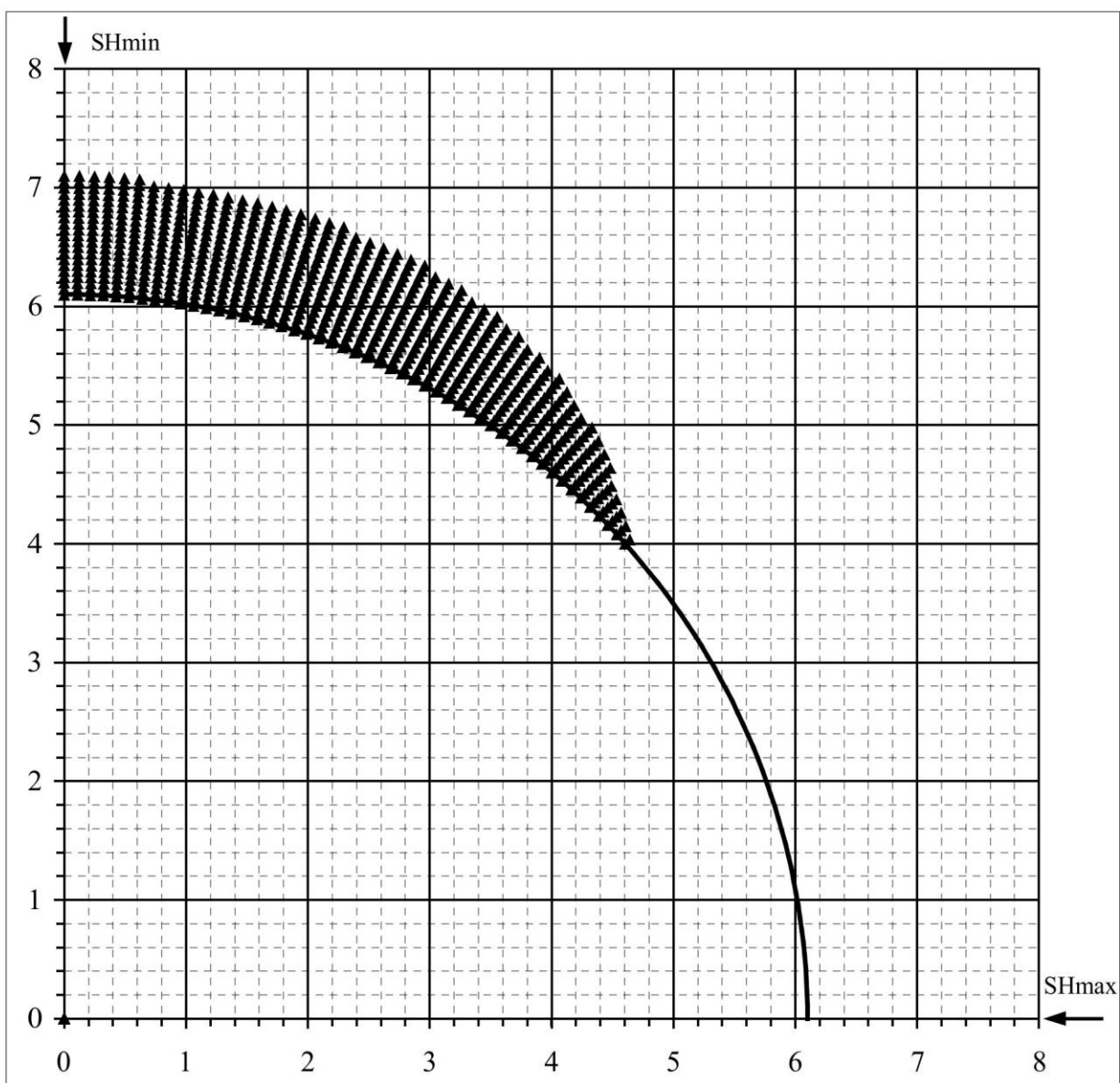
WELL : D-25-61-20-121-45 BREAKOUT ANALYSIS



D-025-61-20-121-45

## Mohr - Coulomb Failure Criterion

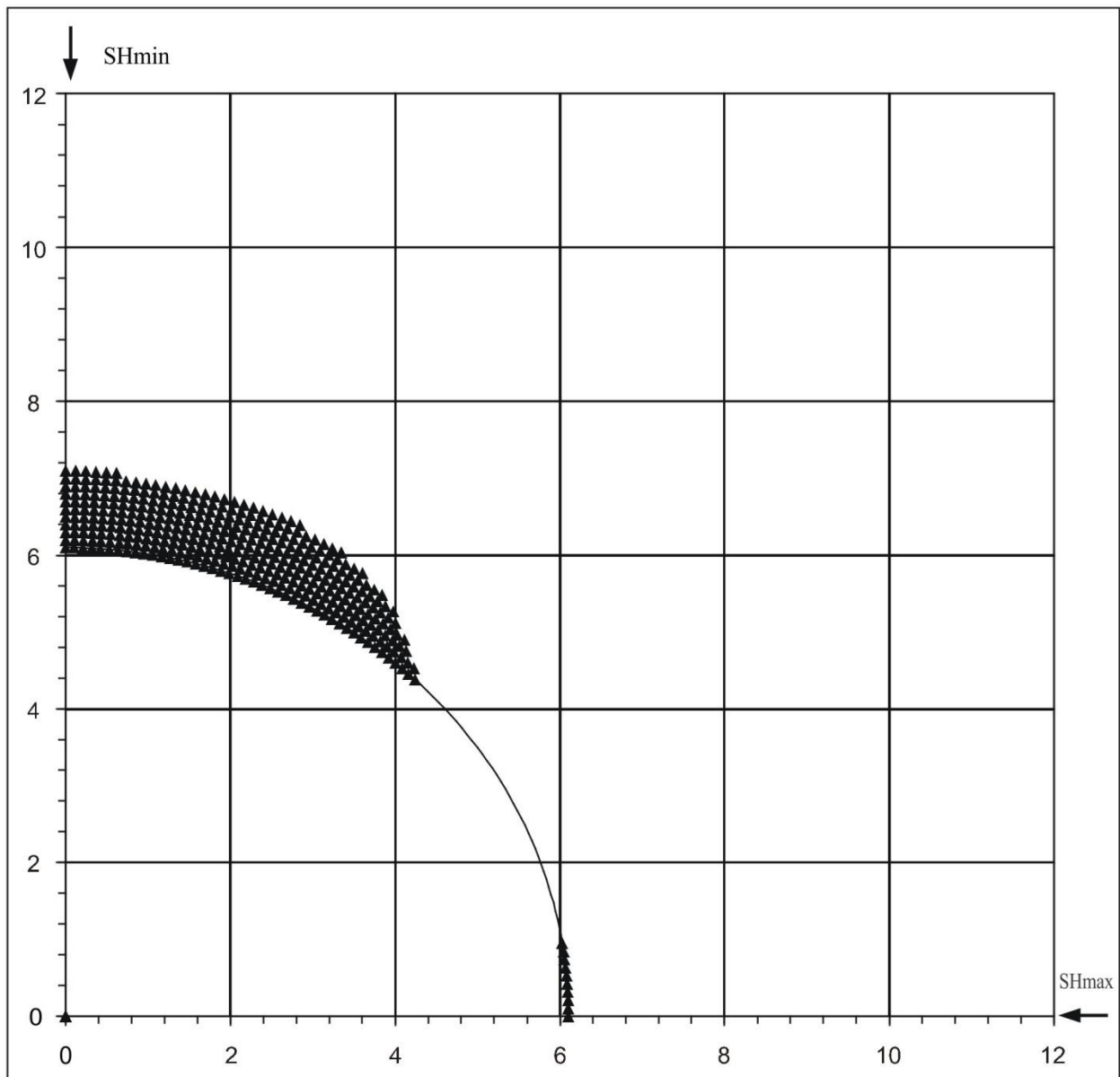
SHmax =	23.5 MPa	u (Coeff. of Friction) =	0.6
SHmin =	13.7 MPa	C (Cohesive Strength) =	5 MPa
Sv =	20.5 MPa	v (Poisson's Ratio) =	0.2
Po (Pore Pressure) =	8.1 MPa	Diameter of Borehole =	12.2 "
Pm (Mud Weight) =	8.1 MPa		
Sensitivity of Figure =	0.05 "	Angle of Max. Breakout =	90 deg
Depth of Max. Breakout =	1 "	Max caliper at 90 deg =	14.2 "
Validity of the results =	TRUE	Max caliper at 0 deg =	8 "



D-025-61-20-121-45

## Extended von-Mises Failure Criterion (Drucker-Prager Failure Criterion)

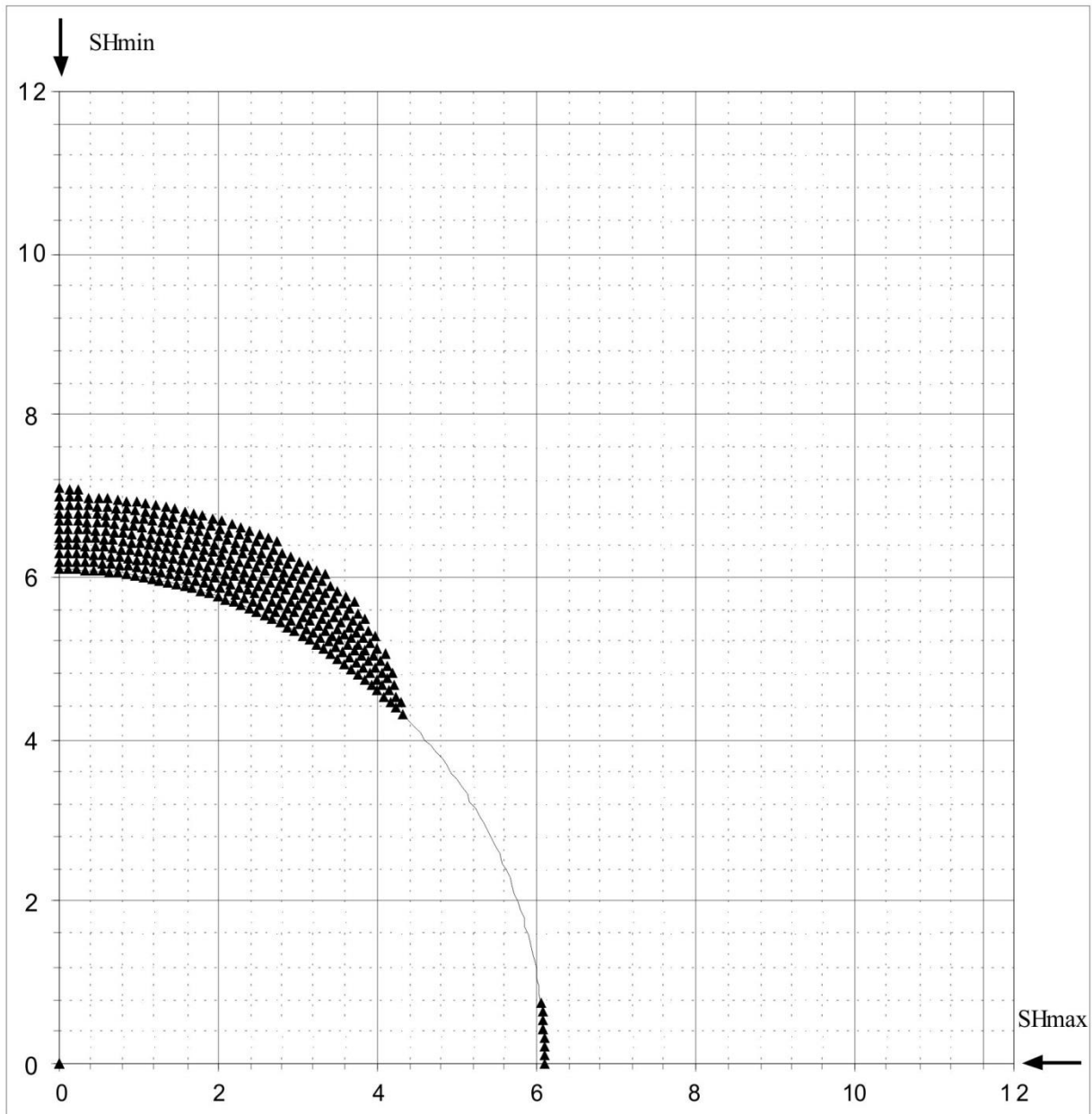
SHmax =	35.6 MPa	u (Coeff. of Friction) =	0.6
SHmin =	13.7 MPa	C (Cohesive Strength) =	5 MPa
Sv =	20.5 MPa	v (Poisson's Ratio) =	0.2
Po (Pore Pressure) =	8.1 MPa	Diameter of Borehole =	12.2 inches
Pm (Mud Weight) =	8.1 MPa	Depth of Max. Breakout =	1 inch
Sensitivity of Figure =	0.05 inches	Angle of Max. Breakout =	90 deg



D-025-61-20-121-45

## Extended Drucker - Prager Failure Criterion (Modified Strain Energy Criterion)

SHmax =	30.3 MPa	u (Coeff. of Friction) =	0.6
SHmin =	13.7 MPa	C (Cohesive Strength) =	5 MPa
Sv =	20.5 MPa	v (Poisson's Ratio) =	0.2
Po (Pore Pressure) =	8.1 MPa	Diameter of Borehole =	12.2 inches
Pm (Mud Weight) =	8.1 MPa	Depth of Max. Breakout =	1 inches
Sensitivity of Figure =	0.05 inches	Angle of Max. Breakout =	90 deg



**SHmax Simulation Commentary – D-057-K/094-N-02**

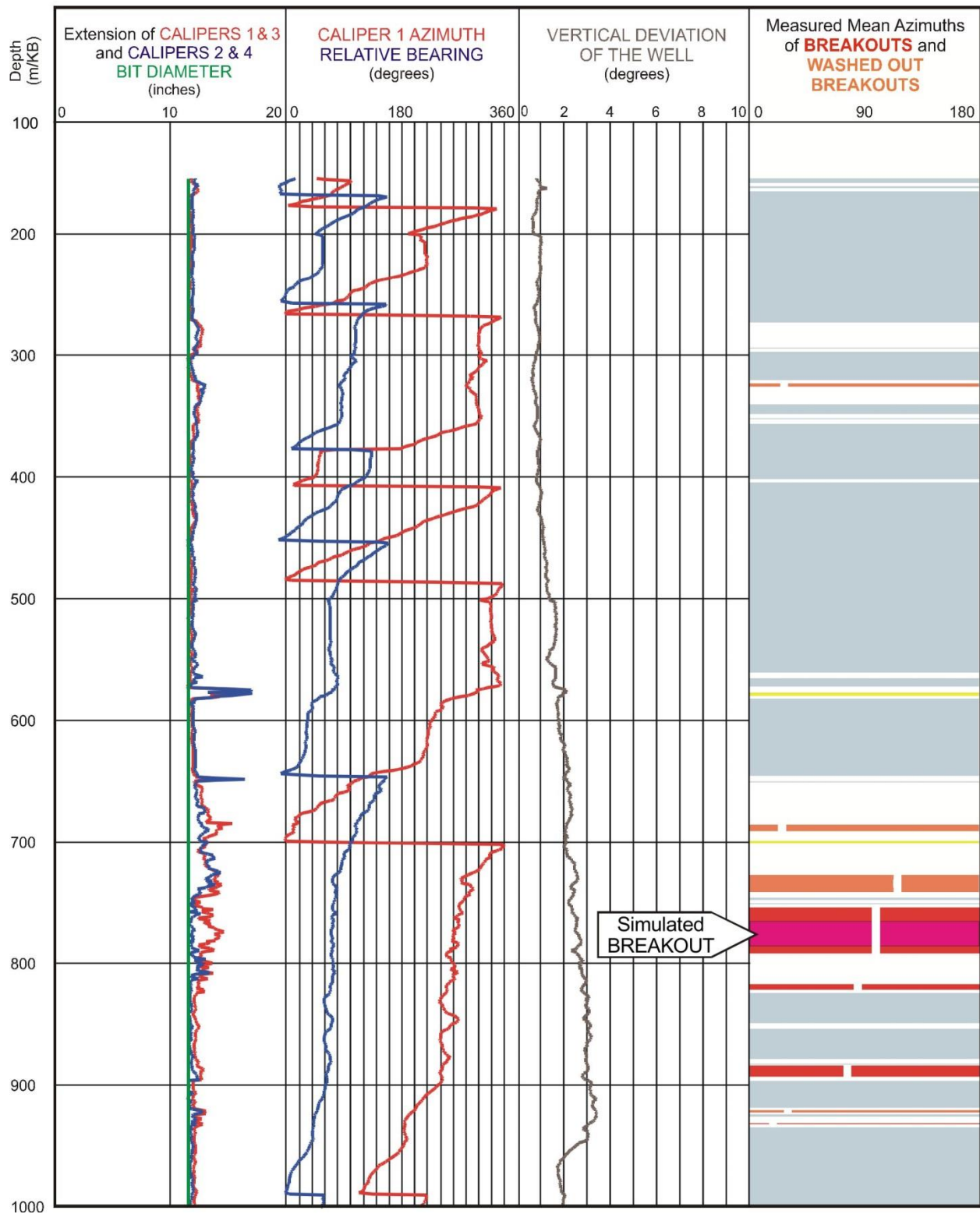
Well: <b>D-057-K/094-N-02</b>	Failure simulation Method				2SHmin-Po
	Mohr Coulomb	Drucker Prager	Modified Strain Energy	3 cycle Mohr Coulomb	
Breakout Interval Top (m KB)	765	765	765	765	
Breakout Interval Base (m KB)	785	785	785	785	
Median depth of Breakout (m KB)	775	775	775	775	
Calipers 1 and 3 extent (inches)	14.53	14.53	14.53	14.53	
Calipers 2 and 4 extent (inches)	12.72	12.72	12.72	12.72	
SHmax (MPa)	<b>21.9</b>	33.5	28.3		20.6
SHmax gradient (kPa/m)	28.3	43.2	36.5		26.6
SHmin (MPa)	14.2	14.2	14.2	14.2	
Sv (MPa)	20.5	20.5	20.5	20.5	
Pore Pressure (MPa)	7.8	7.8	7.8	7.8	
Mudweight (MPa)	7.8	7.8	7.8	7.8	
u (Coefficient of Friction)	0.6	0.6	0.6	0.6	
Cohesive Strength of Rock (MPa)	5.0	5.0	5.0	5.0	
v (Poisson's Ratio)	0.2	0.2	0.2	0.2	
Bit size (inches)	12.25	12.25	12.25	12.25	

The selected portion of Breakout # 4 in well D-057-K/094-N-02 was satisfactorily modelled with all three single cycle simulation routines.

The smallest estimate of  $S_{Hmax}$  magnitude was provided by the Mohr Coulomb failure simulation. With the cohesive strength set at 5 MPa, the Mohr Coulomb failure simulation gave **21.9 MPa** as the  $S_{Hmax}$  magnitude, which is close to the value of 20.6 MPa suggested by the equation  $2S_{Hmin} - P_o$ .

The  $S_v$  magnitude at 775 m KB is well established from the density log.

WELL : D-057-K/094-N-02 BREAKOUT ANALYSIS

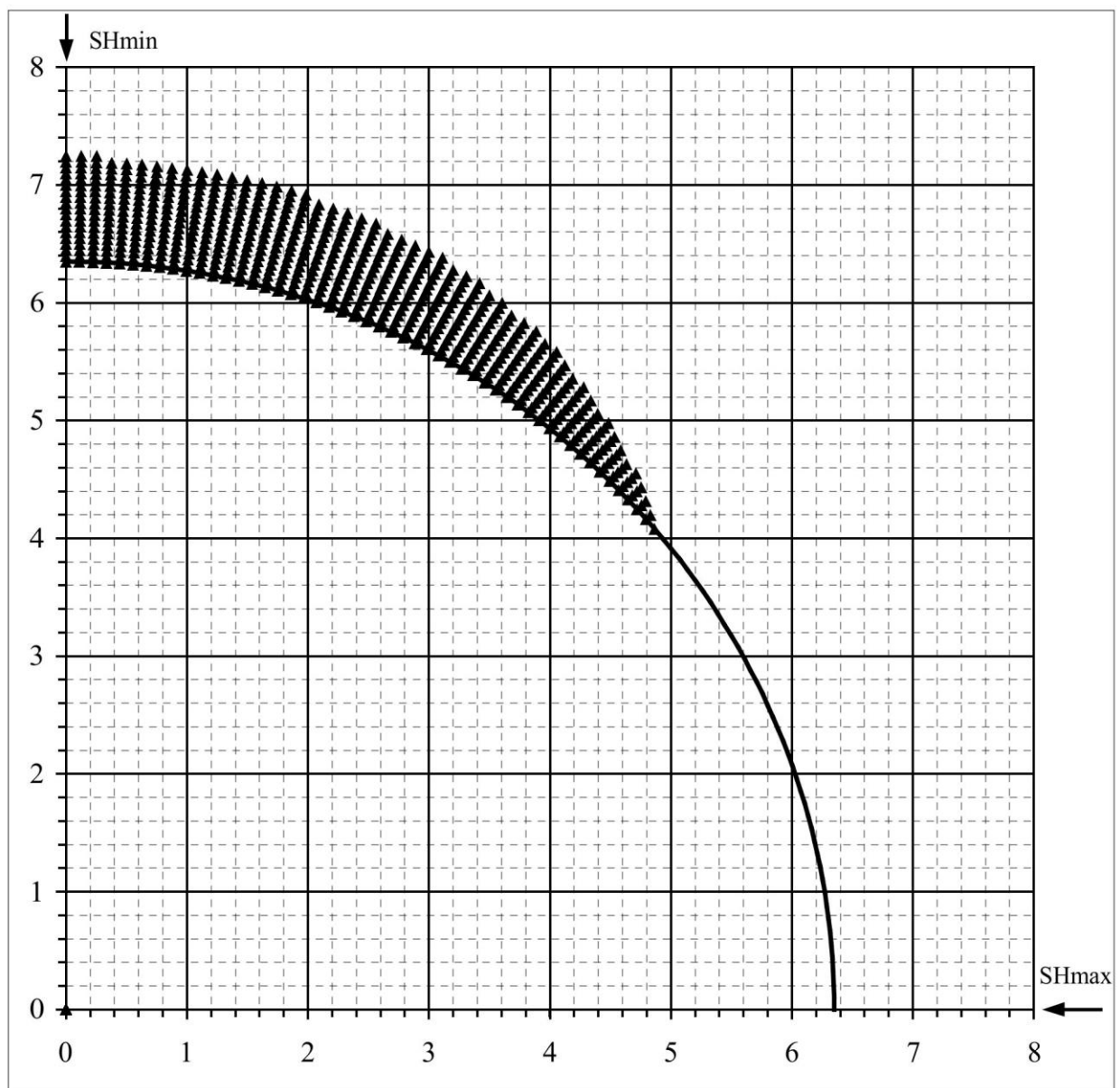




D-057-K/094-N-02

**Mohr - Coulomb Failure Criterion**

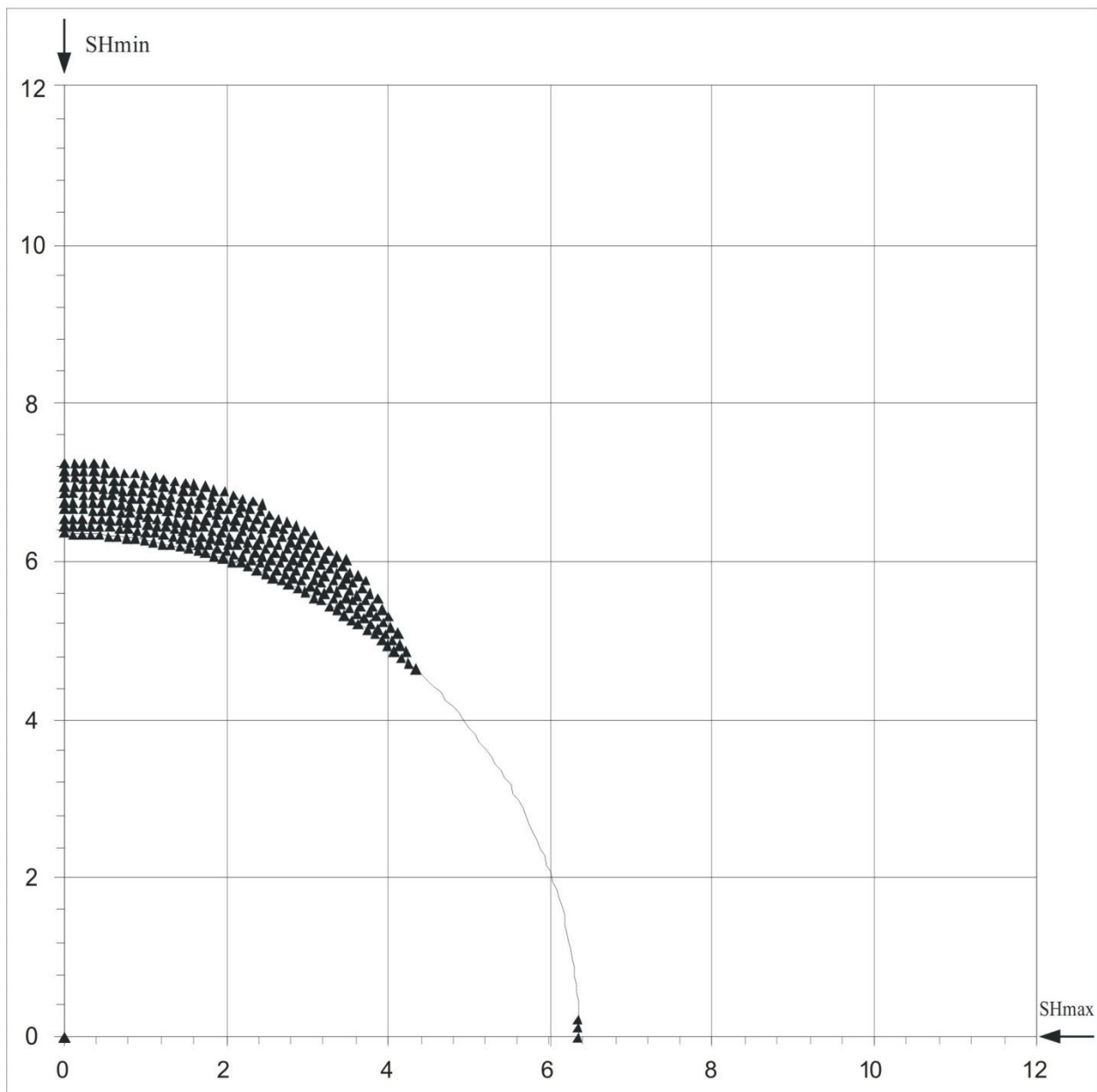
SHmax =	21.9 MPa	u (Coeff. of Friction) =	0.6
SHmin =	14.2 MPa	C (Cohesive Strength) =	5 MPa
Sv =	20.5 MPa	v (Poisson's Ratio) =	0.2
Po (Pore Pressure) =	7.8 MPa	Diameter of Borehole =	12.7 "
Pm (Mud Weight) =	7.8 MPa		
Sensitivity of Figure =	0.05 "	Angle of Max. Breakout =	90 deg
Depth of Max. Breakout =	0.9 "	Max caliper at 90 deg =	14.5 "
Validity of the results =	TRUE	Max caliper at 0 deg =	8 "



D-057-K/094-N-02

## Extended von-Mises Failure Criterion (Drucker-Prager Failure Criterion)

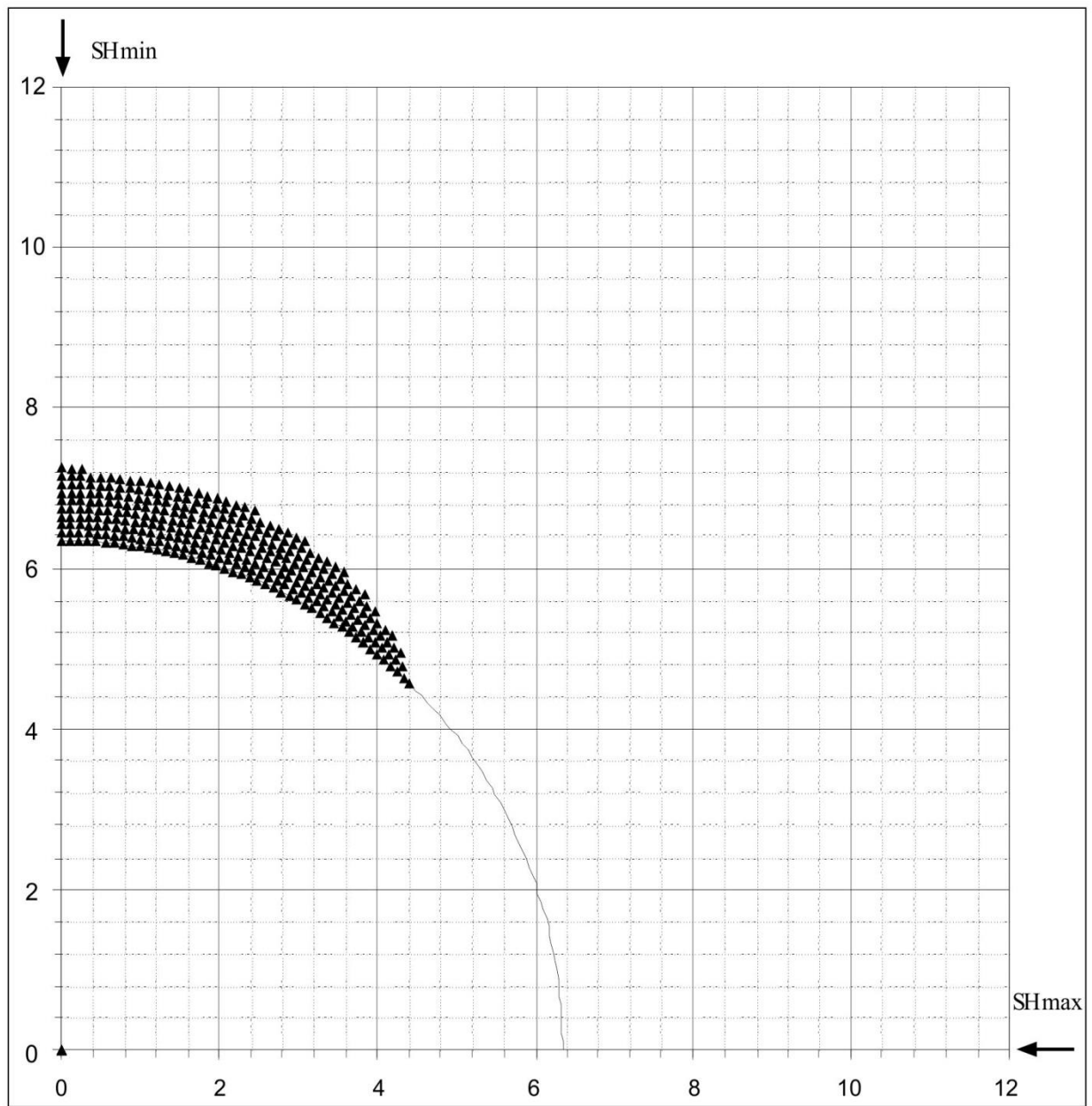
SHmax =	33.5 MPa	u (Coeff. of Friction)=	0.6
SHmin =	14.2 MPa	C (Cohesive Strength) =	5 MPa
Sv =	20.5 MPa	v (Poisson's Ratio) =	0.2
Po (Pore Pressure) =	7.8 MPa	Diameter of Borehole =	12.7 "
Pm (Mud Weight) =	7.8 MPa	Depth of Max. Breakout =	0.9 "
Sensitivity of Figure =	0.05 inches	Angle of Max. Breakout =	90 deg



D-057-K/094-N-02

## Extended Drucker - Prager Failure Criterion (Modified Strain Energy Criterion)

SHmax =	28.3 MPa	u (Coeff. of Friction) =	0.6
SHmin =	14.2 MPa	C (Cohesive Strength) =	5 MPa
Sv =	20.5 MPa	v (Poisson's Ratio) =	0.2
Po (Pore Pressure) =	7.8 MPa	Diameter of Borehole =	12.7 inches
Pm (Mud Weight) =	7.8 MPa	Depth of Max. Breakout =	0.9 inches
Sensitivity of Figure =	0.05 inches	Angle of Max. Breakout =	90 deg



**SHmax Simulation Commentary – D-064-K/094-N-16**

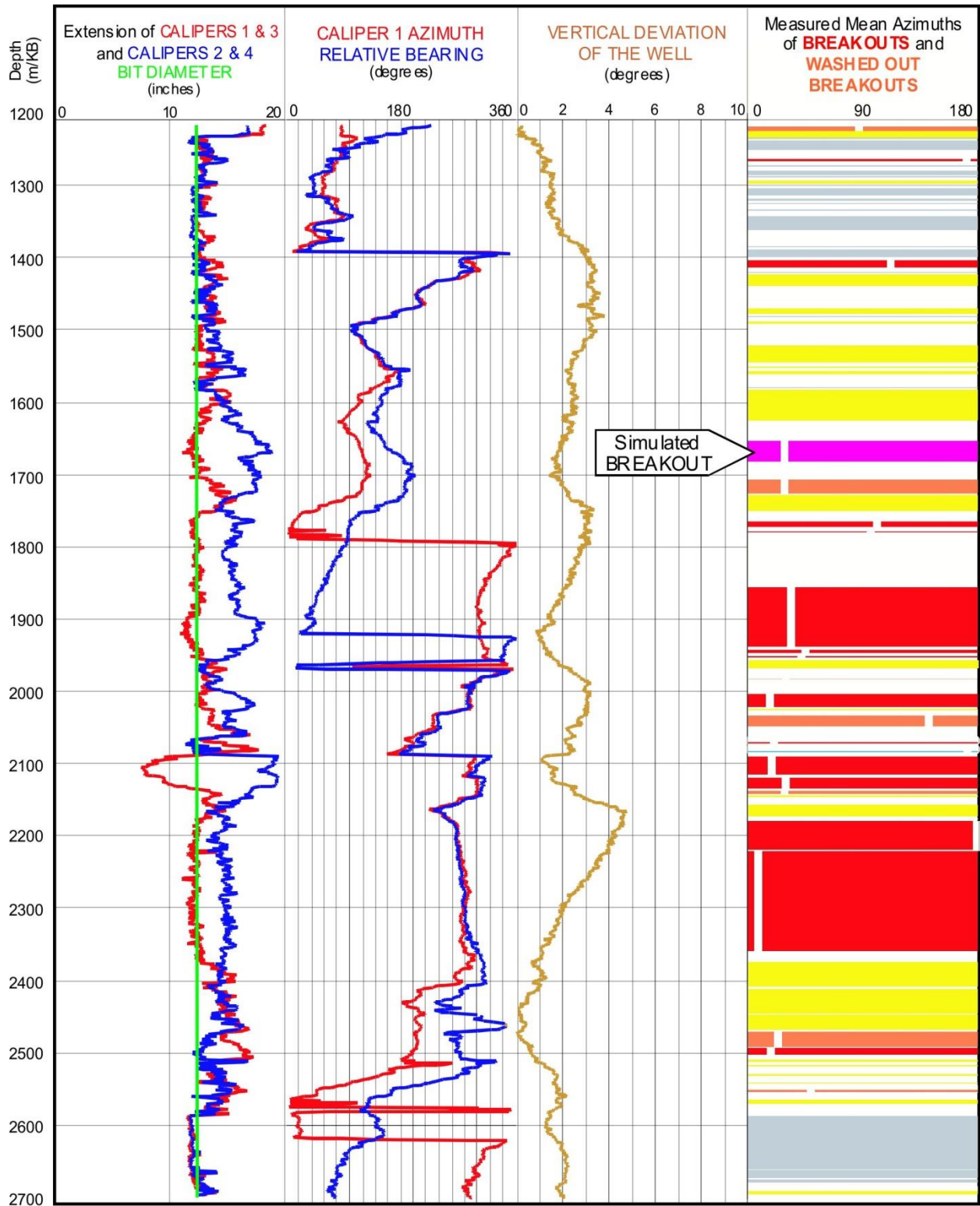
Well: <b>D-064-K/094-N-16</b>	Failure simulation Method				2SHmin-Po
	Mohr Coulomb	Drucker Prager	Modified Strain Energy	3 cycle Mohr Coulomb	
Breakout Interval Top (m KB)	1654	1654	1654	1654	
Breakout Interval Base (m KB)	1684	1684	1684	1684	
Median depth of Breakout (m KB)	1669	1669	1669	1669	
Calipers 1 and 3 extent (inches)	12.13	12.13	12.13	12.13	
Calipers 2 and 4 extent (inches)	17.71	17.71	17.71	17.71	
SHmax (MPa)	53.0*	65.3*	65.6*	<b>50.4</b>	43.7
SHmax gradient (kPa/m)	31.8	39.1	39.3	30.2	26.2
SHmin (MPa)	30.2	30.2	30.2	30.2	
Sv (MPa)	41.2	41.2	41.2	41.2	
Pore Pressure (MPa)	16.7	16.7	16.7	16.7	
Mudweight (MPa)	16.7	16.7	16.7	16.7	
u (Coefficient of Friction)	0.6	0.6	0.6	0.6	
Cohesive Strength of Rock (MPa)	10.0	10.0	10.0	10.0	
v (Poisson's Ratio)	0.2	0.2	0.2	0.2	
Bit size (inches)	12.25	12.25	12.25	12.25	

\* indicates that modelling could not simulate accurate breakout anisotropy

The breakout interval between 1654 and 1684 m was selected for simulation. With a mean maximum diameter of 17.71 inches and a mean minimum diameter of 12.13 inches, it was not possible to generate deep enough breakouts with any of the single cycle routines. However, the 3 cycle Mohr Coulomb routine generated a breakout with these dimensions.

When the cohesive strength was set at 10.0 MPa, the 3 cycle Mohr Coulomb simulation suggested an  $S_{Hmax}$  magnitude of 50.4 MPa, higher than the value predicted by the equation:  $S_{Hmax} = 2(S_{Hmin}) - P_o$ , but one which represents a realistic  $S_{Hmax}$  gradient.

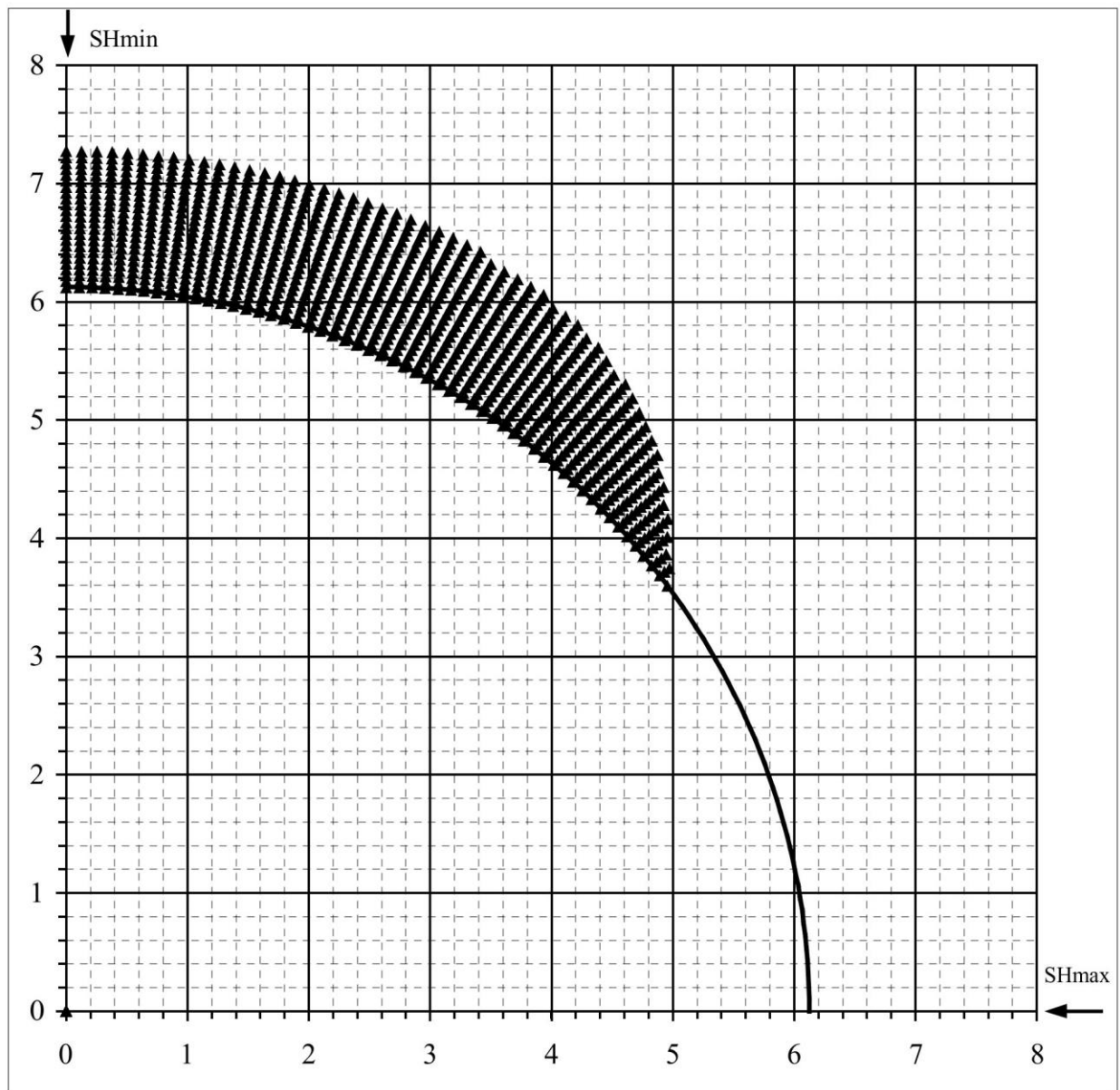
WELL : D-064-K/094-N-16 BREAKOUT ANALYSIS



D-064-K/094-N-16

## Mohr - Coulomb Failure Criterion

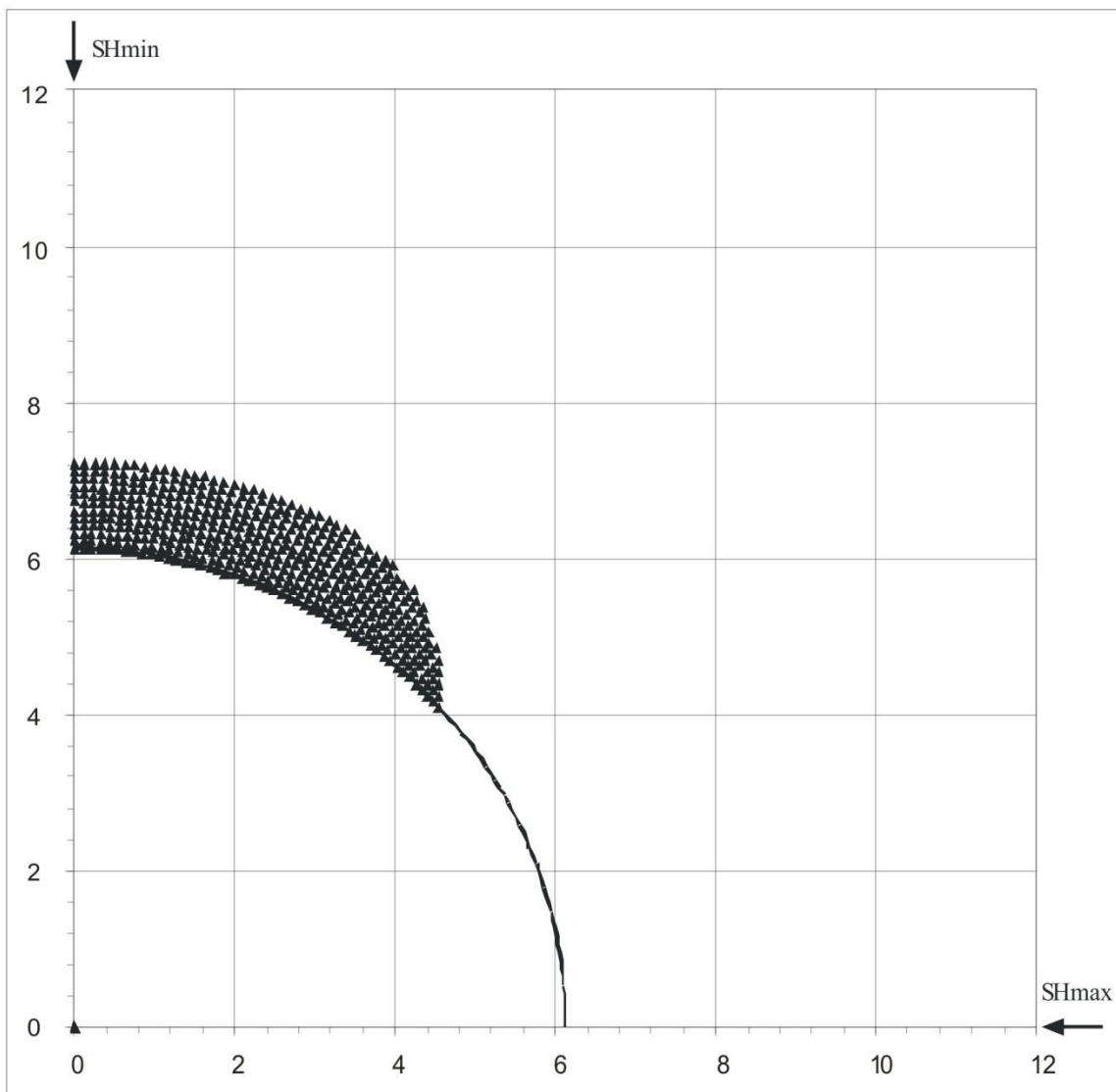
SHmax =	53 MPa	u (Coeff. of Friction) =	0.6
SHmin =	30.2 MPa	C (Cohesive Strength) =	10 MPa
Sv =	41.2 MPa	v (Poisson's Ratio) =	0.2
Po (Pore Pressure) =	16.7 MPa	Diameter of Borehole =	12.25 "
Pm (Mud Weight) =	16.7 MPa		
Sensitivity of Figure =	0.05 "	Angle of Max. Breakout =	90 deg
Depth of Max. Breakout =	1.15 "	Max caliper at 90 deg =	14.55 "
Validity of the results =	TRUE	Max caliper at 0 deg =	12.25 "



D-064-K/094-N-16

## Extended von-Mises Failure Criterion (Drucker-Prager Failure Criterion)

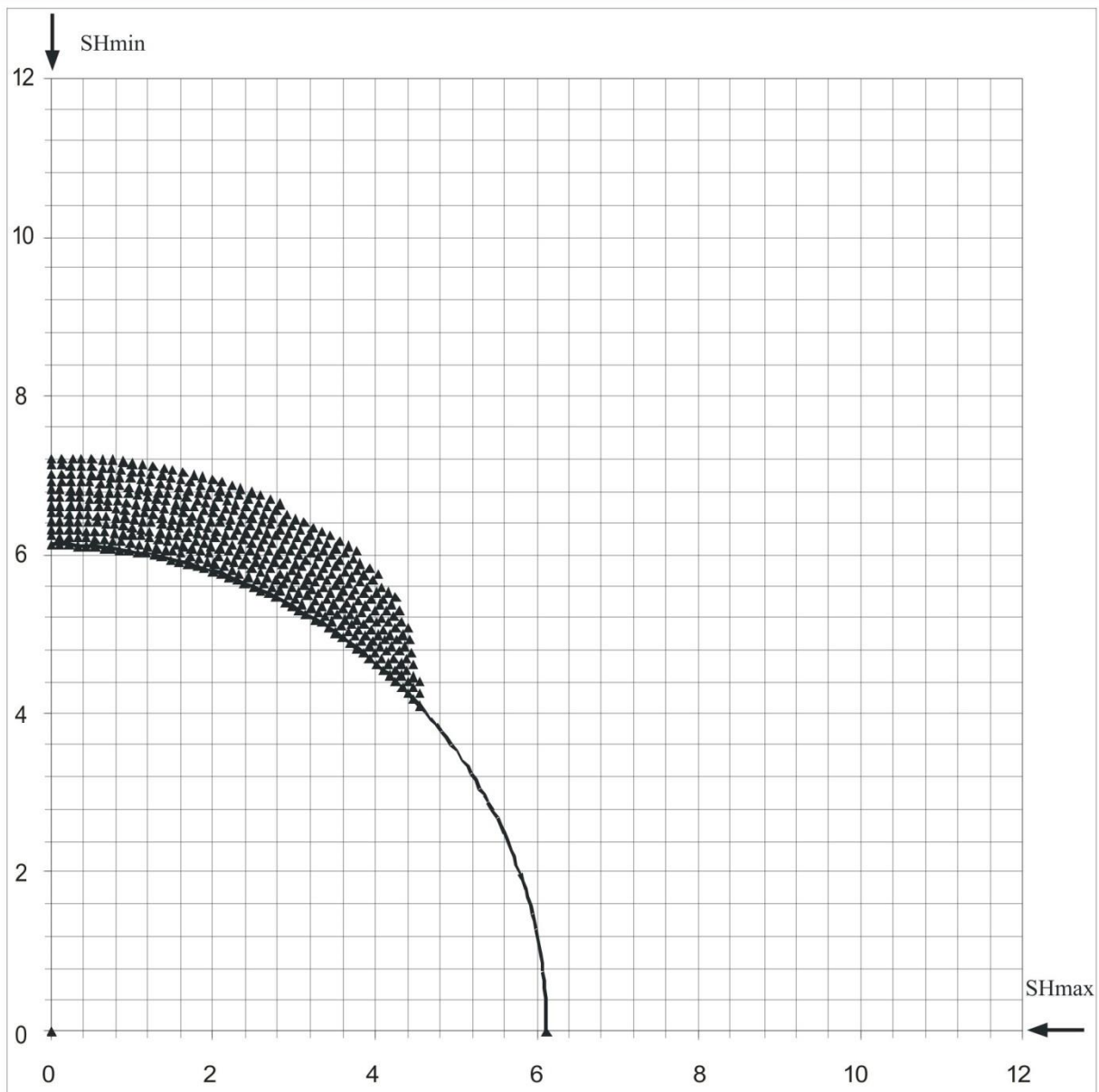
SHmax =	65.3 MPa	u (Coeff. of Friction)=	0.6
SHmin =	30.2 MPa	C (Cohesive Strength) =	10 MPa
Sv =	31.2 MPa	v (Poisson's Ratio) =	0.2
Po (Pore Pressure) =	16.7 MPa	Diameter of Borehole =	12.25 inches
Pm (Mud Weight) =	16.7 MPa	Depth of Max. Breakout =	1.15 inches
Sensitivity of Figure =	0.05 inches	Angle of Max. Breakout =	90 deg



D-064-K/094-N-16

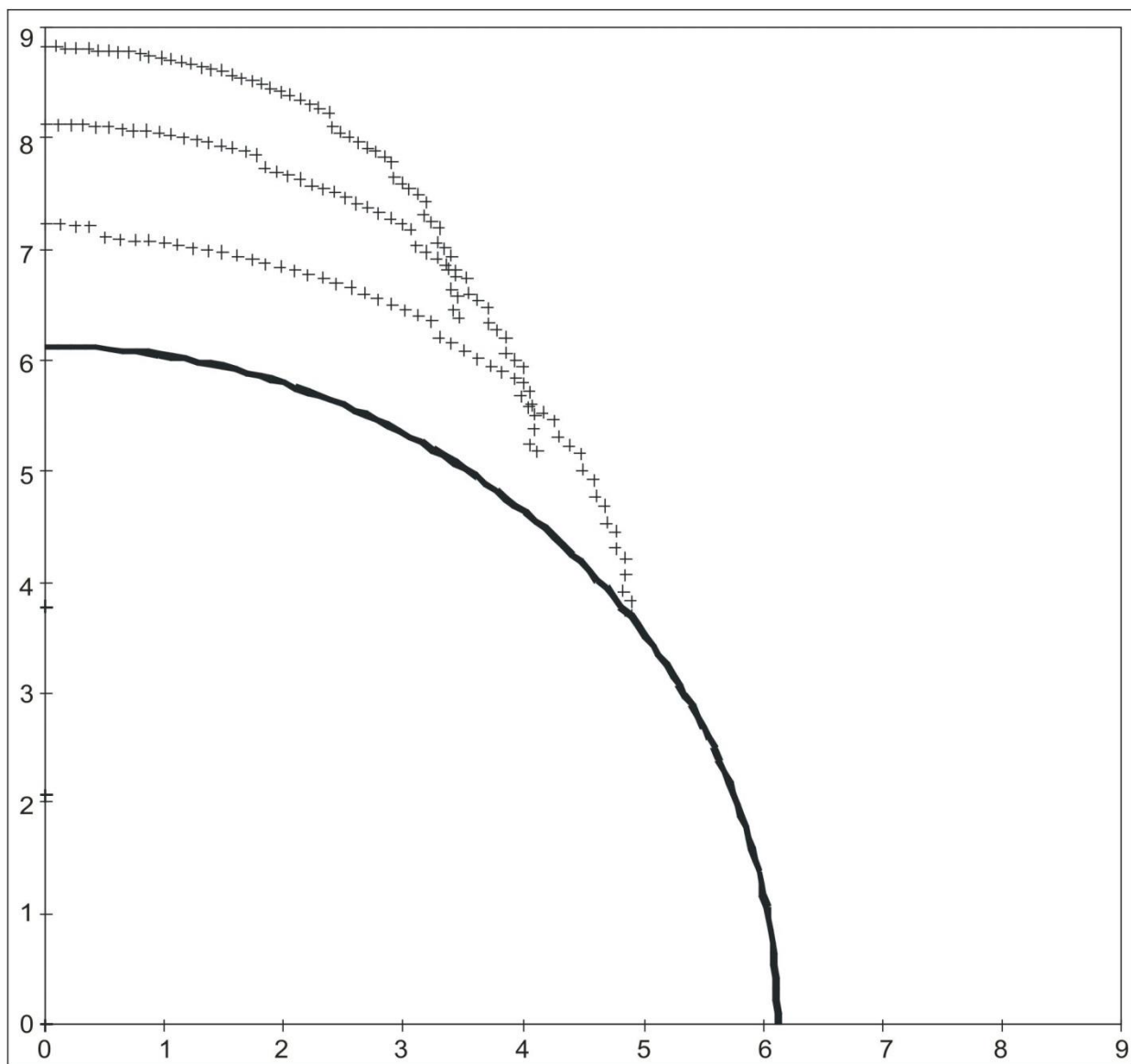
## Extended Drucker - Prager Failure Criterion (Modified Strain Energy Criterion)

SHmax =	65.6 MPa	u (Coeff. of Friction) =	0.6
SHmin =	30.2 MPa	C (Cohesive Strength) =	10 MPa
Sv =	41.2 MPa	v (Poisson's Ratio) =	0.2
Po (Pore Pressure) =	16.7 MPa	Diameter of Borehole =	12.25 inches
Pm (Mud Weight) =	16.7 MPa	Depth of Max. Breakout =	1.1 inches
Sensitivity of Figure =	0.05 inches	Angle of Max. Breakout =	90 deg





D-064-K/094-N-16					
<b>3 Cycle Mohr - Coulomb Failure Criterion</b>					
SHmax =	50.4	MPa	u (Coeff. of Friction) =	0.6	
SHmin =	30.2	MPa	C (Cohesive Strength) =	10	MPa
Sv =	41.2	MPa	v (Poisson's Ratio) =	0.2	
Po (Pore Pressure) =	16.7	MPa	Diameter of Borehole =	12.25	"
Pm (Mud Weight) =	16.7	MPa			
Sensitivity of Figure =	0.05	"			
Depth of Max. Breakout =	2.75	"	Max caliper at 90 deg =	17.75	"
Validity of the results =	TRUE		Max caliper at 0 deg =	12.25	"



## $S_{Hmax}$ Simulation Commentary – D-069-L/094-P-04

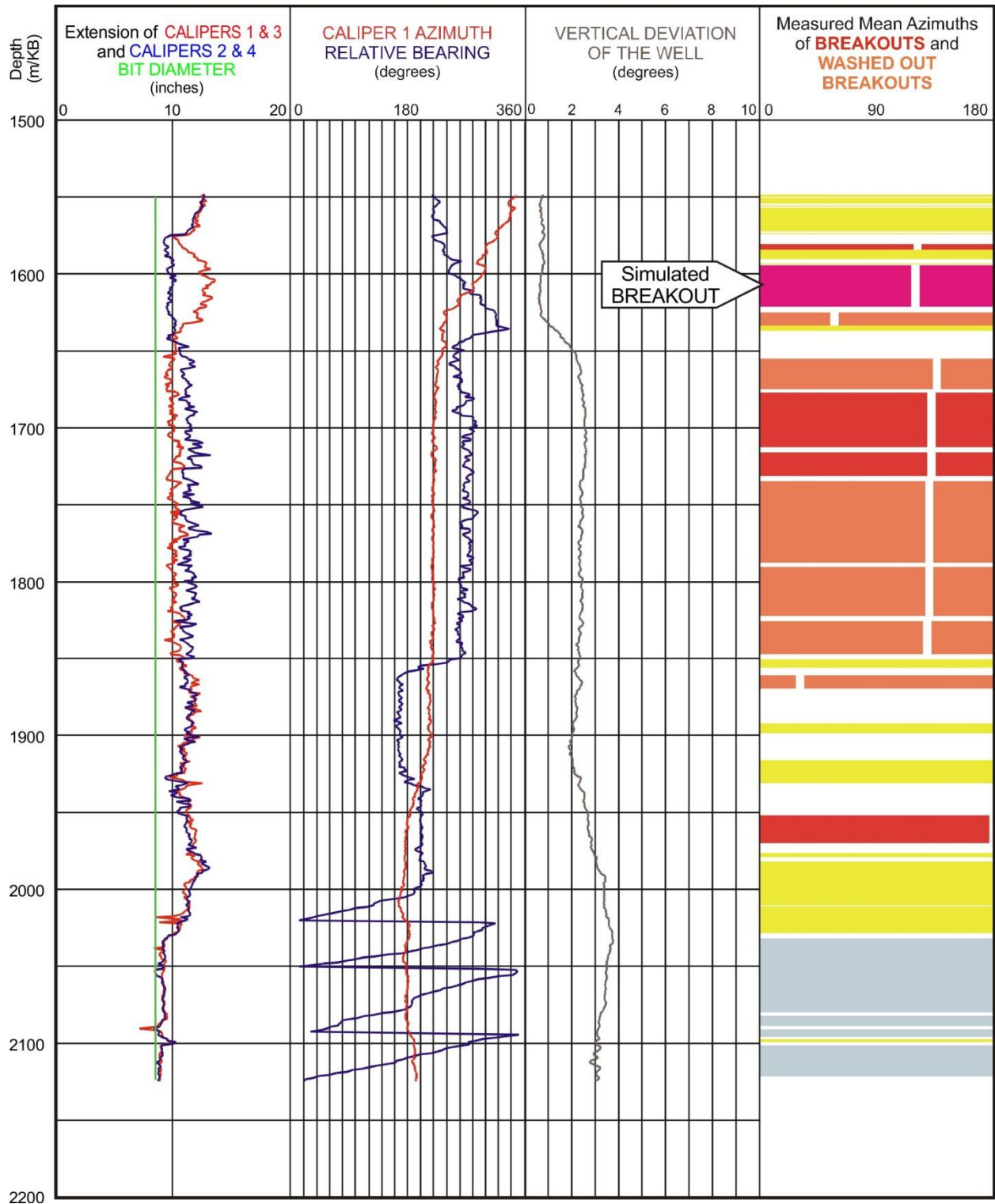
Well: D-069-L/094-P-04	Failure simulation Method				2SHmin-Po
	Mohr Coulomb	Drucker Prager	Modified Strain Energy	3 cycle Mohr Coulomb	
Breakout Interval Top (m KB)	1595	1595	1595	1595	
Breakout Interval Base (m KB)	1635	1635	1635	1635	
Median depth of Breakout (m KB)	1615	1615	1615	1615	
Calipers 1 and 3 extent (inches)	12.65	12.65	12.65	12.65	
Calipers 2 and 4 extent (inches)	9.83	9.83	9.83	9.83	
SHmax (MPa)	50.9*	70.5*	61.7*	<b>46.3</b>	49.4
SHmax gradient (kPa/m)	31.5	43.7	38.2	28.7	30.6
SHmin (MPa)	32.8	32.8	32.8	32.8	
Sv (MPa)	40.3	40.3	40.3	40.3	
Pore Pressure (MPa)	16.2	16.2	16.2	16.2	
Mudweight (MPa)	16.2	16.2	16.2	16.2	
u (Coefficient of Friction)	0.6	0.6	0.6	0.6	
Cohesive Strength of Rock (MPa)	7.0	7.0	7.0	12.0	
v (Poisson's Ratio)	0.2	0.2	0.2	0.2	
Bit size (inches)	8.5	8.5	8.5	8.5	

\* indicates that modelling could not simulate accurate breakout anisotropy

The selected breakout interval (1595-1635 m) is quite deeply spalled. Simulating it using the Mohr Coulomb and Modified Strain Energy routines only generated breakouts with long axes of 12.2 inches. The Drucker-Prager routine generated a breakout with long axis of 12.1 inches. In each case, the cohesive strength was set at 7 MPa. However, the 3 Cycle Mohr Coulomb routine easily generated breakouts with long axes well in excess of 12.6 inches. In order to restrict the long axis dimensions to 12.6 inches, and generate a reasonable value for the magnitude of  $S_{Hmax}$ , it was necessary to raise the cohesive strength to 12 MPa, which is on the high side. It is believed that the true  $S_{Hmax}$  magnitude lies between 50.9 MPa (Mohr Coulomb simulation) and 46.3 MPa (3 Cycle Mohr Coulomb simulation).

The  $S_V$  magnitude for well D-069-L/094-P-04 is well established from the density log.

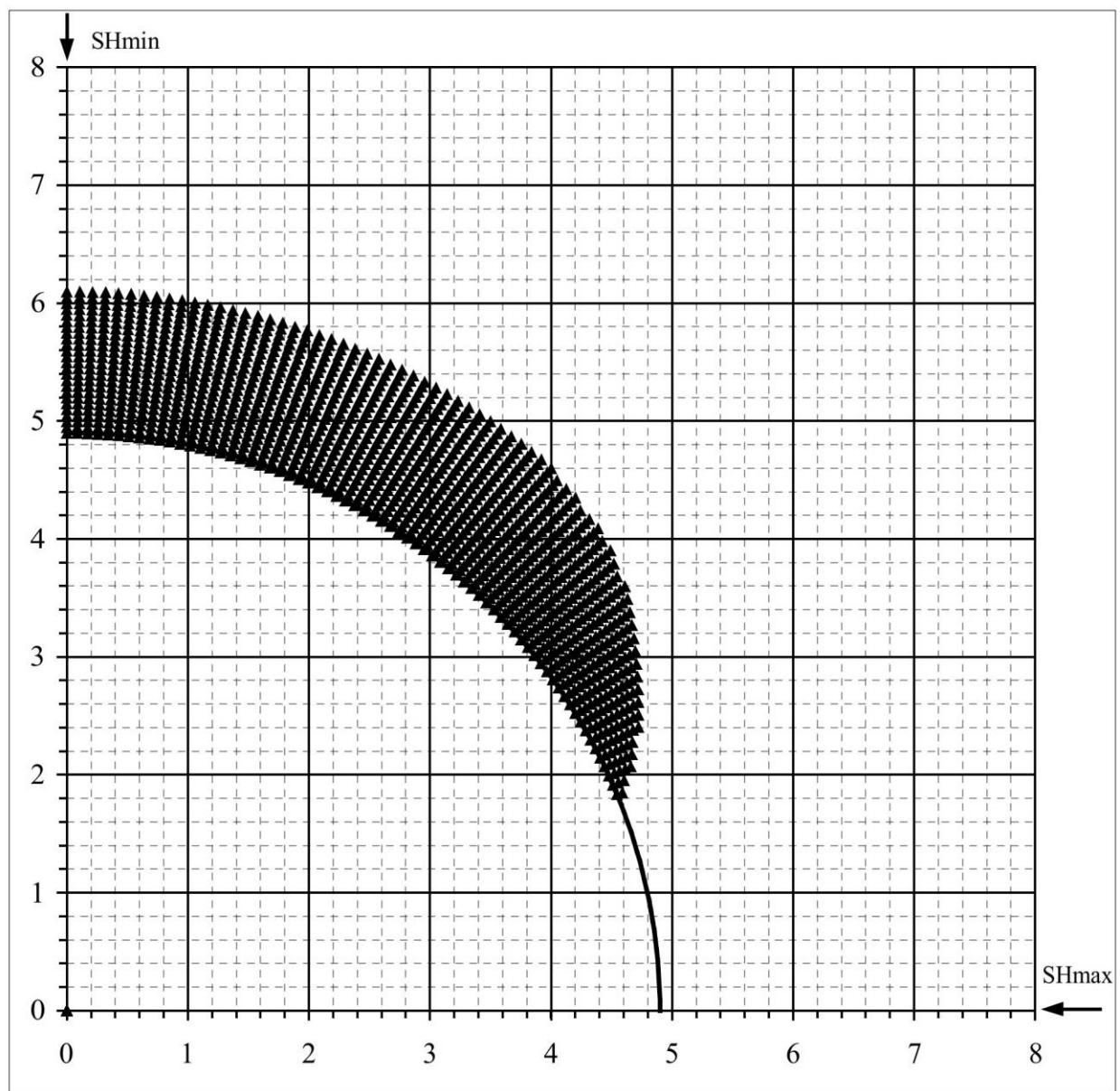
WELL : D-069-L/094-P-04      BREAKOUT ANALYSIS



D-069-L/094-P-04

## Mohr - Coulomb Failure Criterion

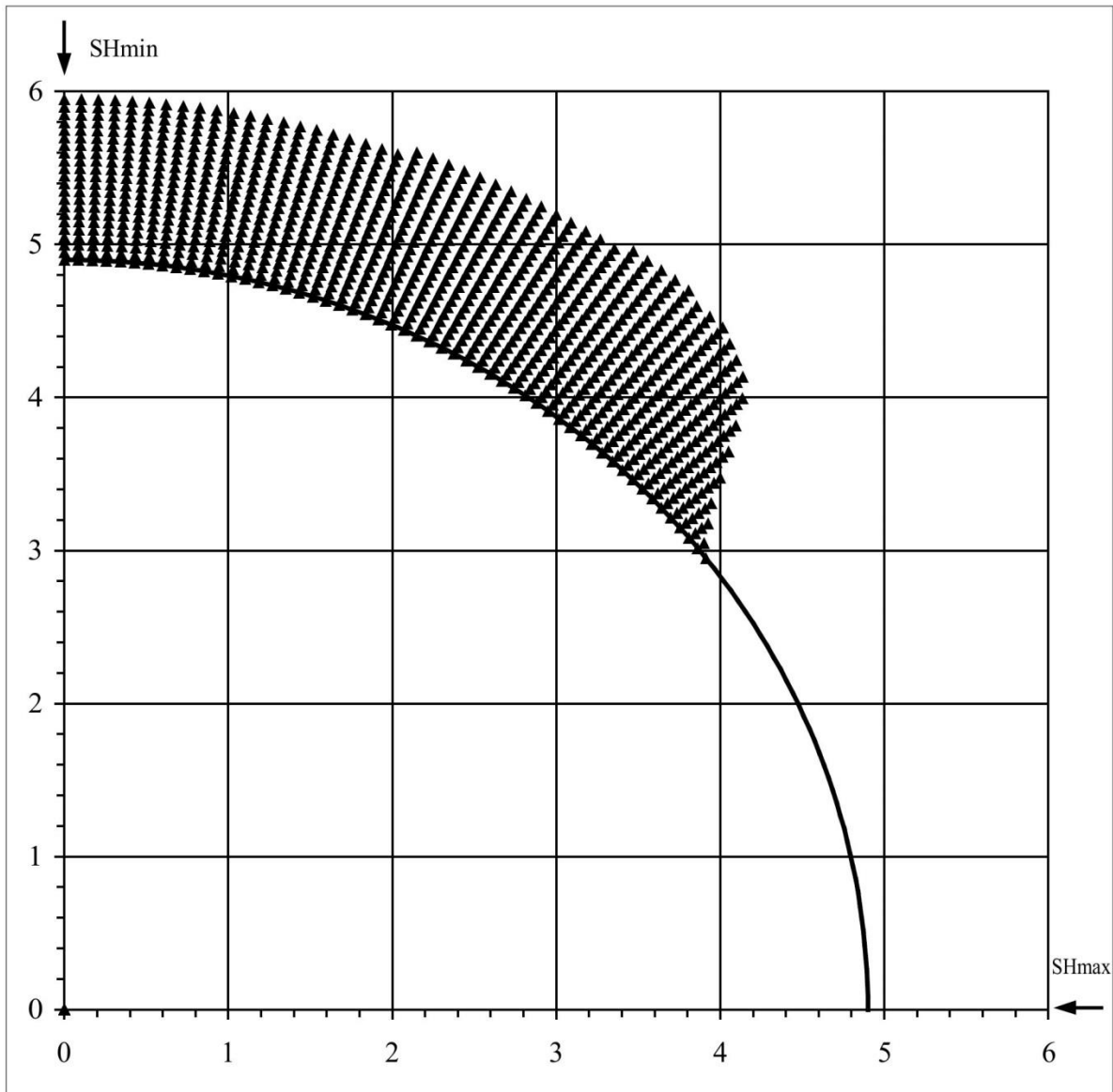
SHmax =	50.9 MPa	u (Coeff. of Friction) =	0.6
SHmin =	32.8 MPa	C (Cohesive Strength) =	7 MPa
Sv =	40.3 MPa	v (Poisson's Ratio) =	0.2
Po (Pore Pressure) =	16.2 MPa	Diameter of Borehole =	9.8 "
Pm (Mud Weight) =	16.2 MPa		
Sensitivity of Figure =	0.05 "	Angle of Max. Breakout =	61 deg
Depth of Max. Breakout =	1.2 "	Max caliper at 90 deg =	12.2 "
Validity of the results =	FALSE	Max caliper at 0 deg =	8 "



D-069-L/094-P-04

## Extended von-Mises Failure Criterion (Drucker-Prager Failure Criterion)

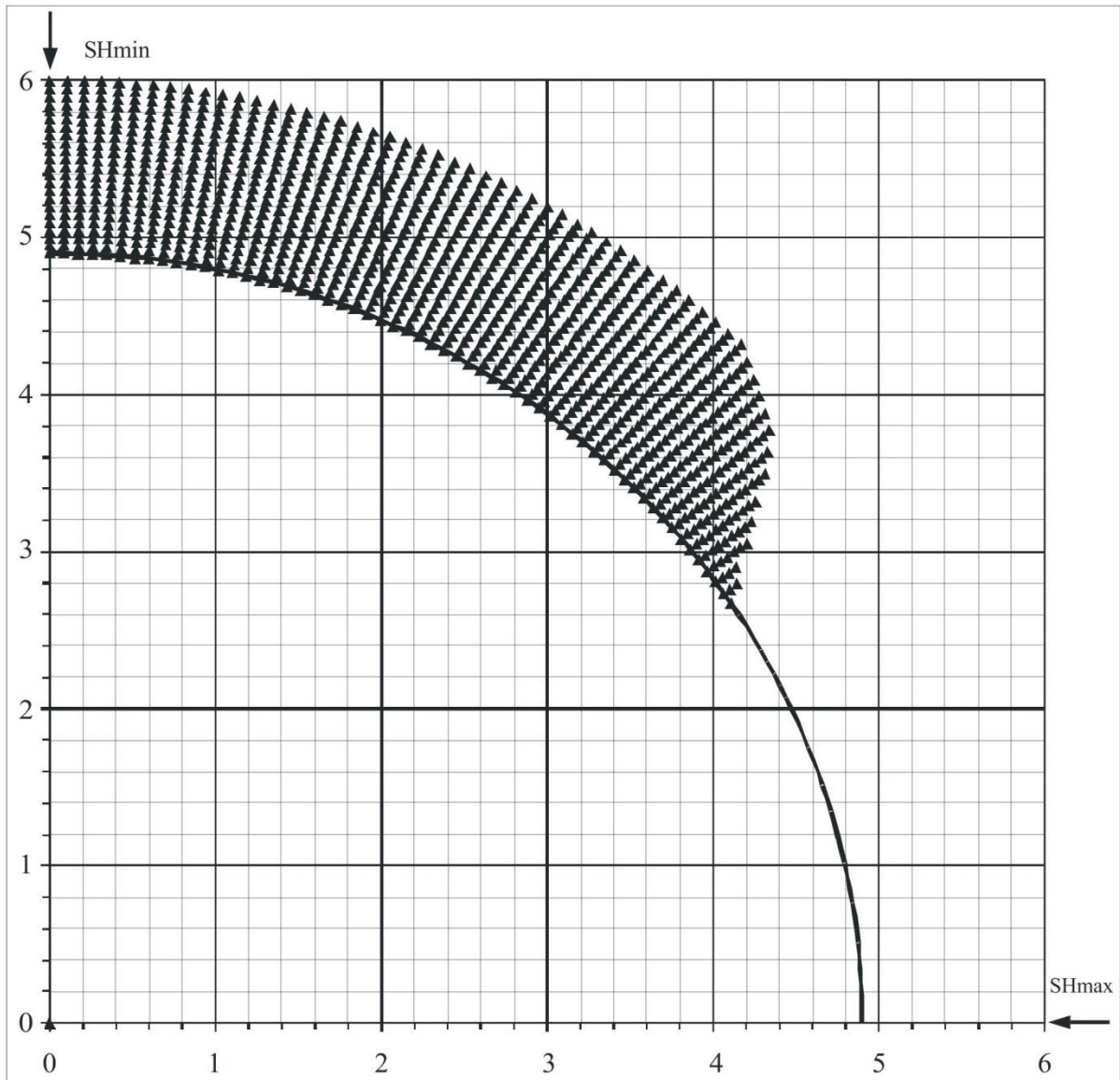
SHmax =	70.5 MPa	u (Coeff. of Friction)=	0.6
SHmin =	32.8 MPa	C (Cohesive Strength) =	7 MPa
Sv =	40.3 MPa	v (Poisson's Ratio) =	0.2
Po (Pore Pressure) =	16.2 MPa	Diameter of Borehole =	9.8 inches
Pm (Mud Weight) =	16.2 MPa	Depth of Max. Breakout =	1.15 inches
Sensitivity of Figure =	0.05 inches	Angle of Max. Breakout =	53 deg



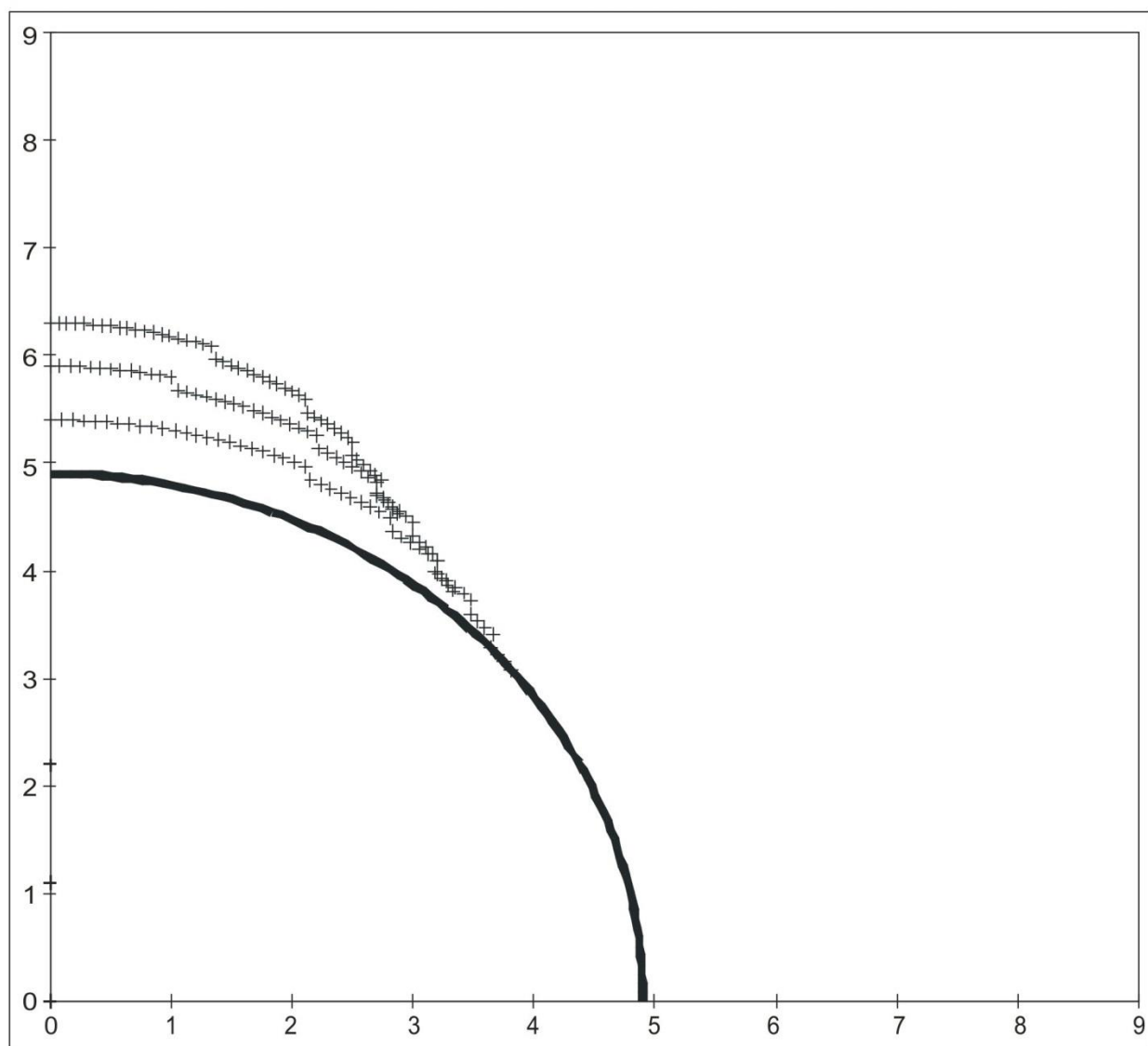
D-069-L/094-P-04

## Extended Drucker - Prager Failure Criterion (Modified Strain Energy Criterion)

SHmax =	61.7 MPa	u (Coeff. of Friction) =	0.6
SHmin =	32.8 MPa	C (Cohesive Strength) =	7 MPa
Sv =	40.3 MPa	v (Poisson's Ratio) =	0.2
Po (Pore Pressure) =	16.2 MPa	Diameter of Borehole =	9.8 inches
Pm (Mud Weight) =	16.2 MPa	Depth of Max. Breakout =	1.2 inches
Sensitivity of Figure =	0.05 inches	Angle of Max. Breakout =	54 deg



D-069-L/094-P-04					
<b>3 Cycle Mohr - Coulomb Failure Criterion</b>					
SHmax =	46.3	MPa	u (Coeff. of Friction) =	0.6	
SHmin =	32.8	MPa	C (Cohesive Strength) =	12	MPa
Sv =	40.3	MPa	v (Poisson's Ratio) =	0.2	
Po (Pore Pressure) =	16.2	MPa	Diameter of Borehole =	9.8	"
Pm (Mud Weight) =	16.2	MPa			
Sensitivity of Figure =	0.05	"			
Depth of Max. Breakout =	1.4	"	Max caliper at 90 deg =	12.6	"
Validity of the results =	TRUE		Max caliper at 0 deg =	9.8	"



## $S_{Hmax}$ Simulation Commentary – D-074-F/094-P-05

Well: D-074-F/094-P-05	Failure simulation Method				2SHmin-Po
	Mohr Coulomb	Drucker Prager	Modified Strain Energy	3 cycle Mohr Coulomb	
Breakout Interval Top (m KB)	290	290	290	290	
Breakout Interval Base (m KB)	305	305	305	305	
Median depth of Breakout (m KB)	297.5	297.5	297.5	297.5	
Calipers 1 and 3 extent (inches)	14.15	14.15	14.15	14.15	
Calipers 2 and 4 extent (inches)	8.61	8.61	8.61	8.61	
SHmax (MPa)	10.3*	13.1*	11.4*	<b>10.2</b>	8.8
SHmax gradient (kPa/m)	34.6	44.0	38.3	34.3	29.6
SHmin (MPa)	5.9	5.9	5.9	5.9	
Sv (MPa)	7.3	7.3	7.3	7.3	
Pore Pressure (MPa)	3.0	3.0	3.0	3.0	
Mudweight (MPa)	3.0	3.0	3.0	3.0	
u (Coefficient of Friction)	0.6	0.6	0.6	0.6	
Cohesive Strength of Rock (MPa)	1.5	1.5	1.5	1.5	
v (Poisson's Ratio)	0.2	0.2	0.2	0.2	
Bit size (inches)	8.5	8.5	8.5	8.5	

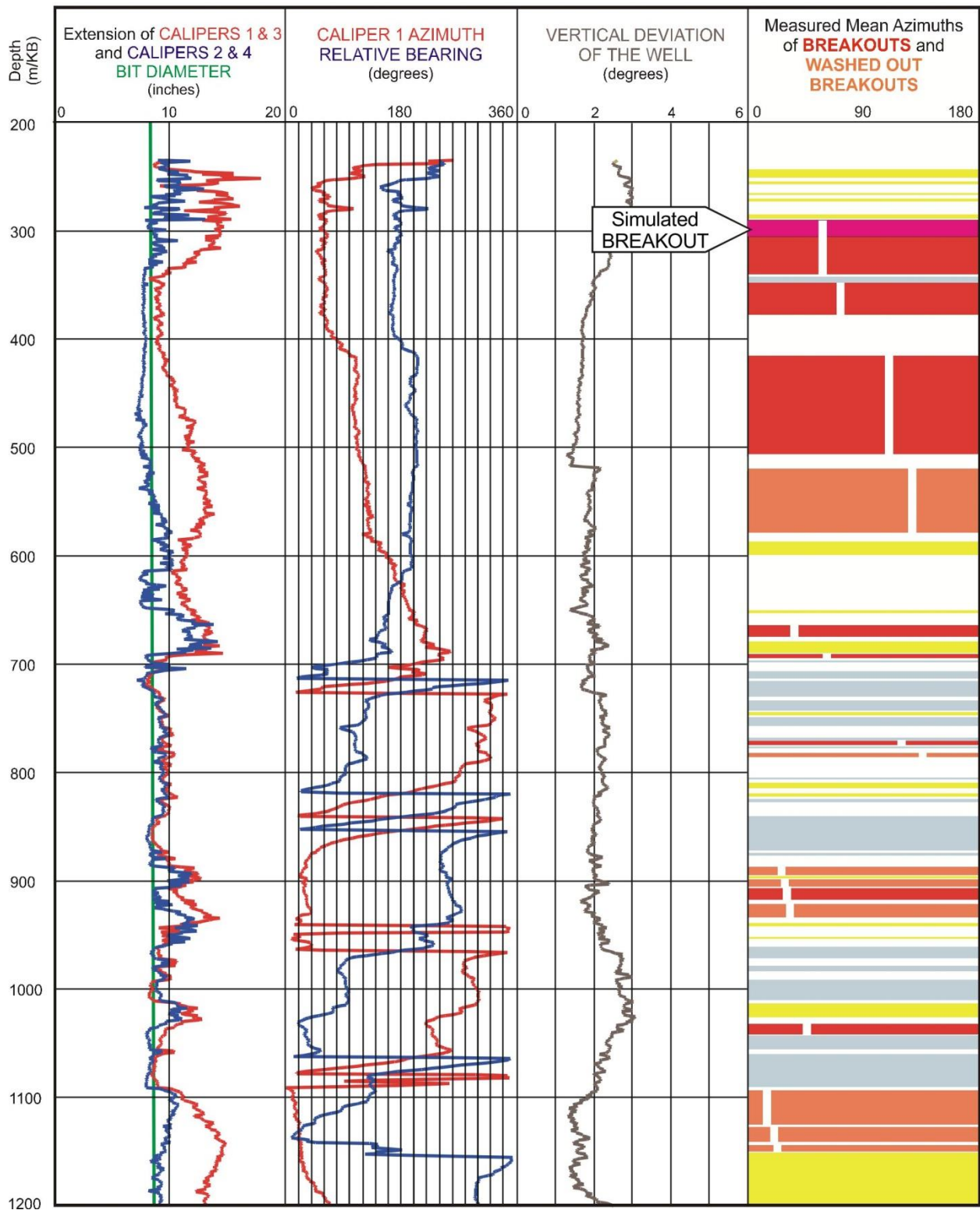
- indicates that modelling could not simulate accurate breakout anisotropy

The breakout interval that was selected for modeling (290-305 m) is the upper part of a longer breakout zone. It was selected because this was the part of the breakout that had exhibited the deepest spalling. It could not be simulated with any of the three single cycle methods, even when the cohesive strength was lowered from 1.5 MPa. Raising  $S_{Hmax}$  to high magnitudes did not generate sufficiently deep breakouts, the maximum being 10.7 inches generated by the Mohr Coulomb routine with an  $S_{Hmax}$  magnitude of 13.1 MPa.

The 3 cycle Mohr-Coulomb simulation modelled a breakout with long axis of 14.1 inches when the cohesive strength was set at 1.5 MPa. The resulting  $S_{Hmax}$  magnitude of **10.2 MPa** is slightly greater than 8.8 MPa, that was suggested by the equation:  $S_{Hmax} = 2(S_{Hmin}) - Po$ .



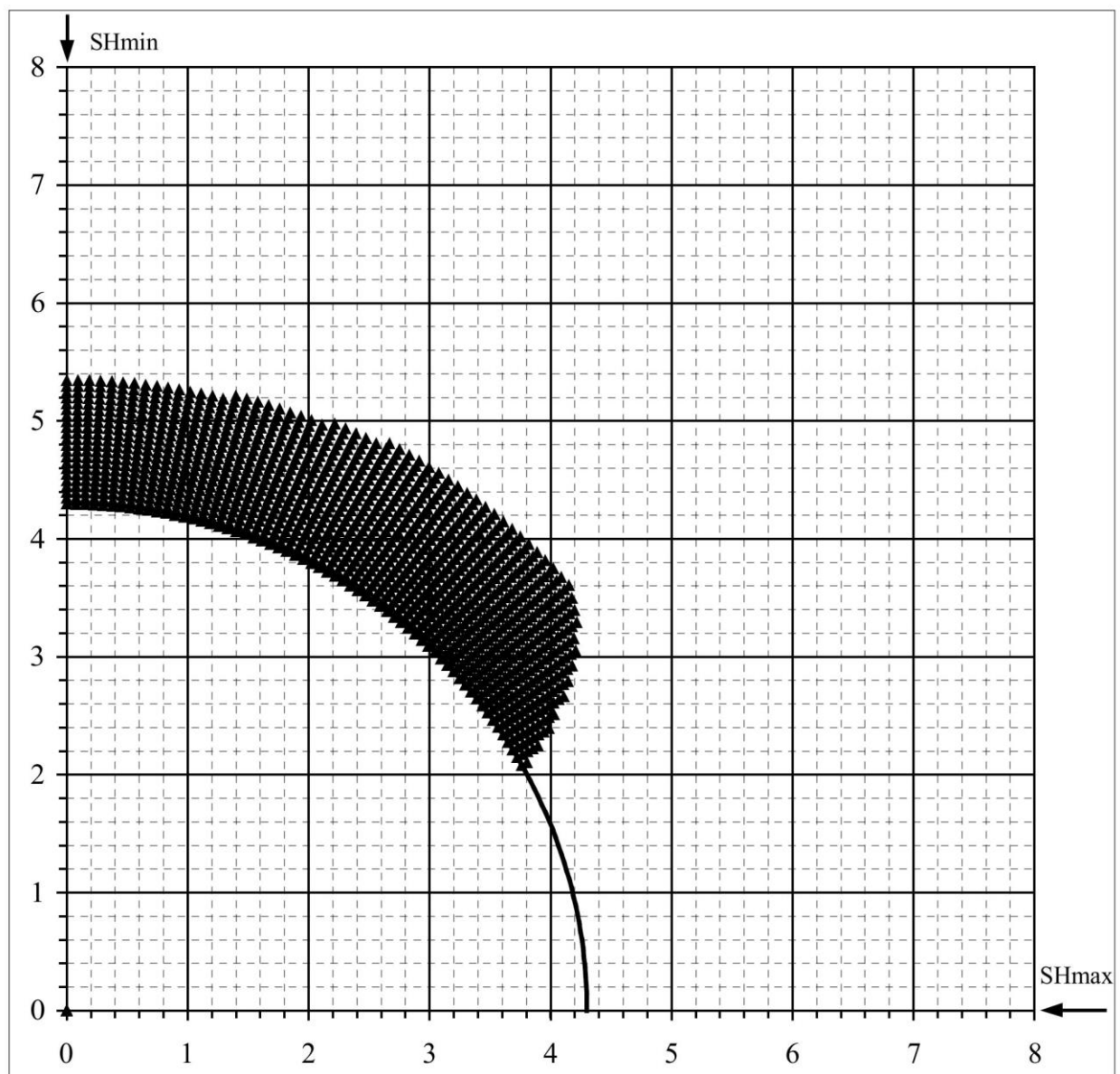
WELL : D-074-F/094-P-05 BREAKOUT ANALYSIS



D-074-F/094-P-05

## Mohr - Coulomb Failure Criterion

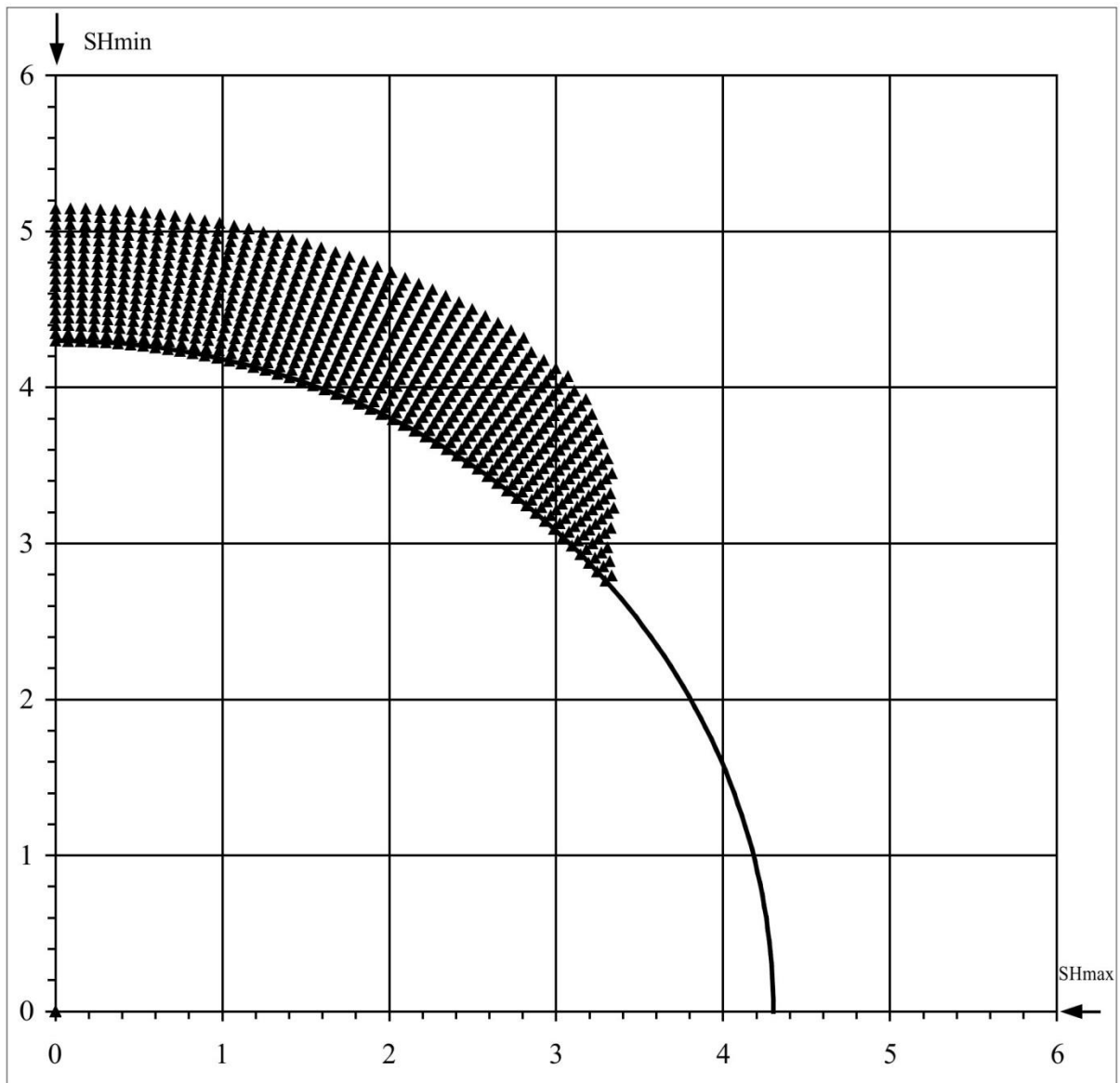
SHmax =	10.3 MPa	u (Coeff. of Friction) =	0.6
SHmin =	5.9 MPa	C (Cohesive Strength) =	1.5 MPa
Sv =	7.3 MPa	v (Poisson's Ratio) =	0.2
Po (Pore Pressure) =	3 MPa	Diameter of Borehole =	8.6 "
Pm (Mud Weight) =	3 MPa		
Sensitivity of Figure =	0.05 "	Angle of Max. Breakout =	50 deg
Depth of Max. Breakout =	1.2 "	Max caliper at 90 deg =	10.7 "
Validity of the results =	FALSE	Max caliper at 0 deg =	8 "



D-074-F/094-P-05

## Extended von-Mises Failure Criterion (Drucker-Prager Failure Criterion)

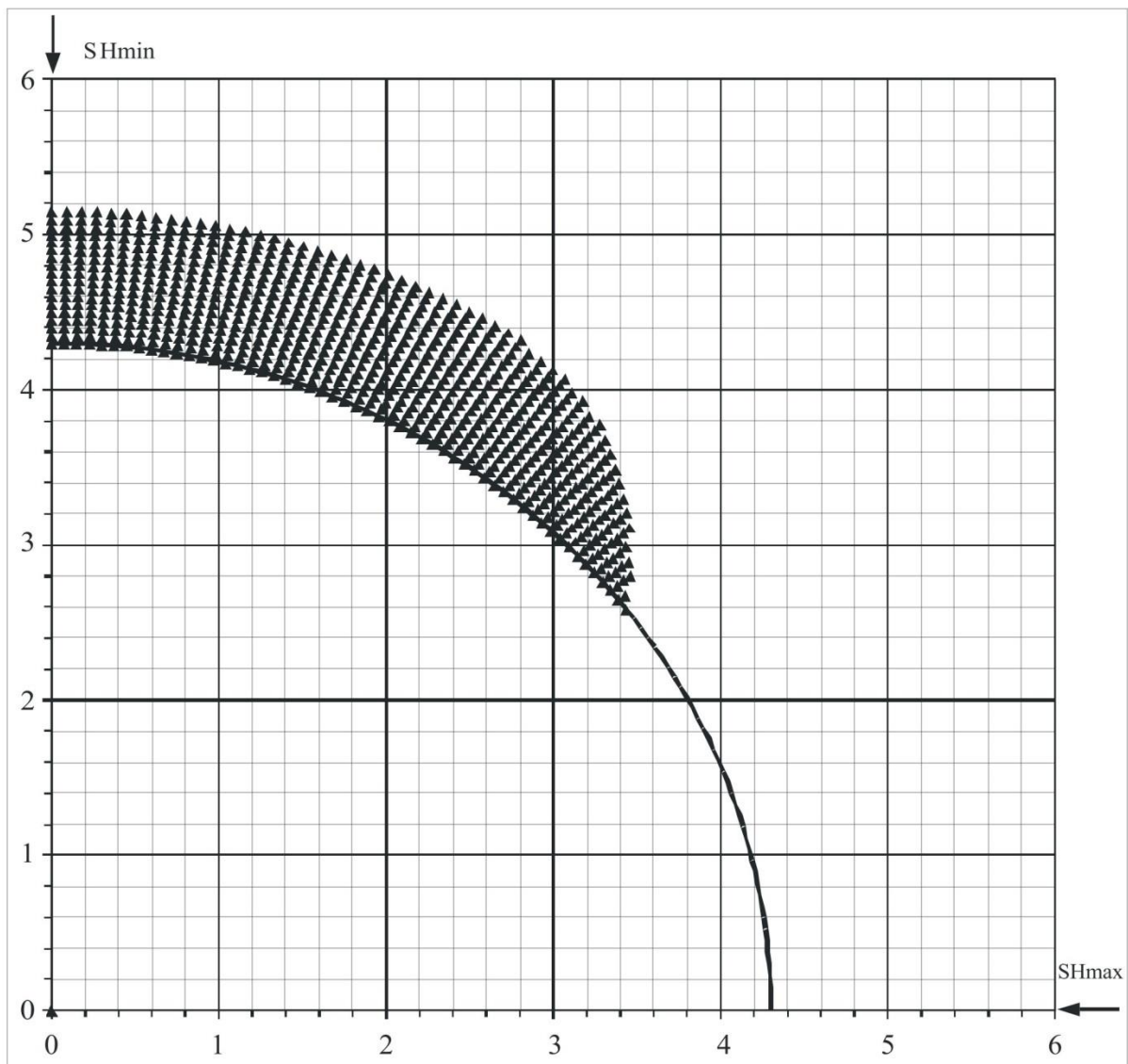
SHmax =	13.1 MPa	u (Coeff. of Friction)=	0.6
SHmin =	5.9 MPa	C (Cohesive Strength) =	1.5 MPa
Sv =	7.3 MPa	v (Poisson's Ratio) =	0.2
Po (Pore Pressure) =	3 MPa	Diameter of Borehole =	8.6 inches
Pm (Mud Weight) =	3 MPa	Depth of Max. Breakout =	0.85 inches
Sensitivity of Figure =	0.05 inches	Angle of Max. Breakout =	90 deg



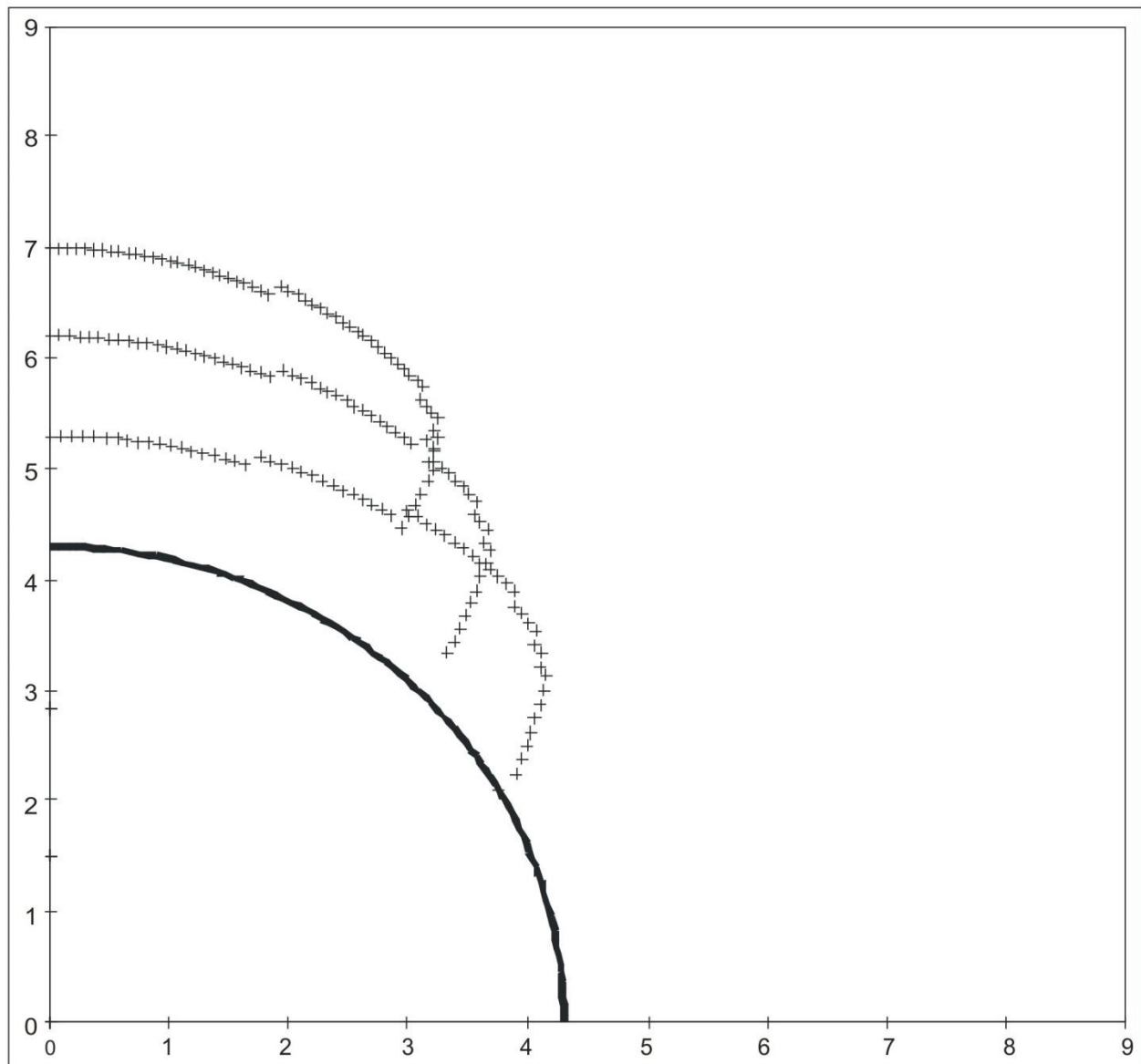
D-074-F/094-P-05

## Extended Drucker - Prager Failure Criterion (Modified Strain Energy Criterion)

SHmax =	11.4 MPa	u (Coeff. of Friction) =	0.6
SHmin =	5.9 MPa	C (Cohesive Strength) =	1.5 MPa
Sv =	7.3 MPa	v (Poisson's Ratio) =	0.2
Po (Pore Pressure) =	3 MPa	Diameter of Borehole =	8.6 inches
Pm (Mud Weight) =	3 MPa	Depth of Max. Breakout =	0.85 inches
Sensitivity of Figure =	0.05 inches	Angle of Max. Breakout =	90 deg



D-074-F/094-P-05					
3 Cycle Mohr - Coulomb Failure Criterion					
SHmax =	10.2	MPa	u (Coeff. of Friction) =	0.6	
SHmin =	5.9	MPa	C (Cohesive Strength) =	1.5	MPa
Sv =	7.3	MPa	v (Poisson's Ratio)=	0.2	
Po (Pore Pressure) =	3	MPa	Diameter of Borehole =	8.6	"
Pm (Mud Weight) =	3	MPa			
Sensitivity of Figure =	0.05	"			
Depth of Max. Breakout =	2.9	"	Max caliper at 90 deg =	14.1	"
Validity of the results =	FALSE		Max caliper at 0 deg =	8.6	"



**SHmax Simulation Commentary – D-087-C /094-P-05**

Well: <b>D-087-C/094-P-05</b>	Failure simulation Method				2SHmin-Po
	Mohr Coulomb	Drucker Prager	Modified Strain Energy	3 cycle Mohr Coulomb	
Breakout Interval Top (m KB)	2001	2001	2001	2001	
Breakout Interval Base (m KB)	2067	2067	2067	2067	
Median depth of Breakout (m KB)	2034	2034	2034	2034	
Calipers 1 and 3 extent (inches)	7.79	7.79	7.79	7.79	
Calipers 2 and 4 extent (inches)	14.9	14.9	14.9	14.9	
SHmax (MPa)	63.4*	82.5*	72.5*	<b>58.7</b>	61.1
SHmax gradient (kPa/m)	31.2	40.6	35.6	28.9	30.0
SHmin (MPa)	40.7	40.3	40.7	40.3	
Sv (MPa)	50.6	50.6	50.6	50.6	
Pore Pressure (MPa)	20.3	20.3	20.3	20.3	
Mudweight (MPa)	20.3	20.3	20.3	20.3	
u (Coefficient of Friction)	0.6	0.6	0.6	0.6	
Cohesive Strength of Rock (MPa)	7.0	7.0	7.0	7.0	
v (Poisson's Ratio)	0.2	0.2	0.2	0.2	
Bit size (inches)	8.5	8.5	8.5	8.5	

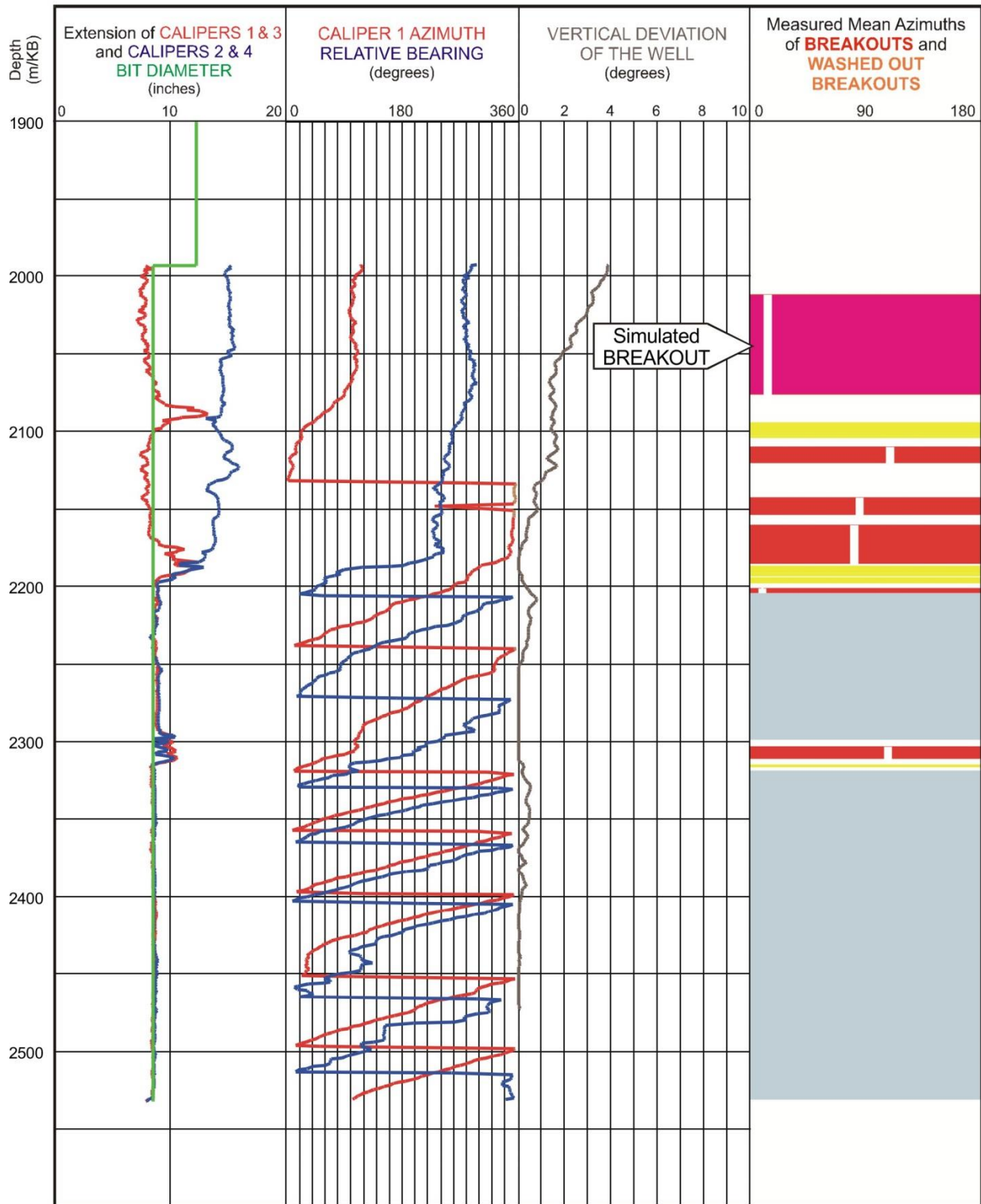
\* indicates that modelling could not simulate accurate breakout anisotropy

The breakout interval that was selected for modelling, 2001-2067 m, exhibits very deep spalling. Raising  $S_{Hmax}$  magnitudes did not generate sufficiently deep breakouts, the maximum being 10.9 inches generated by the Mohr Coulomb routine with an  $S_{Hmax}$  magnitude of 63.4 MPa.

The 3 cycle Mohr-Coulomb simulation modelled a breakout with a long axis of 14.9 inches when the cohesive strength was set at 7.0 MPa. The resulting  $S_{Hmax}$  magnitude of **58.7 MPa** is slightly lower than 61.1 MPa, which was suggested by the equation:  $S_{Hmax} = 2(S_{Hmin}) - Po$ .

The vertical stress,  $S_v$ , is well established at 2034 m depth from the density log.

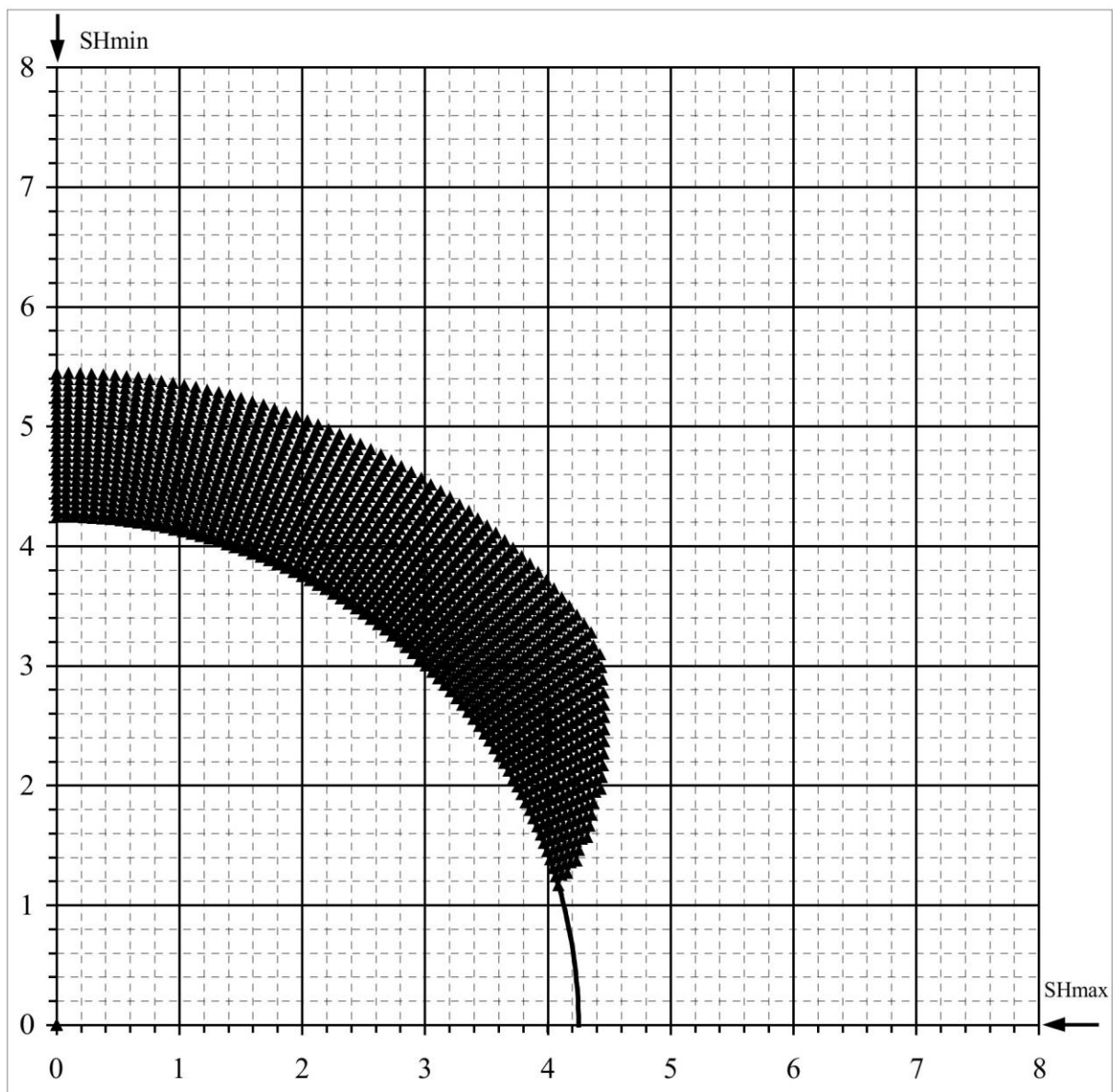
WELL : D-087-C/094-P-05 BREAKOUT ANALYSIS



D-087-C/094-P-05

## Mohr - Coulomb Failure Criterion

SHmax =	63.4 MPa	u (Coeff. of Friction) =	0.6
SHmin =	40.7 MPa	C (Cohesive Strength) =	7 MPa
Sv =	50.6 MPa	v (Poisson's Ratio) =	0.2
Po (Pore Pressure) =	20.3 MPa	Diameter of Borehole =	8.5 "
Pm (Mud Weight) =	20.3 MPa		
Sensitivity of Figure =	0.05 "	Angle of Max. Breakout =	53 deg
Depth of Max. Breakout =	1.2 "	Max caliper at 90 deg =	10.9 "
Validity of the results =	FALSE	Max caliper at 0 deg =	8.5 "

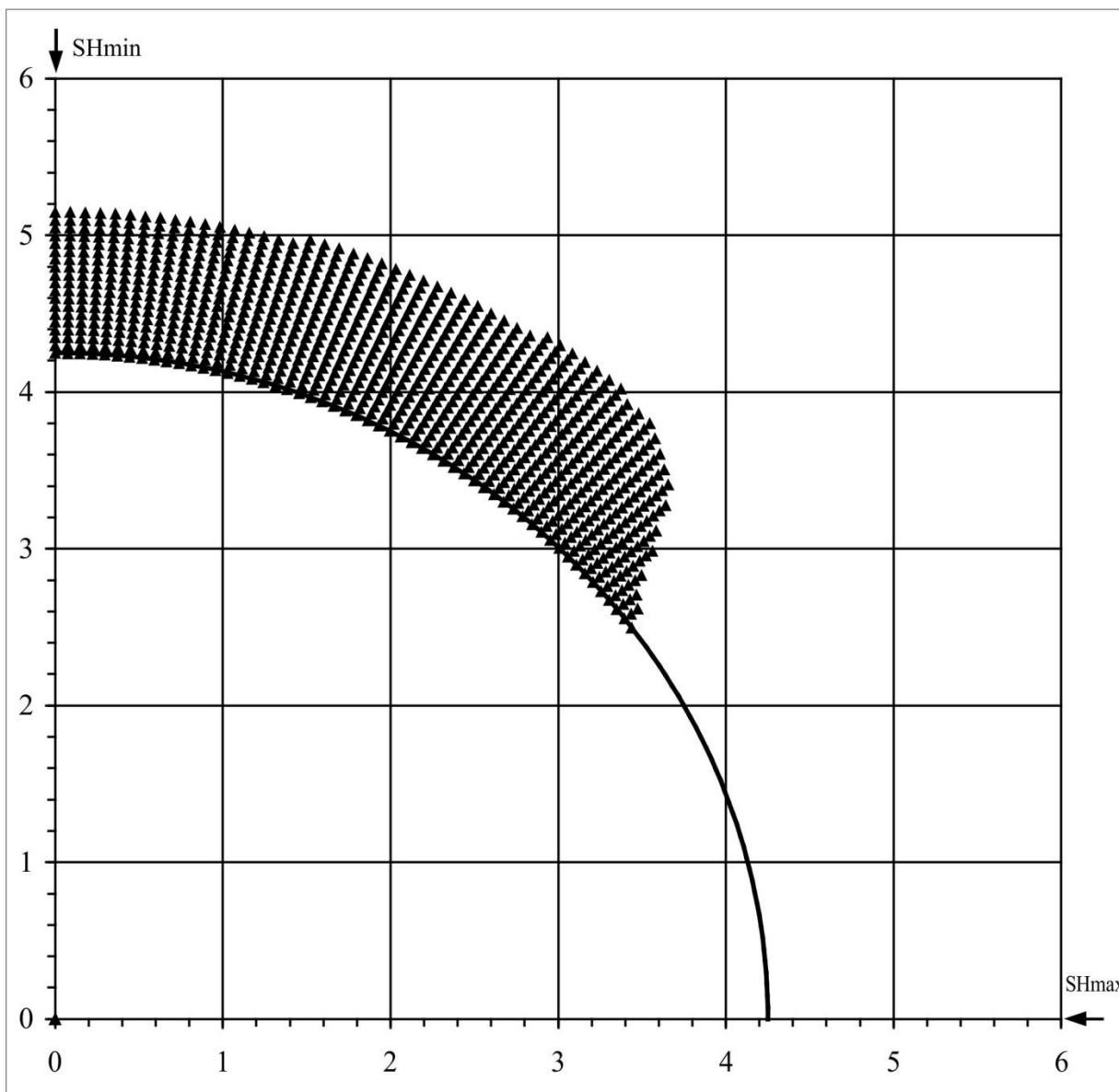




D-087-C/094-P-05

## Extended von-Mises Failure Criterion (Drucker-Prager Failure Criterion)

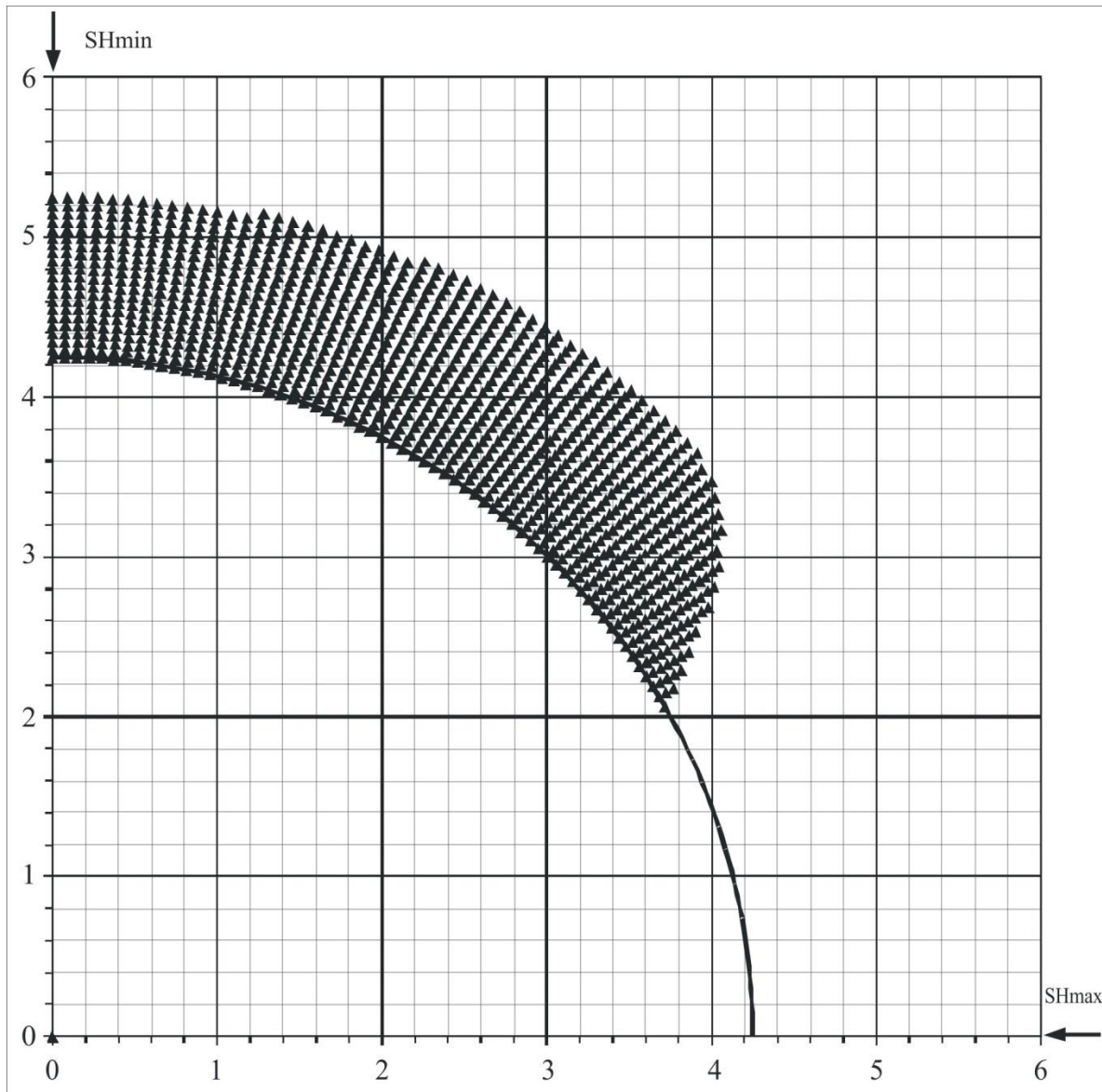
SHmax =	82.5 MP	u (Coeff. of Friction)=	0.6
SHmin =	40.3 MP	C (Cohesive Strength) =	7 MPa
Sv =	50.6 MP	v (Poisson's Ratio) =	0.2
Po (Pore Pressure) =	20.3 MP	Diameter of Borehole =	8.5 inches
Pm (Mud Weight) =	20.3 MP	Depth of Max. Breakout =	1 inches
Sensitivity of Figure =	0.05 inches	Angle of Max. Breakout =	53 deg



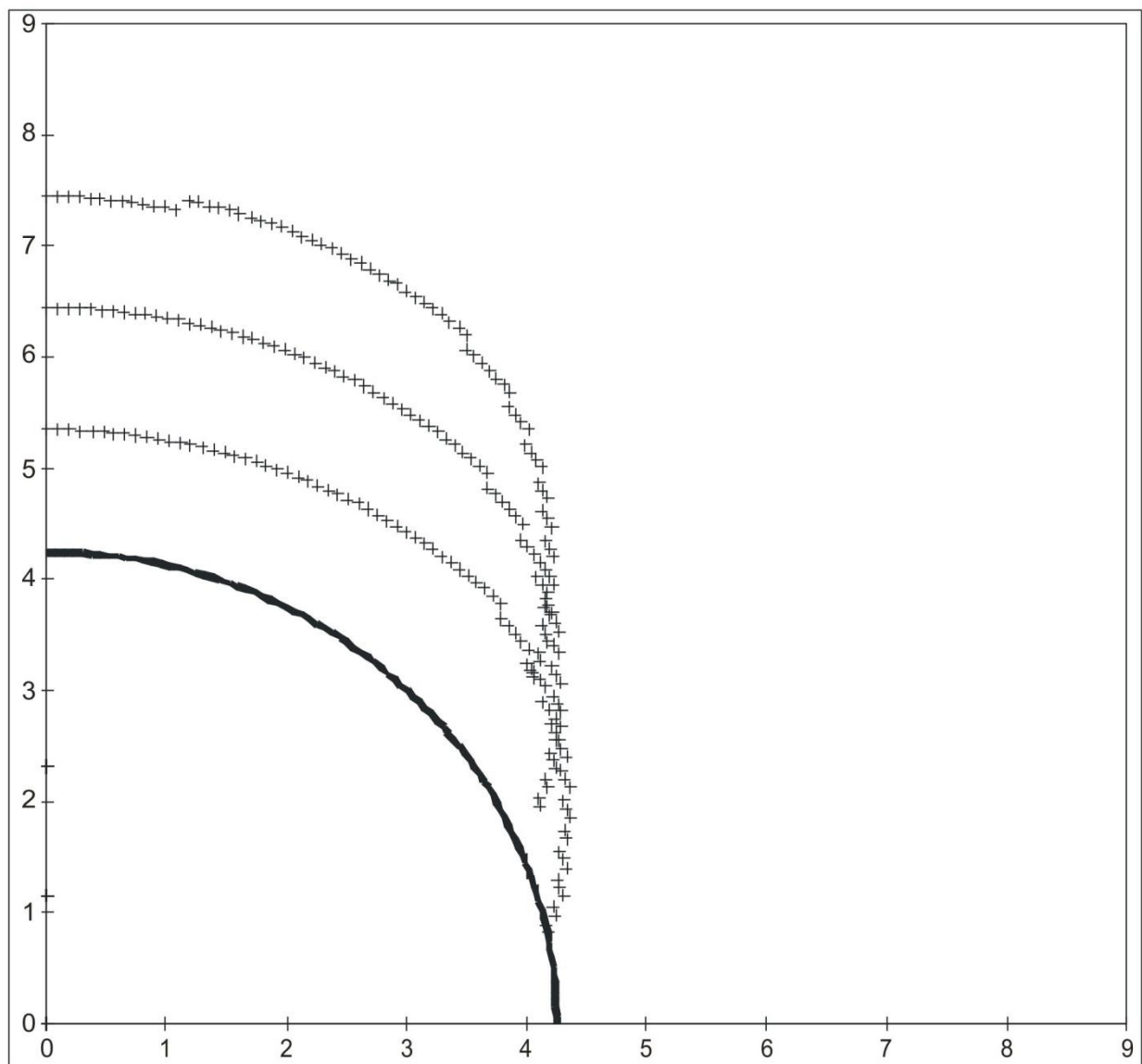
D-087-C/094-P-05

## Extended Drucker - Prager Failure Criterion (Modified Strain Energy Criterion)

SHmax =	72.5 MPa	u (Coeff. of Friction) =	0.6
SHmin =	40.7 MPa	C (Cohesive Strength) =	7 MPa
Sv =	50.6 MPa	v (Poisson's Ratio) =	0.2
Po (Pore Pressure) =	20.3 MP	Diameter of Borehole =	8.5 inches
Pm (Mud Weight) =	20.3 MPa	Depth of Max. Breakout =	1.15 inches
Sensitivity of Figure =	0.05 inches	Angle of Max. Breakout =	51 deg



D-087-C/094-P-05					
<b>3 Cycle Mohr - Coulomb Failure Criterion</b>					
SHmax =	58.7	MPa	u (Coeff. of Friction) =	0.6	
SHmin =	40.3	MPa	C (Cohesive Strength) =	7	MPa
Sv =	50.6	MPa	v (Poisson's Ratio) =	0.2	
Po (Pore Pressure) =	20.3	MPa	Diameter of Borehole =	8.5	"
Pm (Mud Weight) =	20.3	MPa			
Sensitivity of Figure =	0.05	"			
Depth of Max. Breakout =	3.2	"	Max caliper at 90 deg =	14.9	"
Validity of the results =	TRUE		Max caliper at 0 deg =	8.5	"



**SHmax Simulation Commentary – D-087-G /094-O-06**

Well: <b>D-092-J/094-O-06</b>	Failure simulation Method				2SHmin-Po
	Mohr Coulomb	Drucker Prager	Modified Strain Energy	3 cycle Mohr Coulomb	
Breakout Interval Top (m KB)	300	300	300	300	
Breakout Interval Base (m KB)	441	441	441	441	
Median depth of Breakout (m KB)	370.5	370.5	370.5	370.5	
Calipers 1 and 3 extent (inches)	7.49	7.49	7.49	7.49	
Calipers 2 and 4 extent (inches)	10.5	10.5	10.5	10.5	
SHmax (MPa)	13.6*	17.2*	16.1*	<b>10.6</b>	10.1
SHmax gradient (kPa/m)	36.7	46.4	43.5	28.6	27.3
SHmin (MPa)	6.9	6.9	6.9	6.9	
Sv (MPa)	8.6	8.6	8.6	8.6	
Pore Pressure (MPa)	3.7	3.7	3.7	3.7	
Mudweight (MPa)	3.7	3.7	3.7	3.7	
u (Coefficient of Friction)	0.6	0.6	0.6	0.6	
Cohesive Strength of Rock (MPa)	2.5	2.5	2.5	2.5	
v (Poisson's Ratio)	0.2	0.2	0.2	0.2	
Bit size (inches)	7.875	7.875	7.875	7.875	

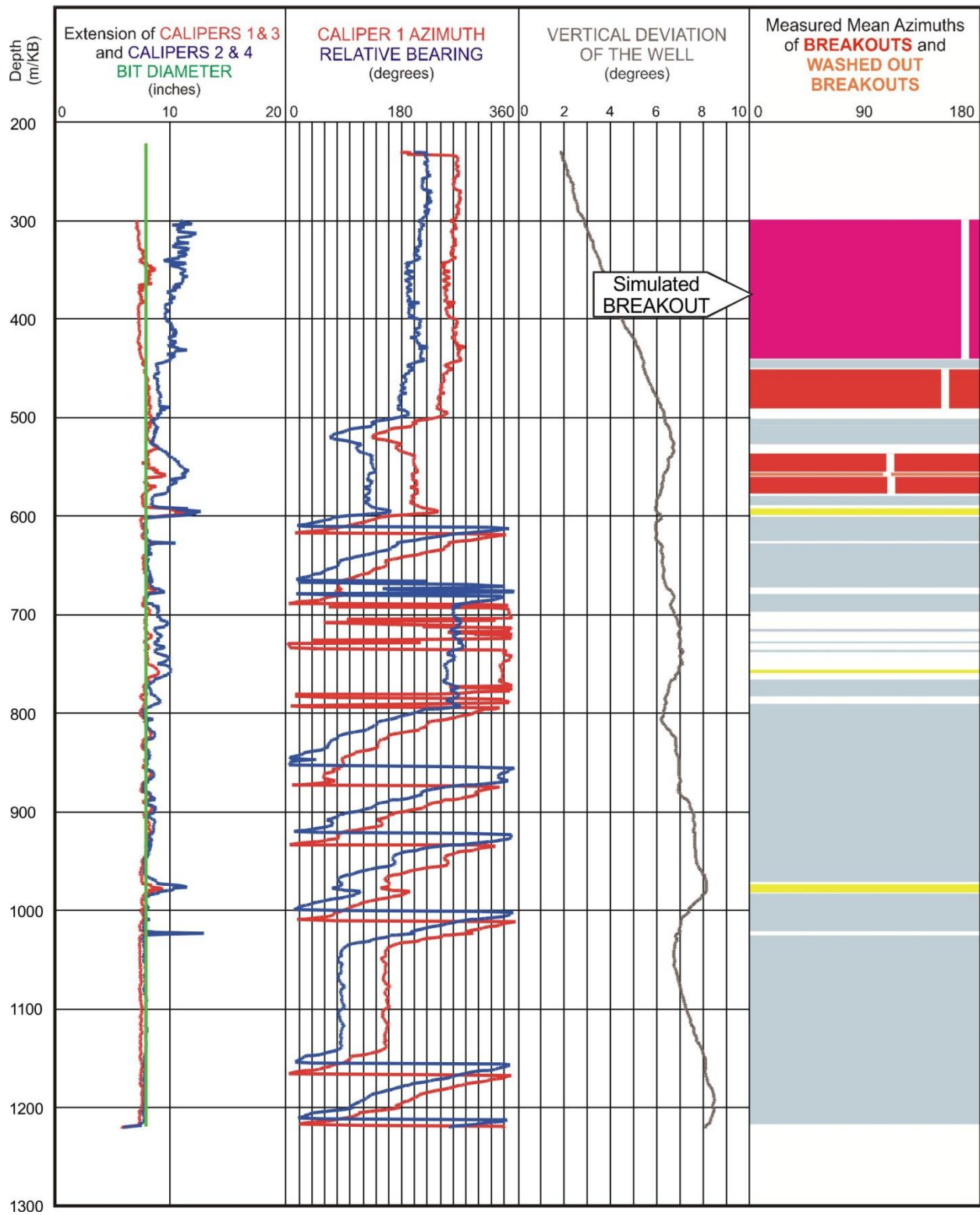
\* indicates that modelling could not simulate accurate breakout anisotropy

The breakout interval that was selected for modelling, 300-341 m, exhibits very deep spalling. Raising  $S_{Hmax}$  magnitudes with the single cycle routines did not generate sufficiently deep breakouts, the maximum being 9.6 inches generated by the Mohr Coulomb routine with an  $S_{Hmax}$  magnitude of 13.6 MPa. This simulation used a cohesive strength of 2.5 MPa.

The 3 cycle Mohr-Coulomb simulation modelled a breakout with a long axis of 10.5 inches, again with the cohesive strength set at 2.5 MPa. The resulting  $S_{Hmax}$  magnitude of **10.6 MPa** is slightly higher than 10.1 MPa that was suggested by the equation:  $S_{Hmax} = 2(S_{Hmin}) - Po$ .

The vertical stress,  $S_v$ , in well D-087-G/094-O-06 is well established at 370.5 m depth from the density log.

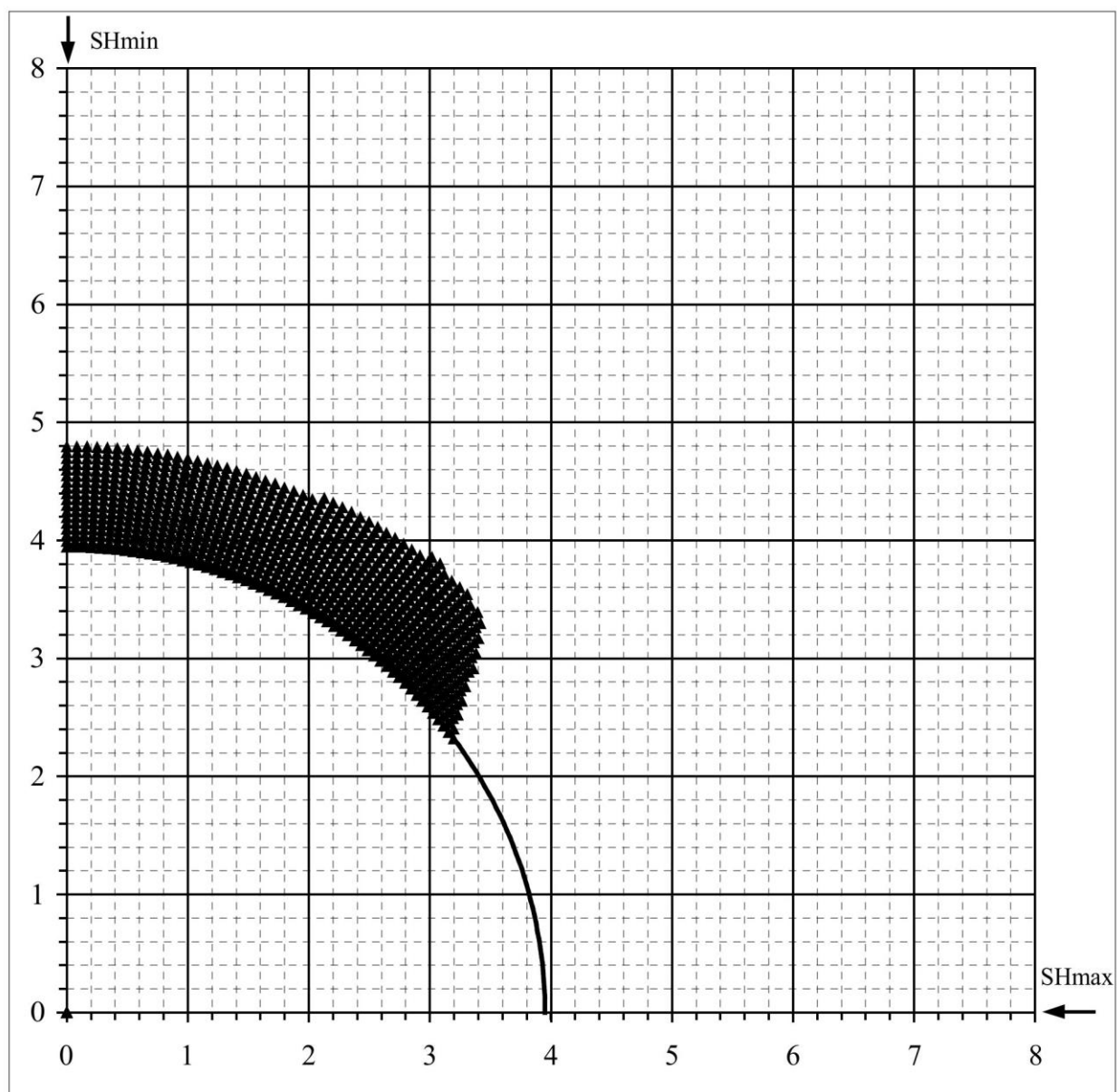
WELL : D-087-G/094-O-06 BREAKOUT ANALYSIS



D-087-G/094-O-06

## Mohr - Coulomb Failure Criterion

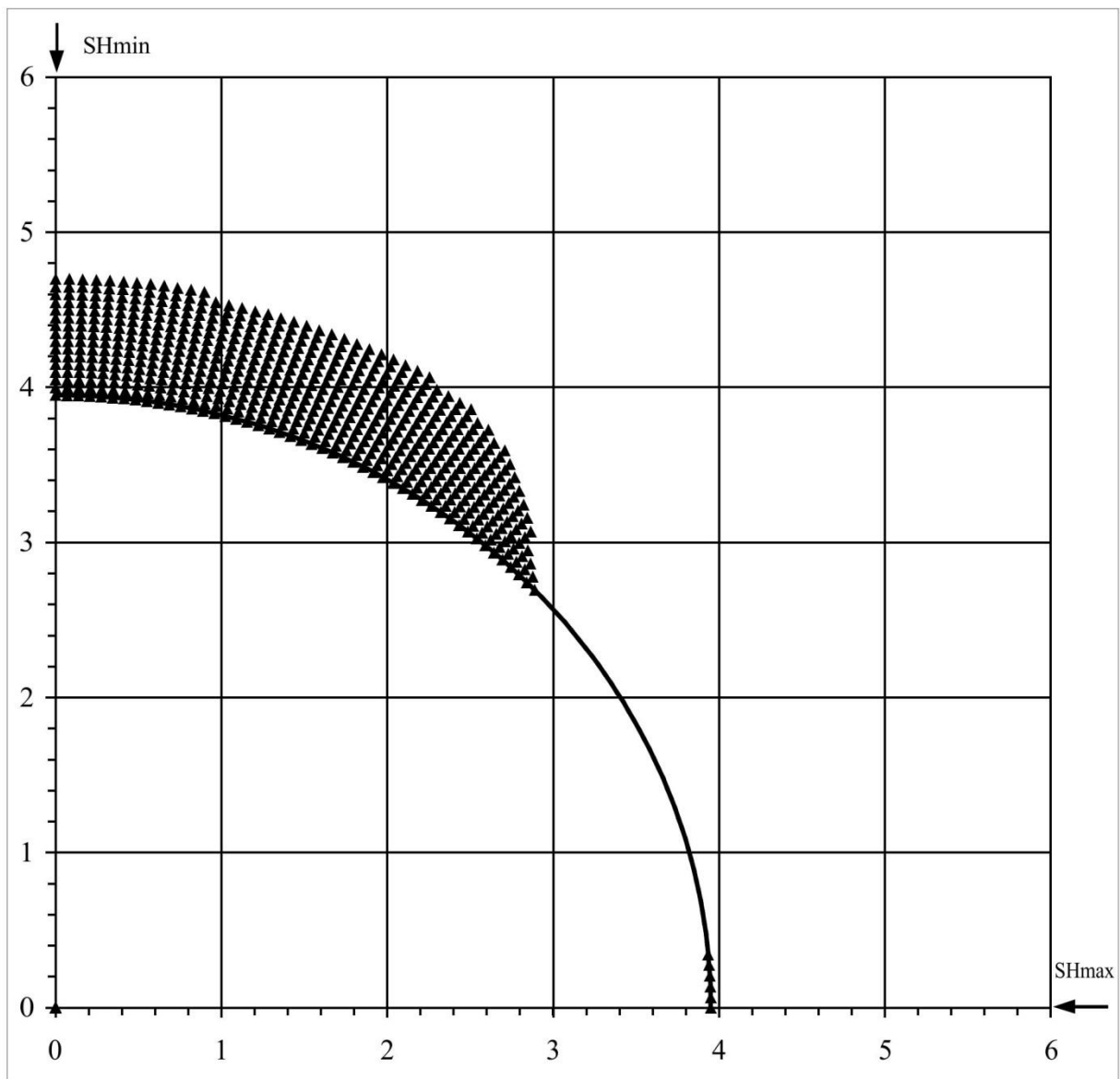
SHmax =	13.6 MPa	u (Coeff. of Friction) =	0.6
SHmin =	6.9 MPa	C (Cohesive Strength) =	2.5 MPa
Sv =	8.6 MPa	v (Poisson's Ratio) =	0.2
Po (Pore Pressure) =	3.7 MPa	Diameter of Borehole =	7.9 "
Pm (Mud Weight) =	3.7 MPa		
Sensitivity of Figure =	0.05 "	Angle of Max. Breakout =	52 deg
Depth of Max. Breakout =	0.95 "	Max caliper at 90 deg =	9.6 "
Validity of the results =	TRUE	Max caliper at 0 deg =	8.5 "



D-087-G/094-O-06

## Extended von-Mises Failure Criterion (Drucker-Prager Failure Criterion)

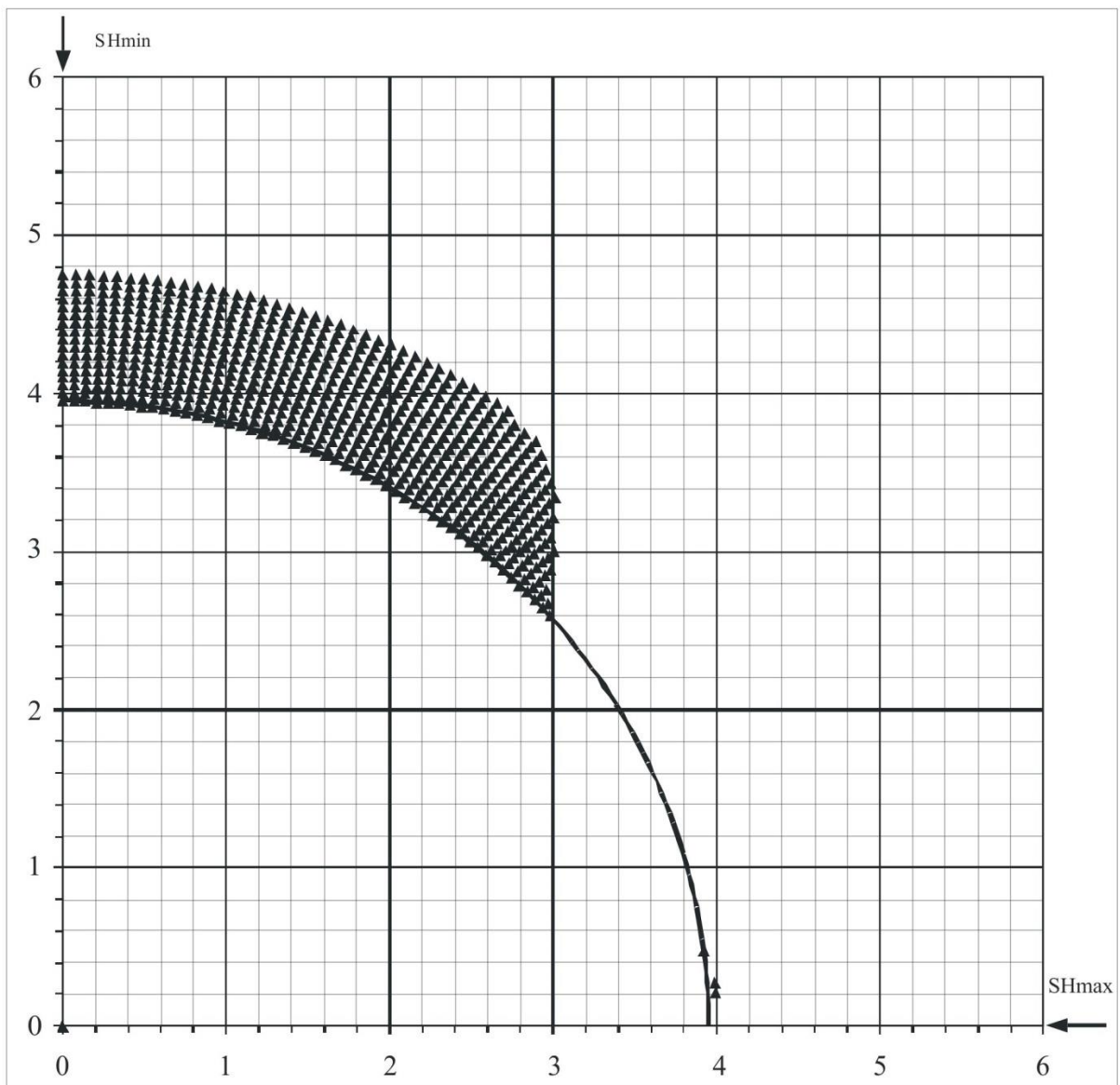
SHmax =	17.2 MPa	u (Coeff. of Friction)=	0.6
SHmin =	6.9 MPa	C (Cohesive Strength) =	2.5 MPa
Sv =	8.6 MPa	v (Poisson's Ratio) =	0.2
Po (Pore Pressure) =	3.7 MPa	Diameter of Borehole =	7.9 inches
Pm (Mud Weight) =	3.7 MPa	Depth of Max. Breakout =	0.75 inches
Sensitivity of Figure =	0.05 inches	Angle of Max. Breakout =	88 deg



D-087-G/094-O-06

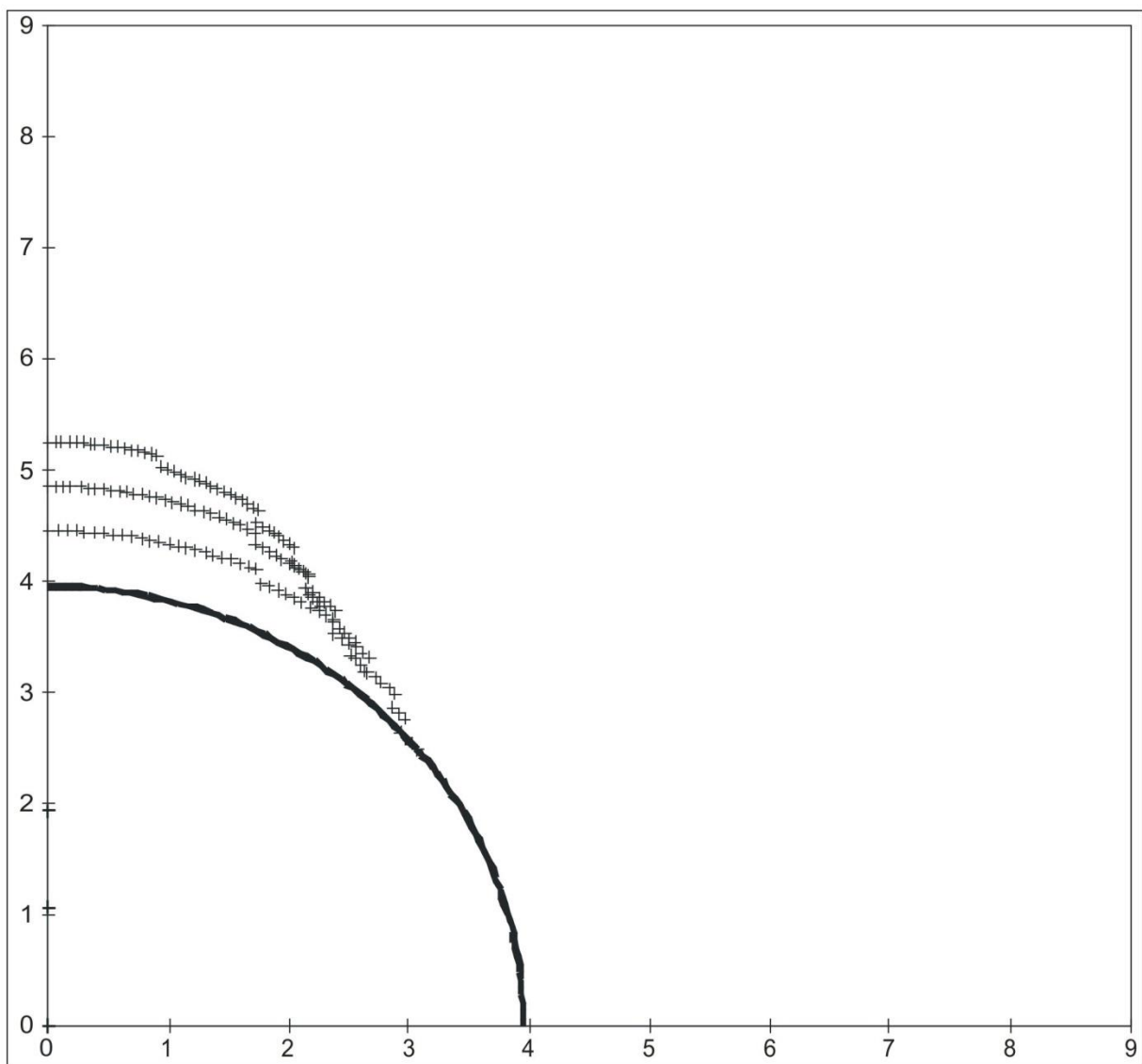
## Extended Drucker - Prager Failure Criterion (Modified Strain Energy Criterion)

SHmax =	16.1 MPa	u (Coeff. of Friction) =	0.6
SHmin =	6.9 MPa	C (Cohesive Strength) =	2.5 MPa
Sv =	8.6 MPa	v (Poisson's Ratio) =	0.2
Po (Pore Pressure) =	3.7 MPa	Diameter of Borehole =	7.9 inches
Pm (Mud Weight) =	3.7 MPa	Depth of Max. Breakout =	0.8 inches
Sensitivity of Figure =	0.05 inches	Angle of Max. Breakout =	70 deg





D-087-G/094-O-06					
<b>3 Cycle Mohr - Coulomb Failure Criterion</b>					
SHmax =	10.6	MPa	u (Coeff. of Friction) =	0.6	
SHmin =	6.9	MPa	C (Cohesive Strength) =	2.5	MPa
Sv =	8.6	MPa	v (Poisson's Ratio)=	0.2	
Po (Pore Pressure) =	3.7	MPa	Diameter of Borehole =	7.9	"
Pm (Mud Weight) =	3.7	MPa			
Sensitivity of Figure =	0.05	"			
Depth of Max. Breakout =	1.3	"	Max caliper at 90 deg =	10.5	"
Validity of the results =	TRUE		Max caliper at 0 deg =	7.9	"



## $S_{Hmax}$ Simulation Commentary – D-092-J /094-O-06

Well: D-092-J/094-O-06	Failure simulation Method				2SHmin-Po
	Mohr Coulomb	Drucker Prager	Modified Strain Energy	3 cycle Mohr Coulomb	
Breakout Interval Top (m KB)	822	822	822	822	
Breakout Interval Base (m KB)	847	847	847	847	
Median depth of Breakout (m KB)	834.5	834.5	834.5	834.5	
Calipers 1 and 3 extent (inches)	14.5	14.5	14.5	14.5	
Calipers 2 and 4 extent (inches)	8.01	8.01	8.01	8.01	
SHmax (MPa)	24.1*	32.2*	27.4*	<b>22.9</b>	22.3
SHmax gradient (kPa/m)	28.9	38.6	32.8	27.4	26.7
SHmin (MPa)	15.3	15.3	15.3	15.3	
Sv (MPa)	19.9	19.9	19.9	19.9	
Pore Pressure (MPa)	8.3	8.3	8.3	8.3	
Mudweight (MPa)	8.3	8.3	8.3	8.3	
u (Coefficient of Friction)	0.6	0.6	0.6	0.6	
Cohesive Strength of Rock (MPa)	2.8	2.8	2.8	2.8	
v (Poisson's Ratio)	0.2	0.2	0.2	0.2	
Bit size (inches)	8.5	8.5	8.5	8.5	

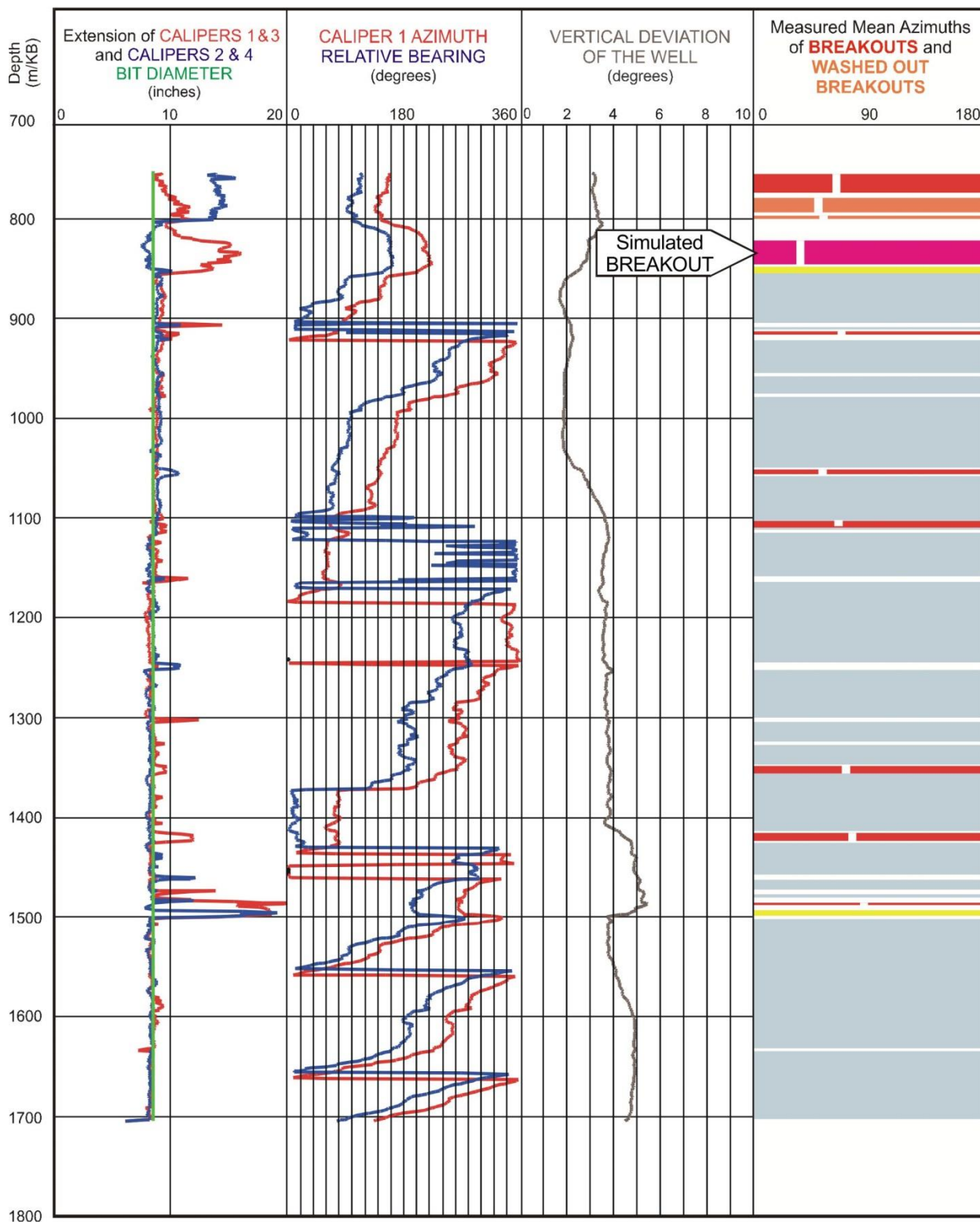
\* indicates that modelling could not simulate accurate breakout anisotropy

The breakout interval that was selected for modelling, 822-847 m, exhibits very deep spalling. Raising  $S_{Hmax}$  magnitudes with the single cycle routines did not generate sufficiently deep breakouts, the maximum being 10.8 inches generated by the Mohr Coulomb routine with an  $S_{Hmax}$  magnitude of 24.1 MPa. This simulation used the low cohesive strength of 2.8 MPa.

The 3 cycle Mohr-Coulomb simulation modelled a breakout with a long axis of 14.5 inches, again with the cohesive strength set at 2.8 MPa. The resulting  $S_{Hmax}$  magnitude of **22.9 MPa** is slightly higher than 22.3 MPa, that was suggested by the equation:  $S_{Hmax} = 2(S_{Hmin}) - Po$ .

The vertical stress,  $S_v$ , in well D-092-J/094-O-06 is well established at 834.5 m depth from the density log.

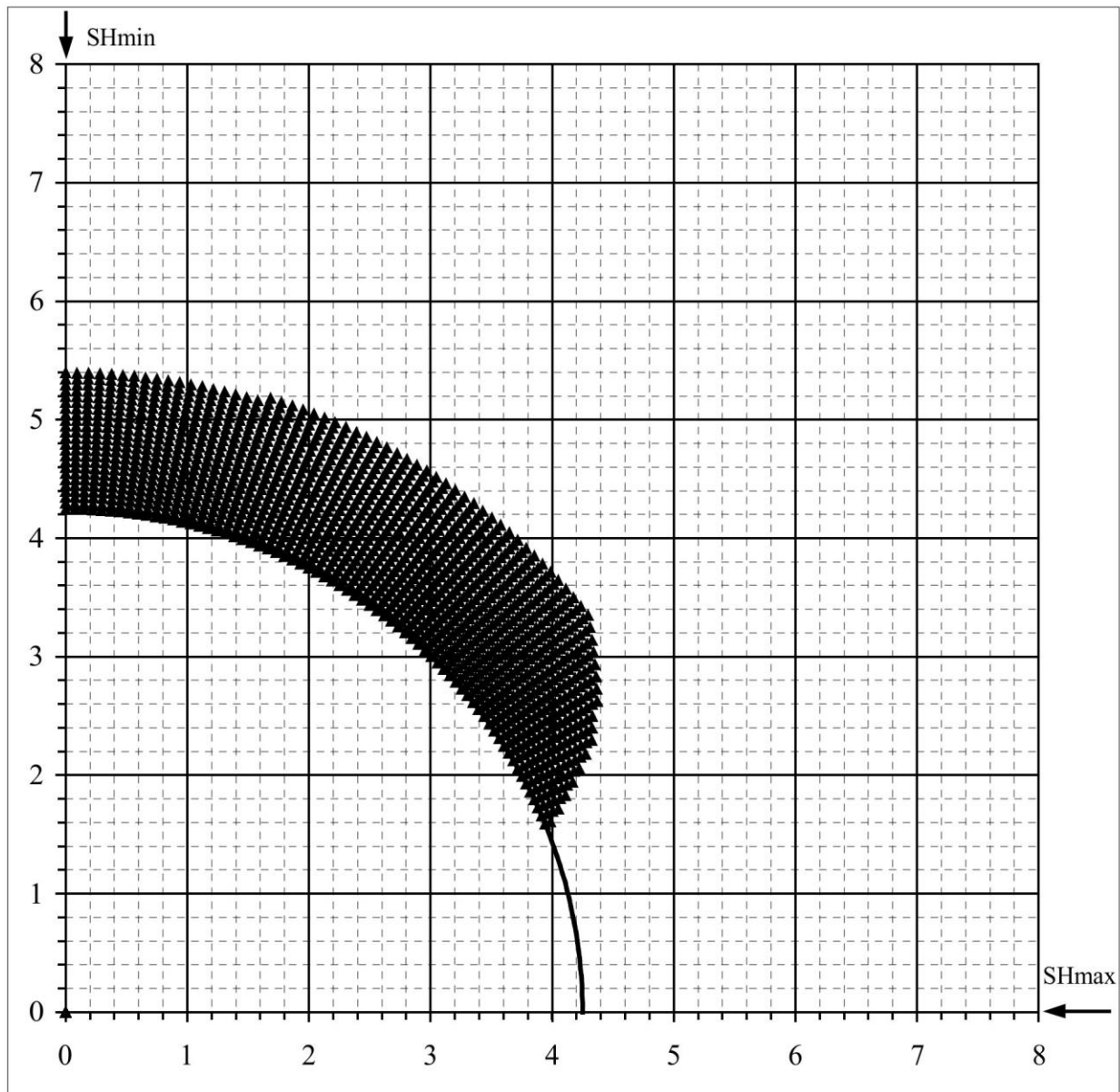
WELL : D-092-J/094-O-06 BREAKOUT ANALYSIS



D-092-J/094-O-106

## Mohr - Coulomb Failure Criterion

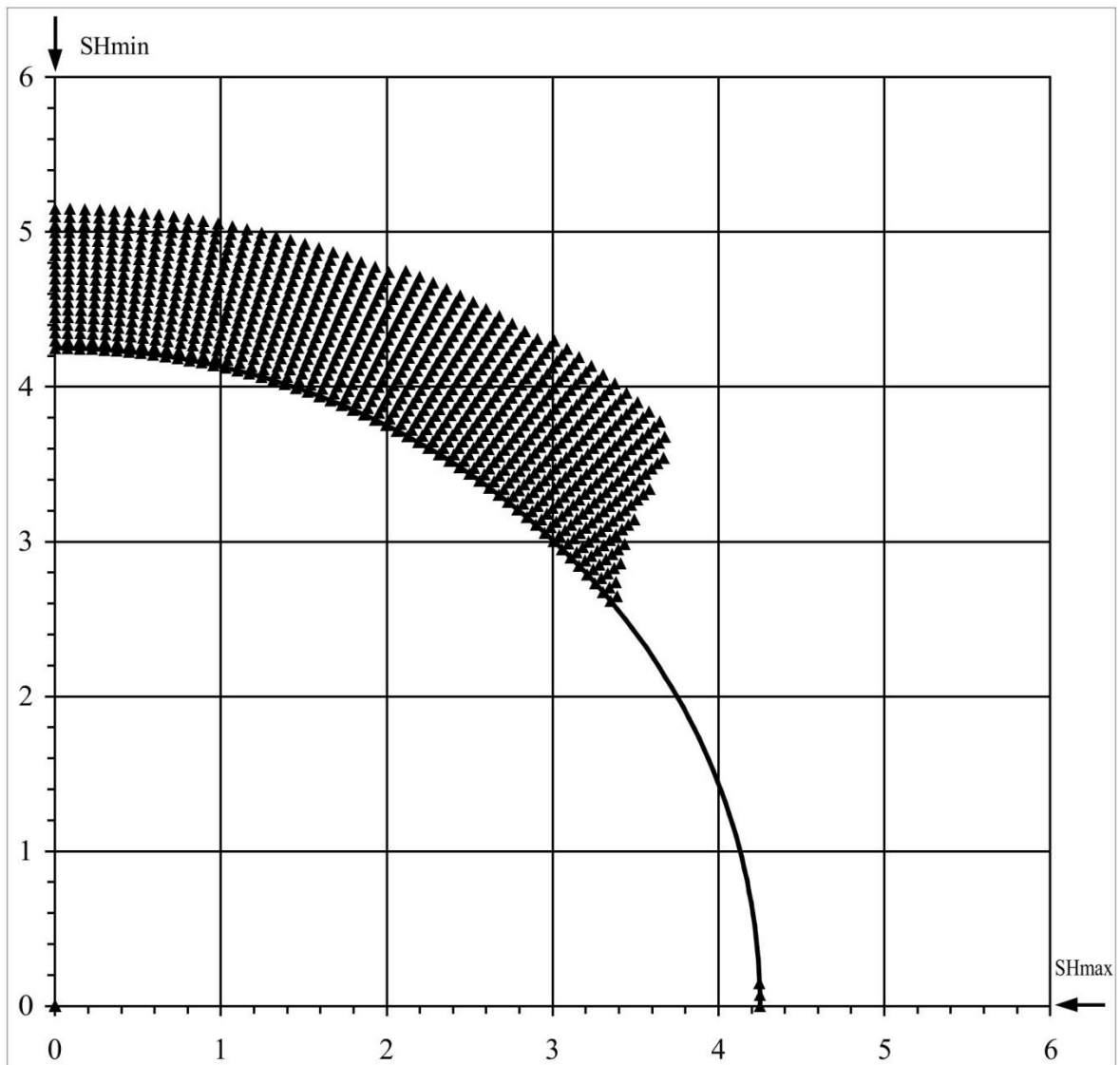
SHmax =	24.1 MPa	u (Coeff. of Friction) =	0.6
SHmin =	15.3 MPa	C (Cohesive Strength) =	2.8 MPa
Sv =	19.9 MPa	v (Poisson's Ratio) =	0.2
Po (Pore Pressure) =	8.3 MPa	Diameter of Borehole =	8.5 "
Pm (Mud Weight) =	8.3 MPa		
Sensitivity of Figure =	0.05 "	Angle of Max. Breakout =	52 deg
Depth of Max. Breakout =	1.2 "	Max caliper at 90 deg =	10.8 "
Validity of the results =	FALSE	Max caliper at 0 deg =	8 "



D-092-J/094-O-06

## Extended von-Mises Failure Criterion (Drucker-Prager Failure Criterion)

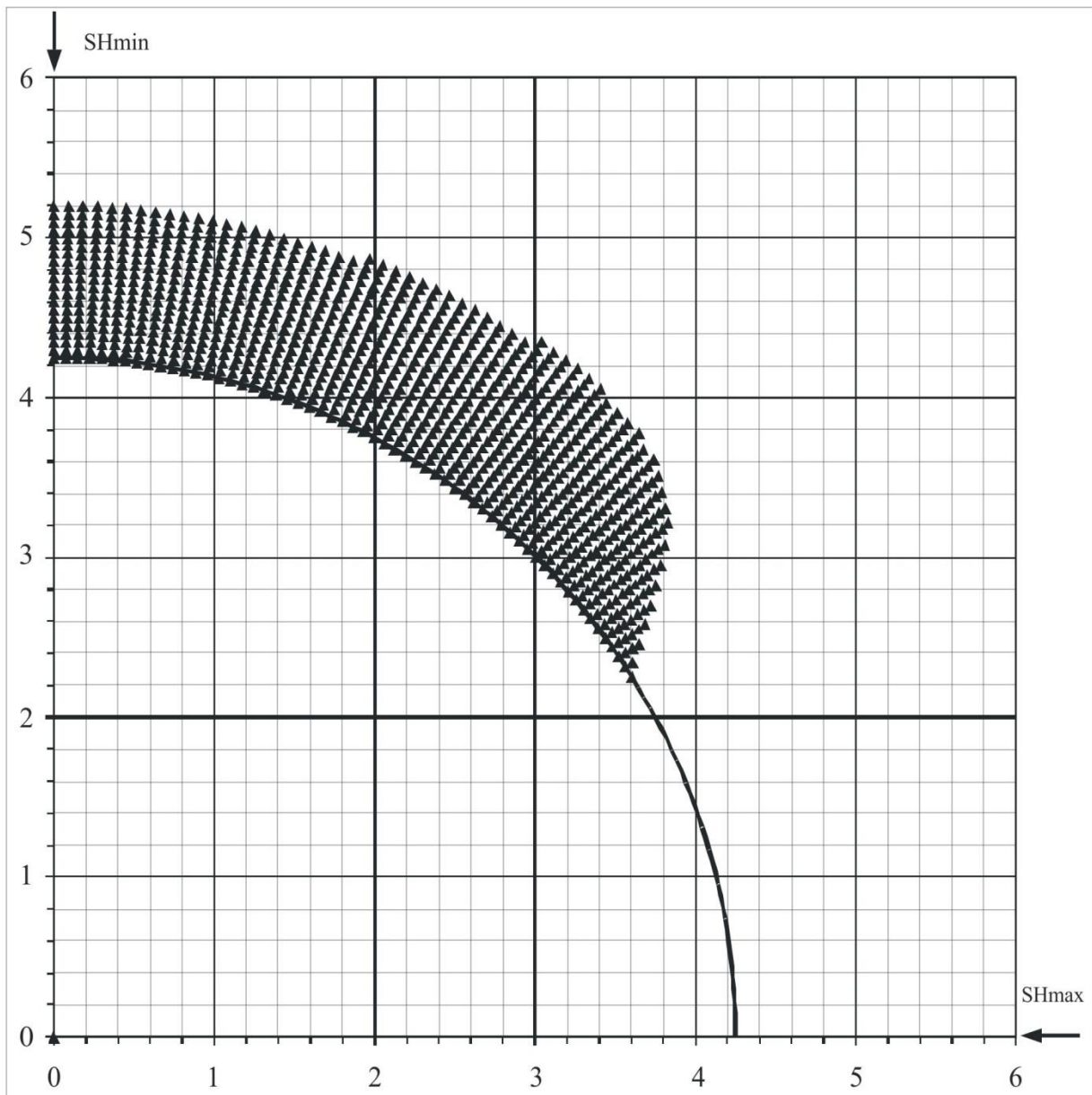
SHmax =	32.2 MPa	u (Coeff. of Friction)=	0.6
SHmin =	15.3 MPa	C (Cohesive Strength) =	2.8 MPa
Sv =	19.9 MPa	$\nu$ (Poisson's Ratio) =	0.2
Po (Pore Pressure) =	8.3 MPa	Diameter of Borehole =	8.5 inches
Pm (Mud Weight) =	8.3 MPa	Depth of Max. Breakout =	1 inches
Sensitivity of Figure =	0.05 inches	Angle of Max. Breakout =	51 deg



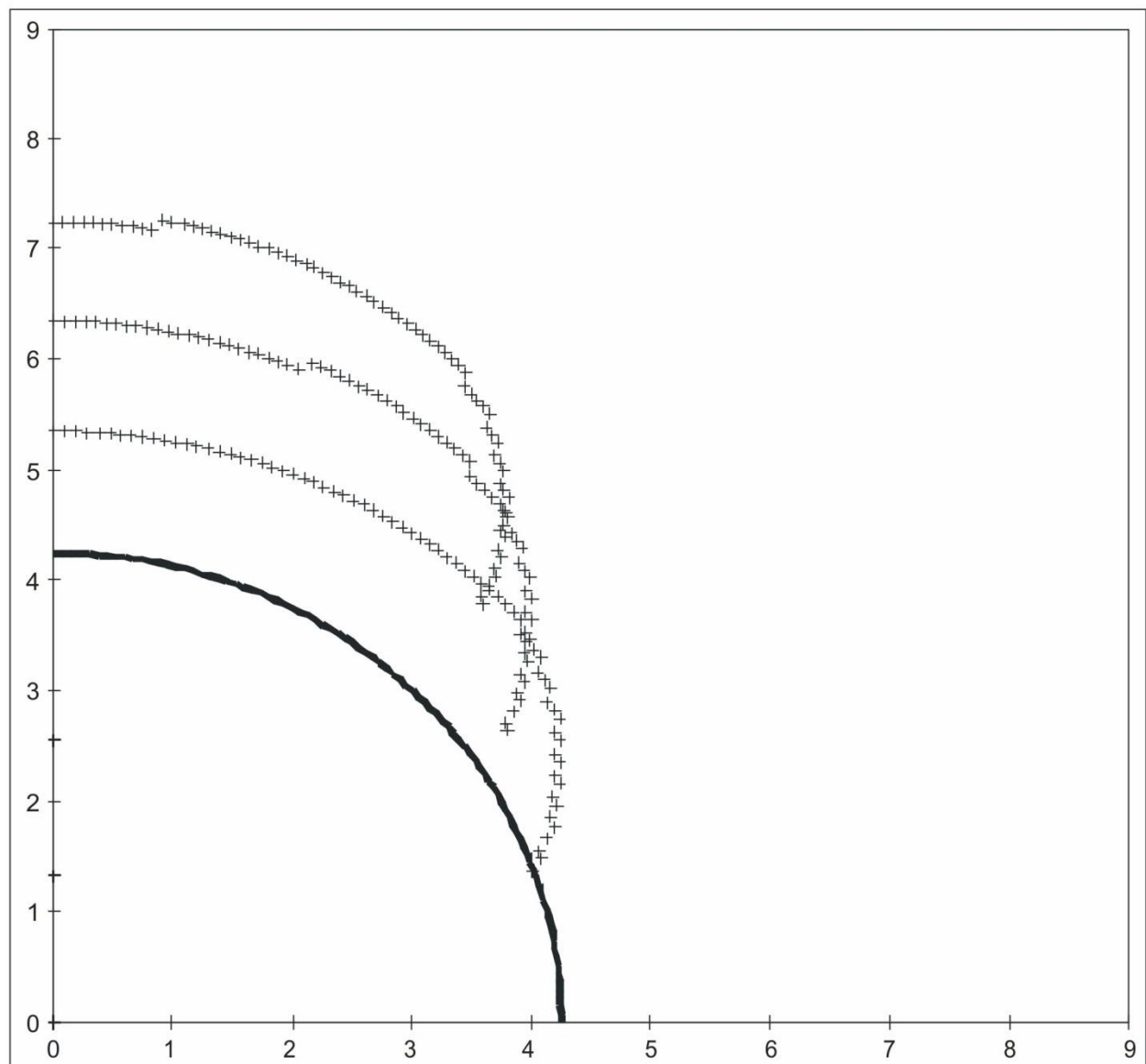
D-092-J/094-O-06

## Extended Drucker - Prager Failure Criterion (Modified Strain Energy Criterion)

SHmax =	27.4 MPa	u (Coeff. of Friction) =	0.6
SHmin =	15.3 MPa	C (Cohesive Strength) =	2.8 MPa
Sv =	19.9 MPa	v (Poisson's Ratio) =	0.2
Po (Pore Pressure) =	8.3 MPa	Diameter of Borehole =	8.5 inches
Pm (Mud Weight) =	8.3 MPa	Depth of Max. Breakout =	1.05 inches
Sensitivity of Figure =	0.05 inches	Angle of Max. Breakout =	52 deg



D-092-J-094-O-06					
3 Cycle Mohr - Coulomb Failure Criterion					
SHmax =	22.9	MPa	u (Coeff. of Friction) =	0.6	
SHmin =	15.3	MPa	C (Cohesive Strength) =	2.8	MPa
Sv =	19.9	MPa	v (Poisson's Ratio)=	0.2	
Po (Pore Pressure) =	8.3	MPa	Diameter of Borehole =	8.5	"
Pm (Mud Weight) =	8.3	MPa			
Sensitivity of Figure =	0.05	"			
Depth of Max. Breakout =	3.05	"	Max caliper at 90 deg =	14.5	"
Validity of the results =	TRUE		Max caliper at 0 deg =	8.5	"



**SHmax Simulation Commentary – F-38-60-30-123-45**

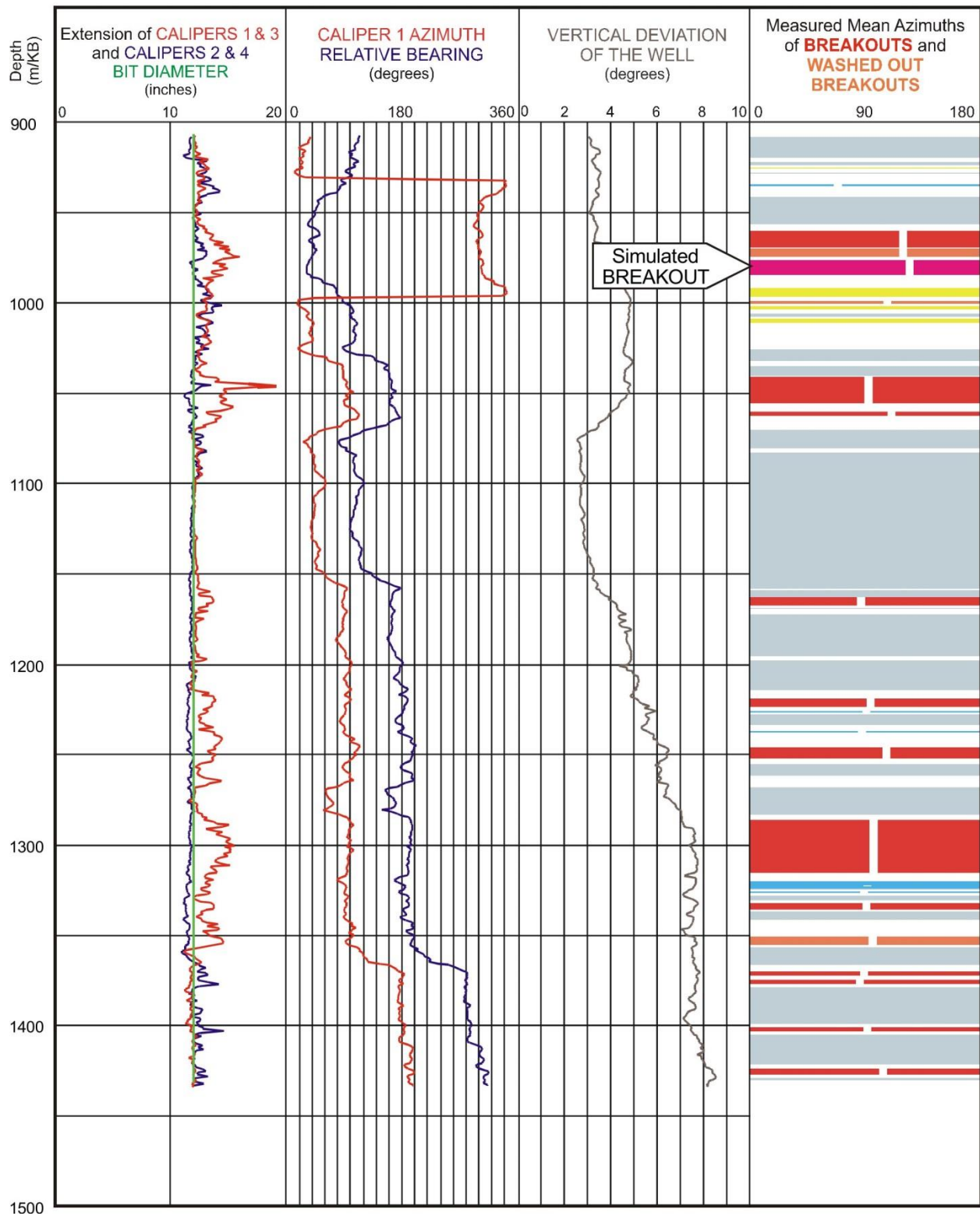
Well: <b>F-038-60-30-123-45</b>	Failure simulation Method				2SHmin-Po
	Mohr Coulomb	Drucker Prager	Modified Strain Energy	3 cycle Mohr Coulomb	
Breakout Interval Top (m KB)	976	976	976	976	
Breakout Interval Base (m KB)	985	985	985	985	
Median depth of Breakout (m KB)	980.5	980.5	980.5	980.5	
Calipers 1 and 3 extent (inches)	14.19	14.19	14.19	14.19	
Calipers 2 and 4 extent (inches)	12.1	12.1	12.1	12.1	
SHmax (MPa)	<b>27.1</b>	42.4	35.4		24.2
SHmax gradient (kPa/m)	27.6	43.2	36.1		24.7
SHmin (MPa)	17.0	17.0	17.0	17.0	
Sv (MPa)	25.1	25.1	25.1	25.1	
Pore Pressure (MPa)	9.8	9.8	9.8	9.8	
Mudweight (MPa)	9.8	9.8	9.8	9.8	
u (Coefficient of Friction)	0.6	0.6	0.6	0.6	
Cohesive Strength of Rock (MPa)	5.0	5.0	5.0	5.0	
v (Poisson's Ratio)	0.2	0.2	0.2	0.2	
Bit size (inches)	12.0	12.0	12.0	12.0	

The breakout interval that was selected for modelling, 976-985 m, exhibits relatively shallow spalling. All the single cycle routines generated sufficiently deep breakouts, with the Mohr Coulomb routine requiring an  $S_{Hmax}$  magnitude of **27.1 MPa**, when the cohesive strength was set at 5 MPa, to generate a breakout with a long axis of 14.2 inches. This value was taken as a reliable estimate of  $S_{Hmax}$  and it compares well with the  $S_{Hmax}$  magnitude of 24.2 MPa, suggested by the equation:  $S_{Hmax} = 2(S_{Hmin}) - Po$ .

The vertical stress,  $S_v$ , in well F-38-60-30-123-45 is well established at 980.5 m depth from the density log.



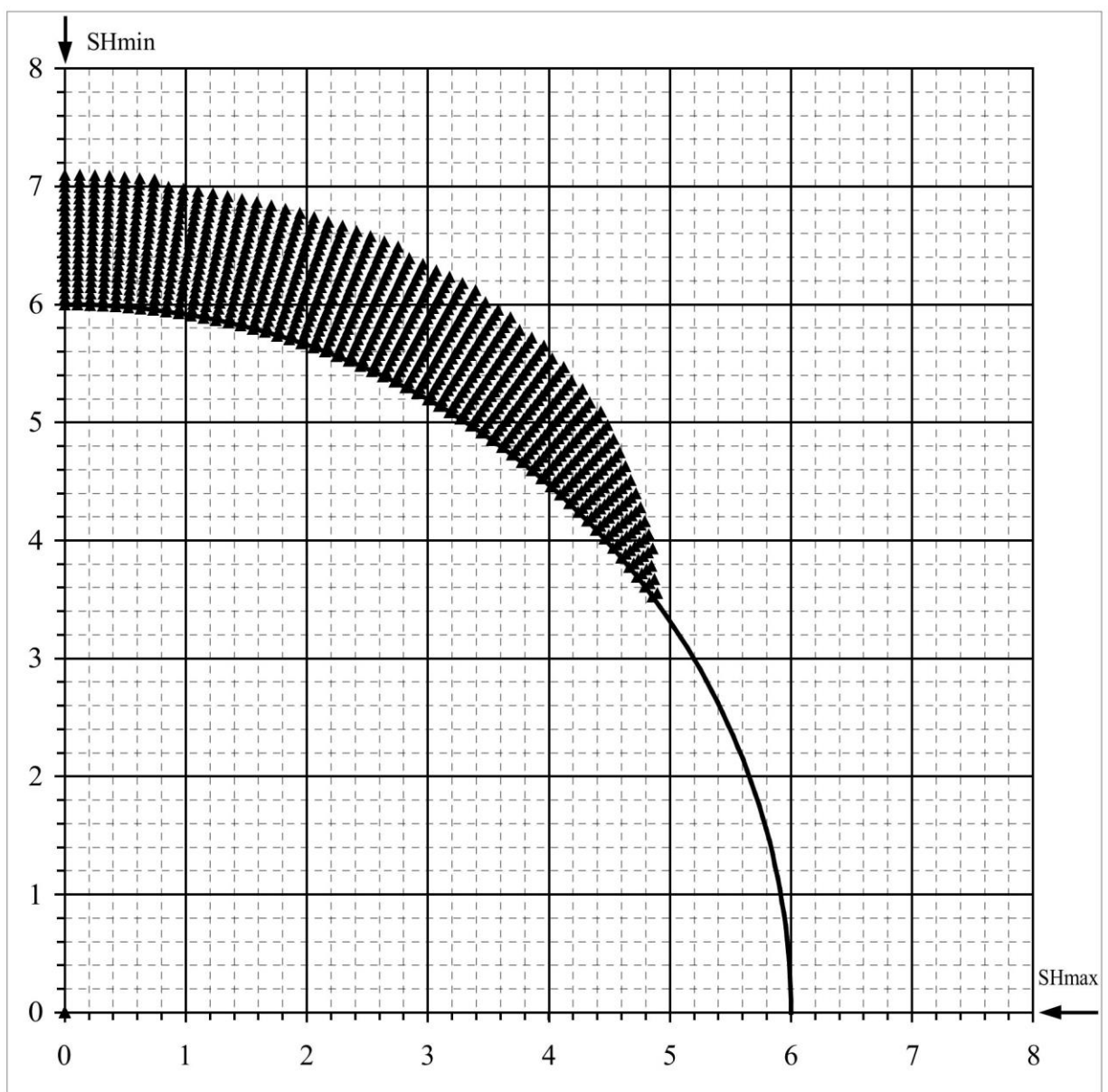
WELL : F-038-60-30-123-45 BREAKOUT ANALYSIS



F-038-60-30-123-45

## Mohr - Coulomb Failure Criterion

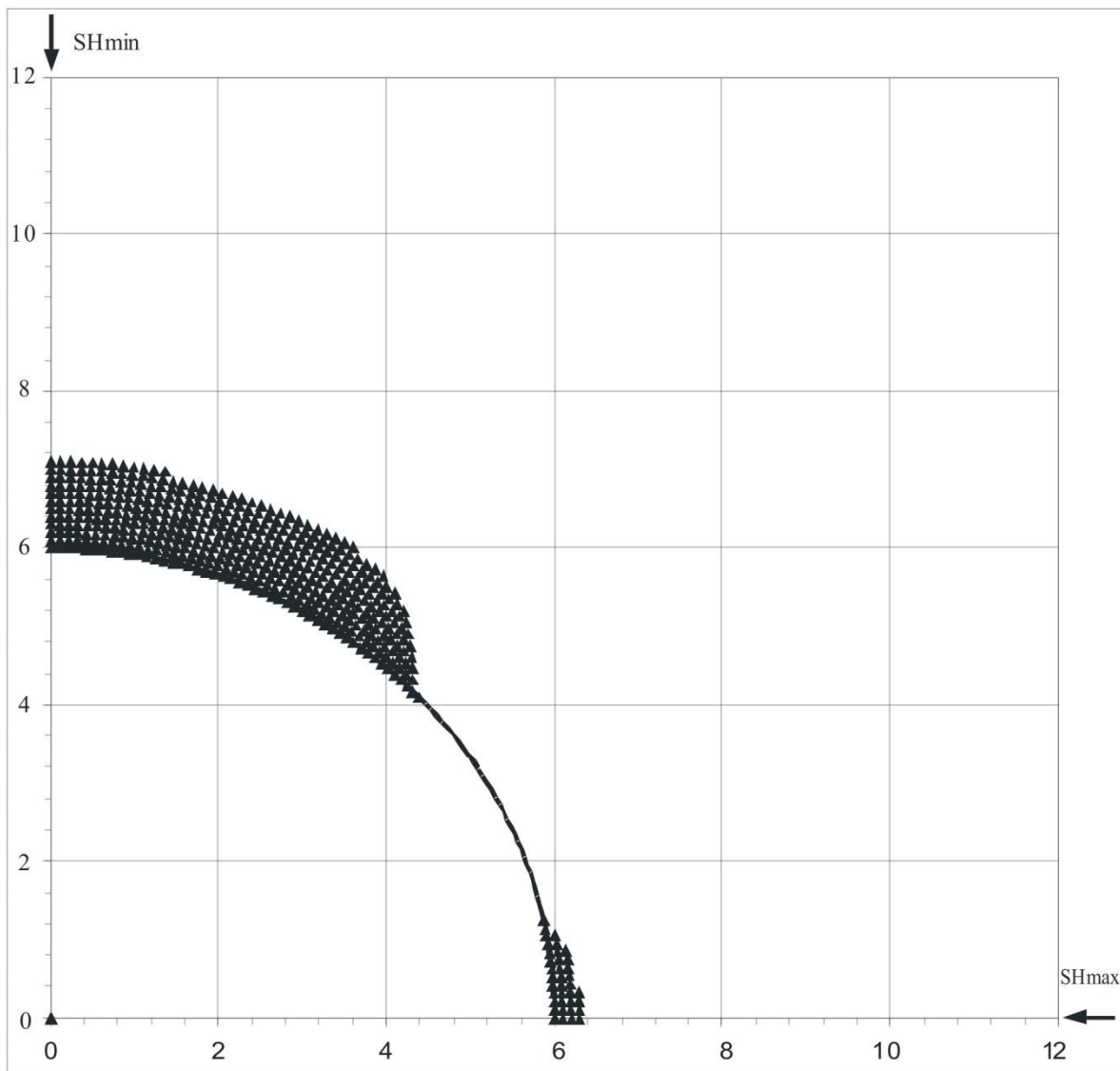
SHmax =	27.1 MPa	u (Coeff. of Friction) =	0.6
SHmin =	17 MPa	C (Cohesive Strength) =	5 MPa
Sv =	25.1 MPa	v (Poisson's Ratio) =	0.2
Po (Pore Pressure) =	9.8 MPa	Diameter of Borehole =	12 "
Pm (Mud Weight) =	9.8 MPa		
Sensitivity of Figure =	0.05 "	Angle of Max. Breakout =	90 deg
Depth of Max. Breakout =	1.1 "	Max caliper at 90 deg =	14.2 "
Validity of the results =	TRUE	Max caliper at 0 deg =	8 "



F-038-60-30-123-45

## Extended von-Mises Failure Criterion (Drucker-Prager Failure Criterion)

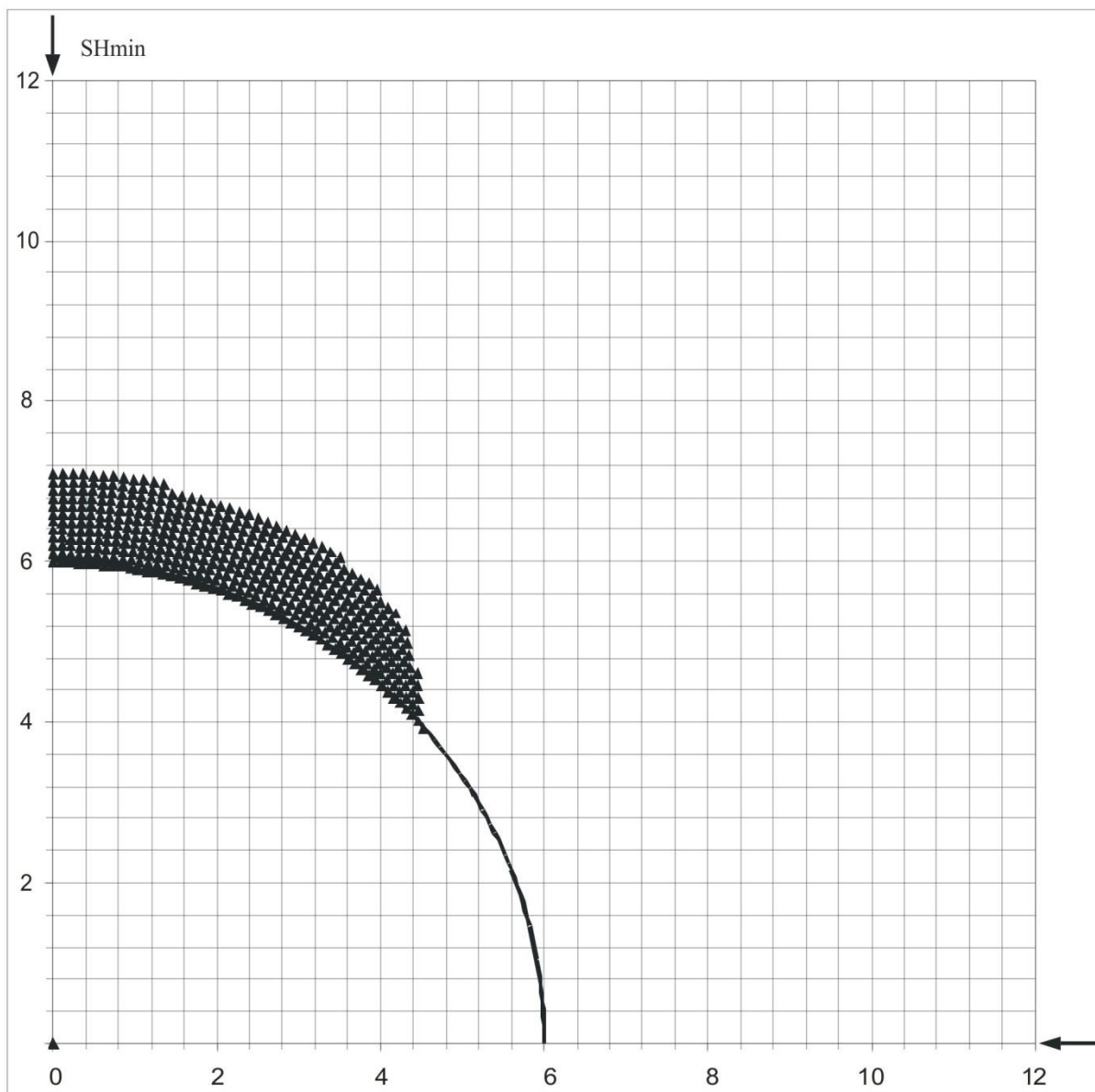
SHmax =	42.4 MPa	u (Coeff. of Friction)=	0.6
SHmin =	17 MPa	C (Cohesive Strength) =	5 MPa
Sv =	25.1 MPa	v (Poisson's Ratio) =	0.2
Po (Pore Pressure) =	9.8 MPa	Diameter of Borehole =	12 inches
Pm (Mud Weight) =	9.8 MPa	Depth of Max. Breakout =	1.1 inches
Sensitivity of Figure =	0.05 inches	Angle of Max. Breakout =	90 deg



F-038-60-30-123-45

## Extended Drucker - Prager Failure Criterion (Modified Strain Energy Criterion)

SHmax =	35.4 MPa	u (Coeff. of Friction) =	0.6
SHmin =	17 MPa	C (Cohesive Strength) =	5 MPa
Sv =	25.1 MPa	v (Poisson's Ratio) =	0.2
Po (Pore Pressure) =	9.8 MPa	Diameter of Borehole =	12 inches
Pm (Mud Weight) =	9.8 MPa	Depth of Max. Breakout =	1.1 inches
Sensitivity of Figure =	0.05 inches	Angle of Max. Breakout =	90 deg



## $S_{Hmax}$ Simulation Commentary – G-01-60-10-124-15

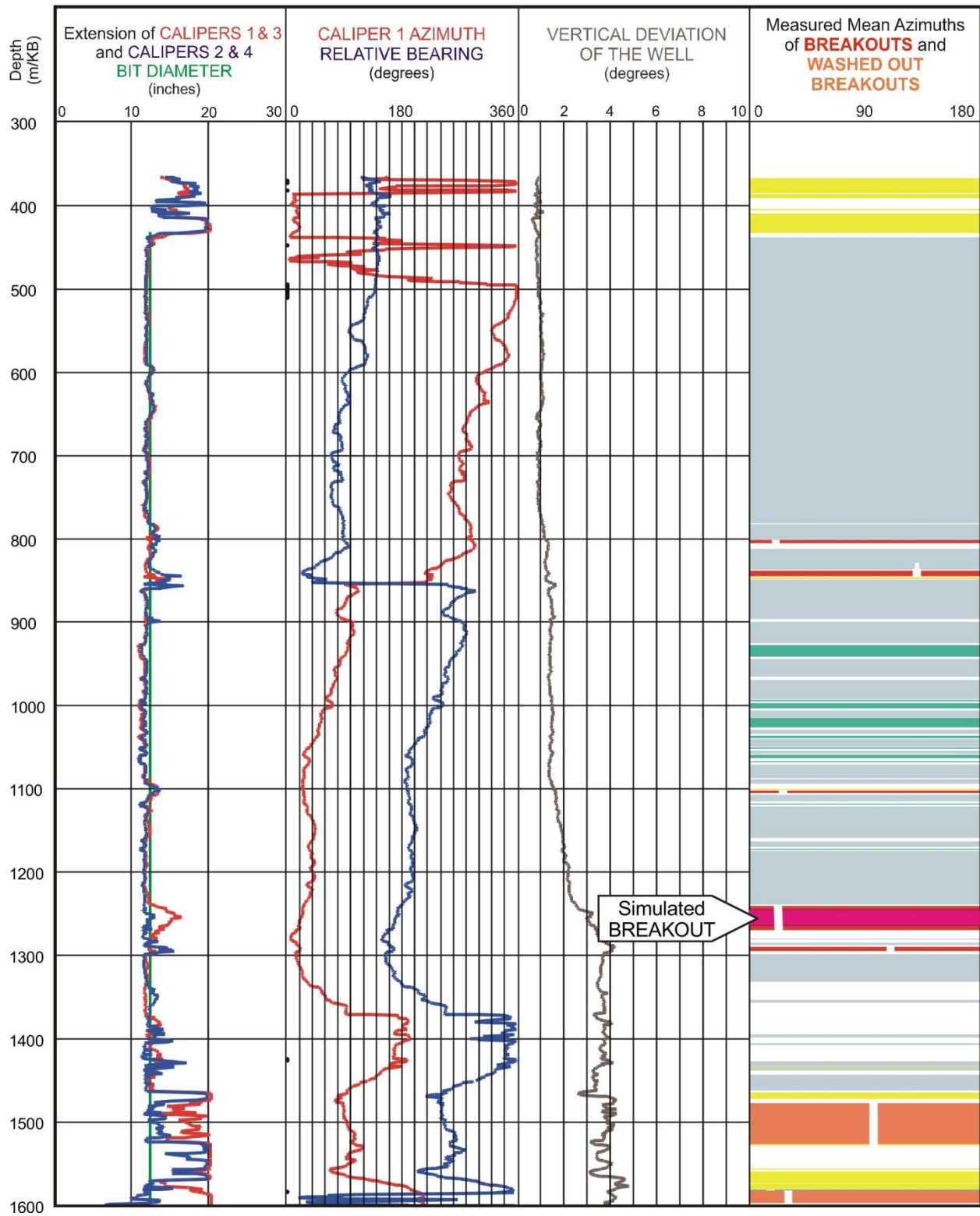
Well: <b>G-001-60-10-124-15</b>	Failure simulation Method				2SHmin-Po
	Mohr Coulomb	Drucker Prager	Modified Strain Energy	3 cycle Mohr Coulomb	
Breakout Interval Top (m KB)	1246	1246	1246	1246	
Breakout Interval Base (m KB)	1264	1264	1264	1264	
Median depth of Breakout (m KB)	1255	1255	1255	1255	
Calipers 1 and 3 extent (inches)	15.27	15.27	15.27	15.27	
Calipers 2 and 4 extent (inches)	12.23	12.23	12.23	12.23	
SHmax (MPa)	43.4*	56.3*	50.5*	<b>33.3</b>	32.9
SHmax gradient (kPa/m)	34.6	44.9	40.2	26.5	26.2
SHmin (MPa)	22.7	22.7	22.7	22.7	
Sv (MPa)	31.1	31.1	31.1	31.1	
Pore Pressure (MPa)	12.5	12.5	12.5	12.5	
Mudweight (MPa)	12.5	12.5	12.5	12.5	
u (Coefficient of Friction)	0.6	0.6	0.6	0.6	
Cohesive Strength of Rock (MPa)	9.0	9.0	9.0	9.0	
v (Poisson's Ratio)	0.2	0.2	0.2	0.2	
Bit size (inches)	12.25	12.25	12.25	12.25	

\* indicates that modelling could not simulate accurate breakout anisotropy

The selected breakout interval, 1246-1264 m, could not be simulated with any of the three single cycle methods. The 3 cycle Mohr-Coulomb simulation modelled the breakout well with a cohesive strength of 9.0 MPa.

The resulting  $S_{Hmax}$  magnitude of **33.3 MPa** compares well with 32.9 MPa, as suggested by the equation:  $S_{Hmax} = 2(S_{Hmin}) - Po$ .

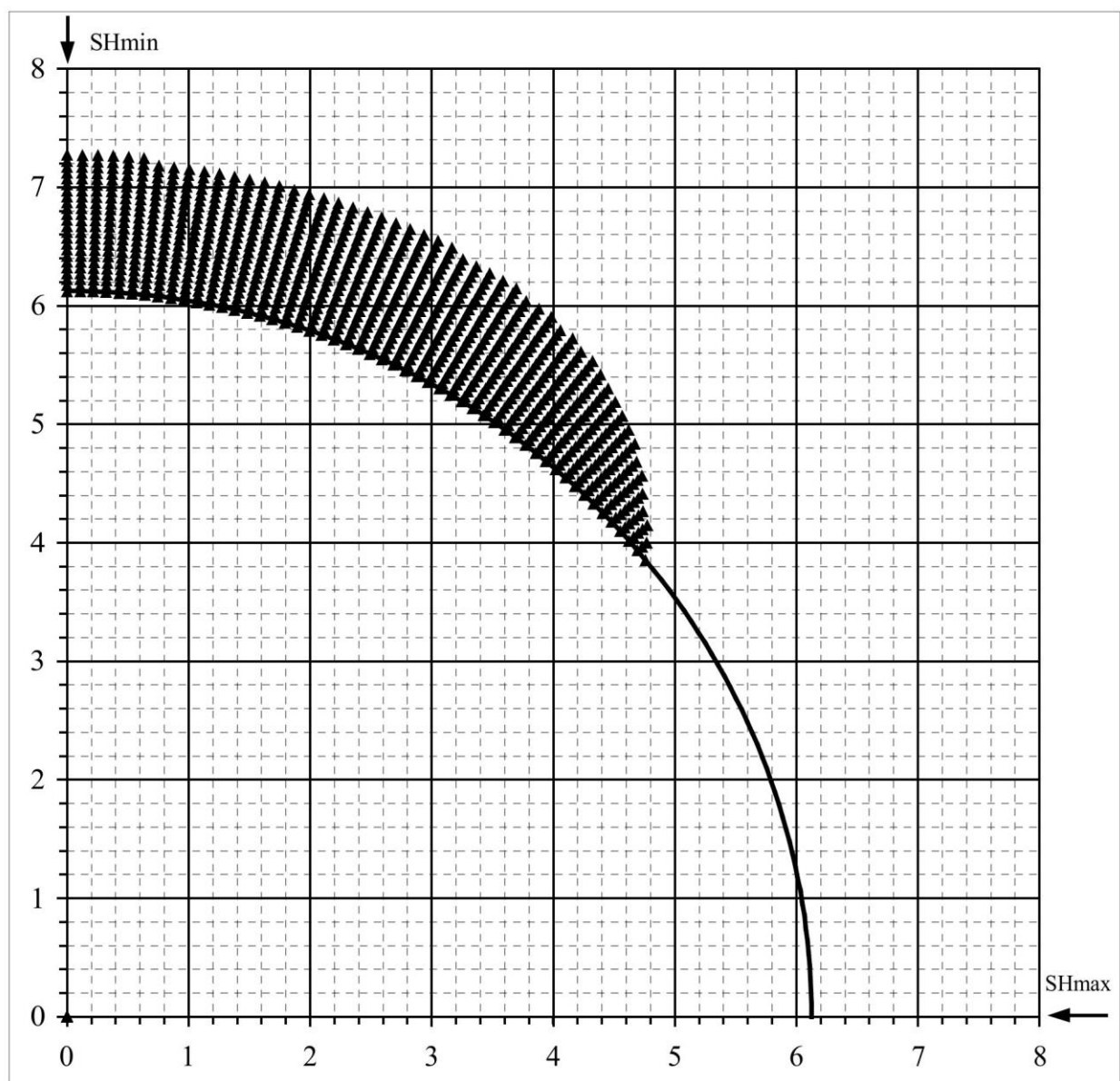
WELL : G-01-60-10-124-15 BREAKOUT ANALYSIS



G-001-60-10-124-15

## Mohr - Coulomb Failure Criterion

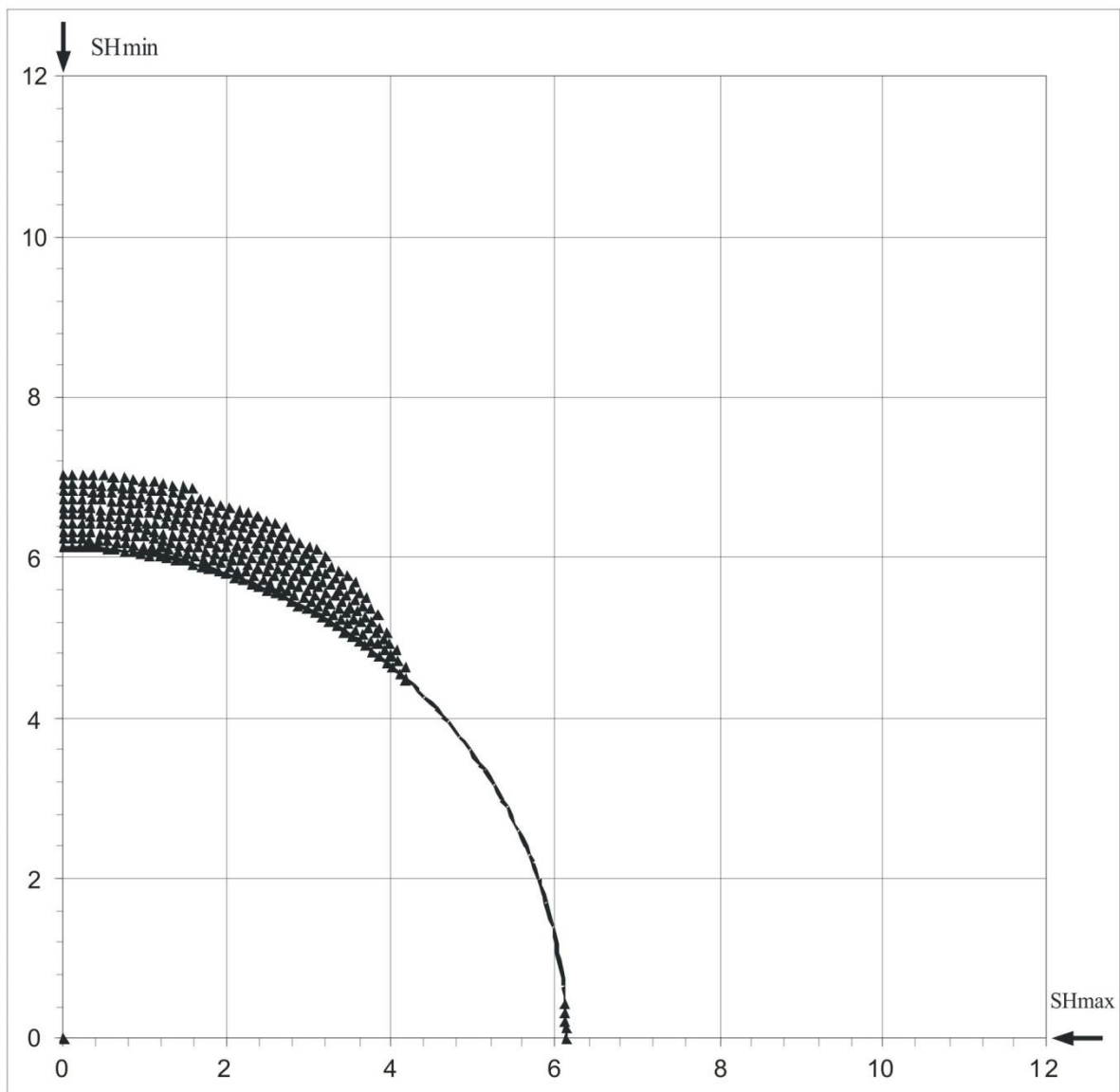
SHmax =	43.4 MPa	u (Coeff. of Friction) =	0.6
SHmin =	22.7 MPa	C (Cohesive Strength) =	9 MPa
Sv =	31.1 MPa	v (Poisson's Ratio) =	0.2
Po (Pore Pressure) =	12.5 MPa	Diameter of Borehole =	12.25 "
Pm (Mud Weight) =	12.5 MPa		
Sensitivity of Figure =	0.05 "	Angle of Max. Breakout =	90 deg
Depth of Max. Breakout =	1.15 "	Max caliper at 90 deg =	14.55 "
Validity of the results =	TRUE	Max caliper at 0 deg =	12.25 "



G-001-60-10-124-15

## Extended von-Mises Failure Criterion (Drucker-Prager Failure Criterion)

SHmax =	56.3 MPa	u (Coeff. of Friction)=	0.6
SHmin =	22.7 MPa	C (Cohesive Strength) =	9 MPa
Sv =	31.1 MPa	v (Poisson's Ratio) =	0.2
Po (Pore Pressure) =	12.5 MPa	Diameter of Borehole =	12.25 inches
Pm (Mud Weight) =	12.5 MPa	Depth of Max. Breakout =	0.9 inches
Sensitivity of Figure =	0.05 inches	Angle of Max. Breakout =	90 deg

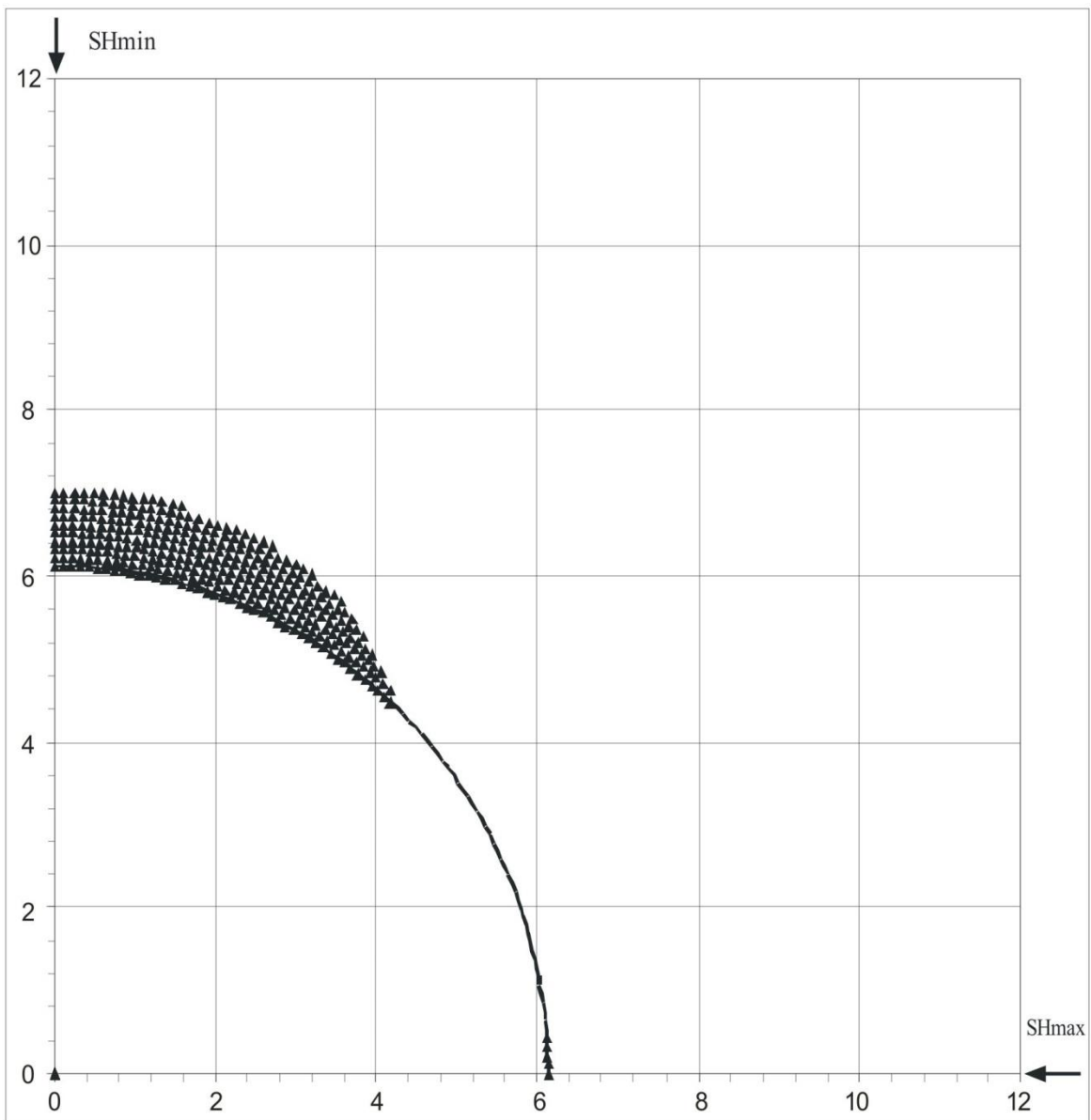




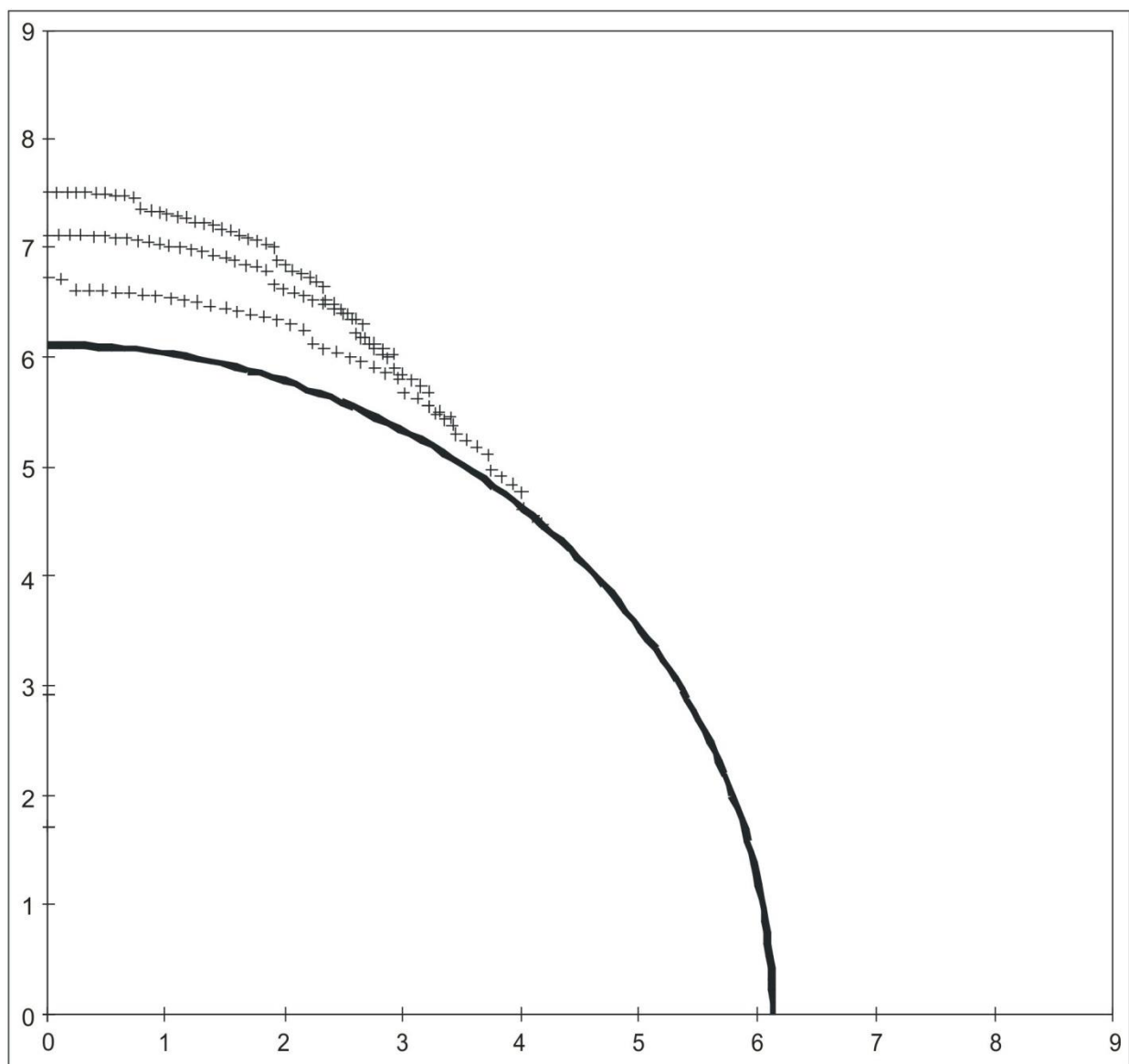
G-001-60-10-124-15

## Extended Drucker - Prager Failure Criterion (Modified Strain Energy Criterion)

SHmax =	50.5 MPa	u (Coeff. of Friction) =	0.6
SHmin =	22.7 MPa	C (Cohesive Strength) =	9 MPa
Sv =	31.1 MPa	v (Poisson's Ratio) =	0.2
Po (Pore Pressure) =	12.5 MPa	Diameter of Borehole =	12.25 inches
Pm (Mud Weight) =	12.5 MPa	Depth of Max. Breakout =	0.95 inches
Sensitivity of Figure =	0.05 inches	Angle of Max. Breakout =	81 deg



G-001-60-10-124-15					
<b>3 Cycle Mohr - Coulomb Failure Criterion</b>					
SHmax =	33.3	MPa	u (Coeff. of Friction) =	0.6	
SHmin =	22.7	MPa	C (Cohesive Strength) =	9	MPa
Sv =	31.1	MPa	v (Poisson's Ratio) =	0.2	
Po (Pore Pressure) =	12.5	MPa	Diameter of Borehole =	12.25	"
Pm (Mud Weight) =	12.5	MPa			
Sensitivity of Figure =	0.05	"			
Depth of Max. Breakout =	1.5	"	Max caliper at 90 deg =	15.25	"
Validity of the results =	TRUE		Max caliper at 0 deg =	12.25	"



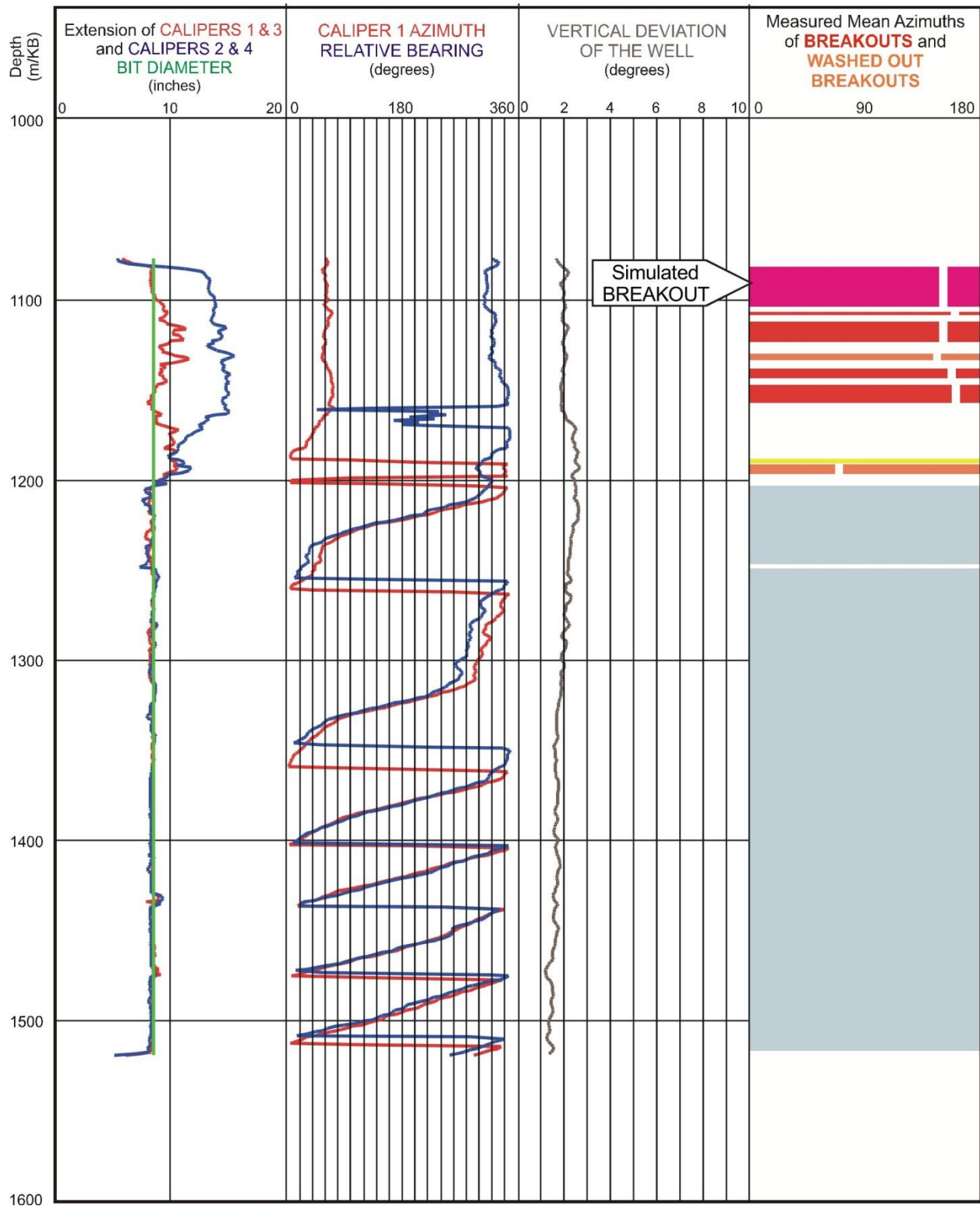
**SHmax Simulation Commentary G-32-61-10-121-15**

Well: <b>G-032-61-10-121-15</b>	Failure simulation Method				2SHmin-Po
	Mohr Coulomb	Drucker Prager	Modified Strain Energy	3 cycle Mohr Coulomb	
Breakout Interval Top (m KB)	1082	1082	1082	1082	
Breakout Interval Base (m KB)	1106	1106	1106	1106	
Median depth of Breakout (m KB)	1094	1094	1094	1094	
Calipers 1 and 3 extent (inches)	8.65	8.65	8.65	8.65	
Calipers 2 and 4 extent (inches)	13.24	13.24	13.24	13.24	
SHmax (MPa)	32.8*	41.5*	38.9*	<b>30.6</b>	26.7
SHmax gradient (kPa/m)	30.0	37.9	35.6	28.0	24.4
SHmin (MPa)	18.8	18.8	18.8	18.8	
Sv (MPa)	26.1	26.1	26.1	26.1	
Pore Pressure (MPa)	10.9	10.9	10.9	10.9	
Mudweight (MPa)	10.9	10.9	10.9	10.9	
u (Coefficient of Friction)	0.6	0.6	0.6	0.6	
Cohesive Strength of Rock (MPa)	5.0	5.0	5.0	5.0	
v (Poisson's Ratio)	0.2	0.2	0.2	0.2	
Bit size (inches)	8.5	8.5	8.5	8.5	

\* indicates that modelling could not simulate accurate breakout anisotropy

The breakout interval that was selected for modelling, 1082-1106 m, exhibits relatively deep spalling, since the long axis of the breakout interval extends to 13.24 inches. The single cycle simulation routines did not generate sufficiently deep breakouts, the maximum diameter achieved being 10.4 inches with the Mohr Coulomb routine. However, the 3 Cycle Mohr Coulomb routine modelled the breakout completely with  $S_{Hmax}$  at **30.6 MPa** and the cohesive strength at 5 MPa. This value was taken as a reliable estimate of  $S_{Hmax}$  and it compares reasonably well with the  $S_{Hmax}$  magnitude of 26.7 MPa, suggested by the equation:  $S_{Hmax} = 2(S_{Hmin}) - Po$ .

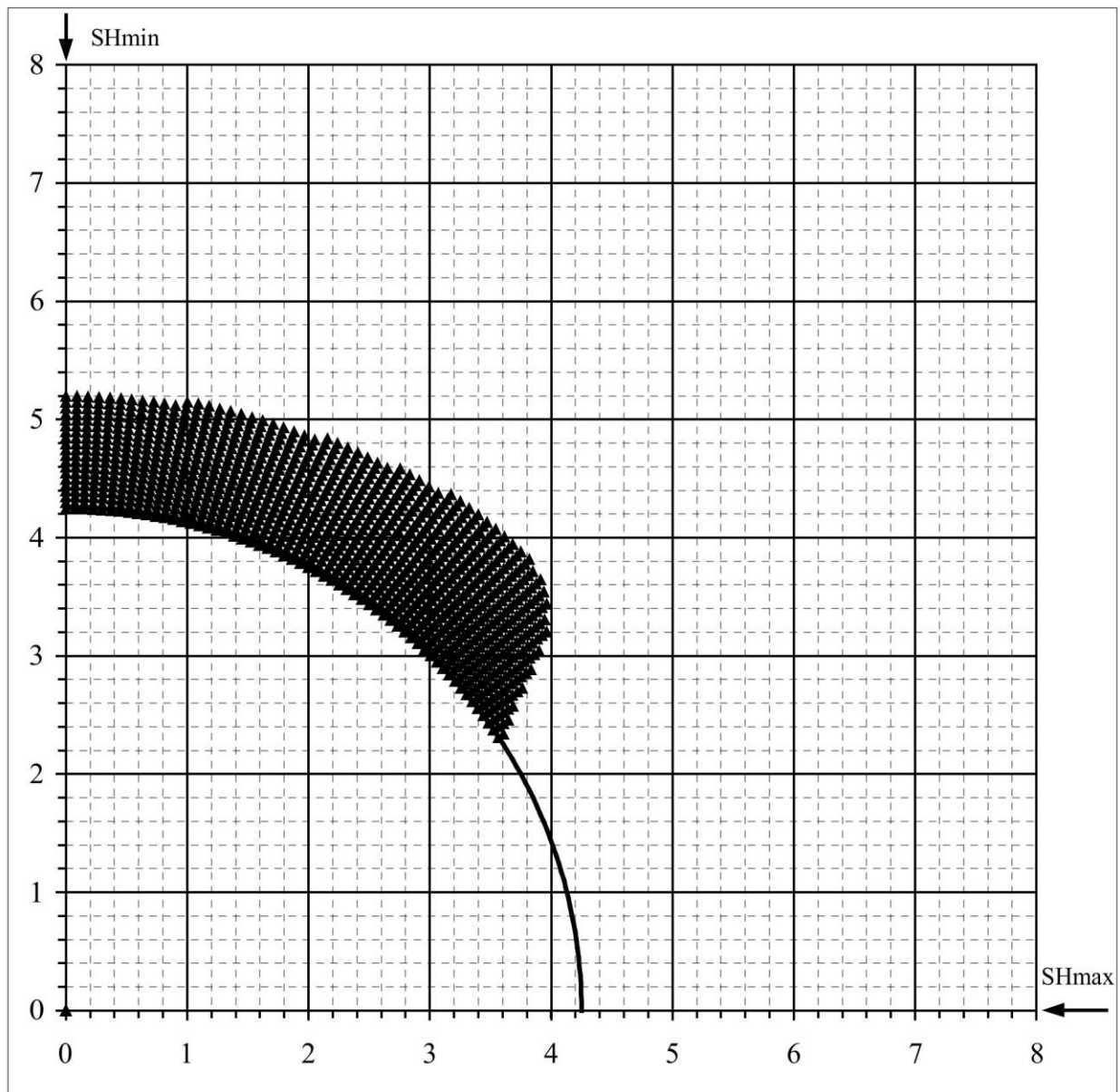
WELL : G-032-61-10-121-15 BREAKOUT ANALYSIS



G-032-61-10-121-25

## Mohr - Coulomb Failure Criterion

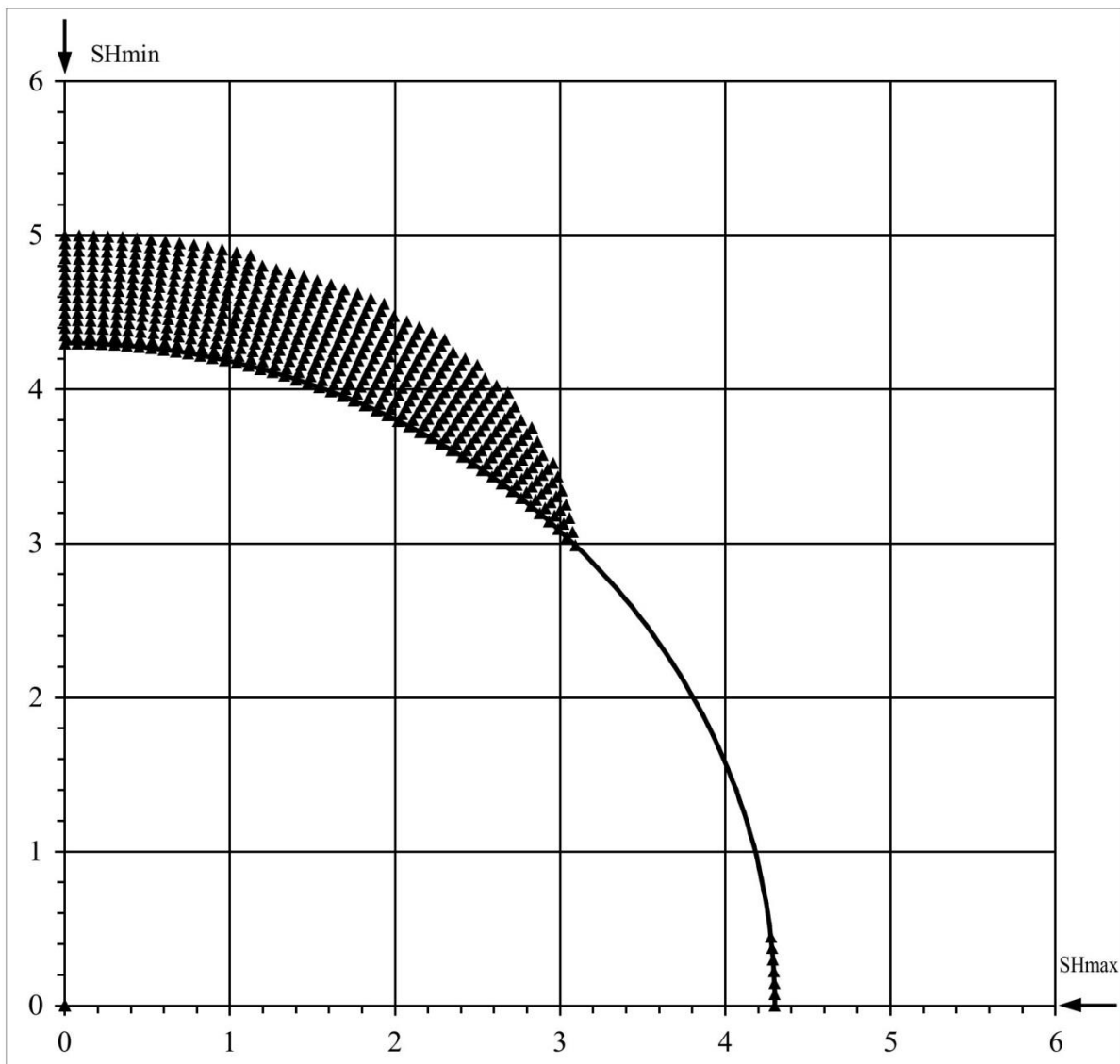
SHmax =	32.8 MPa	u (Coeff. of Friction) =	0.6
SHmin =	18.8 MPa	C (Cohesive Strength) =	5 MPa
Sv =	26.1 MPa	v (Poisson's Ratio) =	0.2
Po (Pore Pressure) =	10.9 MPa	Diameter of Borehole =	8.5 "
Pm (Mud Weight) =	10.9 MPa		
Sensitivity of Figure =	0.05 "	Angle of Max. Breakout =	49 deg
Depth of Max. Breakout =	1.15 "	Max caliper at 90 deg =	10.4 "
Validity of the results =	TRUE	Max caliper at 0 deg =	8 "



G-032-61-10-121-15

## Extended von-Mises Failure Criterion (Drucker-Prager Failure Criterion)

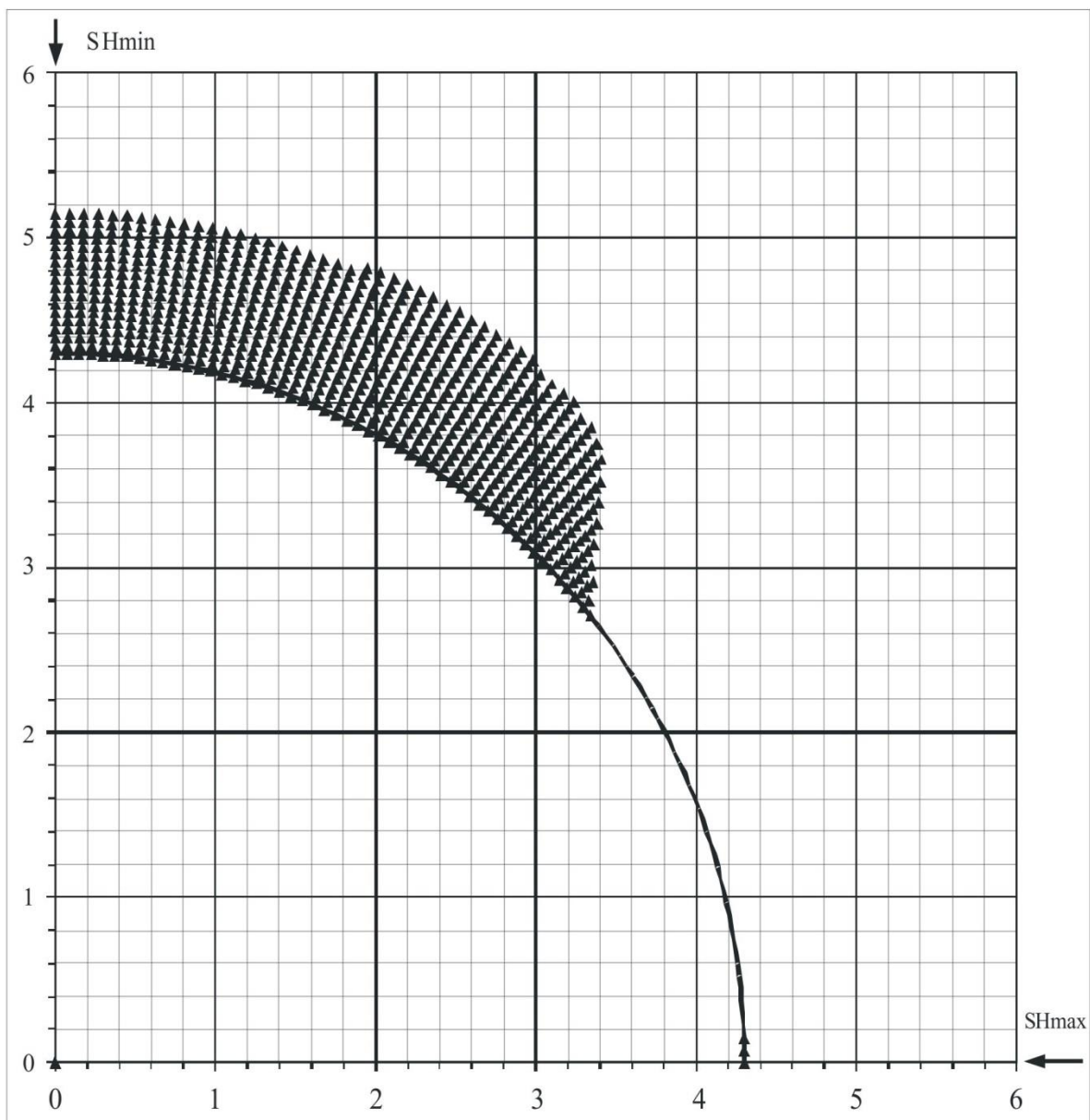
SHmax =	41.5 MPa	u (Coeff. of Friction)=	0.6
SHmin =	18.8 MPa	C (Cohesive Strength) =	5 MPa
Sv =	26.1 MPa	v (Poisson's Ratio) =	0.2
Po (Pore Pressure) =	10.9 MPa	Diameter of Borehole =	8.6 inches
Pm (Mud Weight) =	10.9 MPa	Depth of Max. Breakout =	0.7 inches
Sensitivity of Figure =	0.05 inches	Angle of Max. Breakout =	81 deg



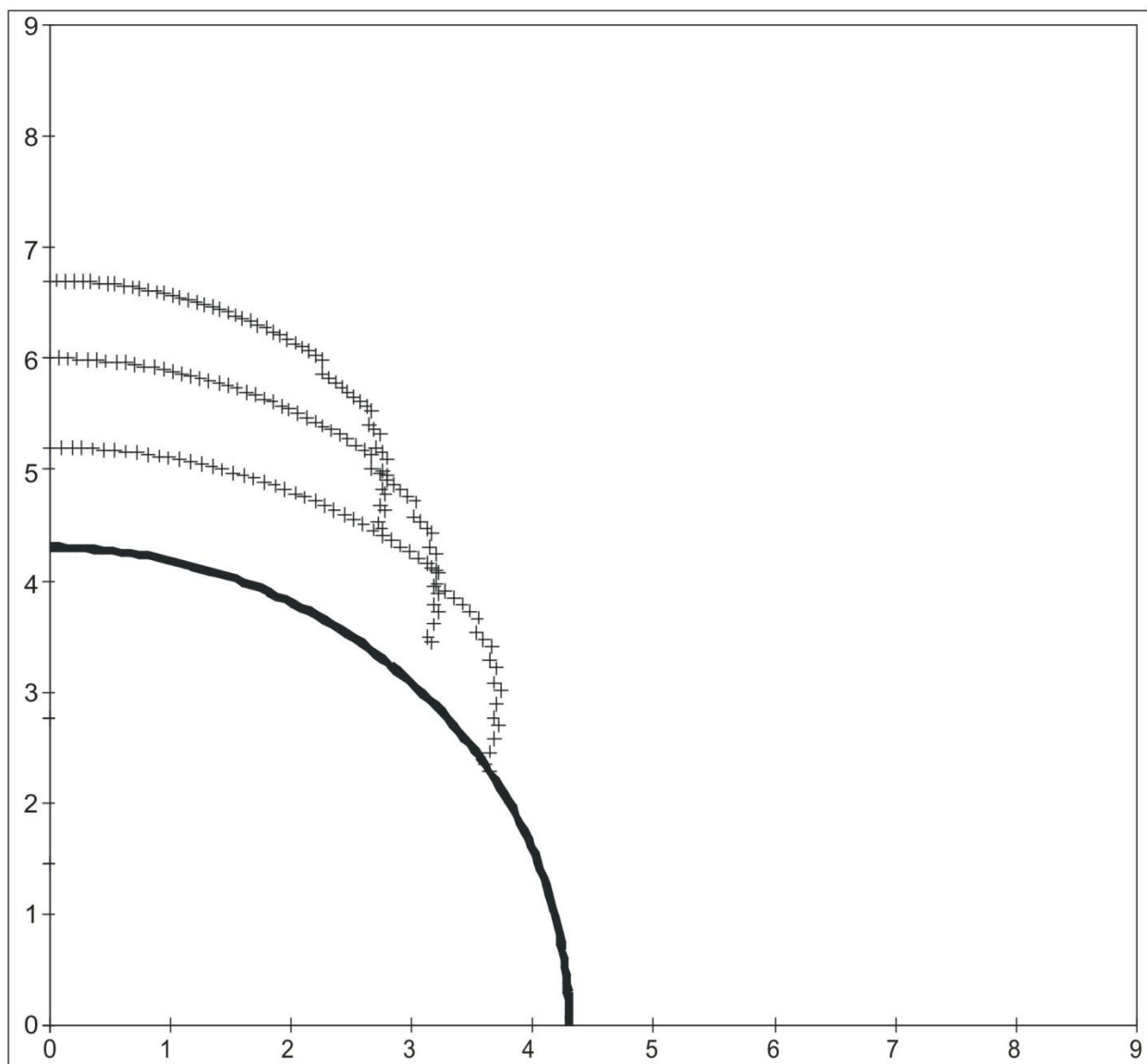
G-032-61-10-121-15

## Extended Drucker - Prager Failure Criterion (Modified Strain Energy Criterion)

SHmax =	38.9 MPa	u (Coeff. of Friction) =	0.6
SHmin =	18.8 MPa	C (Cohesive Strength) =	5 MPa
Sv =	26.1 MPa	v (Poisson's Ratio) =	0.2
Po (Pore Pressure) =	10.9 MPa	Diameter of Borehole =	8.6 inches
Pm (Mud Weight) =	10.9 MPa	Depth of Max. Breakout =	0.9 inches
Sensitivity of Figure =	0.05 inches	Angle of Max. Breakout =	61 deg



G-032-61-10-121-15					
<b>3 Cycle Mohr - Coulomb Failure Criterion</b>					
SHmax =	30.6	MPa	u (Coeff. of Friction) =	0.6	
SHmin =	18.8	MPa	C (Cohesive Strength) =	5	MPa
Sv =	26.1	MPa	v (Poisson's Ratio) =	0.2	
Po (Pore Pressure) =	10.9	MPa	Diameter of Borehole =	8.6	"
Pm (Mud Weight) =	10.9	MPa			
Sensitivity of Figure =	0.05	"			
Depth of Max. Breakout =	2.3	"	Max caliper at 90 deg =	13.2	"
Validity of the results =	TRUE		Max caliper at 0 deg =	8.6	"



**S<sub>Hmax</sub> Simulation Commentary G-042-60-20-121-00**

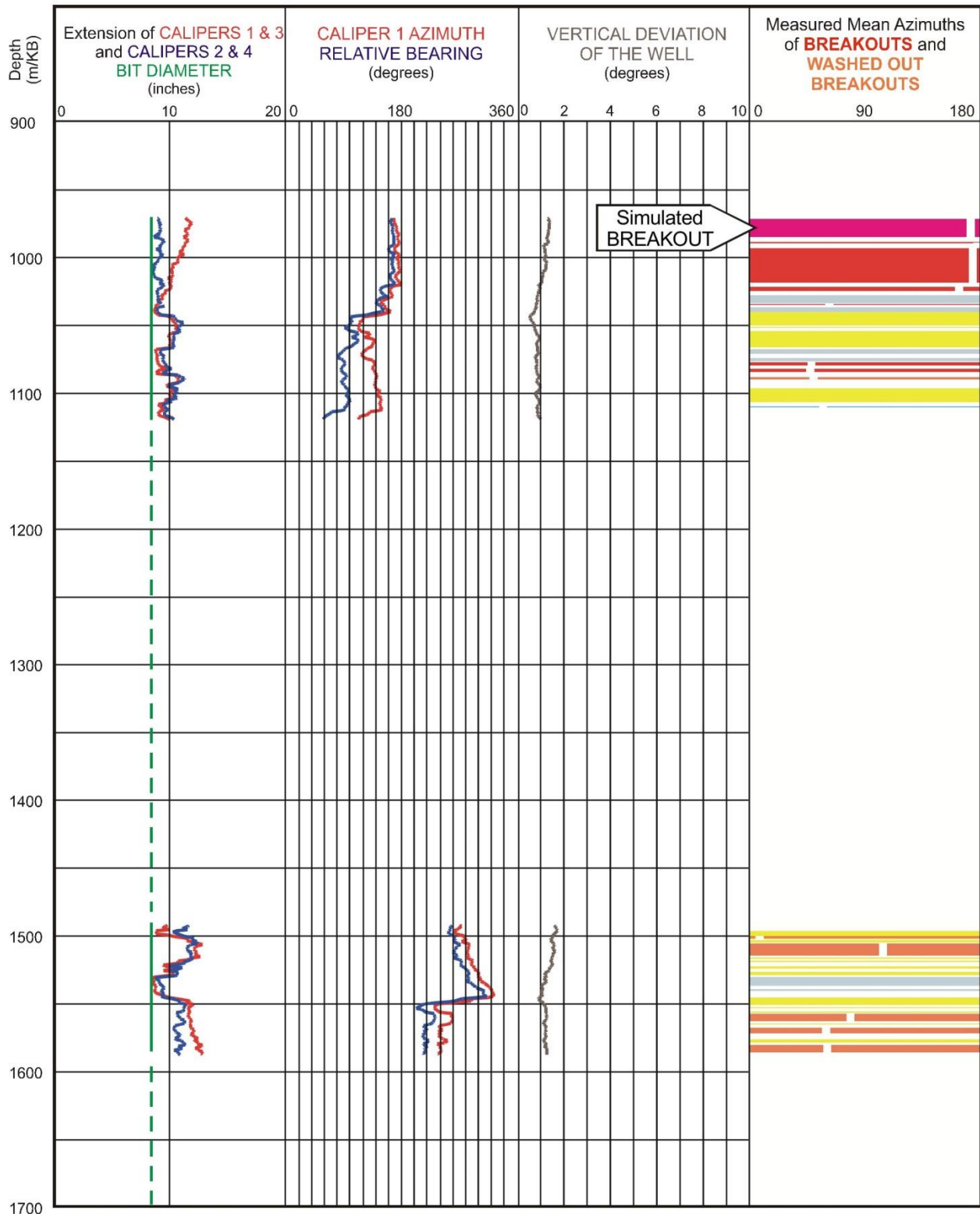


Well: <b>G-042-60-20-121-00</b>	Failure simulation Method				2SHmin-Po
	Mohr Coulomb	Drucker Prager	Modified Strain Energy	3 cycle Mohr Coulomb	
Breakout Interval Top (m KB)	972	972	972	972	
Breakout Interval Base (m KB)	986	986	986	986	
Median depth of Breakout (m KB)	979	979	979	979	
Calipers 1 and 3 extent (inches)	11.57	11.57	11.57	11.57	
Calipers 2 and 4 extent (inches)	9.07	9.07	9.07	9.07	
SHmax (MPa)	29.7*	38.6*	36.1*	<b>27.0</b>	25.0
SHmax gradient (kPa/m)	30.3	39.4	36.9	27.6	25.5
SHmin (MPa)	17.4	17.4	17.4	17.4	
Sv (MPa)	24.2	24.2	24.2	24.2	
Pore Pressure (MPa)	9.8	9.8	9.8	9.8	
Mudweight (MPa)	9.8	9.8	9.8	9.8	
u (Coefficient of Friction)	0.6	0.6	0.6	0.6	
Cohesive Strength of Rock (MPa)	4.5	4.5	4.5	7.0	
v (Poisson's Ratio)	0.2	0.2	0.2	0.2	
Bit size (inches)	8.5	8.5	8.5	8.5	

\* indicates that modelling could not simulate accurate breakout anisotropy

The breakout interval that was selected for modelling, 972-986 m, exhibits relatively deep spalling, since the long axis of the breakout interval extends to 11.6 inches. The single cycle simulation routines were not able to generate sufficiently deep breakouts, although the Mohr Coulomb simulation routine came close with a maximum breakout diameter of 11.2 inches at a cohesive strength of 4.5 MPa (which is on the low side). However, the 3 Cycle Mohr Coulomb routine modelled the breakout completely with  $S_{Hmax}$  set at **27.0 MPa** and the cohesive strength set at 7 MPa. This value was taken as a reliable estimate of  $S_{Hmax}$  and it compares reasonably well with the  $S_{Hmax}$  magnitude of 25.0 MPa, suggested by the equation:  $S_{Hmax} = 2(S_{Hmin}) - P_o$ .

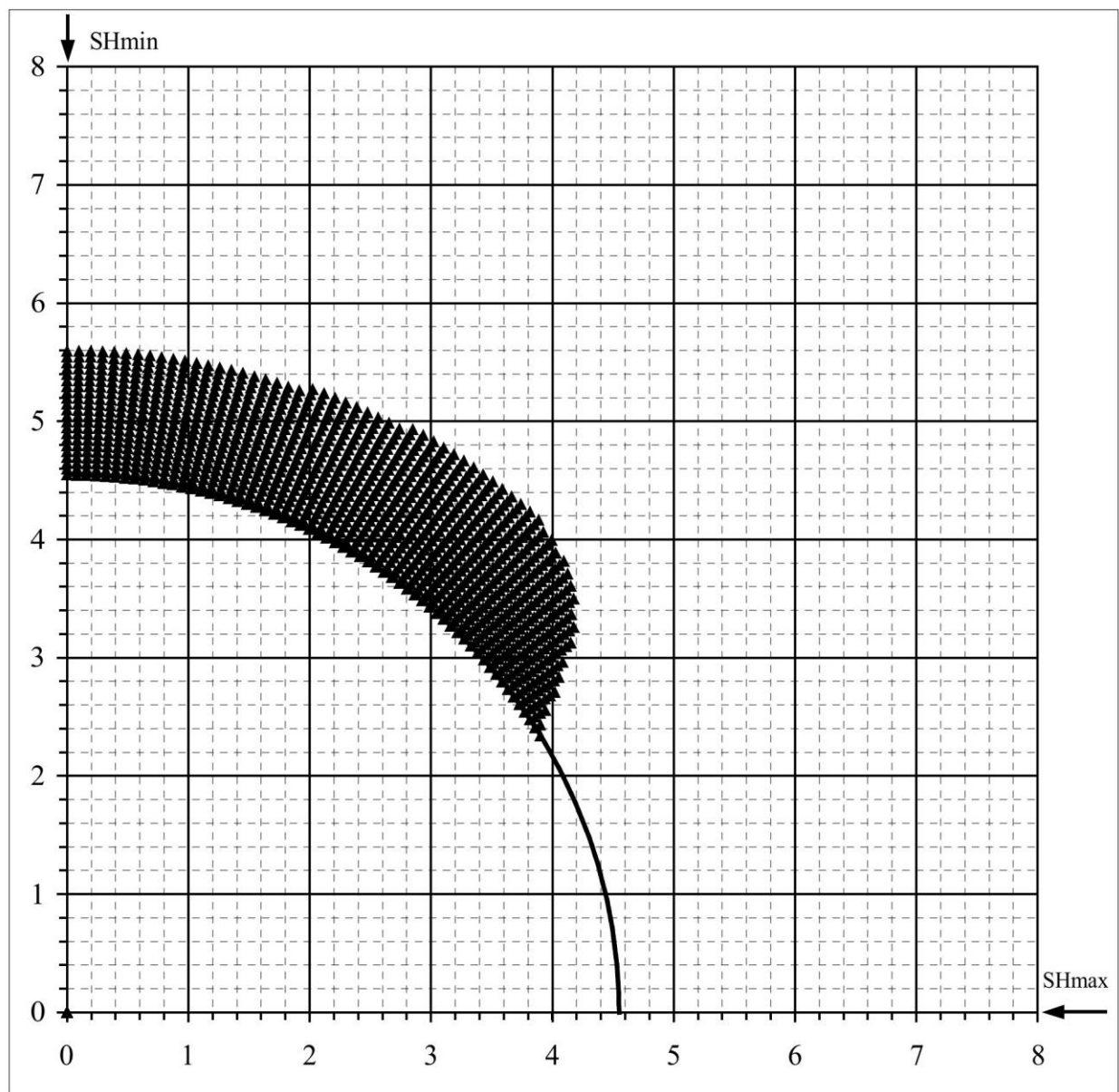
WELL : G-42-60-20-121-00 BREAKOUT ANALYSIS



G-042-60-20-121-00

## Mohr - Coulomb Failure Criterion

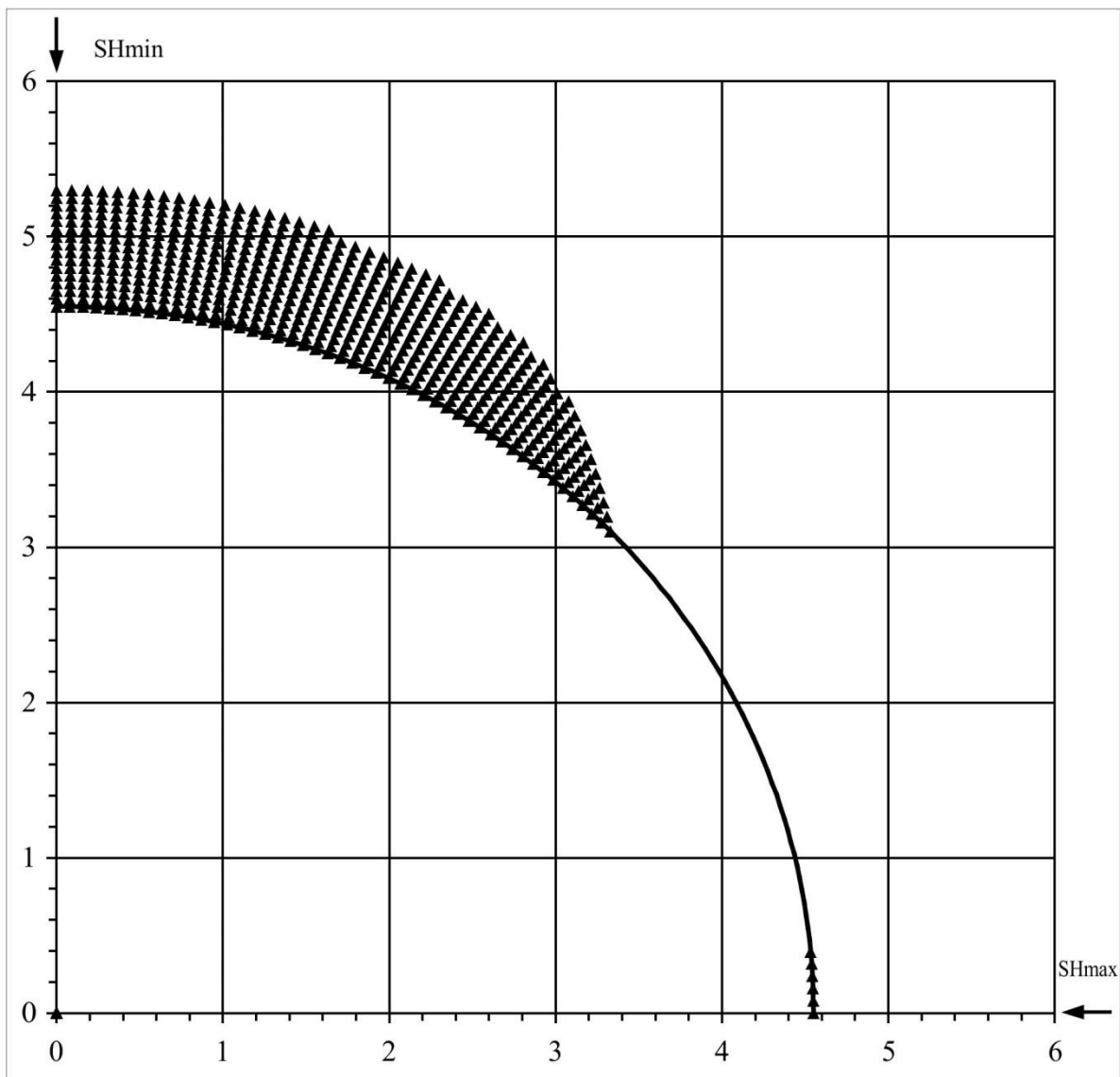
SHmax =	29.7 MPa	u (Coeff. of Friction) =	0.6
SHmin =	17.4 MPa	C (Cohesive Strength) =	4.5 MPa
Sv =	24.2 MPa	v (Poisson's Ratio) =	0.2
Po (Pore Pressure) =	9.8 MPa	Diameter of Borehole =	9.1 "
Pm (Mud Weight) =	9.8 MPa		
Sensitivity of Figure =	0.05 "	Angle of Max. Breakout =	53 deg
Depth of Max. Breakout =	1.15 "	Max caliper at 90 deg =	11.2 "
Validity of the results =	TRUE	Max caliper at 0 deg =	8 "



G-042-60-20-121-00

## Extended von-Mises Failure Criterion (Drucker-Prager Failure Criterion)

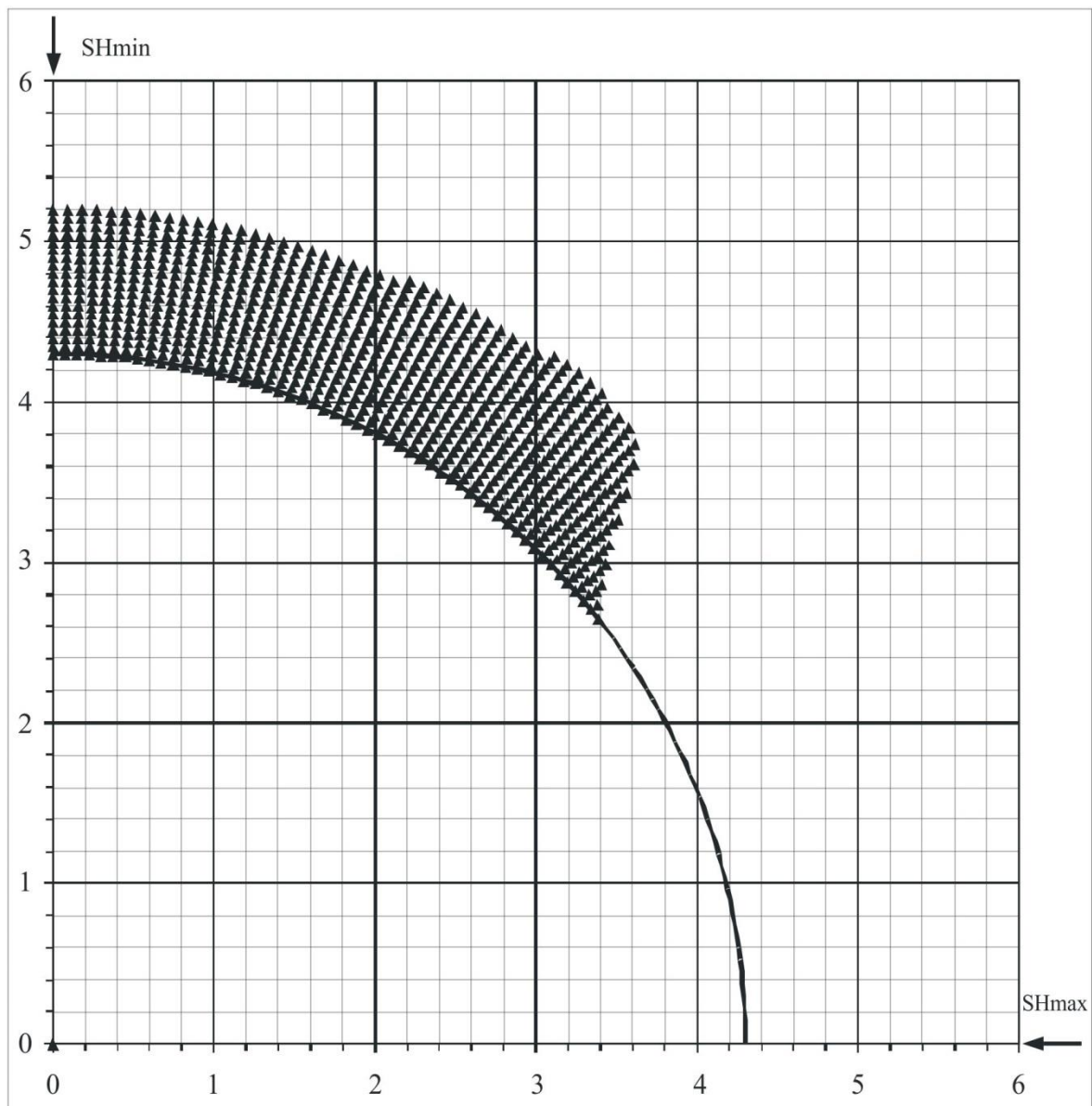
SHmax =	38.6 MPa	u (Coeff. of Friction)=	0.6
SHmin =	17.4 MPa	C (Cohesive Strength) =	4.5 MPa
Sv =	24.2 MPa	v (Poisson's Ratio) =	0.2
Po (Pore Pressure) =	9.8 MPa	Diameter of Borehole =	9.1 inches
Pm (Mud Weight) =	9.8 MPa	Depth of Max. Breakout =	0.75 inches
Sensitivity of Figure =	0.05 inches	Angle of Max. Breakout =	81 deg



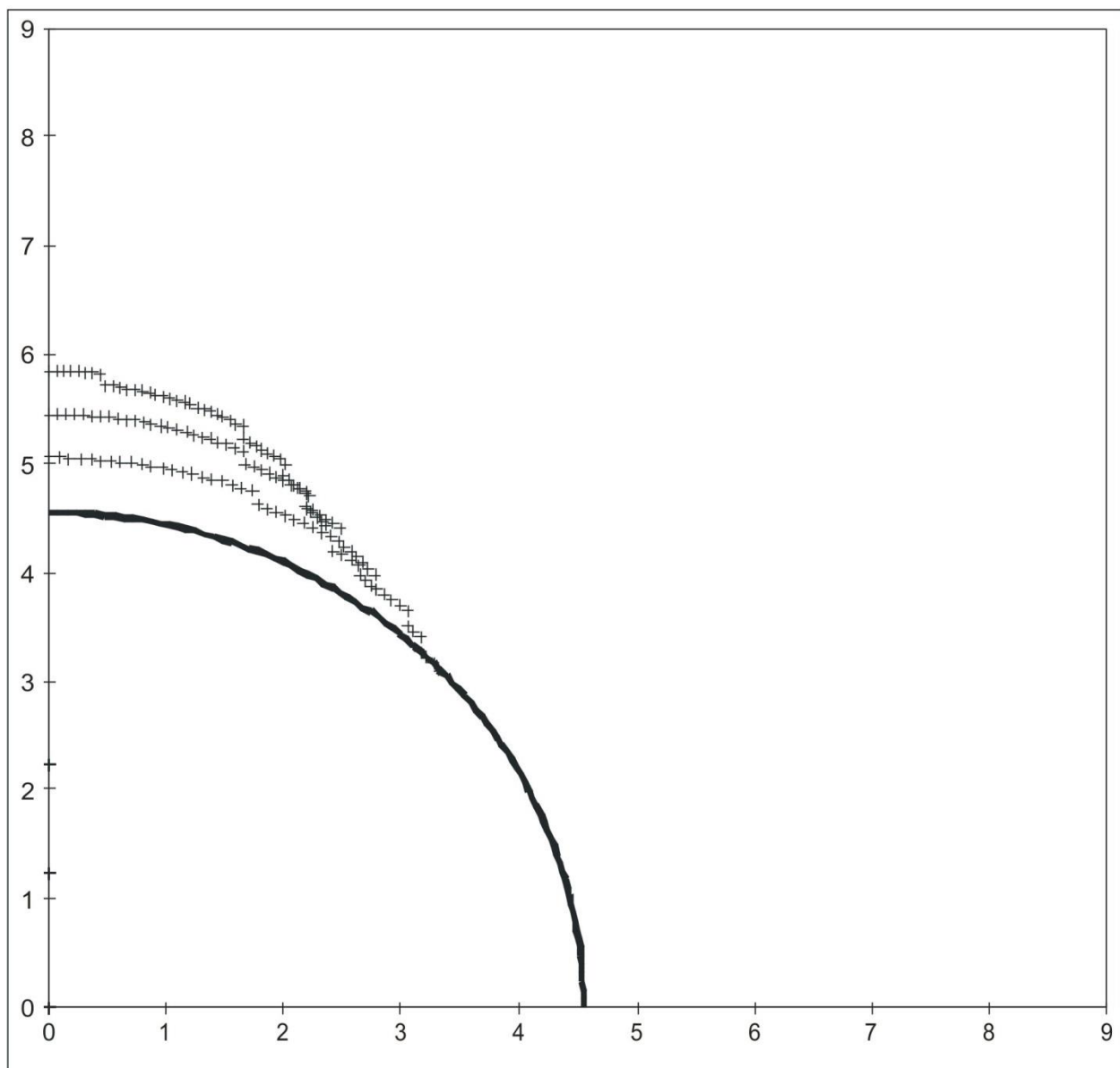
G-042-60-20-121-00

## Extended Drucker - Prager Failure Criterion (Modified Strain Energy Criterion)

SHmax =	36.1 MPa	u (Coeff. of Friction) =	0.6
SHmin =	17.4 MPa	C (Cohesive Strength) =	4.5 MPa
Sv =	24.2 MPa	v (Poisson's Ratio) =	0.2
Po (Pore Pressure) =	9.8 MPa	Diameter of Borehole =	8.6 inches
Pm (Mud Weight) =	9.8 MPa	Depth of Max. Breakout =	1 inch
Sensitivity of Figure =	0.05 inches	Angle of Max. Breakout =	52 deg



G-042-60-20-121-00					
<b>3 Cycle Mohr - Coulomb Failure Criterion</b>					
SHmax =	27	MPa	u (Coeff. of Friction) =	0.6	
SHmin =	17.4	MPa	C (Cohesive Strength) =	7	MPa
Sv =	24.2	MPa	v (Poisson's Ratio) =	0.2	
Po (Pore Pressure) =	9.8	MPa	Diameter of Borehole =	9.1	"
Pm (Mud Weight) =	9.8	MPa			
Sensitivity of Figure =	0.05	"			
Depth of Max. Breakout =	1.25	"	Max caliper at 90 deg =	11.6	"
Validity of the results =	TRUE		Max caliper at 0 deg =	9.1	"



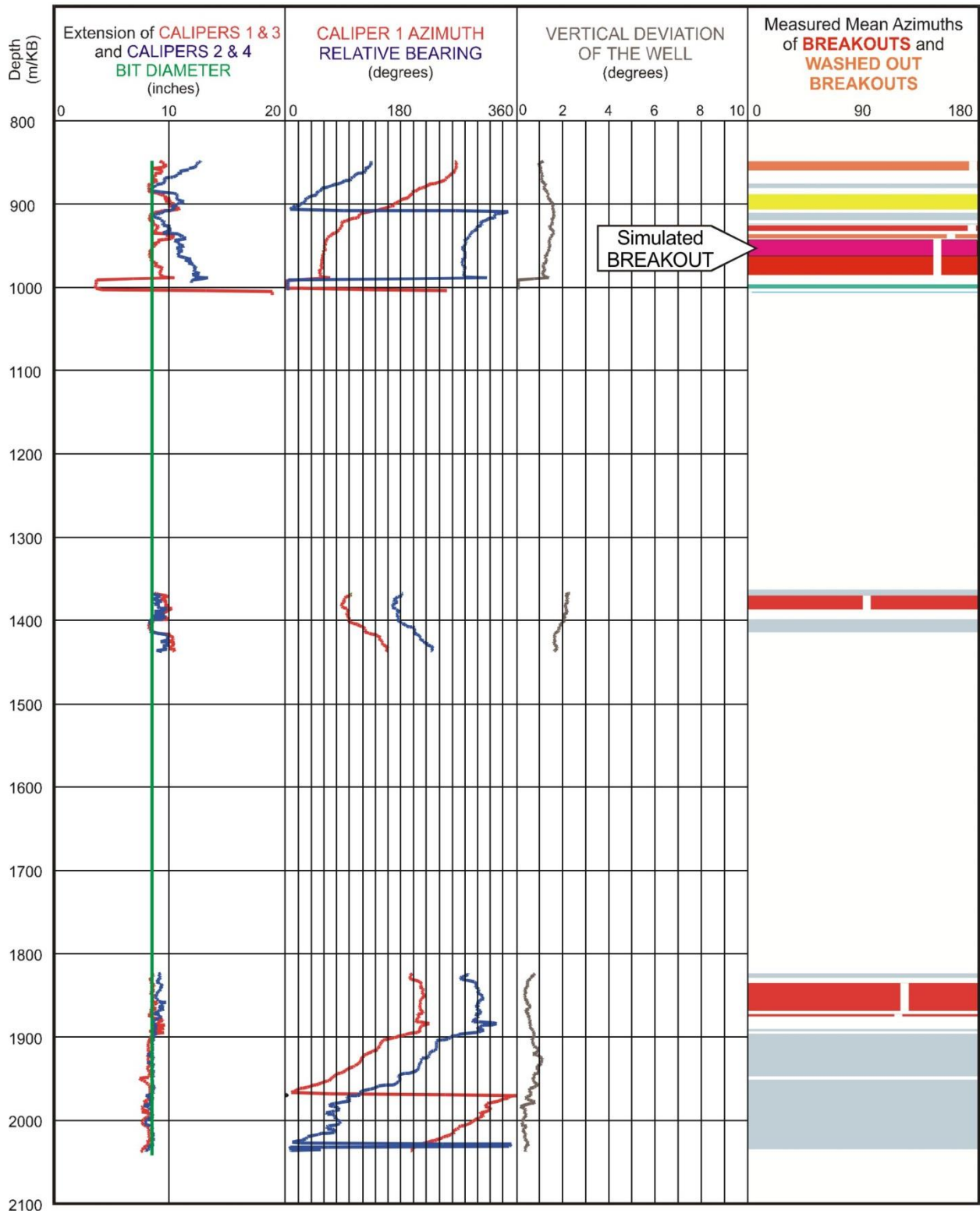
## $S_{Hmax}$ Simulation Commentary M-51-60-30-121-00

Well: M-051-60-30-121-00	Failure simulation Method				2SHmin-Po
	Mohr Coulomb	Drucker Prager	Modified Strain Energy	3 cycle Mohr Coulomb	
Breakout Interval Top (m KB)	944	944	944	944	
Breakout Interval Base (m KB)	964	964	964	964	
Median depth of Breakout (m KB)	954	954	954	954	
Calipers 1 and 3 extent (inches)	8.56	8.56	8.56	8.56	
Calipers 2 and 4 extent (inches)	10.92	10.92	10.92	10.92	
SHmax (MPa)	29.3*	37.5*	35.6*	<b>26.5</b>	24.1
SHmax gradient (kPa/m)	30.7	39.3	37.3	27.8	25.3
SHmin (MPa)	16.8	16.8	16.8	16.8	
Sv (MPa)	23.5	23.5	23.5	23.5	
Pore Pressure (MPa)	9.5	9.5	9.5	9.5	
Mudweight (MPa)	9.5	9.5	9.5	9.5	
u (Coefficient of Friction)	0.6	0.6	0.6	0.6	
Cohesive Strength of Rock (MPa)	4.5	4.5	4.5	7.0	
v (Poisson's Ratio)	0.2	0.2	0.2	0.2	
Bit size (inches)	8.5	8.5	8.5	8.5	

\* indicates that modelling could not simulate accurate breakout anisotropy

The breakout interval that was selected for modelling, 972-986 m, exhibits moderately deep spalling, with the long axis of the breakout interval extending to 10.9 inches. The single cycle simulation routines were not quite able to generate a deep enough breakout, although the Modified Strain Energy simulation routine came close with a maximum breakout diameter of 10.7 inches at a cohesive strength of 4.5 MPa (which is on the low side). However, the 3 Cycle Mohr Coulomb routine modelled the 10.9 inch breakout completely with  $S_{Hmax}$  set at **26.5 MPa** and the cohesive strength raised to 7 MPa. This value was taken as a reliable estimate of  $S_{Hmax}$  and it compares reasonably well with the  $S_{Hmax}$  magnitude of 24.1 MPa, suggested by the equation:  $S_{Hmax} = 2(S_{Hmin}) - P_o$ .

WELL : M-51-60-30-121-00 BREAKOUT ANALYSIS

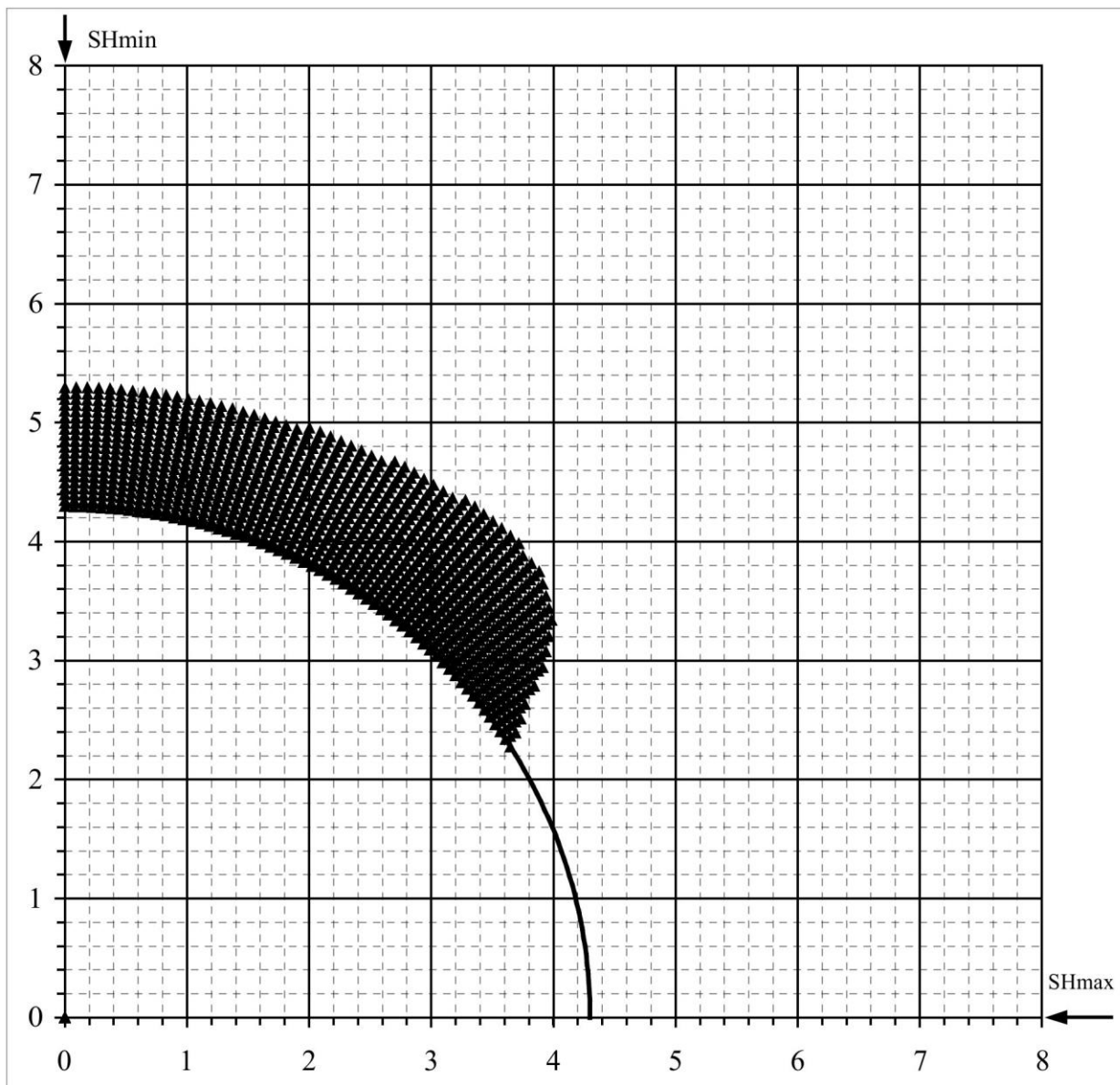




M-051-60-30-121-00

### Mohr - Coulomb Failure Criterion

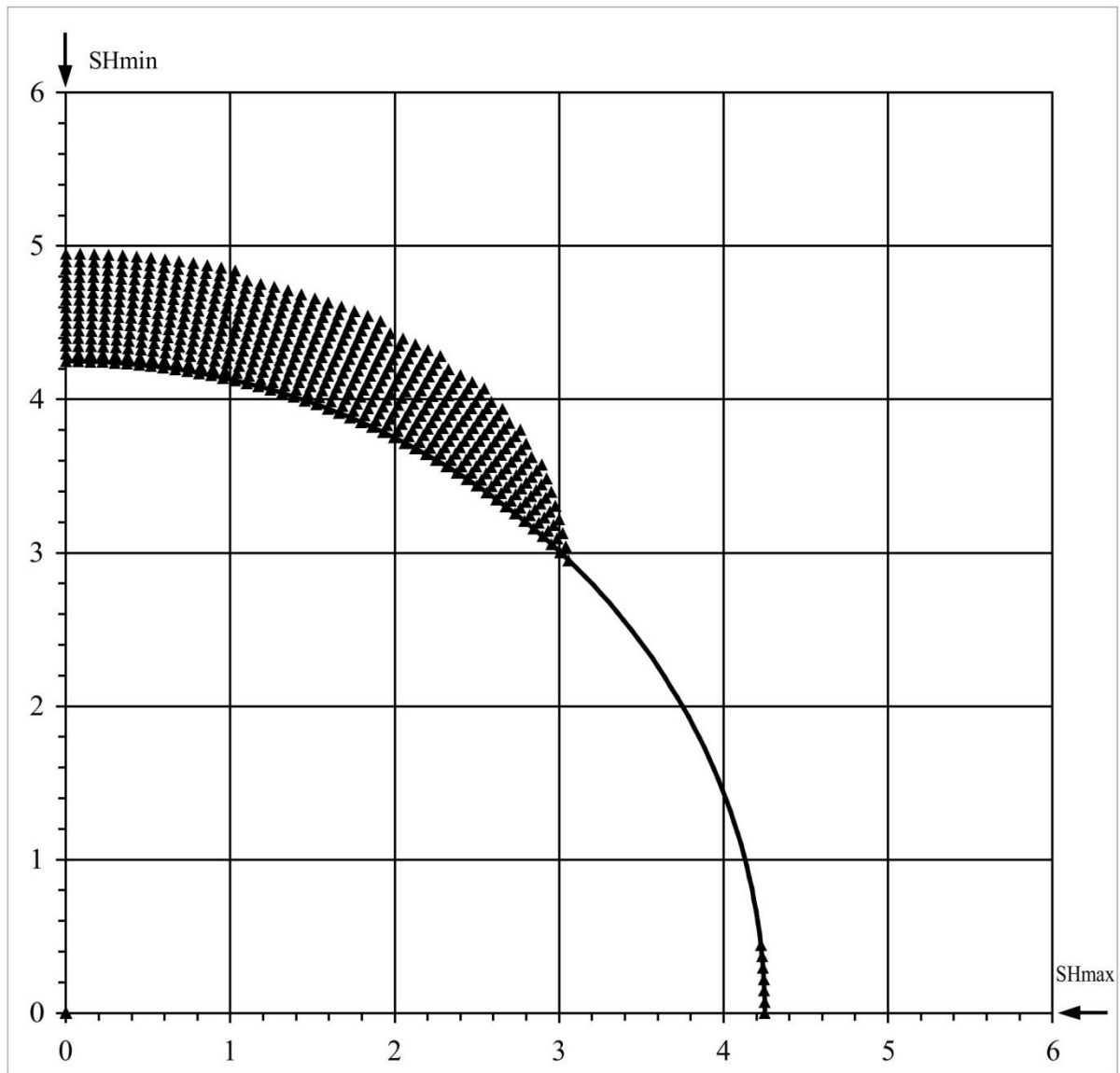
SHmax =	29.3 MPa	u (Coeff. of Friction) =	0.6
SHmin =	16.8 MPa	C (Cohesive Strength) =	4.5 MPa
Sv =	23.5 MPa	v (Poisson's Ratio) =	0.2
Po (Pore Pressure) =	9.5 MPa	Diameter of Borehole =	8.6 "
Pm (Mud Weight) =	9.5 MPa		
Sensitivity of Figure =	0.05 "	Angle of Max. Breakout =	50 deg
Depth of Max. Breakout =	1.15 "	Max caliper at 90 deg =	10.6 "
Validity of the results =	TRUE	Max caliper at 0 deg =	8 "



M-051-60-30-121-00

## Extended von-Mises Failure Criterion (Drucker-Prager Failure Criterion)

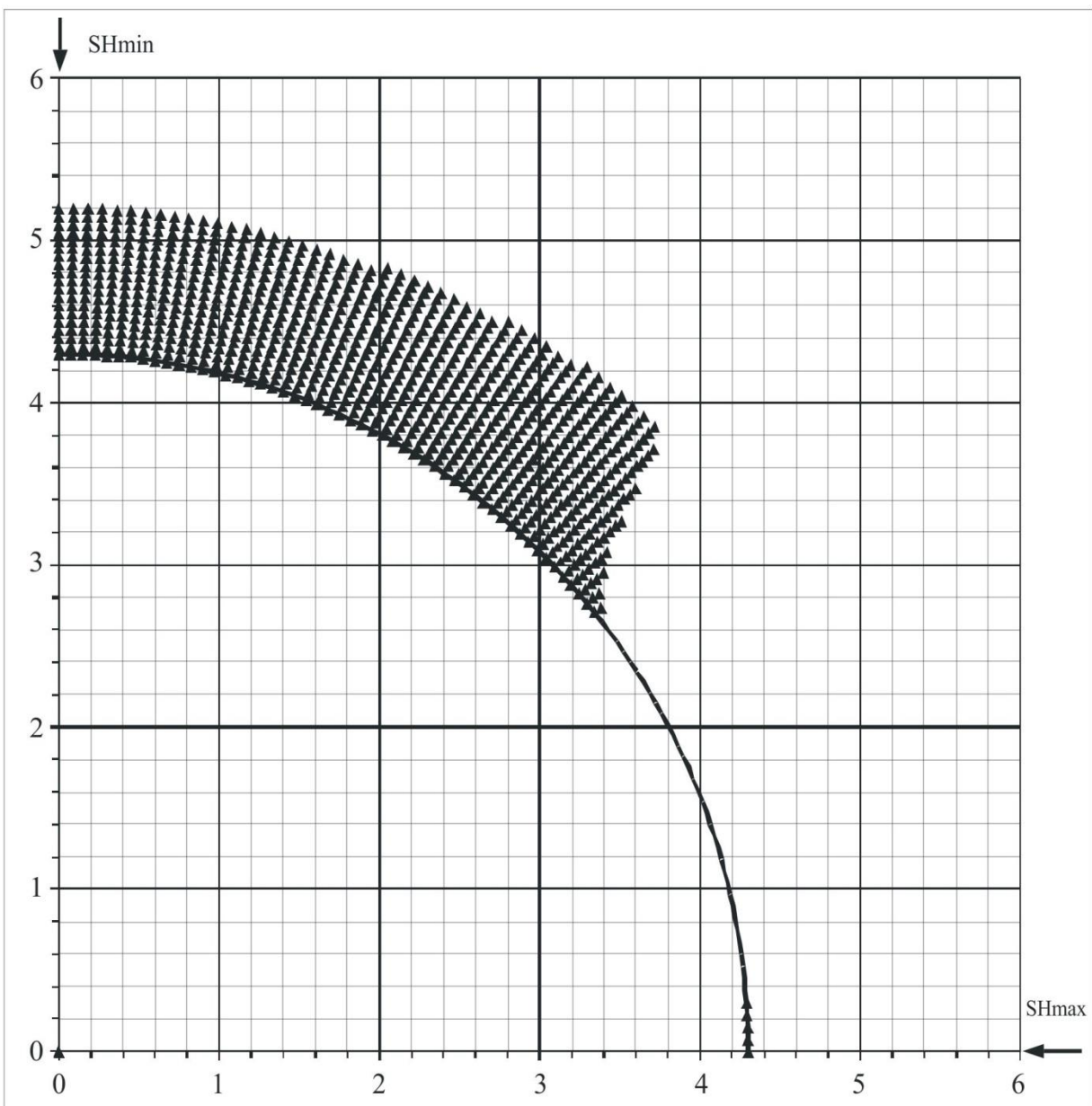
SHmax =	37.5 MPa	u (Coeff. of Friction)=	0.6
SHmin =	16.8 MPa	C (Cohesive Strength) =	4.5 MPa
Sv =	23.5 MPa	v (Poisson's Ratio) =	0.2
Po (Pore Pressure) =	9.5 MPa	Diameter of Borehole =	8.5 inches
Pm (Mud Weight) =	9.5 MPa	Depth of Max. Breakout =	0.7 inches
Sensitivity of Figure =	0.05 inches	Angle of Max. Breakout =	90 deg



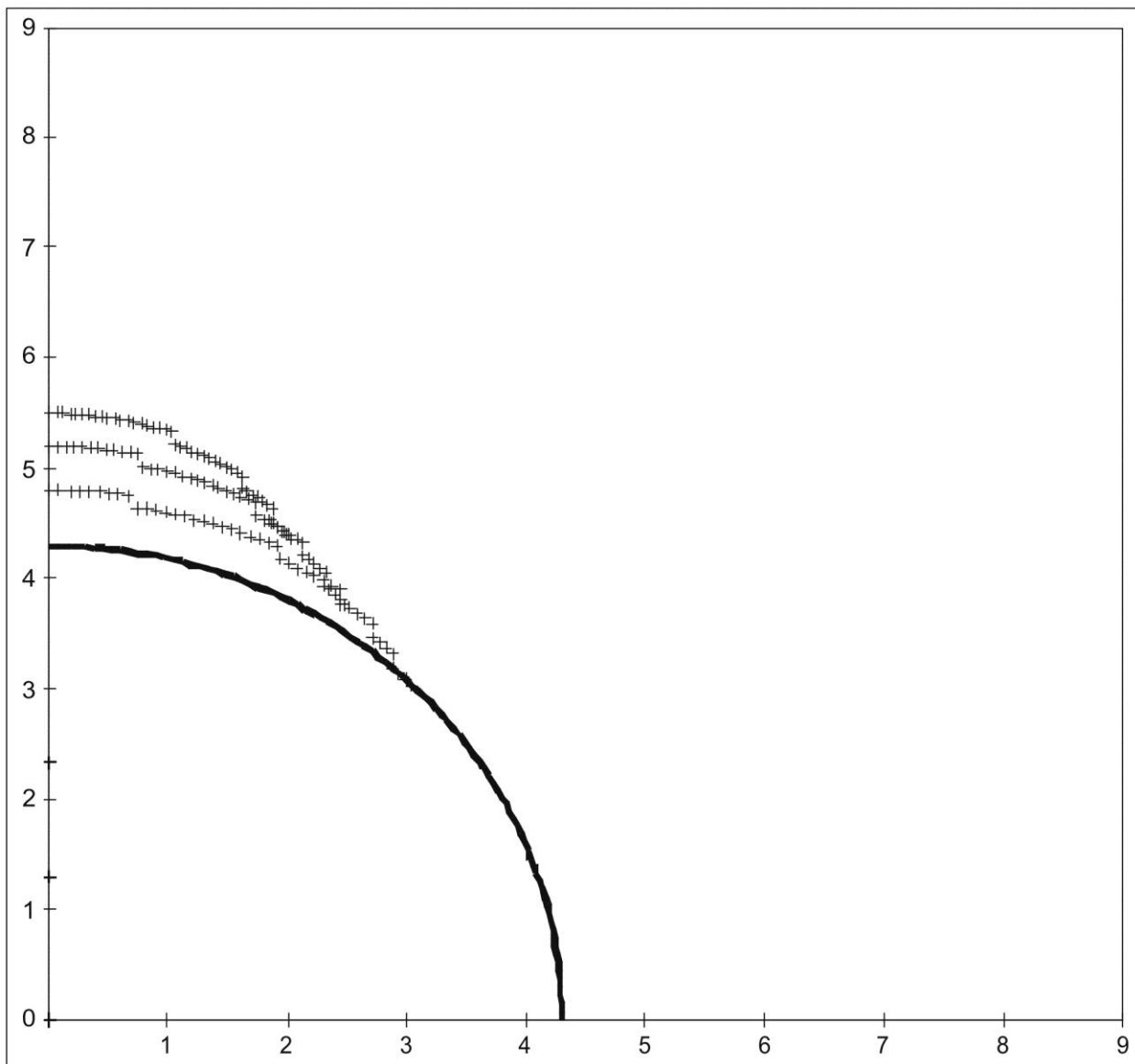
M-051-60-30-121-00

## Extended Drucker - Prager Failure Criterion (Modified Strain Energy Criterion)

SHmax =	35.6 MPa	u (Coeff. of Friction) =	0.6
SHmin =	16.8 MPa	C (Cohesive Strength) =	4.5 MPa
Sv =	23.5 MPa	v (Poisson's Ratio) =	0.2
Po (Pore Pressure) =	9.5 MPa	Diameter of Borehole =	8.6 inches
Pm (Mud Weight) =	9.5 MPa	Depth of Max. Breakout =	1.05 inches
Sensitivity of Figure =	0.05 inches	Angle of Max. Breakout =	49 deg



M-051-60-30-121-00					
3 Cycle Mohr - Coulomb Failure Criterion					
SHmax =	26.5	MPa	u (Coeff. of Friction) =	0.6	
SHmin =	16.8	MPa	C (Cohesive Strength) =	7	MPa
Sv =	23.5	MPa	v (Poisson's Ratio)=	0.2	
Po (Pore Pressure) =	9.5	MPa	Diameter of Borehole =	8.6	"
Pm (Mud Weight) =	9.5	MPa			
Sensitivity of Figure =	0.05	"			
Depth of Max. Breakout =	1.15	"	Max caliper at 90 deg =	10.9	"
Validity of the results =	TRUE		Max caliper at 0 deg =	8.6	"



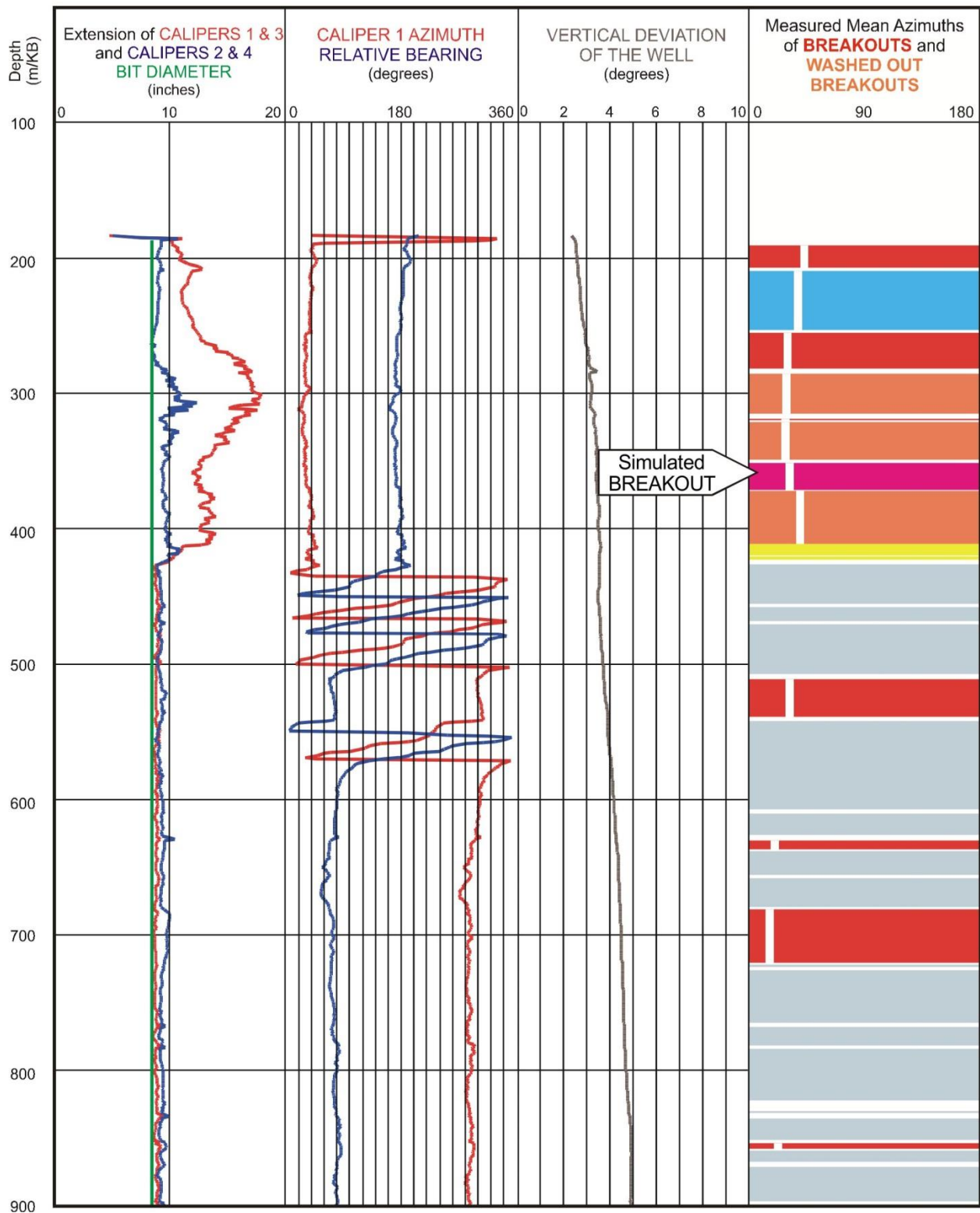
SHmax Simulation Commentary P-24-60-30-123-45

Well: <b>P-024-60-30-123-45</b>	Failure simulation Method				2SHmin-Po
	Mohr Coulomb	Drucker Prager	Modified Strain Energy	3 cycle Mohr Coulomb	
Breakout Interval Top (m KB)	352	352	352	352	
Breakout Interval Base (m KB)	372	372	372	372	
Median depth of Breakout (m KB)	362	362	362	362	
Calipers 1 and 3 extent (inches)	12.48	12.48	12.48	12.48	
Calipers 2 and 4 extent (inches)	9.41	9.41	9.41	9.41	
SHmax (MPa)	12.8*	15.1*	14.1*	<b>10.5</b>	9.0
SHmax gradient (kPa/m)	35.4	41.7	39.0	29.0	24.9
SHmin (MPa)	6.3	6.3	6.3	6.3	
Sv (MPa)	9.1	9.1	9.1	9.1	
Pore Pressure (MPa)	3.6	3.6	3.6	3.6	
Mudweight (MPa)	3.6	3.6	3.6	3.6	
u (Coefficient of Friction)	0.6	0.6	0.6	0.6	
Cohesive Strength of Rock (MPa)	2.5	2.5	2.5	2.5	
v (Poisson's Ratio)	0.2	0.2	0.2	0.2	
Bit size (inches)	8.5	8.5	8.5	8.5	

\* indicates that modelling could not simulate accurate breakout anisotropy

The breakout interval that was selected for modelling, 352-372 m, exhibits moderately deep spalling, with the long axis of the breakout interval extending to 12.5 inches. The single cycle simulation routines were not able to generate a deep enough breakout, although the Mohr Coulomb simulation routine came close with a maximum breakout diameter of 11.3 inches at a cohesive strength of 2.5 MPa. The 3 Cycle Mohr Coulomb routine modelled the 12.5 inch breakout completely with  $S_{Hmax}$  set at **10.5 MPa** and the cohesive strength maintained at 2.5 MPa. This value was taken as a reliable estimate of  $S_{Hmax}$  and it compares reasonably well with the  $S_{Hmax}$  magnitude of 9.0 MPa, suggested by the equation:  $S_{Hmax} = 2(S_{Hmin}) - P_o$ .

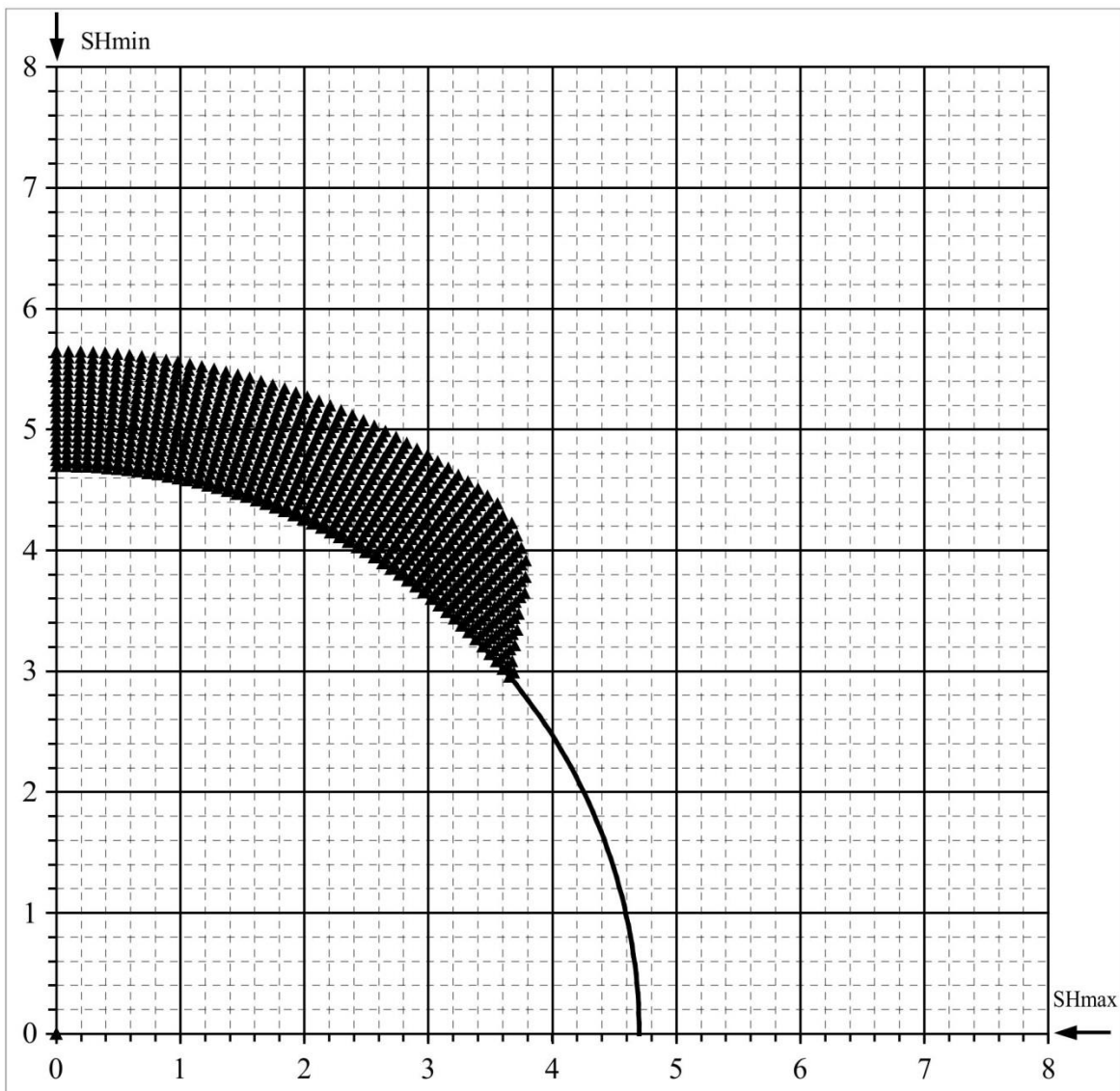
WELL : P-024-60-30-123-45 BREAKOUT ANALYSIS



P-024-60-30-123-45

## Mohr - Coulomb Failure Criterion

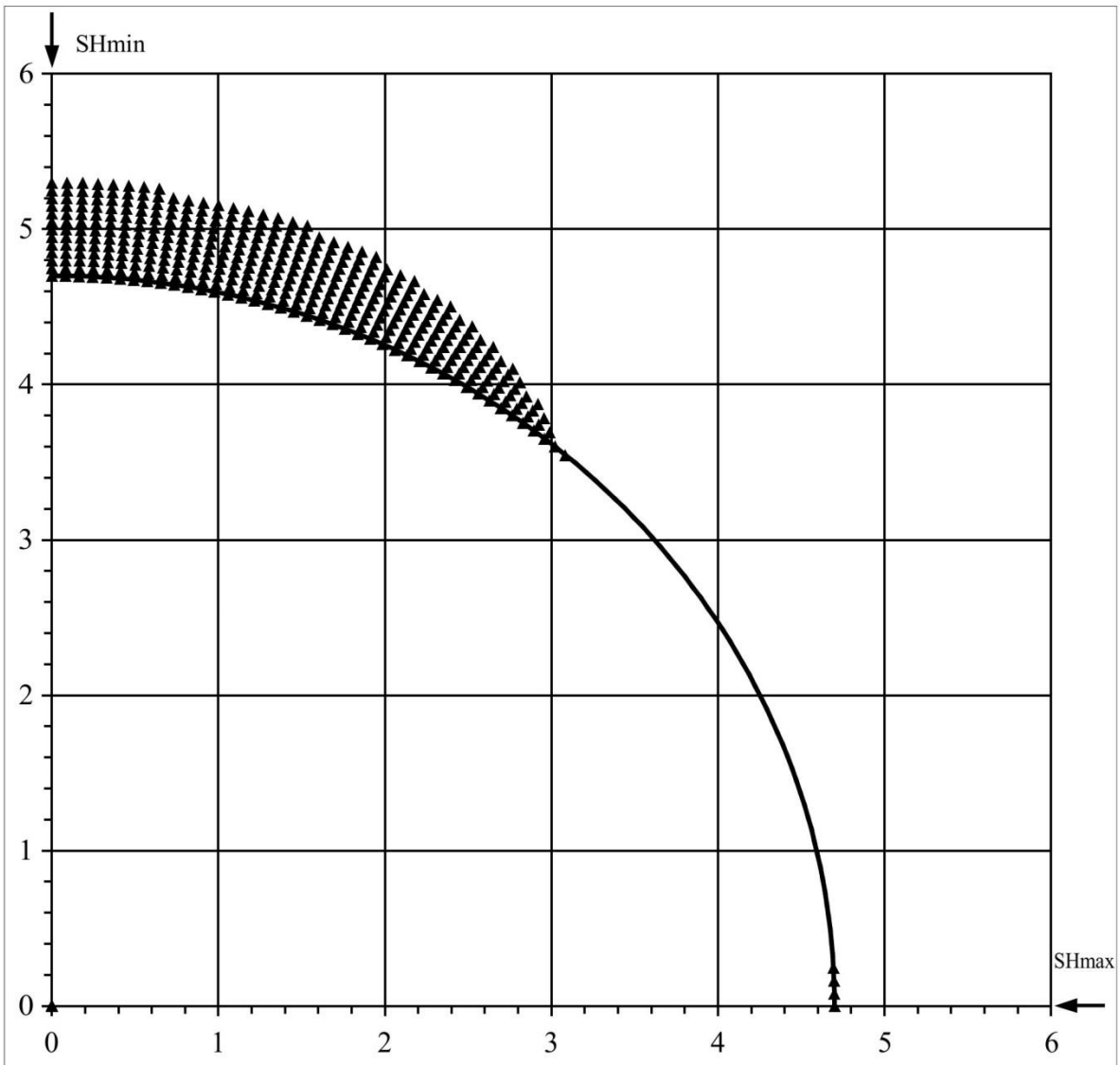
SHmax =	12.8 MPa	u (Coeff. of Friction) =	0.6
SHmin =	6.3 MPa	C (Cohesive Strength) =	2.5 MPa
Sv =	9.1 MPa	v (Poisson's Ratio) =	0.2
Po (Pore Pressure) =	3.6 MPa	Diameter of Borehole =	9.4 "
Pm (Mud Weight) =	3.6 MPa		
Sensitivity of Figure =	0.05 "	Angle of Max. Breakout =	64 deg
Depth of Max. Breakout =	0.95 "	Max caliper at 90 deg =	11.3 "
Validity of the results =	TRUE	Max caliper at 0 deg =	8 "



P-024-60-30-123-45

## Extended von-Mises Failure Criterion (Drucker-Prager Failure Criterion)

SHmax =	15.1 MPa	u (Coeff. of Friction)=	0.6
SHmin =	6.3 MPa	C (Cohesive Strength) =	2.5 MPa
Sv =	9.1 MPa	v (Poisson's Ratio) =	0.2
Po (Pore Pressure) =	3.6 MPa	Diameter of Borehole =	9.4 inches
Pm (Mud Weight) =	3.6 MPa	Depth of Max. Breakout =	0.6 inches
Sensitivity of Figure =	0.05 inches	Angle of Max. Breakout =	90 deg

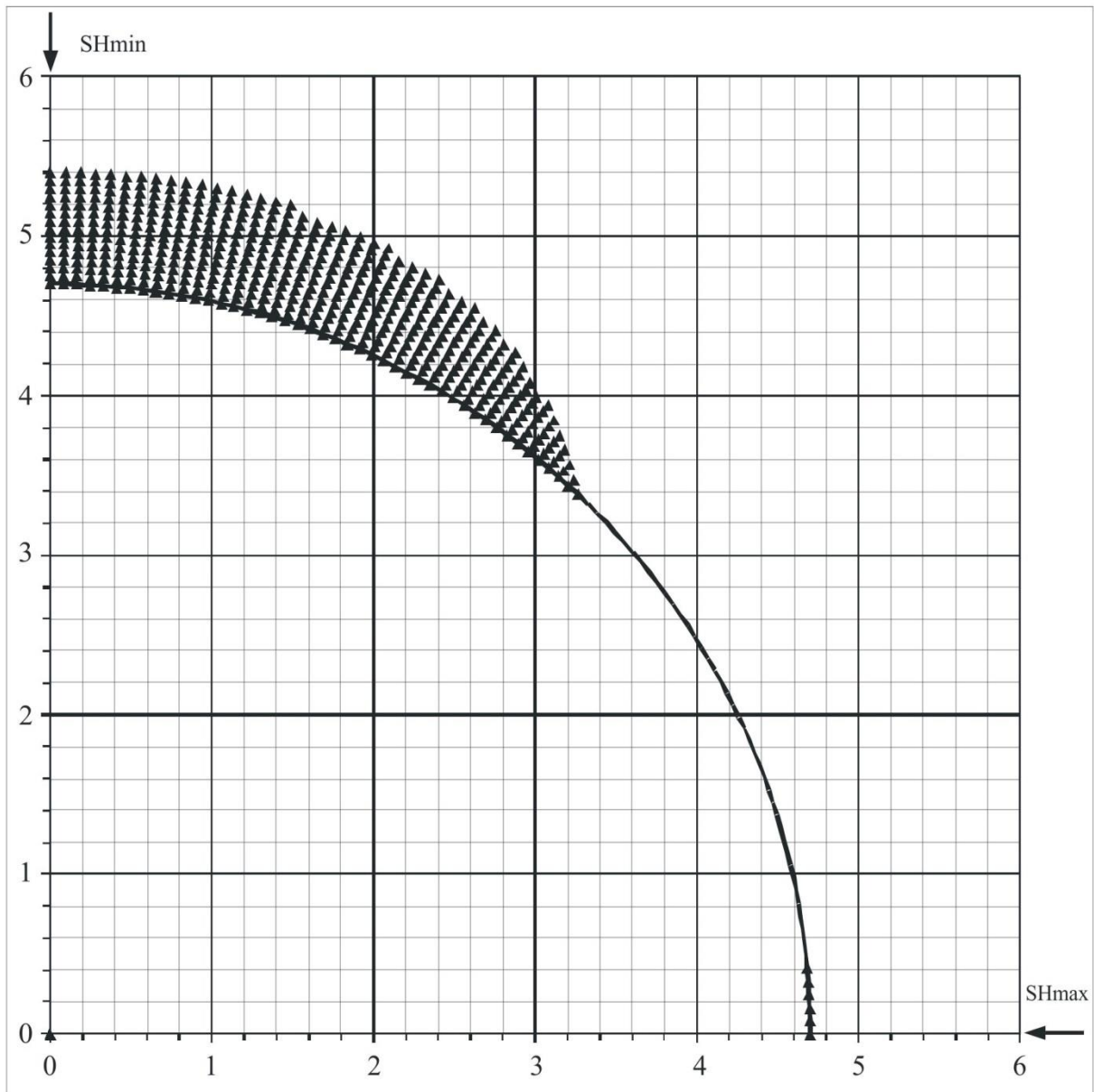




P-024-60-30-123-45

## Extended Drucker - Prager Failure Criterion (Modified Strain Energy Criterion)

SHmax =	14.1 MPa	u (Coeff. of Friction) =	0.6
SHmin =	6.3 MPa	C (Cohesive Strength) =	2.5 MPa
Sv =	9.1 MPa	v (Poisson's Ratio) =	0.2
Po (Pore Pressure) =	3.6 MPa	Diameter of Borehole =	9.4 inches
Pm (Mud Weight) =	3.6 MPa	Depth of Max. Breakout =	0.7 inches
Sensitivity of Figure =	0.05 inches	Angle of Max. Breakout =	79 deg



P-024-60-30-123-45					
<b>3 Cycle Mohr - Coulomb Failure Criterion</b>					
SHmax =	10.5	MPa	u (Coeff. of Friction) =	0.6	
SHmin =	6.3	MPa	C (Cohesive Strength) =	2.5	MPa
Sv =	9.1	MPa	v (Poisson's Ratio)=	0.2	
Po (Pore Pressure) =	3.6	MPa	Diameter of Borehole =	9.4	"
Pm (Mud Weight) =	3.6	MPa			
Sensitivity of Figure =	0.05	"			
Depth of Max. Breakout =	1.55	"	Max caliper at 90 deg =	12.5	"
Validity of the results =	TRUE		Max caliper at 0 deg =	9.4	"

